



THE UNIVERSITY OF
WAIKATO
Te Whare Wānanga o Waikato

Research Commons

<http://waikato.researchgateway.ac.nz/>

Research Commons at the University of Waikato

Copyright Statement:

The digital copy of this thesis is protected by the Copyright Act 1994 (New Zealand).

The thesis may be consulted by you, provided you comply with the provisions of the Act and the following conditions of use:

- Any use you make of these documents or images must be for research or private study purposes only, and you may not make them available to any other person.
- Authors control the copyright of their thesis. You will recognise the author's right to be identified as the author of the thesis, and due acknowledgement will be made to the author where appropriate.
- You will obtain the author's permission before publishing any material from the thesis.

THE NATURE, COMPOSITION AND DISTRIBUTION OF SEDIMENT IN LAKE ROTORUA, NEW ZEALAND

A thesis
submitted in partial fulfilment
of the requirements for the degree of

MASTER OF SCIENCE

at

The University of Waikato

by

LISA KYLE PEARSON



THE UNIVERSITY OF
WAIKATO
Te Whare Wānanga o Waikato

UNIVERSITY OF WAIKATO

2007

ABSTRACT

Lake Rotorua has become increasingly eutrophic over the past 2 to 3 decades. The sediments of the lake have been shown to exert an important influence on this eutrophication process. Chemistry of the sediments has been studied to determine the nature, composition and distribution of elements, through a 1.5 year coring programme. A geophysical survey together with sub-bottom profiling has provided stratigraphic information related to the bathymetry of the lake.

Lake Rotorua has two types of sediments: coarse, dense (density c. 0.5 g/cm^3) sediments comprised of clastic erosion products and coarse rhyolitic airfall components covering approximately 60% of the lake area; and fine, low-density ($\sim 0.02 \text{ g/cm}^3$) diatomaceous ooze that covers the remaining 40% of the lake, accumulated from deposition of biota, predominantly diatom frustules of *Aulacoseira granulata*. The sediment contains a record of volcanic eruptions, with the Tarawera Tephra typically found 0.5 m below the sediment water interface and Kaharoa Tephra typically between 2 to 3 m depth, in water depths of 10-15 m.

Phosphorus concentration in Lake Rotorua sediments decreases with sediment depth. In the centre of the lake phosphorus concentrations in the top 2 cm can exceed 2500 g/tonne and decline to 800 g/tonne at 20 cm depth. Accumulation rate of phosphorus in the sediment based on the nutrient budget is approximately 29.6 t/yr. Iron and manganese concentrations in the sediment depend on the availability of the element and the sedimentation rate of diatom frustules, and are controlled by the redox conditions in the sediment. The average concentration of iron and manganese in the sediment is approximately 8000 g/tonne and between 300 and 400 g/tonne, respectively. Iron accumulates in the sediment at a rate of 385 t/yr and manganese at 17.9 t/yr. Maximum concentrations of arsenic in the sediment are 250 g/tonne but are generally between 50-100 g/tonne, depending on the water depth. Lead concentrations are typically below 15 g/tonne. Sediment concentrations of both arsenic and lead are highly correlated with iron and manganese concentrations in the sediment and mimic the respective concentration profiles. Arsenic and lead

ABSTRACT

accumulate in the sediment at a rate of 3.71 and 0.49 t/yr, respectively. All elements show a peak in concentration in the tephra layers.

The bathymetry of Lake Rotorua is dominated by a curved depression extending from Sulphur Point and almost reaching the Ohau Channel. This depression is probably a structural feature likely associated with the collapse of the caldera, but could be an ancient drainage channel. A series of conical depressions clustered to the north of Sulphur Point and to the east of Mokoia Island are likely to be hydrothermal explosion creators. In the north in the lake at water depths less than 10 m, a series of near-shore terraces are preserved in the sediment.

Sub-bottom echo-sounding shows no return of sonic and seismic signals from most of the lake floor, indicating total absorption by the methane gas-filled sediment. In the shallow lake margin environments, generally <10 m water depth, gas is absent and a detailed stratigraphy of multiple reflectors from tephra layers was observed with sub-bottom profiles. The basin sediments of Lake Rotorua are significantly pockmarked, with deep, circular flat-bottomed depressions c. 20-60 m diameter and 0.5-6 m depth. The pockmarks are located on the lake floor in areas where the sediment is saturated with gas.

ACKNOWLEDGMENTS

Firstly I would like to thank my supervisors, Associate Professor Chris Hendy for his guidance, assistance and advice throughout the course of this thesis, especially the early morning starts coring on Lake Rotorua to the hours answering my numerous questions and Professor David Hamilton, thank you for your help, advice and hours spent editing. Your suggestions have been greatly appreciated.

Thank you to Environment Bay of Plenty for providing funding for the project and a scholarship. Thanks go to Brian Coxhead for driving the EBoP boat and getting your hands dirty helping with the coring. Thank you to the University of Waikato for supporting me with a Masters Research Scholarship.

Olivia Motion, Carmel Mangan, Jake Croall, Sarah Milicich, Manu Edwards, Annie Barker, Tom Whittaker and Shane Carter, you guys are a fantastic coring team, thanks for all your hard work. I would also like to acknowledge Hartly Contractors for the use of their boat.

Thank you to Dirk Immenga, Brad Scarfe and Alexandre Schimel from the Coastal Marine Group for carrying out the geophysical survey. Thanks for the data processing undertaken by Brad Scarfe and Alexandre Schimel to provide useable images for my thesis; it is greatly appreciated especially when you were pushed for time.

Thanks go to Annie Barker for her assistance in lab work and letting me use her lab for numerous digestions and Steve Cameron for running the samples on the ICP. Jake Croall and Sarah Milicich, thanks for the processing of the piston cores. Helen Turner thanks for your assistance with the scanning electron microscope and Wendy Paul for the help with diatom identification. Thank you to Greg Tait for your assistance with the GIS mapping.

Thank you to all the staff in the Earth and Ocean Sciences and Chemistry Departments at the University of Waikato for imparting your knowledge. Cheers to

ACKNOWLEDGMENTS

my fellow Masters students, for the help and making my five years at Waikato most enjoyable.

Finally I would like to thank my family for all the love, support and encouragement they have given to get me this far, especially my parents (Chris and Bev). Thanks Dad for the photography of Lake Rotorua, I had to do a bit of cropping to edit out your rowers and numerous ducks but otherwise they were fantastic.

TABLE OF CONTENTS

TITLE PAGE	i
ABSTRACT	iii
ACKNOWLEDGEMENTS	v
TABLE OF CONTENTS	vii
LIST OF FIGURES AND TABLES	xi
CHAPTER ONE- INTRODUCTION	1
1.0 Introduction	3
1.1 Eutrophication of Rotorua Lakes.....	3
1.2 Lake Rotorua and the Rotorua Region.....	3
1.2.1 Location.....	3
1.2.2 Lake Rotorua.....	4
1.2.3 The Rotorua Catchment.....	5
1.2.4 Rotorua City.....	6
1.2.5 Lake Rotorua Water Quality.....	6
1.3 The Importance of Lake Sediments.....	7
1.4 Research Objectives	8
1.5 Thesis Structure.....	8
References.....	10
CHAPTER TWO- LITERATURE REVIEW.....	13
2.0 Introduction.....	15
2.1 The Rotorua Basin.....	15
2.2 Geological History of Rotorua.....	16
2.2.1 The Taupo Volcanic Zone (TVZ).....	17
2.2.2 The Rotorua Caldera.....	19
2.2.3 The Okatina Volcanic Centre – 1	20
2.2.4 The Okatina Volcanic Centre – 2	21
2.3 Lake Level Changes and Bathymetry.....	23
2.3.1 Lake Level.....	23
2.3.2 Bathymetry.....	26
2.4 Nutrient Inputs to Lake Rotorua.....	27
2.4.1 Stream Inflows.....	28
2.4.2 Groundwater Inflows.....	28
2.4.3 Geothermal Input.....	29
2.4.4 Other Nutrient Sources.....	30
2.4.5 Nutrient Budget.....	31
2.5 Sediment Studies on Lake Rotorua.....	32
2.5.1 Stratigraphy and Sediment Accumulation.....	32
2.5.2 Sediment Composition and the Effect on Lake Water.....	34
2.5.3 Acoustic Studies.....	36
2.6 Summary.....	38
References.....	39
CHAPTER THREE- METHODS.....	45
3.0 Introduction	47
3.1 Coring Methods.....	47

TABLE OF CONTENTS

3.1.1	Piston Coring.....	47
3.1.2	Box Coring.....	50
3.1.3	Gravity Coring	51
3.2	Core Locations.....	53
3.3	Laboratory Methods for Core Analysis	54
3.3.1	Sample Preparation	54
3.3.2	Sediment Digestion using <i>Aqua Regia</i>	54
3.3.3	Sediment Digestion using Ascorbic Acid	55
3.3.4	X-Ray Fluorescence Analysis.....	56
3.3.5	Digestion Analysis.....	57
3.3.6	Carbon and Nitrogen Analysis.....	58
3.3.7	Bulk Density.....	59
3.3.8	Elemental Spatial Mapping.....	59
3.3.9	Sedimentation Rate.....	60
3.3.10	Scanning Electron Microscope (SEM).....	61
3.4	Geophysical Survey.....	62
3.4.1	Multibeam Survey.....	62
3.4.2	Sub-bottom Profiling.....	62
	References.....	64
CHAPTER FOUR-PHYSICAL COMPOSITION		65
4.0	Introduction	67
4.1	Physical Composition of Lake Rotorua Sediments.....	67
4.1.1	Coarse Dense Sediment.....	67
4.1.2	Diatomaceous Ooze.....	67
4.1.3	Tephra Layers.....	69
4.2	Bulk Density of Gravity Cores.....	69
4.3	Sediment Composition under the Scanning Electron Microscope (SEM)...	74
4.3.1	Depth 0-20 cm.....	75
4.3.2	Depth 30-32 cm (Tarawera Tephra).....	77
4.3.3	Depth 92-112 cm.....	79
4.3.4	Depth 132-160 cm.....	81
4.4	Sediment Stratigraphy.....	83
4.5	Summary.....	105
	References.....	106
CHAPTER FIVE-CHEMICAL COMPOSITION		107
5.0	Introduction	109
5.1	Behaviour of Elements in Lake Sediments.....	109
5.1.1	Phosphorus (P).....	109
5.1.2	Iron (Fe).....	110
5.1.3	Manganese (Mn).....	111
5.1.4	Arsenic (As).....	111
5.1.5	Lead (Pb).....	112
5.2	Chemical Composition and Distribution.....	112
5.2.1	Phosphorus (P).....	112
5.2.2	Iron (Fe).....	117

TABLE OF CONTENTS

5.2.3	Manganese (Mn).....	118
5.2.4	Arsenic (As).....	119
5.2.5	Lead (Pb).....	120
5.2.6	Sulfur (S).....	122
5.2.7	Carbon (C) and Nitrogen (N).....	124
5.3	Sediment Accumulation.....	126
5.3.1	Accumulation since the Tarawera eruption.....	126
5.3.2	Phosphorus Budget.....	127
5.4	Discussion.....	128
5.4.1	Composition and Distribution of Rotorua Sediments.....	128
5.4.2	Sediment Accumulation.....	133
5.5	Summary.....	134
	References.....	136
CHAPTER SIX- GEOPHYSICAL SURVEY.....		137
6.0	Introduction.....	139
6.1	The Multibeam System.....	139
6.1.1	Introduction to the Multibeam.....	139
6.1.2	SIMRAD EM3000 Multibeam Echosounding.....	141
6.1.3	Data Collection.....	144
6.1.4	Multibeam Post-Processing.....	144
6.2	Sub-bottom Profiling.....	145
6.2.1	Sub-bottom Profiling Data Collection.....	145
6.2.2	Sub-bottom Profiling Data Analysis.....	146
6.3	Results of the Geophysical Survey.....	147
6.3.1	Bathymetry.....	147
6.3.2	Lake Margins.....	151
6.3.3	Lake Floor.....	151
6.3.4	Outcrops.....	153
6.3.5	Gas in the Sediment.....	155
6.3.6	Pockmarks.....	157
6.3.7	Hydrothermal Activity.....	165
6.4	Summary.....	166
	References.....	168
CHAPTER SEVEN- IMPLICATIONS FOR REMEDIATION.....		171
7.0	Introduction	173
7.1	Restoration of Eutrophic Lakes.....	173
7.1.1	Chemical Application.....	173
7.1.2	Physical Modification.....	174
7.1.3	Biological Manipulations.....	176
7.2	Implications for Restoring Lake Rotorua.....	176
7.2.1	Phosphorus Distribution in Lake Rotorua Sediment.....	177
7.2.2	Nutrient Loading.....	178
7.2.3	Bulk Density.....	181
7.2.4	The Gas Problem.....	181
7.2.5	Biological Possibilities.....	182

TABLE OF CONTENTS

7.2.6	Other Conditions for Restoration Options.....	183
7.3	Recommendations.....	184
7.4	Summary.....	184
	References.....	185
CHAPTER EIGHT- CONCLUSIONS.....		187
8.0	Introduction.....	189
8.1	Physical Composition.....	189
8.2	Chemical Composition.....	190
8.3	Geophysical Survey.....	191
8.4	Remediation Options.....	192
APPENDICES.....		195
Appendix One:	Core Log Data.....	195
Appendix Two:	Bulk Density.....	415
Appendix Three:	Carbon and Nitrogen Analysis.....	443
Appendix Four:	Sub-bottom Tracks.....	447

LIST OF FIGURES AND TABLES

LIST OF FIGURES

CHAPTER ONE- INTRODUCTION	1
1.1 Lakes in the Rotorua Region, Bay of Plenty.....	4
1.2 Lake Rotorua, Central North Island, New Zealand.....	5
CHAPTER TWO- LITERATURE REVIEW.....	13
2.1 The Rotorua Basin showing the distribution of sedimentary and pyroclastic deposits and associated landforms.....	16
2.2 Map of the Taupo Volcanic Zone and the Central Volcanic Zone highlighting the volcanic centres.....	18
2.3 Volcanic lakes in the Rotorua area and simplified structural and volcanic features associated with the Rotorua and Haroharo calderas	20
2.4 Chronology and bulk volume estimates from eruptions from the OVC and the Oruanui eruption from the TVC.....	22
2.5 Probable shorelines of Lake Rotorua between 42 thousand years and the present	24
2.6 Changing levels of Lake Rotorua since ca. 240,000 years ago. Present level is ca. 280 m above sea level.....	25
2.7 Reconstructed shorelines of Rotorua Basin. a) 50 thousand year old shore line and b) area adjacent to Rotorua City 9500 years ago.....	26
2.8 Bathymetry of Lake Rotorua.....	27
2.9 Cycling of a) phosphorus and b) nitrogen in Lake Rotorua expressed as aerial rates ($\text{mg m}^{-2} \text{d}^{-1}$).....	32
2.10 Sediment deposition since the Tarawera Eruption.	33
2.11 Uniboom seismic reflection tracks across southern Lake Rotorua. The hashed area shows strong lake bed multiples indicating gas-filled sediments.....	37
CHAPTER THREE- METHODS.....	45
3.1 Piston coring equipment.....	48
3.2 Schematic of the piston coring process.....	49
3.3 a) Open box corer and b) box coring equipment.....	51
3.4 a) Gravity corer setup, b) gravity corer with sediment showing a closed stopper and piston in the bottom and c) extruding the gravity core into 2 cm horizontal intervals for analysis.....	52
3.5 Core locations sampled on Lake Rotorua.....	53
3.6 Comparisons between ascorbic acid and <i>aqua regia</i> digest methods for arsenic, iron, manganese and phosphorus.....	56
3.7 Comparisons between XRF and <i>aqua regia</i> digest for arsenic, iron, manganese and phosphorus.....	57
CHAPTER FOUR-PHYSICAL COMPOSITION	65
4.1 Location of cores from Lake Rotorua showing the distribution of coarse and diatomaceous sediment in the lake.....	68
4.2 a) Tarawera tephra (Ru 55) b) Kaharoa tephra (Ru 54) and c) reworked	

LIST OF FIGURES AND TABLES

	Kaharoa tephra (Ru 66).....	69
4.3	Bulk density across section A to A', B to B' and C to C' in Lake Rotorua..	70
4.4	Bulk density across section D to D', E to E' and F to F' in Lake Rotorua...	71
4.5	Bulk density across section G to G', H to H', I to I', J to J' and K to K' in Lake Rotorua.....	72
4.6	Core Ru 55 showing sampling depths (cm) for the scanning electron microscope images.....	75
4.7	a) General view for comparison of diatom species found between 0-20 cm depth. b) <i>Aulacoseira granulata</i> , c) <i>Aulacoseira</i> (auxospore), d) <i>Amphora australiensis</i> , e) <i>Pinnularia microstauron</i> (Ehrenberg) Cleve.....	76
4.8	a) General view for comparison of diatom species found between 30-32 cm depth.....	78
	b) Mineral particle in the Tarawera tephra located at 30-32 cm in the sediment core.....	79
4.9	a) General view for comparison of diatom species found between 92-112 cm depth. b) <i>Cyclotella stelligera</i> , c) <i>Cyclotella stelligera</i> , d) <i>Epithemia sp.</i> and e) <i>Achnantheidium sp.</i>	80
4.10	a) General view for comparison of diatom species found between 132-160 cm depth. b) <i>Cyclotella operculata</i> , c) <i>Synedra sp.</i> , d) <i>Cyclostephanos sp.</i> , e) <i>Cymbella sp.</i> , f) <i>Asterionella Formosa</i> Hassall, g) <i>Aulacoseira granulate</i> , h) <i>Stephanodiscus alpinus</i> and i) <i>Achnantheidium sp.</i>	82
4.11	Concentration of phosphorus, iron, manganese, arsenic and lead at Cross-section A to A'	86
4.12	Concentration of phosphorus, iron, manganese, arsenic and lead at Cross-section A to A' gravity cores.....	87
4.13	Concentration of phosphorus, iron, manganese, arsenic and lead at Cross-section B to B'	88
4.14	Concentration of phosphorus, iron, manganese, arsenic and lead at Cross-section B to B' gravity cores.....	89
4.15	Concentration of phosphorus, iron, manganese, arsenic and lead at Cross-section C to C'	90
4.16	Concentration of phosphorus, iron, manganese, arsenic and lead at Cross-section C to C' gravity cores.....	91
4.17	Concentration of phosphorus, iron, manganese, arsenic and lead at Cross-section D to D'	92
4.18	Concentration of phosphorus, iron, manganese, arsenic and lead at Cross-section D to D' gravity cores.....	93
4.19	Concentration of phosphorus, iron, manganese, arsenic and lead at Cross-section E to E'	94
4.20	Concentration of phosphorus, iron, manganese, arsenic and lead at Cross-section E to E' gravity cores.....	95
4.21	Concentration of phosphorus, iron, manganese, arsenic and lead at Cross-section F to F'	96
4.22	Concentration of phosphorus, iron, manganese, arsenic and lead at Cross-section F to F' gravity cores.....	97
4.23	Concentration of phosphorus, iron, manganese, arsenic and lead at Cross-section G to G'	98

LIST OF FIGURES AND TABLES

4.24	Concentration of phosphorus, iron, manganese, arsenic and lead at Cross-section G to G' gravity cores.....	99
4.25	Concentration of phosphorus, iron, manganese, arsenic and lead at Cross-section H to H'	100
4.26	Concentration of phosphorus, iron, manganese, arsenic and lead at Cross-section I to I'	101
4.27	Concentration of phosphorus, iron, manganese, arsenic and lead at Cross-section H to H' and I to I' gravity cores.....	102
4.28	Concentration of phosphorus, iron, manganese, arsenic and lead at Cross-section J to J' piston and box cores.....	103
4.29	Concentration of phosphorus, iron, manganese, arsenic and lead at Cross-section J to J' gravity cores and K to K' piston and gravity cores.....	104
CHAPTER FIVE-CHEMICAL COMPOSITION		107
5.1	Phosphorus concentraion in the top 0-10 cm of Lake Rotorua sediment.....	113
5.2	Phosphorus concentration in the top 10 cm of Lake Rotorua sediment separated into 2 cm intervals.....	115
5.3	Iron concentration in the top 0-10 cm of Lake Rotorua sediment.....	117
5.4	Manganese concentration in the top 0-10 cm of Lake Rotorua sediment.....	118
5.5	Piston core Ru52 showing the distributions in the sediment of a) Fe, b) Mn and c) As. All three elements peak in the Tarawera Tephra.....	119
5.6	a) Linear regression relationships between Fe and As and b) between Mn and As.....	119
5.7	Arsenic concentration in the top 0-10 cm of Lake Rotorua sediment.....	120
5.8	Piston core Ru57 showing the distributions in the sediment of a) Fe, b) Mn and c) Pb.....	121
5.9	a) Linear regression relationships between Fe and Pb and b) between Mn and Pb.....	121
5.10	Lead concentration in the top 0-10 cm of Lake Rotorua sediment.....	122
5.11	a) Location and b) concentration of sulfur in core Ru90 c) Ru91 d) Ru92 e) Ru93 and f) Ru96.....	123
5.12	Sulfur in piston core Ru79 analysed by XRF.....	124
5.13	Carbon concentration in selected piston and box cores.....	124
5.14	Nitrogen concentration in selected piston and box cores.....	125
5.15	a) Carbon, b) nitrogen and c) the carbon to nitrogen mass ratio vs carbon content in gravity core Ru128.....	125
5.16	Phosphorus budget for Lake Rotorua.....	128
5.17	a) Total phosphorus sediment concentration in gravity core Ru136 compared to b) piston core Ru51. c) Iron in Ru136 to d) Ru51 and e) manganese in Ru136 to f) Ru51.....	129
CHAPTER SIX- GEOPHYSICAL SURVEY.....		137
6.1	Research ship R.V. Tangaroa and an artist's depiction of the beam of sound waves mapping the ocean floor using a Simrad EM3000 Multibeam.....	140
6.2	SIMRAD EM 3000 transducer, bow mount on the Coastal Marine Group vessel <i>Tai Rangahau</i>	141

LIST OF FIGURES AND TABLES

6.3	Computer hardware for Multibeam data acquisition and processing inside <i>Tai Rangahau</i>	142
6.4	a) Meridian Altitude and Heading reference System (MAHRS) b) Trimble MS 750 RTK GPS c) AML Sound Velocity Profiler.....	143
6.5	Low frequency echo-sounder track lines.....	146
6.6	Bathymetric map of Lake Rotorua produced from the multibeam survey...	149
6.7	Raw multibeam data of Lake Rotorua showing areas of coverage over the lake.....	150
6.8	Typical stratigraphy visible in lake margins.....	151
6.9	Shallow water lake floor showing a) multibeam image and b) corresponding sub-bottom track and c) small pockmarks.....	153
6.10	Outcrop feature below the northern terraces in Lake Rotorua.....	153
6.11	Outcrops features in Lake Rotorua, showing profile in the sediment.....	154
6.12	Large gas bubble released during gravity core retrieval.....	155
6.13	Sub-bottom return of transition from non-gaseous sediment into gas filled sediment.....	155
6.14	Delta C-13 of bicarbonate in Lake Rotorua porewaters.....	156
6.15	Seismic classification of pockmark genesis.....	158
6.16	Pockmarks in water depths greater than 15 m.....	160
6.17	Pockmarks in water depths less than 15 m.....	162
6.18	Domed pockmark.....	163
6.19	Sub-bottom profile through relict pockmark a) ROT7_003 and b) ROT5_000.....	164
6.20	Depression feature.....	164
6.21	a) Multibeam image of hydrothermal explosion creators and b) cross-section through vents showing water depth.....	165
6.22	Hydrothermal feature to the east of Mokoia Island.....	166
CHAPTER SEVEN- IMPLICATIONS FOR REMEDIATION.....		171
7.1	Area of Lake Rotorua with sediment phosphorus concentration >1500 g/tonne.....	177
7.2	Estimated sewage, stream and total load of phosphorus to Lake Rotorua over the period 1967-2003.....	179
7.3	Estimated sewage, stream and total load of nitrogen to Lake Rotorua over the period 1967-2003.....	179
7.4	Predicted nitrogen loading to Lake Rotorua.....	180

LIST OF FIGURES AND TABLES

LIST OF TABLES

CHAPTER TWO- LITERATURE REVIEW.....	13
2.1 Average water quality of Lake Rotorua.....	28
2.2 Stream total nutrient concentrations in the Rotorua catchment.....	28
2.3 Nutrient loads into Lake Rotorua.....	31
 CHAPTER FIVE-CHEMICAL COMPOSITION	 107
5.1 Total accumulation of selected elements in Lake Rotorua sediments since the Tarawera eruption.....	126
5.2 Sediment mass in 0-10 and 10-20 cm of Lake Rotorua.....	127
5.3 Sediment mass of phosphorus in 2 cm intervals	127
 CHAPTER SIX- GEOPHYSICAL SURVEY.....	 137
6.1 Major tephra formations.....	152

CHAPTER ONE:
INTRODUCTION



1.0 INTRODUCTION

This chapter contains an introduction to Lake Rotorua region and Lake Rotorua; describing the origin, catchment, land use, and water quality of the lakes and their catchments. It highlights the issue of declining water quality and identifies the key areas of research. This chapter concludes with an overview of the structure of this thesis.

1.1 EUTROPHICATION OF ROTORUA LAKES

It has been noted over recent decades, that anthropogenic discharges of nutrients to aquatic systems have accelerated eutrophication in many lakes world wide (Wetzel, 1992). Eutrophication has been particularly evident in shallow lake systems, such as Lake Rotorua, where elevated water column concentrations of nitrogen and phosphorus have led to the formation and persistence of large and potentially toxic cyanobacteria blooms during summer months.

In Lake Rotorua there has been little change in nutrient concentrations and trophic status over the past two decades (Burns *et al.*, 1997). Inputs of phosphorus into the lake have not changed significantly over the past 40 years (Rutherford, 2003). The problem for lake management is why an apparently steady state in phosphorus fluxes should lead to increasing eutrophication. Lake sediments therefore must play a significant role in the recycling of nutrients in the lake.

1.2 LAKE ROTORUA AND THE ROTORUA REGION

1.2.1 Location

The Rotorua region, situated in the central North Island of New Zealand (Figure 1.1), is renowned for spectacular geothermal activity and an abundance of lakes (Figure 1.1) (Chapman, 1981). The reason for both of these attractions is that the region is bisected by the Taupo Volcanic Zone (TVZ), a long thin band of active volcanism caused by the oblique subduction of the Pacific tectonic plate beneath the Indo-Australian tectonic plate, to the east of the North Island (Cox, 1989). The TVZ is a NE-SW oriented zone of volcanic activity that extends from Ruapehu in the south to beyond White Island in the north. It has maximum dimensions of 300 km long x 60 km wide as defined by active volcanic centres (Wilson *et al.*, 1995).

Explosive rhyolitic eruptions have formed numerous calderas and explosion craters, which have subsequently filled up with water. The Rotorua lakes are considered the jewel of the region for their beauty and recreational value, and are popular for fishing, water skiing, swimming and picnicking (Environment Bay of Plenty, 2005).

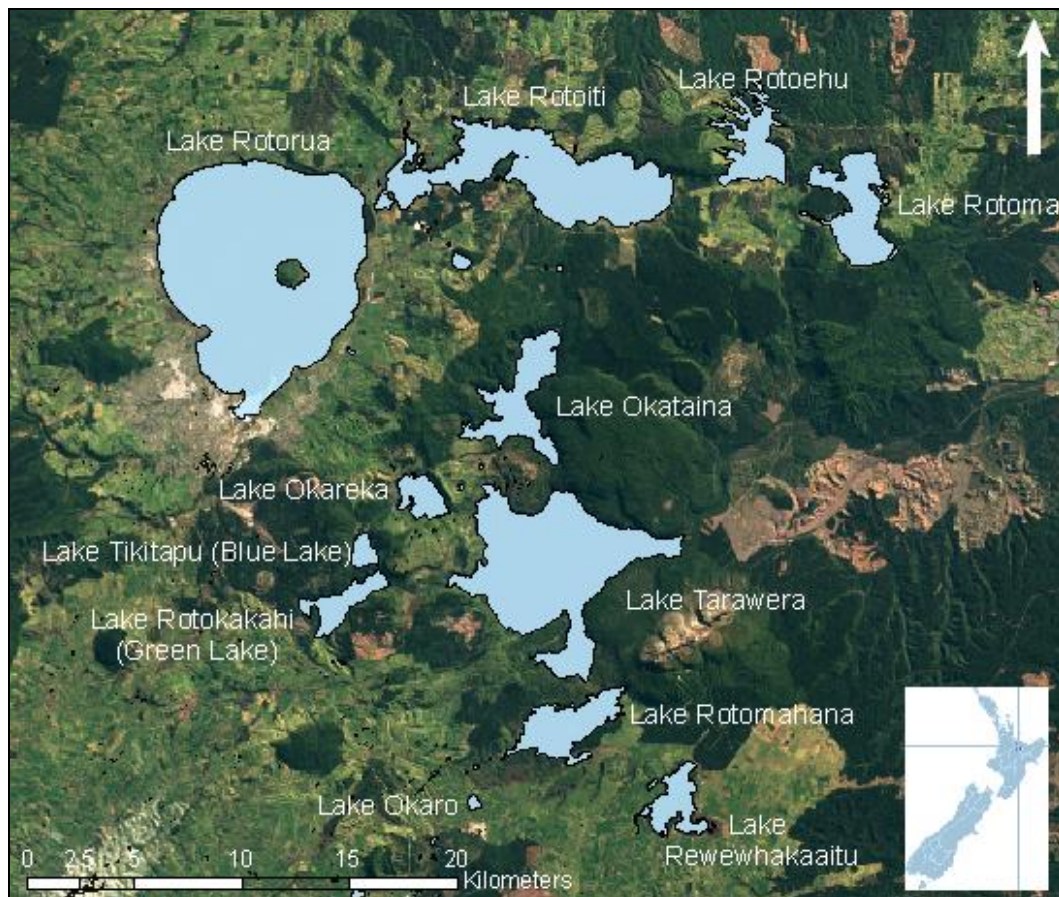


Figure 1.1: Lakes in the Rotorua Region, Bay of Plenty.

1.2.2 Lake Rotorua

Lake Rotorua is the largest of the 14 lakes in the region, with an area of 79 km² (Figure 1.2). It is a shallow eutrophic volcanic lake with an average depth of 10.8 m which formed approximately 220,000 – 240,000 years ago as a result of an eruption in the Mamaku Region, and collapse of the Rotorua caldera (Healy, 1975; White *et al.*, 2004; Esler, 2006). The surrounding area consists of ignimbrite and large rhyolitic extrusions, which also formed Mokoia Island near the centre of the lake. Lake Rotorua is situated adjacent to two geothermal fields; the large Rotorua field (18-28 km²) beneath Rotorua City at the southern margins of the lake and the

Tikitere field, situated north-west of the lake (Gorden *et al.*, 2001; White *et al.*, 2004). Natural discharges of chloride and acid sulphate geothermal waters occur as small inflows or springs at the lake edge (McColl, 1975).



Figure 1.2: Lake Rotorua, Central North Island, New Zealand.

1.2.3 The Rotorua Catchment

The Rotorua lake catchment covers an area of 520 km². Pasture is the prevalent ground cover in the catchment at 51.8%, 25.1% is comprised of indigenous forest/scrub, 14.3% is exotic forest, 8.1% urban and 0.2% is wetlands (Environment Bay of Plenty, 2006). The lake is fed by a number of streams, with the greatest flow from Hamurana stream. Geothermal inputs flow via streams such as the Puarenga and Waiohewa Streams. Hot springs are located around the southern shore of the lake at Sulfur Point and Ohinemutu (Scholes and Bloxham, 2005).

1.2.4 Rotorua City

Rotorua was named by Ihenga of the Te Arawa tribe who discovered Lake Rotoiti, while on a hunting trip from Maketu (Stafford, 1999). Ihenga claimed the area for Te Arawa and discovered Lake Rotorua. The name Rotorua was given to the lake which was thought to be derived by one of two ways. *Roto* – means *lake*, referring to the body of water. *Rua* has multiple meanings, firstly *pit* or *depression*, or *two* or *second*. Therefore the name Rotorua can be taken to mean *lake in a pit* referring to the caldera in which the lake lies or *second lake* referring to the chronology of its discovery after Lake Rotoiti (Stafford, 1999). Maori settled around Lake Rotorua from about 1350, with the major settlements developed at Whakawerawera, Ohinemutu and Mokoia Island.

1.2.5 Lake Rotorua Water Quality

Concern over the water quality in Lake Rotorua arose when the weed *Lagarosiphon major* was discovered in the lake in the mid 1950's. When massive amounts of decomposing weed washed up on the beaches, court action in 1958 resulted in an attempt to get the authority responsible for the lake to improve the condition (Chapman, 1970). Since the 1950's the emphasis has changed from the problem of excessive macrophyte growth to a problem of excessive algal growth. The Parliamentary Commissioner for the Environment (2006) recognises that over the last 30 to 40 years water quality in the Rotorua lakes has declined with algal blooms becoming more common. This has largely been attributed to increased nutrient input to the lakes (mainly nitrogen and phosphorus) from urban and agricultural sources and also increased internal cycling of nutrients from lake sediments (Hamilton, 2003). Decline in lake water quality is of great concern as much of the region's economy is based on tourism, supporting over 1.2 million visitors each year and representing approximately \$260 million dollars of added value to the local economy (Bell *et al.*, 2003). Subsequently a large amount of monitoring and research has been carried out to determine why water quality has declined, subsequent effects, and potential solutions.

Management solutions to improve water quality of Lake Rotorua have focused largely on reducing the external nutrient loads into the lake. However, the lake has become increasingly eutrophic (Rutherford *et al.*, 1996) and prolific cyanobacteria

blooms remain a feature of the lake over the summer months (Burger, 2006). It has become evident that internal nutrient sources derived from benthic fluxes could be more important than external nutrient sources in the lake.

1.3 THE IMPORTANCE OF LAKE SEDIMENTS

The sediment is a vital part of a lake's ecosystem providing both a sink and a source for nutrients. The organisms within the lake are completely dependent on nutrients to survive, with the sediment providing the largest source. Benthic communities often constitute the majority of a lakes total biomass and are reliant on the sediment to support life.

Sediment investigations have been widely used around the world as tools for studying lakes focusing on many different aspects. Deep sediment layers can be used in paleolimnological studies to show changes of acidification and trophic status on a geological time-scale, where as the analysis of the surface layers of the sediment show more recent changes in the lake, such as anthropogenic influences. Lake Rotorua has the ability to provide information on the eruptive history in New Zealand as the lake is situated in an area dominated by tectonics. Lake sediments provide a good record of eruption sequences as the sediments are not as easily eroded as a soil record, where most eruptive records have been developed from.

Chemical analysis of water samples give an instantaneous measure of the water quality, where as analysis of sediment samples integrate a certain period of time depending on the thickness of the sediment layer. In Lake Rotorua the tephra layers provide a vital stratigraphic marker for determining deposition and accumulation of sediment. The Rotorua region has been extensively researched and tephra deposits dated to give a time that the eruptions occurred. Since lake sediments are formed mainly from materials supplied from the terrestrial surroundings of the lake and material synthesised in the lake water, the chemical structure of the lake sediment is a function of the characteristics of the catchment and the lake water. Therefore the lake sediment can provide useful information about the lake, as well as its catchment, depending on sampling techniques and analysis.

The analysis of sediments is also very important when monitoring for substances that appear in very low concentrations in the lake water. Environmental toxins, like heavy metals and hydrophobic organic components, such as polychlorinated biphenyls (PCBs) and dichlorodiphenyltrichloroethane (DDT), as well as nutrients such as nitrogen and phosphorus, readily bind to particulate matter. The factors in the lake that affect this particulate matter will also aid in the distribution of contaminants in the sediments. The concentrations of these substances will also accumulate in the lake sediment in higher concentrations than found in the overlying water. This means that the sediment and benthic community play a vital role in the cycling of nutrients and distribution of contaminants in the ecosystem.

1.4 RESEARCH OBJECTIVES

The principal aim of this study is to understand the distribution of sediments and the nature of the sedimentary processes involved in Lake Rotorua, ultimately aiding in the improvement of lake water quality. Sediment core samples were used to determine the nature, stratigraphy and distribution of the sediments (initially at 1 km intervals), with subsequent analysis of the cored material. Particular attention is given to identifying likely acoustic reflectors such as the Tarawera tephra (Rotomahana mud) of 1886 AD and the Kaharoa pumice (1314 \pm 12 AD). These observations are supported with acoustic sounding using sub-bottom profiling (single beam echo-sounding) and multibeam echo-sounding. The multibeam data is used to produce a bathymetric map of Lake Rotorua. Sub-bottom data is used to identify the depth and thickness of sedimentary sequences. Maps are also constructed to indicate the concentrations of trace elements (phosphorus, iron, manganese, arsenic and lead), quantities of sediment and sedimentation rates. The sediment characteristics are also determined and the sedimentary processes interpreted.

1.5 THESIS STRUCTURE

This chapter is followed by a literature review which introduces the Rotorua Basin, and describes the landscape features and deposits within the basin. It gives a brief summary of work previously undertaken into the geological history of the Rotorua region including its eruptive history, historical lake level changes and

current bathymetry; as well as nutrient inputs and sediment studies relating to stratigraphy, composition and acoustic surveys on Lake Rotorua.

Chapter Three details the coring methods used and the locations of cores on Lake Rotorua. Laboratory techniques for core analysis are described, including sample preparation, digestion and analysis of samples. Methods for bulk density, carbon and nitrogen analysis, scanning electron microscope (SEM) analysis and the calculations for elemental accumulation are included. The chapter also introduces the geophysical survey on Lake Rotorua.

Chapter Four to Chapter Six presents and discusses the results for this study. Chapter Four examines the physical properties of sediments obtained from the extensive coring programme on Lake Rotorua and in particular the distribution of coarse to fine diatomaceous sediments, bulk density, diatom species in the sediment and stratigraphy of the tephra layers present in the cores. Chapter Five describes the chemistry of sediments of Lake Rotorua arising from the coring programme on the lake. Data has been compiled from piston, box and gravity cores to examine the composition and distribution of phosphorus, iron, manganese, arsenic and lead in the bottom sediments. Chapter Six provides details of the bathymetry and stratigraphy of Lake Rotorua, using multibeam and sub-bottom profiling systems. Features are identified around the lake margins and on the lake floor including the location of gas in the sediment, pockmarks and hydrothermal activity.

Chapter Seven examines possible remediation options and discusses the results of this study as they relate to management implications for Lake Rotorua. Remediation options considered were: a reduction in nutrient inputs, sediment capping, dredging and the use of flocculants. Recommendations for possible remediation options for Lake Rotorua are discussed.

Chapter Eight presents conclusions relating to sediments of Lake Rotorua, summarised in terms of the physical and chemical composition of the sediment. The geophysical survey added to the understanding of the sediment and provided a detailed map of the bathymetry and features of interest on the lake floor.

REFERENCES

- Bell, B., Thomas, A., and McRae, A. 2003. An economic evaluation of land use change options. Section B: Economic Impact on Rotorua District and Bay of Plenty Region of water quality induced changes to land use and tourism in Rotorua Lakes catchments. Report to Environment Bay of Plenty. Nimmo-Bell & Company Ltd. Wellington, 21pp.
- Burger, D.F. 2006. Dynamics of internal nutrient loading in a eutrophic, polymictic lake (Lake Rotorua, New Zealand). Ph.D. Thesis. University of Waikato, Hamilton.
- Chapman, V.J. 1970. A history of the weed infestation of the Rotorua Lakes and the Lakes of the Waikato Hydro-electric system. New Zealand Department of Scientific and Industrial Research Information Series. No. 78. 52pp.
- Chapman, V.J. 1981. Handbook of the Rotorua Lakes District. Rotorua: Guardians of the Rotorua Lakes.
- Cox, G. J. 1989. Slumbering Giants: The Volcanoes and Thermal Regions of the Central North Island. Auckland: William Collins Publishers LTD.
- Environment Bay of Plenty. 2005. Rotorua Lakes Recreation Strategy. http://www.ebop.govt.nz/water/media/pdf/Lakes_RotoruaLakesRecreationStrategy.pdf (cited 21/10/06).
- Environment Bay of Plenty. 2006. Lake statistical information. <http://www.ebop.govt.nz/Water/Lakes/Lake-Statistical-Information.asp> (cited 9/10/06).
- Environment Bay of Plenty. 2007. Interactive Map of Bay of Plenty Region. <http://www.ebop.govt.nz-> Interactive Map of Bay of Plenty Region (cited 12/02/07).
- Esler, W.R. 2006. An introduction to Rotorua Basin. In Lowe, D.J. (Ed), Guidebook for 'Land and Lakes' field trip. N.Z. Society of Soil Science Biennial Conference, Rotorua. New Zealand Society of Soil Science, Lincoln, pp. 22-24.
- Gorden, D.A., O'Shaugnessy, B.W., Grant-Taylor, D.G. and Cody, A.D. 2001. Rotorua geothermal field management monitoring. Environment Bay of Plenty, Environmental Report 2001/22. Whakatane. 110pp.
- Hamilton, D.P. 2003. A historical and contemporary review of water quality in the Rotorua Lakes. Report for Environment Bay of Plenty. pp. 1-13.
- Healy, J. 1975. Volcanic Lakes. In V.H. Jolly and J.M.A. Brown (Eds), New Zealand Lakes, Auckland University Press. Auckland. pp. 71-83.

- McColl, R.H.S. 1975 Chemistry of sediments in relation to tropic condition of eight Rotorua lakes. N.Z. Journal of Marine and Freshwater Research, 11 (3): 509-523.
- Parliamentary Commissioner for the Environment. 2006. Restoring the Rotorua Lakes: The ultimate endurance challenge. Wellington: Parliamentary Commissioner for the Environment.
- Rutherford, J.C., Dumnov, S.M. and Hoss, A.H. 1996. Predictions of phosphorus in Lake Rotorua following load reductions. New Zealand Journal of Marine and Freshwater Research, 30: 383-396.
- Rutherford, K. 2003. Lake Rotorua Nutrient Load Targets. NIWA Client Report: HAM2003-155. Prepared for Environment Bay of Plenty.
- Scholes, P. and Bloxham, M. 2005. Rotorua Lakes Water Quality 2005. Environment Bay of Plenty, Environmental Report 2005/24. Whakatane. 71pp.
- Stafford, D. 1999. Pakiwaitara: Te Arawa Stories of Rotorua as told to Don Stafford. Reed Publishing, Auckland, 118pp.
- Wilson, C.J.N., Houghton, B.F., McWilliams, M.O., Lanphere, M.A., Weaver, S.D. and Briggs, R.M. 1995. Volcanic and structural evolution of Taupo Volcanic Zone: a review. Journal of Volcanology and Geothermal Research. 68: 1-28.
- Wetzel, R.G. 1992. Clean water: a fading resource. Hydrobiologia 243/244: 21-30
- White, P.A., Cameron, S.G., Kilgour, G., Mroczek, E., Bignall, G., Daughney, C. and Reeves, R.R. 2004. Review of groundwater in the Lake Rotorua catchment. Report to Environment Bay of Plenty (2004/130). Institute of Geological & Nuclear Sciences. Taupo. 231pp.

CHAPTER TWO:
LITERATURE REVIEW



2.0 INTRODUCTION

This literature review chapter introduces the Rotorua Basin, and describes the landscape features and deposits within the basin. It gives a brief summary of work previously undertaken into the geological history of the Rotorua region including its eruptive history, historical lake level changes and current bathymetry as well as nutrient inputs into Lake Rotorua. Historical and current inflow and outflow data are important in understanding the contribution made by the sediments as both a sink and source for nutrients and other elements. Finally this chapter will investigate previous sediment studies relating to stratigraphy, composition and acoustic surveys on Lake Rotorua.

2.1 THE ROTORUA BASIN

The Rotorua Basin covers an area of 215 km² which includes an area in the Waipa and Kapenga localities south of the Hemo Gorge (Figure 2.1) (Kennedy *et al.*, 1978). Lake Rotorua is surrounded by a series of terraces and fans with the widest of these occupying the east, south-east and south-west of the lake shores. On the northern side of the lake, no terraces occur. Rotorua City occupies the area south-west of the lake and south-east of Mt Ngongotaha. The Rotorua catchment has an area of approximately 520 km². The lake drains through the Ohau Channel into Lake Rotoiti before entering the Kaituna River.

Landscape features and deposits in the Rotorua Basin include terraces, fans, loess or aeolian deposits, lake shore deposits, diatomite deposits and peat deposits (Figure 2.1). Terraces were formed between 42,000 and 22,000 years ago (Kennedy and Pullar, 1981). This age bracket was determined as the Kawakawa Tephra (20 kyr) rests directly on the surface of the lacustrine deposits. Erosion has removed terraces on the northern side of the basin. Fans are made up of the conglomerate of silt, sand, stones and boulders that have been transported by streams. Fans are present around Mt Ngongotaha that deposited around 20 thousand years ago. Modern fans occur mainly on the eastern side of the basin along the foot of the hills. Loess or Aeolian deposits are windblown silt and fine sands deposited generally during periods of colder climate when less vegetation covered the landscape. Kennedy and Pullar (1981) stated that cold climatic

conditions prevailed at the end of the last glaciation, between 20,000 and 15,000 years ago. Lake shore deposits, consisting of sand and rounded pumice gravels, are found up to 10 m above the present lake level. Ancient deposits suggest the lake has been much larger over the eruptive history of the region (Section 2.3). Diatomite deposits, remnants from the millions of siliceous shells of diatom organisms, accumulate on the lake floor to produce a white or greenish-brown, compact, fine textured clay-like deposit when the lake level drops. Peat deposits have occurred in the low-lying poorly drained areas close to the shores of the lake.

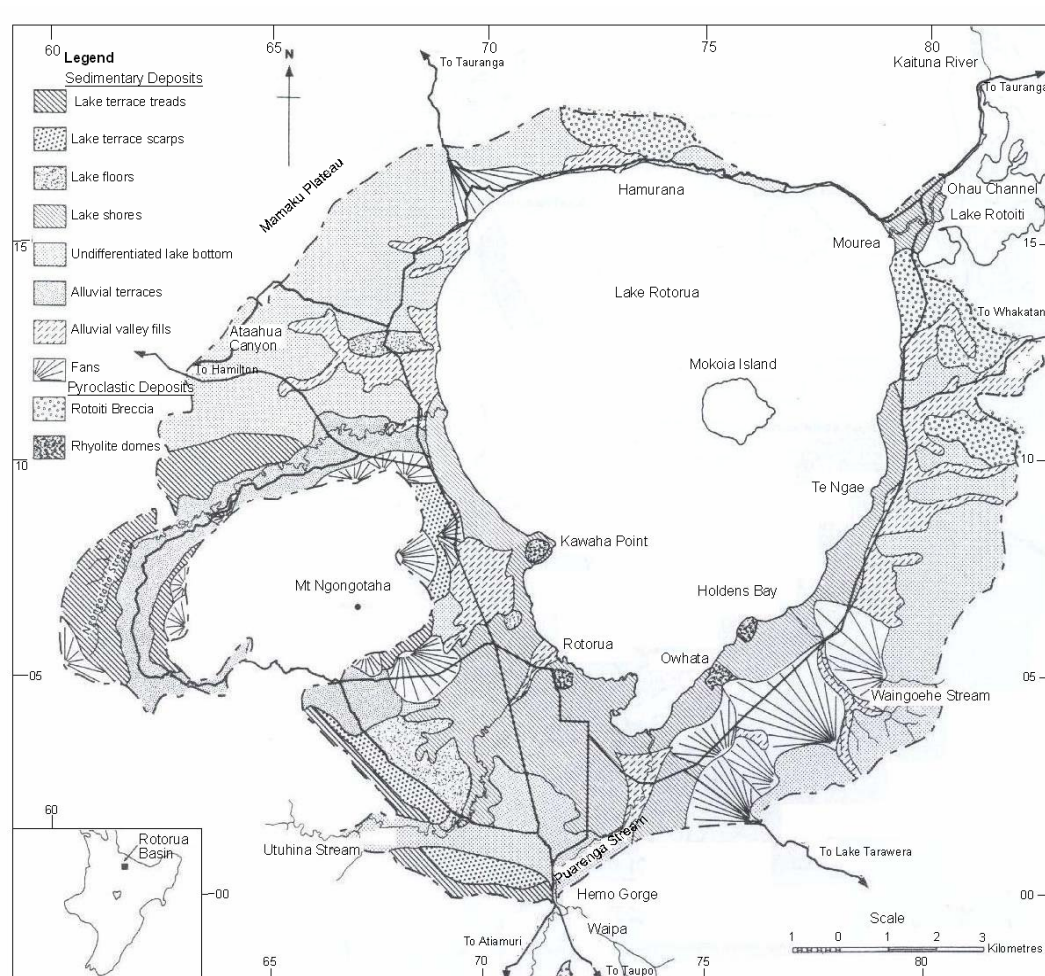


Figure 2.1: The Rotorua Basin showing the distribution of sedimentary and pyroclastic deposits and associated landforms (Kennedy *et al.*, 1978).

2.2 GEOLOGICAL HISTORY OF ROTORUA

A description of the formation and geology of Rotorua has been attempted as early as the 1860s with Hochstetter (1864), in his landmark description of the

geology of New Zealand, describing the hot springs of Rotorua. He suggested that the depression originated through collapse of the ground in the volcanic plateau, rather than being a volcanic crater. The formational processes of the Rotorua depression were also discussed by Park (1910), Marshall (1905, 1912), and Cotton (1922). The formation of Rotorua through a volcanic explosion was favoured by Marshall (1905) and Park (1910), while Marshall (1912) and Cotton (1922) supported the formation by subsidence. Hochsetter's theory was also supported by Grange (1937) who suggested that the depression was formed by structural collapse probably after a volcanic eruption. It was not till Healy (1964) and Thompson (1964) that the depression surrounding Lake Rotorua was referred to as a caldera.

The geological history of Rotorua can be summarised into four main stages of most significant volcanic activity affecting the Rotorua catchment. The first stage coming from the tectonic activity forming the Taupo Volcanic Zone; the second is the Mamaku eruption forming the Rotorua caldera; followed by activity from the Okataina Volcanic Centre, which can be split into two activity periods.

2.2.1 The Taupo Volcanic Zone (TVZ)

The first stage in the geological history of Rotorua comes from the Taupo Volcanic Zone (Figure 2.2) between 2 million and 240 thousand years ago. The earliest eruptions are believed to have occurred around 2.1 million years ago (Carter, 2004). The oldest dated calderas in the TVZ originate from Maroa, Whakamaru and Mangakino. The oldest pyroclastic deposit in the Rotorua area is the Waiotapu Ignimbrite, with an absolute age of 750 thousand years ago (determined by radiometric decay). Stratigraphically below the Waiotapu Ignimbrite is the Akatarewa Ignimbrite and Unit X (Grindley *et al.* 1994), which are as yet undated.

The Whakamaru Group Ignimbrites which erupted out of the Maroa caldera (Figure 2.2) around 330 thousand years ago caused significant crustal readjustment to the north Taupo area due to the explosive nature of the volcanism (Wilson *et al.* 1995).

Thick pyroclastic flows have been deposited around the Rotorua district from the Okataina Volcanic Centre (OVC) (Figure 2.2), dated to be at least 300 thousand years old. Widespread pyroclastic flows from a series of eruptions (Matahina, Pokopoko and Onuku) from the OVC are dated between 300 thousand and 220 thousand years ago. The Haroharo caldera (Figure 2.3) comprises two main volcanic complexes, Haroharo and Tarawera, and lies within the Okataina Volcanic Centre.

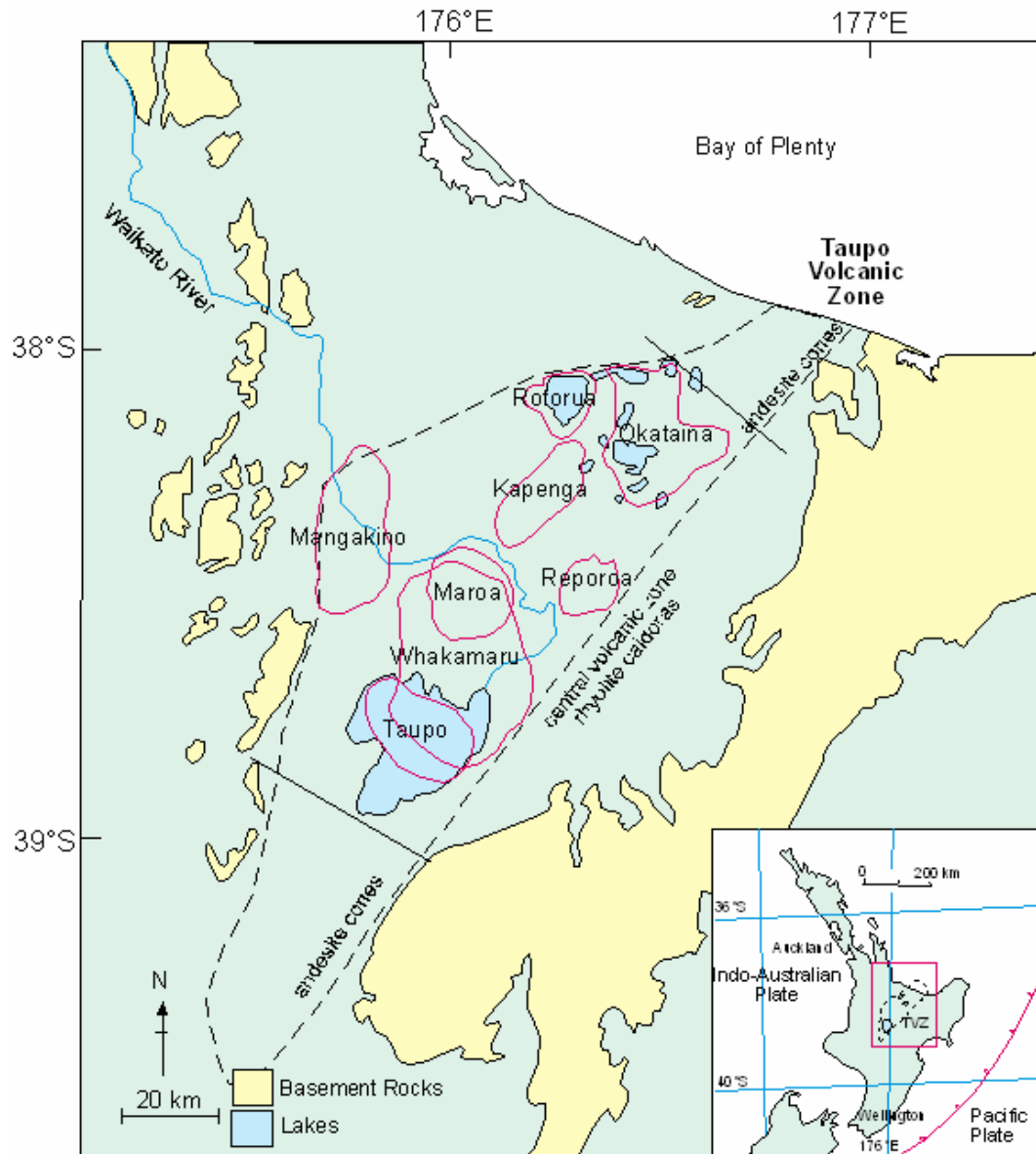


Figure 2.2: Map of the Taupo Volcanic Zone and the Central Volcanic Zone highlighting the volcanic centres (Marx, 2001 adapted from Bibbly *et al.* 2002 and Wilson *et al.* 1995).

2.2.2 The Rotorua Caldera

This stage of the region's history focuses on a period between 240 thousand years to 200 thousand years ago, with the Mamaku eruption associated with the collapse of the Rotorua caldera. It also encompasses the resurgent dome complex of Mt Ngongotaha.

Milner *et al.* (2003) report that the Mamaku eruption was triggered by an andesite intrusion into a pre-existing magma chamber which occurred at a relatively shallow depth. Increased pressure on the crust was created when the relatively hot andesite dyke caused the rhyolite magma to heat and overturn. The increases in pressure led to fault rupture which created pathways for the rapid upward movement of gas and magma. A number of pyroclastic flows erupted horizontally. Block collapse events eventuated from the constant eruption of the rhyolite magma having reduced the buoyancy of the overlying crust. The resulting pyroclastic deposit is greater than 1 km thick within the caldera. The Mamaku ignimbrite covered approximately 3200 km² with an estimated 145 km³ of equivalent magma volume (Milner *et al.* 2003).

Esler (2006) dates the caldera formed by the eruption of the Mamaku Ignimbrite at 240 thousand years ago, with an older caldera formed well before then. Phreatomagmatic deposits at the base of the Mamaku Ignimbrite support the possibility of an early proto-lake Rotorua before the caldera forming eruption (Milner *et al.*, 2002). The Mamaku Ignimbrite is a thin layer (~120m) covering the ancient topography, with some collapse occurring in the south and east of the Basin. Much less than half of the 145 km³ of magma volume previously stated by Milner *et al.* (2003) could have come from the Rotorua Basin; Esler (2006) suggests the rest came from the 'real' caldera which is probably located near the Horohoro Bluffs to the south of Rotorua.

It is believed that the formation of Lake Rotorua began soon after the Mamaku eruption in the ring-faulted depression (Houghton, 1982). Houghton (1982) felt that any record of this early lake would have been buried below tephra and lake sediments. The deposition of lake sediments consisting of the Huka Group fine ash and pumices were believed to be deposited at this time.

Mt Ngongotaha formed from the eruption of a rhyolitic magma well after the Mamaku Ignimbrite. Much of the caldera collapse in the city area came after this intrusion. The timing of the event has not been accurately dated but probably took at least 10 years to grow to its present form (White *et al.* 2004). Mokoia Island and two small lava domes south of the Rotorua airport all pre-date the Rotoiti Ignimbrite of ca. 50 thousand years ago (Esler, 2006).

2.2.3 Okataina Volcanic Centre (OVC) – 1

The third stage of the region's history focuses on a period between 200 thousand years to 45 thousand years ago, a relatively quiet period in the geological history, with subsequent eruptions from the OVC producing thin widely dispersed pyroclastic falls. Lake Rotorua underwent periodic lake level rises followed by an influx of volcanic material during an eruption as there was periodic damming of drainage pathways. The Huka group sediments deposited during this time are widespread and vary in thickness due to the constant changes in lake level (Section 2.2).

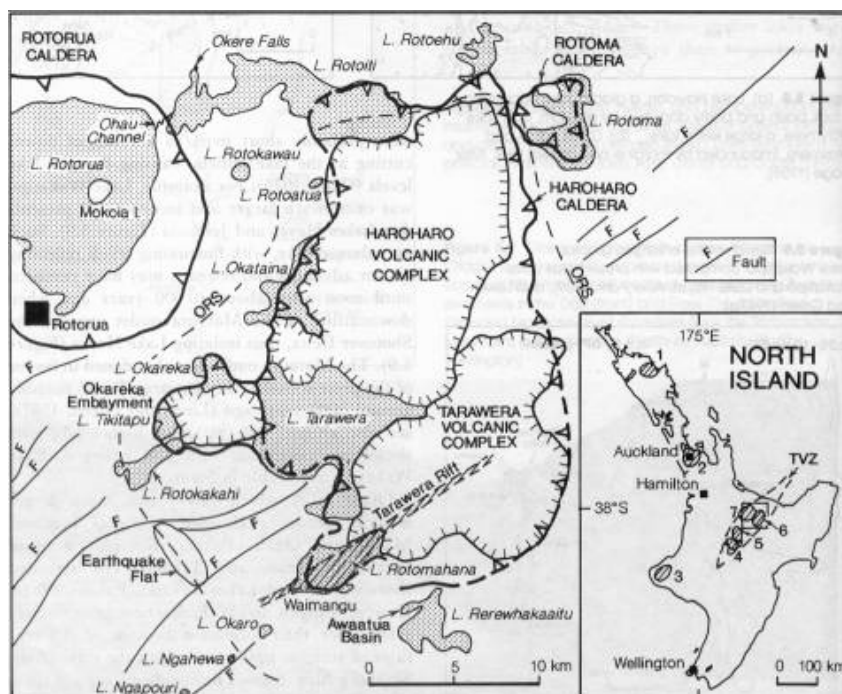


Figure 2.3: Volcanic lakes in the Rotorua area and simplified structural and volcanic features associated with the Rotorua and Haroharo calderas (dashed line marked OVC) (Lowe and Green, 1992).

The formation of the Haroharo complex came from three eruptions. Nairn (2002) identified the thin basal deposit named the Matahi Ash. The other two of the complex are variously named the Rotoehu Ash and Rotoiti Ignimbrite, the Rotoiti Ash and Rotoiti Breccia. The Rotoiti eruption of approximately 50 thousand years ago produced a significant caldera. No age has been obtained directly from the Rotoiti Tephra Formation although attempts have been made from several indirect approaches (Marx, 2004). Numerous non-welded pyroclastic flows were produced with associated air fall throughout the central North Island, particularly the Bay of Plenty.

2.2.4 Okataina Volcanic Centre – 2

The last stage in the eruptive history of the Rotorua region has produced no major caldera-forming eruptions in the last 45 thousand years although relatively smaller airfall deposits have been dispersed throughout the Rotorua area and wider North Island. This stage can be separated into two subgroups; the Mangaone and the Rotorua Subgroup.

Eruptions 30 to 45 thousand years ago from the Haroharo Caldera have been termed the Mangaone Subgroup. The Mangaone subgroup is a series of thick silicic plinian tephra deposits, stratigraphically bracketed between the Rotoiti Tephra Formation and Oruanui eruption products from the TVZ. Jurado-Chichay and Walker (2000) have recognised and described 12 plinian-sized eruptions which dispersed material to the north and east of the OVC. Smith *et al.* (2002) identified two more deposits in the subgroup, bringing the present number of tephra deposits to fourteen.

The Oruanui eruption is the largest most explosive documented eruption from the TVC in the last 250 thousand years. The Kawakawa Tephra Formation consists of the Oruanui Ignimbrite and the Aokautere Ash which are both products of the Oruanui eruption dated 26.5 thousand years ago. Wilson (2001) estimates that an area of 10,000 km² was covered in the fine ash and pumice produced during this eruption.

There have been numerous plinian and sub-plinian eruptions in the past 25 thousand years originating from the OVC and termed the Rotorua Subgroup. Ash plumes have deposited tephras both locally and throughout the wider North Island. The source of the majority of these eruptions has come from the Haroharo caldera (Figure 2.3) within the OVC; with the Haroharo and Tarawera vent zones being the most active. The first eruptions since the Oruanui eruption were the Te Rere (~21 ka) and the Okareka (~18 ka) (Figure 2.4).

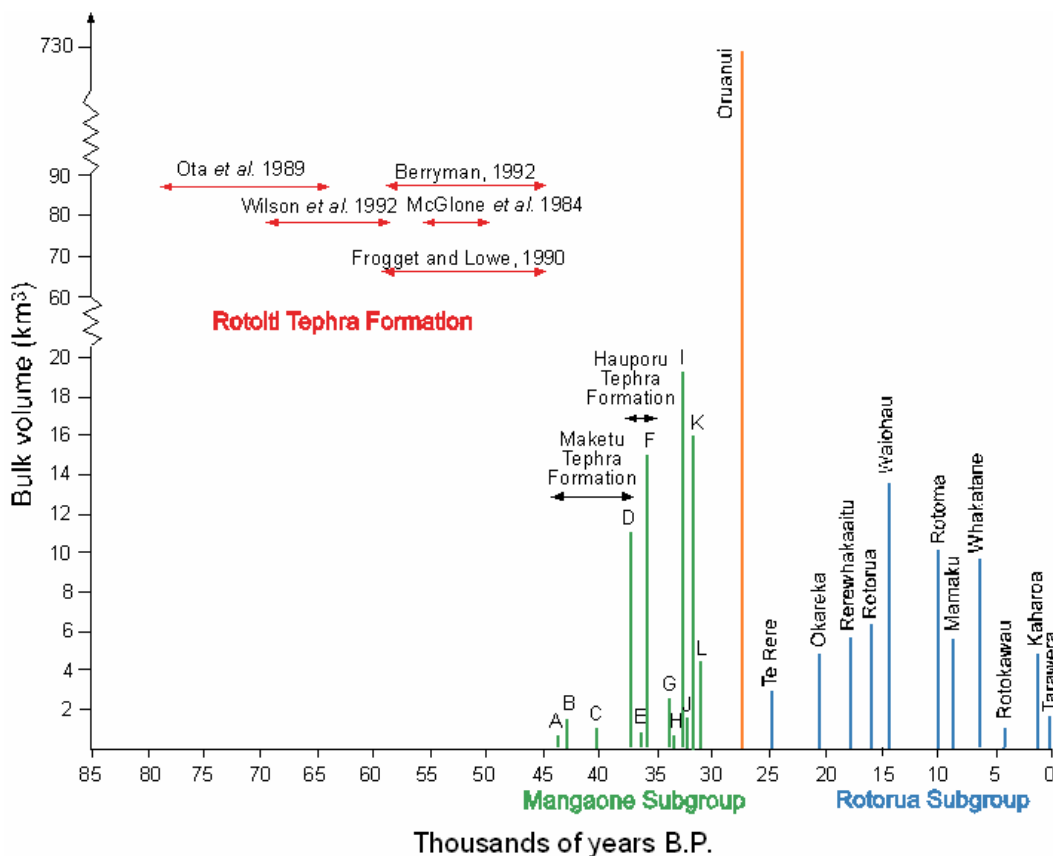


Figure 2.4: Chronology and bulk volume estimates from eruptions from the OVC and the Oruanui eruption from the TVC (Marx, 2004).

The two most recent eruptions have been from Mt Tarawera. The Kaharoa eruption of 1314 ± 12 AD (Hogg *et al.*, 2003) was a large explosive rhyolitic eruption, and there was the explosive basaltic Tarawera eruption of 1886. The Kaharoa eruption occurred from 7 vents along an 8 km linear zone followed by the extrusion of summit lava domes over a period of 4-5 years (Nairn *et al.*, 2001). The Kaharoa Ash is a loose coarse white ash, with hard lapilli (2 mm to 64 mm in diameter) (Pullar and Kennedy, (1981), deposited as far north as Whangarei. The

Tarawera eruption was a violent eruption occurring during the night of 10 June, 1886. The eruption blasted a straight, northeast trending fissure 17 km long, through the crest of Mt Tarawera, through Lake Rotomahana and as far as Waimangu (Ballance, 1981). The ash erupted from this event was different to the typical rhyolite that had previously erupted from the OVC, in that it was basaltic. As well as ash, large amounts of mud from Lake Rotomahana were displaced over the region. The Tarawera Ash and Lipilli is a loose scoriaceous dark coloured coarse material and the Rotomahana mud is a grey to olive grey sandy to silty material (Pullar and Kennedy, 1981). The eruption destroyed the famous Pink and White Terraces and extensively altered Lakes Rotomahana and Lake Tarawera.

2.3 LAKE LEVEL CHANGES AND BATHYMETRY

Lake Rotorua has been subject to many volcanic eruptions in its history, which have altered the lake significantly. Within the lake sediments (from the examination of soil profiles) there are more than 40 recognised tephras preserved. Tephras from Okataina, Taupo, Taranaki, Tongariro, Mayor Island and probably Moroa volcanic centres have been identified. The volcanic eruptions and subsequent change in lake level altered the bathymetry of the lake and it is important when studying the sediments to note the effect of the features on the lake bed.

2.3.1 Lake level

Lake Rotorua has a complex lake level history that has fluctuated considerably since the lake formed. The lake is currently at 280 m above sea level. The variation in lake level has been predominantly due to volcanic or tectonic disruption to the drainage systems. The climatic effect on water inputs is uncertain. Kennedy *et al.* (1978) mapped the probable shorelines of Lake Rotorua since the deposition of the Rotoiti Tephra Formation (Figure 2.5) although these are now realised to be much more complicated than first suggested.

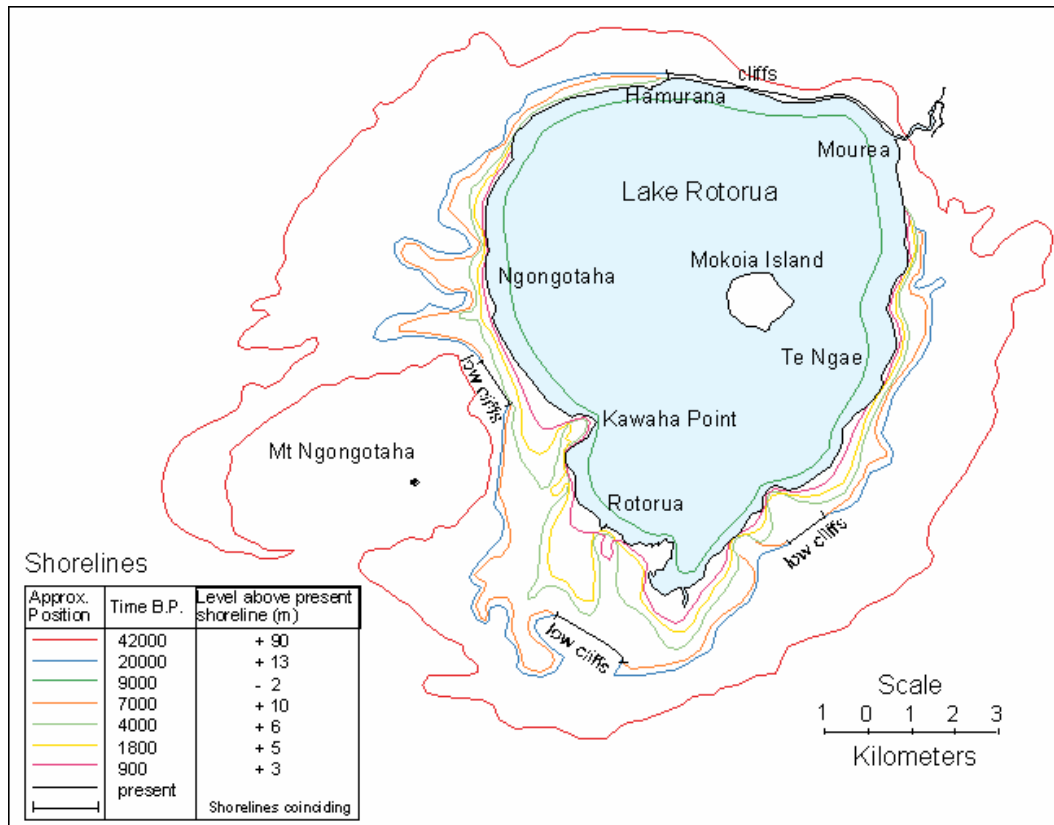


Figure 2.5: Probable shorelines of Lake Rotorua between 42 thousand years and the present (Kennedy *et al.*, 1978).

There have been at least seven periods of very high lake level, up to 120 m above the present level, and the lake has drained completely at least twice (Figure 2.6) (Esler, In Prep). Three of these periods of high lake level post-date the Rotoiti Pyroclasts of 50 thousand years ago. Lake Rotorua has once or twice been part of a huge lake extending to Atiamuri or beyond (Esler, 2006). These drastic changes in water level respond to the geological events occurring at the time. Dravitzki (1999) first recognised evidence for significant lake level fluctuation that occurred between 50 thousand to 26.4 thousand years ago with his work on the sediment characteristics at Paradise Valley. Discharge from the lake has predominantly been seepage of lake water to the thick pumice aquifer beneath the Mamaku Ignimbrite instead of surface discharge (Esler, 2006).

The basin was first breached about 55 -50 thousand years ago at the north-western rim, during the local collapse event in the Tikitere Graben. The Rotoiti Ignimbrite impounded the lake for approximately 20 thousand years, with two internal

drainage periods. During this time the lake reached its highest proven altitude of 400 m, which extended the lake well beyond the Rotorua basin (Figure 2.7a). The Hemo Gorge was larger than the present Lake Rotoiti.

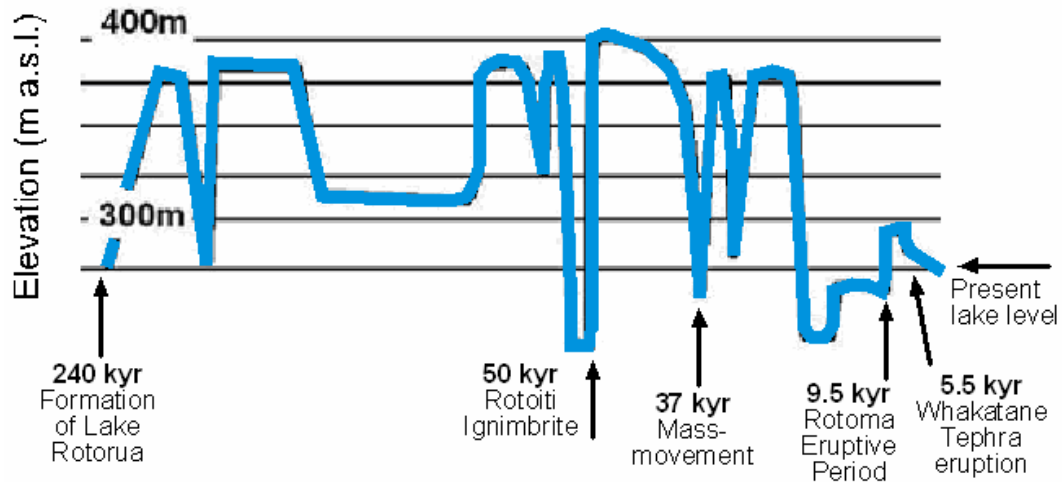


Figure 2.6: Changing levels of Lake Rotorua since ca. 240,000 years ago. Present level is ca. 280 m above sea level. (Adapted from Esler, 2006).

A drastic fall in lake level about 37 thousand years ago caused a gigantic mass-movement of poorly consolidated diatomite into the centre of the basin. Approximately 300 million m³ of sediment was involved (Esler, In Prep). Compacted older diatomite dating from 50 to 40 thousand years ago remained in situ and forms the ‘bedrock’ underlying young lakebed sediments to the north and west of the lake. The last high stand was between 33 and 30 thousand years ago, where the lake reached 380 m above sea level. During this period the prominent high terraces around the Rotorua Basin were formed and the present surface discharge was formed.

Since lavas associated with the Rotoma Tephra (9505 ± 25 cal. yr BP) blocked drainage to the east via Lake Rotoehu, Lake Rotorua level has been controlled by a complex interaction of sudden faulting in the north-east of the basin and the formation and erosion of sunken pumice rafts in the Mourea/Ohau Channel area after each OVC eruption (Esler, In Prep.). The Rotoma lava dams united Lake Rotoiti with Lake Rotorua, 15 m above the present water level. Faulting in the Tikitere Graben has controlled the level of Lake Rotorua, which has fallen

erratically ever since. Figure 2.7b shows the lake shoreline adjacent to Rotorua city during the Rotoma eruptive period. Lake Rotorua dropped nearly 8 m about the time of the Whakatane Tephra eruption (5530 ± 60 cal. yr BP). Esler (2006) predicts that based on present trends, Lake Rotorua will have drained again completely in 6000 years.

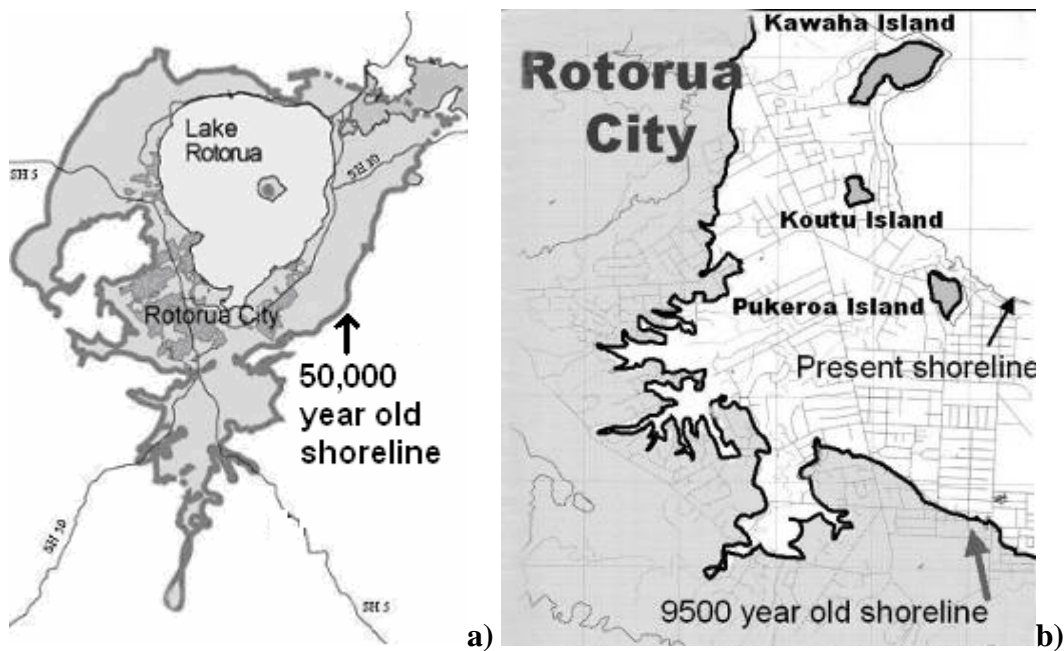


Figure 2.7: Reconstructed shorelines of Rotorua Basin. **a)** 50 thousand year old shore line and **b)** area adjacent to Rotorua City 9500 years ago (Esler, 2006).

There have been many different versions of the timeline of events that have contributed to the deposition of the lacustrine sediments in the Rotorua area. Alternate interpretations of the lake level history include Marx (2004) who supports a ‘caldera breakout flood’ from the present Rotorua Basin. Hodgson and Nairn (2004) suggest the draining of Lake Rotorua into the Okataina Volcanic Centre, and further publications may provide alternate interpretations or differences in timing and magnitude of lake level fluctuations.

2.3.2 Bathymetry

The bathymetry of Lake Rotorua was originally surveyed in November 1966 by the Fisheries Research Division. A provisional bathymetric map was produced by Irwin (1969) by interpolating between a series of echo sound survey tracks across

the lake. It is this map by Irwin that was adjusted to the New Zealand Map Grid and Latitude and Longitude coordinates to be used during this thesis (Figure 2.8).

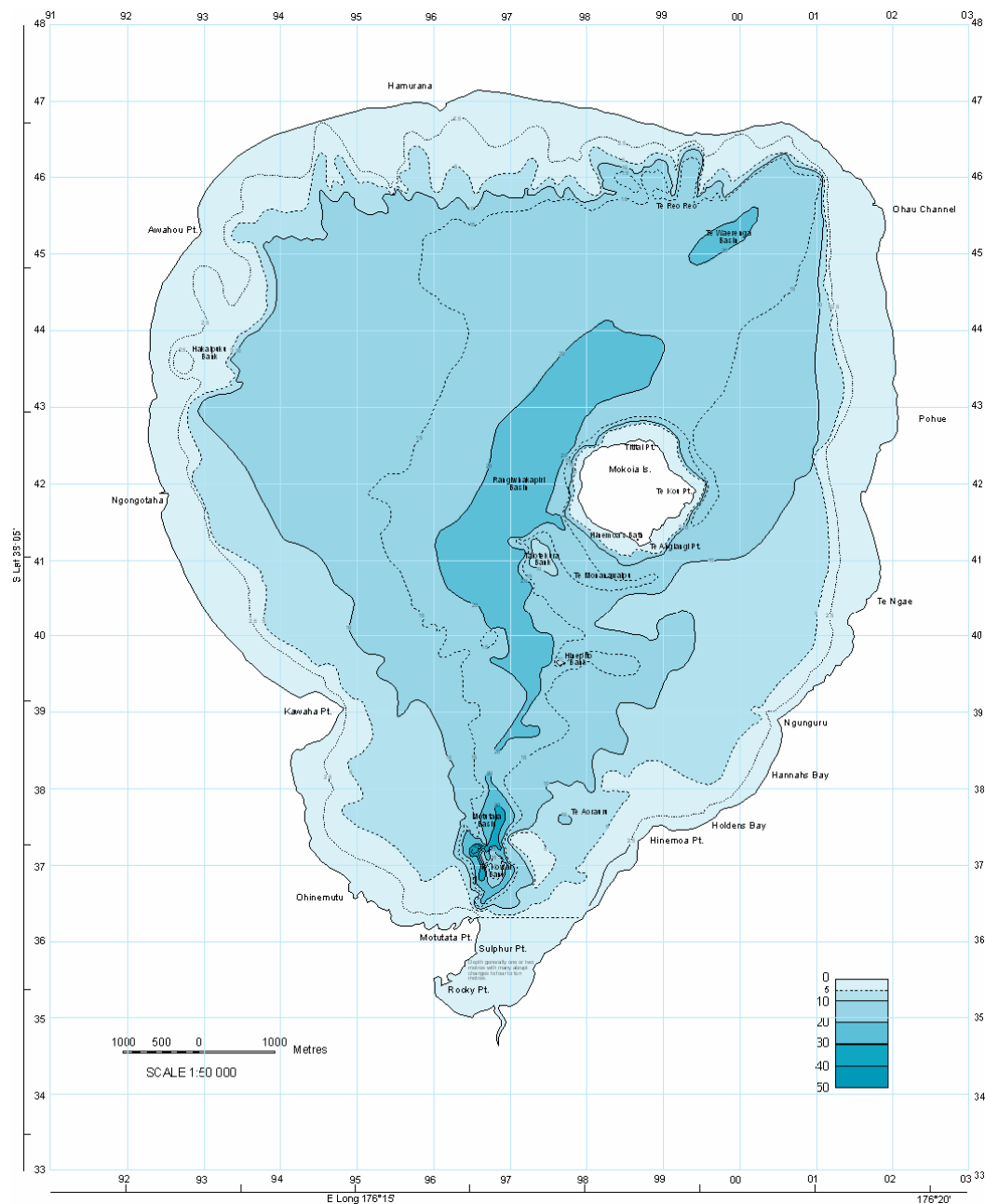


Figure 2.8: Bathymetry of Lake Rotorua (Adapted from Irwin, 1969).

2.4 NUTRIENT INPUTS TO LAKE ROTORUA

Nitrogen and phosphorus concentrations in Lake Rotorua have been studied intensively for several decades (Fish, 1975; Hoare, 1987; Rutherford, 1988; Rutherford *et al.*, 1989). The water quality of the lake is affected by internal processes as well as nutrient inputs from springs, streams, groundwater and

geothermal fields. Rutherford (2003) produced a review of nutrient inputs into Lake Rotorua, concluding that nutrient levels have been increasing over the last few decades (Table 2.1).

Table 2.1: Average water quality of Lake Rotorua (Rutherford, 2003).

	1965	1967-1977	1981-1982	1984-1985
Total Phosphorus (g/m^3)		0.024	0.048	0.079
Total Nitrogen (g/m^3)		0.310	0.519	0.530
Chlorophyll (mg/m^3)		5.5	37.8	22.6
Peak Chlorophyll (mg/m^3)		28	62	58
Secchi Disk (m)	2.5-3	2.3	1.9	1.7
Deoxygenation Rate ($\text{g/m}^3/\text{day}$)		0.4	0.7	0.9

2.4.1 Stream Inflows

There are nine major cold water streams entering Lake Rotorua: Awahou, Hamurana, Ngongotaha, Puarenga, Utuhina, Waiohewa, Waingaehe, Waiteti and Waiowhiro. Stream inflows into Lake Rotorua have been extensively researched (Fish, 1975; Hoare, 1980, 1978, 1987; Rutherford *et al.*, 1989 and Williamson *et al.*, 1996). Monitoring has also been carried out by Environment Bay of Plenty (EBoP). Rutherford (2003) summarised the nutrient concentrations in the streams using data from Hoare (1980), EBoP from 1991 to 1995 and EBoP from 2002 to 2003 (Table 2.2).

Table 2.2: Stream total nutrient concentrations in the Rotorua catchment (Rutherford, 2003).

Site	Total Phosphorus (g/m^3)			Total Nitrogen (g/m^3)		
	Hoare (1980)	EBoP 1991-1995	EBoP 2002-2003	Hoare (1980)	EBoP 1991-1995	EBoP 2002-2003
Awahou	0.072	0.078	0.068	0.120	0.130	0.101
Hamurana	0.086	0.083	0.086	0.090	0.075	0.007
Ngongotaha	0.056	0.063	0.050	0.170	0.313	0.215
Puarenga	0.083	0.098	0.068	0.360	.0390	0.320
Utuhina	0.076	0.070	0.065	0.280	0.267	0.233
Waiohewa	0.089	0.153	0.047	2.110	2.617	1.007
Waingaehe	0.129	0.194	0.104	0.190	0.509	0.121
Waiteti	0.056	0.042	0.071	0.160	0.155	0.370
Waiowhiro	0.058	0.101	0.037		0.417	

2.4.2 Groundwater Inflows

Nitrogen compounds are introduced into the groundwater system both naturally, through microbial fixation, and by human activities, such as agriculture and sewage treatment. Concentrations of nitrogen as nitrate (2 g/m^3), nitrite (0.002

g/m³) and ammonium (0.05 g/m³) are considered low in the groundwater in the Rotorua area (White *et al.*, 2004). No direct groundwater flow via the lake bed has been sampled so far for chemical analysis (Morgenstern and Gordon, 2006). Assumptions were made for the calculation of nitrogen load based on a mean residence time of 37 years with 100% mixed flow and a nitrogen concentration of 1 mg/L (Morgenstern and Gordon, 2006). The direct groundwater flow into Lake Rotorua via the lake bed was estimated to be 4.5 m³/s, by White (In: Morgenstern and Gordon, 2006) using groundwater flow modelling. Hoare (1980) calculated the groundwater direct flow using a mass balance approach, obtaining an inflow of 2.1 m³/s. Morgenstern and Gordon (2006) used an average value between Hoare and White of 3.3 m³/s to calculate the direct groundwater flow to be a minimum of 131 t/year at steady state. Beyá *et al.*, (2005) took a different approach to calculate the contribution of groundwater into Lake Rotorua. Estimations were made from the difference between the total estimated surface flows (minor and major) and the inflow calculated from the lake water balance. The value established could also include a component of ungauged and local surface flows. Groundwater contribution established from this method was 2,396 l/s, which is approximately 15% of the total incoming water to the lake.

White *et al.* (2004) report concentrations of phosphorus in groundwater aquifers to be typically between 0.1 and 0.4 g/m³. Phosphorus is primarily introduced into the groundwater through rock-water interaction as it travels through underground aquifers, therefore increasing in concentration with age in the groundwater system. Phosphorus is also introduced through agricultural practices and waste water treatment. The soils in the Rotorua region contain allophane which has the ability to bind phosphorus. The majority of the phosphorus in the groundwater has a natural rock-derived origin rather than by wastewater or agriculture (White *et al.*, 2004).

2.4.3 Geothermal Input

There are three identified geothermal fluid inputs into Lake Rotorua. Surface flows from the Tikitere Geothermal Field naturally drain into Lake Rotorua via the Waiohewa Stream, on the eastern side of Lake Rotorua. The Rotokawa Geothermal field discharges into Lake Rotorua, east of the Rotorua Airport. The

Rotorua Geothermal Field feeds streams entering Lake Rotorua by overflow of surface springs and shallow aquifers.

Geothermal sources are a significant contribution to the amount of total phosphorus and total nitrogen entering Lake Rotorua. In a review of groundwater in the Rotorua catchment, White *et al.* (2004) estimate that the total input of geothermally-derived total nitrogen and total phosphorus to be 46 t/year and 2.9 t/year respectively. This value was calculated by estimations of inflows from the Tikitere/Waiohewa catchment (Dine, 2004), thermal streams (Donovan and Donovan, 2003), Puarenga Stream (White *et al.*, 2004) and 'missing' geothermal flows to Lake Rotorua (Glover, 1992).

2.4.4 Other Nutrient Sources

The nitrogen and phosphorus concentration of rainfall in the Rotorua region was investigated by Fish (1976). Rain falling onto the surface of the lake is its largest water source, but considered a particularly dilute source of nutrients. Nutrients are introduced into rain from both natural and anthropogenic sources. Fish (1976) concluded that rainfall counts for a small but significant portion of nitrogen and phosphorus input into Lake Rotorua, at 15 % for nitrogen and 5 % for phosphorus inputs.

Sewage has accounted for a significant portion of nitrogen and phosphorus loads entering Lake Rotorua. From 1891 when the first sewers were laid in Rotorua, effluent treatment was by septic tank or discharged into Puarenga stream. During the 1970s and 1980s the sewage nutrient load increased as the population of Rotorua increased and its reticulation system expanded. From 1984-1985 nutrient inputs of treated sewage were as high as 150 t/year and 34 t/year for nitrogen and phosphorus, respectively. After 1991 Lake Rotorua no longer received wastewater from Rotorua City and land disposal of sewage in the Whakawerawera Forest began in an effort to reduce nutrient loads to the lake. The scheme was successful in decreasing nutrient loads from 1991-1993. However, from 1994 the nutrient load has increased again, indicating that the increased nutrients in the groundwater underlying the Whakawerawera Forest took two years to enter the streams

discharging into Lake Rotorua. Table 2.3 gives sewage contributions in the nutrient budget for Lake Rotorua.

2.4.5 Nutrient Budget

Nutrient budgets for the Lake Rotorua catchment have been calculated by Fish (1978), Hoare (1987), Williamson *et al.*, (1996) and Rutherford (2003) (Table 2.2). It was found that the nitrogen and phosphorus inputs to the lake, estimated by multiplying average stream flow rates by average stream nutrient concentrations are dominated by soluble species. Particulate organic nutrients represent a small fraction of total nitrogen and phosphorus entering the lake and do not vary significantly with flow rate. Particulate organic phosphorus and nitrogen was often neglected in the lake's overall nutrient budget. Nitrogen as NO_3 in the stream inflows has been increasing over the past decades associated with change in land use within the catchment compared to NH_4 , which has remained low the major contribution to the lake is geothermal in origin. Phosphorus has remained constant over the past few decades (Hoare, 1987). It was frequently found that the total nutrient input in a lake may be very small compared to the amount already present in the lake, and therefore recycling can provide virtually all the material for biological production within the lake basin (Fish, 1978). Internal nutrient loads are generally associated with stratification of Lake Rotorua during the summer months.

Table 2.3: Nutrient loads into Lake Rotorua (Rutherford, 2003).

Input	Nitrogen			Phosphorus		
	1976-77	1984-85	2002	1976-77	1984-85	2002
Treated sewage (t/y)	73	150	32	7.8	33.8	1
Streams (t/y)	485	415	660	30.4	34	34
Internal (t/y)	0	<260	ND	0	35	ND
Total (t/y)	558	>825	692	42	103	35

Burger (2006) calculated the cycling of phosphorus and nitrogen from the sediments in Lake Rotorua (Figure 2.9). Sedimentation and sediment release rates are expressed as a seasonal mean calculated with the deployment of sediment traps and benthic chambers in Lake Rotorua over four sampling periods. Burger (2006) found that release rates varied between the season and with sample water

depth, indicating important implications for lake sediment removal or capping as a management strategy to reduce internal nutrient loads.

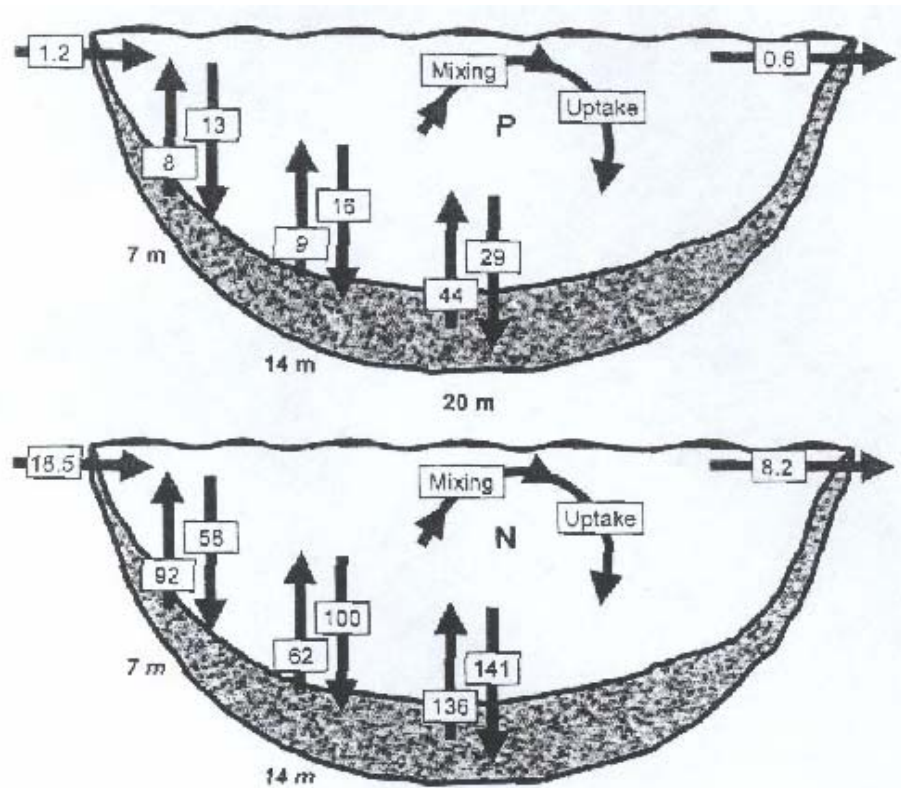


Figure 2.9: Cycling of a) phosphorus and b) nitrogen in Lake Rotorua expressed as aerial rates ($\text{mg m}^{-2} \text{d}^{-1}$) (Burger, 2006).

2.5 SEDIMENT STUDIES ON LAKE ROTORUA

Sediment studies carried out on Lake Rotorua have been primarily related to the accumulation and chemical composition of the accumulated material. Buried tephra layers in the sediment allow the stratigraphy of the sediment to be dated and accumulation rates calculated. Acoustic studies also give an insight into the sedimentation rate and sediment stratigraphy.

2.5.1 Stratigraphy and Sediment Accumulation

Fish (1979) studied the amounts of ejecta from the Tarawera eruption of 1886 deposited over Lake Rotorua. He used 28 sediment cores to determine sedimentation rate and distribution of accumulation. Fish (1979) describes most cores as having a clearly visible layer of volcanic mud which separates upper zone of approximately 50 cm of mottled dark sediment from a lower zone of similar,

more compacted, sediment. Four of his cores contained a layer of white pumice at the bottom. The work by Healy *et al.* (1964) was used to identify the volcanic ash deposits. The upper mud layer was identified as Rotomahana Mud (1886). Smaller, gritty, black basaltic scoria along the base of the Rotomahana Mud was identified as Tarawera Ash. The white pumice layer found between 1 and 1.5 m below the surface of the cores was identified as the Kaharoa Tephra. The intervening material was described as a fine material containing large numbers of diatom frustules, mostly of *Melosira granulata* Ralfs. Figure 2.10 is a map of Lake Rotorua showing where the lake was sampled and isopleths defining the deposition of lake sediments since the Tarawera eruption, produced by Fish (1979).

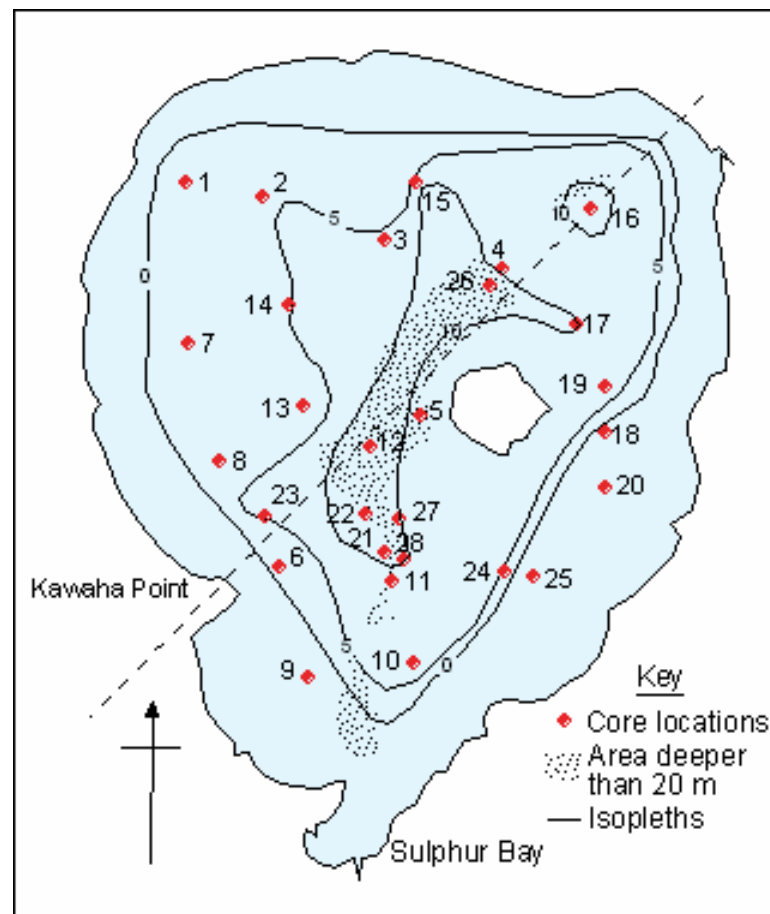


Figure 2.10: Sediment deposition since the Tarawera Eruption (Fish, 1979).

Fish (1979) concluded that the amount of lucustrine sediment deposited since the eruption increased with water depth. In water depth less than 10 m, water movement is too vigorous to permit the permanent settling of the light lake

detritus. This was also found by Hoare (1978) when he studied sediment flows from the catchment into Lake Rotorua. Hoare (1978) concluded from microscopic examinations that the fine material did not contribute to the sediments in the lake beyond the 5 m depth contour. Fish (1979) also identified that the thickness of the Tarawera Tephra decreased in a north-easterly direction across the lake. The mean dry weight of mud and ash from the 1886 eruption sampled from the southeast of the lake is over twice that sampled from the northwest. This is shown by the dashed line in Figure 2.10. Although there was not enough data to make a reliable estimate of the accumulation of sediment between the Kaharoa and Tarawera eruptions, based on what was recovered, Fish (1979) suggests that the sediment deposition rate before the Tarawera eruption was less than at the present time and therefore the present state of Lake Rotorua is correspondingly more eutrophic.

2.5.2 Sediment Composition and the effect on lake water

When organisms die and fall to the bottom of the lake, they carry with them a proportion of their cell contents that become incorporated in the deposition of sediment. The chemical composition of lake sediments in some part reflects the characteristics and the trophic status of the waters in previous times. The nutrients deposited in the sediments are not necessarily sequestered and dissolved nutrients can return to the lake water, especially if the overlying water becomes anoxic. Sediment composition studies are important to ascertain how much of the nutrients are retained in the sediment and how much can be recycled to the overlying lake water.

Fish and Andrew (1978) described the distribution of nitrogen and phosphorus within sediment cores retrieved from Lake Rotorua and determined possible loss rates from the sediment. Ten sediment cores were collected during different seasons and locations to determine whether the vertical distribution of nitrogen and phosphorus was affected by summer stratification or culturally enriched lake inflows. Circulation by wind keeps the waters of Lake Rotorua well oxygenated; however, there are times when the lake becomes thermally stratified for periods of days. Fish and Andrew (1978) found that sediment nutrient concentrations are high at the surface and fall to a more constant value about 20 cm below the sediment-water interface and do not vary significantly with season. Samples taken

below the Rotomahana mud layer have consistently lower concentrations than the sediment deposited above it, suggesting that Lake Rotorua became eutrophic soon after the eruption.

White *et al.* (1978) examined the role of the sediment as a source and sink for plant nutrients in Lake Rotorua. They estimated by a mass balance approach, the nutrient exchanges between the lake sediments and the overlying water column. Rotorua sediments could potentially supply up to half of the total income of phosphorus to the lake, depending upon the extent of summer deoxygenation in the lake water. Phosphorus released from temporarily deoxygenated sediments was estimated at 20-40 mg/m²/d and nitrogen at 250-530 mg/m²/d. Phosphorus sedimentation rate was less than 1 mg/m²/d when the sediment-water interface was oxidised.

Matthews (1979) investigated the probable source of the sediment in various parts of the lake bed, in an attempt to distinguish between different sediment types and the relationship between the sediments. Matthews took core samples from Ngongotaha to Mokoia Island and analysed them using the silica to aluminium ratio, the scanning electron microscope, x-ray diffraction and radiometric dating to determine how far sediment entering the lake off the land is distributed and to determine the sediment composition.

Gifford *et al.* (1993) used divers to collect sediment to investigate the concentrations of pollutants such as penta chlorophenol (PCP), dioxins and several heavy metals in the lake.

Blomkvist and Lundstedt (1995) carried out an investigation on 12 Rotorua lakes as part of the Natural Environment Regional Monitoring Network (NERMN) in the Bay of Plenty region. Three sediment cores were taken on Lake Rotorua and analysed for nitrogen and phosphorus and a number of metals, iron, manganese, arsenic, mercury, cadmium, chromium, copper lead and zinc. Phosphorus concentrations in the three cores averaged ~1750 g/tonne and total nitrogen concentrations between 9500-10500 g/tonne. Lake Rotorua has low iron and manganese concentrations compared with other lakes analysed in the Rotorua

region, with a value of 3300 g/tonne and around 240 g/tonne, respectively. Arsenic concentrations are as high as 50 g/tonne and lead at 13 g/tonne.

Burger (2006) investigated variations in sedimentation rates of total particulate matter, total phosphorus, total nitrogen and chlorophyll-*a* using cylindrical sediment traps at three different depths in Lake Rotorua. Sedimentation rate of particulate inorganic material increased with depth indicating that sediment resuspension is an important process in the lake. It is estimated to contribute up to 71 % of total particulate matter at the shallowest site. Sedimentation rate increased during the summer. Burger (2006) found that the nutrient budget for Lake Rotorua indicated that internal nutrient sources derived from benthic fluxes are more important than external nutrient sources to the lake (Figure 2.9).

2.5.3 Acoustic studies

Acoustic surveys have increasingly been used as a method for determining sediment stratigraphy and to identify sub-bottom features. As advances in technology enable clearer and faster data acquisition, increasingly complex areas are able to be mapped. Irwin (1969) produced a bathymetric map of Lake Rotorua by interpolating between a series of echo sound survey tracks across the lake.

In 1990, three one-day trials were conducted on Lake Taupo, Lake Rotorua and the Waikato River using uniboom seismic reflection. Marine seismic reflection profiles were obtained in the southern end of Lake Rotorua in order to aid in the understanding of the Rotorua Geothermal System (Davy, 1992). The original target of the profiling was delineation of faults that might be associated with circulation of geothermal hot water. The survey was run in track lines as shown in Figure 2.11.

Davy (1992) recognised gas in the sediments by the negative polarity of the initial pulse reflected at the lake floor, and the constant phase of lake floor-lake surface multiples. Another important feature identified by Davy (1992) is a pockmark. It was found that the strong multiple reflections terminated in the pockmark on the lake floor. Pockmarks in hydrocarbon gas-charged sedimentary environments are indicative of gas leakage into the water column (Hovland, 1981).

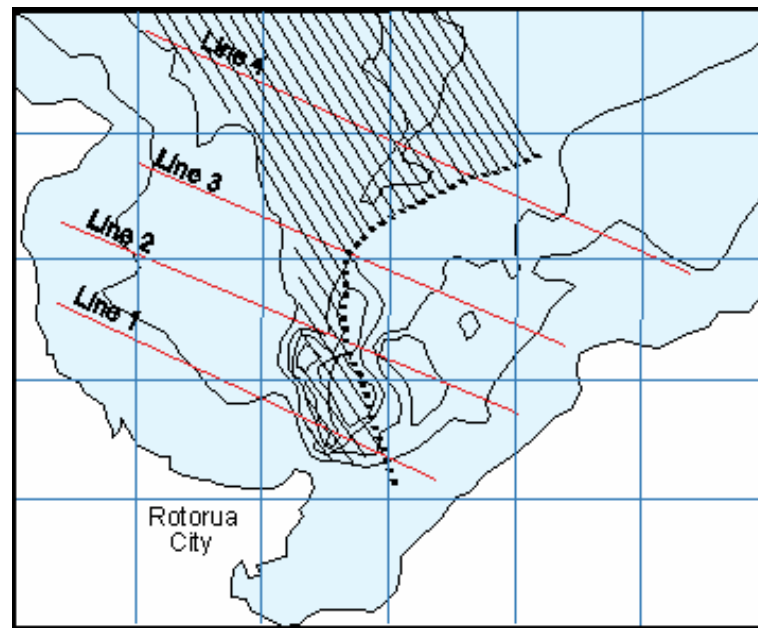


Figure 2.11: Uniboom seismic reflection tracks across southern Lake Rotorua. The hashed area shows strong lake bed multiples indicating gas-filled sediments (Davy, 1992).

Shallow seafloor and lake floor gas has been widely reported elsewhere in the world by numerous authors (King and MacLean, 1970; Otis *et al.*, 1977; Anderson and Hampton, 1980; Hovland, 1981; and Rodgers *et al.*, 2006). Pockmarks were first described as ‘concave, crater-like depressions that occur in profusion on mud bottoms across the Scotian Shelf’ (King and MacLean, 1970). They can reach hundreds of meters and depths of tens of meters. Pockmarks are recognised in a variety of continental margin settings, deltas, and areas of petroleum production or tectonic activity, all over the world (Rodgers *et al.*, 2006). Gas is not usually observed directly beneath a pockmark, allowing imaging of sub-bottom reflectors beneath pockmarks that are obscured by gas nearby. This relationship suggests that the escape of the gas and associated pore waters formed the pockmark (Rodgers *et al.*, 2006).

Davy (1992) suggests that the origin of the gas in the sediments of Lake Rotorua could be sourced by either biogenic production or thermal outgassing. If the gas in the sediments is biogenic in origin the gas is likely to be methane and other higher order hydrocarbons. If the gas in the sediments is sourced geothermally the gas is

expected to be a mixture of carbon dioxide and hydrogen sulphide. With information from Bibby *et al.* (1992), Davy (1992) favoured a deeper geothermal origin as the source mechanism for the gas but without further examination their findings are inconclusive.

Pickrill (1993) carried out a seismic survey on Lake Rotoiti using an echo-sounder and seismic reflection profiler. Gas filled sediments and pockmarks, similar to those found in Lake Rotorua by Davy (1992) are found in the much deeper Lake Rotoiti. Pickrill (1993) used tephrochronology, established from the surrounding catchments, correlating it with the seismic stratigraphy markers found in Lake Rotoiti. Reflectors from eight major eruptions over the last 11850 years were able to be identified. Due to the close proximity of Lake Rotoiti to Lake Rotorua it may be possible to use Pickrill's (1993) identification of the tephra layers to identify stratigraphic markers in Lake Rotorua. Pickrill also determined different stages of pockmark genesis which show pock marks grow, decay, migrate and persist over several thousand years.

2.6 SUMMARY

Lake Rotorua has a long complex history of eruption sequences which have had drastic effects the level of the lake. Over thousands of years diatomaceous sediments have been accumulating in the lake bed interlaying with Tephra deposits from the Taupo Volcanic Zone. The most recent of these deposits are the Kaharoa (1314 ± 12 yr) and the Tarawera eruption (June 1886). Both are identifiable in the sediments of Lake Rotorua through core samples and acoustic reflections. The presence of a large quantity of gas in the sediment is recognised during sub-bottom surveying.

The water quality of the lake is affected by internal processes as well as nutrient inputs from springs, streams, groundwater and geothermal fields. A nutrient budget for Lake Rotorua suggests that internal nutrient sources derived from benthic fluxes are more important than external nutrient sources to the lake. Therefore the sediments play a vital role in recycling nutrients into the lake and any future remediation options will need to deal directly with the source.

REFERENCES

- Anderson, A.L. and Hampton, L.D. 1980. Acoustics of gas bearing sediment. *Journal of the Acoustical Society of America*. 67: 1865-1903.
- Balance, P.F. 1981. Geology and Landforms of the Rotorua Lakes Area. In: Chapman, V.J. (ed), *Handbook of the Rotorua Lakes District. The Guardians of the Rotorua Lakes*.
- Beyá, J., Hamilton, D. and Burger, D. 2005. Analysis of catchment hydrology and nutrient loads for lakes Rotorua and Rotoiti. Centre for Biodiversity and Ecology Research, University of Waikato, Hamilton.
- Bibby, H.M., Dawson, G.B., Rayner, H.H., Bennie, S.L. and Bromley, C.J. 1992. Electrical resistivity and magnetic investigations of the geothermal systems in the Rotorua area, New Zealand. *Geothermics*. 21: 43-64.
- Bibby, H.M., Risk, G.F. and Caldwell, T.G. 2002. Long offset tensor apparent resistivity surveys of the Taupo Volcanic Zone, New Zealand. *Journal of Applied Physics*. 49: 17-32.
- Blomkvist, D. and Lundstedt, L. 1995. Sediment investigation of the Rotorua Lakes. Environment Bay of Plenty Environmental Report No. 95/23.
- Burger, D.F. 2006. Dynamics of internal nutrient loading in a eutrophic, polymictic lake (Lake Rotorua, New Zealand). Ph.D Thesis. University of Waikato, Hamilton.
- Carter, L., Alloway, B., Shane, P. and Westgate, J.A. 2004. Deep-ocean record of major Late Cenozoic rhyolite eruptions from New Zealand. *New Zealand Journal of Geology and Geophysics* 47 (3): 481-500.
- Cotton, C.A. 1922. *Geomorphology of New Zealand*. Government printer, Wellington.
- Davy, B. 1992. Seismic reflection profiling on southern Lake Rotorua – Evidence for gas-charged lakefloor sediments. *Geothermics*. 21 (1/2): 97-108.
- Dine, P. 2004. Tikitere Diversion. Rotorua District Council. Internal Report T-12814.
- Donovan, C.L. and Donovan, W.F. 2003. Estimate of the geothermal nutrient inputs to twelve Rotorua lakes. Bioresearchers report for Environment Bay of Plenty. pp52.
- Dravitzki, D.N.R. 1999. The volcanic history and lake sediment characteristics of Paradise Valley, Rotorua. MSc. Thesis, Earth Science Department, University of Waikato, Hamilton.

- Esler, W.R. 2006. An introduction to Rotorua Basin. In: Lowe, D.J. (ed), Guidebook for 'Land and Lakes' fieldtrip, N.Z. Society of Soil Science Biennial Conference, Rotorua. New Zealand Society of Soil Science, Lincoln, pp. 22-24.
- Esler, W.R. (In Prep). The tephrostratigraphy and paleogeography of the Rotorua Basin, North Island, New Zealand. Ph.D. Thesis. Department of Earth and Ocean Sciences, University of Waikato, Hamilton.
- Fish, G.R. 1975. A Nutrient Budget for Lake Rotorua. In: Jolly, V.H. and Brown, J.M.A. (eds), New Zealand Lakes. Auckland/Oxford University Press.
- Fish, G.R. 1976. Nitrogen and phosphorus analysis of rainfall at Rotorua, New Zealand. New Zealand Journal of Hydrology. 15: 17-26.
- Fish, G.R. 1979. Recent stratigraphy of sediments in Lake Rotorua. New Zealand Journal of Marine and Freshwater Research. 13(4): 529-532.
- Fish, G.R. and Andrew, I.A. 1980. Nitrogen and phosphorus in the sediments of Lake Rotorua. New Zealand Journal of Marine and Freshwater Research. 14(2): 121-128.
- Gifford, J.S., Hannus, I.M., Judd, M.C., McFarlane, P.N., Anderson, S.M. and Amoamo, D.H. 1993. Assessment of chemical contaminants in the Lake Rotorua catchment. New Zealand Forest Research Institute.
- Glover, R.B. 1992. Integrated heat and mass discharges from the Rotorua Geothermal System. Geothermics. 21: 89-96.
- Grange, L.I. 1937. The geology of the Rotorua-Taupo subdivision: Rotorua and Kaimanawa divisions. New Zealand Geological Survey Bulletin, No. 37, 132p.
- Grindley, G.W., Mumme, T.C. and Kohn, B.P. 1994. Stratigraphy, paleomagnetism, geochronology and structure of silicic volcanic rocks, Waiotapu/Paeroa range area, New Zealand. Geothermics 23: 473-499.
- Healy, J. 1964. Volcanic mechanisms in Taupo Volcanic Zone, New Zealand. New Zealand Journal of Geology and Geophysics. 7: 6-23.
- Healy, J., Vucetich, C.G. and Pullar, W.A. 1964. Stratigraphy and chronology of Lake Quaternary volcanic ash in Taupo, Rotorua and Gisborne district. New Zealand Geological Survey Bulletin 73.
- Hoare, R.A. 1978. Particulate matter in tributaries of Lake Rotorua. Proceedings of the 25th Anniversary Conference on 'Erosion assessment and control in New Zealand'. New Zealand Association of Soil Conservators. 244-51.
- Hoare, R.A. 1980. Inflows into Lake Rotorua. New Zealand Journal of Hydrology. 19: 49-59.

- Hoare, R.A. 1987. Nitrogen and Phosphorus in the Catchment of Lake Rotorua. Water Quality Centre Publication 11. Ministry of Works and Development, Hamilton, New Zealand.
- Hochsetter, F. von. 1864. Geology of New Zealand: Contributions to the Geology of the provinces of Auckland and Nelson. Translated from German and edited by C.A. Fleming. 1959. R.E. Owen, Government printer, Wellington. 319p.
- Hodgson, K.A. and Nairn, I.A. 2004. The sedimentation and drainage history of the Harohoro Caldera and the Tarawera river system, Taupo Volcanic Zone, New Zealand. Environment Bay of Plenty Operations Publication 2004/03. August 2004.
- Hogg, A.G., Higham, T.F.G., Lowe, D.J., Palmer, J.G., Reimer, P.J. and Newnham, R.M. 2003. A wiggle-match date for Polynesian settlement of New Zealand. *Antiquity*. 77: 116-125.
- Hovland, M. 1981. Characteristics of Pockmarks in the Norwegian Trench. *Marine Geology*. 39: 103-117.
- Irwin, J., 1969. Lake Rotorua Provisional Bathymetry. Lake Series, 1:15,840. Fisheries Research Division, New Zealand Marine Department.
- Jurado-Chichay, Z. and Walker, G.P.L. 2000. Stratigraphy and dispersal of the Mangoane Subgroup deposits, Okataina Volcanic Centre, New Zealand. *Journal of Volcanology and Geothermal Research*. 104(1-4): 319-380.
- Kennedy, N.M. and Pullar, W.A. 1981. Landscape Features and Deposits in the Lake Rotorua Basin. In: Chapman, V.J. (ed), *Handbook of the Rotorua Lakes District. The Guardians of the Rotorua Lakes*.
- Kennedy, N.M., Pullar, W.A. and Pain, C.A. 1978. Lake Quaternary land surfaces and geomorphic changes in the Rotorua basin, North Island, New Zealand. *New Zealand Journal of Science*. 21: 249-264.
- King, L.H. and MacLean, B. 1970. Pockmarks on the Scotian Shelf. *Geological Society of America Bulletin*. 81: 3141-3148.
- Lowe, D.J. and Green, J.D. 1992. Lakes. In: Soons, J.M.; Selby, M.J. (eds) *Landforms of New Zealand: Second Edition*. Auckland, Longman Paul, 107-143.
- Marshall, P. 1905. *The Geography of New Zealand*. Whitcombe and Tombs, Wellington, New Zealand.
- Marshall, P. 1912. *Geology of New Zealand*. Government printer, Wellington, New Zealand. p 107-114.

- Marx, R.S. 2004. The Evolution of Lake Rotorua. M.Sc. Thesis. University of Otago, Dunedin, New Zealand.
- Matthews, R.J. 1979. Chemical analysis of Lake Rotorua sediments. M.Sc. Thesis. University of Waikato, Hamilton, New Zealand.
- Milner, D.M. 2001. The Structure and Eruptive History of Rotorua Caldera, Taupo Volcanic Zone, New Zealand. Ph.D. Thesis. University of Canterbury, New Zealand. p 434.
- Milner, D.M., Cole, J.W. and Wood, C.P. 2002. Asymmetric, multiple block collapse at Rotorua Caldera, Taupo Volcanic Zone, New Zealand. *Bulletin of Volcanology*. 64: 134-149.
- Milner, D.M., Cole, J.W. and Wood, C.P. 2003. Mamaku Ignimbrite: a caldera-forming ignimbrite erupted from a compositionally zoned magma chamber in Taupo Volcanic Zone. *Journal of Volcanology and Geothermal Research* 122: 243-264.
- Morgenstern, U. and Gordon, D. 2006. Prediction of Future Nitrogen Loading to Lake Rotorua. GNS Science. Consultancy Report: 2006/10.
- Nairn, I.A., Self, S., Cole, J.W., Leonard, G.S. and Scutter, C. 2001. Distribution stratigraphy and history of proximal deposits from the c. AD 1305 Kaharoa eruptive episode at Tarawera volcano, New Zealand. *New Zealand Journal of Geology and Geophysics*. 44: 467-484.
- Nairn, I.A. 2002. Geology of the Okataina Volcanic Centre. Institute of Geological and Nuclear Sciences. Lower Hutt, New Zealand. p156.
- Otis, R.M., Smith, R.B. and Wold, R.J. 1977. Geophysical surveys of Yellowstone Lake, Wyoming. *Journal of Geophysical Research*. 82 (26): 3705-3717.
- Pickrill, R.A. 1993. Shallow seismic stratigraphy and pockmarks of a hydrothermally influenced lake, Lake Rotoiti, New Zealand. *Sedimentology*. 40: 813-828.
- Park, J. 1910. Geology of New Zealand. Whitcome and Tombs, Wellington, New Zealand. p 116-181.
- Pullar, W.A. and Kennedy, N.M. 1981. Tephra Deposits in the Rotorua Lakes District. In: Chapman, V.J. (ed), *Handbook of the Rotorua Lakes District. The Guardians of the Rotorua Lakes*.
- Rodgers, J.N., Kelley, J.T., Belknap, D.F., Gontz, A. and Barnhardt, W.A. 2006. Shallow-water pockmark formation in temperate estuaries: A consideration of origins in the western gulf of Maine with special focus on Belfast Bay. *Marine Geology*. 225: 45-62.

- Rutherford, J.C., Pridmore, R.D. and White, E. 1989. Management of phosphorus and nitrogen inputs to Lake Rotorua, New Zealand. *Journal of Water Resources, Planning and Management*. 115(4): 431-439.
- Rutherford, J.C. 1989. Internal nitrogen and phosphorus loads in Lake Rotorua, New Zealand. *International Association of Theoretical and Applied Limnology*. 23(2): 828-831.
- Rutherford, K. 2003. Lake Rotorua Nutrient Load Targets. NIWA Client Report: HAM2003-155. Prepared for Environment Bay of Plenty.
- Smith, V.C., Shane, P. and Smith, I.A. 2002. Tephrastratigraphy and geochemical fingerprinting of the Mangaone Subgroups Tephra beds, Okataina Volcanic Centre, New Zealand. *New Zealand Journal of Geology and Geophysics*. 45: 207-219.
- Thompson, B.N. 1964. Quaternary volcanism of the Central Volcanic Region. *New Zealand Journal of Geology and Geophysics*. 7: 45-65.
- White, E., Don, B.J., Downes, M.T., Kemp, L.J., MacKenzie, A.L. and Payne, G.W. 1978. Sediments of Lake Rotorua as sources and sinks for plant nutrients. *New Zealand Journal of Marine and Freshwater Research*. 12(2): 121-130.
- White, P.A., Cameron, S.G., Kilgour, G., Mroczek, E., Bignall, G., Daughney, C. and Reeves, R.R. 2004. Review of groundwater in the Lake Rotorua catchment. Report prepared by the Institute of Geological and Nuclear Sciences for Environment Bay of Plenty. Client Report 2004/130.
- Williamson, R.B., Smith, C.M. and Cooper, A.B. 1996. Watershed Riparian Management and its Benefits to a Eutrophic lake. *Journal of Water Resources, Planning and Management*. 122: 24-32.
- Wilson, C.J.N., Houghton, B.F., McWilliams, M.O., Lanphere, M.A., Weaver, S.D. and Briggs, R.M. 1995. Volcanic and structural evolution of Taupo Volcanic Zone, New Zealand: a review. *Journal of Volcanology and Geothermal Research*. 68: 1-28.
- Wilson, C.J.N. 2001. The 26.5 ka Oruanui eruption, New Zealand: an introduction and overview. *Journal of Volcanology and Geothermal Research*. 112(1-4): 133-174.

CHAPTER THREE:

METHODS



3.0 INTRODUCTION

The coring methods and location of cores on Lake Rotorua are described in this chapter. Laboratory techniques for core analysis are described in detail including sample preparation, digestion and analysis of samples. Bulk densities of the gravity core samples were also determined. One core (Ru128) was also analysed for carbon and nitrogen. Core Ru55 was examined using a scanning electron microscope (SEM) for determination of diatom species. A geophysical survey was also undertaken on Lake Rotorua using a multibeam echo-sounder and sub-bottom profiler with a low-frequency echo-sounder. This chapter includes a description of the equipment and methods used to carry out the survey.

3.1 CORING METHODS

The main aim of the field work was to determine the distribution and nature of the sedimentary processes involved in Lake Rotorua. To do this sediment cores were collected from Lake Rotorua on a 1 km by 1 km grid pattern. Three different coring methods (piston, box and gravity) were used to capture the sediment, each with its own advantages and limitations. At each site the coring method, water depth, location (latitude and longitude), core length and description of the nature of the material were recorded. Core photos were also taken at the time of sampling. The coring program began in January 2005 and cores were labelled sequentially (Ru1-Ru163).

3.1.1 Piston Coring

The piston coring system is an adaptation of the Livingston corer (Livingston, 1965; Wright, 1967) consisting of a medium wall 3 m long, 50 mm diameter stainless steel tube core barrel fitted for wire line piston coring (Figure 3.1). Either a conventional piston or a locking piston, which was released when thrust was applied to the piston wire, was used. The corer was assembled with a wire attached to the piston, passing through the core barrel, an anvil at the top of the core barrel and a guide tube in the centre of the anvil (Figure 3.2). The driving force was supplied by a 20 kg annular hammer which slid up and down the guide tube. A rope was attached to the hammer. The entire drill string was gently lowered to the lake floor and the piston wire attached to the boat. The hammer

rope was used to raise the hammer about 1.8 m before the hammer was dropped to drive the core barrel into the sediments. The process was repeated until the piston wire tautened indicating that the core barrel was fully extended. The piston wire was then attached to the drill string and both were winched from the sediments. On the boat the anvil and guide tube were removed from the core barrel and a hand winch was used to force a rod through the core barrel from the anvil end, extruding the sediment into 1 m long split 50 mm PVC pipes. As each segment of core was extruded it was photographed, described and covered with a second split pipe, labelled, sealed and secured for removal to the laboratory.

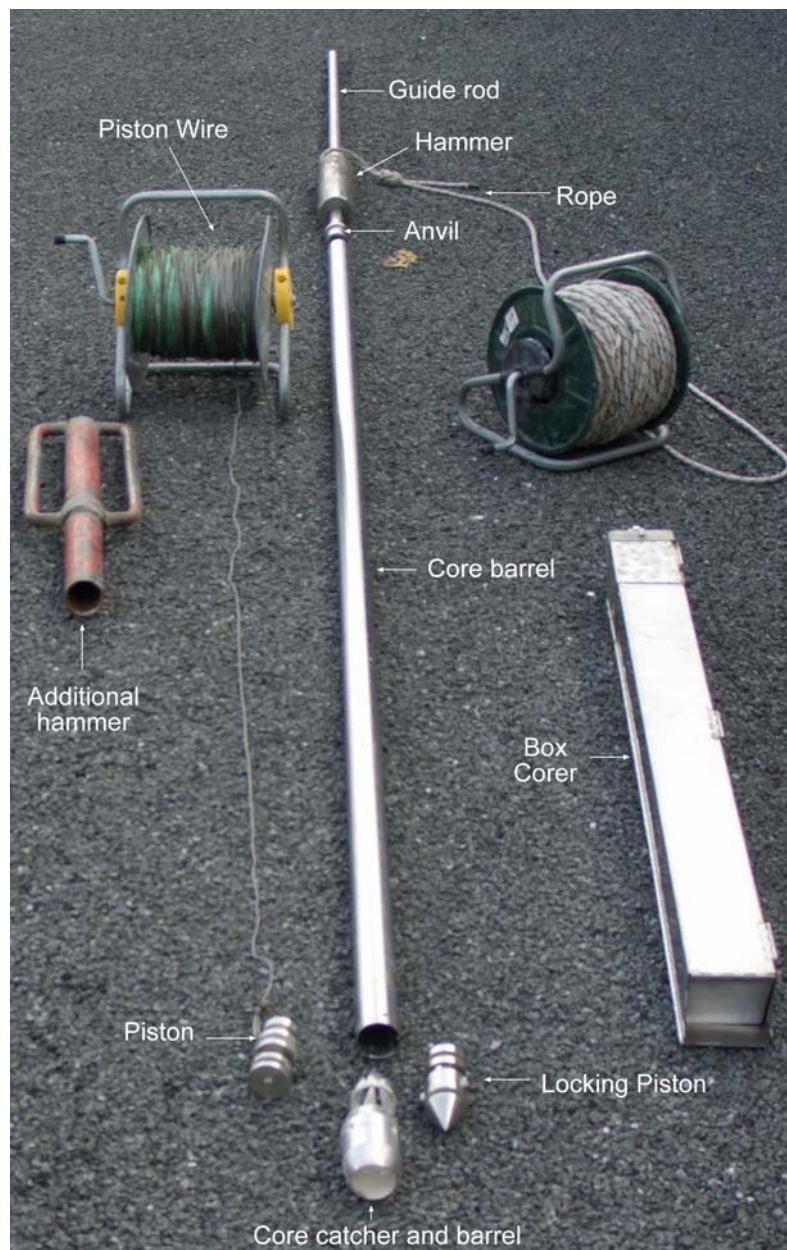


Figure 3.1: Piston coring equipment

The locking piston was employed when coring was intended to start below the lake/sediment interface. A core catcher (Figure 3.1) consisting of sprung stainless steel teeth mounted on a ring and fitted between the core cutter and core barrel was trialled but discontinued when it was found to have completely disturbed the stratigraphy.

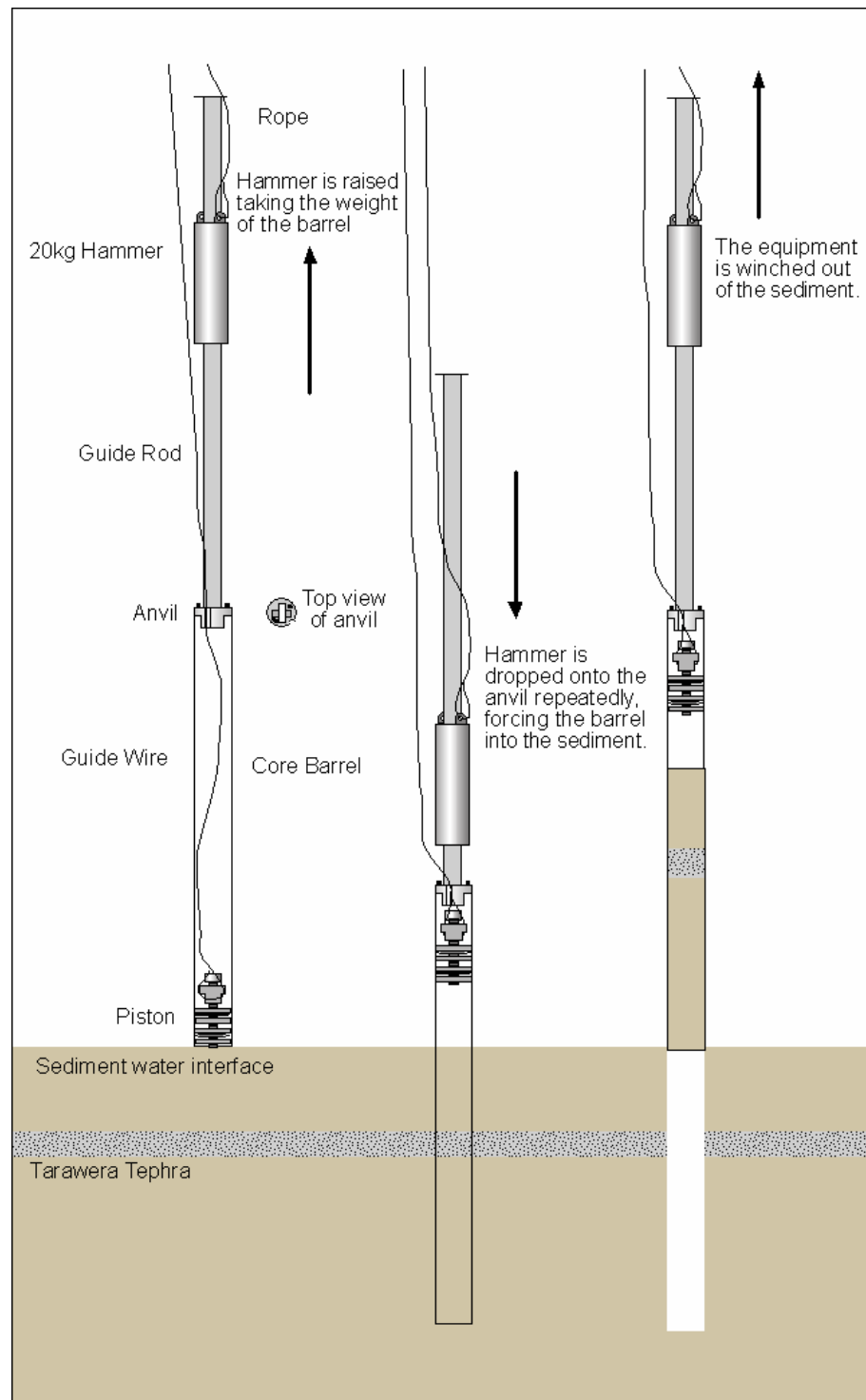


Figure 3.2: Schematic of the piston coring process

The application of the piston core is limited by the gas present in the sediment and its inability to capture the low density diatomaceous material. As described above, the piston corer was lowered over the side of the boat, until the sediment is felt below, and hammered into the sediment. It was only possible to detect the piston entering the denser sediment; therefore low density diatomaceous ooze was often lost off the top of the core. The high water content of the sediment also inhibited accurate collection of the sediment as it did not stay intact when being extruded from the core barrel. As the core was brought up from the lake bottom gas expanded as the hydrostatic pressure was reduced. Gas that escaped forced the sediment out of the core barrel. Gas also escaped when the core was being extruded, which could have altered the stratigraphy of the sediment record.

3.1.2 Box Coring

Box coring is similar to piston coring, with a box (10 x 10 cm) used to capture 1.2 m of sediment. The box core was made of 1.2 mm stainless steel walls with a hinged side and gravity-closing trap door (Figure 3.3a). It was driven into the sediment with a 20 kg annular hammer mounted on a guide tube through the anvil at the top of the corer (Figure 3.3b). Once on the boat the box core was laid on its side, opened, photographed and sampled.

The box corer is useful when large volumes of sediment are required or the material has high water or gas content. It was used in Lake Rotorua in shallower areas (<10 m) that have coarse sediment, where the longer 3 m core was not practicable. It was limited by not being able to keep an intact sample, to be used as a reference, as the entire core was split and bagged for analysis. The box coring method also lost the top of the sediment sample as loose diatomaceous ooze could be extruded through the top of the box corer if driven too far into the sediment or when the corer was laying down.

Box coring began at the same time as piston coring began and was dependent on the type of sediment and water depth as to which coring method was used.

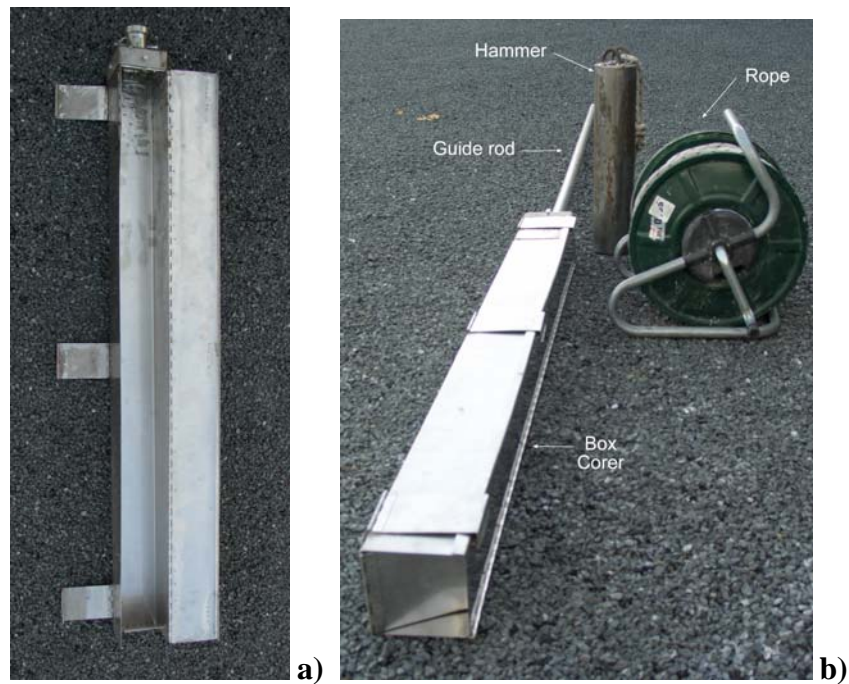


Figure 3.3: a) Open box corer and b) box coring equipment

3.1.3 Gravity Coring

A gravity corer is used to capture the low density diatomaceous sediment. It consists of a clear Perspex (plexiglass) core barrel 62.5 mm in diameter and 60 mm in length with a trapping mechanism fitted to the top (Figure 3.4a). A gravity core was collected by lowering the corer over the side of the boat until the sediment was felt. It was then raised 1-2 m above the sediment and released, allowing the weight of the corer to drive the barrel into the sediment. The trigger was released as the corer penetrated the sediment closing the stopper, which prevented water from re-entering the top of the core barrel and thus holding the sediment in the barrel as it was extracted from the lake floor. Before raising the core above water level a piston was inserted into the bottom of the barrel to catch the sediment (Figure 3.4b). The core was then labelled, photographed and described before extruding the core into a sealed chamber. Two cm intervals were extruded at a time and forced with a plunger into 50ml centrifuge tubes (Figure 3.4c). After measuring the pH and Eh these were sealed, stored at 0°C and returned the laboratory for pore water separation by centrifugation.

The gravity core enabled the recovery of the high water content, low density diatomaceous sediments that were previously unobtainable using the other coring

methods. By adjusting the weights attached to the core barrel, the corer was used to capture the sediment water interface and sometimes also captured the nepheloid layer above the interface. In very low density sediment it was not always possible to catch the top of the sediment as it was too soft to support the weight of the corer to trigger the stopper. Cores in the deeper part of the lake were affected by this limitation. It was recorded in the core description if core tops were present.



Figure 3.4: a) Gravity corer setup, b) gravity corer with sediment showing a closed stopper and piston in the bottom and c) extruding the gravity core into 2 cm horizontal intervals for analysis.

A transect of gravity cores from Sulphur Point to the Ohau Channel was taken in April 2005. It became evident when comparing the chemistry of sediment material with that of the piston cores that the highest concentrations of phosphorus were in the top of the sediment at the sediment-water interface. The gravity core samples are significantly higher, in several nutrient and metal concentrations, especially phosphorus, due to inability of the piston corer to capture the top portion of

diatomaceous ooze. In January 2006, gravity coring was used when revisiting sites where piston cores had been taken from, in order to capture the top of the sediment for chemical analysis (Ru102-Ru163).

3.2 CORE LOCATIONS

The location of the cores and type of coring equipment used is shown in Figure 3.5. For full details of core locations including grid references see Appendix 1.

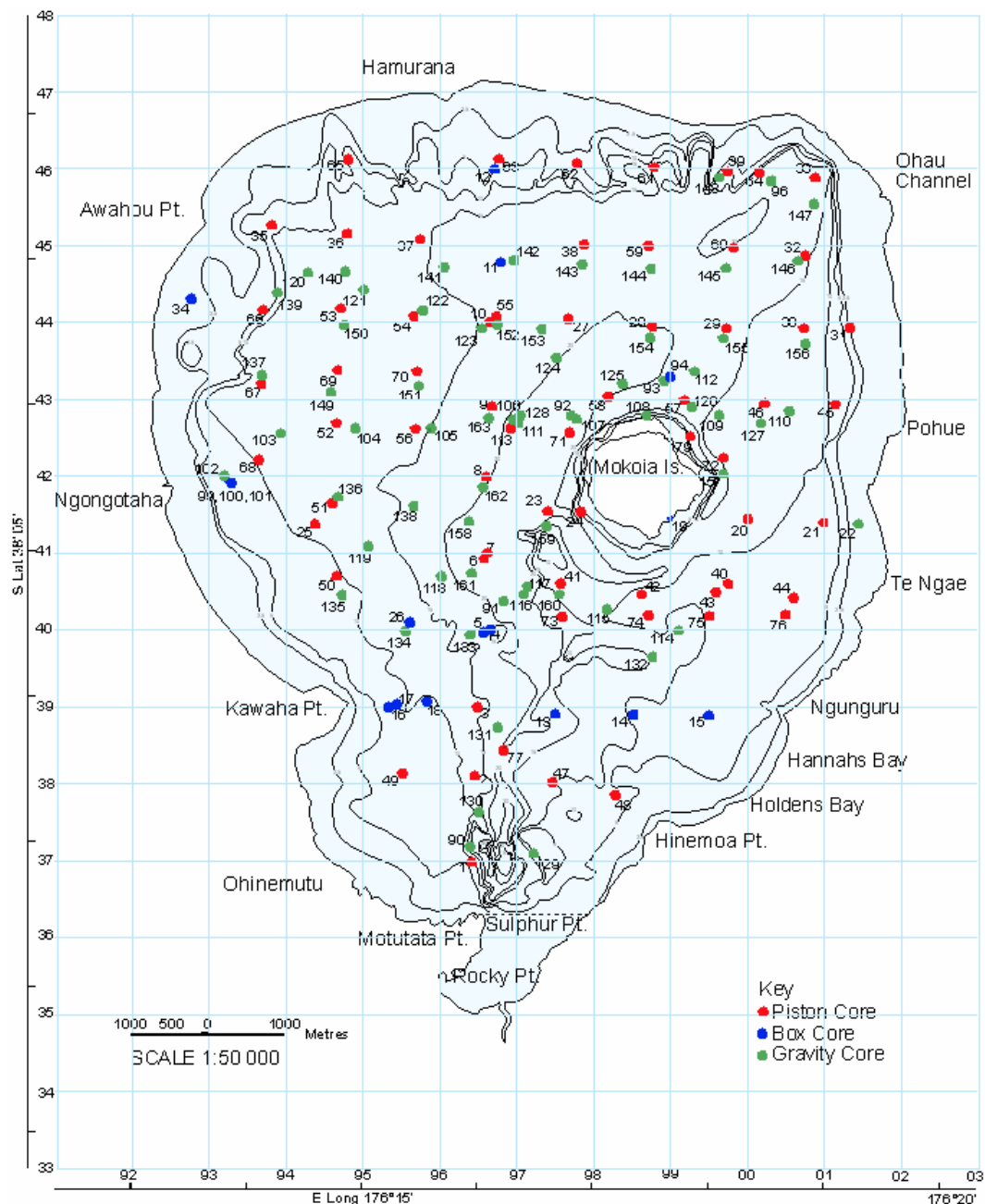


Figure 3.5: Core locations sampled on Lake Rotorua.

3.3 LABORATORY METHODS FOR CORE ANALYSIS

3.3.1 Sample Preparation

Piston core samples were split down the middle to give a reference half, which was stored in the refrigerator at 4°C. The working half was used for analysis. The whole box core sample was used for analysis, as these cores were split and stored in bags at the time of sampling. The piston cores were split into 20 cm intervals or where there were obvious sediment boundaries. The sediment was then dried at 50-80 °C in the oven, crushed using a mortar and pestle and stored in zip-lock bags. Initial samples were sent to a commercial laboratory (Hill Laboratories) for analysis. Subsequent samples were analysed at The University of Waikato by the author as described below. No significant differences were observed between the results from the two laboratories.

Gravity core samples were weighed before centrifuging at 4000 rpm for 20 min to separate the pore water from the sediment. The pore water was then decanted off and stored in 100 ml plastic containers. The sediment was then reweighed to give an indication of the pore water that was recovered. The centrifuge tubes were then placed in an oven at 50 °C until dry. Once dry, the sediment was reweighed for bulk density calculations before the dry sediment was then transferred from the centrifuge tubes, crushed using a mortar and pestle, and stored in zip-lock bags.

3.3.2 Sediment Digestion using *Aqua Regia*

Piston and box core sediments were digested using *aqua regia* (3 HCl:1 HNO₃). Two grams of sample were weighed into 50 ml centrifuge tubes, with 3 ml HNO₃ and 9 ml HCl, to form *aqua regia*. The lids on the centrifuge tubes were replaced loosely and left standing to pre-digest over night. The samples were then placed in a pre-heated water bath at 80 °C and digested for 1 hour. After digestion the samples were allowed to cool before filtering the digested sediment into 50 ml volumetric flasks. The filter unit consisted of firstly a membrane filter to catch the fine sediment, then a glass-fibre filter to retain the bulk of the sediment. The mix of acid and sediment was filtered and rinsed thoroughly with deionised water, before making the flask up to the 50 ml mark with deionised water. The samples were stored in acid-washed 100 ml plastic bottles. A 20 ml sample of the digest

was put into ICP tubes. Piston and box core samples were run on the Inductively Coupled Plasma – Optical Emission Spectrometer (ICP-OES).

Gravity core sediments were digested using reverse *aqua regia* (3 HNO₃:1 HCl). One gram of the dried sample was weighed into a 50 ml centrifuge tube, with 15 ml HNO₃ and 5ml HCl reverse *aqua regia*. The lids were replaced loosely and left standing to pre-digest over night. The samples were then placed in a pre-heated water bath at 50 °C or on a digestion block heated to 50 °C, and digested for 3 hours. Once digested the samples were allowed to cool before centrifuging at 4000 rpm for 15 minutes. A 0.5 ml sample of the centrifuged mixture was pipetted into a 15 ml tube and diluted with 10 ml of deionised water for analysis by the Inductively Coupled Plasma – Mass Spectrometer (ICP-MS). The remaining acid solution was decanted into 30 ml plastic storage containers. A blank reagent and quality assurance solution were run with each of the sample batches.

3.3.3 Sediment Digestion using Ascorbic Acid

To estimate the likely availability of trace elements in anoxic pore waters a second digestion method was carried out on the piston cores. Reduction digestion was carried out using one gram of dried sediment with a 1% (w/v) solution of ascorbic acid. Samples were filtered through 0.12 µm millipore membrane filters after centrifugation, and extracts were stored frozen (to prevent the growth of micro-organisms) until analysis using the ICP-OES.

Comparison of results from the two methods of digestion (Figure 3.6) show that slightly more phosphorus was extracted by *aqua regia* than by the ascorbic acid method, but that significantly greater quantities of arsenic and manganese were extracted by the ascorbic acid digestion. Iron was quite variable.

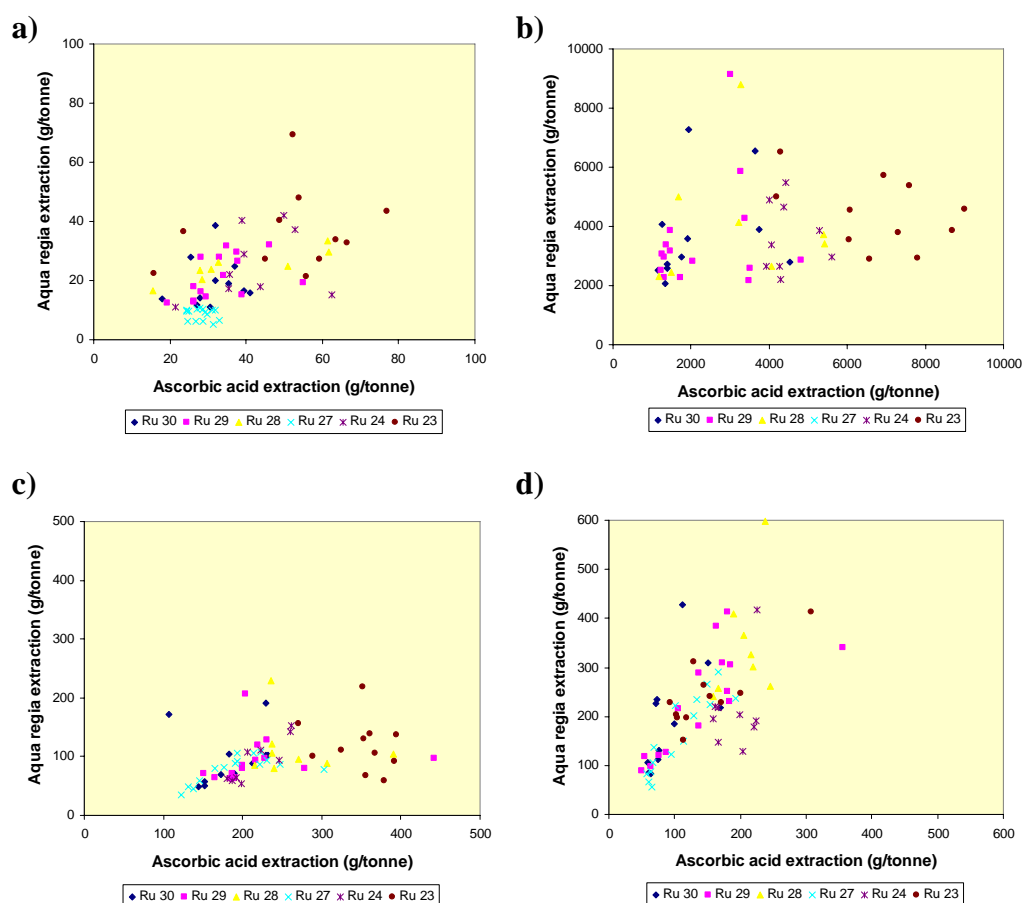


Figure 3.6: Comparisons between ascorbic acid and *aqua regia* digest methods for a) arsenic b) iron c) manganese and d) phosphorus.

3.3.4 X-Ray Fluorescence (XRF) Analysis

XRF was carried on core Ru79 at the University of Waikato using a SPECTRO X-LAB 2000, which is a polarizing energy dispersive X-ray fluorescence spectrometer. The dried ground samples were palletised using PVA and compressed and run through the XRF.

A comparison of the XRF analysis results and *aqua regia* digestion for Ru79 shows that iron, arsenic and phosphorus gave a good correlation between the two techniques, while manganese was consistently underestimated by *aqua regia* extractions (Figure 3.7).

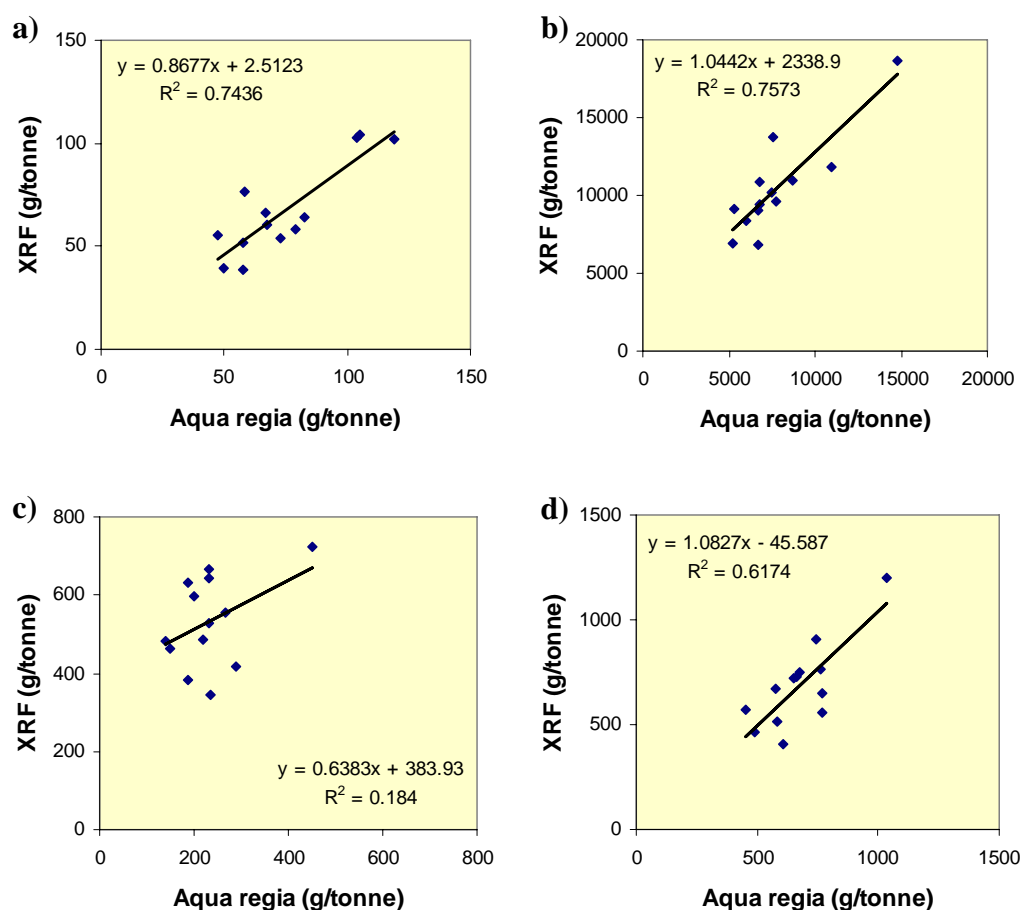


Figure 3.7: Comparisons between XRF and *aqua regia* digest for **a)** arsenic **b)** iron **c)** manganese and **d)** phosphorus.

3.3.5 Digestion Analysis

Analysis of the sediment cores focused on five main elements: phosphorus, iron, manganese, arsenic and lead. Phosphorus was chosen as it is a key nutrient; iron and manganese are involved with binding and/or the release of phosphorus to and from the sediment; and arsenic and lead are heavy metals that may potentially be toxic in the sediments.

Concentrations of elements from ICP-OES and ICP-MS analysis were calculated using the amount of material digested and dilution used for the analysis as follows: The concentration of an element ($C_{x(s)}$) is equal to the ICP-OES result ($R_{x(ICP)}$) (ug/ml) times the total volume of solution made up to ($V_{(final)}$) (ml) times the volume of *aqua regia* acid used for digestion ($V_{(aqua\ regia)}$) (ml) divided by the aliquot of acid digest taken (V_A) (ml) divided by the weight of the dry sediment

digested (M_s) (g). The concentrations from the ICP-MS are reported in units of $\mu\text{g/l}$, and thus these values were then divided by 1000 to give units of g/tonne.

$$C_{x(s)} = R_{x(\text{ICP})} * V_{(\text{final})} * V_{(\text{aqua regia})} / V_A / M_s$$

Concentrations of phosphorus, iron, manganese, arsenic and lead were graphed against sample depth. The large amount of data enabled vertical and spatial distribution of the elements in the sediments over the lake to be plotted. Once the ICP-MS became available the number of elements determined increased to about 40, but only phosphorus, iron, manganese, arsenic and lead were considered significant. Severe interferences with oxygen made sulfur too insensitive to measure accurately by ICP-MS.

3.3.6 Carbon and Nitrogen Analysis

Carbon and nitrogen analysis was carried out on core Ru128 using a LECO TruSpec CN Carbon/Nitrogen Determinator. Dried diatomaceous sediment of weight 0.15 g for each depth separation was put out into a tin foil cup and twisted to seal the contents in the foil. The sample was then placed in the CN analyzer and underwent the three phases in the analysis cycle: purge, combust and analyse. In the purge phase the encapsulated sample was placed in the loading head, sealed and purged of any atmospheric gases that may have entered during sample loading (LECO Corporation, 2006). The sample was then dropped into a hot furnace (950°C) and flushed with oxygen for a very rapid and complete combustion. The products of the combustion phase were passed through a secondary furnace (850°C) for further oxidation and particulate removal. In the analysis phase, oxygen was mixed with the combustion gases and purged through a CO_2 infrared detector and a 3cc aliquot loop (LECO Corporation, 2006). Once the gases had equilibrated, carbon was measured as carbon dioxide by the CO_2 detector. The gases in the aliquot loop were transferred to a helium carrier flow, swept through hot copper to remove oxygen and change NO_x to N_2 , and then through 'Lecosord' and 'Anhydron' to remove carbon dioxide and water, respectively (LECO Corporation, 2006). A thermal conductivity cell was used to determine nitrogen content. The final results were calculated and expressed as percentage of carbon and nitrogen in the dried sample.

3.3.7 Bulk Density

Bulk densities of the diatomaceous sediments were calculated from the weights recorded from the gravity coring. Samples were weighed to give a total sediment weight/porewater before the samples were centrifuged to separate the porewater from the sediment. Once the porewater was separated, the sediment samples were weighed again to give a percentage of pore water recovered. The samples were then dried and reweighed to give the dry weight of the sediment. Total porewater was calculated as sediment and porewater weight minus the dry sediment weight.

Bulk density was calculated by the dry sediment weight (g) divided by the volume of the sample (cm³). Ru102-Ru138 used a slightly larger core barrel with an internal volume for the 2 cm separations of 61.36 cm³. Cores Ru139-Ru163 used a barrel with an internal volume of 52.84 cm³ for the 2 cm separations.

The accuracy of the bulk densities calculated was affected by the sampling method used when coring. Two cm of sediment is extruded from the core and squeezed into the box on the core barrel (Figure 3.4c) and forced into a 50ml centrifuge tube. When the sediment becomes firmer it is harder to force the whole sample into the centrifuge tube. A small portion of the previous sample is left in the box or is discarded to the ground. This error in density calculations is shown as the depth increases down the core it was expected that the density of the sediment also increases but this was not always the case.

3.3.8 Elemental Spatial Mapping

Piston cores were used for the elemental spatial mapping as the core tops were retrieved intact. A square grid of 0.2 x 0.2 km of Lake Rotorua was used to identify locations of core sites. Concentration data for each element was entered into appropriate location for each of the gravity cores. The gravity cores were used for spatial mapping as core tops were retained during sampling, compared to piston and box coring which lost the core top. Land areas were given values of 0 and locations where there were no cores, a value of -99. This data was then transferred into Fortner Transform software and a krigging algorithm was used to fill the missing data (values of -99) between the core sample values. This procedure allowed spatial maps of the elemental distribution in the sediments to

be produced over the lake area. This method was carried out for each element analysed for depths of 0-10 and 10-20 cm. Phosphorus distribution was examined in 2 cm intervals down to 10 cm.

The total amount of an element in the depth interval was calculated by: the sum of all the squares in the grid was divided by the number of squares (1958) to get an average of all the cells. The average value was timed by the area of the lake (78 km²) times the depth interval (0.1 m) times the average density (0.08) to give the total amount for the element (tonnes).

3.3.9 Sedimentation Rate

Due to the loss of the sediment from the piston corer, determination of the sedimentation rate in the lake was difficult. By comparing the concentration of phosphorus in the piston core data with the closest gravity core phosphorus concentration an estimate was made of how much sediment was lost from the top of the piston cores.

The amount added onto the piston core is calculated by: the amount in the piston core (t) added to the estimated missing interval (t). The amount in the piston core is equal to the concentration (g/tonne) times the depth (2 cm) times the bulk density (0.1) times 0.001 to convert to tonnes. The estimated missing interval is equal to the estimated depth missing from the top of the piston core times the density factor (3.09) times 0.001 to convert to tonnes times the average concentration between the gravity core bottom and the piston core top.

The amount of material accumulated above the Tarawera tephra in the piston cores was adjusted by the density factor (3.09) and added to the above result to give the total amount of an element accumulated since the Tarawera eruption in tonnes.

To calculate the rate of accumulation for each element, the values were plotted into the grid used previously for calculating the amount in the top 10 cm of sediment. Concentration data for each element was entered into appropriate location for each of the gravity cores. Land areas were given values of 0 and locations where there were no cores, a value of -99. This data was then transferred

into Fortner Transform software and a krigging algorithm applied to fill the missing data (values of -99) between the core sample values. The total amount of an element accumulated since the Tarawera eruption was calculated by: the sum of all the squares in the grid was divided by the number of squares (1958) to get an average of all the cells. The average value was timed by the area of the lake (78 km²) to give the total amount accumulated for the element (tonnes).

The rate of accumulation since the Tarawera eruption in tonnes per year is equal to the total amount accumulated divided by the number of years since the eruption (121).

3.3.10 Scanning Electron Microscope (SEM)

A piston core (Ru55) was chosen to be examined using a scanning electron microscope to identify the diatom composition of the sediment. The electron microscope facility is a Hitachi s-4100 Field Emission Scanning Electron Microscope. The samples selected from the core were taken at 0-20, 30-32 (Tarawera tephra), 92-112 and 132-160 cm. Sample preparation involved covering a small mounting stub with double-sided carbon tape, and a small portion of the sample was placed on top. A handheld pump was used to remove excess sediment from the tape before the stub was placed in a Hitachi Sputter (Platinum) Coater. The chamber containing the samples is pumped to high vacuum and a potential applied between a platinum plate and a cathode. This strips platinum from the plate and coats the sample, which provides a conductive surface preventing electron charging of the sample surface in the SEM. The mounting stub, containing the sample coated in platinum, is screwed onto the mounting plate in the SEM and introduced into the sample chamber. Hand controls are used to navigate around the sample to identify the different diatoms in the sample. An image is taken by slowing the image capture rate of the SEM and pressing the capture buttons on the capture computer and export computer. Images were taken to get a representative sample at a lower magnification before increasing magnification to focus on single diatoms in the sample.

3.4 GEOPHYSICAL SURVEY

A geophysical survey began on Lake Rotorua in August 2006. It consisted of two echo-sounding techniques run simultaneously. A multibeam survey was conducted to give the bathymetry of Lake Rotorua, while sub-bottom profiling gave a record of the sediment layers. The sediment layers of greatest interest were tephra sequences which enable sedimentation rates to be calculated between eruption events.

3.4.1 Multibeam Survey

A multibeam survey was undertaken on Lake Rotorua between August and November 2006 by Dirk Immenga, Brad Scarfe and Alex Schimel, from the Coastal Marine Group at the University of Waikato. The multibeam survey used a SIMRAD EM3000 Multibeam Echo-sounder at 300 kHz. The system transmits 127 beams perpendicular to the vessel track that use a maximum ping frequency of 20 s^{-1} . The multibeam system comprises of two major components: The EM3000 echo sounder which is fixed to the hull of the boat and houses the transducers that emit and receive the swath of ultrasonic energy, and the data acquisition and processing system, which receives the raw data and allows for real-time and post processing.

The multibeam was run in track lines from the 10 m water depth contour on the University of Waikato vessel, *Tai Rangahu*. A single beam low frequency echo sounder was also run simultaneously to the multibeam survey. Data acquisition took place on an onboard system using Triton Elics Software. Further details of the multibeam system, results and data processing are detailed in Chapter 6.

3.4.2 Sub-bottom Profiling

Sub-bottom profiling was carried out on Lake Rotorua using a low-frequency single beam echo-sounder (KNUDEN 320 MP). The frequencies that were used were 33 and 200 kHz. Positional information was recorded by Real Time Kinematic GPS accurate to $\pm 0.05 \text{ m}$. The echo-sounder was run in track lines from the shore to the 10 m water depth contour. The echo-sounder was also run in the centre of the lake but was unable to give a complete sediment record due to the interference by gas trapped in the sediment. Analysis of the profiles was

carried out using a program called ‘Post Survey’ which is part of the Sounder Suite. Details of the Sub-bottom profiling analysis and methodology are continued in Chapter 6.

REFERENCES

- LECO Corporation. 2006. TruSpec CN Carbon/Nitrogen Determinator, Instruction Manual. LECO Corporation. United States.
- Livingston, D. 1965. The use of filament tape in raising long cores from soft sediment. *Limnology and Oceanography* 12: 346-348.
- Wright, H.E.J. 1967. A square rod piston sampler for lake sediments. *Journal of Sediment Petrology* 37: 975-976.

CHAPTER FOUR:

PHYSICAL COMPOSITION OF LAKE
ROTORUA SEDIMENT



4.0 INTRODUCTION

This chapter examines the physical properties of sediments obtained from the extensive coring programme on Lake Rotorua and in particular the distribution of coarse to fine diatomaceous sediments, and identification and stratigraphy of the tephra layers present in the cores. The bulk density of the gravity cores is analysed across sections of the lake. Scanning electron microscope images have been produced to examine and identify the diatom frustules preserved in the sediment.

4.1 PHYSICAL COMPOSITION OF LAKE ROTORUA SEDIMENTS

Lake Rotorua has two types of sediments: coarse, dense sediments and fine, low-density diatomaceous ooze. The top of the piston, box and gravity cores were examined to produce a distribution map of the coarse to diatomaceous sediment distribution in Lake Rotorua (Figure 4.1). Buried under the accumulating diatomaceous ooze are tephra layers of variable depths.

4.1.1 Coarse Dense Sediment

The coarse sediment is comprised of clastic erosion products and coarse rhyolitic airfall components. It is concentrated in water depths generally less than 10 m as wave action prevents the finer material settling out and keeps it suspended in the water column. The coarse sand and gravel sized pumice covers approximately 60% of the lake area. The coarse material is low in nutrients and contributes very little to the recycling of phosphorus in the lake (see Chapter 5).

4.1.2 Diatomaceous Ooze

Diatomaceous ooze dominates the remaining 40% of the lake area, at depths greater than 10 m. It is comprised of the fine, low density material accumulated by the decomposition of biota within the lake. Nutrients entering the lake are taken up from the water column by algae. The free-floating (pelagic) component of the algal assemblage is phytoplankton, which take up the nutrients, die or are consumed by higher trophic levels, or settle to the sediments. The cyanobacteria and many other phytoplankton appear to leave little material to accumulate in the bottom sediments but diatom frustules remain largely intact to dominate the fine, low density component of the sediment. Once in the sediments, the nutrients may

be recycled back into the water column (e.g. via porewater releases or disturbance by resuspension) or progressively buried. Diatomaceous ooze accumulates rapidly and carries the majority of phosphorus and nitrogen to the lake sediment (see Chapter 5).

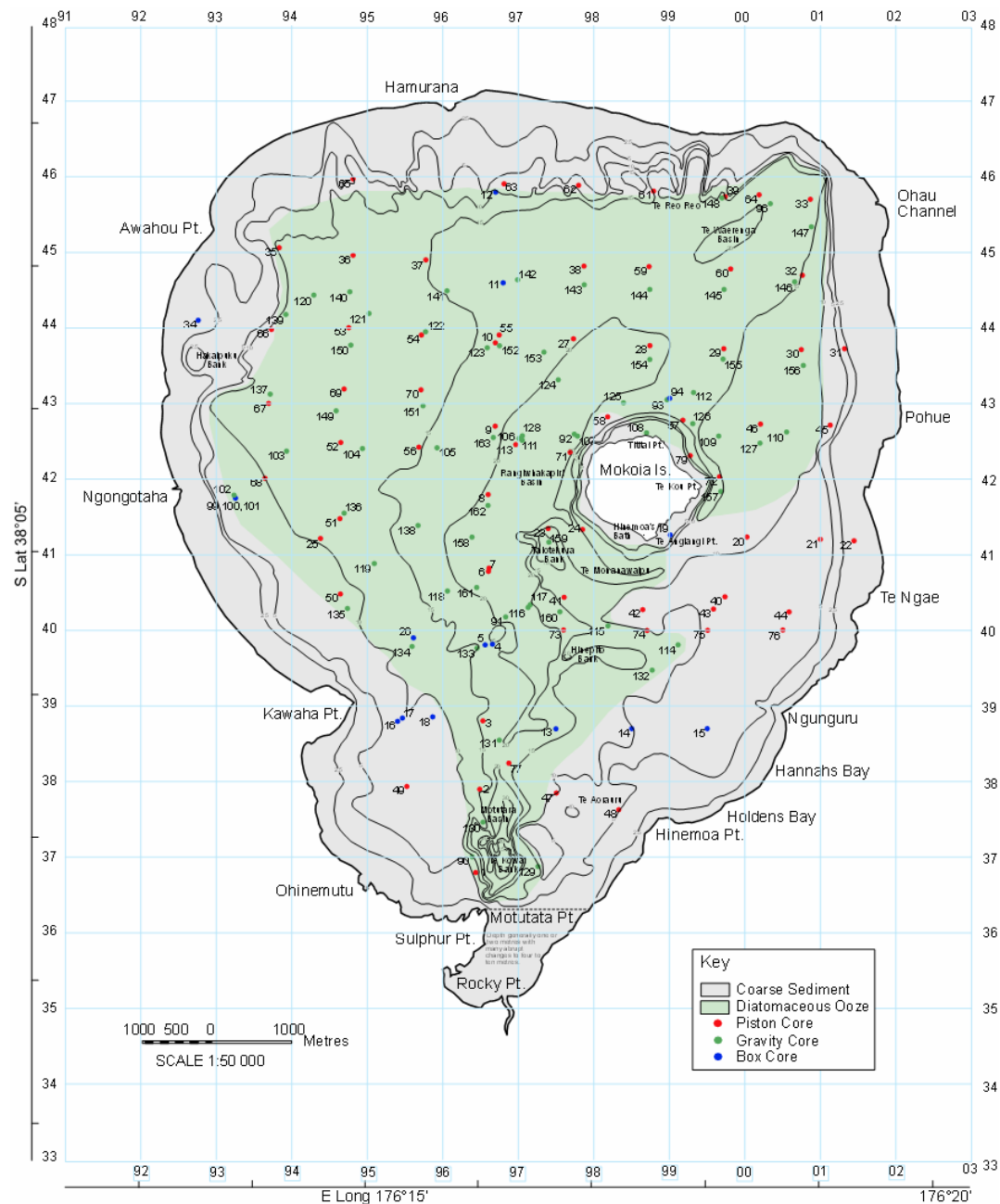


Figure 4.1: Location of cores from Lake Rotorua showing the distribution of coarse and diatomaceous sediment in the lake.

4.1.3 Tephra layers

Ejecta from the Tarawera eruption (1886 AD) and the Kaharoa eruption (1314 \pm 12 AD) were observed in the core samples. The Tarawera tephra is a grey layer of volcanic mud. The tephra often has two distinctive layers. The upper mud layer is Rotomahana Mud (1886) which covered the landscape as superheated sediment was forced from Lake Rotomahana during the Tarawera eruption. The smaller, gritty, black basaltic scoria along the base of the Rotomahana Mud is Tarawera Ash (Figure 4.2a). The Tarawera tephra is typically 2 cm thick and found 20 to 120 cm below the sediment water interface. Separated from the Tarawera tephra by the accumulation of diatomaceous ooze is the coarser Kaharoa tephra consisting of sand and pumice (Figure 4.2b). It is typically found between 2-3 m below the surface in water depths greater than 10 m in the lake. In shallower water depths, Kaharoa or reworked Kaharoa material often make up the surface sediments (Figure 4.2c). These shallow water sites also contain abundant shells of freshwater mussels as well as macrophyte remains.

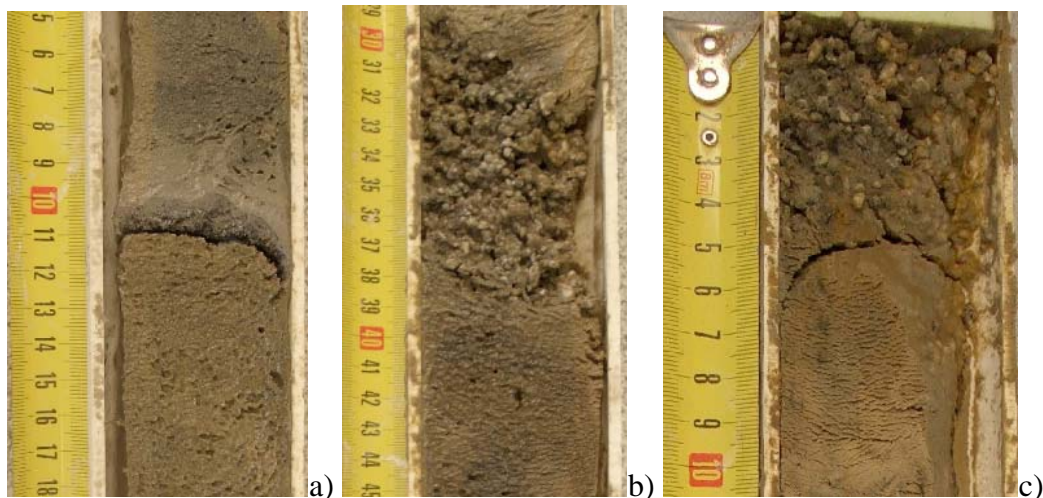
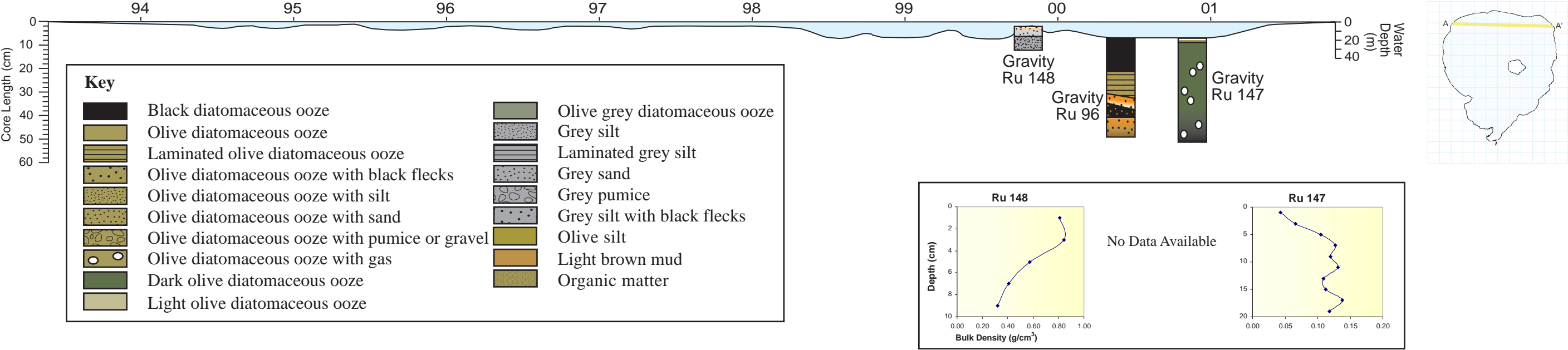


Figure 4.2: a) Tarawera tephra (Ru 55) b) Kaharoa tephra (Ru 54) and c) reworked Kaharoa tephra (Ru 66).

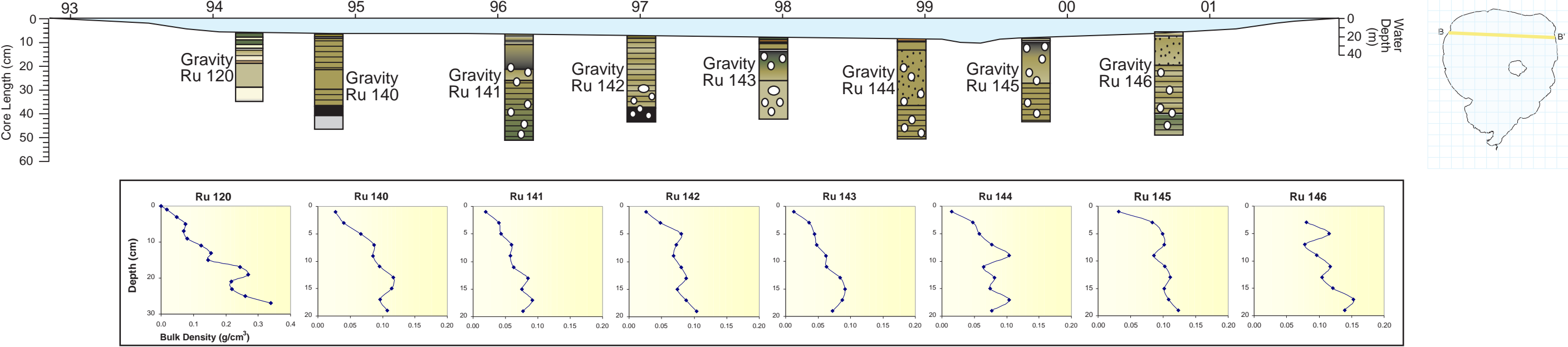
4.2 BULK DENSITY OF GRAVITY CORES

The bulk density of the sediment was calculated from the gravity core samples (Ru102-Ru163) as a known volume of sample was obtained when the cores were extruded. Figures 4.3 to 4.5 display the bulk density results as cross-sections across Lake Rotorua.

Cross Section A to A' Gravity Cores



Cross Section B to B' Gravity Cores



Cross Section C to C' Gravity Cores

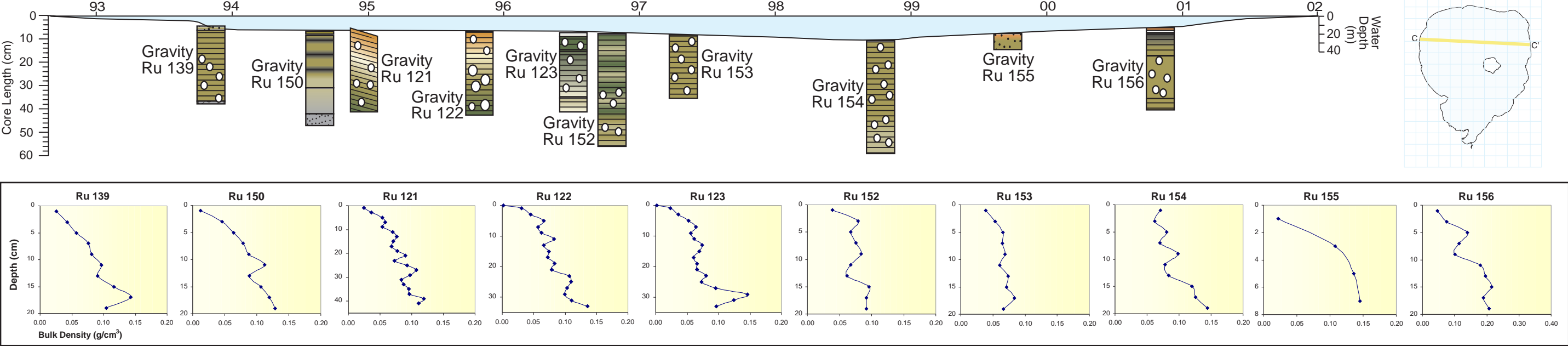
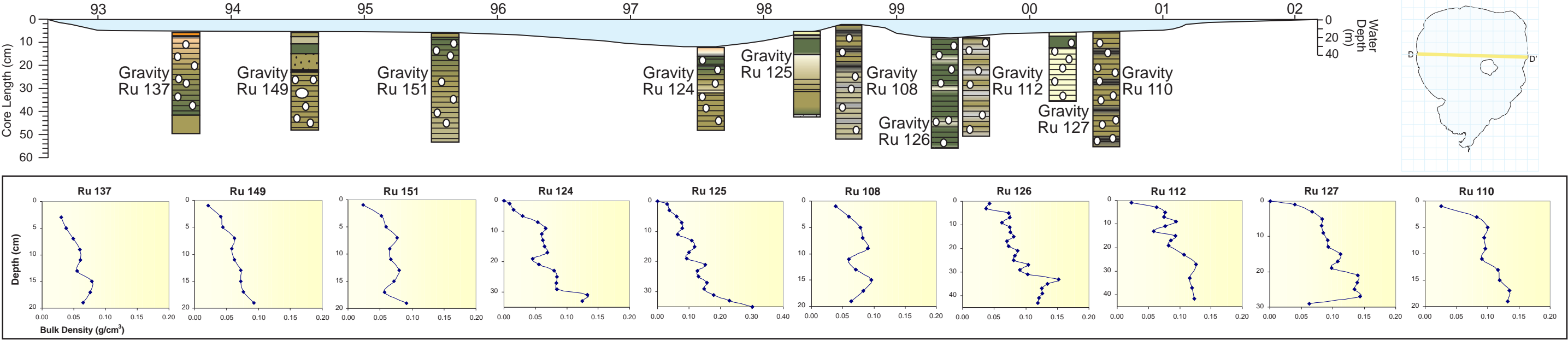
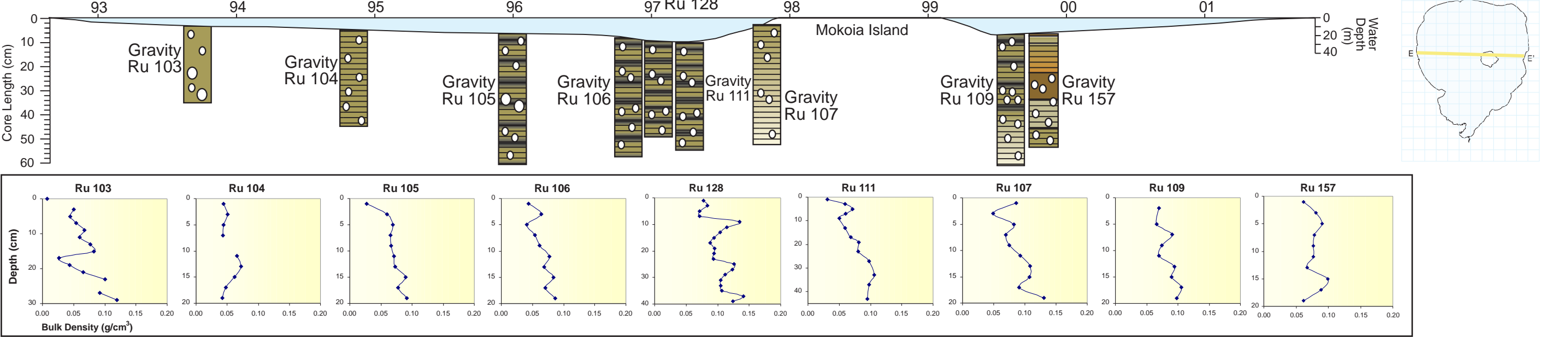


Figure 4.3: Bulk density across section A to A', B to B' and C to C' in Lake Rotorua.

Cross Section D to D' Gravity Cores



Cross Section E to E' Gravity Cores



Cross Section F to F' Gravity Cores

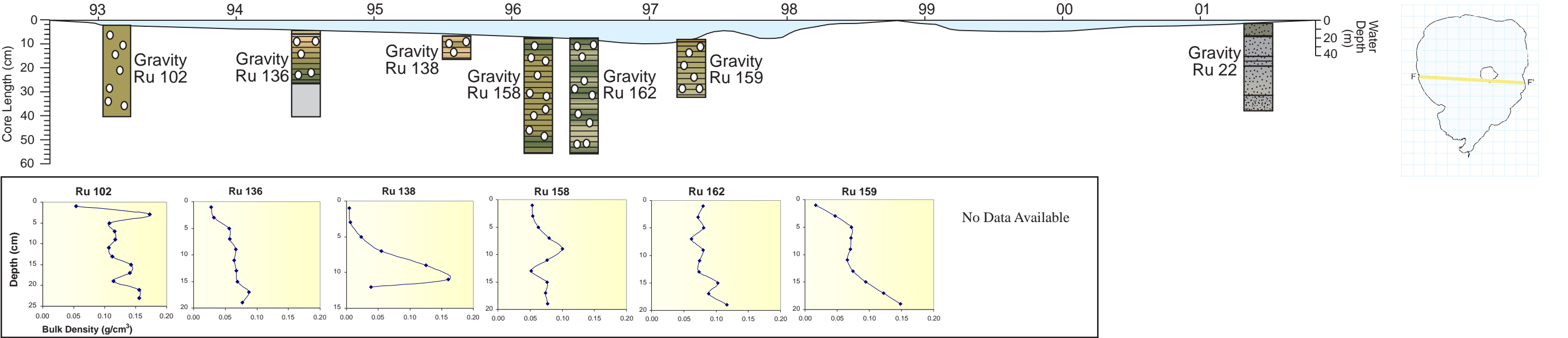
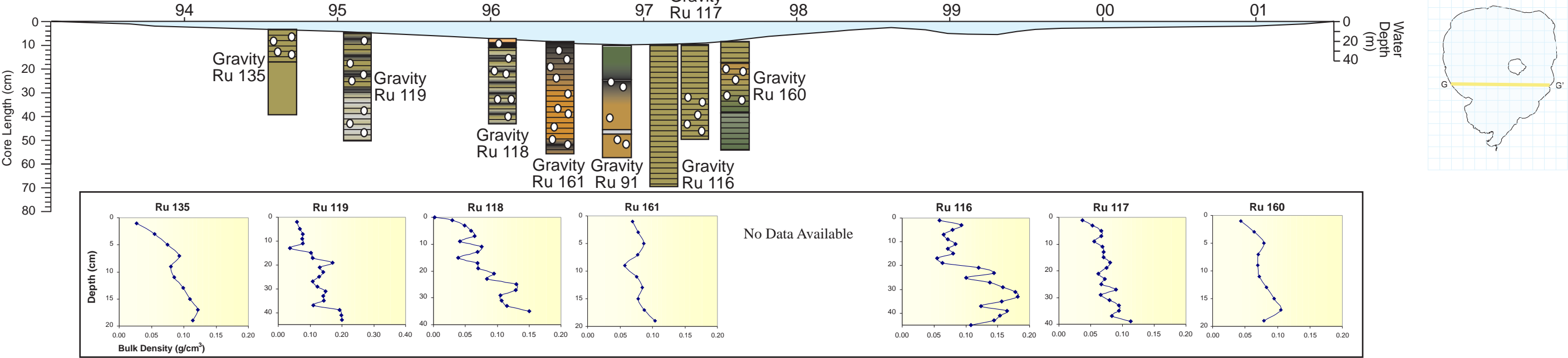
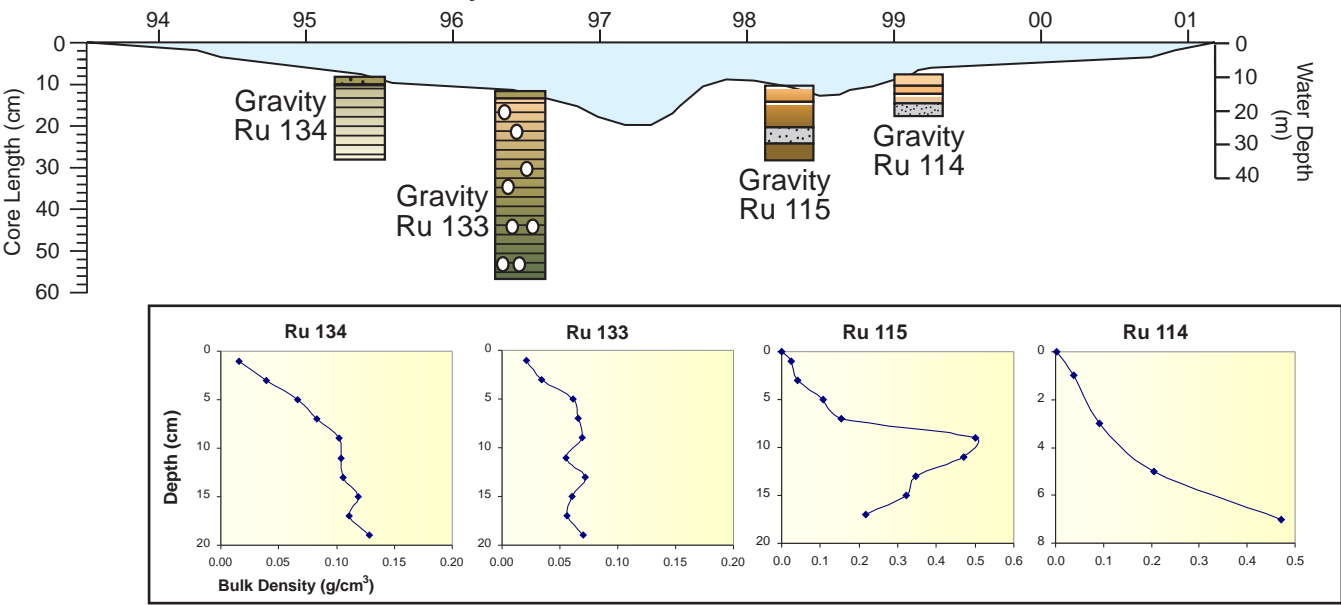


Figure 4.4: Bulk density across section D to D', E to E' and F to F' in Lake Rotorua.

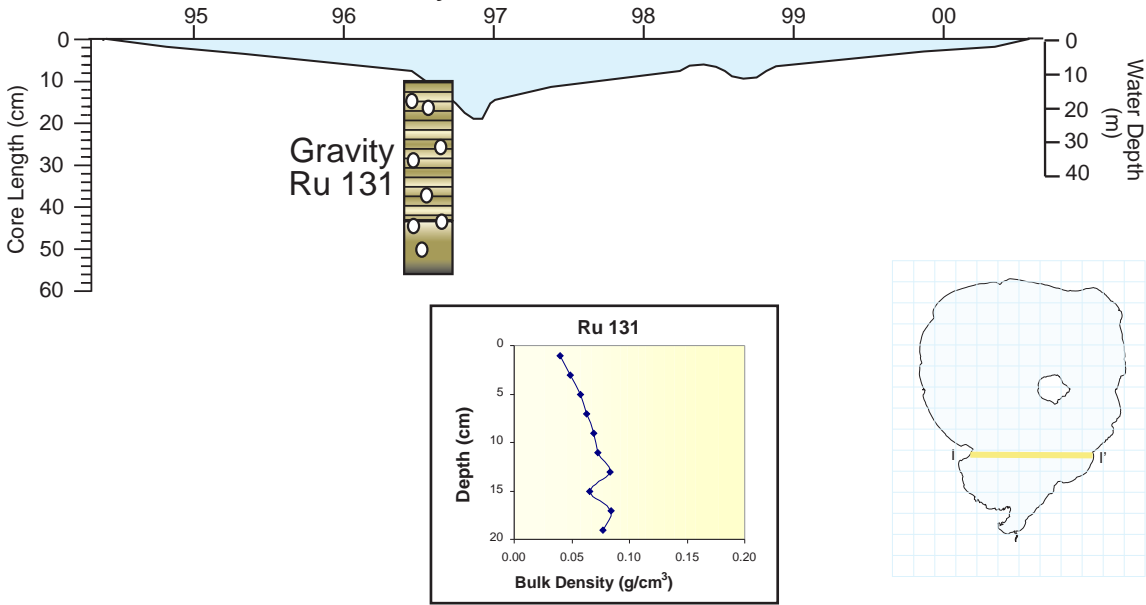
Cross Section G to G' Gravity Cores



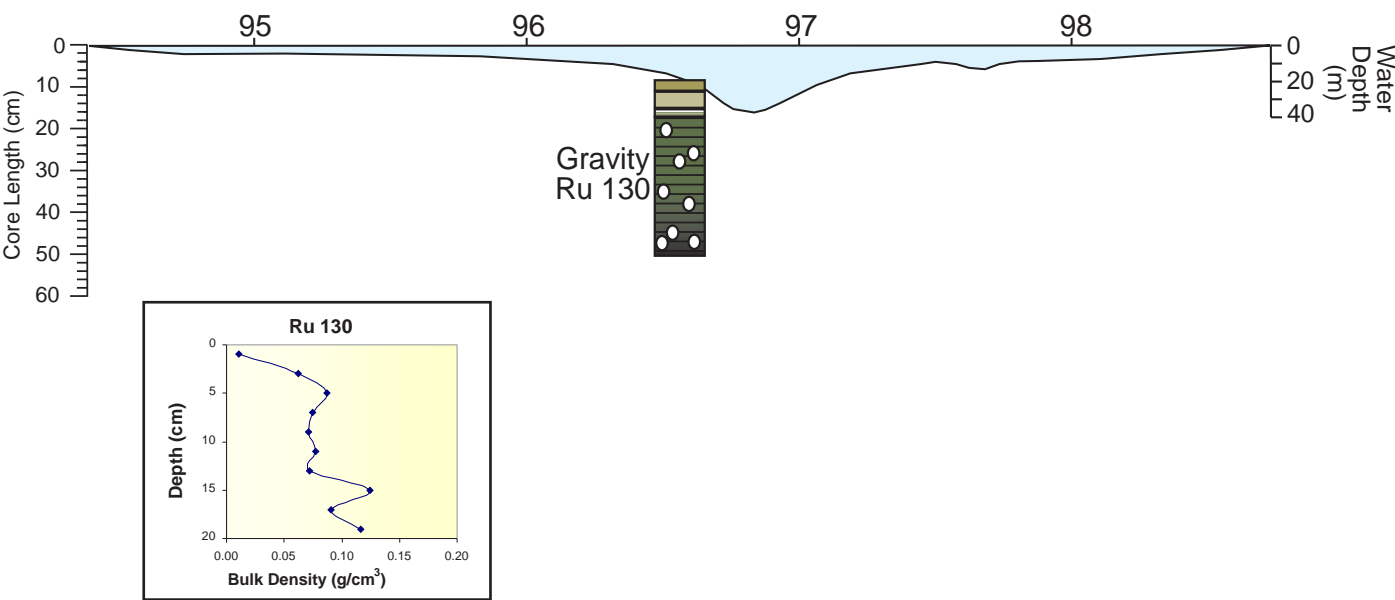
Cross Section H to H' Gravity Cores



Cross Section I to I' Gravity Cores



Cross Section J to J' Gravity Cores



Cross Section K to K' Gravity Cores

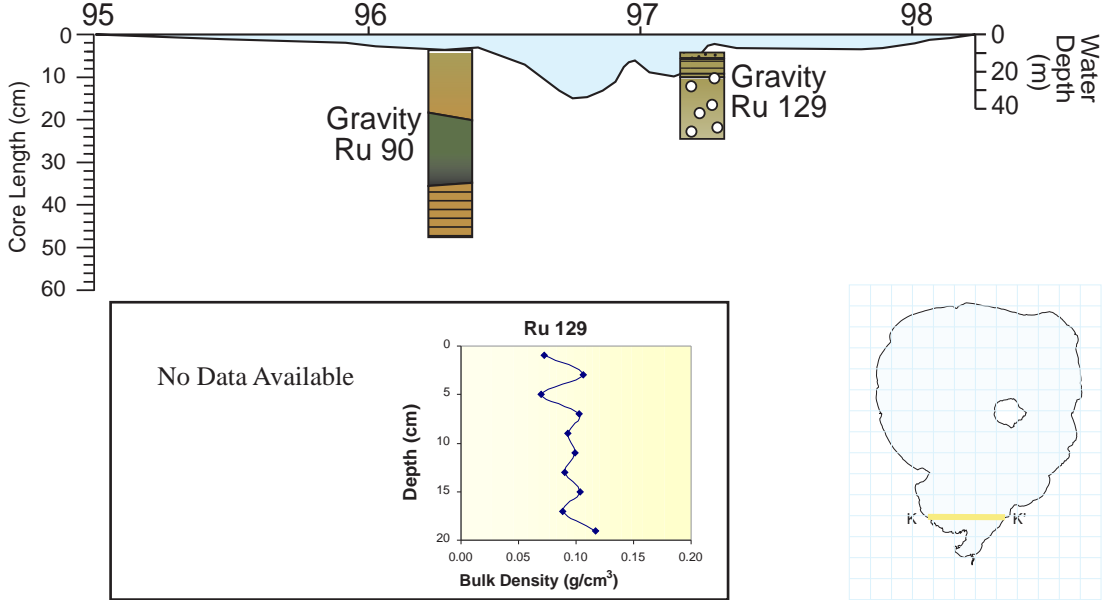


Figure 4.5: Bulk density across section G to G', H to H', I to I', J to J' and K to K' in Lake Rotorua.

The bulk density of the sediment ranges from less than 0.02 g/cm^3 below the sediment-water interface in the diatomaceous ooze to 0.5 g/cm^3 in the coarse, sandy material nearer the lake shore. The bulk density of the material rapidly declines as the transition from a sandy lake bed to diatomaceous material occurs. Even lower bulk densities were found in surficial sediments from deep water near the centre of the lake where. This layer may not be easily distinguished from the turbid (nepheloid) slurry immediately above the sediments.

In cross section A to A' (Figure 4.3) the difference in surface sediment is apparent by comparison of bulk density in the top 2 cm of the cores. The graph of Ru148 (Figure 4.3) does not give an accurate representation of the density profile with increasing depth as the material recovered during core extrusion in the field overfilled the 50 ml centrifuge tube and part of the sample was lost. A further problem occurs when the bulk density of the material is higher than approximately 0.15 g/cm^3 . Coarse sand de-waters in the extruder and results in an apparent steep decline in density at the base of the core as part of the sample remains trapped in the extruder box.

Cross-sections B to B' and C to C' (Figure 4.3) show the trends across the lake well and are not affected by the location of Mokoia Island. Close to the shore the density is higher than the cores sampled in greater than 10 m water depth in the diatomaceous sediment, reaching values of 0.35 g/cm^3 . Deeper in the sediment profile the gas contained in the sediment affects the bulk density. Gas was released from the sediment as the cores were brought up from the lake floor under lower atmospheric pressure, which was likely to disturb the bulk density of the core. The effect of the gas exaggerates the steep rise and fall of the bulk density approximately 10 cm below the sediment-water interface in the density profiles.

Figure 4.4 shows the bulk density through cross-sections D to D', E to E' and F to F'. Coring to the west of Mokoia Island in water depths greater than 15 m was difficult as there is a substantial nepheloid layer present above the sediment-water interface. The material has low density that it makes it very difficult to capture the top of the sediment during gravity coring. The diatomaceous material was not dense enough to support the weight of the gravity corer to trigger the stopper,

which prevented the material leaving the core barrel, and ultimately resulted in a loss of sediment from the top of the core.

The bulk density of the Tarawera tephra observed in core Ru136 (Figure 4.4 F to F') and Ru114 and Ru115 (Figure 4.5 H to H') varied depending on the core location. The Rotomahana mud has a lower density than the Tarawera ash, which is a much coarser material. The bulk density of Ru136 was less than 0.1 g/cm^3 compared to values reaching 0.5 g/cm^3 for Ru114 and Ru115.

4.3 SEDIMENT COMPOSITION UNDER THE SCANNING ELECTRON MICROSCOPE (SEM)

Lake sediments contain the remains of a variety of organisms such as cyanobacteria, chrysophytes, chironomid larvae, terrestrial vegetation (pollen and spores), sponges, and most commonly diatoms. Diatom productivity is dependent on the season, and the largest populations are commonly found in autumn to early spring (Cassie-Cooper, 1996). Although most of the organic component of organisms decomposes and leaves little evidence of the biota, diatom frustules, which are composed of silica, remain largely intact to dominate the accumulating sediment. The large amount of volcanic material deposited in Lake Rotorua, the discharge of silica-laden geothermal waters and groundwaters high in silica from the ignimbrite aquifers have maintained moderate levels of soluble silicic acid, preventing the diatom frustules from dissolving (Rawlence, 1984). The sediments contain a record of changes to the diatom population that provides valuable paleolimnological information about changes in the trophic status of a lake over time. Diversity within the diatom population is subject to change as natural and anthropogenic influences affect the lake catchment and productivity within the lake.

Samples taken from the top, middle and bottom of piston core Ru55 were examined under the scanning electron microscope to identify diatom species and other materials present in the sediment. A sample of Tarawera tephra within the core was also examined. Due to the bulking of dry sediment which was taken for chemical analysis, only a depth range is able to be given for the location of the

samples (Figure 4.6). Identification of diatom species present was made using taxonomic guides and scanning electron photographs from Cassie (1984), Round *et al.* (1990), Cassie-Cooper (1996), John (2000) and Edwards (In Prep.).

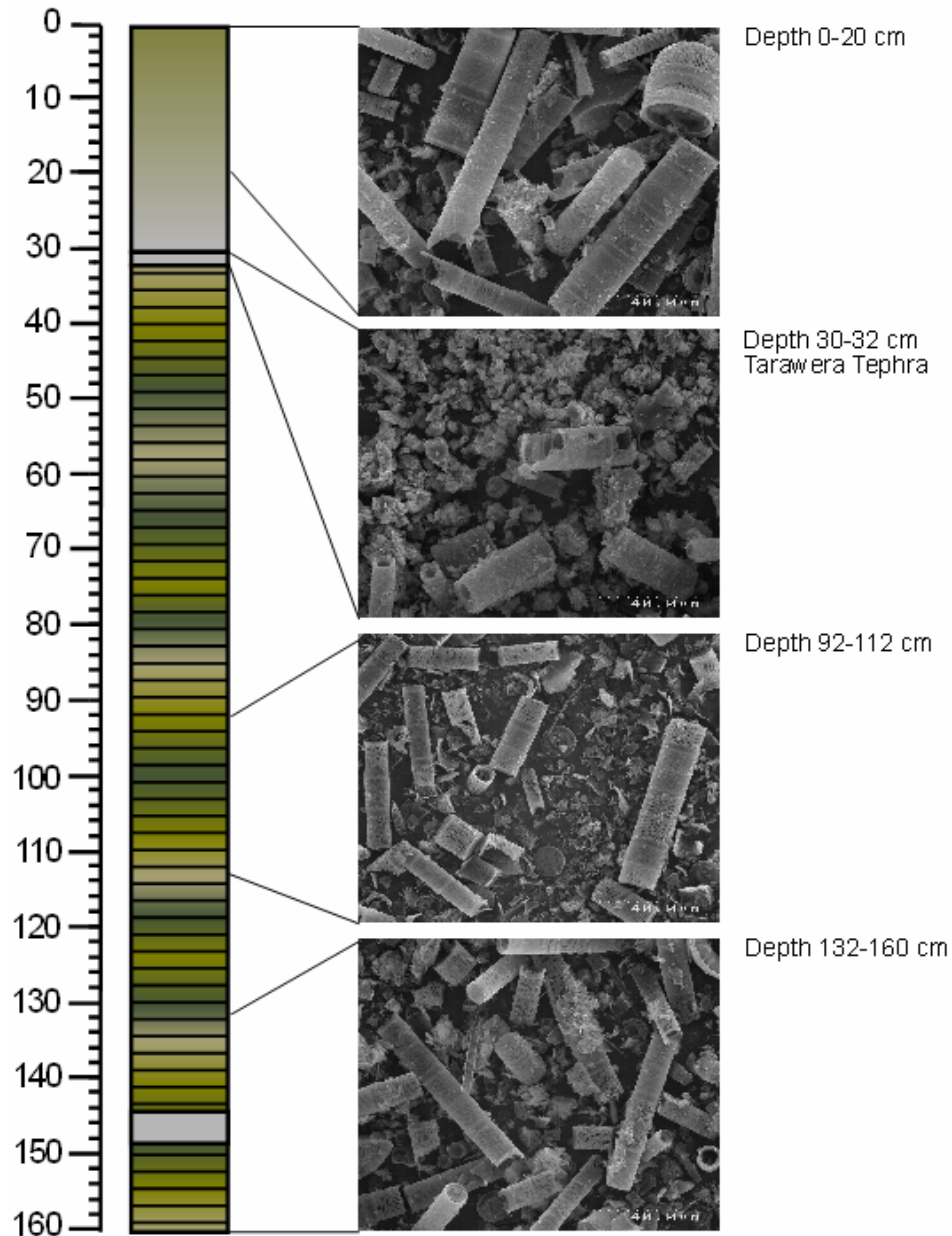


Figure 4.6: Core Ru 55 showing sampling depths (cm) for the scanning electron microscope images.

4.3.1 Depth 0-20 cm

The 0-20 cm sample represents post-Tarawera eruption sedimentation. Compared with the other images in Figure 4.6 the diatom frustules appear to be larger. Figure

4.7 a) shows a general view of the sample and b) to e) show some of the diatom species present in the sample.

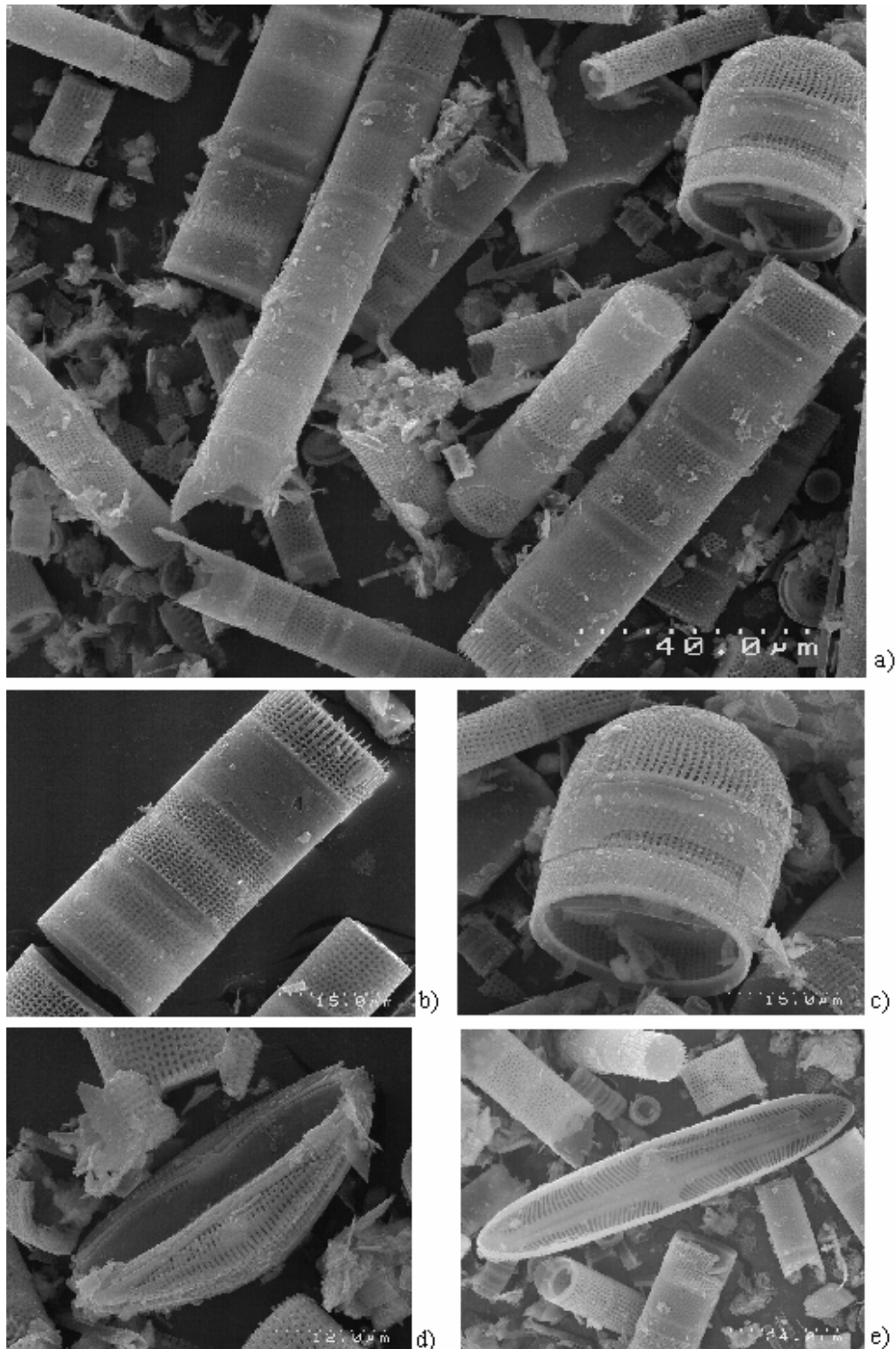


Figure 4.7: a) General view for comparison of diatom species found between 0-20 cm depth. b) *Aulacoseira granulata*, c) *Aulacoseira* (auxospore), d) *Amphora australiensis*, e) *Pinnularia microstauron* (Ehrenberg) Cleve.

The SEM images produced from the top 20 cm of the sediment are dominated by diatom frustules, most commonly *Aulacoseira granulata*, which is the dominant diatom species present in Lake Rotorua sediments. Visual examination by SEM of sediment samples taken from Lake Rotorua by Edwards (In Prep.) indicates that more than 97% of the diatomaceous sediment is composed of diatoms. In excess of 99% of the sample diatom material was *Aulacoseira* (Edwards, In Prep.).

The cylindrical-celled chains shown in Figure 4.7b were previously placed in the *Melosira* genus, not *Aulacoseira* (Cassie-Cooper, 1996). *Aulacoseira* has been described by Foged (1979) as being a cosmopolitan, alkilophilous element in the plankton as it has various reactions to nutrient enrichment in the water from indifferent to preferring eutrophic waters. Figure 4.7c shows an auxospore which is found on the end of the *Aulacoseira* chain (Round *et al.* 1990). Auxospores are formed for cell multiplication and are not commonly found in the sediment. The frequency of valve separation in *Aulacoseira* controls the filament length, which in turn influences the density of the diatom. *Aulacoseira ambigua* and *Aulacoseira angustissima* are also present in Lake Rotorua sediments. The tubes formed in these species are smaller in size and have different separation valves to those of *Aulacoseira granulata* (Round *et al.* 1990; Edwards, In Prep.). *Cytotella stelligera* is visible above the scale bar in Figure 4.7a. It is a round, dish-shaped diatom that is found consistently through the core. It is considered a cosmopolitan species characteristic of eutrophic through to oligotrophic conditions (Rawlence, 1985).

4.3.2 Depth 30-32 cm (Tarawera Tephra)

A noticeable shift from diatom dominance in the sediment to mineral particles occurred from depths 30-32 cm in the sediment core, observed in the SEM images. The Tarawera tephra (Figure 4.8) contains a large amount of former lake silt (Rotomahana mud). The diatom frustules are dominated by *Aulacoseira granulata*. They are significantly more damaged compared with frustules above and below the tephra, which is expected given the destruction caused by the Tarawera eruption. Rawlence (1984) reported that a significant amount of terrestrial vegetation, lake weeds or non-siliceous phytoplankton was deposited into the lake during the eruption. The suspended particles in the water column that slowly settle to accumulate in the sediment would have been settled out by the

addition of the fine tephra. Close inspection of Figure 4.8b reveals the presence of diatoms (possibly *Aulacoseira granulata* and *Cyclotella stelligera*) incorporated into the mineral particles. This suggests the material originated from Lake Rotomahana or flocculated diatoms from the water column during deposition to the lake sediments. Higher nitrogen and phosphorus levels in the post-Tarawera sediment were recorded by Fish and Andrew (1980), who reported that there was an increase in eutrophication immediately after the ash fall. Rawlence (1984) stated that there is no evidence of increased abundance of diatoms in Lake Rotorua immediately following the eruption.

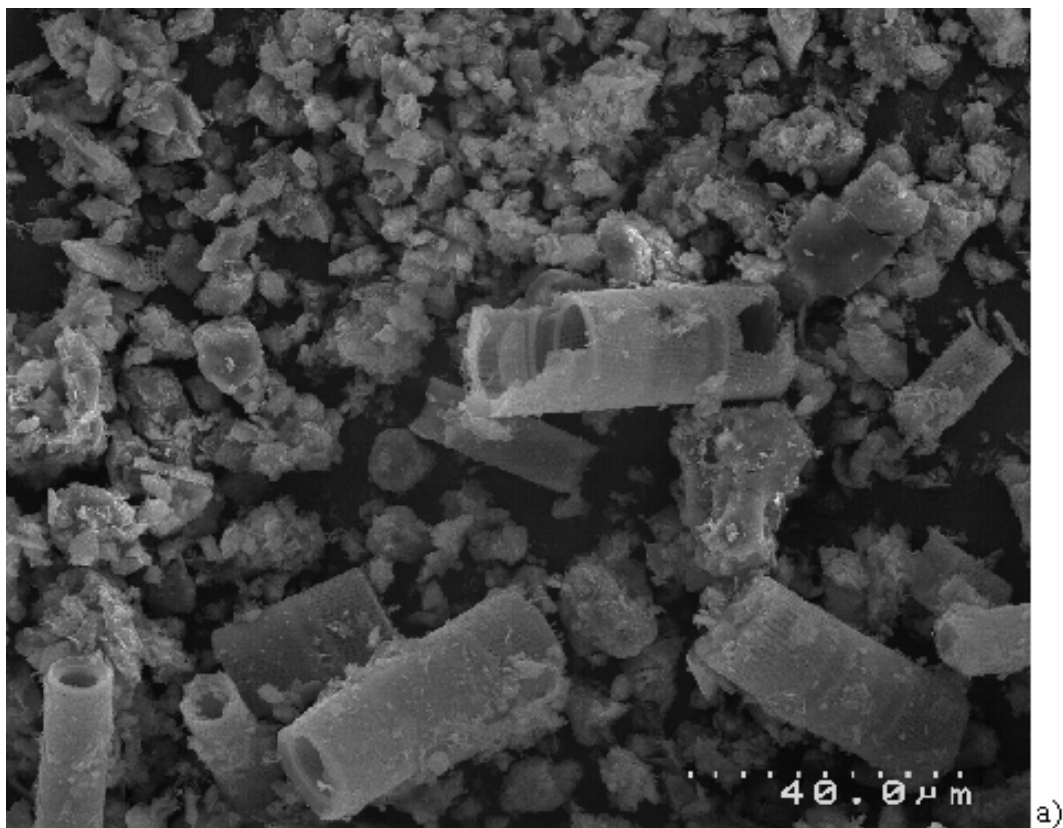


Figure 4.8: a) General view for comparison of diatom species found between 30-32 cm depth.

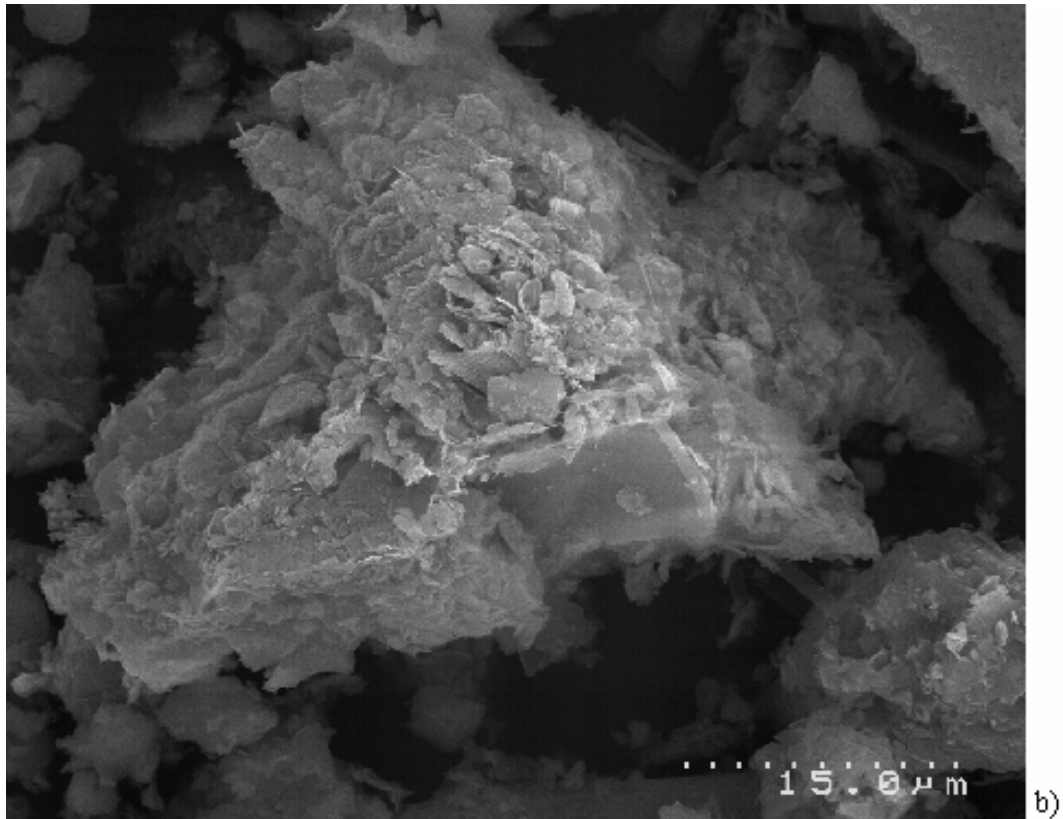


Figure 4.8: b) Mineral particle in the Tarawera tephra located at 30-32 cm in the sediment core.

4.3.3 Depth 92-112 cm

Pre-Tarawera eruption sediments of depth 92-112 cm show a notable increase in the diversity of species found in the sediment compared with higher sediments (Figure 4.9) although these sediments are still dominated by *Aulacoseira granulata*. The *A. granulata* chains become more separated and the longer chains observed at depths 0-20 cm (Figure 4.7a) are no longer evident. The diatom frustules become more degraded with increasing depth. The location of the sample in Figure 4.9 is between the Kaharoa and the Tarawera tephra. A rough age estimate is that the sample is between 120 and 700 years old due to the deposition between the Kaharoa and the Tarawera tephra layers. Bulking of sediment during sampling makes a more precise age impossible with this analysis.

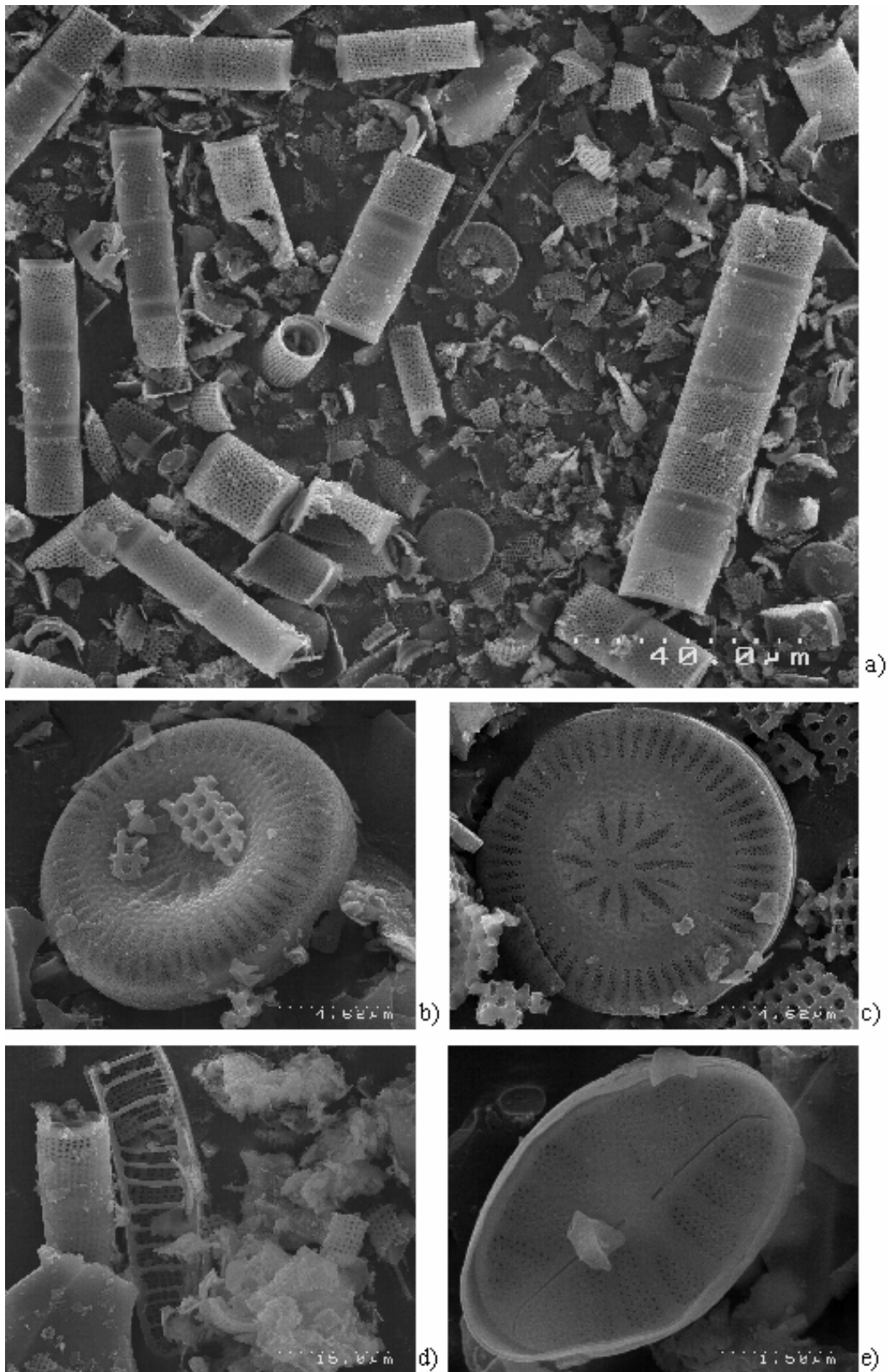
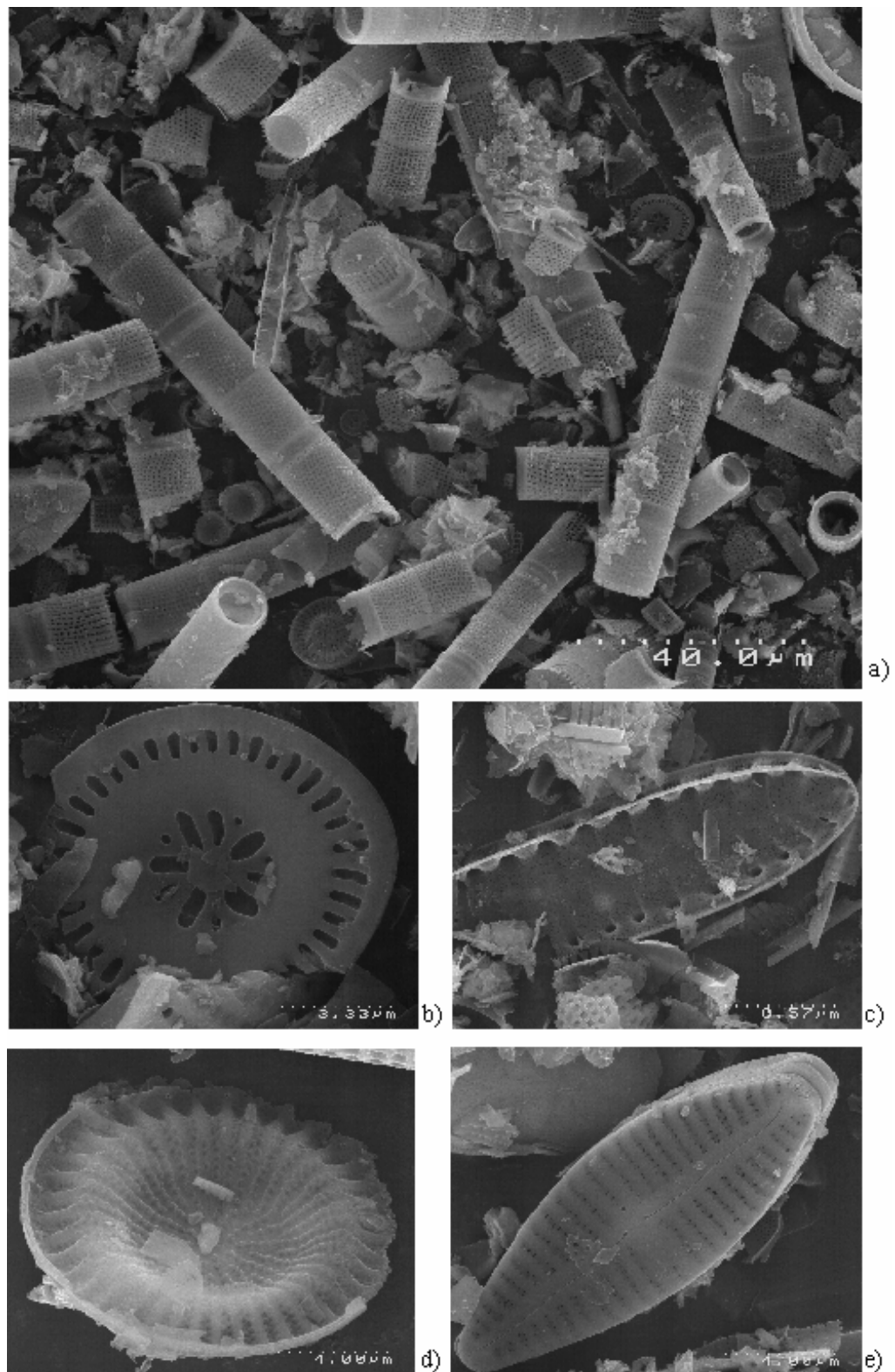


Figure 4.9: a) General view for comparison of diatom species found between 92-112 cm depth. b) *Cyclotella stelligera*, c) *Cyclotella stelligera*, d) *Epithemia* sp. and e) *Achnanthisdium* sp.

4.3.4 Depth 132-160 cm

The deepest sample from 132-160 cm showed the largest diversity of diatom species preserved in the sediment. Figure 4.10 shows some of the diatom species found in the sample.



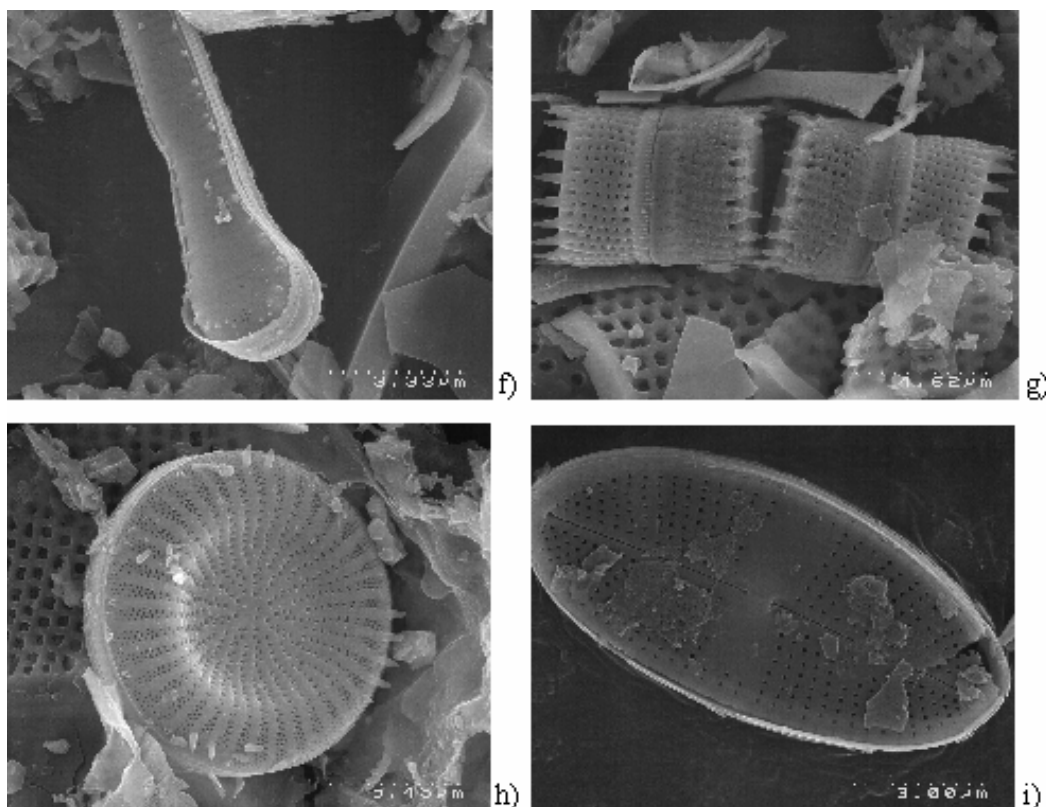


Figure 4.10 a) General view for comparison of diatom species found between 132-160 cm depth. b) *Cyclotella operculata*, c) *Synedra* sp., d) *Cyclostephanos* sp., e) *Cymbella* sp., f) *Asterionella Formosa* Hassall, g) *Aulacoseira granulate*, h) *Stephanodiscus alpinus* and i) *Achnantheidium* sp.

Asterionella formosa Hassall cells are elongated and form abundant star-shaped colonies. The image in Figure 4.10f is the end of a single cell. *Asterionella formosa* is reported to be characteristic of mesotrophic to eutrophic conditions. *Cytotella* is also present. It is characteristic of eutrophic and oligotrophic conditions (Rawlence, 1985). Based upon the large range of trophic conditions of these two diatom species it is not possible to give an accurate estimation of the water quality in Lake Rotorua during the time the sediment was deposited.

The SEM images of Figure 4.7 to 4.10 provide evidence that diversity of diatom species decreased in Lake Rotorua after the Tarawera eruption. However, only one core was examined during this analysis and diatom species that had been identified by Rawlence (1984) and Matthews (1979) were not found in the core. Rawlence (1984) stated that it is debatable whether the diatom flora of Lake Rotorua is characteristic of eutrophic conditions or just tolerant of nutrient

enrichment. Increases in nutrient levels in the lake have come from anthropogenic changes in the catchment, discharge of Rotorua City effluent into the lake and the widespread clearing of land for agriculture and farming activities, are resulting in a gradual decline in water quality of Lake Rotorua. The interpretation of the diatom record in relation to trophic status of the lake is an imprecise indicator. There are a number of ecological forms of the species *Aulacoseira granulata* that are morphologically distinct to those found in Lake Rotorua, identified by Rawlence (1984) in other lakes in the region.

4.4 SEDIMENT STRATIGRAPHY

The sediment stratigraphy is interpreted by comparing the depth of Tarawera and Kaharoa tephras in the sediment cores. Due to the difficulty of capturing the low-density diatomaceous material with the piston and box corer the depths of the tephra layers can vary by as much as 20 cm. Cross-sections showing the stratigraphy of the sediment (Figure 4.11-4.29) have been produced from the coring program and are supported with chemical analysis (Chapter 5) and sub-bottom profiling (Chapter 6). Cross-section profiles are labelled alphabetically from A in the north to K to the south and cover a west to east direction across the lake (Figure 4.11-4.29).

In section A to A' (Figure 4.11 and 4.12) the stratigraphy of the sediment is not well defined. This area is shallow and subject to frequent mixing by wind, which reduces material settling to the bottom and washes finer material into the deeper waters. The top of the cores is mostly reworked Kaharoa tephra or sands and gravels derived from catchment runoff. The finer material in the majority of the cores is composed of a mixture of diatomaceous ooze and silts. Kaharoa tephra is buried by a thin layer of diatomaceous ooze in the central part of the section as the water depth increases. There is no sign of the Tarawera tephra in this section. The eastern portion of A to A' is close to the only discharge of Lake Rotorua, the Ohau Channel, which discharges into Lake Rotoiti. Much of the finer material suspended in the water column is transported down the Ohau Channel. Regular dredging of the channel occurs to keep access for boats.

Cross-section B to B' (Figure 4.13 and 4.14) is a transect of increasing water depth, allowing for a larger amount of diatomaceous ooze to accumulate above the Tarawera tephra layer. Laminations in the diatomaceous sediment are observed. Laminations are typically 1-2 cm thick. The Tarawera tephra is mostly comprised of fine mud material from Lake Rotomahana and for this reason is not visible in core samples located close to the lake shore. With the exception of piston cores Ru35 and Ru36 the Kaharoa tephra is not seen as it is located deeper than the core depth. The effect of losing the fine diatomaceous material from the top of the core is visible across the section as it would be expected that the Kaharoa tephra is located deeper in the core with increasing water depth. In cross-section B to B' the Kaharoa tephra is located deeper in the near shore core. This is caused by the diatomaceous sediment becoming less compacted, making it easily washed away from the top of the cores during sampling, thereby distorting the apparent stratigraphy of the sediment.

In section C to C' (Figure 4.15 and 4.16) the Tarawera tephra is visible in all cores across the lake transect. It is noticeable that when the water depth is greater than 10 m diatomaceous ooze accumulates on the lake floor and the Tarawera tephra layer is deeper in cores taken in deeper water, indicating a higher sedimentation rate. The Kaharoa tephra is located below the depth of the bottom of all cores in the transect.

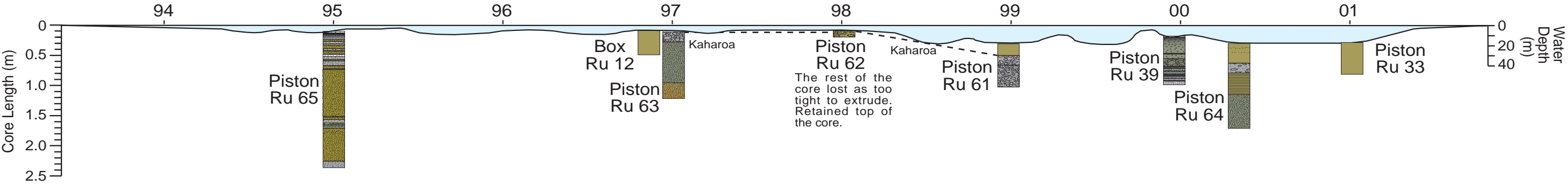
In cross-sections D to D' (Figure 4.17 and 4.18), E to E' (Figure 4.19 and 4.20), F to F' (Figure 4.21 and 4.22) and G to G' (Figure 4.23 and 4.24) the stratigraphy is not as well defined. The amount of diatomaceous ooze accumulated since the Tarawera tephra has increased significantly compared to transects north of Mokoia Island (Figure 4.11-4.16). Cores taken near Mokoia Island have sand and gravel surfaces similar to those observed in near-shore core samples. There is a steeper gradient into deeper water around Mokoia Island than around the lake shore, which results in a zone of net deposition in these near-shore samples. Wind comes predominantly from a southerly direction and tends to shelter an area to the north of Mokoia Island, enhancing settling of diatomaceous material. To the south-east of Mokoia Island the water depth becomes shallow and the sediment is typically sandy (Figure 4.21). The western side of Mokoia Island is much deeper,

with water depths greater than 20 m. Diatomaceous ooze has accumulated rapidly in this area, which was hard to core due to the low density and high water content of the sediment. An accurate record of the stratigraphy is not possible due to inability to capture the surface sediment.

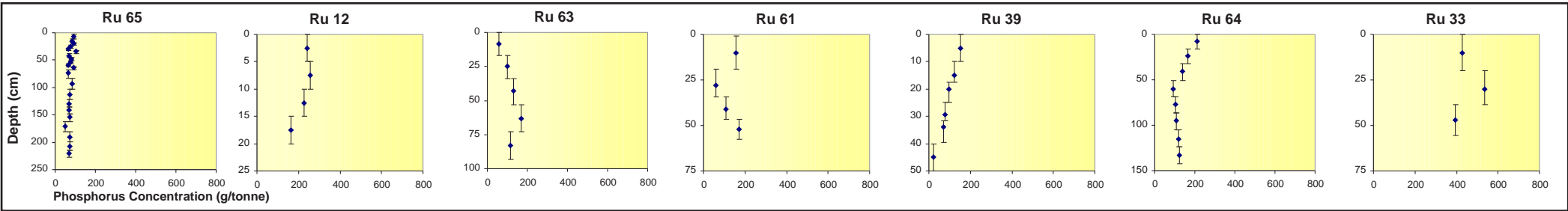
The southern end of the lake, encompassed by cross-sections H to H' and I to I' (Figure 4.25, 4.26 and 4.27) J to J' and K to K' (Figure 4.28 and 4.29), has two different sedimentation rates. The stratigraphy shows evidence of mixing and resuspension in the shallow, eastern side of the lake. The Tarawera tephra, observed in gravity cores, is between 10-15 cm below the sediment-water interface in Ru114 and Ru115 on the east side of the lake (Figure 4.27). North of Sulphur Point is the deepest part of the lake. The box and gravity cores taken in this area were not sufficiently deep to show the tephra layers.

It would have been interesting to core in the Sulphur Point area to examine for differences in the sediment that is strongly influenced by geothermal activity in this area. Boiling mud pools are found within 10 m from the edge of the lake and discharge geothermal water into the lake. The lake water is highly turbid and there is a strong smell of sulfur in the area. Unfortunately due to the abrupt changes in water depth in the area, coring was not possible.

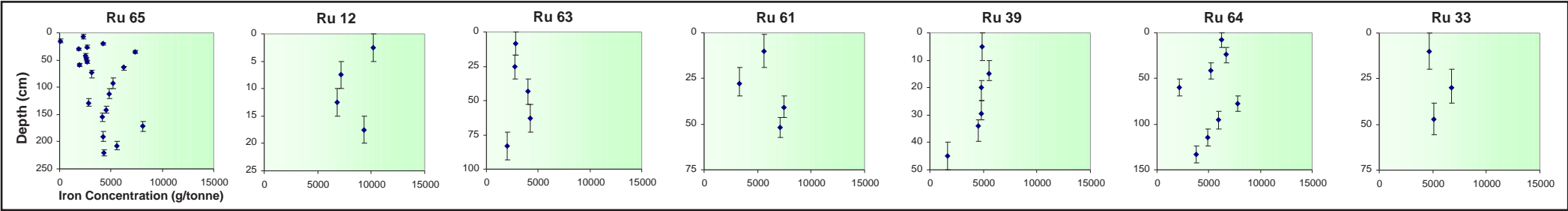
Cross Section A to A' Piston and Box Cores



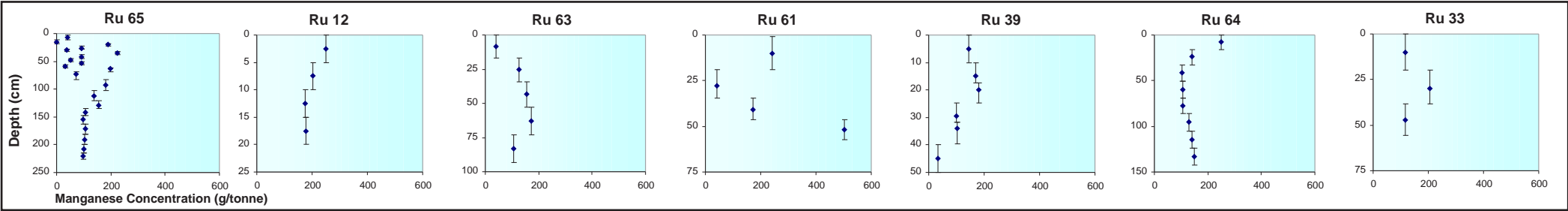
Phosphorus



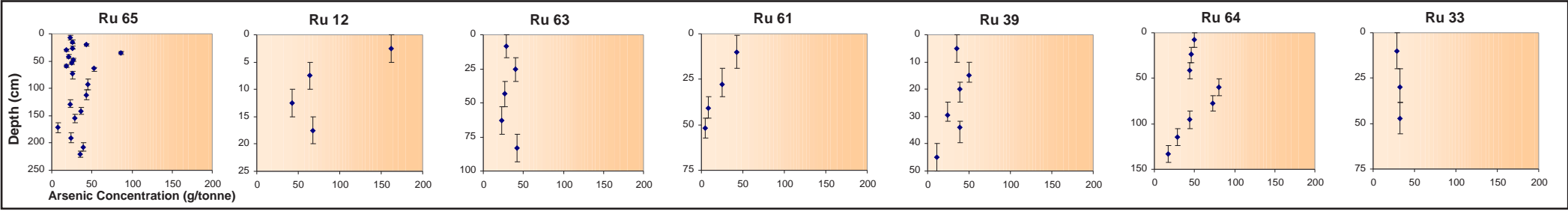
Iron



Manganese



Arsenic



Lead

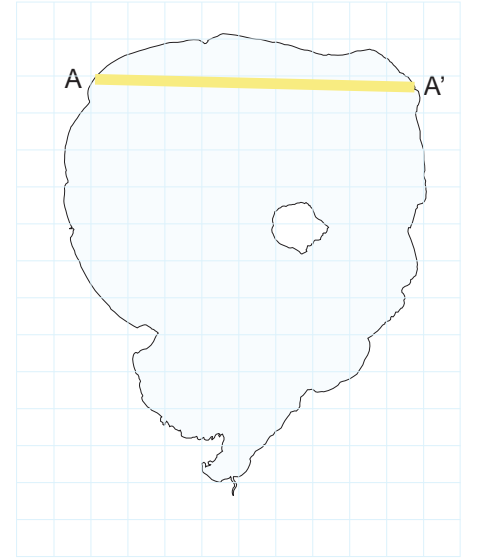
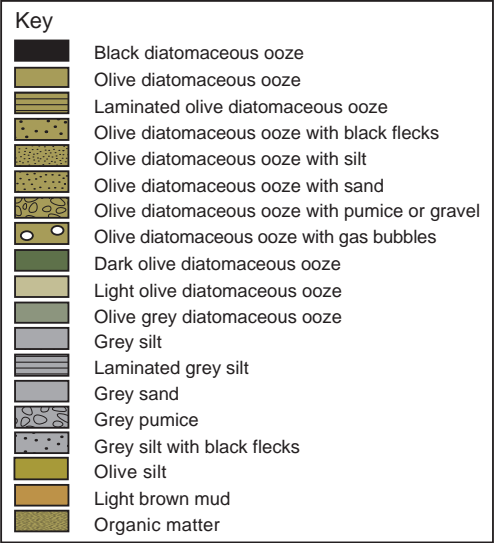
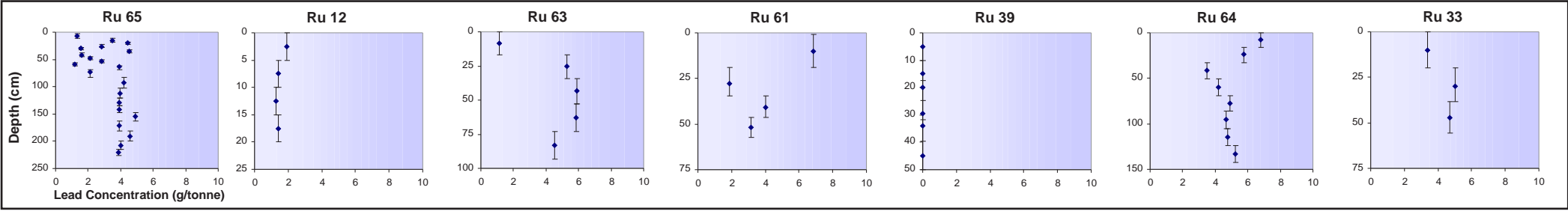
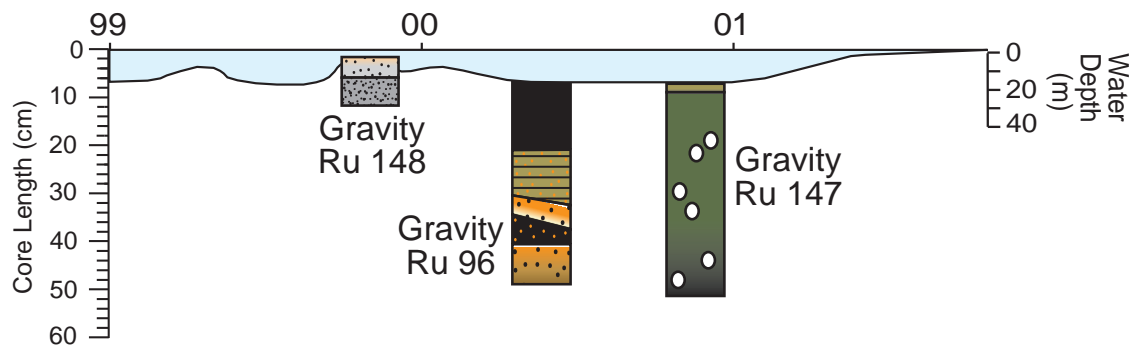
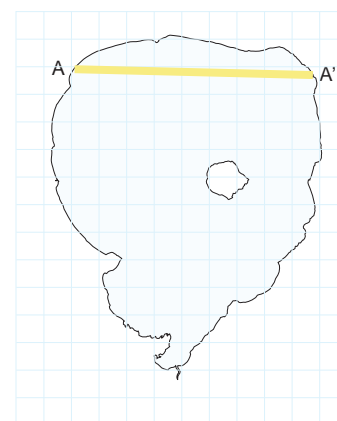
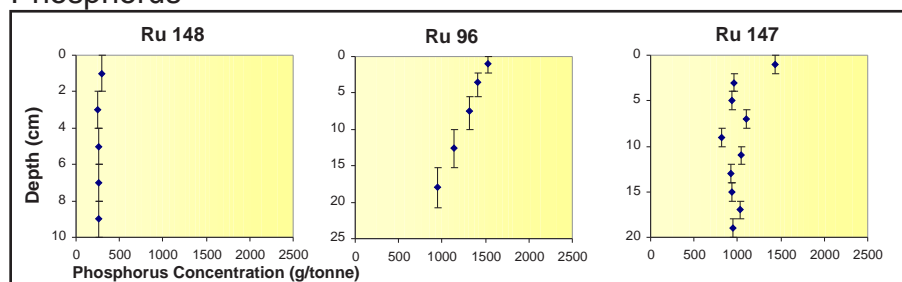


Figure 4.11: Concentration of phosphorus, iron, manganese, arsenic and lead at cross-section A to A'.

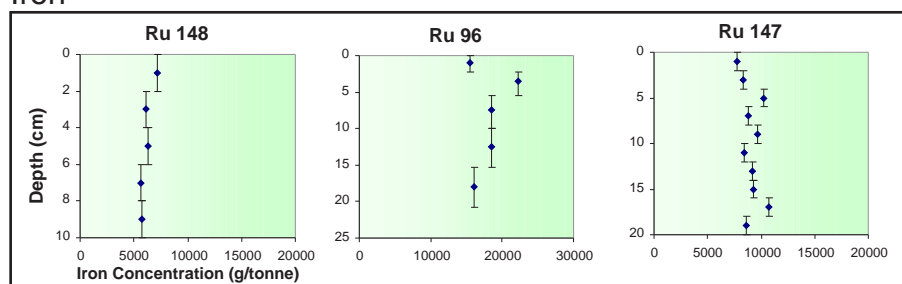
Cross Section A to A' Gravity Cores



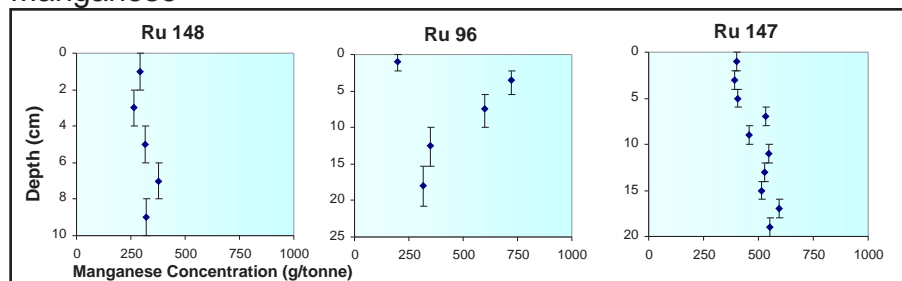
Phosphorus



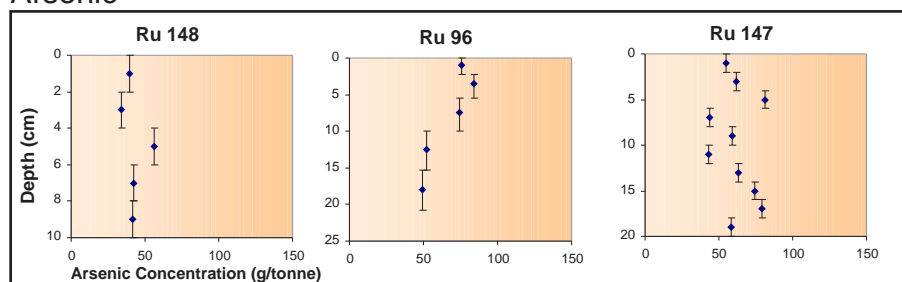
Iron



Manganese



Arsenic



Lead

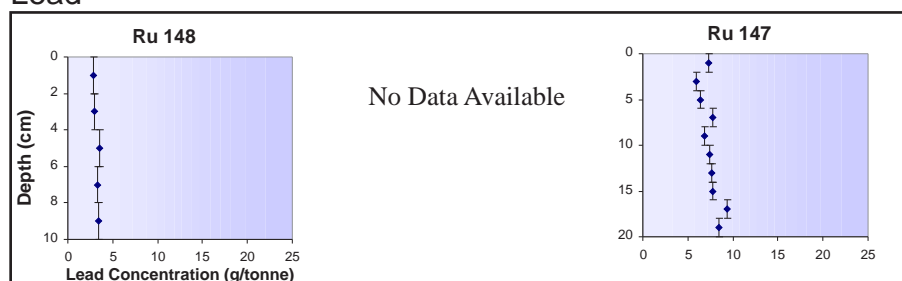


Figure 4.12: Concentration of phosphorus, iron, manganese, arsenic and lead at cross-section A to A' gravity cores.

Cross Section B to B' Piston and Box Cores

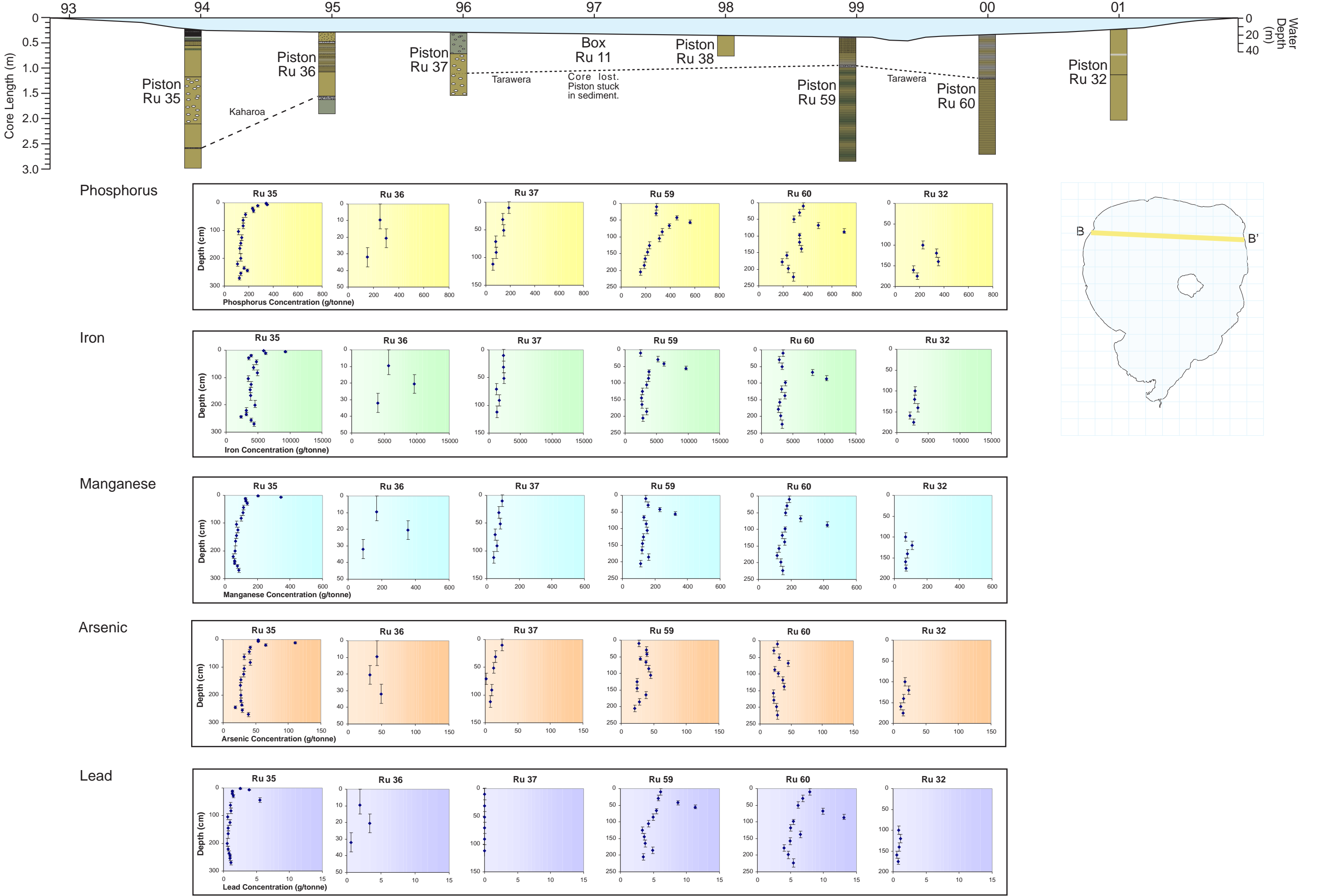


Figure 4.13: Concentration of phosphorus, iron, manganese, arsenic and lead at cross-section B to B'.

Cross Section B to B' Gravity Cores

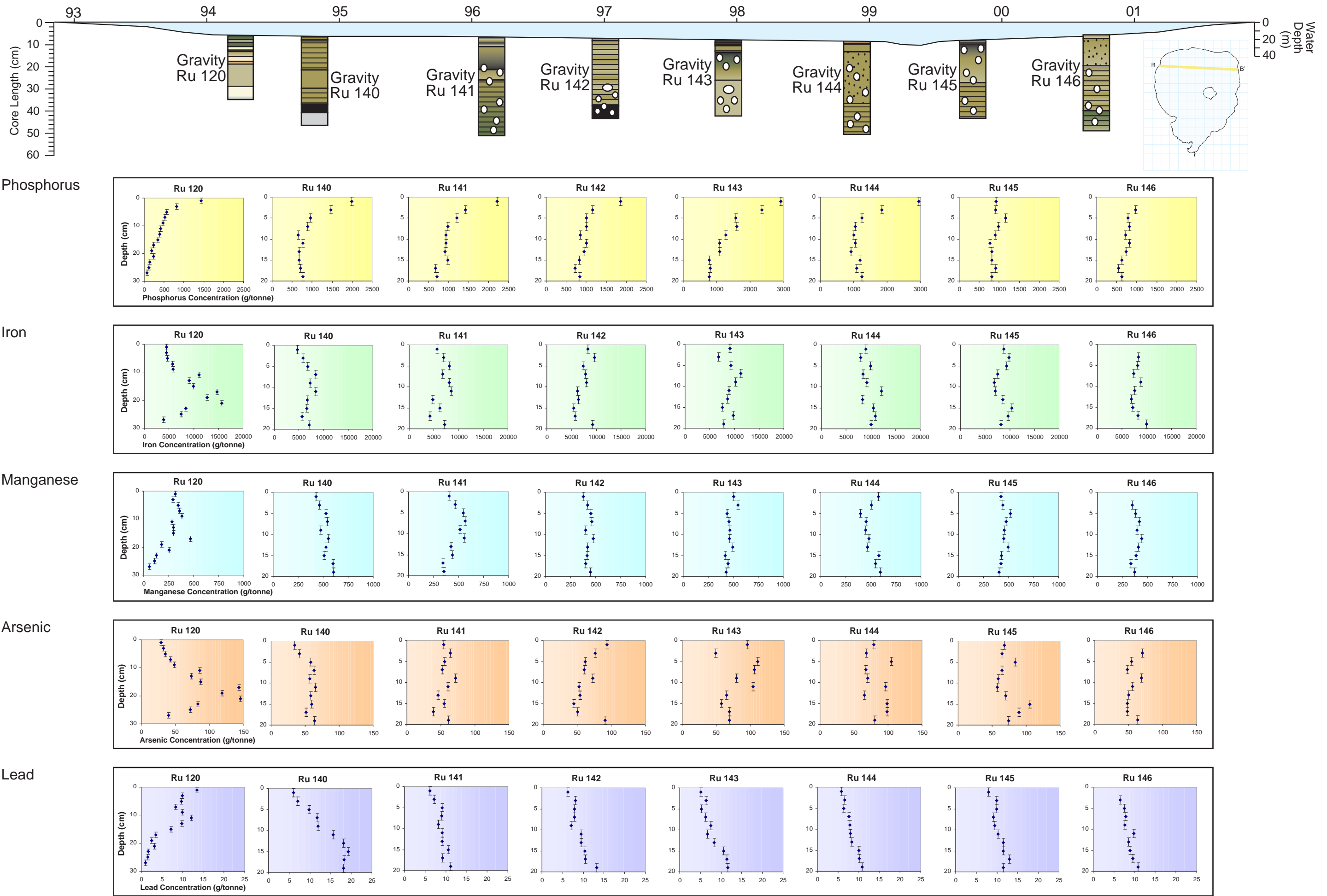
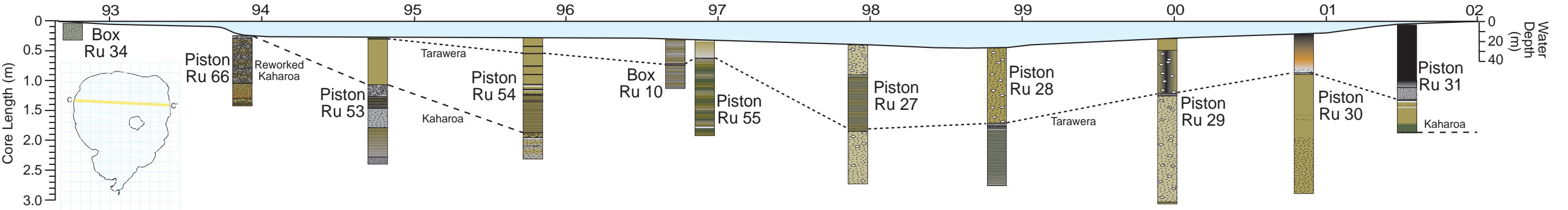
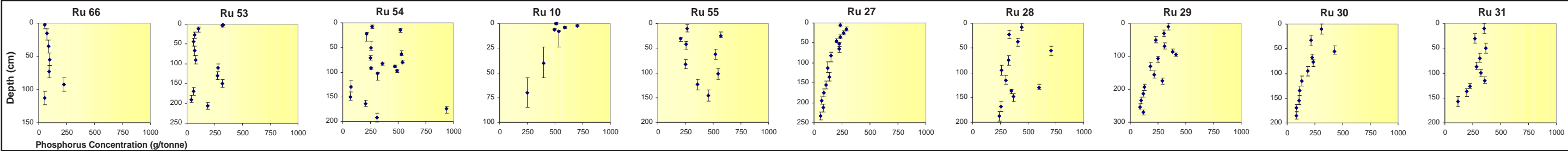


Figure 4.14: Concentration of phosphorus, iron, manganese, arsenic and lead at cross-section B to B' gravity cores.

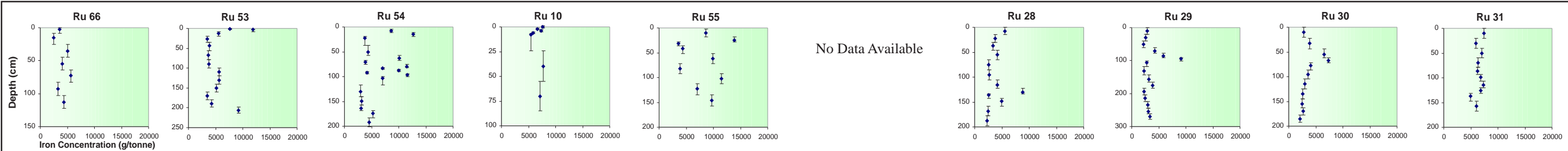
Cross Section C to C' Piston and Box Cores



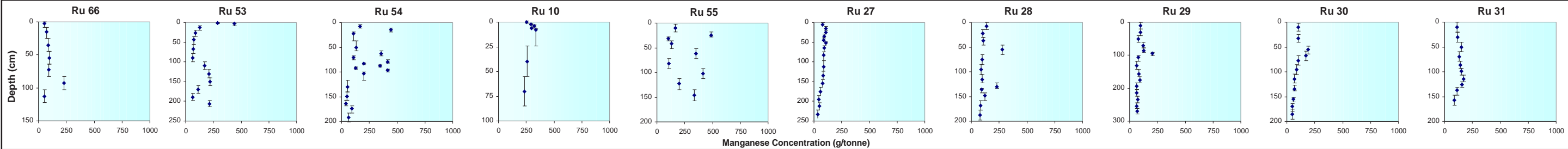
Phosphorus



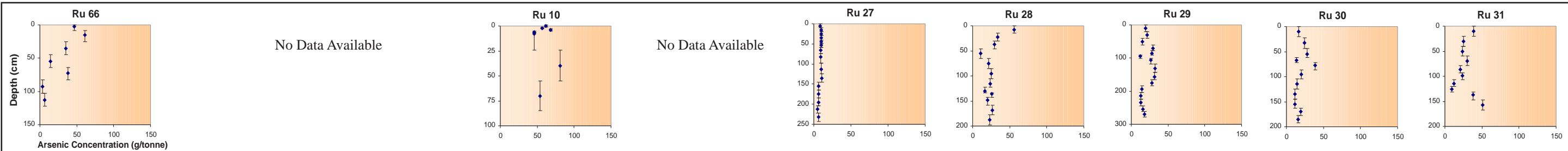
Iron



Manganese



Arsenic



Lead

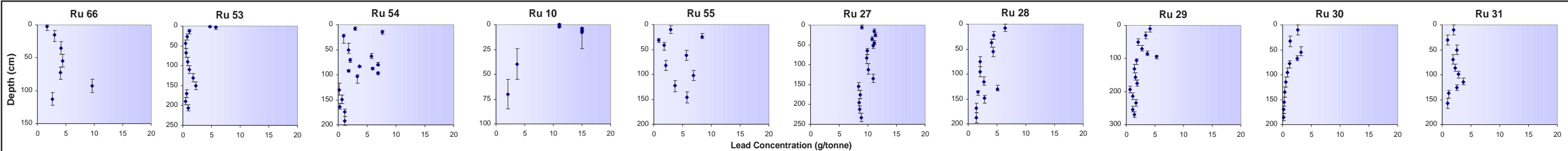
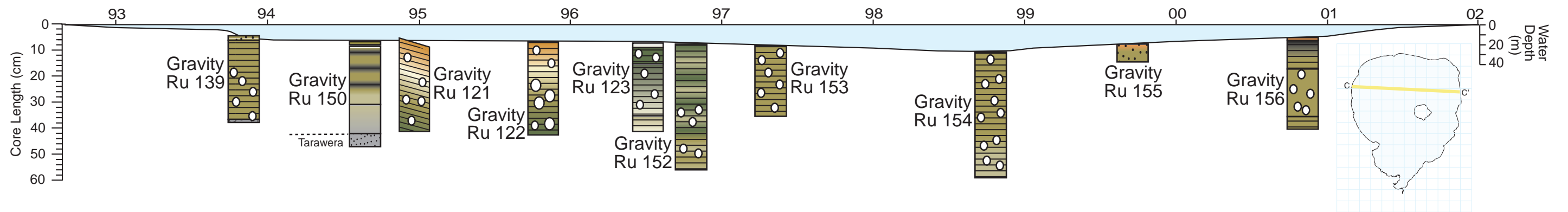
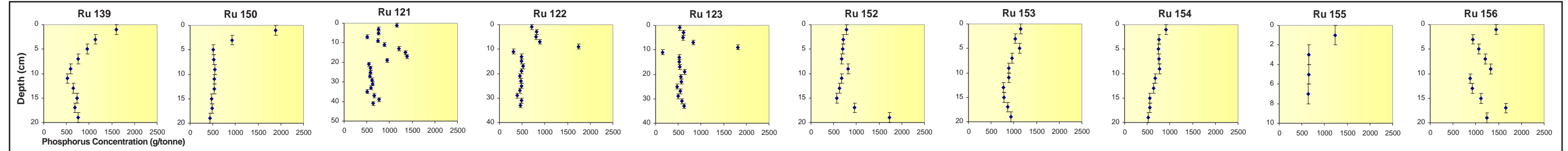


Figure 4.15: Concentration of phosphorus, iron ,manganese, arsenic and lead at cross-section C to C'.

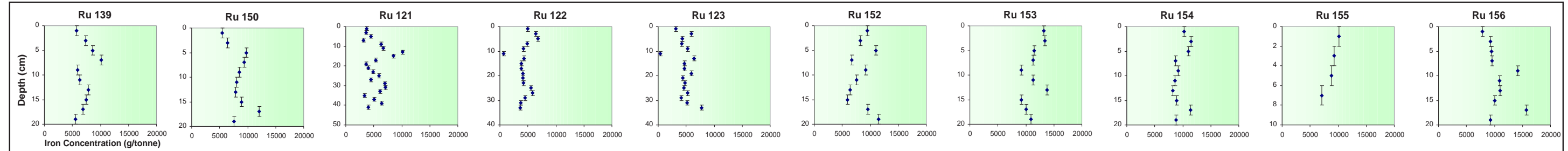
Cross Section C to C' Gravity Cores



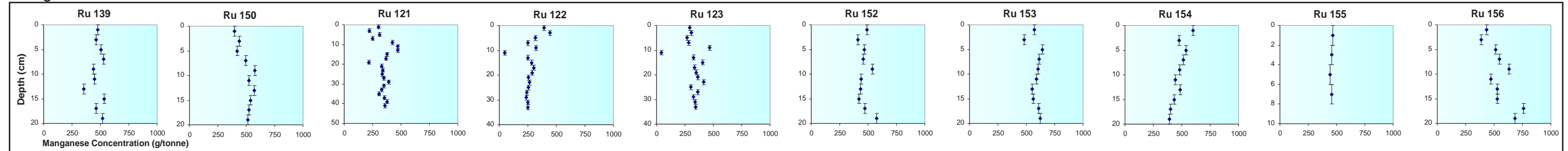
Phosphorus



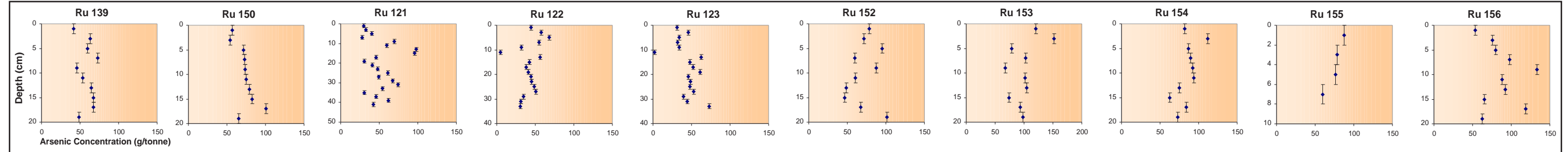
Iron



Manganese



Arsenic



Lead

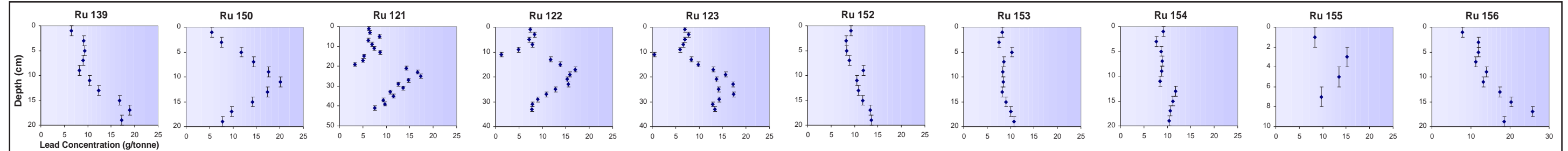
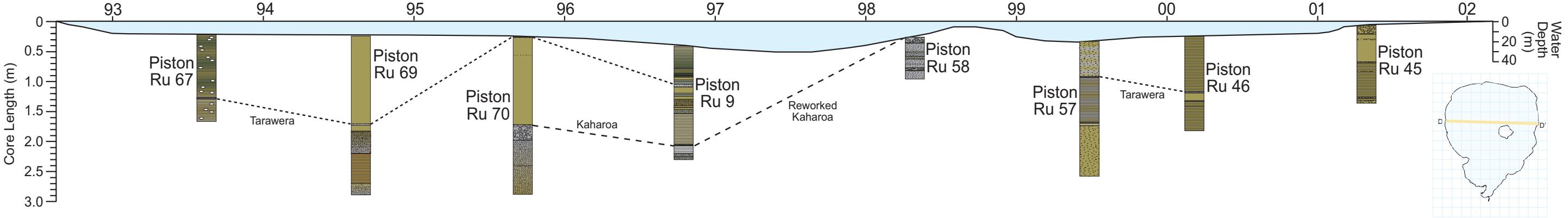
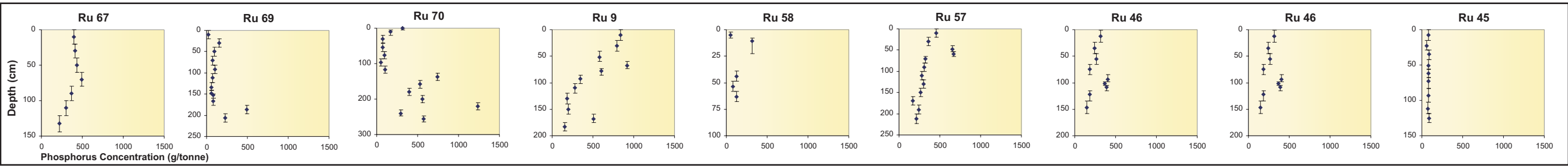


Figure 4.16: Concentration of phosphorus, iron, manganese, arsenic and lead at cross-section C to C' gravity cores.

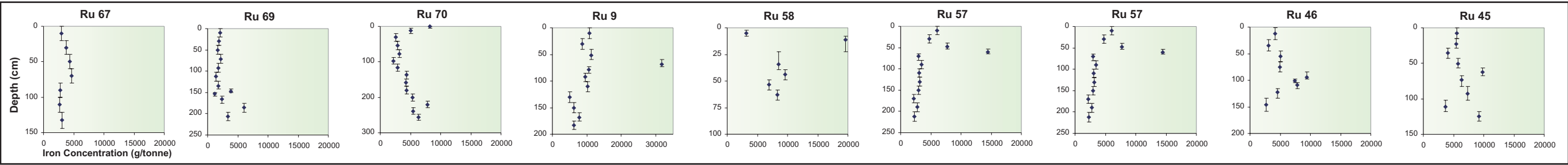
Cross Section D to D' Piston and Box Cores



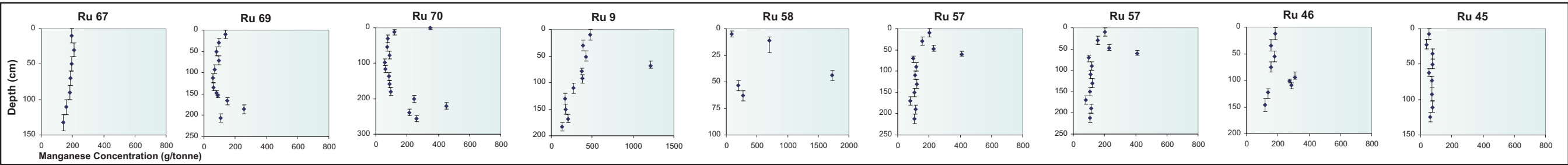
Phosphorus



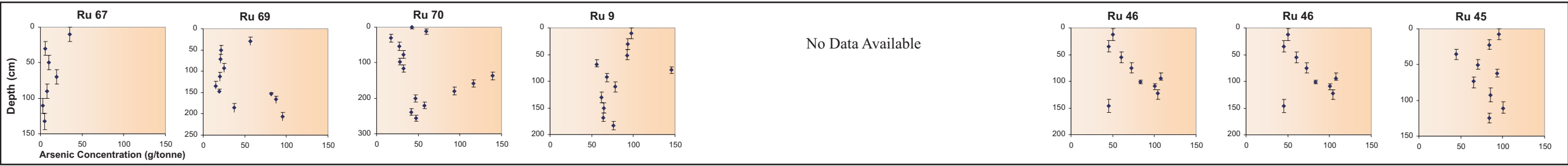
Iron



Manganese



Arsenic



Lead

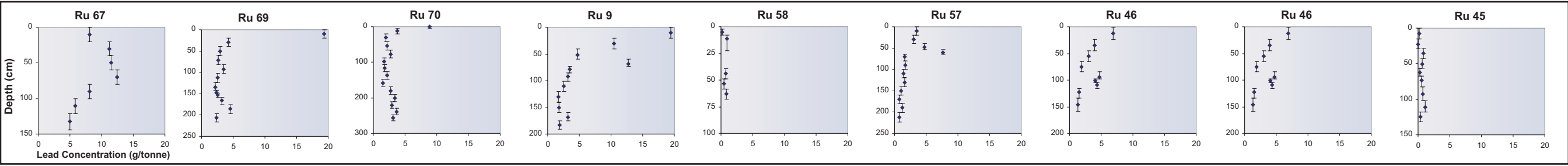
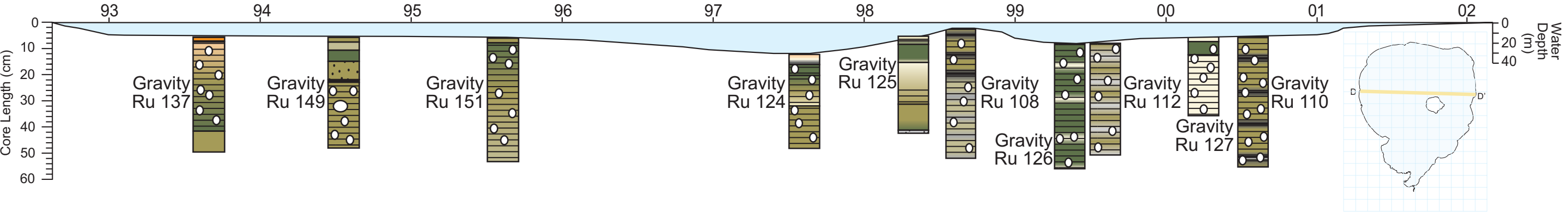
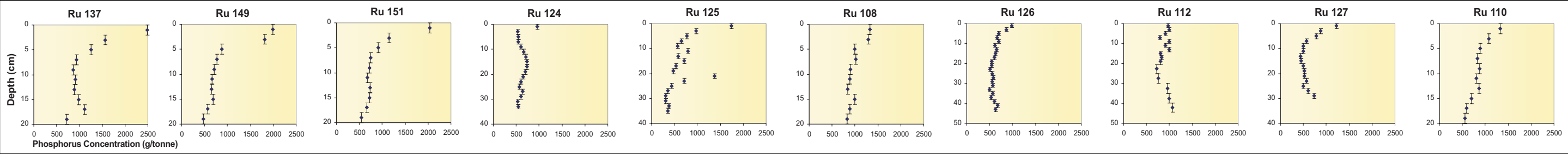


Figure 4.17: Concentration of phosphorus, iron, manganese, arsenic and lead at cross-section D to D'.

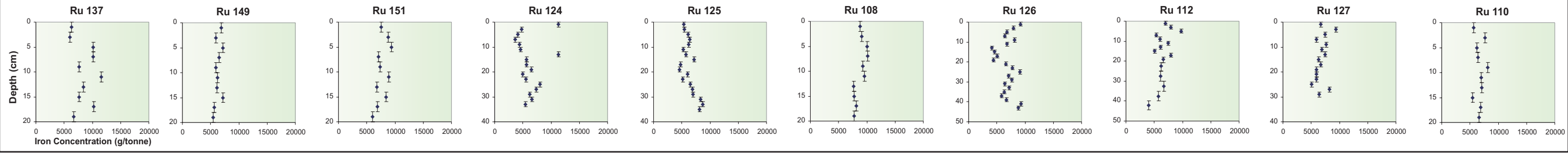
Cross Section D to D' Gravity Cores



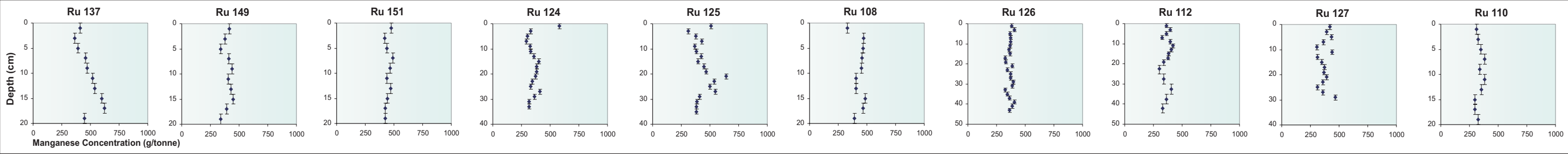
Phosphorus



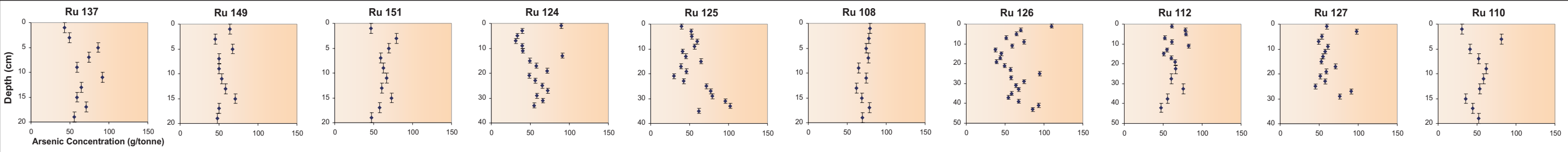
Iron



Manganese



Arsenic



Lead

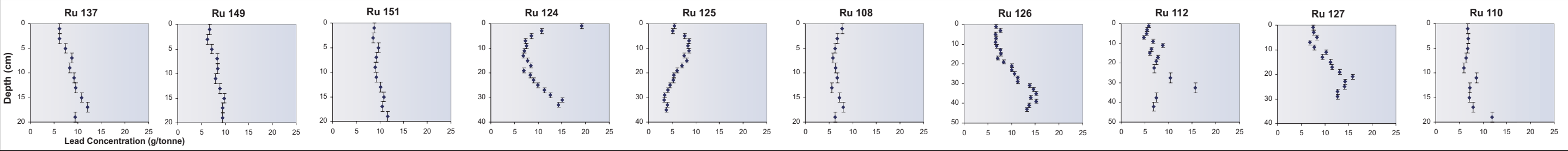


Figure 4.18: Concentration of phosphorus, iron, manganese, arsenic and lead at cross-section D to D’ gravity cores.

Cross Section E to E' Piston and Box Cores

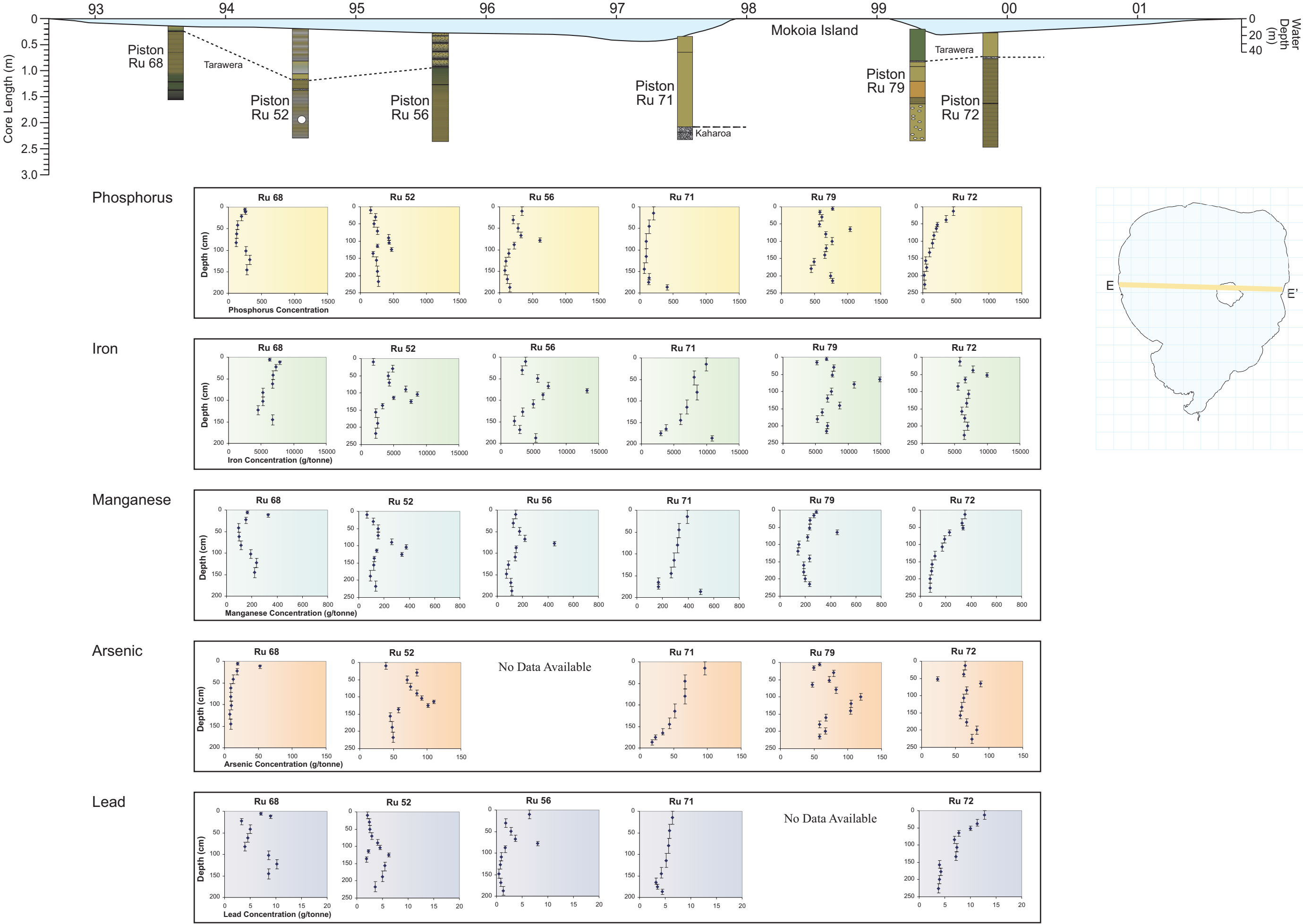


Figure 4.19: Concentration of phosphorus, iron, manganese and lead at cross-section E to E'.

Cross Section E to E' Gravity Cores

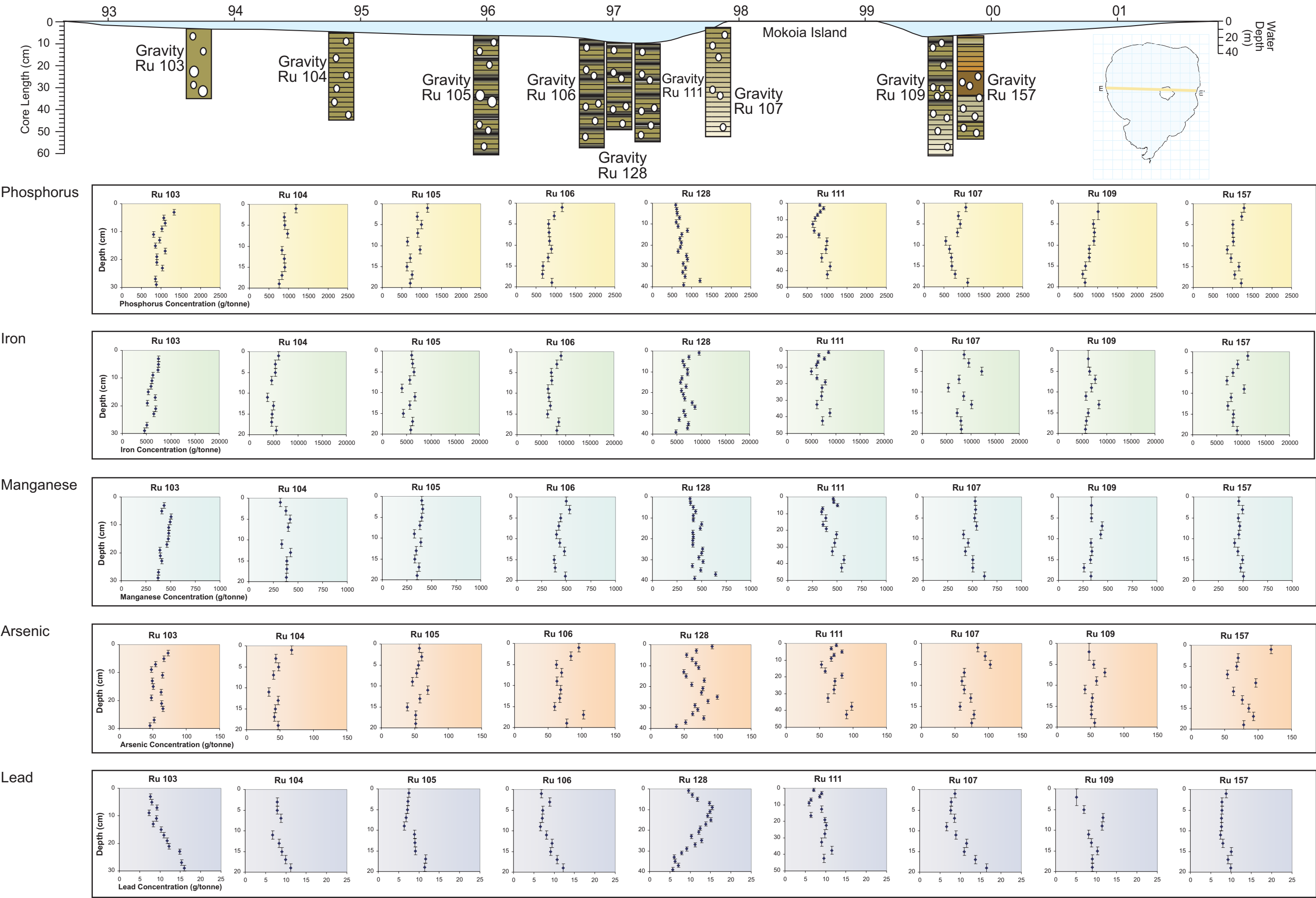


Figure 4.20: Concentration of phosphorus, iron, manganese, arsenic and lead at cross-section E to E' gravity cores.

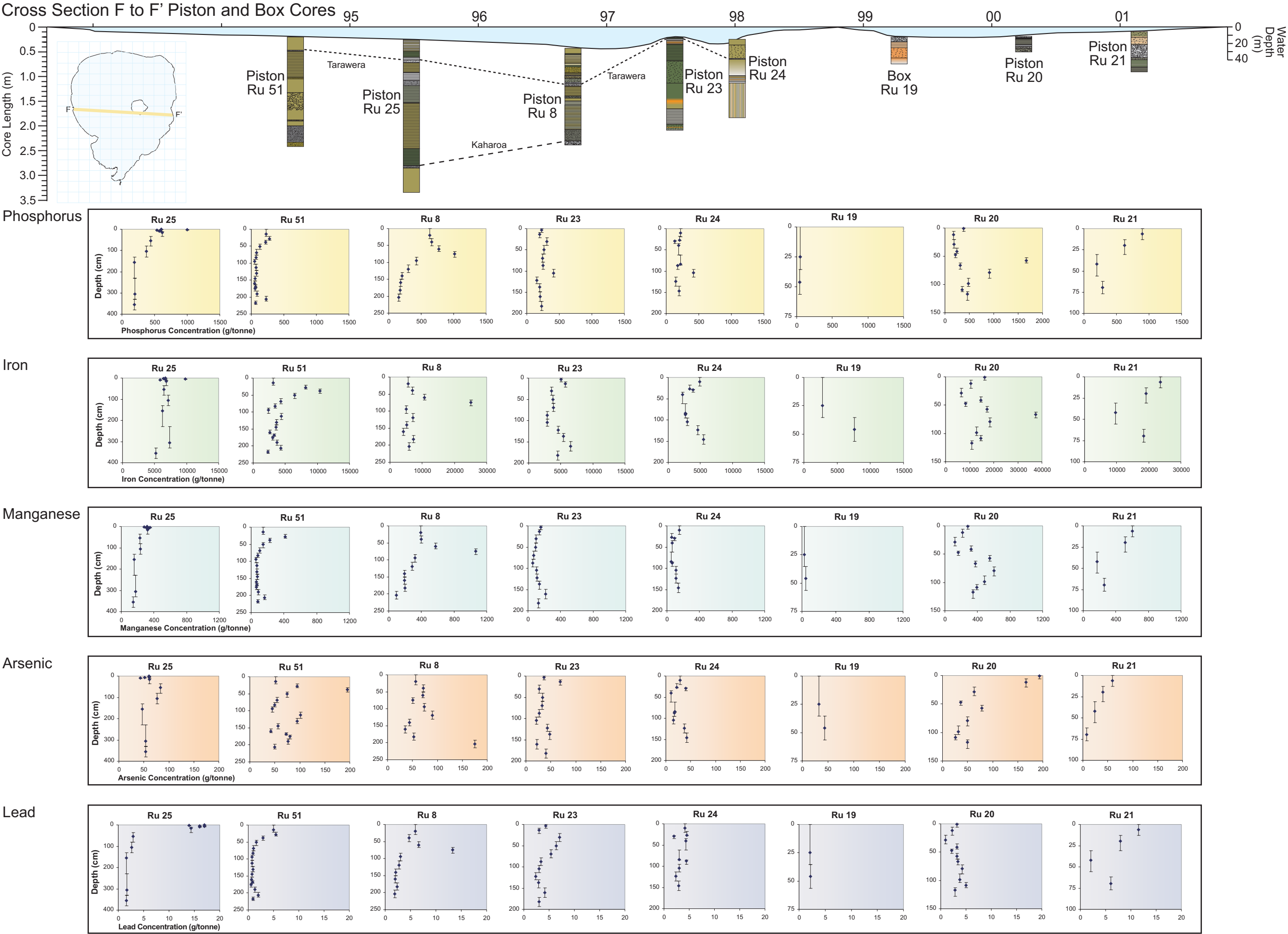


Figure 4.21: Concentration of phosphorus, iron, manganese and lead at cross-section F to F'.

Cross Section F to F' Gravity Cores

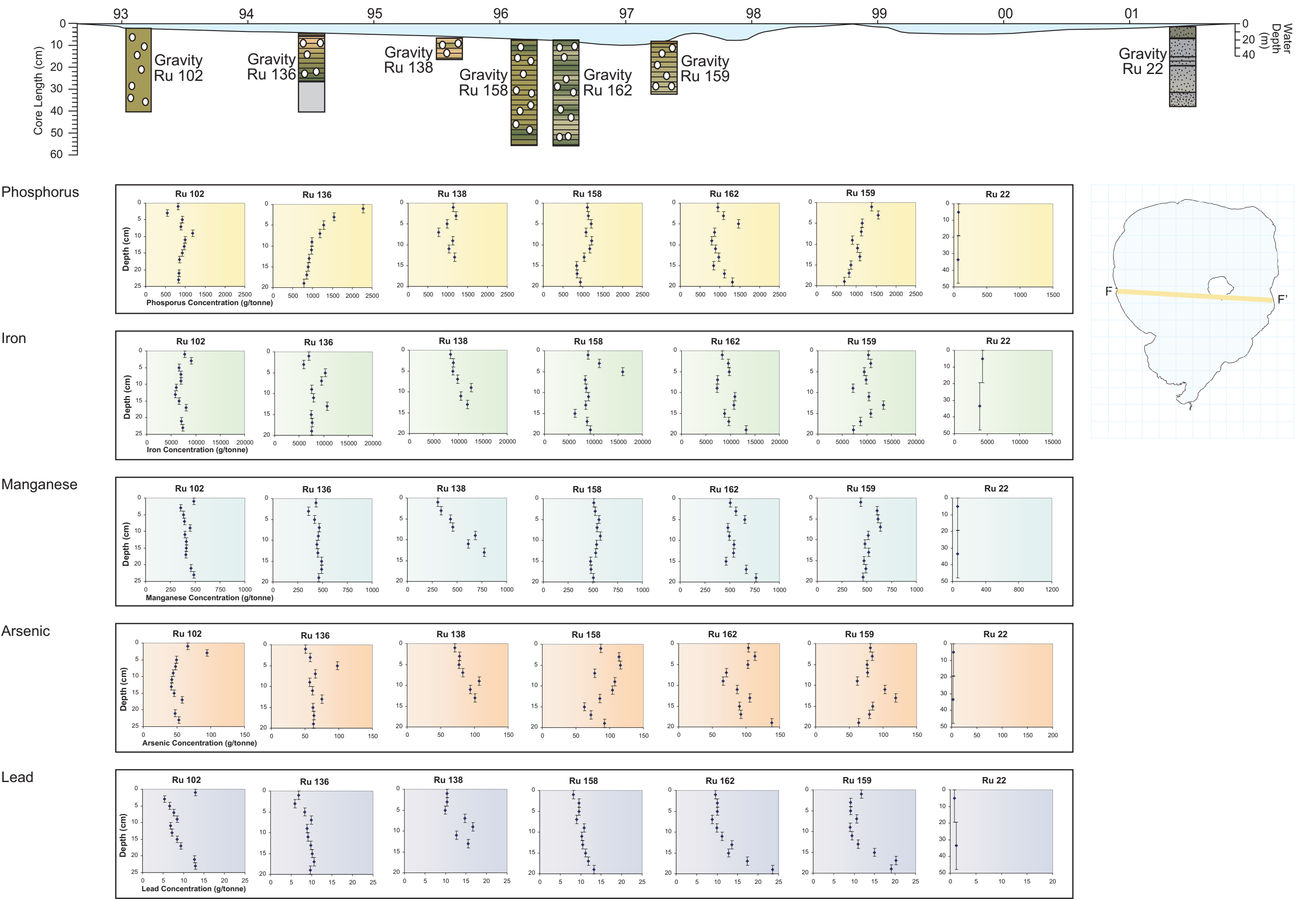


Figure 4.22: Concentration of phosphorus, iron, manganese, arsenic and lead at cross-section F to F' gravity cores.

Cross Section G to G' Piston and Box Cores

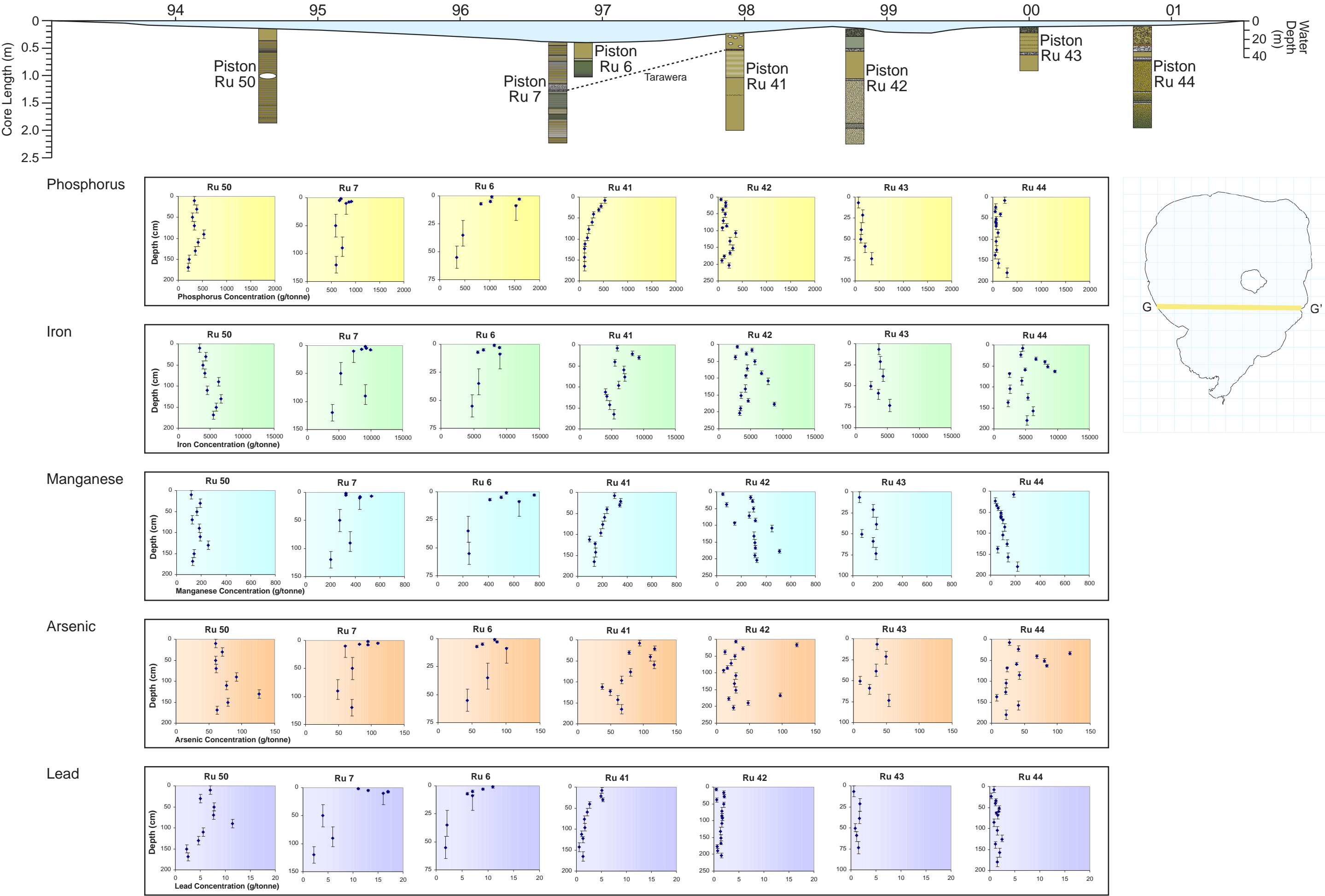


Figure 4.23: Concentration of phosphorus, iron, manganese and lead at cross-section G to G'.

Cross Section G to G' Gravity Cores

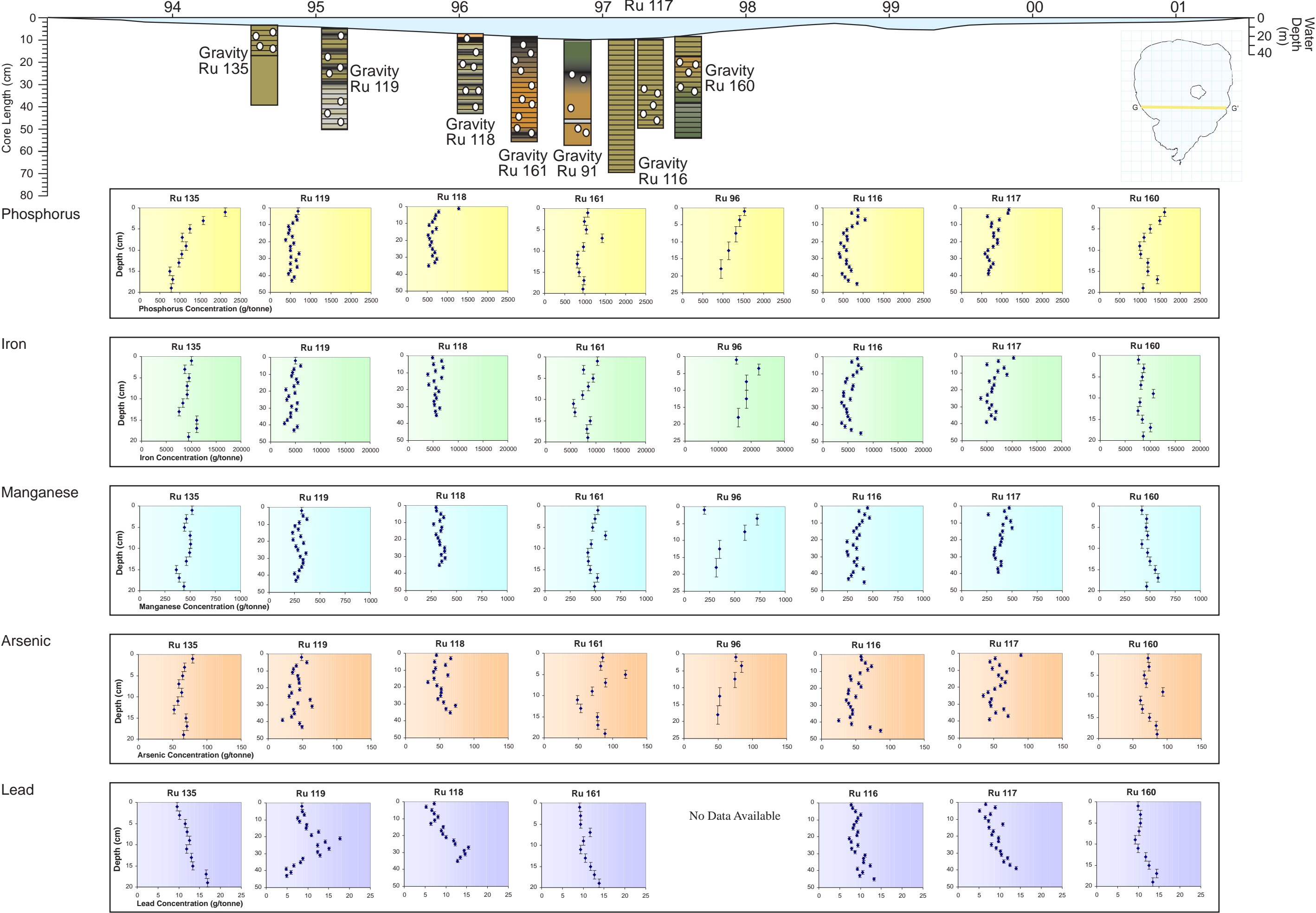


Figure 4.24: Concentration of phosphorus, iron, manganese, arsenic and lead at cross-section G to G' gravity cores.

Cross Section H to H' Piston and Box Cores

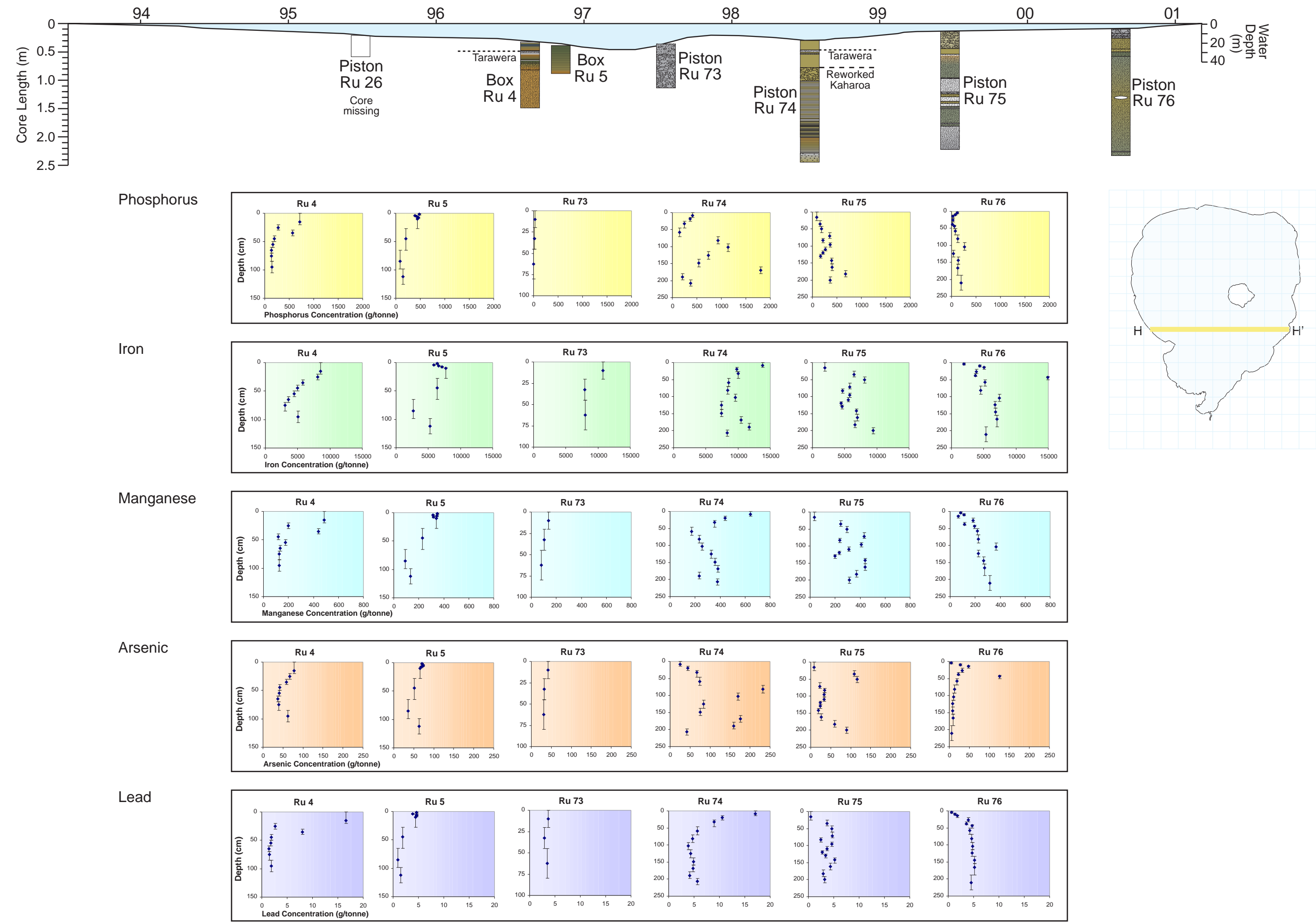
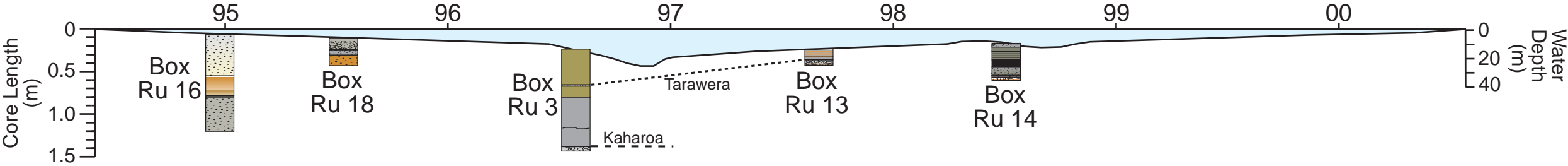
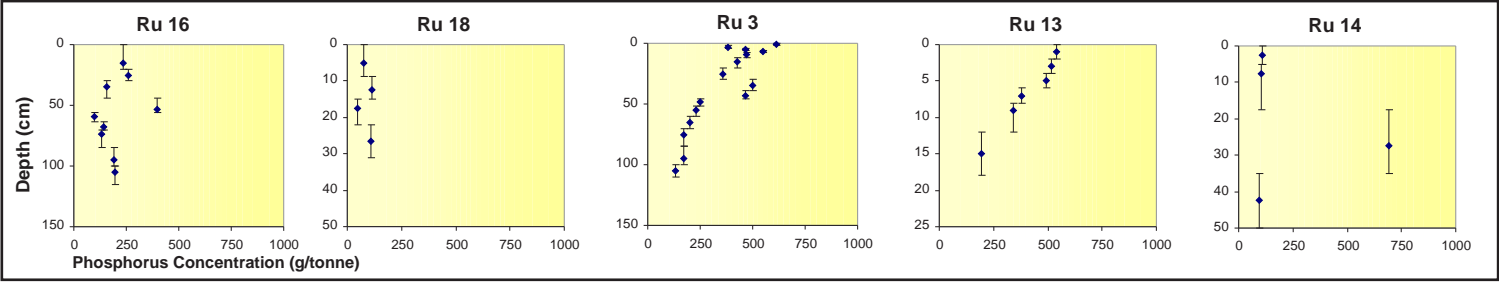


Figure 4.25: Concentration of phosphorus, iron, manganese and lead at cross-section H to H'.

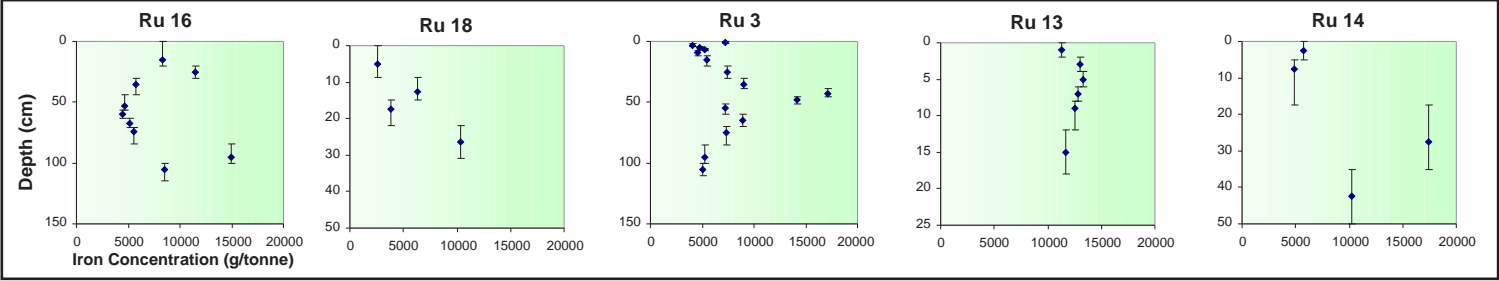
Cross Section I to I' Piston and Box Cores



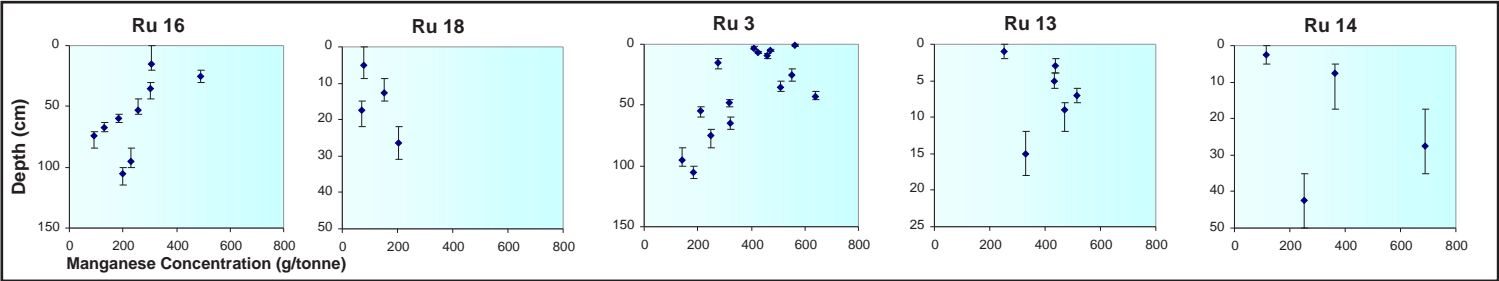
Phosphorus



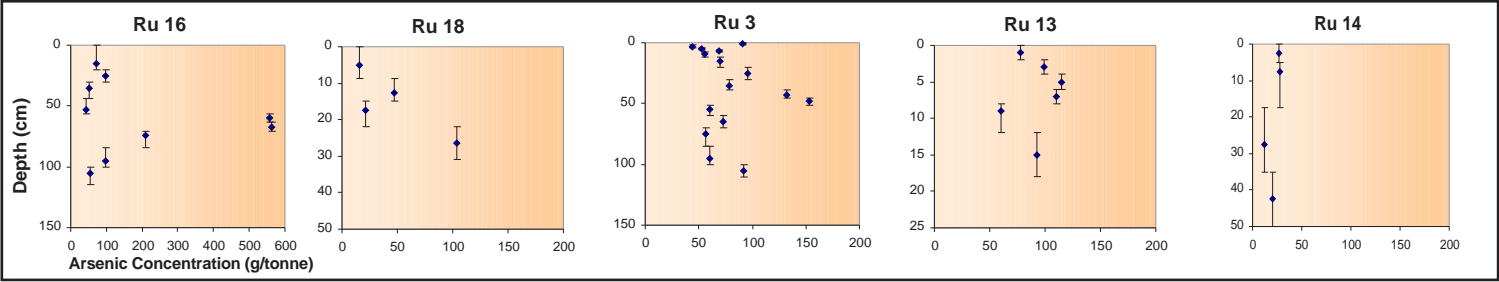
Iron



Manganese



Arsenic



Lead

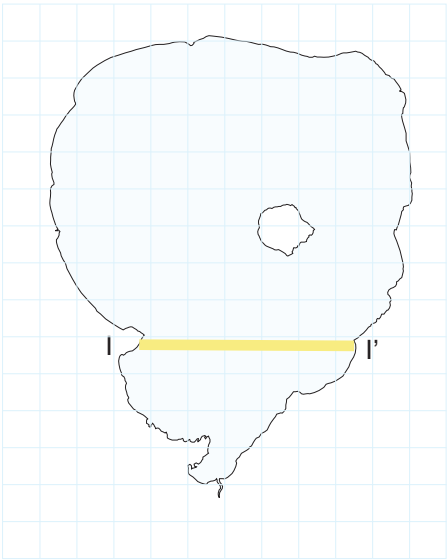
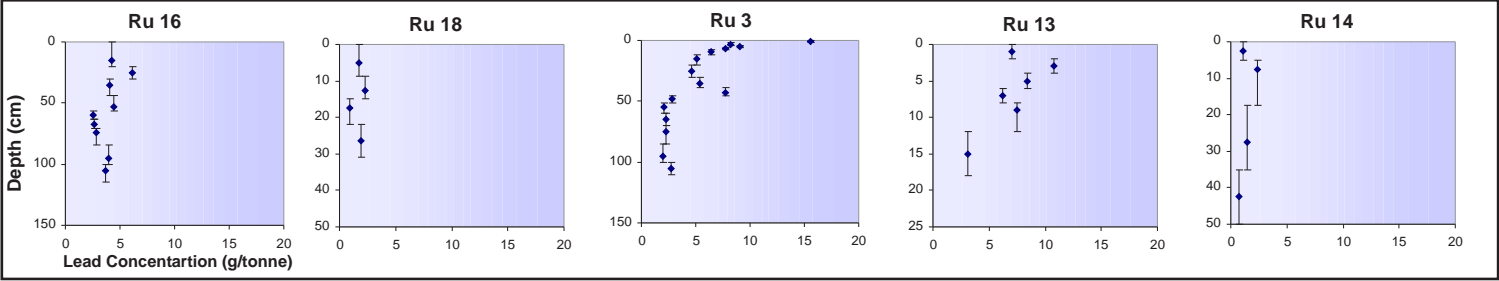
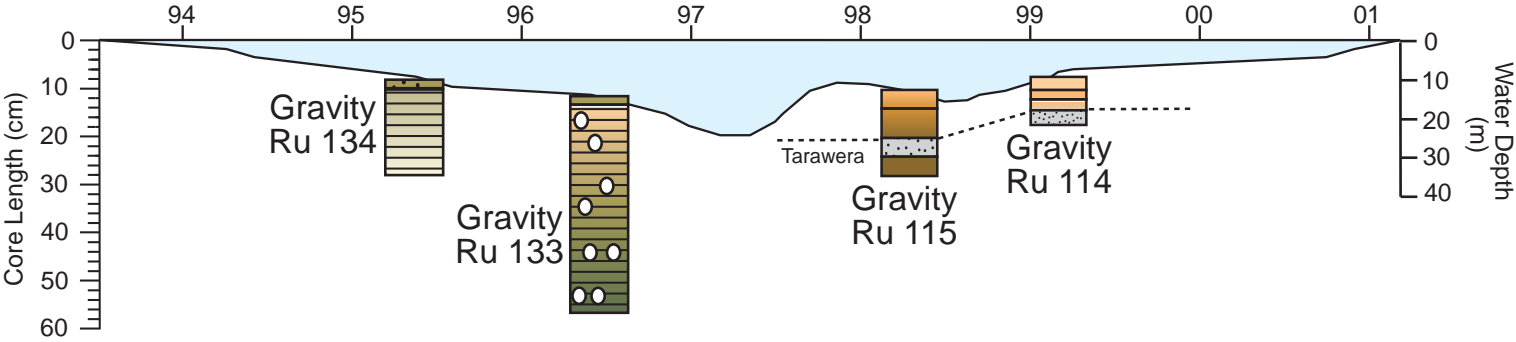
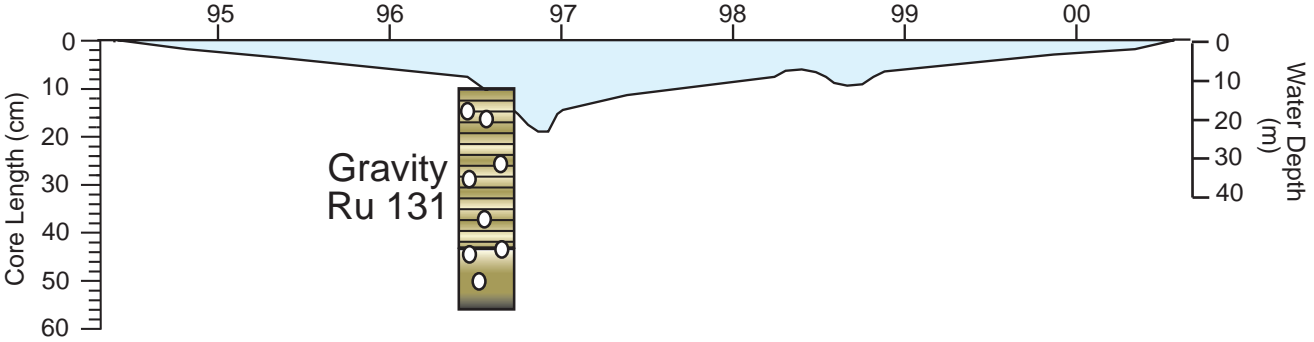


Figure 4.26: Concentration of phosphorus, iron, manganese and lead at cross-section I to I'.

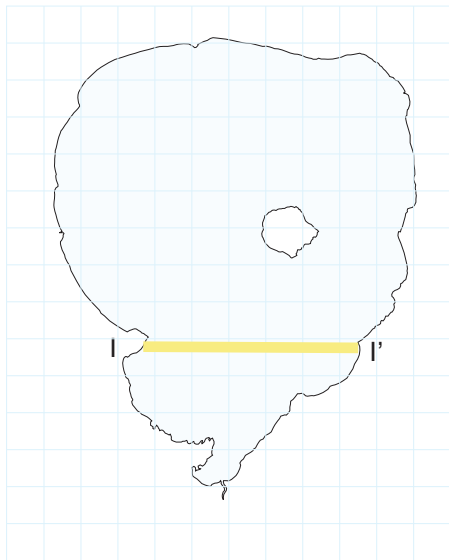
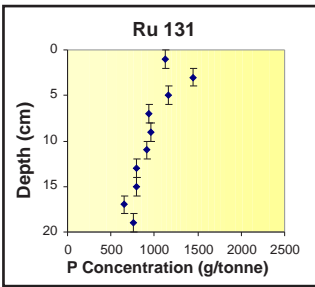
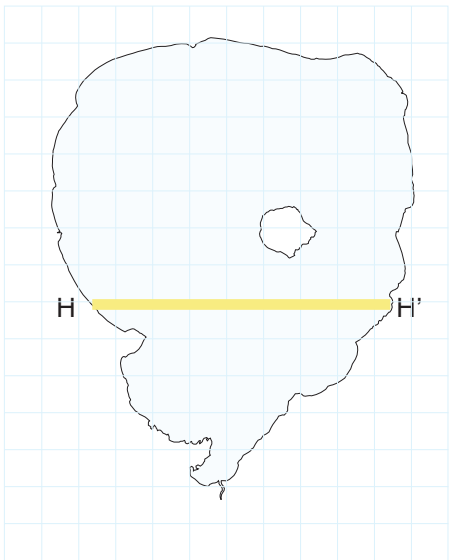
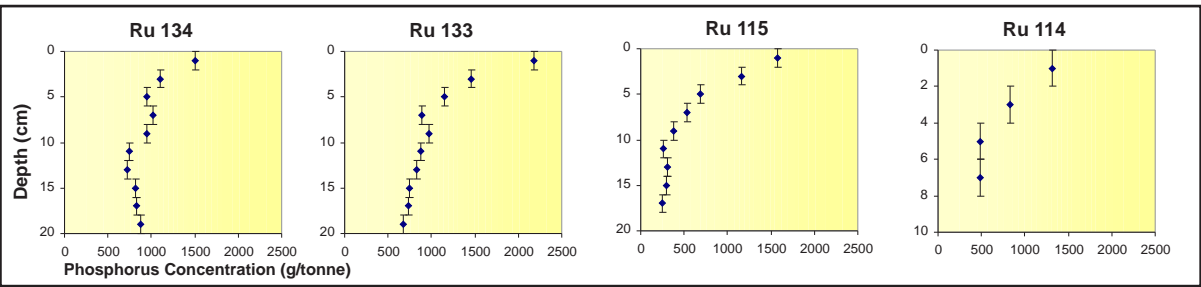
Cross Section H to H' Gravity Cores



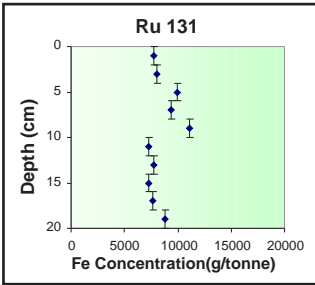
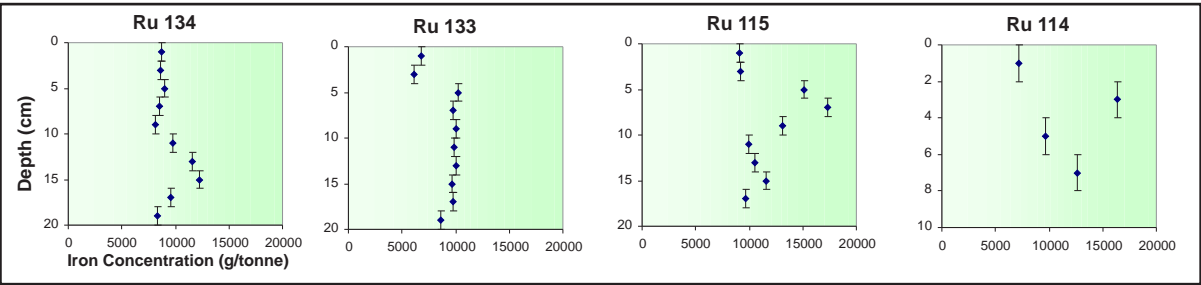
Cross Section I to I' Gravity Cores



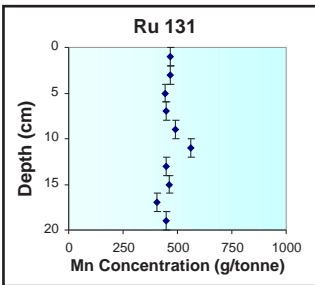
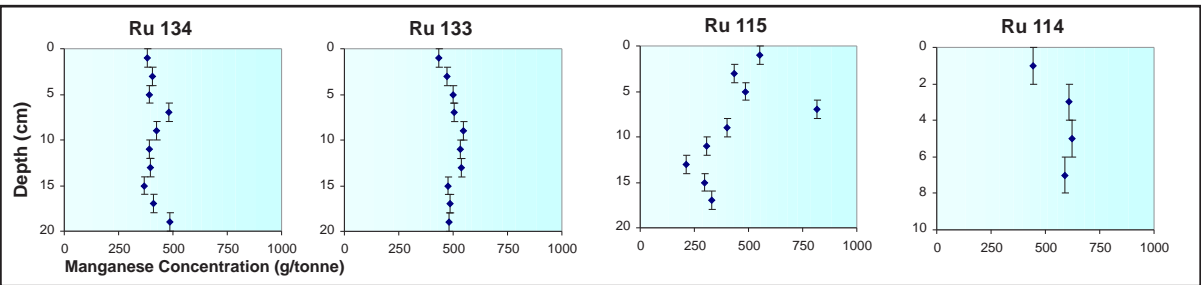
Phosphorus



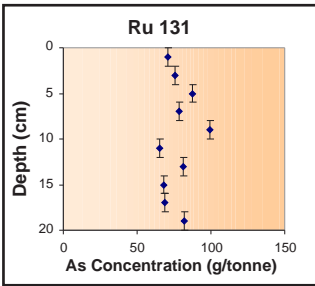
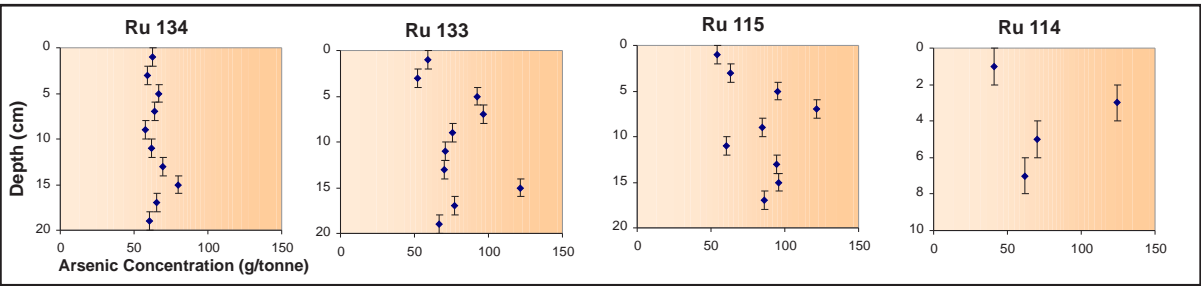
Iron



Manganese



Arsenic



Lead

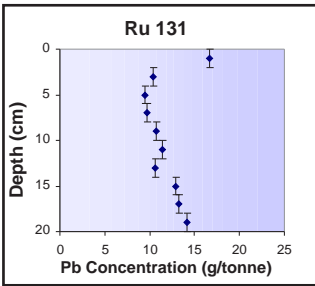
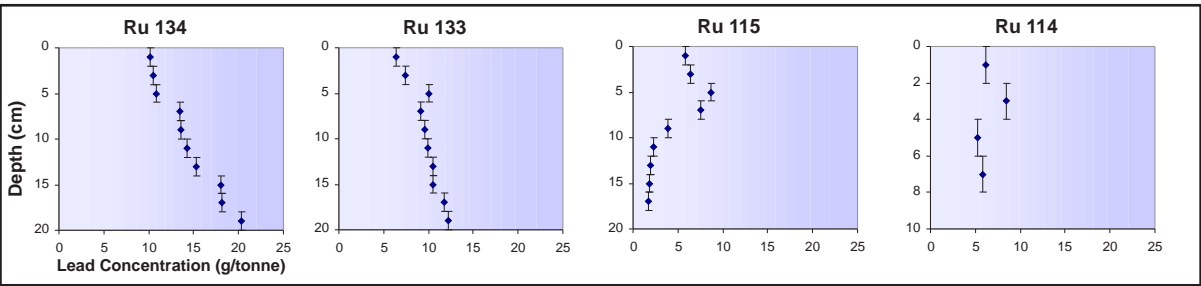
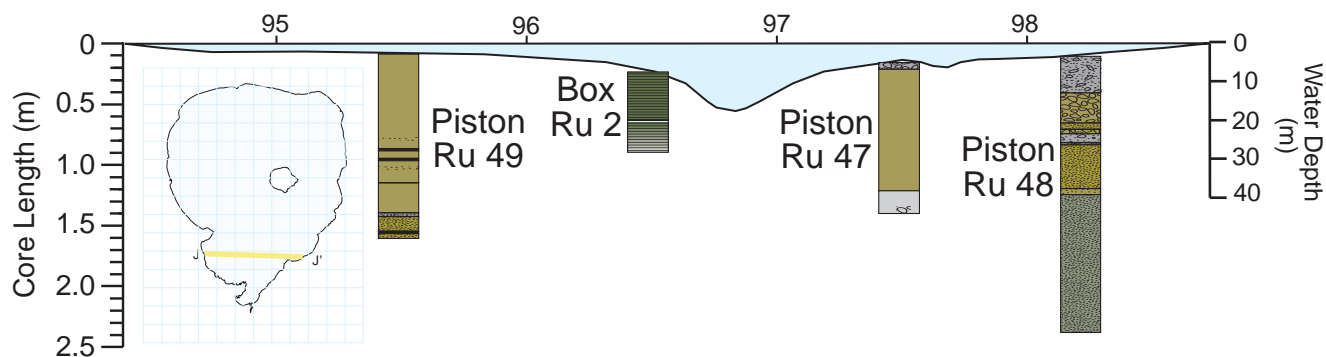
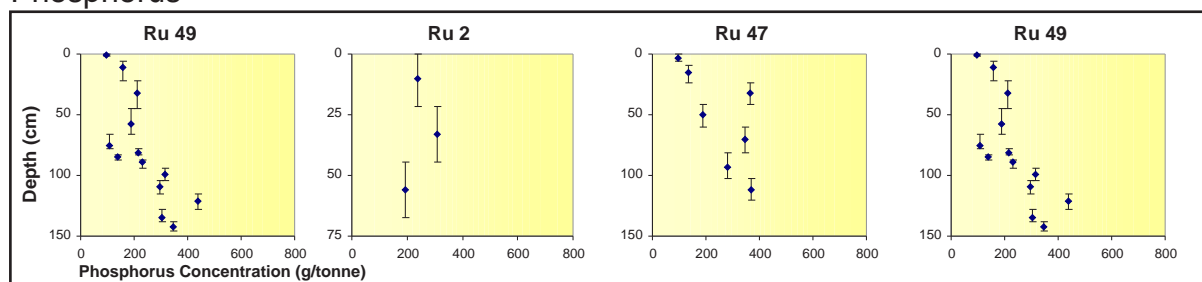


Figure 4.27: Concentration of phosphorus, iron, manganese, arsenic and lead at cross-section H to H' and I to I' gravity cores.

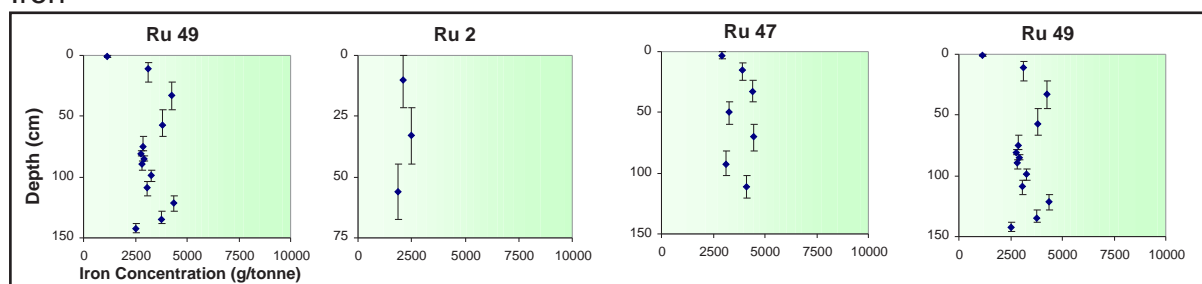
Cross Section J to J' Piston and Box Cores



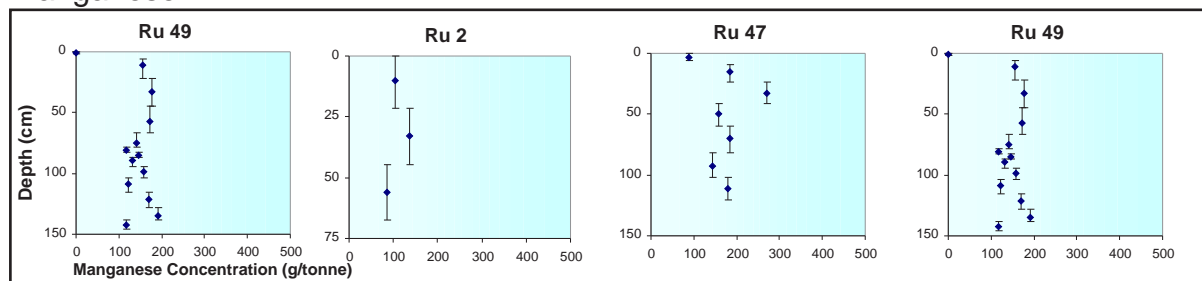
Phosphorus



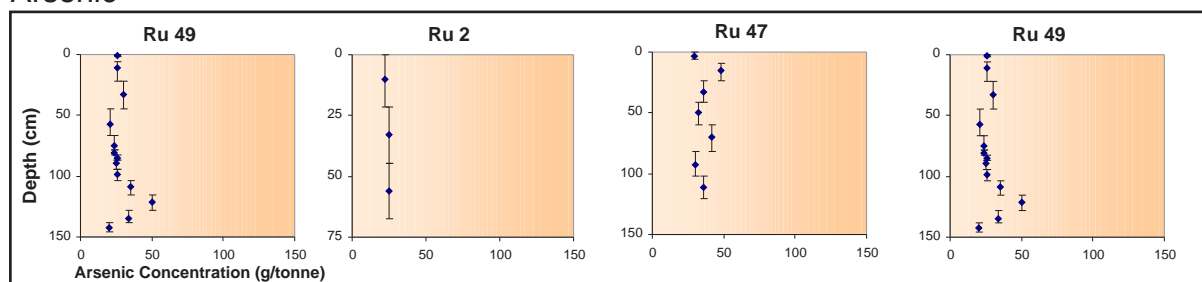
Iron



Manganese



Arsenic



Lead

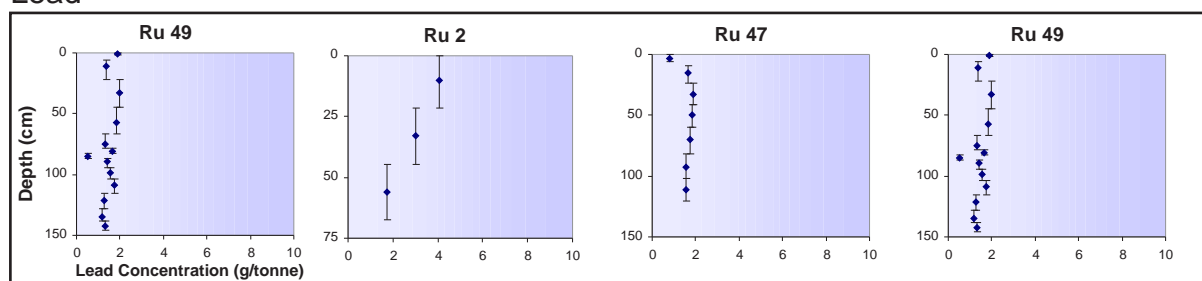
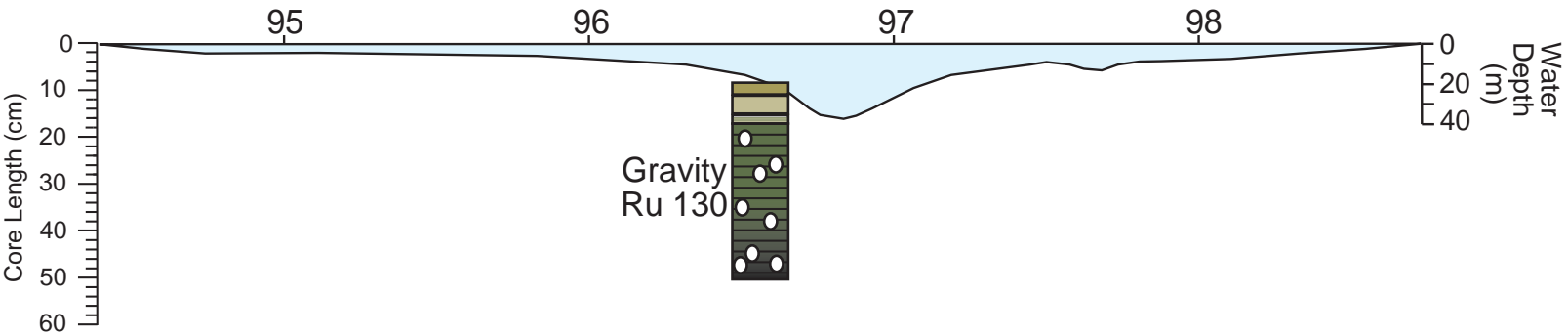
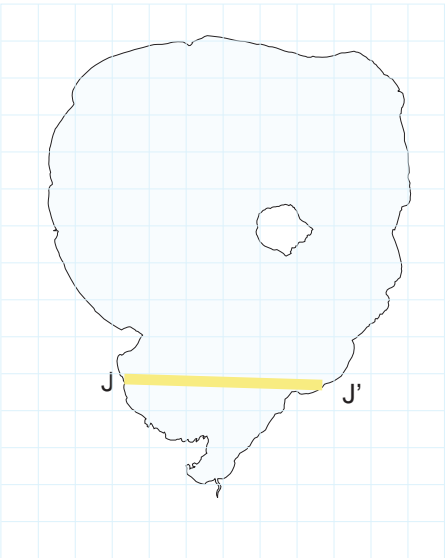
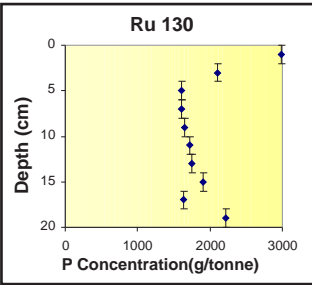


Figure 4.28: Concentration of phosphorus, iron, manganese, arsenic and lead at cross-section J to J' piston and box cores.

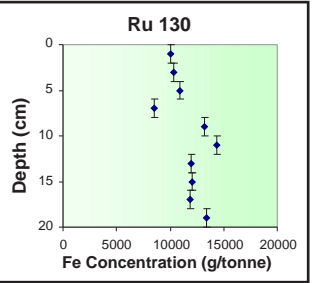
Cross Section J to J' Gravity Cores



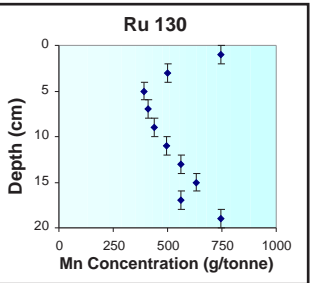
Phosphorus



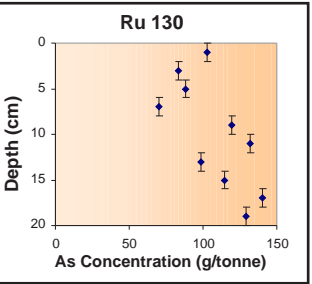
Iron



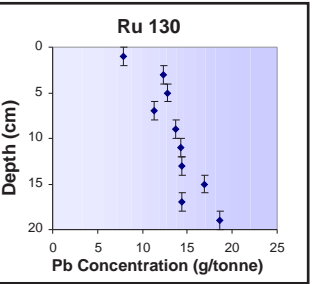
Manganese



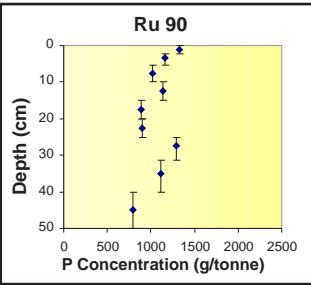
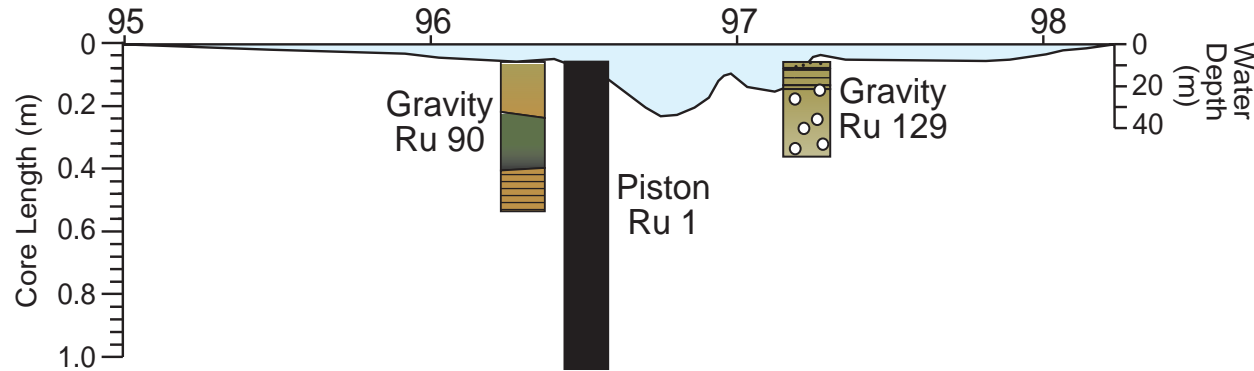
Arsenic



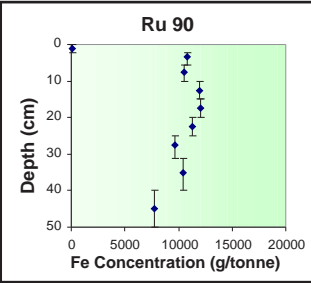
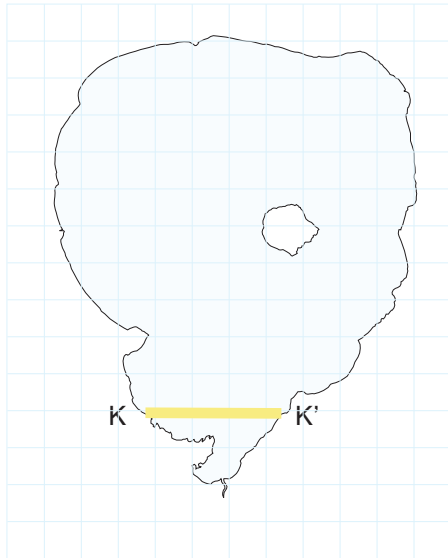
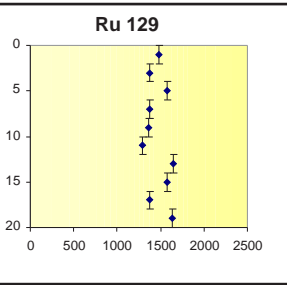
Lead



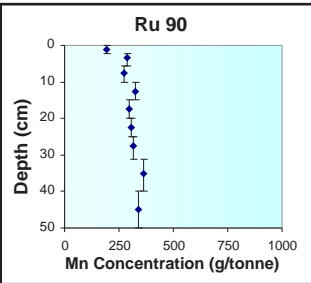
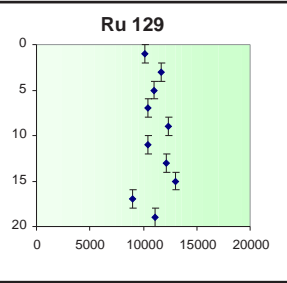
Cross Section K to K' Piston and Gravity Cores



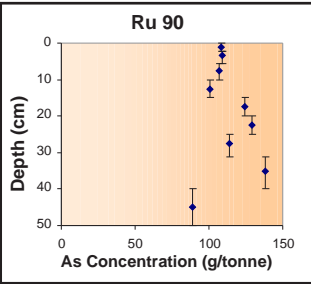
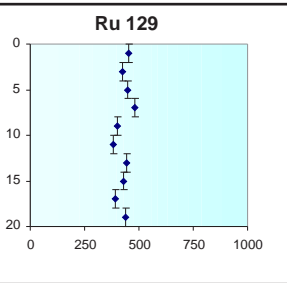
No Data Available



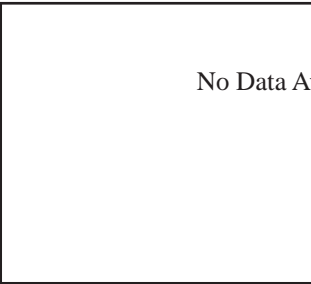
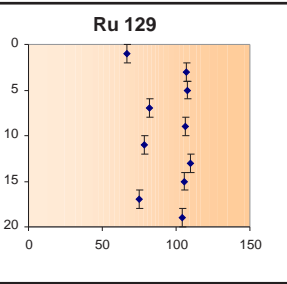
No Data Available



No Data Available



No Data Available



No Data Available

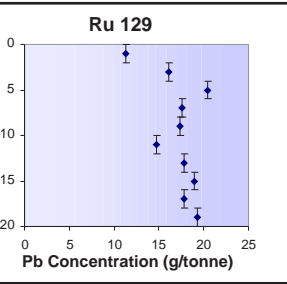


Figure 4.29: Concentration of phosphorus, iron, manganese, arsenic and lead at cross-section J to J' gravity cores and K to K' Piston and Gravity Cores.

4.5 SUMMARY

Lake Rotorua has two types of sediments: coarse, dense sediments and fine, low density diatomaceous ooze. The coarse sediment is comprised of clastic erosion products and coarse rhyolitic airfall components. The diatomaceous ooze is comprised of material accumulated from deposition of biota within the lake. The diatom frustules present in the sediment are dominated by *Aulacoseira granulata* (formerly *Melosira granulata*). The sediment contains a record of volcanic eruptions which deposited ejecta over the region. From cores taken from Lake Rotorua, the Tarawera tephra and Kaharoa tephra can be identified at typically 0.5 m and between 2 to 3 m depth, respectively, in water depths of 10-15 m. The bulk density of the sediment ranges from less than 0.02 g/cm³ immediately below the sediment-water interface in the diatomaceous ooze to 0.5 g/cm³ in the coarse sandy material nearer the lake shore. The bulk density of the material declines rapidly in a transect line from the sandy near-shore lake bed to where diatomaceous material occurs in water depths greater than 10 m.

REFERENCES

- Cassie, V. 1984. Checklist of the Freshwater Diatoms of New Zealand. *Bibliotheca Diatomologica* Band 4. Vaduz, Cramer. 125pp.
- Cassie-Cooper, V. 1996. *Microalgae: Microscopic Marvels*. Riverside Books. Hamilton, New Zealand. 164pp.
- Edwards, M.M. In Prep. Historical trophic status of seven Rotorua lakes based on sediment profile composition. M.Sc. Thesis. University of Waikato, Hamilton, New Zealand.
- Fish, G.R. and Andrew, I.A. 1980. Nitrogen and phosphorus in the sediments of Lake Rotorua. *New Zealand Journal of Marine and Freshwater Research*. 14: 121-128.
- Foged, N. 1979. Diatoms in New Zealand, the North Island. *Bibliotheca Phycologica*. 47:1-224.
- John, J. 2000. National River Health Program, The urban sub-program: A guide to diatoms as indicators of urban stream health. Land and Water Resources Research and Development Corporation.
- Matthews, R.J. 1979. Chemical analysis of Lake Rotorua sediments. M.Sc. Thesis. University of Waikato, Hamilton, New Zealand.
- Rawlence, D.J. 1984. A study of pigment and diatoms in a core from Lake Rotorua, North Island, New Zealand, with emphasis on recent history. *Journal of the Royal Society of New Zealand*. 14(2):119-132.
- Rawlence, D.J. 1985. Post-Tarawera eruption (A.D. 1886) diatom stratigraphy of Lake Rotoiti, North Island, New Zealand. *New Zealand Journal of Marine and Freshwater Research*. 19: 391-397.
- Round, F. E., Crawford, R. M. and Mann, D. G. 1990. *The Diatoms : Biology and Morphology of the Genera*. Cambridge University Press, Cambridge. 747pp.

CHAPTER FIVE:

CHEMICAL COMPOSITION OF LAKE
ROTORUA SEDIMENT



5.0 INTRODUCTION

This chapter describes the chemistry of sediments of Lake Rotorua arising from the extensive coring programme on the lake. Data has been compiled from piston, box and gravity cores taken on Lake Rotorua between January 2005 and August 2006 to provide an extensive examination of the composition and distribution of phosphorus, iron, manganese, arsenic and lead in the bottom sediments. Calculations have been made of accumulation of these elements in the sediment since the Tarawera eruption is also calculated.

5.1 BEHAVIOUR OF ELEMENTS IN LAKE SEDIMENTS

The composition of the sediment focuses on the elements phosphorus, iron, manganese, arsenic and lead. These elements are considered to make the most significant contribution (by mass and interaction with other elements) to the overall composition of the sediment. Phosphorus was chosen as it is a key nutrient; iron and manganese are involved with binding and/or the release of phosphorus to and from the sediment; and arsenic and lead are heavy metals that may potentially be toxic. Carbon, nitrogen and sulfur play an important role in the sediments but due to analytical costs and technical difficulties these elements were not as extensively examined as the other elements.

5.1.1 Phosphorus (P)

The retention of phosphorus in aquatic sediments is a major factor regulating the trophic state of the overlying waters in a wide variety of environments (Katsev *et al.* 2006). Phosphorus can be released from the sediments by a number of factors. The classical model (Mortimer, 1941) describes seasonal phosphorus release upon the onset of sediment anoxia. Phosphorus efflux is linked to redox conditions at the sediment-water interface which in turn are controlled by dissolved oxygen concentrations in the bottom water. Oxidic sediment surfaces promote strong adsorption of dissolved phosphate to solid iron oxyhydroxides, which prevents phosphate diffusion into the water column from deeper reduced sediment. Under anoxic conditions the iron oxyhydroxides dissolve, which releases phosphate into the water column. Long term phosphorus retention is relatively insensitive to the dynamics of phosphorus cycling near the sediment-water interface and is

determined by the effectiveness of phosphorus retention in deep reduced sediment (Katsev *et al.* 2006). Wetzel (2001) lists other factors that have the potential to influence sediment phosphorus retention including: pH of the overlying water (by affecting the strength of ionic phosphate sorption to solid sediment surfaces); quality and quantity of organic carbon input; inputs of phosphorus-bearing minerals; bioturbation; epipellic photosynthesis; rooted plant activity; in-sediment concentrations of organic matter; reactive iron; dissolved sulfate; calcite; and other sediment characteristics.

5.1.2 Iron (Fe)

Iron plays a major role in the geochemical cycling of many elements in freshwater systems (Hilton *et al.* 1986). Most of the iron entering lakes via rivers is in particulate form (Davison, 1993). Iron is present in the lattice of clay minerals and unavailable for reaction in solution, therefore it sinks to the sediment, as does some of the Fe III which is in the form of oxyhydroxides, either as free particles, adsorbed onto mineral particles or associated with the diatom frustules.

Iron is subject to release from the sediment depending on the redox conditions present in the sediment. Iron has two oxidation states of importance to aquatic chemistry, Fe II and Fe III. When an oxidized particulate material encounters the redox boundary it is reduced into the soluble divalent form. At the redox boundary there is a point source of soluble metal. The soluble metal diffuses (by either eddy or molecular diffusion) upwards or downwards away from this point source. As it diffuses upwards it re-enters the oxic region where it is oxidized back into the insoluble particulate form. Larger particles may also sink due to gravity. The complete redox cycle has been termed the “Ferrous Wheel”. Therefore, enrichment at the sediment surface occurs by immobilization upwards from the deeper sediment and re-precipitation due to oxidizing conditions from the water column. There is a greater chance of the reduction occurring in the sediment, because it is usually a highly reducing environment due to the decomposition of organic material which has settled out of the water column (Davison, 1993). Particulate material, which binds iron, is removed from the system by being mixed into surface waters and lost via outflows or by sinking through the redox boundary to accumulate in the sediment. Biological processes of bioturbation,

ingestion and decomposition greatly influence the transport of solids and dissolved substances within the sediments, but ultimately a downward transport of solids within the sediment is accommodated by mineral formation processes. The main effect of iron cycling is to chemically focus the metals from shallower to deeper sediments (Benoit and Hemond, 1990).

Ferric and ferrous iron form a variety of complexes and compounds in the sediment (Mackay *et al.*, 2002). Iron II forms complexes with hydroxyl to produce ferrous hydroxide ($\text{Fe}(\text{OH})_2$) and sulfate forming ferrous sulfide (FeS). Iron III forms insoluble oxyhydroxides (Davison, 1993) and complexes with inorganic sulfate (SO_4^{2+}), phosphate (PO_4^{3+}) and organic material (Luther, 2005). Granina *et al.* (2004) state that sulfide released by sulfate reduction in the sediments acts as a major reducing agent for iron.

5.1.3 Manganese (Mn)

Manganese has three oxidation states of importance to aquatic chemistry; Mn II, Mn III and Mn IV (Davison, 1993). Manganese enters lakes through inflows and is thought to be derived from two distinct sources. Firstly from weathering, which produces suspended sediment and secondly due to an influx of soluble reduced Mn II leached from oxygen-deficient soil and groundwater. Manganese II is present in many rock forming minerals where it replaces iron in the crystal lattice, although there is generally a much larger amount of iron. As with iron most of the particulate matter which enters the lake will settle to accumulate in the sediment.

5.1.4 Arsenic (As)

Arsenic occurs naturally in lake waters as a result of rock and soil weathering or geothermal activity. It can also be introduced anthropogenically through herbicide and pesticide use and the combustion of fossil fuels. The mobility of arsenic is primarily determined by processes at mineral surfaces, particularly precipitation, dissolution, adsorption and desorption controlled by geochemical parameters such as pH, Eh, ionic composition, and mineral type (Bauer and Blodau, 2006). Under neutral pH and oxidised conditions, arsenic is immobilized by sorption or co-precipitated with metal oxides. A low pH and reduced redox potential cause the dissolution of metal oxides, increasing arsenic mobility. The formation of sulfide

minerals, in strongly reducing conditions, controls the concentration of arsenic. Competition for absorption sites with phosphate, bicarbonate and other anions reduces the sorption of arsenic (Bauer and Blodau, 2006).

5.1.5 Lead (Pb)

Compared with most other pollutants, lead has a long residence time in the environment. As a result, lead compounds tend to accumulate in sediments where, due to low lead solubility and relative freedom from microbial degradation, it remains accessible (Davies, 1990). Lead alkyls were used as an additive in petrol to prevent uneven combustion in engines and were phased out approximately 10 years ago.

5.2 CHEMICAL COMPOSITION AND DISTRIBUTION

The bulk of the sediment is made up of diatom frustules composed of silica, therefore the composition of other elements in the sediments can be related to the lake composition at the time of diatom deposition. As diatoms grow they extract nutrients (C, H, O, P, N, Si and trace elements) from the surrounding water in approximate proportion to the Redfield ratio. As they are metabolised, most of the organic matter is remineralised leaving silicified material with a very large surface area. This material provides sites for adsorption and ion exchange so that the settling frustules also transport iron and manganese oxides and hydroxides and many co-precipitated and adsorbed trace metals from the water column to the sediments.

5.2.1 Phosphorus

Phosphorus concentration in Lake Rotorua sediments decreases with depth (Figure 4.11-4.29). A peak in concentration is observed at the tephra layers. In the centre of the lake, phosphorus concentrations in the top 2 cm can reach 2500 g/tonne but decline to 800 g/tonne by 20 cm depth. Around the lake margin in sandy sediment, the phosphorus concentrations are less than 250 g/tonne and do not show the characteristic peak at the sediment surface.

Sediment with high concentrations of total phosphorus in the top 10 cm of the sediment are focussed in waters deeper than 15 m. Phosphorus distribution (Figure 5.1) was mapped from the gravity core data as it gives a more realistic representation of the concentrations in the top 10 cm of the sediment than the piston cores, however, towards the centre of the lake, even the gravity cores failed to capture the sediment-water interface due to the low bulk density and high water content of the diatomaceous material.

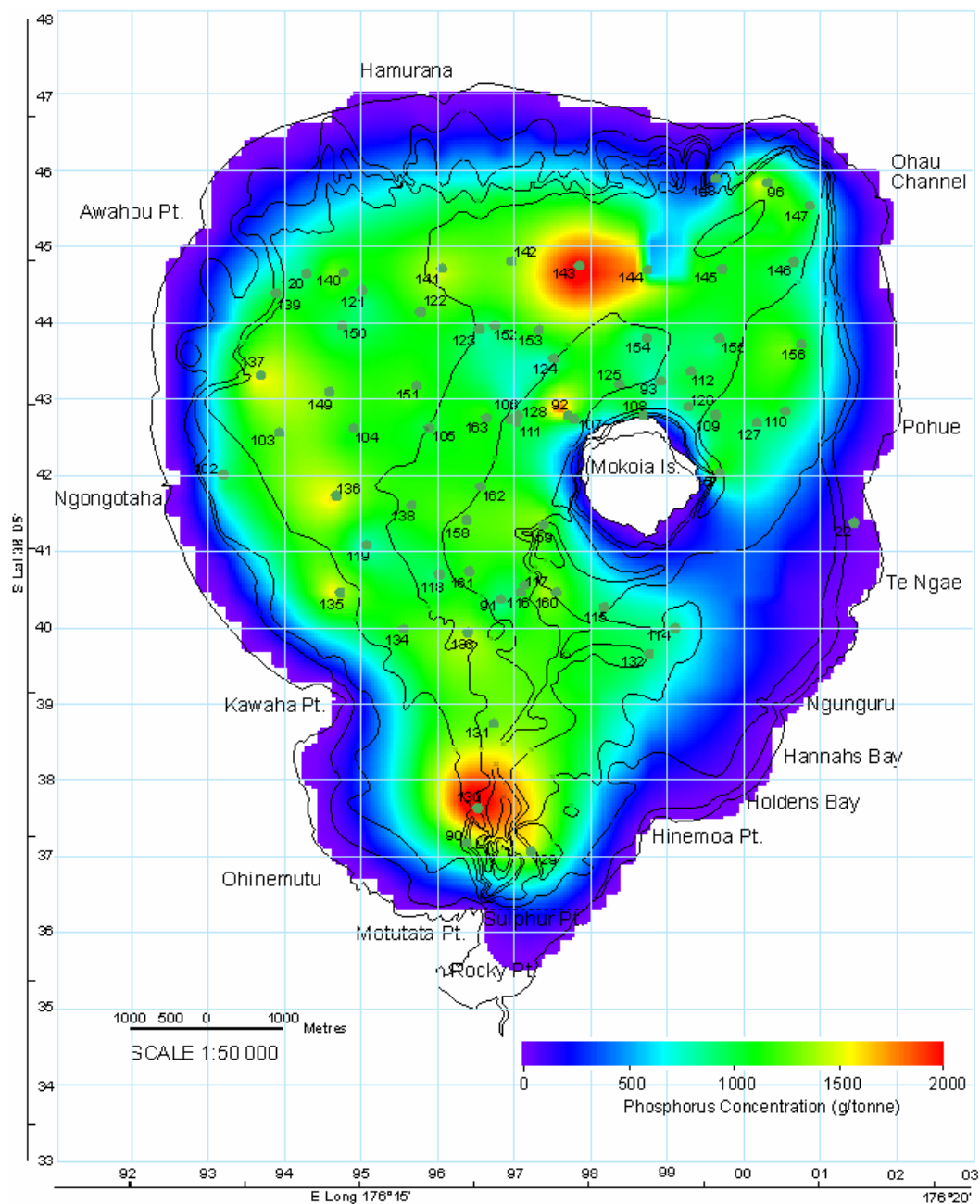


Figure 5.1: Total phosphorus concentrations in the top 0-10 cm of Lake Rotorua sediment.

Figure 5.2 shows the distribution of the phosphorus concentrations of the top 10 cm of sediment separated into the 2 cm sampling intervals. The highest phosphorus concentrations occur in the top 0-2 cm of the sediment and then decrease fairly uniformly with depth. The hashed symbol indicates the area where samples of the surface of the core were unobtainable. From the physical core descriptions it is known that the area with water depths greater than 15 m have a high accumulation rate of sediment as the Tarawera tephra is located deeper than 1 m from the sediment-water interface.

Core tops unobtainable in this area due to the soft nature of the sediment. Phosphorus concentrations are expected to be between 2000-3000 g/tonne. The effect of the sediment loss is seen in each map.

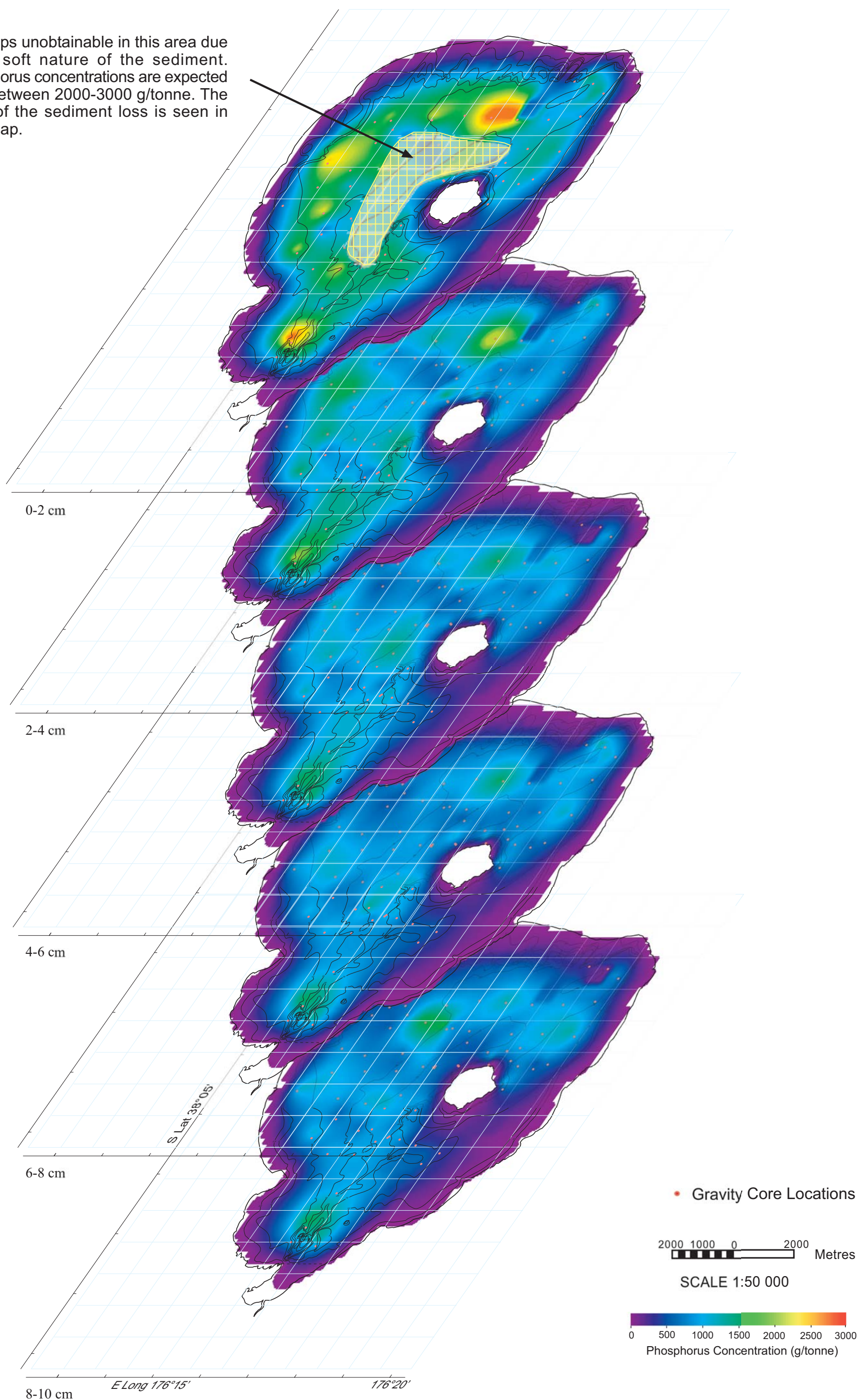


Figure 5.2: Phosphorus concentration in the top 10 cm of Lake Rotorua sediment separated into 2 cm intervals

5.2.2 Iron

Iron concentration in the sediment of Lake Rotorua is mostly dependent on sediment transitions in form of iron and the sedimentation rate of diatom frustules into the sediment. The average concentration of iron in the diatomaceous sediment is approximately 8000 g/tonne (Figure 4.11-4.29), with the Tarawera Tephra exceeding 15 000 g/tonne. The sediments with the highest iron concentrations in the top 10 cm (Figure 5.3) are focused in areas of deep water, with the exception of the area south of Mokoia Island which is influenced by the presence of the Tarawera tephra in the top 10 cm (cores Ru114 and Ru115).

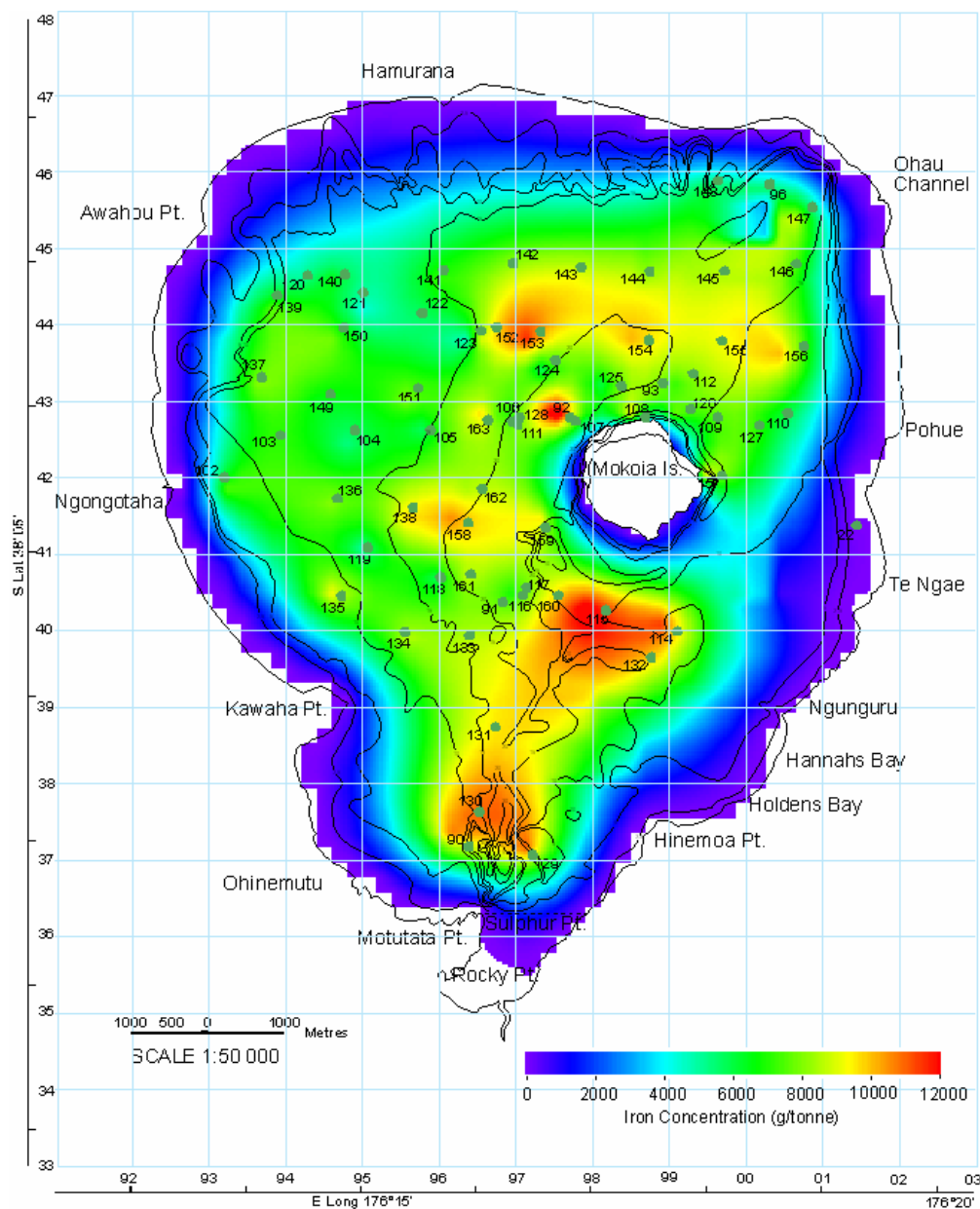


Figure 5.3: Iron concentrations in the top 0-10 cm of Lake Rotorua sediment.

5.2.3 Manganese

Manganese concentrations in the sediment follow the same trends as this metal responds similarly to redox conditions in the sediments (Figure 4.11-4.29). As with iron, manganese also peaks in the tephra layers. The average concentration of manganese in the sediment is approximately 300 to 400 g/tonne. High manganese concentrations are distributed mostly in the top 10 cm of the sediment, focused in the deeper water (Figure 5.4).

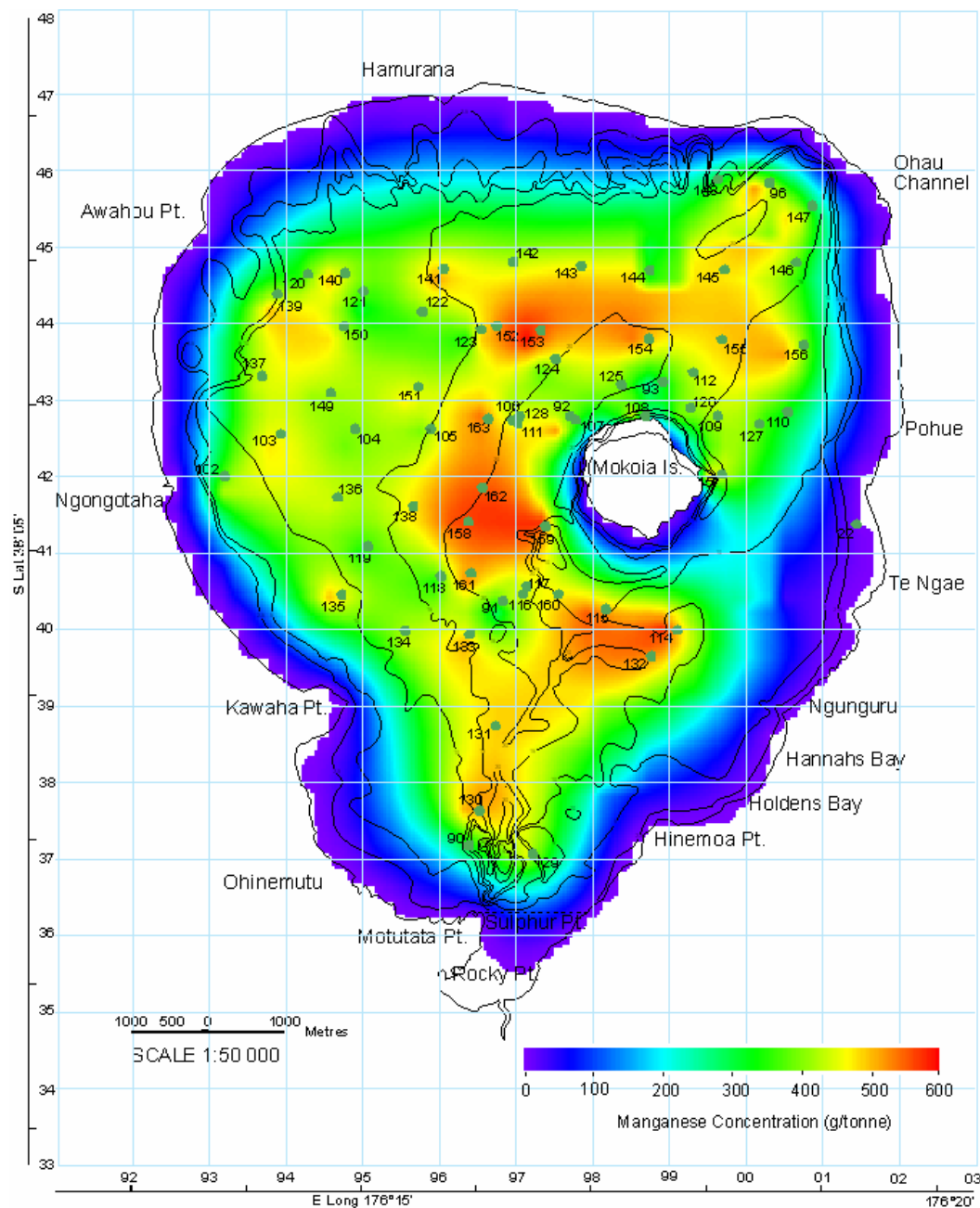


Figure 5.4: Manganese concentrations in the top 0-10 cm of Lake Rotorua sediment.

5.2.4 Arsenic

Concentrations of arsenic in the sediment reach a maximum of 250 g/tonne but are generally between 50-100 g/tonne, depending on the location (Figure 4.11-4.29). A typical profile of arsenic concentration in the sediment follows the trends of iron and manganese (Figure 5.5). Arsenic concentrations in box core Ru16 in the southwestern end of the lake, off Kawaha Point in 7.2 m water depth (Figure 4.26) reach 560 g/tonne in a layer which was observed as a dark, gingery mud which lightens to a pale brown to light cream down the profile. Arsenic concentrations peak in tephra layers. In Figure 5.5, the Tarawera tephra is located between in 103-105 cm in core Ru52.

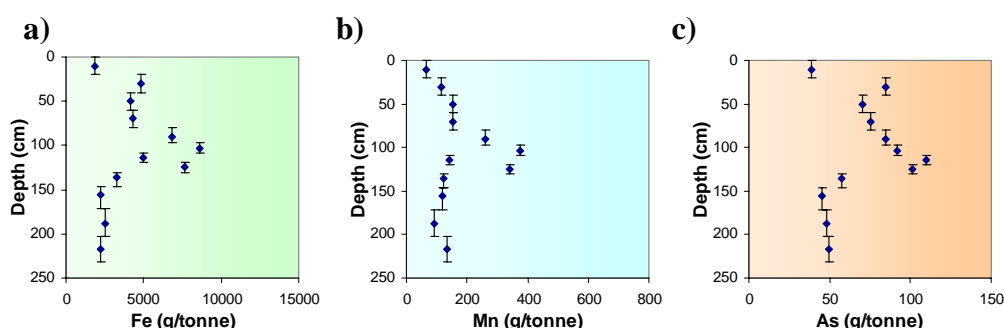


Figure 5.5: Piston core Ru52 showing the distributions in the sediment of **a)** Fe, **b)** Mn and **c)** As. All three elements peak in the Tarawera Tephra.

The associated linear regressions between iron and arsenic (Figure 5.6a) and manganese and arsenic (Figure 5.6b) show a high correlation at lower arsenic concentrations. The correlation coefficient between iron and arsenic at 0.71 ($p < 0.01$) is higher than that of manganese at 0.42 ($p < 0.01$).

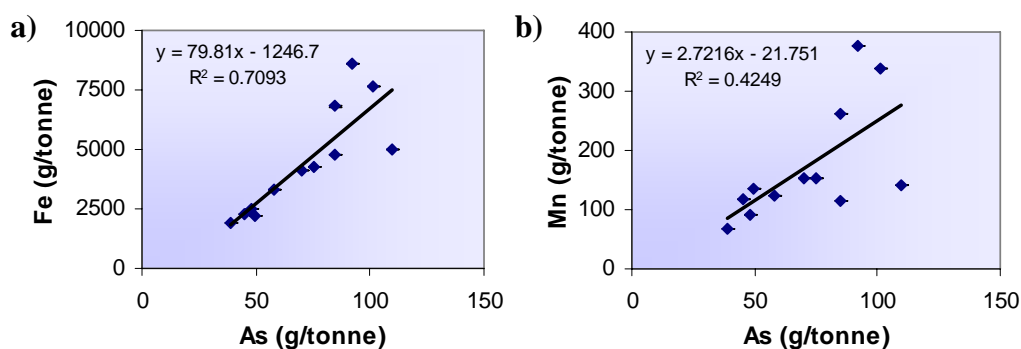


Figure 5.6: **a)** Linear regression relationships between Fe and As and **b)** between Mn and As.

The distribution of arsenic in the top 10 cm of the sediment indicates that its accumulation is focussed in areas with water depth greater than 10 m, in common with the diatomaceous ooze (Figure 5.7).

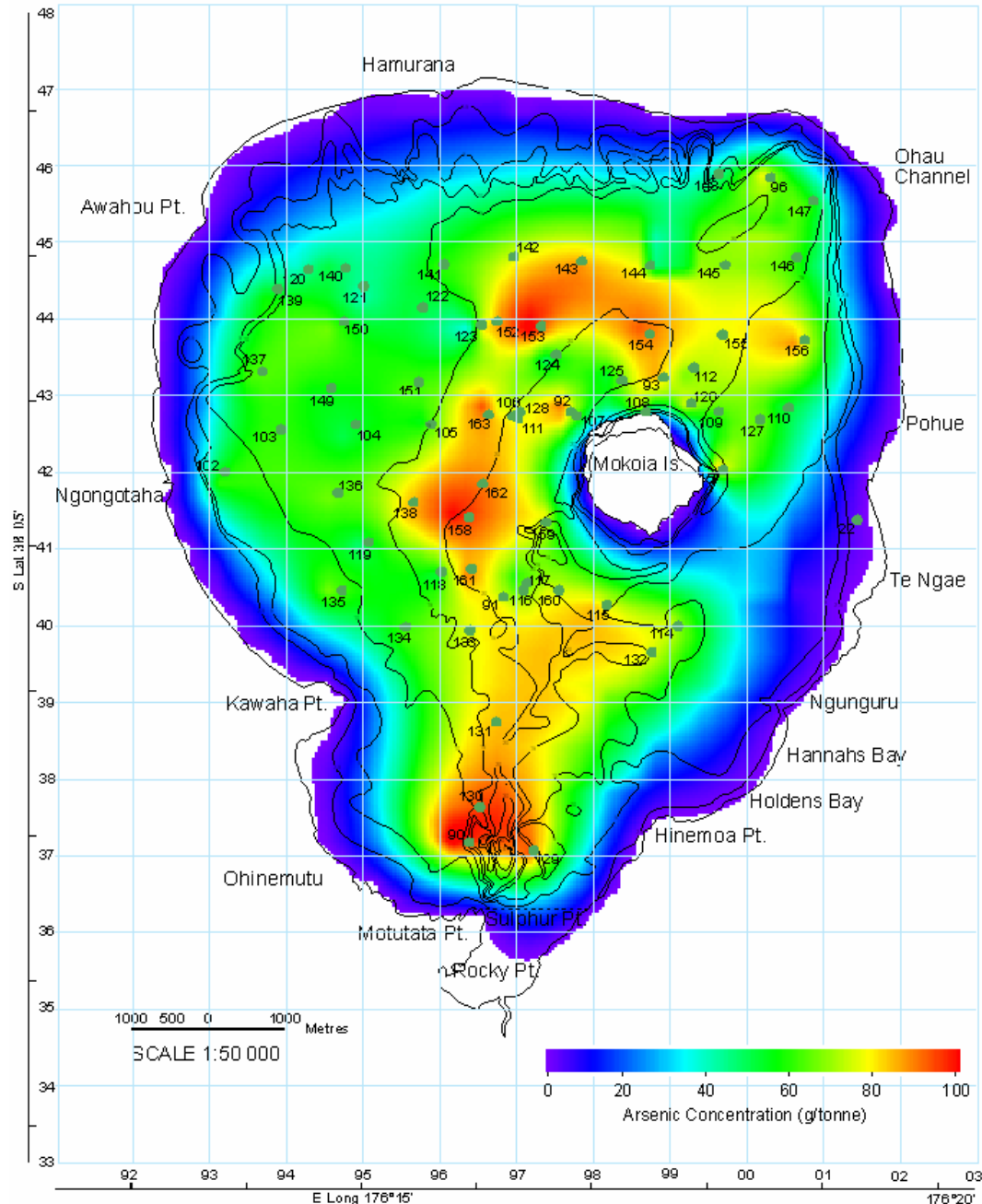


Figure 5.7: Arsenic concentrations in the top 0-10 cm of Lake Rotorua sediment.

5.2.5 Lead

Lead concentrations in the sediment of Lake Rotorua are typically less than 15 g/tonne (Figure 4.11-4.29). Lead is influenced by the concentration of iron and

manganese in the sediment and distributions tend to mimic those of iron and manganese (Figure 5.8). Lead concentrations also peak in the tephra layers, which is consistent with other elements.

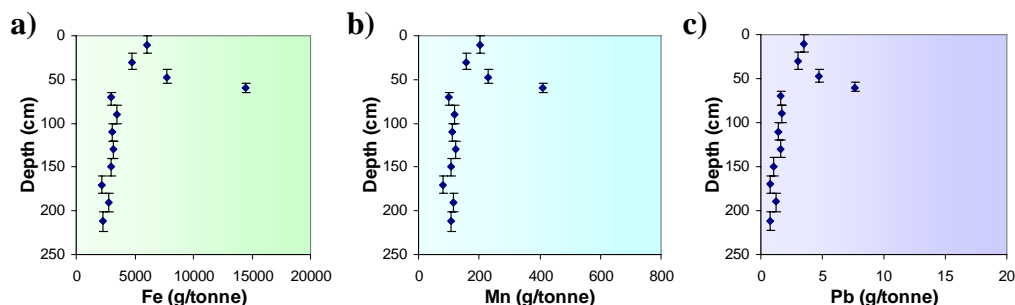


Figure 5.8: Piston core Ru57 showing the distributions in the sediment of **a)** Fe, **b)** Mn and **c)** Pb.

The regression relationships between iron and lead (Figure 5.9a) and manganese and lead (Figure 5.9b) are very close, with correlation coefficient of 0.97 and 0.96, respectively. This suggests that lead is bound in the sediment by iron and manganese, therefore mobilisation of lead is possible if redox conditions change.

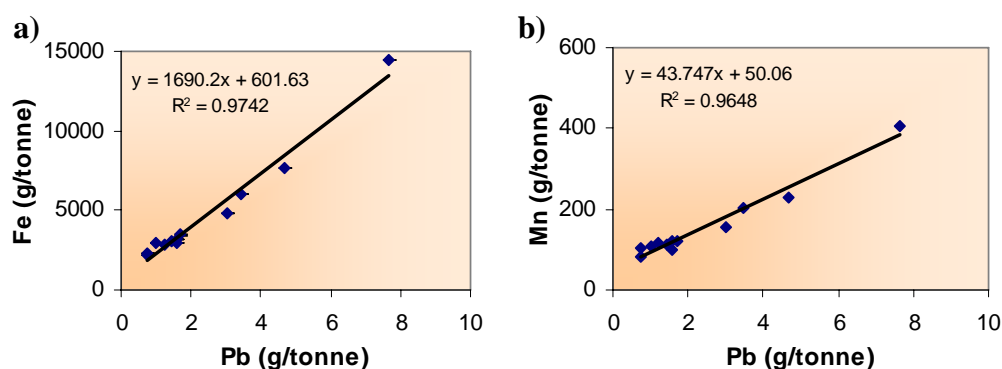


Figure 5.9: **a)** Linear regression relationships between Fe and Pb and **b)** between Mn and Pb.

The distribution of lead in the top 10 cm of the sediment in Lake Rotorua is concentrated in the deep area north of Sulfur Point (Figure 5.10). In the remainder of the lake area lead concentrations in the diatomaceous ooze are typically between 5-10 g/tonne.

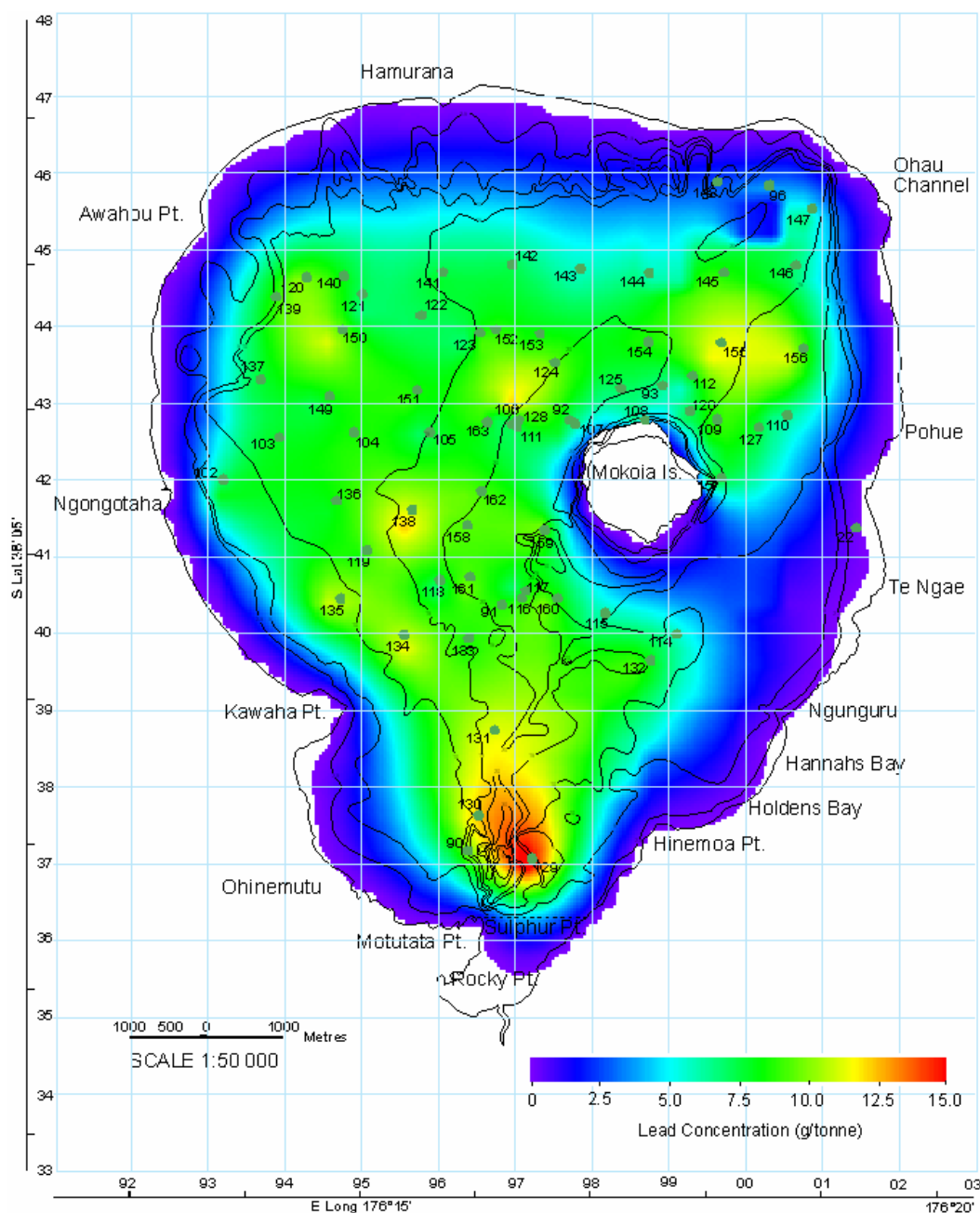


Figure 5.10: Lead concentrations in the top 0-10 cm of Lake Rotorua sediment.

5.2.6 Sulfur (S)

A gravity core transect from the Ohau Channel (Ru96) in the north to Sulphur Point (Ru90) in the south was taken to show the concentration and distribution of sulfur in the sediment (Figure 5.11). The majority of sulfur entering Lake Rotorua is of geothermal origin. Core Ru90 is taken in the deepest part of the lake off Sulphur Point, which receives inflows from the Rotorua geothermal field discharging into the lake. The water around this area is cloudy and there is often a strong sulfur smell. All cores in the transect line were taken in water depths

greater than 15 m and have high sediment accumulation rates (Figure 5.11a). The concentration of sulfur observed in the top 50 cm of the sediment is typically between 5000 and 7500 g/tonne. There is no consistent trend of sulfur concentration with depth over the top 50 cm. The trend of the sulfur concentration in the sediment across the transect line shows a decrease to the north of the lake with increasing distance from the main geothermal source around Sulphur Point.

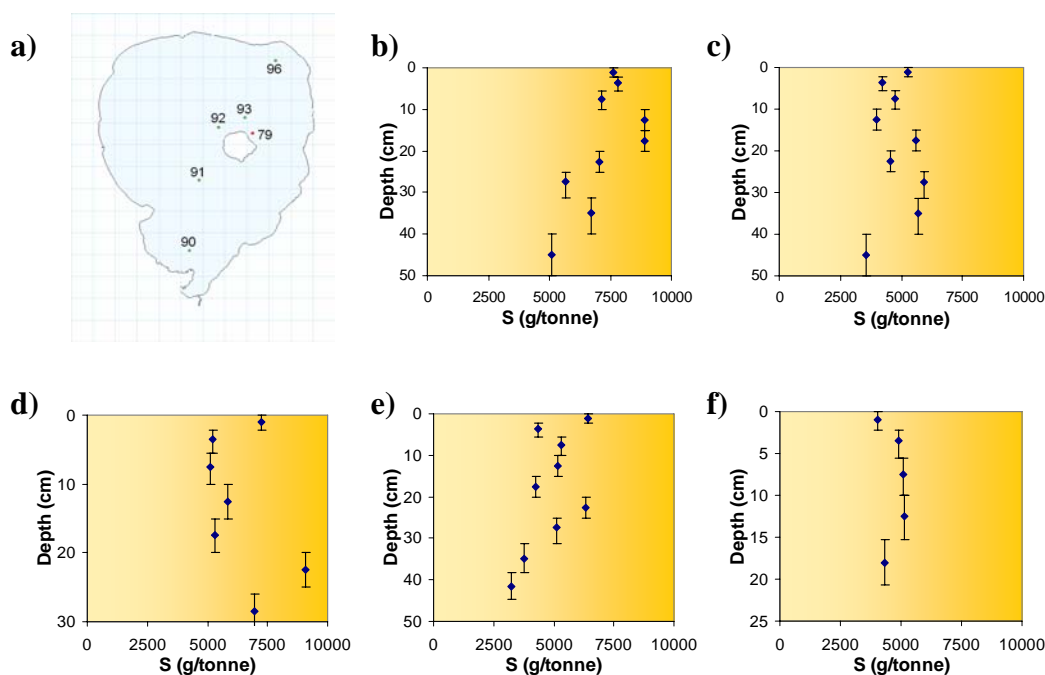


Figure 5.11: a) Location and b) concentration of sulfur in core Ru90 c) Ru91 d) Ru92 e) Ru93 and f) Ru96.

Core Ru79 was analysed by XRF giving a profile for sulfur to a depth of 220 cm in the sediment (Figure 5.12). This core was sampled to the east of Mokoia Island where there is a lower sediment accumulation rate, and therefore there is not the high sulfur concentration observed in the top 50 cm of the gravity core samples to the west of Mokoia Island (Figure 5.11a). The peak in sulfur concentration in Ru79 at 50 cm is associated with the Tarawera tephra. The sulfur concentration in the sediment is two times higher in the Rotomahana mud layer than in the sediment accumulated in Lake Rotorua. Below this depth sulfur concentrations exceed those above the Tarawera tephra. This could be the result of either an increase in sulfur availability or a decrease in the diatom sedimentation rate.

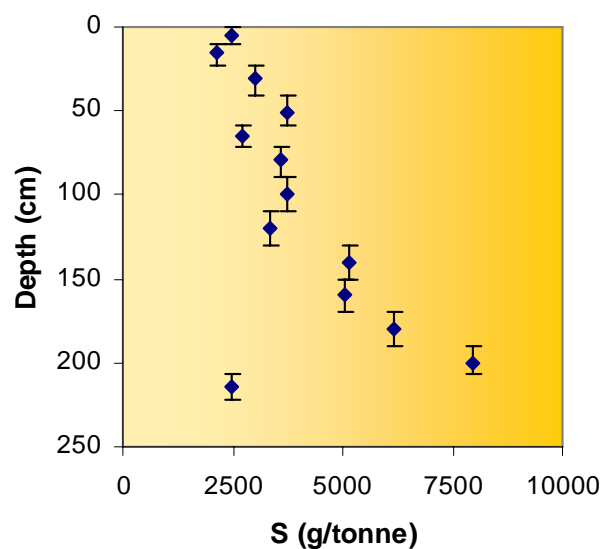


Figure 5.12: Sulfur in piston core Ru79 analysed by XRF.

5.2.7 Carbon (C) and Nitrogen (N)

Carbon and nitrogen concentrations in the sediment decrease rapidly within the top 50 cm. Carbon concentration at the top of the sediment is between 3-6 % and decreases to less than 2% by 50 cm sediment depth (Figure 5.13 and 5.15a). Nitrogen concentration in the sediment decreases from 0.8% to less than 0.4% within the top 50 cm (Figure 5.14 and 5.15b).

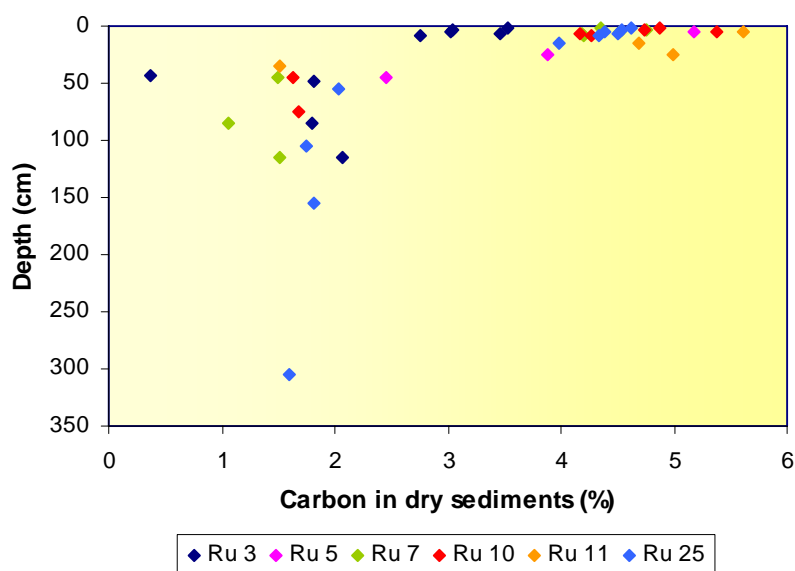


Figure 5.13: Carbon concentration in selected piston and box cores.

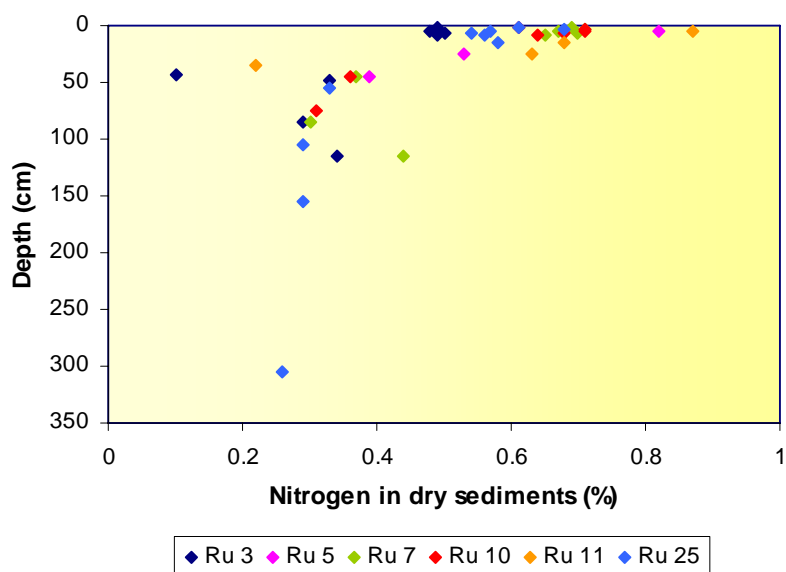


Figure 5.14: Nitrogen concentration in selected piston and box cores.

Figure 5.15 shows that carbon and nitrogen are remineralised together but the changing ratio shows that carbon is remineralised preferentially to nitrogen.

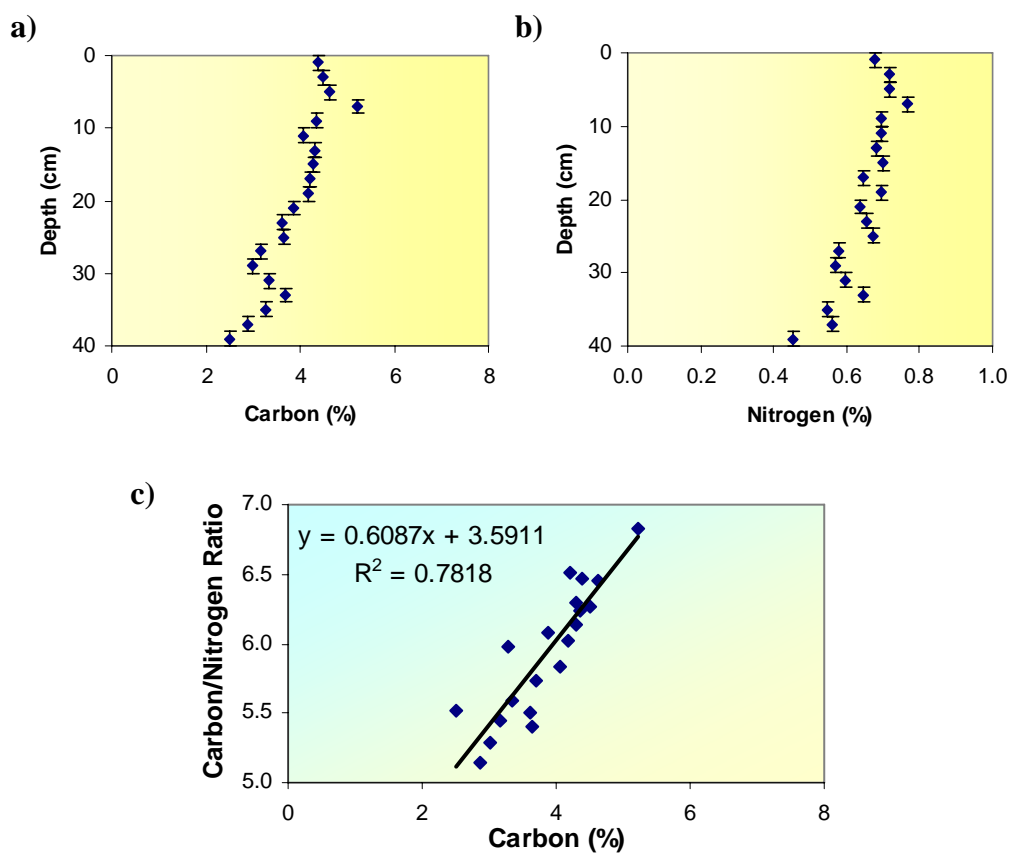


Figure 5.15: a) Carbon, b) nitrogen and c) the carbon to nitrogen mass ratio vs carbon content in gravity core Ru128.

5.3 SEDIMENT ACCUMULATION

Sedimentation is an important component of the internal nutrient cycle in lakes as it regulates loss of organic and inorganic particulate material from the water column and controls the supply of nutrients to the bottom sediments (Gálvez and Niell, 1992). Sediment in Lake Rotorua is focused by wave action into deeper waters, generally greater than 15 m as seen by the cross sections in the previous chapter. The accumulation of phosphorus, iron, manganese, arsenic and lead can be calculated from the sediment concentration and the amount of sediment. The accumulation rate of each element in the sediment has been calculated: since the Tarawera eruption; within the top 0-10cm; and 10-20 cm in the sediment (see Chapter 3 for methodology).

5.3.1 Accumulation since the Tarawera eruption

The Tarawera tephra provides an excellent marker in the sediment stratigraphy for calculating the accumulation of sediment in the lake. The Tarawera eruption, occurred on 10 June, 1886. The total amount of each element in the sediment has been estimated since the Tarawera eruption based on corresponding accumulation rates (Table 5.1).

Table 5.1: Total accumulation of selected elements in Lake Rotorua sediments since the Tarawera eruption.

Element	Total (tonnes)	Accumulation Rate (tonnes/year)
Phosphorus	3575.6	29.6
Iron	46209.1	385.1
Manganese	2161.5	17.9
Arsenic	445.4	3.7
Lead	58.7	0.49

The accumulation of each element within the top 0-10 and 10-20 cm is shown in Table 5.2. Phosphorus accumulation in the sediment decreases with depth (Table 5.3) as recycling from the sediment keeps phosphorus mobilised at the sediment-water interface. Due to the recycling of phosphorus from the lake sediment, the concentration in the 0-10 and 10-20 cm intervals exceeds what is expected from the estimated accumulation rate. The accumulation of iron and manganese in the sediment has not changed significantly. The increase in arsenic and lead

concentration from the 0-10 cm to 10-20 cm is associated with the binding of iron in the sediment, which prevents remobilisation.

Table 5.2: Sediment mass in 0-10 and 10-20 cm of Lake Rotorua.

Element	0-10 cm (tonnes)	10-20 cm (tonnes)
Phosphorus	442	334
Iron	3417	3481
Manganese	180	178
Arsenic	28.62	28.72
Lead	3.53	4.32

Table 5.3: Sediment mass of phosphorus in 2 cm intervals.

Depth (cm)	Phosphorus (tonnes)	Accumulated P (tonnes)
0-2	122.3	122.3
2-4	94.3	216.5
4-6	78.9	295.4
6-8	73.4	368.8
8-10	70.9	439.7

5.3.2 Phosphorus Budget

A phosphorus budget has been constructed for Lake Rotorua (Figure 5.16). Inputs of phosphorus into Lake Rotorua come from stream and groundwater flows and rainfall. Outputs of phosphorus from the lake are from the Ohau Channel. Evaporation is not considered to have an effect on phosphorus losses from the lake.

Total phosphorus in stream (gauged) inflows is c. 35 t/yr (Rutherford, 2003; Beyá, 2005; Burger, 2006). Groundwater flow into the lake can be calculated in two ways: Morgenstern and Gordon (2006) estimated a flow rate of 3.3 m³/s and a concentration of 0.1 g/m³ (White, 2004). On the basis of these assumptions, the total phosphorus load in the groundwater entering Lake Rotorua is 10.41 t/yr. Beyá (2005) estimated the total input to be 12.8 t/year for ungauged inflows from the difference between the total estimated surface flows (minor and major) and the inflow calculated from the lake water balance. This value includes groundwater and ungauged local surface flows, which also contribute to phosphorus inputs into the lake. Phosphorus input to Lake Rotorua from rainfall was estimated at 1.3 t/yr from the 'Kaituna at Whakawerawera' climate station data and adjusted for mean

lake surface area (Beyá *et al.*, 2005). The average discharge of phosphorus down the Ohau Channel is 19.3 tonnes/year (Beyá *et al.*, 2005). Figure 5.14 shows the phosphorus concentration in the inflows and outflow from Lake Rotorua.

From the phosphorus budget, the amount of phosphorus retained in Lake Rotorua each year is 29.8 tonnes. The majority of the phosphorus is accumulating into the sediment, with significant internal recycling from the sediment to the water column.

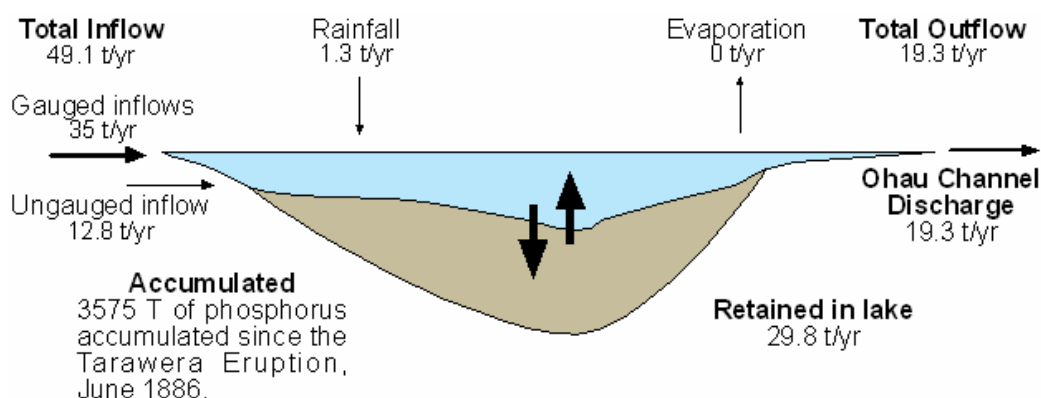


Figure 5.16: Phosphorus budget for Lake Rotorua

5.4 DISCUSSION

5.4.1 Composition and Distribution of Rotorua Sediments

The bulk of the sediment in Lake Rotorua is made up of diatom frustules composed of silica; therefore the composition of other elements in the sediments can be related to the lake composition at the time of diatom deposition. Lake Rotorua contains very little carbonate (a few molluscs), its bottom waters can become anoxic during stratification periods over the summer (although it is more likely to become hypoxic during stratification events) and it contains no rooted plants below 10 m water depth.

The inability to capture the surficial sediments with piston coring is obvious by comparing the surface phosphorus concentration of gravity cores with those of adjacent piston cores (Figures 5.17). In this case it would appear that piston coring failed to capture the upper 20 cm of the sediment. The loss of sediment is not as

obvious when examining the profiles of the other elements as there is not a rapid decrease in concentration within the top 20 cm of sediment and the concentration does not peak at the sediment-water interface. The concentration of iron in the top 20 cm is approximately 2000 g/tonne higher in the gravity core than it is in the associated piston core. As for manganese, this difference in sediment concentration equates to approximately 300 g/tonne. To account for the loss of sediment, only the gravity core data was used in producing the distribution maps and calculating the accumulation of each element in the sediment.

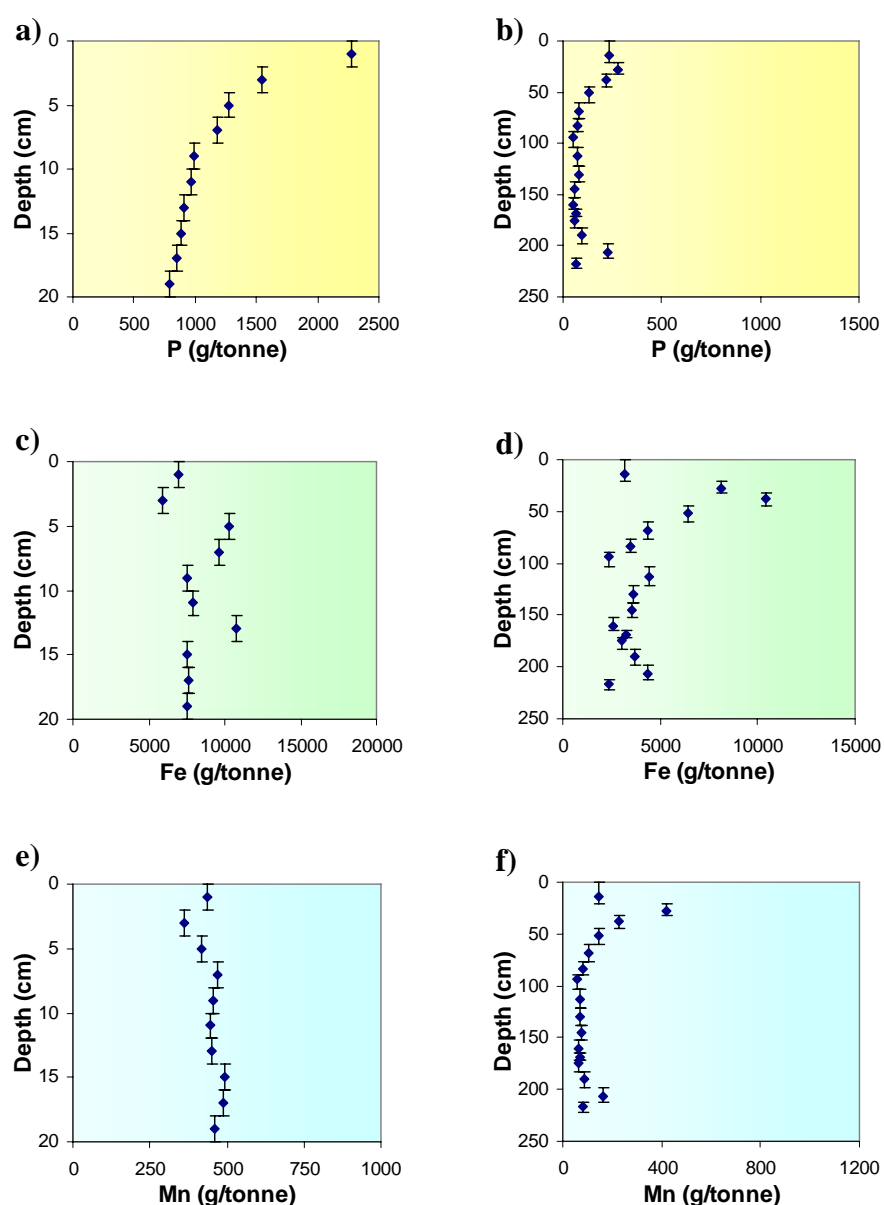


Figure 5.17: a) Total phosphorus sediment concentration in gravity core Ru136 compared to b) piston core Ru51. c) Iron in Ru136 to d) Ru51 and e) manganese in Ru136 to f) Ru51.

The distribution maps for all the elements studied showed high concentrations in the sediment located off Sulfur Point. The water depth in this area reaches 46 m and is the deepest area in the lake (see Chapter 6). Although none of the cores taken in this area was long enough to penetrate to the Tarawera tephra, it is expected from the location of the Tarawera tephra in other deep water areas that it would be greater than 1 m. A high accumulation rate in this area is from the focusing of diatomaceous material from water depths >10 m which results in progressively greater deposition rate with water depth. Between 1973 and 1991, Lake Rotorua received sewerage discharge from Rotorua City (population 60,000) with the outlet into Puarenga stream, entering the Sulphur Bay south of Sulphur Point (Hoare, 1980; Rutherford *et al.*, 1996). This could account for the high concentration of phosphorus accumulated in the deep water north of Sulphur Point. Lead in the sediment is concentrated in the deep area north of Sulfur Point suggesting that the source of the lead into the lake is predominantly from the Rotorua City area. One possibility is through the discharge of storm water into the lake. Lead alkyls were used as an additive in petrol to prevent uneven combustion in the engine and were phased out beginning around the 1990. Stormwater systems would then have transported contaminants into Lake Rotorua. The other possible source of lead is through geothermal discharges, as lead shows similar deposition patterns off Sulphur Point to those of arsenic.

From the early 1960s, chemical controls containing arsenic were used to combat the increasing weed problem in Lake Rotorua, but anthropogenic inputs into Lake Rotorua will be masked by the large natural geothermal contributions of arsenic into the lake. There are three identified geothermal fluid inputs into Lake Rotorua, which are the main source of arsenic and sulfur to the lake. Surface flows from the Tikitere geothermal field naturally drain into Lake Rotorua via the Waiohewa Stream, on the eastern side of Lake Rotorua. The Rotokawa geothermal field discharges into Lake Rotorua, east of the Rotorua Airport. The Rotorua geothermal field feeds streams entering Lake Rotorua by overflow of surface springs and shallow aquifers at the southern end of the lake.

Peaks in the concentration of all elements in the sediment profiles correspond to tephra layers buried in the sediment. The Tarawera tephra formed from super-

heated sediment ejected from Lake Rotomahana and covered the landscape during the Tarawera eruption (1886). Lake Rotomahana has large geothermal contributions of inflows to the lake and therefore high concentrations of sulfur and arsenic are likely to have accumulated in the sediments of this lake. Iron and manganese concentrations peak in both the Tarawera and Kaharoa tephra layers, probably as a result of the higher abundance of iron and manganese containing minerals. The sediment profile shows a rise in concentration from deeper sediments up to the tephra layer. Above the tephra layer concentration decreases. This suggests that the diagenetic processes causing upwards mobilisation of iron and manganese are impeded by the tephra. Below the Tarawera tephra sulfur concentrations exceed those above the tephra layer. This could be the result of either an increase in sulfur availability or a decrease in the diatom sedimentation rate.

Sediment retention of phosphorus appears to be mostly controlled by iron, manganese and sulfur diagenesis (Mangan, In Prep.) Research by Burger (2006) indicates that there may be several iterations of sedimentation and release before nutrients are either buried permanently or discharged through outflows from the lake. In general only a relatively small proportion of incoming nutrients are discharged via the outflows; c. 18 % of total phosphorus in Lake Rotorua. Under certain conditions, recycling becomes the dominant source of nutrients to the overlying water (Burger et al., 2005). Arsenic can be extensively recycled once it is introduced into an aquatic environment (Belzile and Tessier, 1990) largely in association with iron and manganese cycling in the lake, but unlike phosphorus, which decreases with depth in the sediment, there is little evidence of this in Lake Rotorua.

Burger (2006) estimated that the total phosphorus sediment release rates increased from 8.8 to 26.3 mg m⁻² day⁻¹ during a stratification period lasting 19 days in February, 2003. The high release rates occurred on days in the stratification period coinciding with a general decrease in dissolved oxygen in the bottom waters of the lake. From a mass balance for nutrients in Lake Rotorua, Beyá (2005) estimated the net retention of total phosphorus to be 2.1 mg m⁻² yr⁻¹ in the bottom sediments. This value is approximately 10 times lower than that calculated by

Burger (2006) which suggests that phosphorus is recycled many times between the water column and the sediment before it is either lost via the outflow or buried in the sediment.

The slower rate of oxidation of manganese, compared with iron, leads to a peak of particulate manganese higher in the sediment than that of iron (Mayer *et al.* 1982) although in Lake Rotorua concentrations of both elements peak within the top 1 cm of the sediment, so are not distinguishable in the sediment data, in contrast to other lakes in the Rotorua region, such as Lake Tarawera and Rotoma (Carminie and Hendy, 2004; Barker and Hendy, 2006). An orange-brown layer was observed on the surface of some gravity cores (Appendix 1: Ru137), which is likely to be due to ferric oxyhydroxide. Iron II may diffuse upwards in the sediment profile and is likely to be trapped by oxidation in the surficial sediments.

Carbon and nitrogen are principal components of organic matter brought with the accumulating sediment by both diatoms and other phytoplankton along with contributions from other allochthonous and autochthonous sources. This material tends to be rapidly remineralised by decomposers. While there is sufficient dissolved oxygen available, this will be utilised, but as pore waters become anoxic during stratified periods, sulfate, ferric and manganate will be reduced. As other electron acceptors are exhausted anaerobic fermentation can convert much of the remaining organic matter into methane and carbon dioxide. Gas bubbles were observed in the diatomaceous material of the sediment cores. High supply rates of organic matter to the bottom sediments may be important in sustaining high rates of sediment nutrient release, particularly in eutrophic lakes (Søndergaard *et al.*, 2003).

The Redfield atomic ratio for diatoms is about 50 atoms of silicon, 106 atoms of C and 15 atoms of N (Redfield, 1937; Goldman, 1980). At these ratios diatoms settling into the sediment would produce sediment containing by mass approximately 40% C and 7% N. Figure 5.13 shows approximately 4% carbon and 0.7% nitrogen are retained in the surface 40 cm of the sediment indicating that more than 90% of the carbon and nitrogen is recycled within the water column. Along with iron and manganese, organic matter competes for the binding

or sorption of trace metals, with the overall importance of each component related to its abundance relative to other components of the sediments (Bendell Young and Harvey, 1992). Remineralisation of the organic matter will release the adsorbed trace metals and contribute to their recycling.

A linear increasing trend in mean baseflow of nitrate concentration has been identified in 8 of the 9 major stream inflows over the period 1968-2002 (Rutherford, 2003). Organic nitrogen mineralisation produces ammonium ions, which may then be nitrified to nitrate, and denitrification may subsequently reduce nitrate to nitrogen gas (McCarthy *et al.*, submitted 2007). McCarthy *et al.*, (2007) found that denitrification in Lake Rotorua was fuelled primarily by overlying water nitrate rather than nitrate from nitrification. No potential dissimilatory nitrate reduction to ammonium was observed in Lake Rotorua. The porewater samples analysed by Motion (In Prep.) were taken from the sediment cores used for this study. Most of the porewater nitrogen is converted to ammonium ions, which then can be transported back into the overlying water column. Diffusion, bioturbation, gas ebullition and sediment resuspension all contribute to the movement of ammonium through the sediment (Song *et al.* 2003).

5.4.2 Sediment Accumulation

Highest sediment accumulation rates are in areas with water depths greater than 20 m. Burger (2006) estimated the fraction of total particulate matter derived from resuspension to be up to 71% at a site in 7 m water depth. Since 34% of the lake area is less than 7 m deep there is a large potential for sediment resuspension. In deeper water, Burger (2006) estimated that 47 % of the total particulate matter captured in 20 m water depth was contributed by resuspension. Therefore, resuspension of particulate matter is highest in the shallow water.

The accumulation of phosphorus in the sediments calculated from the coring programme is 29.6 t/yr (Table 5.1). This is very close to the difference between inflows and outflows from the lake of 29.8 t/yr from the phosphorus budget (Section 5.3.2). Internal nutrient loads are thought to represent a substantial portion of the total lake nutrient load (Fish, 1975; Rutherford *et al.*, 1996),

particularly in association with summer stratification events and rapid reductions in bottom water concentrations of dissolved oxygen. Beyá (2005) estimated the net internal cycling to be 24 t/yr or 30% of the total inflow. Burger (2006) showed that sedimentation rate of total particulate material (TPM) is in the range 1.8 to 8.2 g m⁻² d⁻¹ and variations within the range were due to the season and water depth. The material sedimenting has a high total phosphorus content of 4.2 mg P g TPM⁻¹ (Burger, 2006).

5.5 SUMMARY

Sediment accumulation is generally highest in Lake Rotorua in water depths greater than 15 m. Wave action keeps fine material suspended in the shallower water and it is deposited in areas of lower turbulence. The bulk of the sediment is made up of diatom frustules composed of silica; therefore the composition of other elements in the sediments is related to the lake composition at the time of diatom deposition, although diagenesis in the sediment differentially changes elemental concentration. Diatoms extract elements (C, H, O, P, N, Si and trace elements) from the surrounding water in approximate proportion to their Redfield ratios. As these elements are metabolised most of the organic matter is remineralised, leaving silica minerals with a very large surface area. This material provides sites for adsorption and ion exchange so that the settling frustules also transport iron and manganese oxides/hydroxides and many co-precipitated and adsorbed trace metals from the water column to the sediments.

Phosphorus concentration in Lake Rotorua sediments decreases with sediment depth. In the centre of the lake phosphorus concentrations in the top 2 cm can reach 2500 g/tonne and decline to 800 g/tonne by 20 cm depth. Accumulation rate of phosphorus in the sediment is 29.6 t/yr. Iron and manganese concentrations in the sediment are dependent on the availability of the element and the sedimentation rate of diatom frustules, and are controlled by the redox conditions in the sediment. The average concentration of iron and manganese in the sediment is approximately 8000 g/tonne and between 300 and 400 g/tonne, respectively. Iron accumulates at a rate of 385.1 t/yr and manganese 17.9 t/yr in the sediment. Maximum concentrations of arsenic in the sediment are 250 g/tonne but are generally between 50-100 g/tonne, depending on the water depth. Lead

concentrations are typically below 15 g/tonne. Sediment concentrations of both arsenic and lead are highly correlated with iron and manganese in the sediment and mimic the concentration profiles. Arsenic and lead accumulate in the sediment at a rate of 3.71 and 0.49 t/yr, respectively. Sulfur concentrations typically reach 8000 g/tonne in the centre of the lake. Below the Tarawera tephra, sulfur concentrations exceed those observed above the tephra. All elements show a peak in concentration in the tephra layers.

Concentrations of carbon and nitrogen in the surface sediment are typically c. 5 % and 0.7 %, and decline with depth to <2 % and 0.4 %, respectively. The rapid decrease in carbon and nitrogen concentration in the sediment shows that most of the remineralisation and recycling through diagenesis takes place within the top 50 cm, but mostly within the top 10 cm.

REFERENCES

- Barker, A. and Hendy C.H. 2006. The accumulation of phosphorus and trace elements in the sediment of Lake Rotoma. New Zealand Freshwater Sciences Society Conference, Rotorua.
- Bauer, M. and Blodau, C. 2006. Mobilization of arsenic by dissolved organic matter from iron oxides, soils and sediments. *Science of the Total Environment*. 354: 179-190.
- Belzile, N. and Tessier, A. 1990. Interactions between arsenic and iron hydroxides in lacustrine sediments. *Geochimica et Cosmochimica Acta*. 54:103-109.
- Bendell Young, L. and Harvey, H.H. 1992. The relative importance of manganese and iron oxides and organic matter in the sorption of trace metals by surficial lake sediments. *Geochimica et Cosmochimica Acta*. 56: 1175-1186.
- Benoit, G. and Hemond, H.F. 1990. Po and Pb remobilization from lake sediments in relation to iron and manganese cycling. *Environmental Science and Technology*. 24:1224-1234.
- Beyá, J., Hamilton, D. and Burger, D. 2005. Analysis of catchment hydrology and nutrient loads for lakes Rotorua and Rotoiti. Centre for Biodiversity and Ecology Research, University of Waikato, Hamilton.
- Burger, D. B., 2006. Dynamics of internal nutrient loading in a eutrophic polymictic lake. Ph.D. Thesis, Department of Biological Sciences, University of Waikato.
- Burger, D. F., Hamilton D.P., Pilditch C.A., Gibbs M.M., and Hall J.A., 2005. Sediment phosphorus release during stratification in polymictic Lake Rotorua, New Zealand. *Verhandlung Internationale Vereinigung de Limnologie* 29: 811-814.
- Carmine, M. and Hendy, C.H. 2004. Trace element distribution in Lake Tarawera sediment. New Zealand Freshwater Sciences Society Conference, Rotorua.
- Davies, B.E. 1990. Lead. In Alloway, B.J. *Heavy Metals in Soils*. Blackie and Sons Ltd. London. pp177-194.
- Davison, W. 1993. Iron and manganese in lakes. *Earth-Science Reviews*. 34: 119-163.
- Fish, G.R. 1975. Lakes Rotorua and Rotoiti, North Island, New Zealand: Their trophic status and studies for a nutrient budget. Fisheries Research Division, New Zealand Ministry of Agriculture and Fisheries. Wellington. 72p.
- Gálvez, J.A. and Niell, F.X. 1992. Sediment resuspension in a monomictic eutropic reservoir. *Hydrobiologia*. 235/236: 133-141.

- Goldman, J.C. 1980. Physiological processes, nutrient availability and the concept of relative growth rate in marine phytoplankton ecology. In: Falkowske, P.G. *Primary Production in the Sea*. Plenum Publishing Corporation. pp 179-193.
- Hilton, J., Long, G.J., Chapman, J.S. and Lishman, J.P. 1986. Iron mineralogy in sediments. A Mössbauer study. *Geochimica et Cosmochimica Acta*. 50: 2147-2151.
- Hoare, R.A. 1980. The sensitivity to phosphorus and nitrogen loads, of Lake Rotorua, New Zealand. *Progress in Water Technology*. 12: 897-904.
- Katesv, S., Tsandev, I., L'Heureux, I. and Rancourt, D.G. 2006. Factors controlling long-term phosphorus efflux from lake sediments: Exploratory reactive-transport modelling. *Chemical Geology*. 234:127-147.
- Luther, G.W., Kostka, J.E., Church, T.M., Sulzberger, B. and Stumm, W. 2003. Seasonal iron cycling in the salt-marsh sedimentary environment: the importance of ligand complexes with Fe(II) and Fe(III) in the dissolution of Fe(III) minerals and pyrite, respectively. *Marine Chemistry Journal*. 40(1-2):81-203.
- MacKay, K.M., MacKay, R.A. and Henderson, W. 2002. *Introductions to Modern Inorganic Chemistry*. 6th Edition. Nelson Thornes Ltd. Cheltenham, UK.
- Mangan, C.M. In Prep. *The Sequestration of Phosphorus by Iron Phases in Sediments from Lake Rotorua, New Zealand*. MSc Thesis, Department of Chemistry, University of Waikato.
- Mayer, L.M., Liotta, F.P. and Norton, S.A. 1982. Hypolimnetic redox and phosphorus cycling in hyper-eutrophic Lake Sebasticook, Maine. *Water Research*. 16:1189-1196.
- McCarthy, M.J., Burger, D.F. Hamilton, D.P., Hendy, C.H. and Gardner, W.S. 2007. Sediment-water interface nitrogen transformations in lakes Rotorua and Rotoiti (North Island, New Zealand): Does dissimilatory nitrate reduction to ammonium (DNRA) contribute to water column ammonium accumulation? 30th Congress of the International Association of Theoretical and Applied Limnology, taking place August 12-18th, 2007.
- Morgenstern, U. and Gordon, D. 2006. *Prediction of Future Nitrogen Loading to Lake Rotorua*. GNS Science. Consultancy Report: 2006/10.
- Mortimer, C.H. 1941. The exchange of dissolved substances between mud and water in lakes. *Journal of Ecology*. 29:280-329.
- Redfield A.C., 1937. On the proportions of organic derivations in seawater and their relation to the composition of plankton. In: Daniel R.J. (ed.) *James Johnson Memorial Volume*. University Press of Liverpool, pp. 177-192.

- Rutherford, J.C., Dumnov, S.M. and Ross, A.H. 1996. Predictions of phosphorus in Lake Rotorua following load reductions. *New Zealand Journal of Marine and Freshwater Research*. 30: 383-396.
- Rutherford, K. 2003. Lake Rotorua Nutrient Load Targets. NIWA Client Report: HAM2003-155. Prepared for Environment Bay of Plenty.
- Søndergaard, M., Kristensen, P., and Jeppesen, E. 1992. Phosphorus release from resuspended sediment in the shallow and wind-exposed Lake Arresø, Denmark. *Hydrobiologia*. 228: 91-99.
- Song, J., Luo, Y., Zhao, Q. and Christie, P. 2003. Novel use of soil moisture samplers for studies on anaerobic ammonium fluxes across lake sediment-water interfaces. *Chemosphere*. 50: 711-715.
- Wetzel, R.G. 2001. *Limnology – Lake and River Ecosystems*. 3rd Edition. Academic Press, USA. 1006pp.

CHAPTER SIX:

GEOPHYSICAL SURVEY



6.0 INTRODUCTION

This chapter provides details of the bathymetry and stratigraphy of Lake Rotorua using multibeam and sub-bottom profiling systems. It includes an introduction to the multibeam and sub-bottom profiling systems and presents a survey carried out with these instruments on Lake Rotorua. It explains how the multibeam and sub-bottom profiling systems are operated and methodology of the survey. Features are identified around the lake margins and on the lake floor including the location of gas in the sediment, pockmarks and hydrothermal activity.

6.1 THE MULTIBEAM SYSTEM

A multibeam survey was undertaken to determine the bathymetry of Lake Rotorua and identify features on the lake bed. A comparison can be made between the bathymetry mapped by Irwin (1969) (Figure 2.8) by interpolating between a series of echo sound survey tracks across the lake and the multibeam technique.

6.1.1 Introduction to the Multibeam

Multibeam technology has been in use since the 1960s, by the US Military. Declassification of multibeam seafloor sounding systems in the 1980s and the recent emergence of computer hardware capable of processing the vast amount of data collected, multibeam systems have become a highly efficient means of obtaining a “full coverage” survey of the sea floor (Hughes-Clark *et al.*, 1996; Blacquiere and van Woerde, 1998). Thus instead of interpolating between a series of survey tracks, dense soundings can be collected from the entire seafloor and virtually no interpolation is required to produce the physiographic surface (Gardner *et al.*, 2003), as depicted in Figure 6.1.

A multibeam ecosounder works by emitting sound pulses from a transducer perpendicular to the vessel track. The returning echoes from the ensonified sea bed are averaged based on a central point in the beam footprint, to give an individual depth point (Miller *et al.*, 1997). Multibeam frequencies are between 100 and 450 kHz, with beams emitted from the transducer at typically 120° (port-starboard direction). In the fore-aft direction the beams are emitted at only 1.5°, creating a narrow ray of sonar beams (Blacquiere and van Woerde, 1998). The

width of the fan causes the outer beams to reach the seafloor later and at a larger angle than the inner beams, generally resulting in higher accuracy for beams that are closer to the nadir region. The beam location is calculated by taking into account the elapsed time, angle and strength of the returning signal to the transducer (Mallace, 2002).

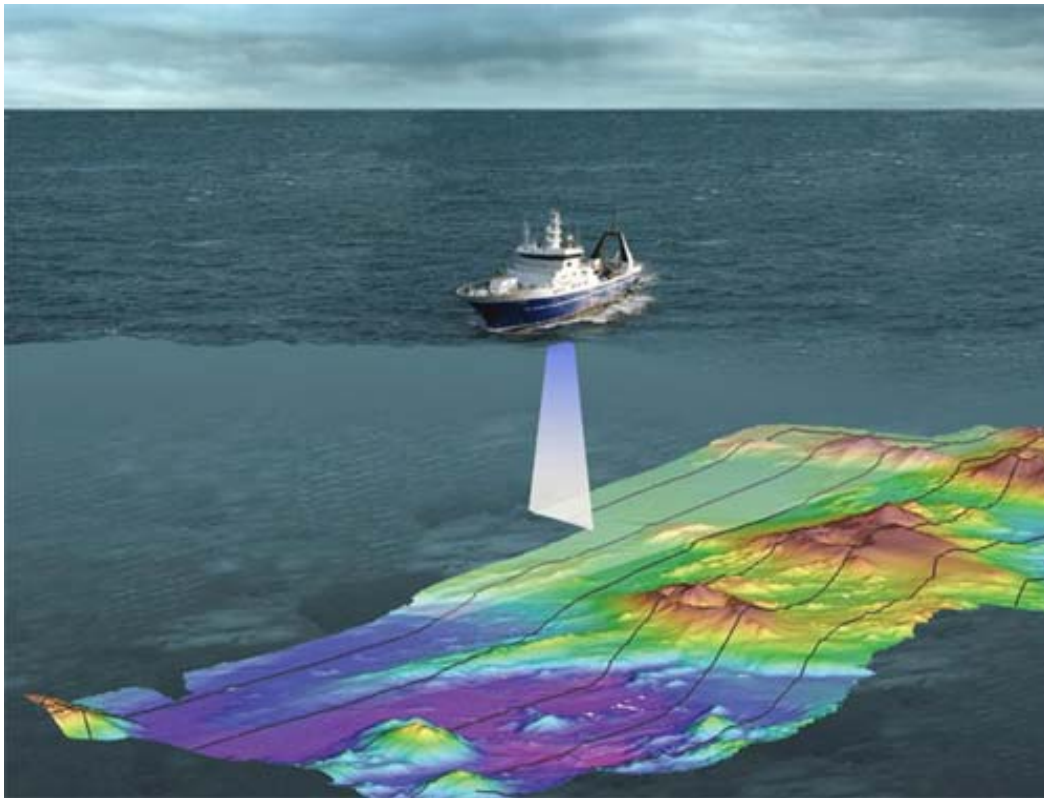


Figure 6.1: Research ship R.V. Tangaroa and an artist's depiction of the beam of sound waves mapping the ocean floor using a Simrad EM3000 Multibeam (Pickrill and Barnes, 2003).

Multibeam systems are used mostly in marine settings, but they are not confined to this environment. Lakes, estuaries and rivers are all suitable environments for a multibeam surveys. Since 2003, The University of Waikato, Coastal Marine Group has carried out a number of surveys using the SIMRAD EM3000 Echo Sounder. Multibeam echo soundings have been conducted of the Tauranga Harbour and Mt Manganui Beach (Scarfe, 2002; Spiers, 2005) and the Karapiro to Ngaruawahia reach of the Waikato River (Wood, 2006).

6.1.2 SIMRAD EM3000 Multibeam Echosounding

The SIMRAD EM3000 Multibeam Echo-sounder is a 300 kHz, beam-forming system capable of obtaining full bottom coverage at depths of 0.5 to 150 m (Flood *et al.*, 1999). The EM3000 has a swath width of 120°, which typically corresponds to 3.5-4 times the water depth and a narrow beam width of 1.5°. The system transmits 127 beams perpendicular to the vessel track at a maximum ping rate of 20 times per second (Flood *et al.*, 1999; Coastal Marine Group, 2004). The multibeam system comprises of two major components; the EM3000 echo-sounder which is fixed to the hull of the boat and houses the transducers that emit and receive the swath of ultrasonic energy (Figure 6.2); and the TEI (Triton Elics International) data acquisition and processing system, which receives the raw data and allows for real-time and post processing (Figure 6.3).



Figure 6.2: SIMRAD EM 3000 transducer, bow mount on the Coastal Marine Group vessel *Tai Rangahau* (Coastal Marine Group, 2004).



Figure 6.3: Computer hardware for Multibeam data acquisition and processing inside *Tai Rangahau* (Coastal Marine Group, 2004).

The multibeam system also requires a number of constituents to obtain accurate data. An altitude and heading system is required to attain the exact heading and boat motion information. A TSS MAHRS (Meridian Altitude and Heading Reference System) (Figure 6.4a) has a built-in motion sensor which is used to determine the pitch, roll and heave of the boat. The internal gyroscope compass determines the heading and corrections are applied to the data during post processing. Exact position is accounted for by the Trimble MS 750 RTK (Real-Time Kinematic) GPS (Global Positioning System) (Figure 6.4b). The fast update rate (up to 20 Hz) is necessary for use in shallow water and provides accurate positioning, to ~ 0.02 m (Trimble Ltd, 2005). The RTK GPS provides X and Y axis positions and also Z axis for tidal control and heave corrections. The speed of

sound can vary through the water column with changes in water pressure (depth), salinity and temperature. These changes can cause refraction of the sonar beams passing through the water column, altering interpretation of the returning sound signal. Compensation for the errors are corrected by taking repeated sound velocity profiles using an AML Sound Velocity Profiler (SVP) (Figure 6.4c). The SVP details the changes to the speed of sound in the water column and inputs the data into the system prior to and during surveying.

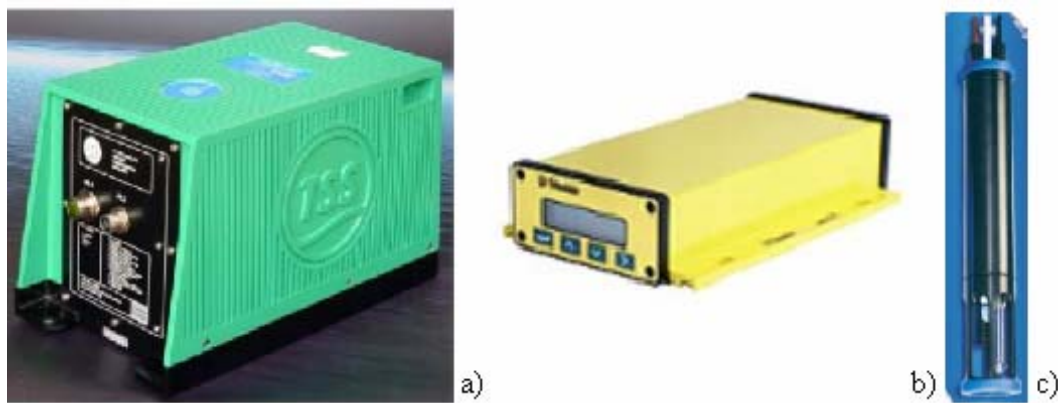


Figure 6.4: a) Meridian Altitude and Heading reference System (MAHRS) b) Trimble MS 750 RTK GPS c) AML Sound Velocity Profiler (Coastal Marine Group, 2004).

Despite best efforts to minimize errors, several factors can affect data resolution and accuracy, resulting in misleading artifacts in the data or incomplete coverage. Long period horizontal accelerations (i.e. line turns) are unable to be completely compensated for by the motion sensor, resulting in inaccurate roll corrections in the data (Hughes-Clark *et al.*, 1996). This effect can be minimized by: only collecting data when the vessel is traveling in straight lines, by turning off the transmitter when the boat is turning until it is aligned on the next track. In shallow water and with smaller survey vessels, the wave height can also affect the ability of the motion sensor to record accurate data. Data collection in this study was restricted to days with calmer weather to minimize inaccuracies data. The ping repetition rate and vessel speed affect the beam coverage and resolution. The faster the vessel speed the lower the amount of pings able to be transmitted and received, therefore lowering the resolution (Miller *et al.*, 1997). During the

survey the boat speed on Lake Rotorua was less than 5 knots during data collection to ensure a high data resolution.

6.1.3 Data Collection

A multibeam survey was undertaken on Lake Rotorua between August and December 2006 by Dirk Immenga, Brad Scarfe and Alex Schimel, Coastal Marine Group at the University of Waikato. The multibeam was run in track lines from the 10 m water depth contour on the University of Waikato vessel, *Tai Rangahu*. A single beam low frequency echo sounder was also run simultaneously with the multibeam survey. Data acquisition took place on an onboard system using Triton Elics Software.

6.1.4 Multibeam Post-Processing

Multibeam data post-processing was carried out by Brad Scarfe and Alex Shimel from the Coastal Marine Group at the University of Waikato using software by Triton Imaging Inc. ISIS Sonar software is used to identify ‘bad’ data by running the coverage map, where the path of the vessel and the lake bed sonified by the multibeam are displayed. The map is determined by the GPS position recorded, so that in areas where full GPS dropout (no signal from autonomous or DGPS) occurs the anomaly in the visualisation and can be manually removed. *Bathyprow* software is used to process the multibeam files from an .xtf file extension to a visual information file (dds.vif) which enables the information to be viewed in *Delphmap*. Processing parameters carried out in *Bathyprow*, which require corrections are: vessel navigation settings, gyro (TSS MAHRS), suppressing the bad beam quality data and applying a tide correction. The data output settings are also determined at this stage. Small holes in the data set are filled by smoothing the grid resolution of the multibeam soundings where a text file output of XYZ coordinates are recorded with those of neighbouring data in the final processing of the data set.

Two output files are produced from the post-processing. A text file contains the northing, easting and elevation (XYZ) and can be used in most GIS software programmes, when converted into an Arc Raster file (for use in *ArcMap*). The second output file is a Visual Information File (VIF), which can be used in

Delphmap. The imagery files in *Delphmap* are displayed according to the geocoding that accompanies the file creating a mosaic. GeoTIFF images, which are a raster file format that holds the geographic position information for the image and can be exported and used for display in *ArcMap*. *Delphmap* enables 3D contact images to be produced which were used for identifying the sub-bottom features.

6.2 SUB-BOTTOM PROFILING

Single beam echo-sounders have been in use considerably longer than multibeam sounders and have been used extensively around the world to map the bathymetry of many marine and freshwater environments. The bathymetry of Lake Rotorua was originally surveyed in November 1966 by the Fisheries Research Division. A provisional bathymetric map was produced by Irwin (1969) by interpolating between a series of echo-sound survey tracks across the lake. Sub-bottom profiling was carried out on Lake Rotorua in 1990, by the DSIR Division of Geology and Geophysics. Research by Davy (1992) identified a strong lake floor reflector which masked almost all underlying reflectors. The strong reflector was interpreted as a layer of gas-charged sediments. Other gas characteristics were observed such as pockmarks in association with the reflector.

6.2.1 Sub-bottom Profiling Data Collection

Sub-bottom profiling was carried out simultaneously with the Multibeam survey on Lake Rotorua using a low-frequency single beam echo-sounder (KNUDEN 320 MP). The frequencies that were used are 33 and 200 kHz. Positional information was recorded by Real Time Kinematic GPS, accurate to ± 0.05 m. The single beam was run in track lines (Figure 6.5) from the shore to the 10 m water depth contour on the 6 m long University of Waikato vessel *Taitimu*, before being transferred to the larger, 9 m long, *Tai Rangahu*, which was used to cover the remainder of the lake. A complete sediment record was unobtainable due to the interference of gas trapped in the sediment. Analysis of the track lines were carried out using *Post Survey* which is part of the 'Sunder Suite'.

6.2.2 Sub-bottom Profiling Data Analysis

Data processing of the sub-bottom profile tracks was undertaken by Brad Scarfe, Coastal Marine Group. The sub-bottom data was saved as text files and converted into *ArcGIS* format to produce an *ArcMap* file and *ArcGIS* geodatabase file, which was used to locate the sub-bottom profile tracks (Figure 6.5) (See Appendix 4 for close up images with track lines identified).

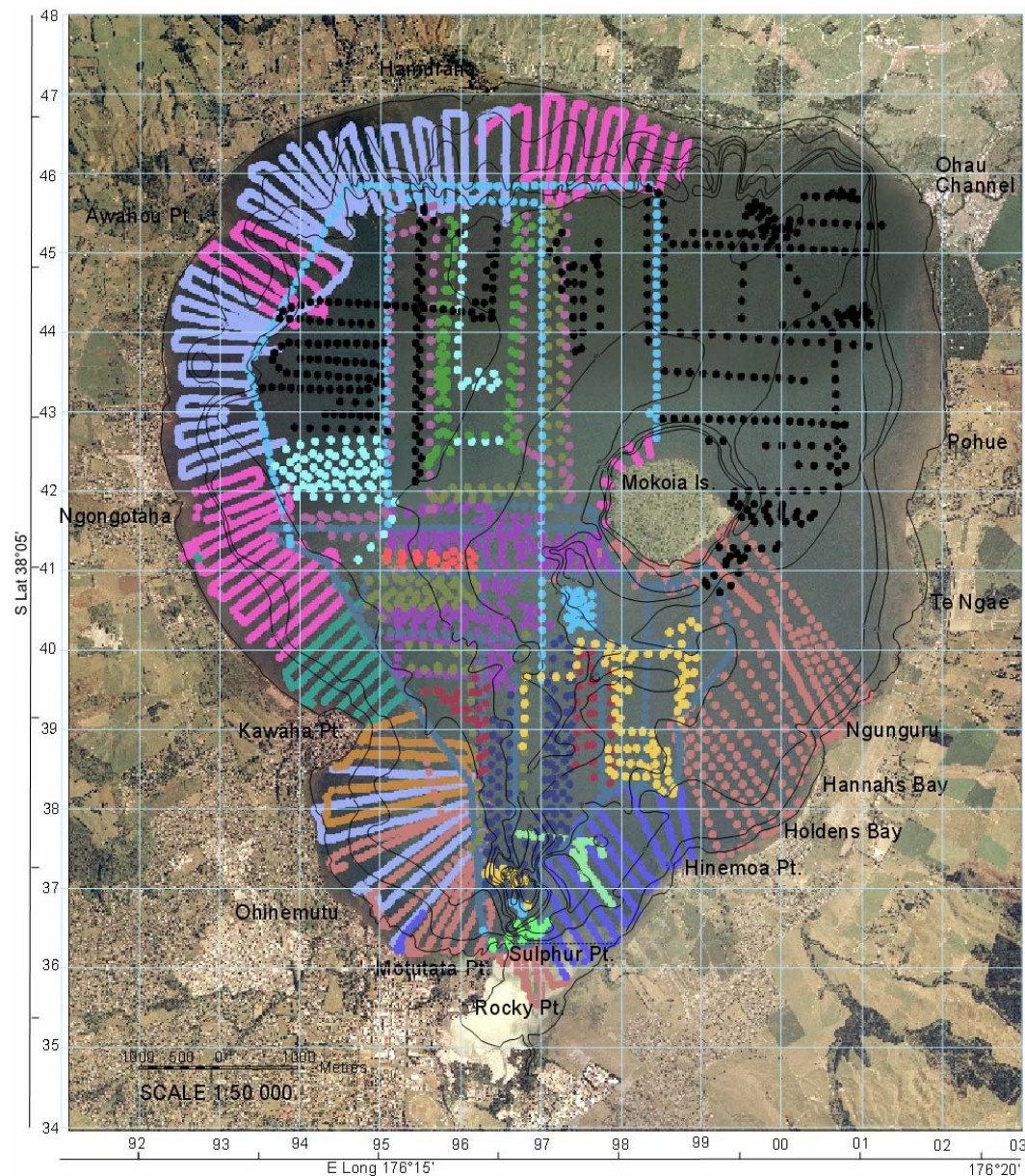


Figure 6.5: Low frequency echo-sounder track lines.

Post Survey was used to view the tracks from the echo-sounder to describe the tracks (Appendix 4) and identify features of interest on the lake bed. Once a

feature was identified the date and time parameter in NZST or NZDT was recorded and converted to UTC (NZST-12h or NZDT-13h). Multibeam data was then able to be played back using ISIS software to match the time of the sub-bottom feature. In *Delphmap*, an image and grid reference of the feature surveyed by the multibeam was produced to match the track from the sub-bottom profiling.

6.3 RESULTS OF THE GEOPHYSICAL SURVEY

The results of the geophysical survey are used to determine the bathymetry, stratigraphy of the sediment and the significance of gas in the sediment of Lake Rotorua. The bathymetric map of the lake produced by the multibeam shows a large amount of detail, allowing some characteristics of the sediment to be identified. The sub-bottom profiling survey allows the identification of buried tephra layers in the sediment, revealing the stratigraphy to a greater coverage than the coring programme. Gas generation in the sediments of Lake Rotorua is a significant factor influencing features found on the lake floor.

6.3.1 Bathymetry

Lake Rotorua is currently at 280 m above sea level. It has had a complex history of fluctuating lake levels caused by volcanic activity which have altered Lake Rotorua significantly since its formation. Variations in lake level have been predominantly due to volcanic or tectonic disruption to the drainage systems and down-cutting of outlet channels.

The bathymetry of Lake Rotorua (Figure 6.6) is dominated by a curved depression extending from Sulphur Point and almost reaching the Ohau Channel. This depression is probably a structural feature likely associated with the collapse of the caldera, but could be an ancient drainage channel. Infilled material from the Rotoehu eruption (~65 kyr) was naturally eroded to form the Ohau Channel. For the depression to be a drainage channel, lake level has to be at least 25 m (255 m asl) shallower than it is now. Esler (In Prep) has identified at least two periods when lake level was less than 260 m asl.

Mokoia Island is surrounded by a depressed ring typically 800 m from the shore of the island. This ring is possibly a crustal depression associated with the formation of the rhyolite dome (Mokoia Island), which stands at 451 m asl (170 m above lake level). A ring shaped bathymetric high (270 m asl) occurs approximately 1.5 km off Mokoia Island in the south and east of the lake. This could also be related to the local crustal depression associated with the rhyolite dome. Ring faulting may have occurred as chains of pockmarks are found in the depression around Mokoia Island. The pockmarks could result from methane loss, spring discharges and hydrothermal explosion creators, as both flat-bottomed and cylindrical pockmarks were identified during the multibeam survey.

Terraces in the north show the underlying structure of cross-cutting and eroded tephra unconformities. These terraces are possibly formed by the collapse of the northern margin (Esler, In Prep.), where spires that were eroded at the lake level are now positioned 10 m below the lake level. Terraces are also found up to 13 m above lake level on Mt Ngongotaha at the southern end of the lake (Figure 2.5).

The raw multibeam data map (Figure 6.7) produced from the survey shows the areas of full to partial coverage with the multibeam. Areas in red are in less than 10 m water depth and the blue areas are greater than 20 m. The multibeam data processing is at 5 m resolution which results in a loss of bathymetric detail in Figure 6.6. Further processing of the data needs to be completed to achieve a higher resolution bathymetric map, but unfortunately was not completed in time for this thesis.

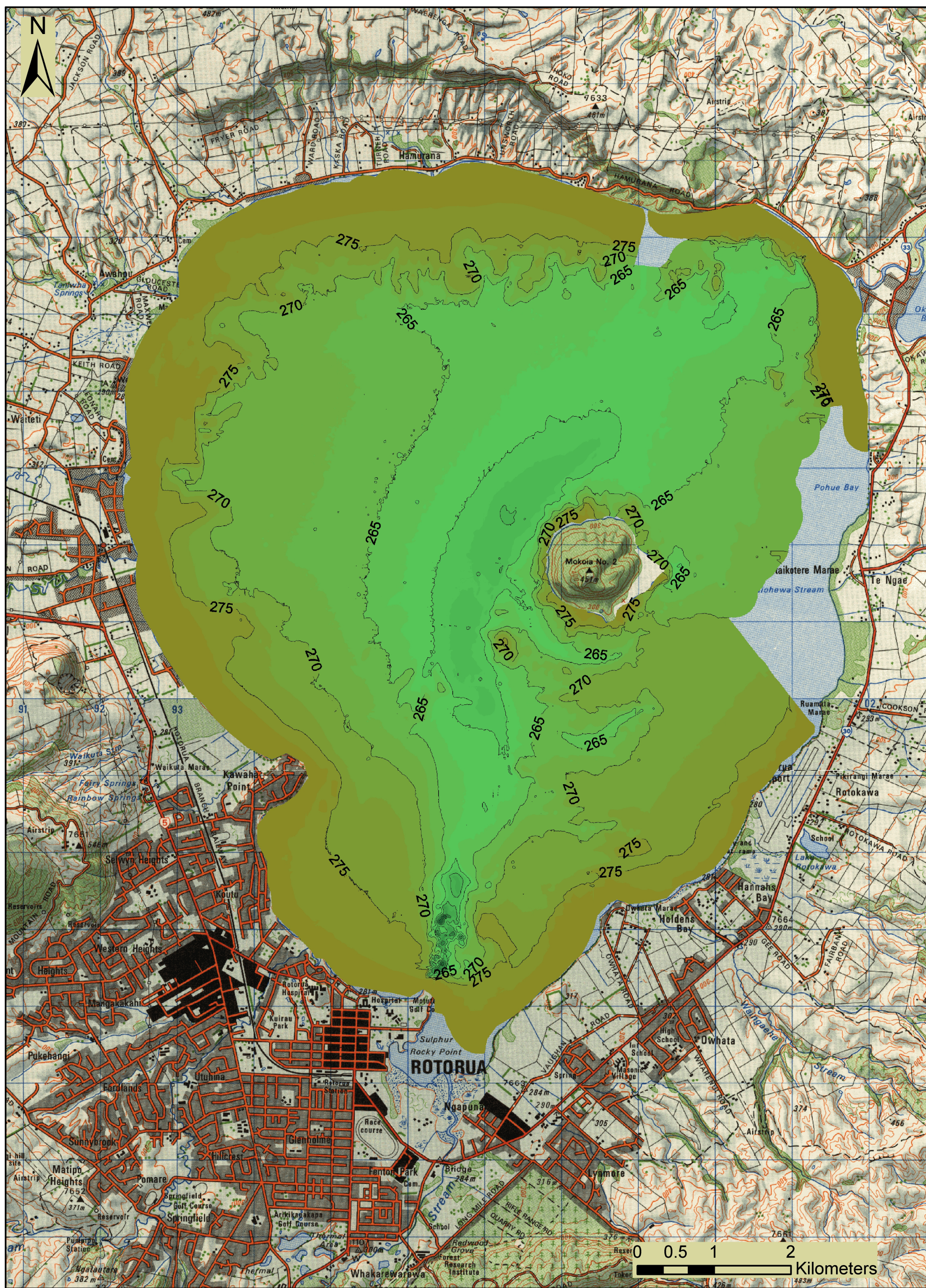


Figure 6.6: Bathymetric map of Lake Rotorua produced from the multibeam survey

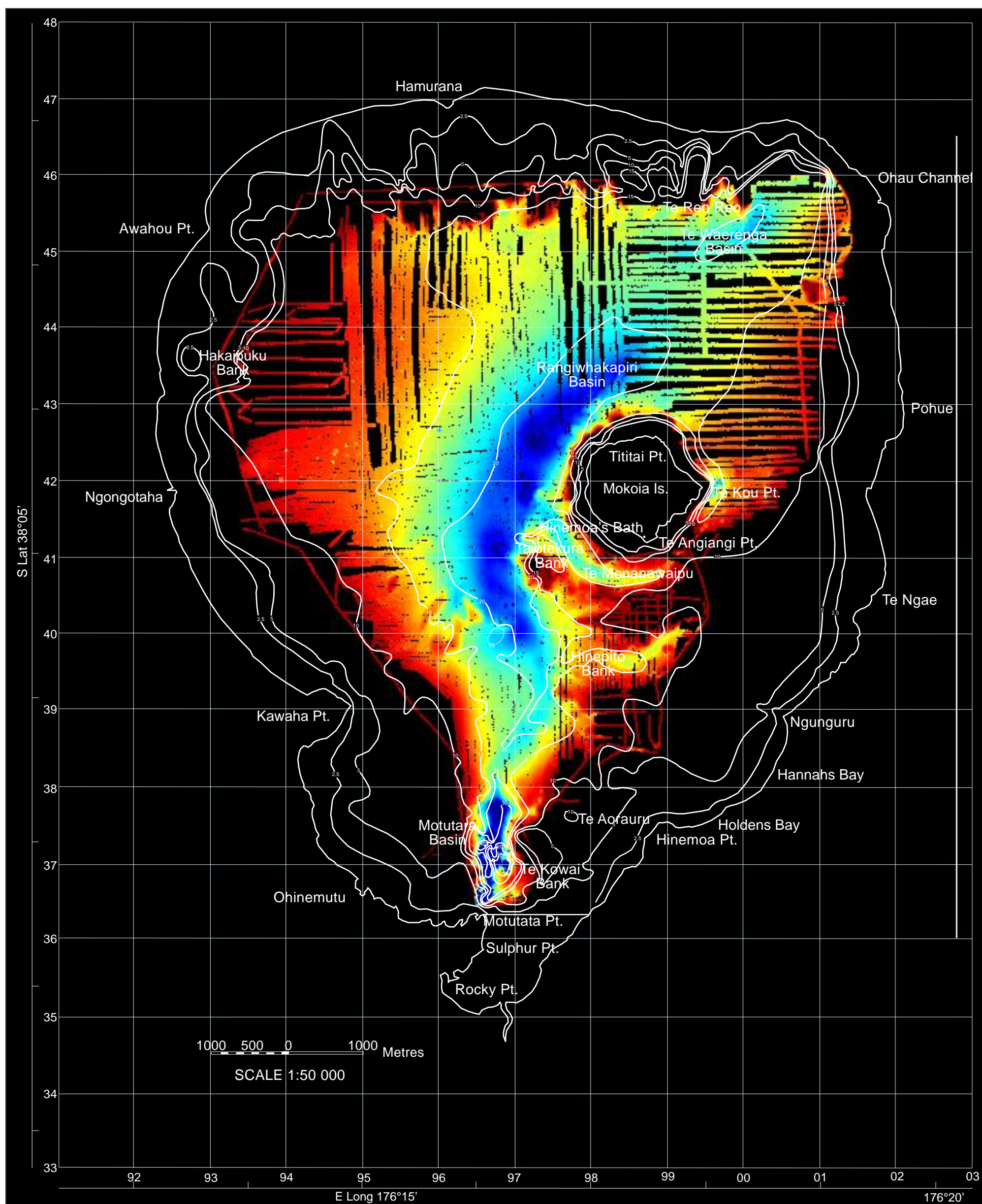


Figure 6.7: Raw multibeam data of Lake Rotorua showing areas of coverage over the lake.

6.2.1 Lake Margins

Around the lake margins the coring programme established that the sediment is predominantly coarse sandy material and reworked tephra. Limited seismic penetration is recorded in the lake margins (Figure 6.8). It is possible that the Tarawera Tephra occurs approximately 0.5 m below the sediment surface and the Kaharoa, 3 m below the sediment surface.

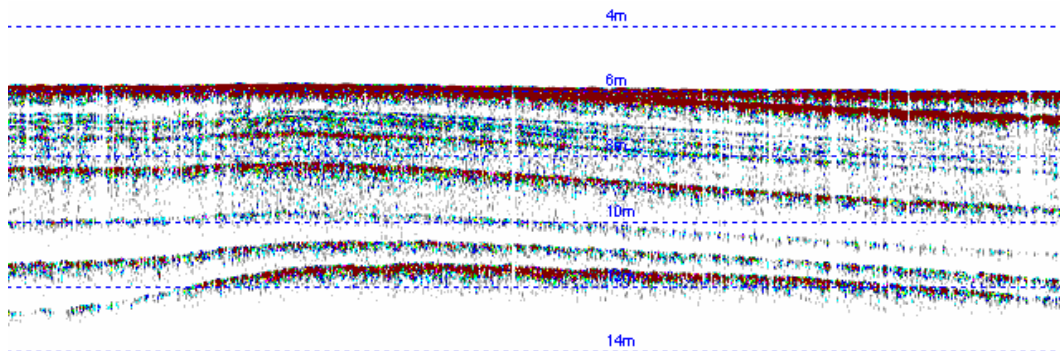


Figure 6.8: Typical stratigraphy visible in lake margins of Lake Rotorua.

In water depths less than 10 m a series of nearshore terraces is preserved in the sediment to the north in the lake. The terraces have formed in response to wave action at different lake levels. Kennedy *et al.* (1978) reported that from 17 000 to 9000 years B.P. the lake level of Rotorua was approximately 3 m lower than the present level. Similar terraces have been found by Pickrill (1993) in Lake Rotoiti and Nelson (1983) in Lake Rotoma. The terraces in Lake Rotorua and Lake Rotoiti were probably cut during the time of low lake level between 17 000-9000 years B.P.

6.3.3 Lake Floor

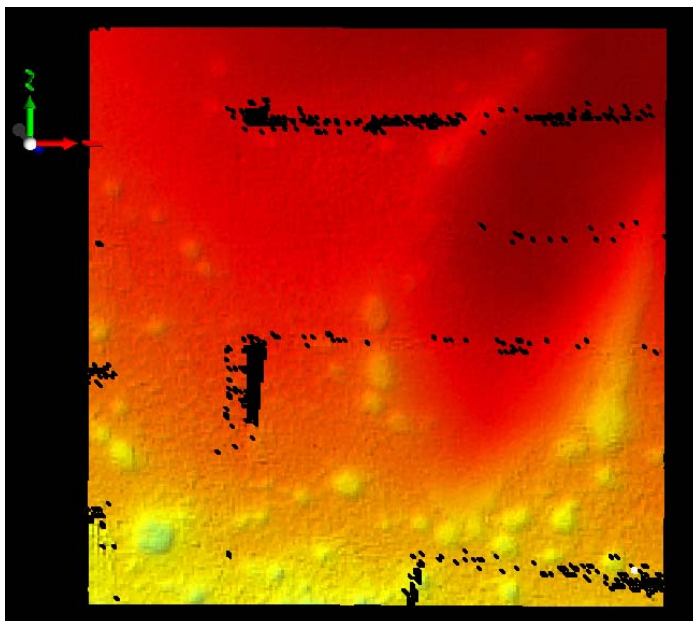
The lake floor is covered in diatomaceous ooze. Diatomaceous sediment accumulates faster in areas of deeper water (see Chapter 4) and sub-bottom profiles are dependent on the water depth. As water depth increases diagenetic processes in the sediment produce methane gas. Gas accumulation in the sediment masks sonic reflectors. Davy (1992) recognised the presence of gas in Lake Rotorua sediments by the negative polarity of the initial pulse reflected at the lake floor, and the constant phase of lake floor-lake surface multiples during a uniboom seismic reflection trial in 1990.

Volcanism influences the sedimentation of Lake Rotorua as there have been at least eight major airfall events in the last 11 850 years (Froggatt and Lowe, 1990). Tephra layers have been deposited from both subaerial and subterranean sources. Pickrill (1993) correlated the sub-bottom reflectors seen in Lake Rotoiti with those described by Froggatt and Lowe (1990) (Table 6.1) from soil profiles in the region. Unfortunately sub-bottom penetration in Lake Rotorua is generally <10 m into the sediment and reveals down to the Taupo tephra.

Table 6.1: Major tephra formations (Froggatt and Lowe, 1990).

Tephra name	Approximate age (years)	Thickness (cm)
Tarawera Tephra	105	5-20
Kaharoa Tephra	770	30-100
Taupo Tephra	1850	20
Rotokawau Tephra	3440	30-60
Whakatane Tephra	4830	40
Mamaku Tephra	7250	70-220
Rotoma Tephra	8530	40-300
Waiohau Tephra	11 850	250

In shallow water environments (depth ~12 m) the lake floor is typically covered in small pockmarks. The stratigraphy observed by sub-bottom profiling is either thin tephra or depositional sand layers similar to those in the lake margins (Figure 6.8) or gaseous diatomaceous sediment (Figure 6.9). Small dome features were observed corresponding to diatomaceous ooze accumulating over tephra deposits.



a)

Location of feature:
38° 05 21 S
176° 17 11 E
Sub-bottom track:
ROT7_010

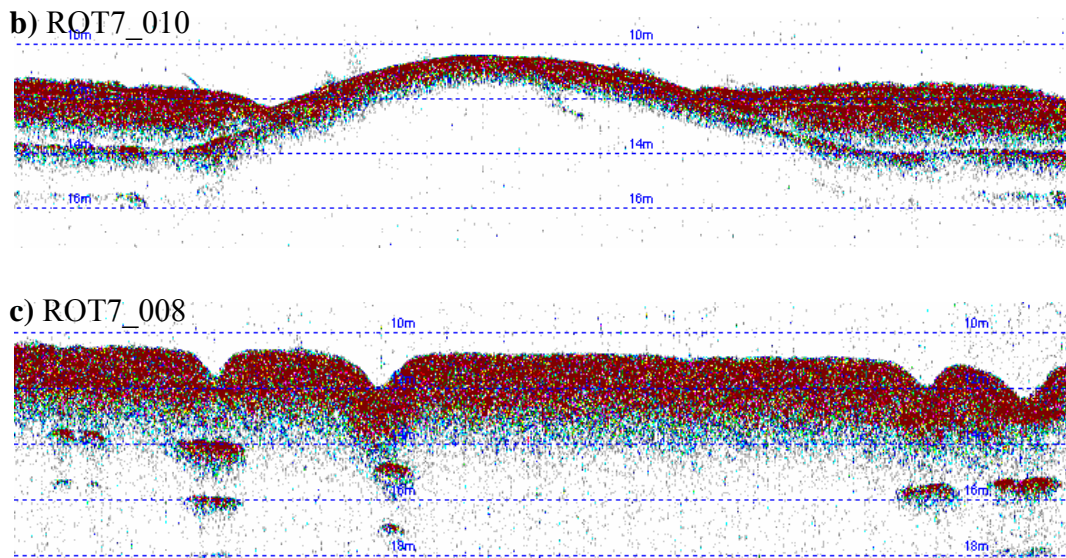


Figure 6.9: Shallow water lake floor showing **a)** multibeam image and **b)** corresponding sub-bottom track and **c)** small pockmarks.

6.3.4 Outcrops

Isolated dome structures are found in Lake Rotorua in water depths typically greater than 12 m (Figure 6.10 and 6.11). The domes in Figure 6.11 are between 50-150 m in length and are covered in diatomaceous ooze. Moats around the structures suggest that water flow is enhanced around the outcrop which, is likely to to reduce sedimentation around the structure. Similar structures are found in Lakes Rotoiti (Pickrill, 1993) and Rotoma (Nelson, 1983). Nelson (1993) reports that the dome structures are thought to be the tops and margins of rhyolitic domes and coulees.

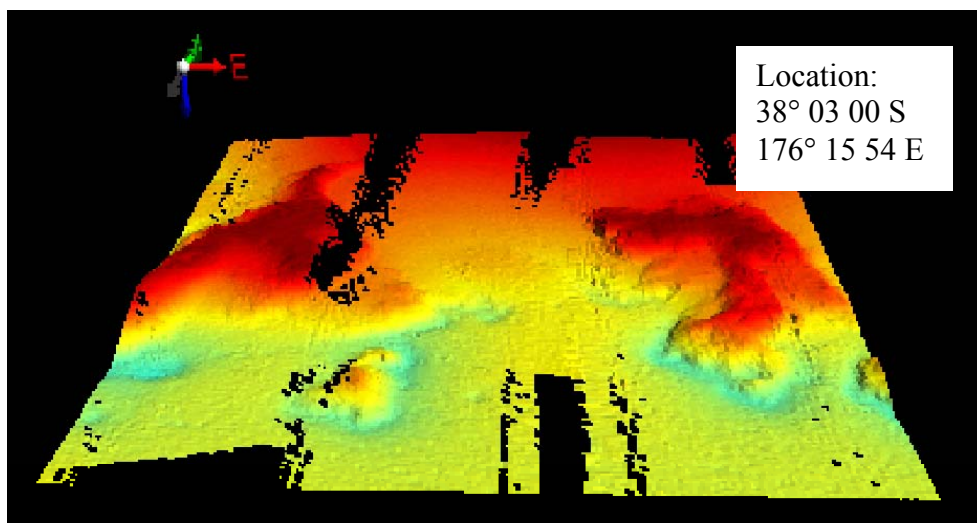


Figure 6.10: Outcrop feature below the northern terraces in Lake Rotorua.

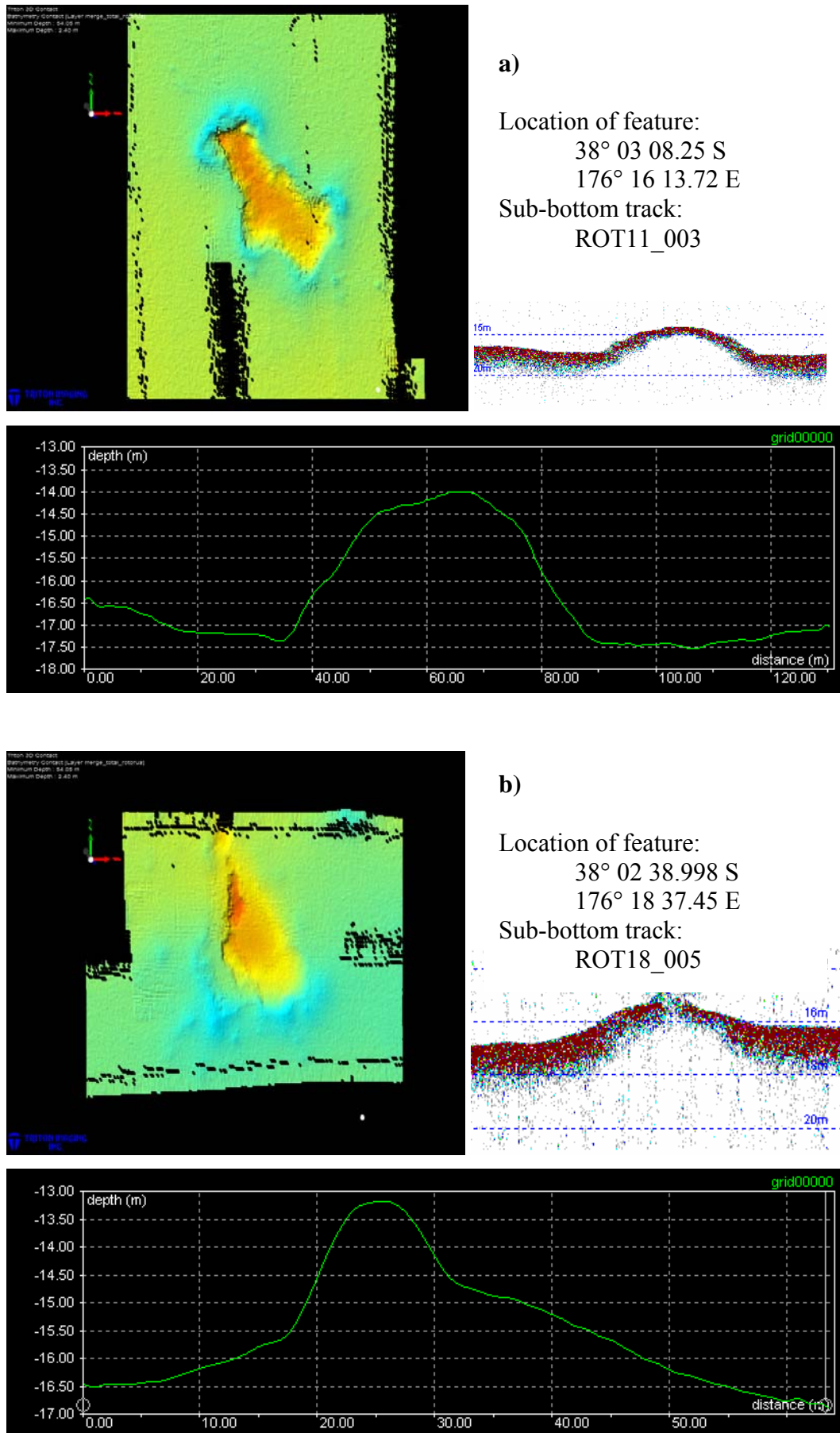


Figure 6.11: Outcrops features in Lake Rotorua

6.3.5 Gas in the Sediment

Lake Rotorua has long been known to discharge gas. Bubbles are frequently observed rising to the surface under calm conditions, and can be easily stimulated by dropping objects onto the sediments, such as anchors, or during coring (Figure 6.12).



Figure 6.12: Large gas bubble released during gravity core retrieval.

Sub-bottom echo-sounding shows no return of sonic and seismic signals from most of the lake floor indicating total absorption by the gas filled sediment. In the shallow lake margin environments, generally <10 m water depth, gas is absent and a detailed stratigraphy of multiple reflectors from tephra layers was observed by sub-bottom profiling. The transition from nongaseous sediment to gaseous sediment can be traced through the sub-bottom tracks (Figure 6.13).

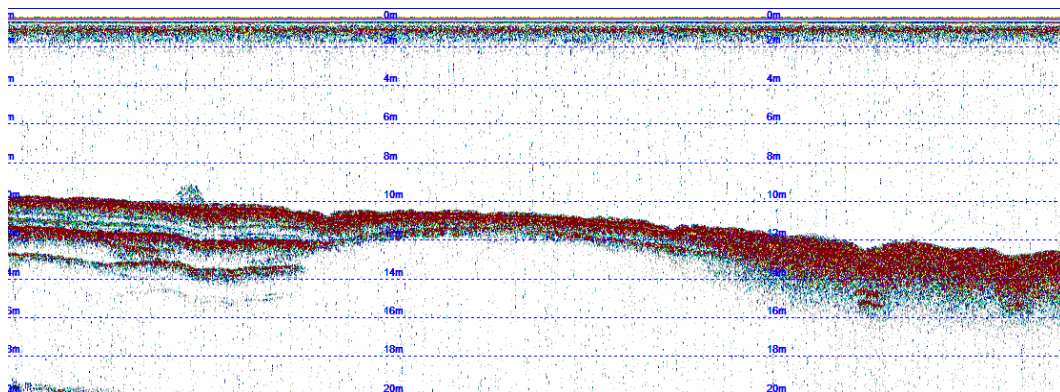


Figure 6.13: Sub-bottom return of non gaseous sediment into gas filled sediment.

The origin of the gas was speculated to have a geothermal source based on the distribution of the gas in the sediment (Davy, 1992) and resistivity surveys by Bibby *et al.* (1992). Gas was captured from an area to the west of Mokoia Island on Lake Rotorua by stimulation with water injection. The composition of the gas determined by Motion (In, Prep) was 97.7% methane and 2.3% carbon dioxide. The methane has a delta C-13 value of -64.3 and the carbon dioxide a delta C-13 of +10.6 per mille. This indicates that the source of the gas is anaerobic fermentation with most of the carbon dioxide dissolving in the pore waters enriching the bicarbonate to +18 per mille (Figure 6.14) (Motion, In Prep).

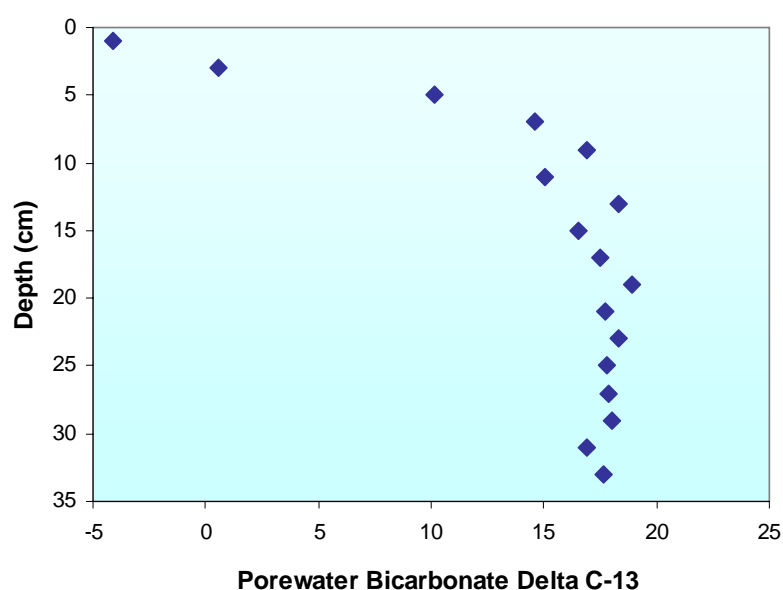


Figure 6.14: Delta C-13 of bicarbonate in Lake Rotorua porewaters (Motion, In Prep).

Carbon loss from the incoming sediments is equal to 3 mg/cm²/year. Over the 40 km² of gaseous sediment this is equivalent to a loss of 1.25 x 10⁶ m³ of methane per year. The measured rate of gas generation in the sediment is 1-3 x 10⁶ m³ of methane per year, most of which is generated between 20 and 40 cm depth in the sediment as carbon concentration declines rapidly in the sediment.

Methane ebullition from the sediments is likely to displace porewaters, which would contribute significantly to the cycling of nutrients from the sediment back into the water column. Methane ebullition is also reported to contribute to

destratification and the artificial oxygenation of the hypolimnion in lake systems by creating greater mixing (Romero *et al.*, 1996).

6.3.6 Pockmarks

The basin sediments of Lake Rotorua have many pockmarks of 20-60 m diameter, 0.5-6 m deep circular flat bottomed depressions. The pockmarks are usually located on the lake floor in areas where there sediment contains gas. Shallow seafloor and lake floor gas has been widely reported elsewhere in the world by numerous authors (King and MacLean, 1970; Otis *et al.*, 1977; Anderson and Hampton, 1980; Hovland, 1981; and Rodgers *et al.*, 2006). Pockmarks were first described as ‘concave, crater-like depressions that occur in profusion on mud bottoms across the Scotian Shelf’ (King and MacLean, 1970). They can reach hundreds of meters and depths of tens of meters, although in Lake Rotorua they are relatively small in comparison. Pockmarks are recognised in a variety of continental margin settings, deltas, and areas of petroleum production or tectonic activity, all over the world (Rodgers *et al.*, 2006). Gas is not usually observed directly beneath a pockmark, allowing imaging of sub-bottom reflectors beneath pockmarks that are obscured by gas nearby. This observation suggests that the escape of the gas and associated pore waters formed the pockmark (Rodgers *et al.*, 2006).

Pickrill (1993) describes stages in pockmark genesis based on the assumption that pockmarks are created by degassing or dewatering at the sediment surface. The preservation in seismic records of pockmarks reflects the history of the pockmark development over time. The seven stages of pockmark formation identified by Pickrill (1993) for Lake Rotoiti are shown in Figure 6.15.

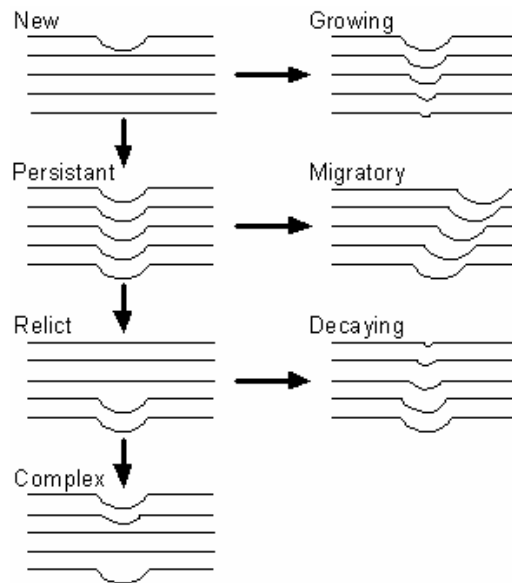
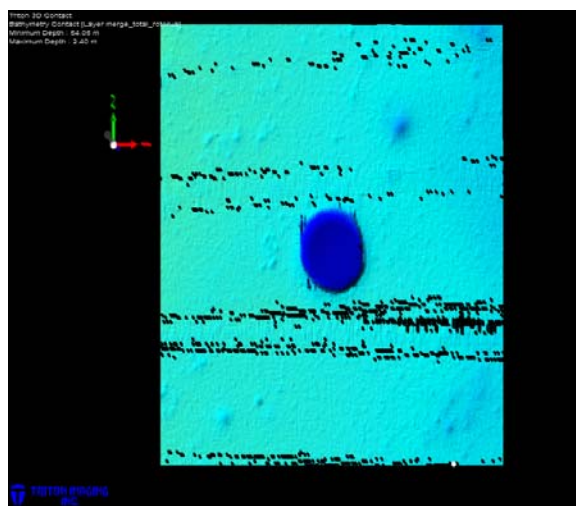


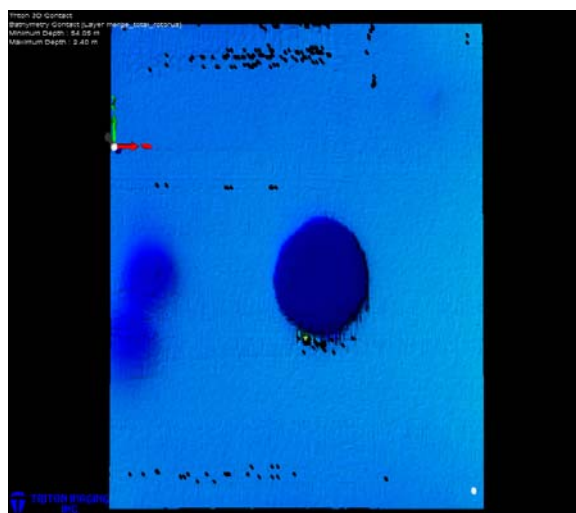
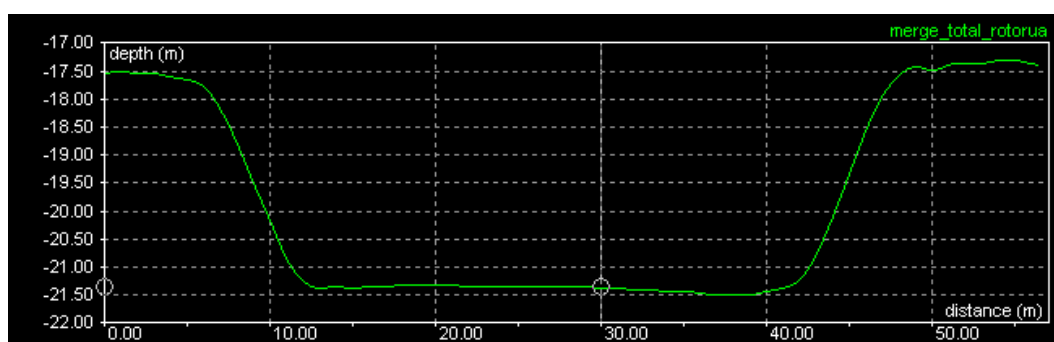
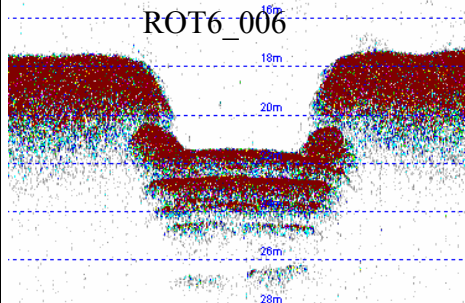
Figure 6.15: Seismic classification of pockmark genesis (Pickrill, 1993).

Other potential causes of depressions in lacustrine sediments include hydrothermal craters, spring discharges, block faulting and turbulence surrounding solid objects on the lake floor. Each of these will have characteristic features such as mounding of ejected material surrounding craters or rectilinear edges to block faulting which can be used to distinguish their origins.

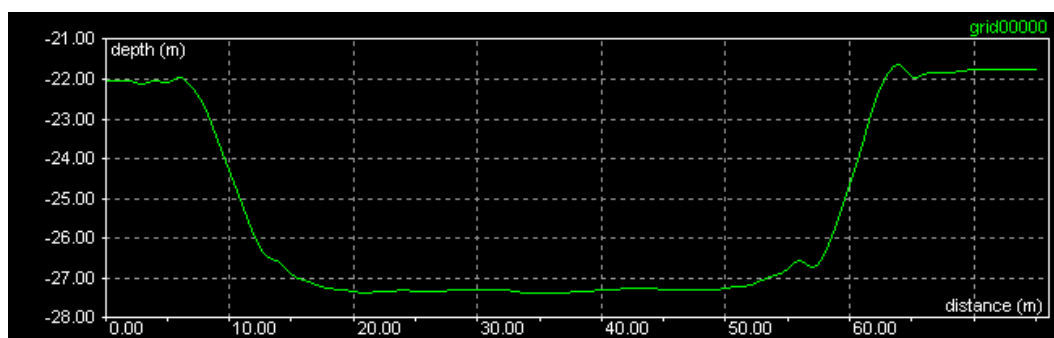
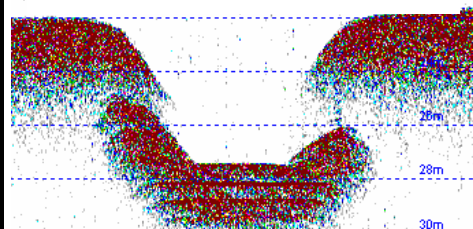
Deep pockmarks are found in water depths greater than 15 m and show a 3-5 m decrease in the sediment surface elevation (Figure 6.16). The sub-bottom profiles of the pockmarks show that gas has been lost from the overlying sediment making the stratigraphy visible in the pockmark. The stratigraphy of the underlying tephra layers buried in the sediment appears to be undisturbed which suggests a slow release of gas from the sediment. However the deposition of recent tephra layers such as the Tarawera Tephra, would be younger than the large pockmarks and would have deposited in the depression. Deeper sub-bottom penetration into the sediment may show disturbance of older stratigraphic layers allowing an approximate age for the formation of the pockmark to be assigned. The deep water pockmarks could be classified as persistent as the pockmark is present through multiple tephra layers. The presence of gas in the surrounding sediment masks the sonic signal so the change in stratigraphy of the sediment caused by the creation of the pockmark cannot be fully described.

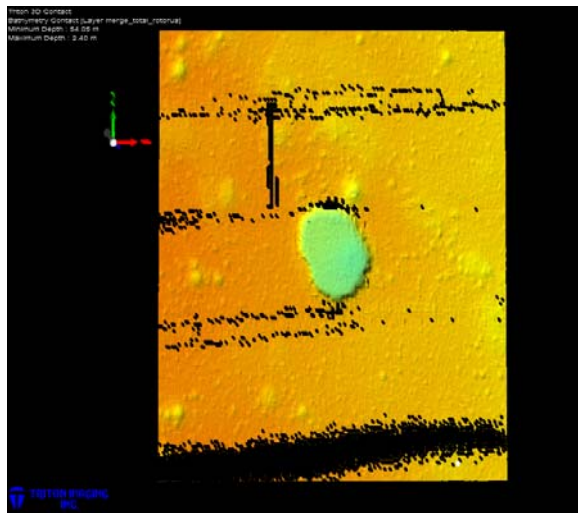


a)
Location of feature:
38° 04 52.82 S
176° 15 30.82 E
Sub-bottom track:
ROT6_006



b)
Location of feature:
38° 05 37.41 S
176° 16 12.99 E
Sub-bottom track:
ROT7_012





c)

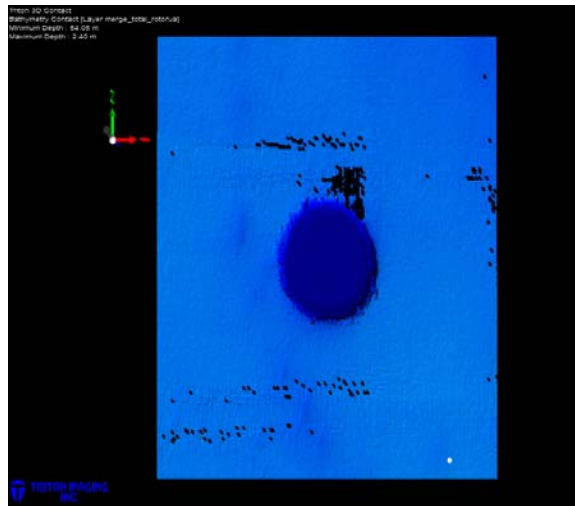
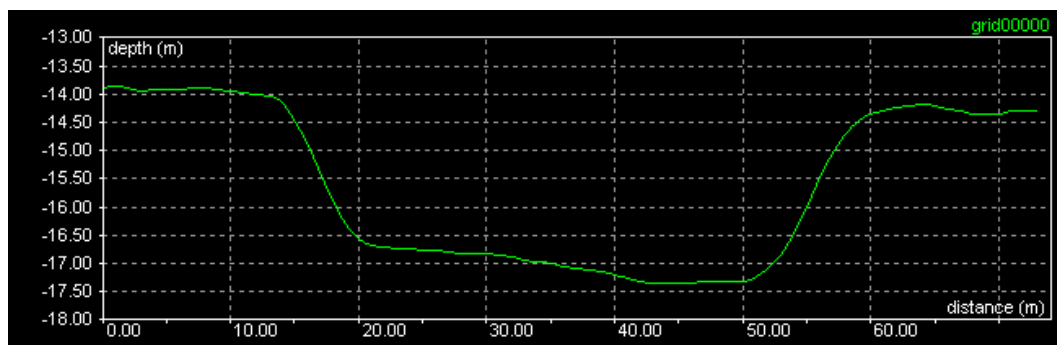
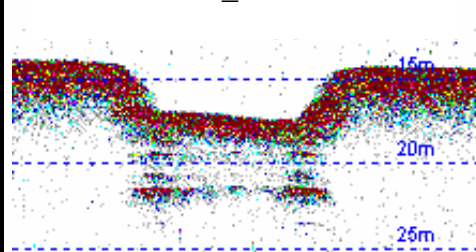
Location:

38° 04 53.06 S

176° 16 09.89 E

Sub-bottom track:

ROT9_021



d)

Location:

38° 04 53.06 S

176° 16 09.89 E

Sub-bottom track:

ROT8_010

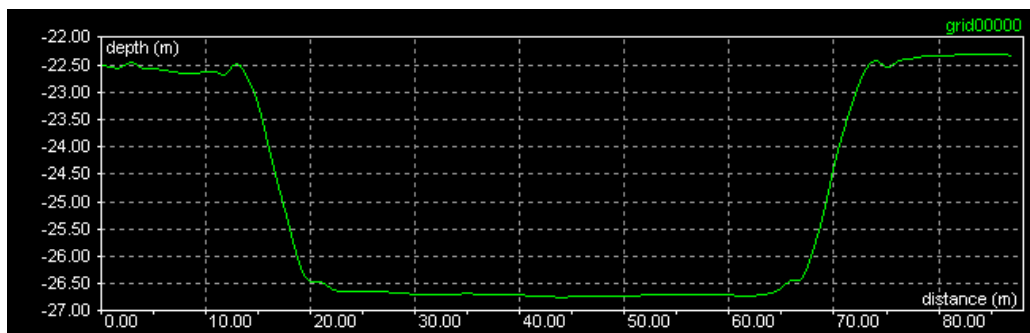
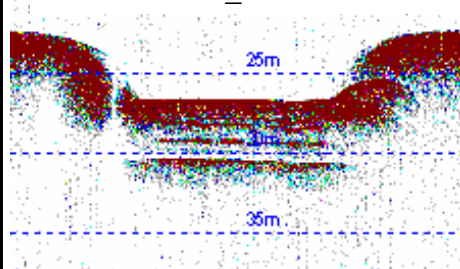
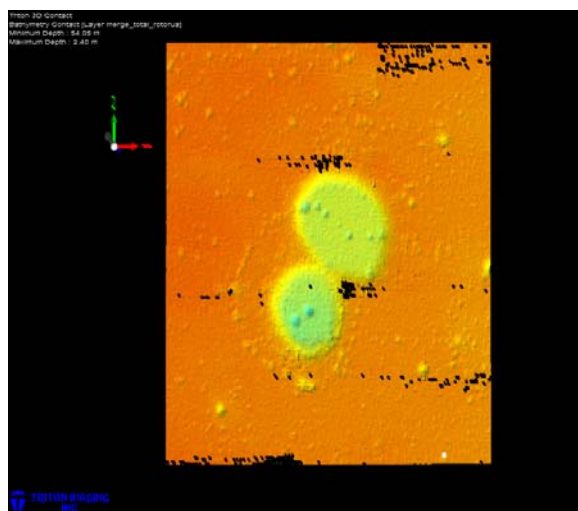


Figure 6.16: Pockmarks in water depths greater than 15 m.

An estimation of the amount of gas lost from the pockmark can be calculated from the volume ($\pi r^2 x$) of the pockmark (where r is the radius of the pockmark and x is the depth). The pockmark in Figure 6.16 d is 50 m in diameter ($r = 25$) and 4 m ($x = 4$) below the surrounding surface at a water depth of 22.5 m, representing a loss of 7850 m³ of gas ($\pi * 25^2 * 4$) (and water) from the sediment. If this volume was all gas, the volume at atmospheric pressure is approximately 25,500 m³ which could form an explosive mixture of approximately 400,000 m³ with air. Extended across the 40 km² of gas rich sediment the total quantity of available methane is approximately 520 x10⁶ m³ (c. 23,000 tonnes).

Pockmarks in shallow water appear similar to the deep water pockmarks from the multibeam image, except the stratigraphy of the underlying sediment is not visible in the sub-bottom profiles (Figure 6.17). This observation suggests that the pockmarks are relatively new and the sediment has not lost enough gas to become transparent. Alternatively the pockmark could be decaying. Due to the size of the pockmarks (up to 60 m in diameter), it is most likely the latter, as the underlying tephra layers are not visible in the sub-bottom profiles due to diagenetic processes in the sediment producing methane. The decaying pockmarks are likely to have formed thousands of years ago when the lake level was much higher. In the majority of small shallow-water pockmarks (>10 m diameter) stratigraphy of the underlying sediment is visible. The theory of regeneration of gas in the sediment is supported by the presence of small pockmarks occurring in larger pockmarks (Figure 6.17a).



a)

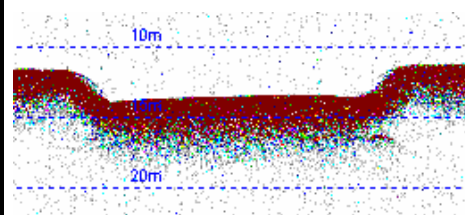
Location of feature:

38° 04 32.81 S

176° 16 43.34 E

Sub-bottom track:

ROT14_001



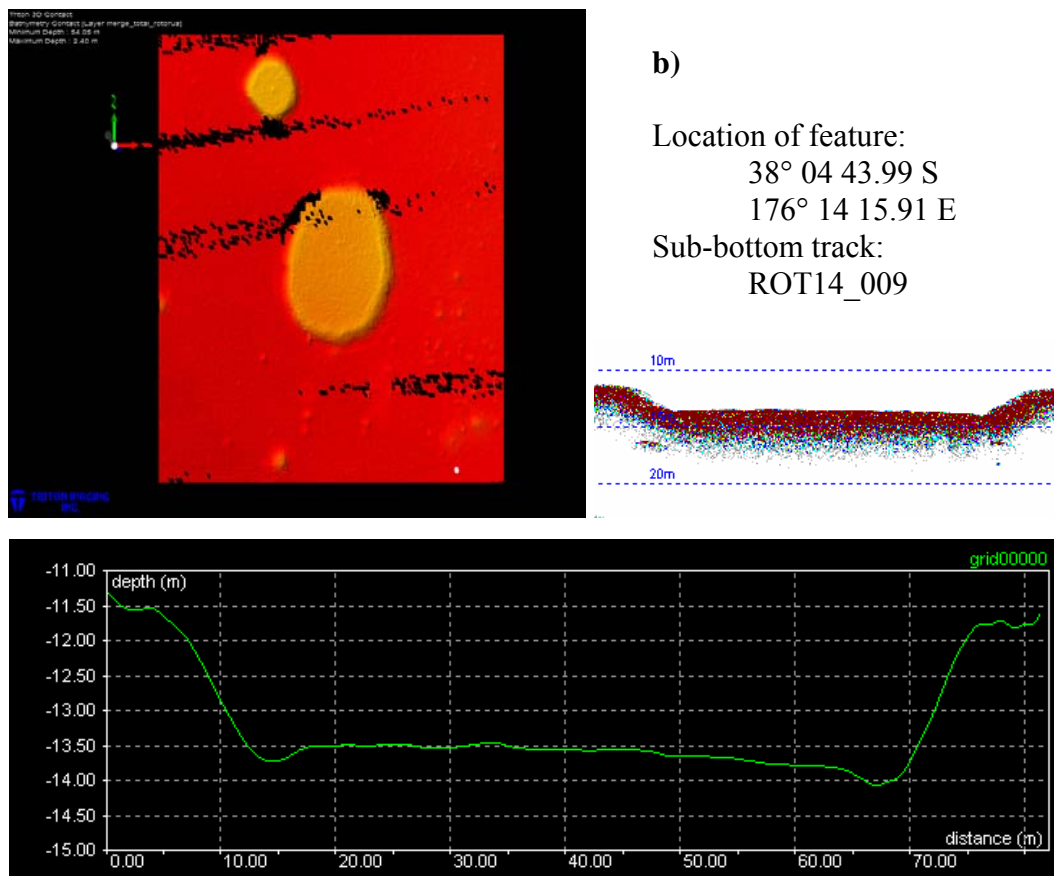


Figure 6.17: Pockmarks in water depths less than 15 m.

The location of the pockmark below (Figure 6.18) is to the east of Te Kou Point of Mokoia Island. Here pockmarks are approximately 1.5 m deep and 40 m wide. The centre of the pockmark is not depressed. The transect profile is taken through both pockmarks. Unfortunately, the sub-bottom track only captures a portion of the depression ring. The origin of the domed pockmarks is not easily assigned. Without a sub bottom profile through the centre of the pockmark it is not possible to determine whether the depression is from lost gas or disturbance. The ring around the mound is gas-free and could be the result of a number of smaller pockmarks coalescing, as there are a few small pockmarks in the mound of one of the rings. Why small pockmarks should coalesce in a ring is not obvious.

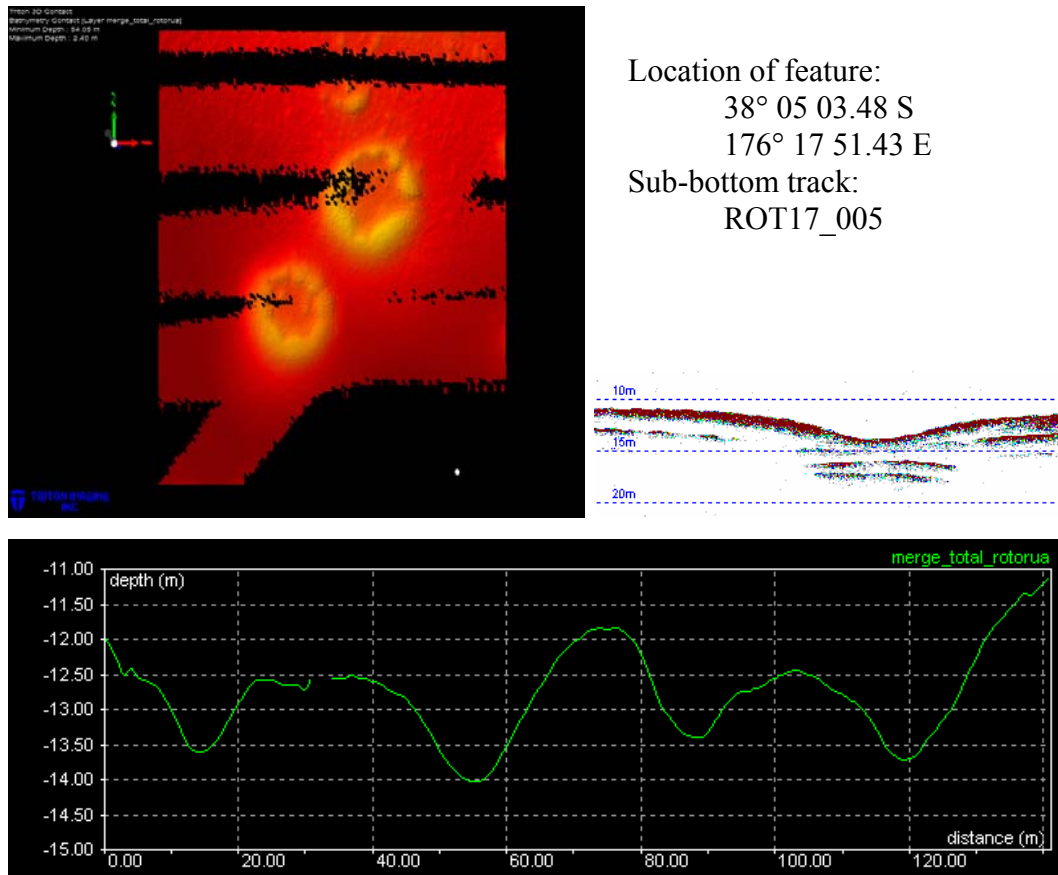


Figure 6.18: Domed pockmark.

Depressions in the underlying stratigraphy are possibly relict pockmarks, where there is no surface expression of the pockmark (Figure 6.19). The deeper reflectors show depressions that have been infilled. The pockmarks would have been active when the buried tephras formed at the sediment surface, but with a decrease in activity the pockmark has infilled and tephra layers above show no evidence of the former pockmark. The above pockmark (Figure 6.18) may be in the process of infilling but it is impossible to know for sure without seeing the stratigraphy of the surrounding area. In Figure 6.19a only a 1 m depression remains at the sediment surface.

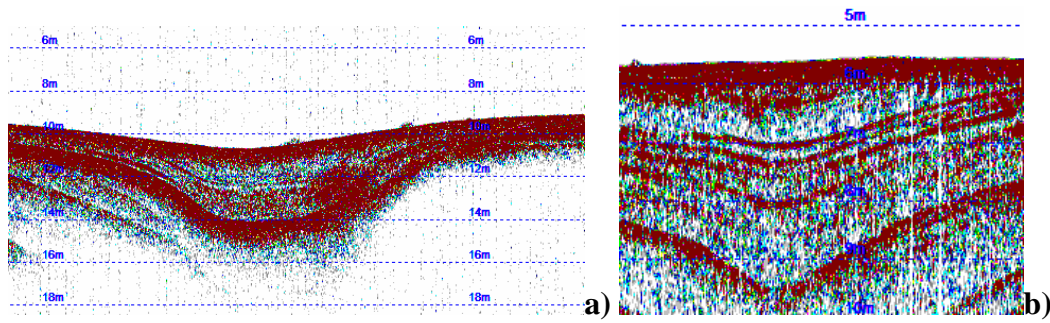
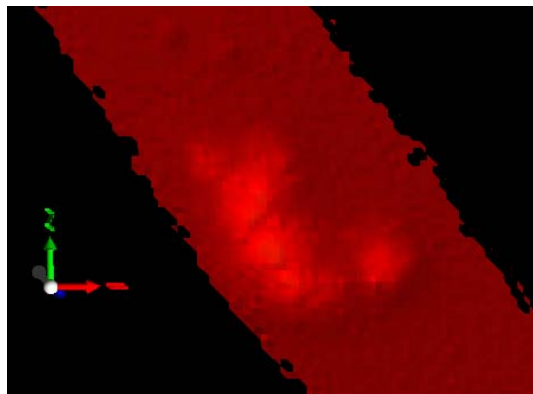


Figure 6.19: Sub-bottom profile through relict pockmark **a)** ROT7_003 and **b)** ROT5_000.

The depression formed by the loss of gas from the sediment in Figure 6.20 is in 9.8 m water depth. It is a shallow depression (>1.2 m). The sub-bottom track shows the stratigraphy of the sediment surrounding the depression but the reflectors are absent in the centre. Distortion and downward curving of the reflector layers towards the centre of the depression could be the result of a sub-aqueous spring.



Location of feature:

38° 06 12.49 S

176° 15 15.36 E

Sub-bottom track:

ROT6_007

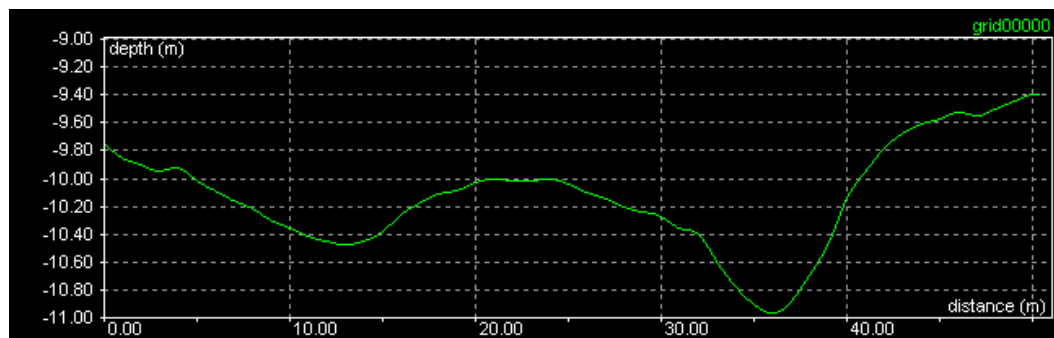
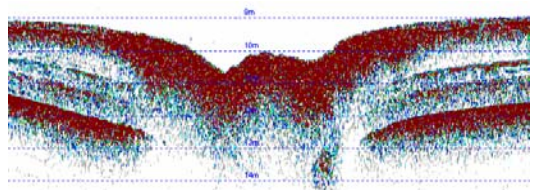
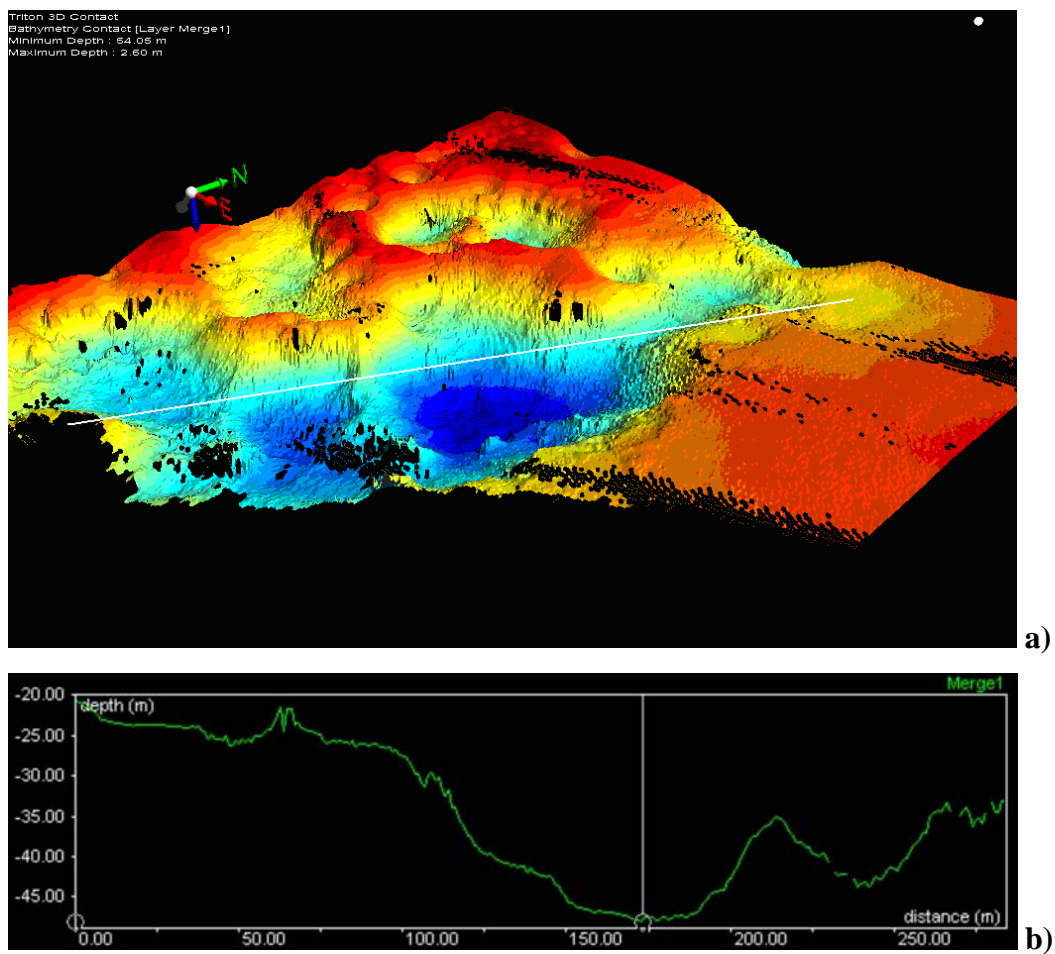


Figure 6.20: Depression feature**6.3.7 Hydrothermal Activity**

A series of depressions clustered to the north of Sulphur Point are clearly different to the methane pockmarks in that they are conical rather than flat bottomed and are surrounded by mounds (Figure 6.21). These are likely to be hydrothermal explosion craters and appear to be actively discharging water and gas.

**Figure 6.21:** a) Multibeam image of hydrothermal explosion creators and b) cross-section through vents showing water depth.

A small group of depressions, surrounded by small pockmarks, located off Te Kou Point on Mokoia Island are possibly hydrothermal as they collectively form a

significant hole in otherwise shallow waters close to the island (Figure 6.22). They are irregular in shape compared to the circular pockmarks.

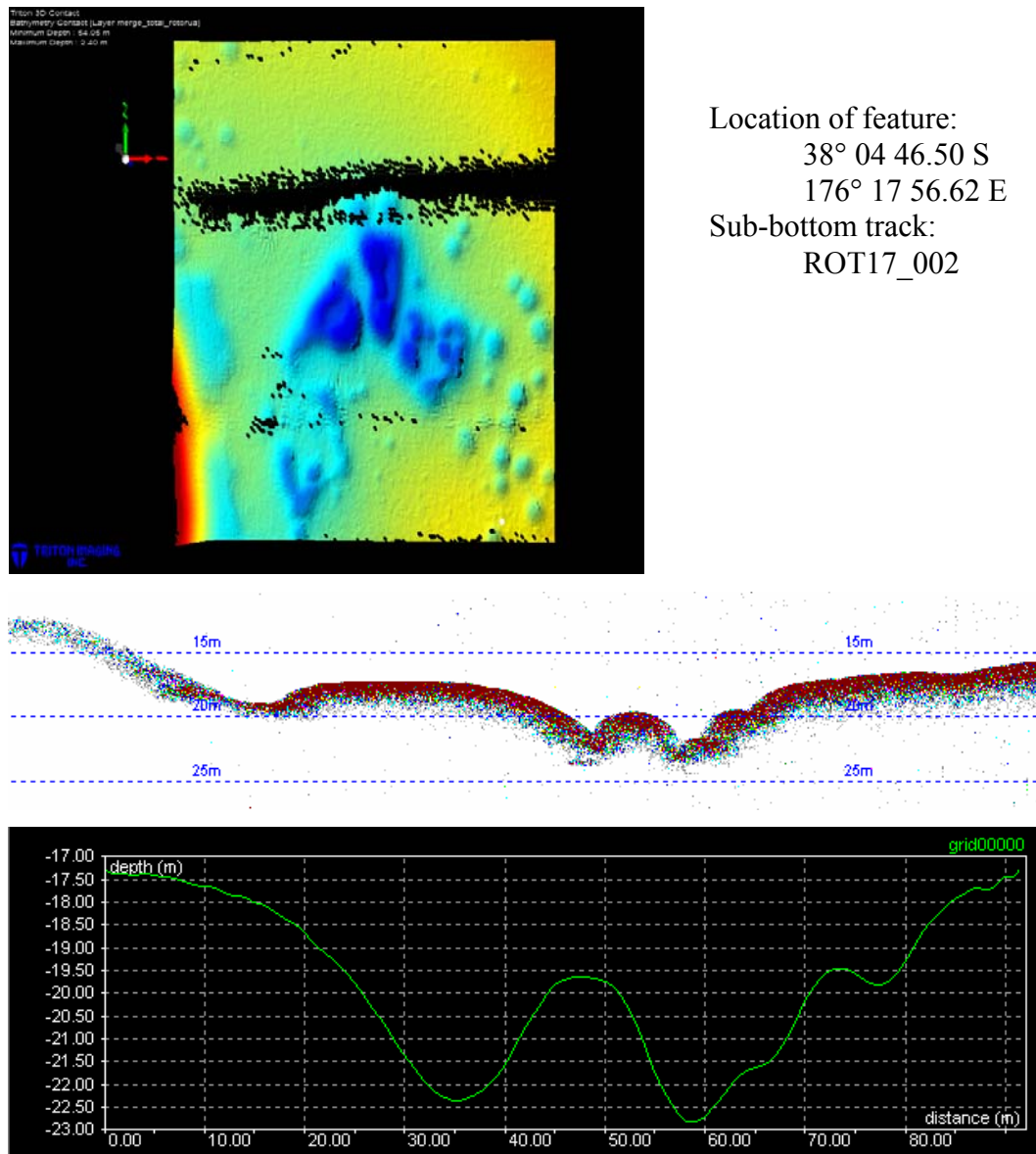


Figure 6.22: Hydrothermal feature to the east of Mokoia Island.

6.4 SUMMARY

Lake Rotorua is currently at 280 m above sea level. The bathymetry of Lake Rotorua is dominated by a curved depression extending from Sulphur Point and almost reaching the Ohau Channel outlet. This depression is probably a structural feature likely associated with the collapse of the caldera, but could be an ancient drainage channel. In less than 10 m water depth, a series of nearshore terraces are preserved in the sediment to the north in the lake. A series of conical depressions

clustered to the north of Sulphur Point and to the east of Mokoia Island are likely to be hydrothermal explosion creators and appear to be actively discharging water and gas.

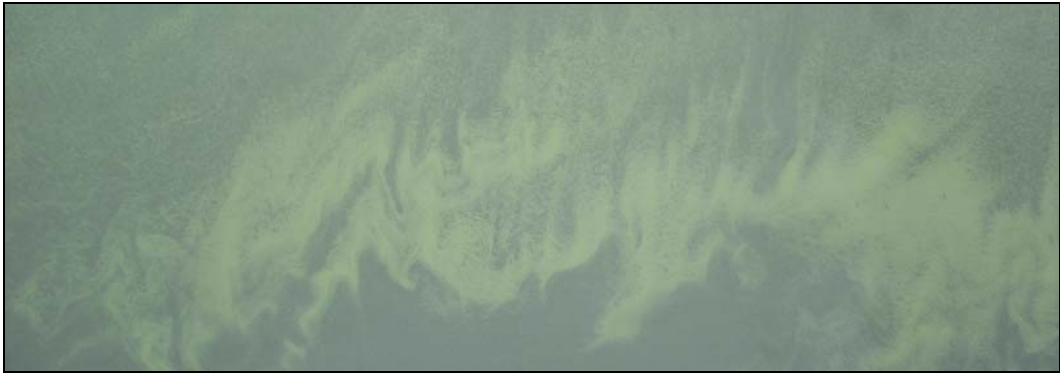
Sub-bottom echo-sounding shows no return of sonic and seismic signals from most of the lake floor, indicating total absorption by the gas filled sediment. In the shallow lake margin environments, generally <10 m water depth, gas is absent and a detailed stratigraphy of multiple reflectors from tephra layers was observed by sub-bottom profiling. The basin sediments of Lake Rotorua have significant circular, flat bottomed pockmarks of 20-60 m diameter and 0.5-6 m depth. The pockmarks are located on the lake floor in areas where the sediment is saturated with gas. The gas has a composition of 97.7% methane and 2.3% carbon dioxide and is formed by anaerobic fermentation in the sediment. In Lake Rotorua sediment, the total quantity of available methane is approximately $520 \times 10^6 \text{ m}^3$ (c. 23,000 tonnes).

REFERENCES

- Anderson, A.L. and Hampton, L.D. 1980. Acoustics of gas bearing sediment. *Journal of the Acoustical Society of America*. 67: 1865-1903.
- Bibby, H.M., Dawson, G.B., Rayner, H.H., Bennie, S.L. and Bromley, C.J. 1992. Electrical resistivity and magnetic investigations of the geothermal systems in the Rotorua area, New Zealand. *Geothermics*. 21: 43-64.
- Blacquiere, G. and van Woerde, K., 1998. Multibeam Echosounding: Beamforming versus Interferometry. *Oceanology International* Vol. 2. Brighton. pp. 353-356.
- Coastal Marine Group, 2004. The Multibeam Hydrographic Survey System. Department of Earth Sciences, University of Waikato. pp29
- Davy, B. 1992. Seismic reflection profiling on southern Lake Rotorua – Evidence for gas-charged lakefloor sediments. *Geothermics*. 21 (1/2): 97-108.
- Esler, W.R. (In Prep). The tephrostratigraphy and paleogeography of the Rotorua Basin, North Island, New Zealand. Ph.D. Thesis. Department of Earth and Ocean Sciences, University of Waikato, Hamilton.
- Flood, R.D., Nitttrouer, C., and Mayer, L.A., 1999. A shallow-water swath bathymetry system. In: *Geology and Geophysics Program Summary FY 1998*. Contract report for Office of Naval Research, Department of the Navy, Arlington. Report No. ONR 32299-6. 4p.
- Froggatt, P.C. and Lowe, D.J. 1990. A review of late Quaternary silicic and some other tephra formations from New Zealand: their stratigraphy, nomenclature, distribution, volume and age. *New Zealand Journal of Geology and Geophysics*. 33: 89-109.
- Gardner, J.V., Dartnell, P., Mayer, L.A., and Hughes-Clark, J.E., 2003. Geomorphology, acoustic backscatter, and processes in Santa Monica Bay from multibeam mapping. *Marine Environmental Research*, 56: 15-46.
- Hovland, M. 1981. Characteristics of pockmarks in the Norwegian Trench. *Marine Geology*. 39: 103-117.
- Hughes-Clark, J., Mayer, L.A. and Wells, D.E., 1996. Shallow-water imaging multibeam sonar; a new tool for investigating seafloor processes in the coastal zone and on the continental shelf. *Marine Geophysical Research*, 18: 607-629.
- Irwin, J., 1969. Lake Rotorua Provisional Bathymetry. Lake Series, 1:15,840. Fisheries Research Division, New Zealand Marine Department.

- Kennedy, N.M., Pullar, W.A. and Pain, C.A. 1978. Lake Quaternary land surfaces and geomorphic changes in the Rotorua basin, North Island, New Zealand. *New Zealand Journal of Science*. 21: 249-264.
- King, L.H. and MacLean, B. 1970. Pockmarks on the Scotian Shelf. *Geological Society of America Bulletin*. 81: 3141-3148.
- Mallace, D., 2002. A comparison of Shallow water Multibeam Systems from a commercial view point. *Proc. 13th Biennial International Hydrographic symposium (Hydro, 2002)*, Kiel, Germany. 32p.
- Miller, J.E., Hughes-Clark, J. and Paterson, J., 1997. How effectively have you covered your bottom? *The Hydrographic Journal*, 83: 3-10.
- Motion, O.J. In Prep. Early Diagenesis in Lake Rotorua Sediment. MSc Thesis, Department of Chemistry, University of Waikato.
- Nelson, C.S. 1983. Bottom sediments of Lake Rotoma. *New Zealand Journal of Geology and Geophysics*. 17:185-204.
- Otis, R.M., Smith, R.B. and Wold, R.J. 1977. Geophysical surveys of Yellowstone Lake, Wyoming. *Journal of Geophysical Research*. 82 (26): 3705-3717.
- Pickrill, R. and Barnes, P. 2003. Managing the seabed with multibeam mapping: Learning from the Canadian Experience. *Water and Atmosphere*, (11) 4: 7-9.
- Rodgers, J.N., Kelley, J.T., Belknap, D.F., Gontz, A. and Barnhardt, W.A. 2006. Shallow-water pockmark formation in temperate estuaries: A consideration of origins in the western gulf of Maine with special focus on Belfast Bay. *Marine Geology*. 225: 45-62.
- Romero, J.R., Patterson, J.C. and Melack, J.M. 1996. Simulation of the effect of methane bubble plumes on vertical mixing in Mono Lake. *Aquatic Sciences* 58(3): 210-233.
- Scarfe, B. E., 2002. Categorising surfing manoeuvres using wave and reef characteristics. MSc Thesis, Department of Earth Sciences, University of Waikato. 181 p.
- Spiers, C., 2005. Continued Beach Renourishment from Dredge Spoil Deposit. MSc Thesis, Department of Earth Sciences, University of Waikato. 241 p.
- Trimble Ltd, 2005. <http://www.trimble.com/ms750.html>, Accessed 1/10/2006.
- Wood, A.P., 2006. Morphodynamic Channel and Stability of the Waikato River: Karapiro to Ngaruawahia Reach. MSc Thesis, Department of Earth Sciences, University of Waikato. 393 p.

CHAPTER SEVEN:
IMPLICATIONS FOR REMEDIATION



7.0 INTRODUCTION

This chapter examines possible remediation options and discusses the results of this study as they relate to management implications for Lake Rotorua. Remediation options considered were: a reduction in nutrient inputs, sediment capping, dredging and the use of flocculants. Recommendations for possible remediation options for Lake Rotorua are also discussed.

7.1 RESTORATION OF EUTROPHIC LAKES

During the past century increased urbanisation and sewage disposal, reclamation of wetlands and removal of stream riparian regions, as well as more intensive farming practices have greatly increased the nutrient loading in many shallow lakes world-wide (Jeppesen *et al.*, 2003). The reduction of phosphorus and nitrogen loads is usually the main goal of restoring a eutrophic lake (Harper, 1992; Rowe, 2004). Cooke *et al.* (1993) reviewed restoration and management options but focused primary on North American lakes. The problems and methods applicable to New Zealand lakes tend to differ from North American and European lakes (Rowe, 2004). Several restoration techniques have been developed to reduce phosphorus and nitrogen, including chemical applications, physical modification and biological manipulations within the lake environment.

7.1.1 Chemical Application

Chemical restoration involves the flocculation or precipitation of suspended solids, including phytoplankton and nutrients. Treatment requires dosing the lake with a surface spray of compounds such as aluminium sulphate, iron chloride, calcium or zirconium salts (Cooke *et al.*, 1993). Rowe (2004) suggests physically sealing the sediment by covering the affected areas of the lake bottom with sand, mineral soils, fly ash, hydrous and metal oxides and clay minerals.

The efficiency of a material for nutrient removal depends on the cation exchange capacity and the adsorption capacity. For clay minerals the cation exchange capacity is derived from isomorphic substitution or by dissociation of aluminol groups. Isomorphic substitution occurs in the tetrahedral and/or octahedral sheets of the clay mineral layer and is considered to be insensitive to the pH of a system.

The dissociation of aluminol groups occurs on the edges of clay sheets and is dependent on the pH.

Clay minerals have very good sorption properties for a number of substances. The sorption capacity of clays is dependent on: the total number of charges on the clay mineral surface and the charge density; acidity and the number of hydroxyl groups and oxygen atoms on the clay mineral surface; and the specific surface area of the clay mineral.

There are many factors that need to be considered before adding a chemical substance into a lake ecosystem. The pH of the material usually needs to be maintained around 6-8 throughout the treatment. The longevity of the material is important to determine the long-term effects of the additive. The timing of application is dependent on the lake conditions. Kleeberg *et al.* (2001) found that 90% elimination of phosphorus following an alum treatment is only reached if the application occurs when the hypolimnetic P-concentration is at a maximum, or at the end of thermal stratification. Wind exposure and mixing regime can make it difficult to achieve even chemical application over the lake (Cooke *et al.*, 1993). The toxicity and risk to biota limit the materials available for remediation.

7.1.2 Physical Modification

Physical modifications can be carried out either by different *in situ* methods or by removal of bottom sediments. *In situ* methods include capping and aeration of bottom waters. Sediment capping involves the deposition of a layer of solids over the lake bottom. The capping layer needs to be sufficiently thick to prevent biological mixing of the capped underlying sediment. The capping material used needs to be coarser than the underlying sediment to prevent mixing or disruption of the cover by wind and wave activity. Capping is rarely used as a remediation option in lakes because of the difficulty of placing a uniform cover in the sub-aqueous environment. Aeration has been used as a remediation method to eliminate anoxia in the bottom water by releasing air or other mixtures with oxygen or strong oxidising agents at the sediment-water interface. Destratification of the water column can also be achieved by the physical mixing of the overlying

lake water, which disrupts the formation of anoxia in the bottom waters and reduces sediment nutrient release.

Sediment removal is recommended in cases when the internal nutrient load needs to be reduced, recreational activities are impaired due to sediment build-up, for macrophyte control or to remove toxic substances present in the lake bed (Cooke *et al.*, 1993). Dredging can remove all of the sediment contained within an area of a known volume in a lake or reservoir. However, a single lake dredging may not be a permanent solution due to sedimentation and ongoing external nutrient inputs, dredging will most likely have to be repeated. Dredging methods are well known and understood and the selection of dredging techniques and equipment should be based on the accuracy of sediment removal, speed of removal, and on minimizing the resuspension and/or loss of particles to the water column. Dredging can be carried out by dragliner, bucket dredge, or hydraulic suction dredge, depending on the lake depth (Cooke *et al.*, 1993).

There are several factors that need to be taken into consideration before deciding to dredge. The amount of sediment removed is dependent on the desired outcome. To reduce the nutrient load, the amount of sediment removed is dependent on the vertical nutrient profile of the sediment; or to deepen the lake, the amount of material removed depends on the requirements for recreation (Faithfull *et al.*, 2005). The characteristics of the newly exposed sediment affect how successful the sediment removal is at reducing nutrient loads. If the sediment exposed has the same nutrient release characteristics then there will be no decrease in nutrient loading (Gulati and van Donk, 2002). Dredging alters the physical and chemical character of the sediments, which can potentially mobilise contaminants that were stable prior to disturbance (Davidson *et al.*, 2005). Freshwater sediments are not typically high in sulphide minerals, and dramatic changes in pH are not common, however increases in redox potential can still be large resulting in an increased rate of organic decomposition and transformation of redox-sensitive elements to oxidised states. Therefore before dredging it is important to evaluate the potential for mobilisation of contaminants currently sequestered in the lake sediments. Dredging can also release phosphorus into the water column stimulating algal blooms (Faithfull *et al.*, 2005). Disposal of the sediment is essential to the

restoration effort. If the sediment has low concentrations of toxic metals and/or organic compounds then it can be used as a fertilizer or soil conditioner on agricultural soils. However, if the sediment contains toxic elements and compounds then disposal on soil or to a downstream river or lake should not be allowed. Sediment with concentrations of elements and compounds exceeding the Ministry of the Environment guidelines are regarded as contaminated and should be disposed of in landfills or in containment areas. The containment is sealed to prevent leaching of nutrients and contaminants back into the surrounding environment.

7.1.3 Biological Manipulations

Biological actions can involve the use of microbial bioremediation agents for biological nutrient removal, or the removal of biological pests that influence nutrient transformations and availability (e.g. carp) or biomanipulation to also influence the way in which nutrients are cycled within the system. Biomanipulation of the food web to improve lake trophic state is an experimental procedure and many interactions are unknown or poorly understood (Cooke *et al.*, 1993).

The function of fish removal is to reduce predation on zooplankton, which is intended to result in higher zooplankton consumption of phytoplankton and reduced biomass (Faithfull *et al.*, 2005). Fish removal can also reduce phosphate release from the lake sediments as fish disturb the sediments stimulating phosphorus release. Herbivorous fish reduce the erosion resistance of the sediment by reducing the abundance of macrophytes; thus indirectly contributing to sediment resuspension (Faithfull *et al.*, 2005). The reestablishment of macrophytes can result in a reduction of phosphorus release from the lake sediments, as they assimilate phosphorus from both the water column and sediment for plant growth.

7.2 IMPLICATIONS FOR RESTORING LAKE ROTORUA

Factors influencing considerations of remediation options for Lake Rotorua are the distribution and composition of nutrient rich sediment in the lake, nutrient

loading and recycling of nutrients from the sediment, sediment bulk density and presence of methane gas in the sediment.

7.2.1 Phosphorus Distribution in Lake Rotorua Sediment

The distribution of phosphorus in the sediment dictates areas where physical and chemical remediation activities will have the greatest benefit. From the results discussed in this thesis, it was found that the highest concentrations of phosphorus (>1500 g/tonne) in the sediment are located in areas with water depths >15 m (Figure 7.1). These areas also have a high sediment accumulation rate. Figure 7.1 includes the area where core tops were unobtainable by gravity coring as phosphorus concentrations are likely to exceed 1500 g/tonne.

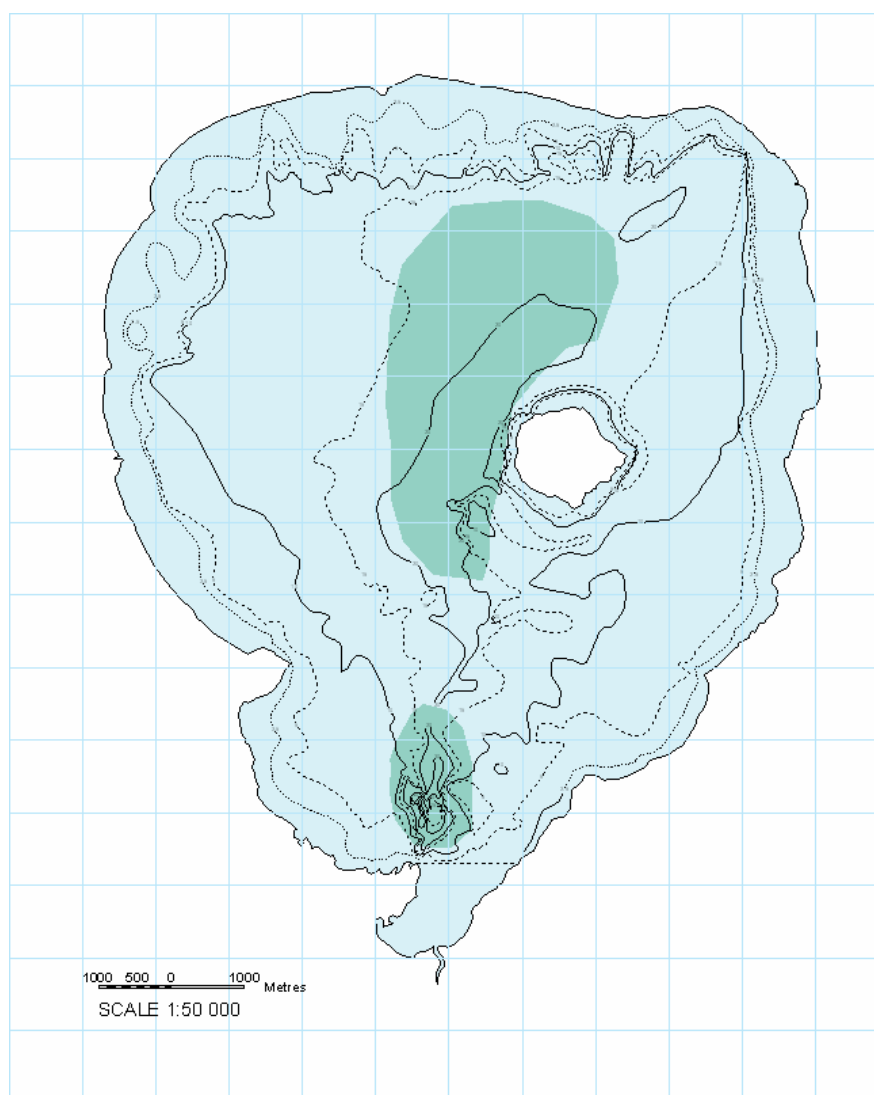


Figure 7.1: Area of Lake Rotorua with sediment phosphorus concentration >1500 g/tonne.

The amount of phosphorus, iron, manganese, arsenic and lead in the sediment is shown in Table 5.2. Dredging of the top 10 cm of sediment over the whole lake area will remove approximately 442 tonnes of phosphorus, 3417 tonnes of iron, 180 tonnes of manganese, 28 tonnes of arsenic and 3.5 tonnes of lead. However, to significantly reduce phosphorus recycling from the lake sediment, removal or capping of the shaded area in Figure 7.1 would be sufficient.

7.2.2 Nutrient Loading

The mean phosphorus content of a lake should decrease roughly in proportion to the reduction in phosphorus input (Marsden, 1989). The amount of phosphorus entering Lake Rotorua has declined significantly since the diversion of sewage in 1991 (Figure 7.2) (Rutherford, 2003) and the present load complies with nutrient target loads established in the 1980s. Nitrogen inflows to the lake however have continued to increase over recent decades (Figure 7.3). Part of this increase is associated with ‘leakage’ from the land associated with the sewage disposal site but the majority is associated with increasing nitrate in streams draining agricultural land (Rutherford, 2003). Streams contribute approximately 75% of total nitrogen inflow into Lake Rotorua (Morgenstern and Gordon, 2006). Total nitrogen loads would need to be reduced by ~250 t-N/y to comply with the target loads. Sewage diversion was followed by significant improvements in lake water clarity, nutrient and chlorophyll concentrations from 1993-95, but since then lake water quality has again deteriorated (Rutherford, 2003). The Kaituna Catchment Control Scheme was implemented in the 1980s when sewage was diverted from Lake Rotorua to reduce and control non-point sources of nutrients entering through tributary streams from activities such as farming. The scheme encouraged the gradual planting of native trees along the edges of many of the main inflowing streams (Rowe, 2004). The control measures have reduced sediment, total phosphorus and particulate nitrogen inputs to the lake, but have not controlled nitrate inputs (Rutherford, 2003).

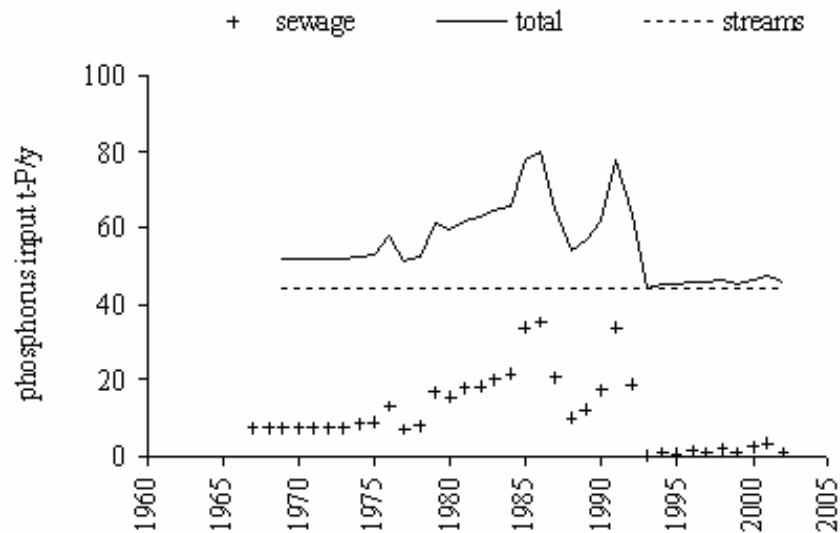


Figure 7.2: Estimated sewage, stream and total load of phosphorus to Lake Rotorua over the period 1967-2003 (Rutherford, 2003).

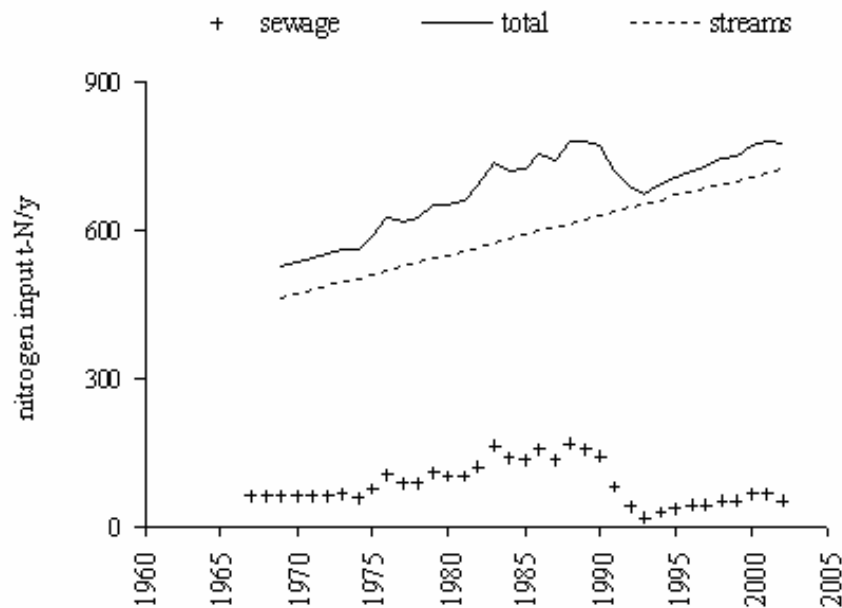


Figure 7.3: Estimated sewage, stream and total load of nitrogen to Lake Rotorua over the period 1967-2003 (Rutherford, 2003).

Nitrogen loading via direct groundwater contributions is approximately 20% of total nitrogen to the lake. Due to the large aquifer system, groundwater has a long residence time and nitrogen loading has not yet reached a steady state in respect to land use change 55 years ago (Morgenstern and Gordon, 2006). Nitrate generated through land clearance and the development of agriculture in the Rotorua

catchment may only now be reaching the lake and is expected to increase by approximately 40% before reaching a steady state (Figure 7.4).

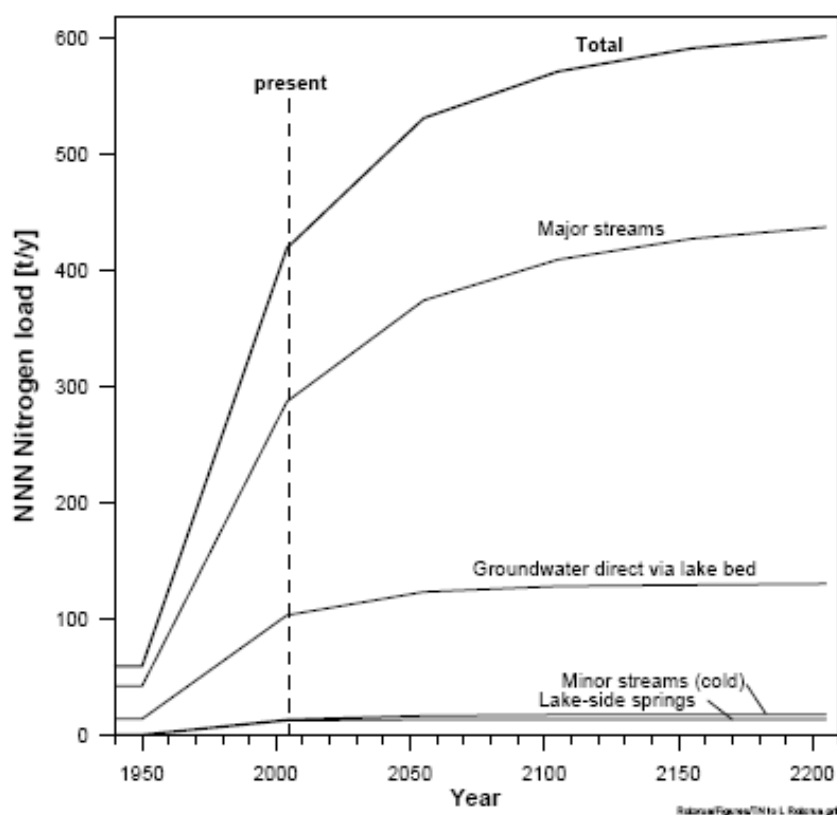


Figure 7.4: Predicted nitrogen loading to Lake Rotorua (Morgenstern and Gordon, 2006).

The high rate of internal recycling of phosphorus in Lake Rotorua suggests that improvements in lake water quality will be delayed after reductions in external nutrient loads, which was observed after sewage removal in the 1990s (Rutherford, 2003). High rates of organic matter sedimentation and subsequent decomposition at the sediment-water interface may be important for enhancing sediment release of nitrogen and phosphorus back into the water column under certain environmental conditions (Marsden, 1989). Resuspension processes may also be important for directly remobilising dissolved nutrients from the sediment porewater back into the overlying water column (Søndergaard, 1992). Howard-Williams and Kelly (2003) estimated that just four days of anoxic conditions over the lakes sediments would produce the same amount of nitrogen and phosphorus that are brought into the lake by all external sources for an entire year. Scenarios

of external and internal load reductions developed by Burger (2006) indicate that the internal sediment nutrient flux is currently more important in influencing nutrient loads in Lake Rotorua than external nutrient sources. Reducing the internal nutrient load is therefore a more effective management strategy to achieve short-term improvements in water quality than external load reductions under the present loading rates. The major methods for reducing internal concentrations and recycling are listed in Rowe (2004) and include: dilution, or flushing and the selective abstraction of nutrient rich waters from the lake; sediment removal; chemical treatment of the lake water to precipitate phosphorus; treatment of the sediment to physically seal phosphorus within them; chemical treatment to bind phosphorus in the sediment and prevent its release when anoxic conditions occur; and sediment oxidation.

7.2.3 Bulk Density

The bulk density of the diatomaceous material is an important factor that needs to be taken into consideration for chemical and physical restoration techniques. The bulk density of the sediment in Lake Rotorua ranges from less than 0.02 g/cm³ below the sediment-water interface in the diatomaceous ooze to 0.5 g/cm³ in the coarse, sandy material nearer the lake shore. Restoration with flocculent materials, to prevent fluxes of nutrients from the sediment re-entering the water column, have to be located where the material has the greatest ability to bind nutrients in the sediment or extract nutrients from the water column. If the density of the material used is much higher than the diatomaceous ooze it will sink into the sediment, reducing the effectiveness of the material. For a sediment removal remediation method, such as dredging, the bulk density is important for disposal of the sediment. The percentage of water in the diatomaceous sediment is >90% (Appendix 2), therefore a suitable location for dewatering, drying and disposal is required.

7.2.4 The Gas Problem

The presence of gas in the sediment has the potential to affect remediation options. Motion (In Prep) estimated the natural rate of ebullition from Lake Rotorua sediment to be $1.38 \times 10^6 \text{ m}^3 \text{ yr}^{-1}$. Ebullition contributes nutrient rich porewater back into the overlying water column at a rate higher than diffusion.

The presence of gas limits physical remediation options for Lake Rotorua. Dredging or ploughing the sediment would trigger a release of gas transporting nutrient rich porewater into the lake. The large influx of nutrients from the porewater would have a negative effect on lake water quality. The influx of nutrients in the lake water would also affect water quality in Lake Rotoiti from discharge through the Ohau Channel. Sediment capping would also be limited as ebullition from the sediment could compromise the integrity of the capping layer.

A possibility for remediation is to stimulate the sediment to a desired depth by flushing water or air into the sediment to release gas, porewater and to suspend the fine diatomaceous sediment. Capturing the gas and water for removal may be a problem but if solved the gas could be separated, the water treated to remove nitrogen and phosphorus before being returned to the lake and the suspended sediment removed and placed in landfill.

7.2.5 Biological Possibilities

Manipulation of the trophic state of a lake without chemicals and machinery is rich in possibilities and requires a long term commitment. Various types of biomanipulation can be used to alleviate eutrophication by developing methods to address the weed problems, reduce algal blooms, reduce species and populations of problem fish, or combat nutrient cycling and sediment resuspension (Rowe, 2004).

Phillips (2006) investigated the potential for freshwater mussels to reduce phytoplankton abundance in the Rotorua Lakes. Freshwater mussels have the potential to reduce phytoplankton abundance by filter-feeding phytoplankton out of the water column. However practical considerations (such as low growth rates requiring high stocking densities) and biotic factors (such as calcium limitation) are likely to limit the use of freshwater mussels in practice. Freshwater mussel shells found in the core samples from Lake Rotorua were brittle and poor quality, suggesting that the lake does not contain sufficient calcium to support the stocking densities required to improve water quality.

7.2.6 Other Conditions for Restoration Options

Certain criteria must be considered when establishing remediation options, such as the effectiveness of the material or remediation strategy, the costs and adverse effects on the environment.

The cost of a remediation method strongly influences the options for remediation. Physical modification methods, such as dredging, require contractors and the time required to carry out the operation budgeted for. Miller (2005) stated that when two chemical remediation materials show similar promise, the material that can be obtained more cheaply is given preference. Naturally occurring and locally available materials may be obtained more cost efficiently than others.

The most important factor for chemical restoration materials is the ability to bind and retain major nutrients under both oxic and anoxic conditions. Yang *et al.* (2004) found that modified zeolite (clay mineral) had the ability to achieve >95% phosphate removal and >50% nitrate removal through the use of incubation studies. It was found that the binding of phosphate is largely irreversible under natural pH and temperature conditions. Özkundakci (2006) investigated the efficiency of sediment capping materials and flocculants for nutrient removal in Lake Okaro, New Zealand. Özkundakci (2006) found none of the materials trialled (allophane, alum, iron slag, lime, PhoslockTM and zeolite) in mesocosm chambers in the lake reduced dissolved or total species significantly over the trial period, and concluded that further trials were needed before using the material in other lakes in the Rotorua Region.

The effect of the remediation effort on the environment is an important limiting factor. The toxicity of a chemical material to the ecosystem, and the potential effects on flora and fauna need to be extensively researched before application or operation. The ‘down-stream’ effect of physical modification, chemical application and biological actions on the environment needs to be considered. The outflow from Lake Rotorua discharges through the Ohau Channel into Lake Rotoiti before entering the Kaituna River and transported out to sea.

7.3 RECOMMENDATIONS

The reduction of nutrients into Lake Rotorua from the removal of sewage resulted in an improvement of water quality for a short period but other nutrient sources have increased in the catchment since then. A sustained effort to reduce nitrogen and phosphorus loading to the lake is required if longer term improvements to water quality are to occur.

The results obtained from this thesis raise the question of suitability in regard to some of the remediation options discussed. The presence of methane gas in the sediment compromises traditional dredging options as physical disturbance will trigger the release of gas and an influx of nutrients from the porewater into the lake. Sediment removal as a remediation option is still a possibility if solutions to the gas problem are found. Sediment capping is also limited by the natural ebullition of methane from the sediment. The use of flocculants also remains a suitable option to retain phosphorus in the sediment and reduce the internal cycling of phosphorus in Lake Rotorua, but is likely to have little effect on nitrogen recycling.

7.4 SUMMARY

The implications raised during the course of this study limit the use of remediation options available for Lake Rotorua. The high rate of internal cycling of nutrients from the sediment back into the water column minimises the effects resulting from reducing external nutrient sources, such as sewage diversion. Physical and chemical restoration techniques, such as sediment removal or capping would be most beneficial where the sediment has a high phosphorus concentration (>1500 g/tonne) in water depths greater than 15 m. The sediment in these areas in Lake Rotorua has a low bulk density and a large volume of methane trapped within the diatomaceous sediment supplying a significant contribution of nutrients to the overlying lake water which increases during anoxic conditions. The physical and chemical properties of the sediment reduce the feasibility of certain restoration options.

REFERENCES

- Burger, D. B., 2006. Dynamics of internal nutrient loading in a eutrophic polymictic lake. Ph.D. Thesis, Department of Biological Sciences, University of Waikato.
- Cooke, G.D., Welch, E.B., Peterson, S.A. and Newroth, P.R. 1993. Restoration and Management of Lakes and Reservoirs. 2nd Edition. CRC Press Incorporated. Lewis Publishers. Boca Raton. 548pp.
- Davidson, G.R., Bennett, S.J., Beard III, W.C. and Waldo, P. 2005. Trace elements in sediments of an aging reservoir in rural Mississippi: Potential for mobilisation following dredging. *Water, Air and Soil Pollution*. 163: 281-292.
- Faithfull, C.L., Hamilton, D.P. and Burger, D.F. 2005. Waikato peat lakes sediment nutrient removal scoping exercise. Centre for Biodiversity and Ecology Research, University of Waikato. Prepared for Environment Waikato. Technical Report 2006/15.
- Gulati, R.D. and van Donk, E. 2002. Lakes in the Netherlands, their origin, eutrophication and restoration: State-of-the-art-review. *Hydrobiologica*. 479: 73-108.
- Harper, D. 1992. Eutrophication of waters, principles, problems and restoration. Chapman Hall. London.
- Howard-Williams, C. and Kelly, D. 2003. Local perspectives in Lake Restoration and Rehabilitation. In: Kumangai, M. and Vincent, W.F. (Eds) *Freshwater Management: Global Versus Local Perspectives*. Springer. 153-175.
- Jeppesen, E., Søndergaard, M., Jensen, J.P. and Lauridsen, T.L. 2003. Recovery from Eutrophication. In: Kumangai, M. and Vincent, W.F. (Eds) *Freshwater Management: Global Versus Local Perspectives*. Springer. 135-151.
- Kleeberg, A., Hammerling, R. and Nixdorf, B. 2001. Effect of hypolimnetic discharge on the faster deprivation of phosphorus from lake sediment (Lake Jabel, north-east Germany). *Lakes and Reservoirs: Research and Management*. 6: 289-295.
- Marsden, M.W. 1989. Lake restoration by reducing external phosphorus loading: the influence of sediment phosphorus release. *Freshwater Biology*. 21: 139-162.
- Miller, N. 2005. Locally available adsorbing materials, sediment sealing and flocculants for chemical restoration of lake and stream water. Report prepared for Environment Bay of Plenty. Analytical and Environmental Consultants. Rotorua. 82pp.

- Morgenstern, U. and Gordon, D. 2006. Prediction of Future Nitrogen Loading to Lake Rotorua. GNS Science. Consultancy Report: 2006/10.
- Motion, O.J. In Prep. Early Diagenesis in Lake Rotorua Sediment. MSc Thesis, Department of Chemistry, University of Waikato.
- Özkundakci, D. 2006. Efficiency of sediment capping materials and flocculants for nutrient removal as a lake restoration technique: Case study on Lake Okaro, New Zealand. *Diplom* Thesis. University of Waikato, New Zealand and University of Applied Sciences, Germany.
- Phillips, N. 2006. Review for the potential for biomanipulation of phytoplankton abundance by freshwater mussels (Kakahi) in the Rotorua lakes. NIWA Client Report: HAM2006-125. Prepared for Environment Bay of Plenty.
- Rowe, D. 2004. Lake Restoration. In: Harding, J., Mosley, P., Pearson, C. and Sorrell, B. Freshwaters of New Zealand. New Zealand Hydrological Society Inc. and New Zealand Limnological Society Inc. Caxton Press. Christchurch, New Zealand. 764pp.
- Rutherford, K. 2003. Lake Rotorua Nutrient Load Targets. NIWA Client Report: HAM2003-155. Prepared for Environment Bay of Plenty.
- Søndergaard, M., Kristensen, P., and Jeppesen, E. 1992. Phosphorus release from resuspended sediment in the shallow and wind-exposed Lake Arresø, Denmark. *Hydrobiologia*. 228: 91-99.
- Yang, Z., van den Heuvel, M.R. and Stuthridge, T.R. 2004. Assessment of the performance of nutrient reduction treatments for the Rotorua lakes. Eco-Smart Technologies, Forest Research. Prepared for Environment Bay of Plenty. Contract R02445.

CHAPTER EIGHT:

CONCLUSIONS



8.0 INTRODUCTION

The sediment of Lake Rotorua is a vital part of the ecosystem of the lake, providing both a sink and a source for nutrients. Conclusions drawn from this thesis in relation to sediments of Lake Rotorua are summarised in terms of the physical and chemical composition of the sediment resulting from the extensive coring programme. The geophysical survey added to the understanding of the sediment and provided a detailed map of the bathymetry and features of interest on the lake floor.

8.1 PHYSICAL COMPOSITION

There are two types of sediments found in Lake Rotorua. In the lake margins, up to ~10 m water depth, the sediment is dominated by coarse clastic erosion products and coarse rhyolitic airfall components. Wave action prevents the finer material from settling out and currents then focus these sediments towards deeper areas of the lake. The coarse sand and gravel-sized pumice covers approximately 60% of the lake area. In the remaining 40% of the lake area with water depths greater than 10 m the sediments is dominated by diatomaceous ooze. It is comprised of the fine, low-density material accumulated by decomposition of biota within the lake. The cyanobacteria and many other phytoplankton appear to leave little material to accumulate in the bottom sediments but diatom frustules remain largely intact and resistant to decay, and therefore dominate the bulk of the sediment. The diatom frustules present in the sediment are dominated by *Aulacoseira granulata* (formerly *Melosira granulata*). The sediment contains a record of volcanic eruptions from deposited ejecta. From the 3 m piston cores taken from Lake Rotorua, the Tarawera Tephra and Kaharoa Tephra can be identified at typically 0.5 m and between 2 to 3 m depth, respectively, in water depths of 10-15 m.

The bulk density of the sediment ranges from less than 0.02 g/cm³ below the sediment-water interface in the diatomaceous ooze to 0.5 g/cm³ in the coarse, sandy material nearer the lake shore. The bulk density of the material declines rapidly as the transition occurs from a sandy lake bed to diatomaceous material.

Even lower bulk densities were found in surficial sediments from deep water sites near the centre of the lake.

8.2 CHEMICAL COMPOSITION

The bulk of the sediment is silica composed from diatom frustules, therefore the composition of other elements in the sediments is related to the lake composition at the time of diatom deposition, although diagenesis in the sediment differentially changes elemental concentration. Diatoms extract elements (C, H, O, P, N, Si and trace elements) from the surrounding water in approximate proportion to the Redfield ratio. As these elements are metabolised most of the organic matter is remineralised, leaving silica minerals which have a very large surface area. This material provides sites for adsorption and ion exchange so that the settling frustules also transport iron and manganese oxides/hydroxides and many co-precipitated and adsorbed trace metals from the water column to the sediments. The nutrients in the sediments may be recycled back into the water column or progressively buried.

The retention of phosphorus in aquatic sediments is a major factor regulating the trophic state of the overlying waters in a wide variety of environments. Phosphorus concentrations in Lake Rotorua sediments decrease with sediment depth. In the centre of the lake phosphorus concentrations in the top 2 cm can reach 2500 g/tonne and decline to 800 g/tonne by 20 cm depth. Since the Tarawera eruption (1886 AD), 3576 tonnes of phosphorus have accumulated in the sediment, equating to an accumulation rate of 29.6 t/yr. Iron and manganese concentrations in the sediment are dependent on the availability of these elements and the sedimentation rate of diatom frustules, and mobilisation is controlled by the redox conditions in the sediment. The average concentration of iron and manganese in the sediment is approximately 8000 g/tonne and between 300 and 400 g/tonne, respectively. Iron accumulates at a rate of approximately 385 t/yr and manganese at 17.9 t/yr in the sediment. Maximum concentrations of arsenic in the sediment are 250 g/tonne but are generally between 50-100 g/tonne, depending on the water depth. Lead concentrations are typically below 15 g/tonne. Sediment concentrations of both arsenic and lead are highly correlated with iron and manganese in the sediment and mimic the respective concentration profiles.

Arsenic and lead accumulate in the sediment at a rate of 3.71 and 0.49 t/yr, respectively. Sulfur concentrations typically reach 8000 g/tonne in the centre of the lake. Below the Tarawera tephra, sulfur concentrations exceed those observed above the tephra. All elements show a peak in concentration in the tephra layers.

Concentrations of carbon and nitrogen in the surface sediment are typically c. 5 % and 0.7 %, and decline with depth to <2 % and 0.4 %, respectively. The rapid decrease in carbon and nitrogen concentration in the sediment shows that most of the remineralisation and recycling through digenesis takes place within the top 50 cm, but mostly within the top 10 cm.

8.3 GEOPHYSICAL SURVEY

Lake Rotorua is currently at 280 m above sea level. The bathymetry of Lake Rotorua is dominated by a curved depression extending from Sulphur Point and almost reaching the Ohau Channel. This depression is probably a structural feature likely associated with the collapse of the caldera, but could be an ancient drainage channel. At water depths less than 10 m, a series of near shore terraces are preserved in the sediment to the north in the lake. A series of conical depressions clustered to the north of Sulphur Point and to the east of Mokoia Island are likely to be hydrothermal explosion craters and appear to be actively discharging water and gas.

Sub-bottom echo-sounding shows no return of sonic and seismic signals from most of the lake floor, indicating total absorption of the signal by the gas-filled sediment. In the shallow lake margin environments, generally <10 m water depth, gas is absent and a detailed stratigraphy of multiple reflectors from tephra layers is observed in sub-bottom profiles. The basin sediments of Lake Rotorua are significantly pockmarked, with these circular, flat-bottomed depressions approximately 20-60 m diameter and 0.5-6 m deep. The pockmarks are located on the lake floor in areas where the sediment is saturated with gas. The gas has a composition around 97.7% methane and 2.3% carbon dioxide and is likely to be formed by anaerobic fermentation in the sediment. Over the entire lake sediments the quantity of available methane is approximately 520 million m³ (23,000 tonnes).

Carbon loss from the incoming sediments equates to around 3 mg/cm²/year. Over the 40 km² of gaseous sediment this figure represents is a loss of 1.25 x 10⁶ m³ of methane per year. The measured rate of gas generation in the sediment is 1-3 x 10⁶ m³ of methane per year, most of which is generated between the surface and around 20 to 40 cm depth in the sediment. Methane ebullition from the sediments is likely to displace porewaters, which would be likely to contribute significantly to the recycling of porewater nutrients from the sediment back into the water column.

8.4 REMEDIATION OPTIONS

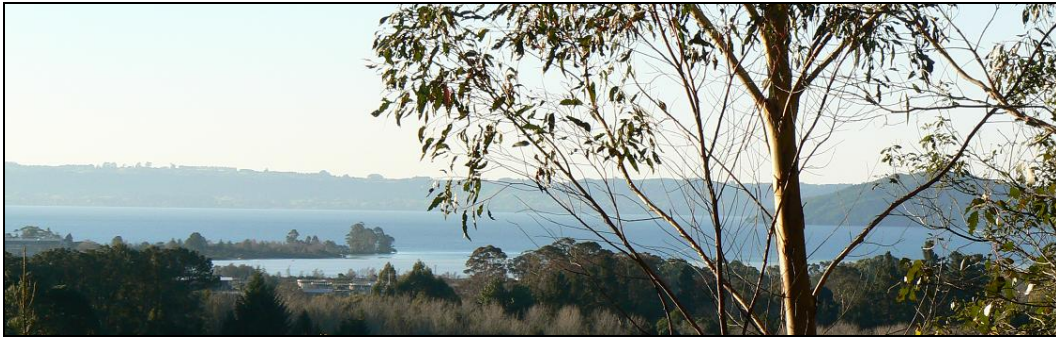
This study indicates that remediation options for Lake Rotorua may be restricted by practical considerations. Lake Rotorua has a high rate of internal cycling of nutrients from the sediment back into the water column, which minimises the benefits of reducing external nutrient sources. The distribution of phosphorus in the sediment dictates areas where physical and chemical remediation activities will have the greatest benefit. From the results discussed in this thesis, it was found that the highest concentrations of phosphorus in the sediment (>1500 g/tonne) are located in areas with water depths >15 m. These areas also have a high sediment accumulation rate, at ~1 cm per year. The sediment in these areas also has a low bulk density and there is a large volume of methane gas trapped within the diatomaceous sediment. The diatomaceous sediment makes a significant contribution of nutrient inputs to the overlying lake water, which increases during anoxic conditions.

The physical and chemical properties of the sediment reduce the feasibility of certain restoration options, such as dredging or sediment capping. The presence of methane gas in the sediment compromises traditional dredging options as physical disturbance will trigger the release of gas and an influx of nutrients from the porewater into the lake. Sediment capping is limited by the natural ebullition from the sediment, as gas release could compromise the integrity of the capping layer. The use of flocculants remains a suitable option to retain phosphorus in the sediment and reduce the internal cycling of phosphorus in Lake Rotorua, but is likely to have little effect on nitrogen recycling.

A possibility for remediation is to mix the sediment to a desired depth by flushing water or air into it to release gas, porewater and to resuspend the fine diatomaceous sediment. Capturing the gas and water for removal may be a problem but if solved, the gas could be separated for commercial benefits, the water treated to remove nitrogen and phosphorus before returning it to the lake, and the suspended sediment removed and dried for possible application as a filter material, building material or for landfill.

APPENDIX ONE:

CORE LOG DATA



APPENDIX ONE- CORE LOG DATA

















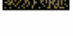

Appendix One contains the core log data for sediment samples from Lake Rotorua. Recorded in the log for each core is as follows:

- Core Number
- Site location in latitude and longitude
- New Zealand Map Grid reference
- Water depth
- Core length
- Core stratigraphy – includes core photos taken at the time of sampling (unless stated otherwise), a description of the core, core type (piston, box or gravity) and observations made during sampling and a location map.
- Chemical analysis of the concentration of phosphorus, iron, manganese, arsenic and lead in the cores.

Chemical analysis of the cores has been carried out at the University of Waikato unless stated otherwise. Initial core samples were sent to Hills Laboratory and have been noted in the core log for the appropriate cores. Many of the initial cores sent to Hills Laboratory have been reanalysed at the University and the core logs retain both results. The concentration data was obtained by primarily using an *aqua regia* digestion of the dry sediment before being run through the ICP-OES or ICP-MS. A number of the cores were also digested using ascorbic acid and those concentrations are included also in the core log.





Core Ru79, in addition to digestion, the sediment was analysed using XRF and the results are recorded in the core log.

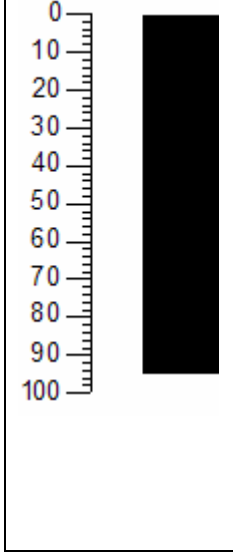

Key for Stratigraphic Column

	Black diatomaceous ooze		Olive grey diatomaceous ooze
	Olive diatomaceous ooze		Grey silt
	Laminated olive diatomaceous ooze		Laminated grey silt
	Olive diatomaceous ooze with black flecks		Grey sand
	Olive diatomaceous ooze with silt		Grey pumice
	Olive diatomaceous ooze with sand		Grey silt with black flecks
	Olive diatomaceous ooze with pumice or gravel		Olive silt
	Olive diatomaceous ooze with gas		Light brown mud
	Dark olive diatomaceous ooze		Organic matter
	Light olive diatomaceous ooze		

Core ID	Site Location	Grid S Grid E	Water Depth (m)	Core Length (m)
Ru 1	38 07 36.5875 S	6336794	21.00	0.95
	176 15 56.8485 E	2796438		



Core Stratigraphy

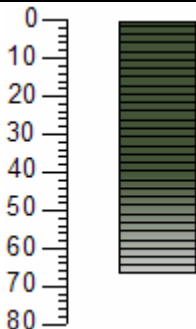
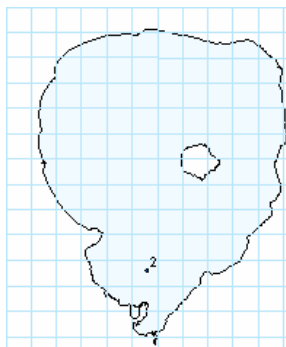
0-26	28-54	54-80	80-95
			

Stratigraphic Column	Description	Location Map
	<p>Piston Core</p> <p>0-95cm Uniform black ooze</p>	

Core ID	Site Location	Grid S Grid E	Water Depth (m)	Core Length (m)
Ru 2	38 07 0.8237 S	6337897	20.20	0.64
	176 15 56.4908 E	2796470		

Core Stratigraphy

0-32	32-64
	

Stratigraphic Column	Description	Location Map
	<p>Piston Core</p> <p>0-40cm Dark olive diatomaceous ooze with thick black banding</p> <p>40-67cm Dark olive diatomaceous ooze with dark grey to black laminations.</p>	

Concentrations Aqua Regia (g/tonne)

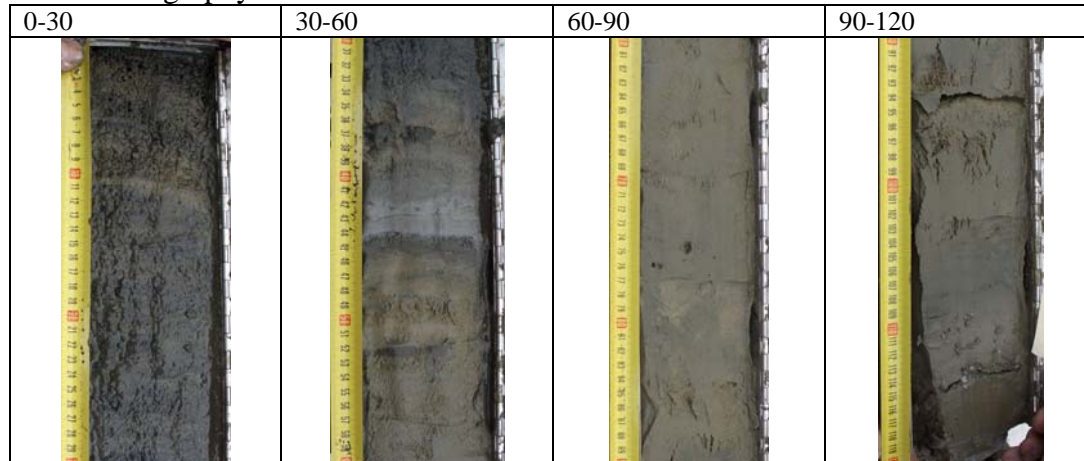
Depth (cm)	As	Fe	Mn	P	Pb
10	22.1	2110	104	238	4.06
33	25	2490	137	310	3
56	25.1	1864	86	193	1.72

Concentrations Ascorbic Acid (g/tonne)

Depth (cm)	As	Fe	Mn	P
10	63	3851	324	68
32	66	3866	365	36
56	72	3859	290	91

Core ID	Site Location	Grid S Grid E	Water Depth (m)	Core Length (m)
Ru 3	38 06 31.2228 S 176 15 57.5504 E	6338808 2796531	15.81	1.2

Core Stratigraphy



Stratigraphic Column	Description	Location Map
	<p>Box Corer</p> <p>0-42cm Diatomaceous ooze</p> <p>42-44cm Grey silt layer (Tarawera Tephra)</p> <p>44-57cm Diatomaceous ooze</p> <p>57 cm onwards becomes more compact</p> <p>Break in sediment at 93 cm</p> <p>115-120 Hard grey pumice (Kaharoa)</p>	

Concentrations (g/tonne) (Hill Laboratories)

Depth (cm)	As	Fe	Mn	P	Pb
1	77	6080	339	524	14
3	53	5650	385	549	11.2
5	56	5450	361	506	10
7	72	6100	396	657	9.3
9	58	4730	341	465	6.4
42.5	21	12400	518	359	8.2
47.5	83	7730	234	245	2.1
85	100	9040	187	172	1.9
115	168	6960	148	148	2.3

Tonnes per square km in top 1 m

As	Fe	Mn	P	Pb
23.3	2279	90	109	1.73

Tonnes per square km above Tarawera tephra

As	Fe	Mn	P	Pb
7.7	641	45	63	0.95

Concentrations Aqua Regia (g/tonne) (Waikato University)

Depth (cm)	As	Fe	Mn	P	Pb
1	90.6	7236	563	615	15.6
3	44.0	4024	410	383	8.2
5	52.4	4781	472	467	9.1
7	68.7	5218	426	547	7.7
9	55.4	4529	458	471	6.4
15	70.0	5410	276	425	5.1
25	95.7	7377	551	358	4.6
35	78.9	9019	511	498	5.4
43	131.7	17139	638	466	7.7
48	152.8	14113	317	251	2.8
55	60.6	7222	212	232	2.1
65	72.8	8866	322	199	2.3
75	56.8	7376	250	172	2.3
95	59.9	5199	142	174	2.0
105	92.1	5018	182	131	2.7

Tonnes per square km in top 1 m



As	Fe	Mn	P	Pb
21.6	2202	99	90	1.2

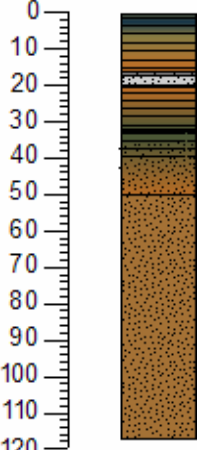
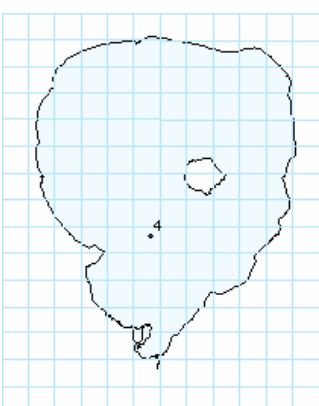
Concentrations Ascorbic Acid (g/tonne)

Depth (cm)	As	Fe	Mn	P	Pb
1	90.6	7236	563	615	15.6
3	44.0	4024	410	383	8.2
5	52.4	4781	472	467	9.1
7	68.7	5218	426	547	7.7
9	55.4	4529	458	471	6.4
15	70.0	5410	276	425	5.1
25	95.7	7377	551	358	4.6
35	78.9	9019	511	498	5.4
43	131.7	17139	638	466	7.7
48	152.8	14113	317	251	2.8
55	60.6	7222	212	232	2.1
65	72.8	8866	322	199	2.3
75	56.8	7376	250	172	2.3
95	59.9	5199	142	174	2.0
105	92.1	5018	182	131	2.7

Core ID	Site Location	Grid S Grid E	Water Depth (m)	Core Length (m)
Ru 4	38 05 58.0928 S 176 16 01.3717 E	6339824 2796660	18.4	1.19

Core Stratigraphy

0-25	25-45	
		Rest of photos are missing

Stratigraphic Column	Description	Location Map
	<p>Box Corer</p> <p>0-16 cm Diatomaceous ooze laminated, dark blue/black to orangey brown</p> <p>16-17.5cm Silty sediment with dark laminations</p> <p>17.5-20cm Pale grey very fine silt (Rotomahana mud, Tarawera tephra)</p> <p>20-32cm laminated orange brown to dark olive</p> <p>32 cm 5mm bright orange band</p> <p>32-50cm laminations fade becoming more silty</p> <p>50-119cm massive light brown silt</p>	

Concentrations (g/tonne) (Hill Laboratories)

Depth (cm)	As	Fe	Mn	P	Pb
0-2	70	6360	347	479	4.6
2-4	73	5880	312	390	3.9
4-6	73	6630	343	435	4.6
6-8	68	7130	319	457	4.6
8-10	66	7720	341	437	4.4
40-50	51	6400	229	204	1.9
80-90	36	2700	90	87	0.9
110-120	63	5240	135	150	1.5

Tonnes per square km in top 1 m

As	Fe	Mn	P	Pb
17.2	1791	75	85	0.84

Tonnes per square km above Tarawera tephra

As	Fe	Mn	P	Pb
3.7	387	18	24	0.24

Concentrations Aqua Regia (g/tonne) (Waikato University)

Depth (cm)	As	Fe	Mn	P	Pb
15	78.2	8520	485	714	16.6
25	66.9	8103	198	275	2.6
35	58.2	5784	441	568	8.0
45	42.3	5000	119	198	1.9
55	40.1	4470	175	168	1.8
65	36.9	3547	134	138	1.4
75	39.4	3008	126	134	1.5
95	62.6	5027	128	149	1.9

Tonnes per square km in top 1 m

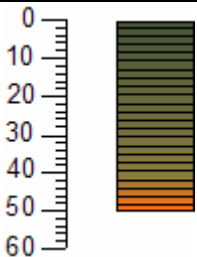

As	Fe	Mn	P	Pb
17.4	1832	76	102	1.7

Concentrations Ascorbic Acid (g/tonne)

Depth (cm)	As	Fe	Mn	P
15	45	3141	430	190
26	33	1503	208	72
35	35	1947	153	65
35*	45	2726	403	139
55	31	1349	188	55
65	32	1091	174	51
75	30	930	166	48
75	34	975	162	47
95	41	1958	89	53
105	40	1314	138	57

Core ID	Site Location	Grid S Grid E	Water Depth (m)	Core Length (m)
Ru5	38 05 58.8834 S 176 15 57.2527 E	6339803 2796560	18.4	0.50

Core Stratigraphy

Stratigraphic Column	Description	Location Map
	<p>Box Corer</p> <p>0-50 cm sloppy laminated dark olive green to orange diatomaceous ooze.</p> <p>No indication of Tarawera Tephra</p>	

Concentrations (g/tonne)

Depth (cm)	As	Fe	Mn	P	Pb
0-10	69	7410	330	713	11
20-30	100	7440	417	770	14.5
40-50	61	5480	358	530	5.2

Tonnes per square km in top 1 m

As	Fe	Mn	P	Pb
18.7	1704	100	166	2.09

Tonnes per square km above Tarawera tephra (more than)

As	Fe	Mn	P	Pb
12.3	1087	57	108	1.74

Core ID	Site Location	Grid S Grid E	Water Depth (m)	Core Length (m)
Ru 6	38 05 26.9820 S 176 15 57.7123 E	6340786 2796604	22.36	0.63

Core Stratigraphy

0-20	20-40	40-63

Stratigraphic Column	Description	Location Map
	<p>Piston Core</p> <p>0-29cm olive diatomaceous ooze</p> <p>29-34cm olive diatomaceous ooze with dark patch</p> <p>34-63cm dark olive/black diatomaceous ooze</p> <p>No evidence of Tarawera Tephra</p>	

Concentrations (g/tonne)

Depth (cm)	As	Fe	Mn	P	Pb
1	83	8080	542	1040	11
3	87	8870	760	1590	9
5	65	6490	499	1010	7
7	57	5590	412	828	6
9	101	8960	642	1530	7
35	73	5740	241	461	2.1
55	43	4740	248	339	1.8

Tonnes per square km in top 1 m









As	Fe	Mn	P	Pb
18.4	1791	106	192	1.15

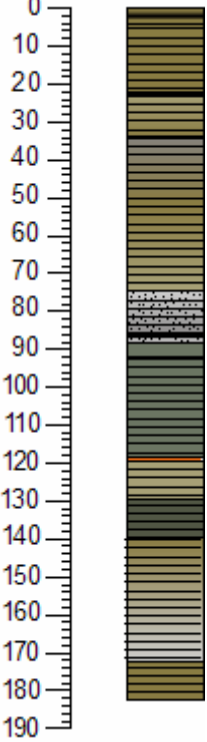

Tonnes per square km above Tarawera tephra (at least)

As	Fe	Mn	P	Pb
13.1	1206	75	150	0.93

Core ID	Site Location	Grid S Grid E	Water Depth (m)	Core Length (m)
Ru 7	38 05 26.2975 S 176 15 57.7165 E	6340807 2796604	22.5	1.80

Core Stratigraphy

0-24	24-48	50-74	70-93
			
93-117	117-151	151-165	163-186
			

Stratigraphic Column	Description	Location Map
	<p>Piston Core</p> <p>0-5cm olive diatomaceous ooze with black band 3-4cm thick</p> <p>5-22.5cm olive diatomaceous ooze with thick black bands</p> <p>22.5-34cm light olive diatomaceous ooze with dark olive laminations</p> <p>34-75cm grey to light olive sesto with dark grey banding</p> <p>75-87cm pale grey to dark grey laminated silty diatomaceous ooze</p> <p>87-89 pale grey silt with sharp upper and lower contacts (Tarawera)</p> <p>89-93.5 pale olive grey diatomaceous ooze</p> <p>90-119cm pale olive grey diatomaceous ooze with dark grey laminations</p> <p>119-120cm thin orange (olive?) band</p> <p>120-130cm pale olive with light grey laminations</p> <p>130-140 cm dark olive grey diatomaceous ooze with black laminations</p> <p>140—173cm olive diatomaceous ooze with light grey laminations</p> <p>173-183cm olive diatomaceous ooze with dark grey laminations</p>	

Concentrations (g/tonne)

Depth (cm)	As	Fe	Mn	P	Pb
0-2	95	9120	327	700	11
2-4	110	9280	327	669	13
4-6	82	8570	532	912	17
6-8	95	9950	439	865	17
8-10	60	7260	438	803	16
40-50	71	5300	277	589	4
80-90	49	9120	361	730	5.9
110-120	70	3960	203	600	2.2

Tonnes per square km in top 1 m


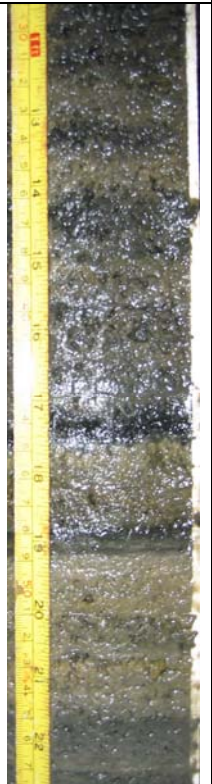


As	Fe	Mn	P	Pb
22.7	2311	108	216	2.69

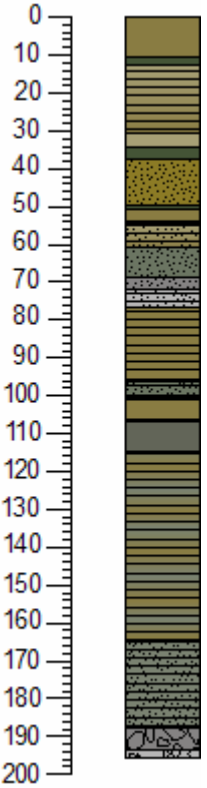

Tonnes per square km above Tarawera tephra

As	Fe	Mn	P	Pb
20.8	1944	93	186	2.45

Core ID	Site Location	Grid S Grid E	Water Depth (m)	Core Length (m)
Ru 8	38 04 53.7814 S 176 15 56.2719 E	6341810 2796609	21.20	2.12

Core Stratigraphy

9-38	38-57	57-91	91-105	
				2 nd half barrel not photographed

Stratigraphic Column	Description	Location Map
	<p>Piston Core</p> <p>0-11cm olive diatomaceous ooze</p> <p>11-13cm dark olive diatomaceous ooze</p> <p>13-31cm olive/light olive laminated diatomaceous ooze</p> <p>31-35cm light olive diatomaceous ooze</p> <p>35-38cm dark olive diatomaceous ooze</p> <p>38-38.5cm laminated dark olive/olive ooze</p> <p>38.5-50 olive silt</p> <p>50-51cm dark olive diatomaceous ooze</p> <p>51-54 olive diatomaceous ooze</p> <p>54-55cm laminated dark grey silt</p> <p>55-61cm light olive laminated diatomaceous ooze</p> <p>61-69cm olive grey diatomaceous ooze, more silty</p> <p>69-72.5cm grey diatomaceous ooze with silt</p> <p>72.5-77cm light grey laminated silt, bottom contact sharp, upper contact gradational (Tarawera)</p> <p>77-97 cm olive laminated diatomaceous ooze</p> <p>97-101cm olive grey laminated diatomaceous ooze with thin grey silt laminations</p> <p>101-104cm olive diatomaceous ooze</p> <p>110-115cm grey olive diatomaceous ooze</p> <p>115-123.5cm dark grey diatomaceous ooze</p> <p>123.5-173.5cm light olive grey diatomaceous ooze with olive laminations</p> <p>173.5-196cm light olive grey silt with dark grey laminations (Kaharoa)</p> <p>196-202.5cm rice bubble sized pumice</p> <p>202.5-204cm sandy pumice</p>	

Concentrations Aqua Regia (g/tonne)

Depth (cm)	As	Fe	Mn	P	Pb
20	56.4	5651	391	629	5.9
40	71.5	6916	396	660	4.7
61	70.4	10687	573	772	6.6
75	51.1	25122	1065	1018	13.3
94	73.9	5006	323	428	3.0
120	90.0	7155	286	298	2.7
140	44.1	5140	195	204	2.1
160	35.4	4196	191	181	2.0
182	53.0	7265	199	174	2.4
204	174.9	6010	92	158	1.9

Tonnes per square km in top 1 m

As	Fe	Mn	P	Pb
20.5	2422	139	198	1.7

Tonnes per square km above Tarawera tephra

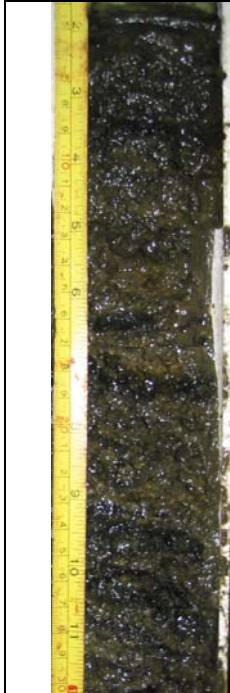

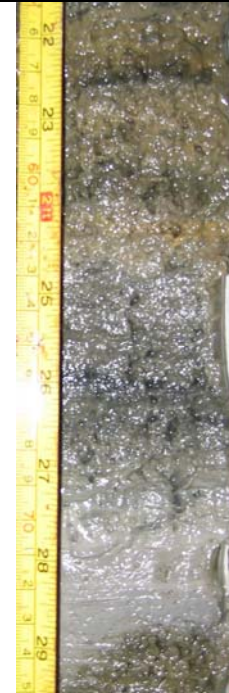




As	Fe	Mn	P	Pb
14.2	1637	96.9	147	1.14

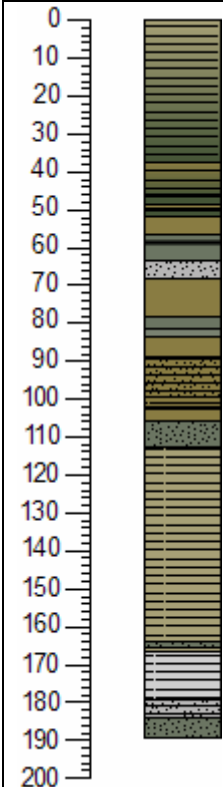

Concentrations Ascorbic Acid (g/tonne)

Depth (cm)	As	Fe	Mn	P
20	55	3625	307	220
40	46	3735	231	144
66	86	7461	414	345
75	19	3688	317	203
89	43	3650	165	146
120	62	4035	193	120
140	85	7684	330	209
160	36	3840	156	84
182	47	3839	140	51
202	94	3804	45	87

Core ID	Site Location	Grid S Grid E	Water Depth (m)	Core Length (m)
Ru 9	38 04 23.1244 S	6342753	19.45	1.9
	176 15 59.0582 E	2796712		

Core Stratigraphy

0-30	30-55	55-75	75-100
			
100-132	132-164	164-193	
			

Stratigraphic Column	Description	Location Map
	<p>Piston Core</p> <p>0-38cm diatomaceous ooze, laminated, light olive-dark olive</p> <p>38-47cm diatomaceous ooze, laminated, olive-dark olive</p> <p>47-49.5cm dark olive laminated diatomaceous ooze</p> <p>49.5-50cm olive diatomaceous ooze</p> <p>50-52.5cm dark olive diatomaceous ooze</p> <p>52.5-57.5 cm olive diatomaceous ooze</p> <p>57.5-64.5cm olive grey diatomaceous ooze, dark band at 61.5</p> <p>64.5-69cm light grey silt. Upeer contact gradational, lower contact unconformable. (Tarawera)</p> <p>69-79.5cm olive diatomaceous ooze</p> <p>79.5-82cm olive grey diatomaceous ooze</p> <p>82-84.5cm light olive diatomaceous ooze</p> <p>84.5-89.5cm olive diatomaceous ooze</p> <p>89.5 – 100cm olive silt with darker laminations</p> <p>100-103cm olive silt with darker laminations</p> <p>103-106.5 olive diatomaceous ooze</p> <p>106.5-113cm olive grey diatomaceous ooze, more silty</p> <p>113-164.5cm light olive laminated diatomaceous ooze</p> <p>164.5-166cm olive grey silt (Tephra?)</p> <p>166-167.5cm light olive diatomaceous ooze</p> <p>167.5-180cm grey laminated silt, gradational contacts (Kaharoa)</p> <p>180-185cm silt dark and light grey laminations</p> <p>185.5-190cm olive grey silt</p>	

Concentrations Aqua Regia (g/tonne)

Depth (cm)	As	Fe	Mn	P	Pb
10	97.5	10689	478	835	19.4
30	93.0	8749	391	794	10.5
52	92.8	11287	422	581	4.7
68	55.7	31759	1218	921	12.7
78.5	146.0	10544	372	603	3.5
92.5	68.3	9487	378	343	3.2
110	78.5	10253	268	280	2.5
130	61.4	5062	169	187	1.7
150	64.8	6161	173	200	1.8
168	640.2	7745	208	511	3.2
183	76.4	6233	131	155	1.9

Tonnes per square km in top 1 m

As	Fe	Mn	P	Pb
29.1	3687	148	207	2.8

Tonnes per square km above Tarawera tephra

As	Fe	Mn	P	Pb
18.7	2038	85	144	2.2

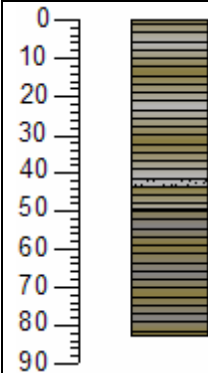

Concentrations Ascorbic Acid (g/tonne)

Depth (cm)	As	Fe	Mn	P
10	65.4	6515.4	363.1	212.0
30	48.2	4703.8	300.7	197.4
50	52.2	4575.0	214.3	159.7
50*	53.4	4389.5	216.7	160.9
68	24.4	4832.3	280.4	198.2
79	49.4	3966.9	183.6	180.5
92	32.9	3840.1	173.7	87.8
110	46.9	5516.8	178.6	79.8
130	45.0	4226.7	136.5	65.3
150	38.8	4268.4	118.4	76.7
167	66.9	5203.1	115.7	75.7
182	58.0	4894.7	99.5	57.1

Core ID	Site Location	Grid S Grid E	Water Depth (m)	Core Length (m)
Ru 10	38 03 48.2003 S 176 15 59.4563 E	6343828 2796761	16.2	0.82

Core Stratigraphy

0-28	28-56	56-83
		

Stratigraphic Column	Description	Location Map
	<p>Piston Core</p> <p>0-42cm olive diatomaceous ooze with grey laminations</p> <p>42-44cm grey silt (Tarawera)</p> <p>44-50cm olive diatomaceous ooze with grey laminations</p> <p>53-83 olive diatomaceous ooze with dark grey laminations</p>	

Concentrations (g/tonne)

Depth (cm)	As	Fe	Mn	P	Pb
0	62	7600	252	508	11
2	57	6610	295	700	11
4	68	7370	321	589	15
6	46	5820	299	497	15
8	46	5410	337	533	15
40	81	7770	260	395	3.7
70	54	7110	236	248	2.1

Tonnes per square km in top 1 m

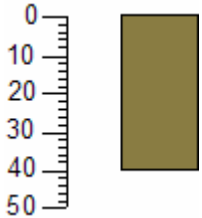

As	Fe	Mn	P	Pb
19.4	2190	83	129	2.19

Tonnes per square km above Tarawera tephra

As	Fe	Mn	P	Pb
7.4	859	39	72	1.68

Core ID	Site Location	Grid S Grid E	Water Depth (m)	Core Length (m)
Ru 11	38 03 15.8824 S	2796761	15.6	0.4
	176 16 01.3092 E	6343828		

Core Stratigraphy

Stratigraphic Column	Description	Location Map
	<p>Box Core</p> <p>0-40 cm Uniform diatomaceous ooze</p> <p>No sign of Tarawera Tephra</p>	

Concentrations (g/tonne)

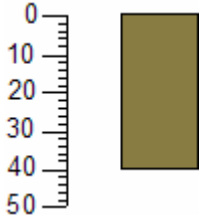

Depth (cm)	As	Fe	Mn	P	Pb
5	60	7300	308	785	8
15	57	6160	290	555	10
25	62	6170	294	546	15.3
35	26	2390	127	233	4.7

Tonnes per square km in top 1 m

As	Fe	Mn	P	Pb
5.6	561.8	27.5	54.3	1.0

Core ID	Site Location	Grid S Grid E	Water Depth (m)	Core Length (m)
Ru 12	38 02 44.1657 S 176 15 57.3697 E	6345801 2796781	9.86	0.4

Core Stratigraphy

Stratigraphic Column	Description	Location Map
	<p>Box Core</p> <p>0-40 cm Uniform olive diatomaceous ooze.</p>	

Concentrations (g/tonne)

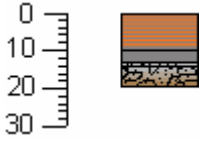

Depth (cm)	As	Fe	Mn	P	Pb
2.5	162	10200	251	241	1.9
7.5	64	7170	202	255	1.4
12.5	43	6840	174	228	1.3
17.5	68	9310	178	162	1.4

Tonnes per square km in top 1 m

As	Fe	Mn	P	Pb
22	2819	56	54	0

Core ID	Site Location	Grid S Grid E	Water Depth (m)	Core Length (m)
Ru 13	38 06 31.3051 S	6338768	14.09	0.2
	176 16 38.5561 E	2797529		

Core Stratigraphy

Stratigraphic Column	Description	Location Map
	<p>Box Core</p> <p>0-10cm banded orange and dark grey diatomaceous ooze</p> <p>10-13cm dark massive mud</p> <p>13cm grey tephra (tarawera?) mm sized pumice fragments</p> <p>13-20cm mixed pumice material and mud</p>	

Concentrations (g/tonne) (Hill Laboratories)

Depth (cm)	As	Fe	Mn	P	Pb
1	78	11300	253	541	7
3	99	13000	438	515	10.8
5	115	13300	434	494	8.4
7	110	12800	516	381	6.2
9	60	12500	471	340	7.5
15	93	11700	329	193	3.1

Tonnes per square km in top 1 m



As	Fe	Mn	P	Pb
52	6535	186	115	2

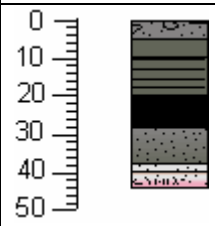

Tonnes per square km above Tarawera tephra

As	Fe	Mn	P	Pb
3.7	497.2	16.1	15.8	0.3

Core ID	Site Location	Grid S Grid E	Water Depth (m)	Core Length (m)
Ru 14	38 06 31.6681 S 176 17 19.3150 E	6338719 2798519	8.53	0.44

Core Stratigraphy

0-20	20-44
	

Stratigraphic Column	Description	Location Map
	<p>Box Core</p> <p>0-5cm Coarse sand, fine gravel + mussels – black layer</p> <p>5-10cm Grey mud</p> <p>10-20cm grey mud + black bands</p> <p>20-28cm mostly black mud + grey patches</p> <p>28-38cm sand coarsening downwards, dark grey colour</p> <p>38-40cm pale grey almost white medium particle sized sand</p> <p>40-44cm orange/grey med sand. Terminates in a pale pink sand with 2/3mm white grains + 1cm sized pumice grains</p> <p>NOTE – Suspect the top of the sediment is being reworked by wave action due to shallowness of site.</p>	

Concentrations (g/tonne)

Depth (cm)	As	Fe	Mn	P	Pb
2.5	27	5780	114	110	1.1
7.5	28	4870	362	104	2.4
27.5	12	17400	689	692	1.5
42.5	20	10200	250	95	0.7
110-120	63	5240	135	150	1.5

Tonnes per square km in top 1 m


As	Fe	Mn	P	Pb
5.3	3131	96	64	0.3

Concentrations Ascorbic Acid (g/tonne)

Depth (cm)	As	Fe	Mn	P
12.5	49.2	5005.5	297.3	26.8
22.5	53.1	4974.6	331.5	183.2
32.5	51.6	7587.1	539.5	89.6
37.5	20.9	3259.2	223.5	16.9




Core ID	Site Location	Grid S Grid E	Water Depth (m)	Core Length (m)
Ru 15		6338700 2799500	5.50	0

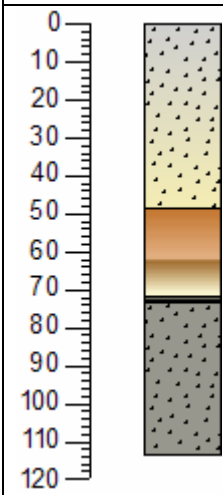

Core Stratigraphy

Stratigraphic Column	Description	Location Map
	<p>Box Corer used</p> <p>Lost the box corer over the side, so very minimal sample recovered.</p> <p>Collected 1 bag of gravel and possibly tarawera ash from this site.</p> <p>Due to the type of sediment (ie gravel) we are not continuing with this site the bottom substrate.</p>	

Core ID	Site Location	Grid S Grid E	Water Depth (m)	Core Length (m)
Ru 16	38 06 31.8787 S 176 15 13.6058 E	6338825 2795459	7.23	1.14

Core Stratigraphy

0-35	35-70	70-106
		

Stratigraphic Column	Description	Location Map
	<p>Box Corer</p> <p>0-49cm appears to have been cored in a previous attempt.</p> <p>Very fine mud that is pale grey to pale yellow with dark flex</p> <p>49cm Sharp boundary to a dark gingery mud (diatomaceous ooze?) gradually lightening towards 63 cm where it becomes pale brown to light cream at 72cm</p> <p>72cm Abrupt transition to a dark grey mud (72-73cm)</p> <p>73-114cm pale grey mud with horizontal grey flex.</p> <p>No sign of Tarawera tephra, mud all the way through.</p> <p>NOTE - Mussels at the top of the core.</p>	

Concentrations (g/tonne) (Hill Laboratories)

Depth (cm)	As	Fe	Mn	P	Pb
5	75	8980	207	157	2.8
45	16	3870	211	409	2.7
85.5	34	5570	134	113	2.1
115	32	6040	175	210	2.4

Tonnes per square km in top 1 m

As	Fe	Mn	P	Pb
12.1	1822	58	75	0.8

Concentrations Aqua Regia (g/tonne) (Waikato University)

Depth (cm)	As	Fe	Mn	P	Pb
15	72.0	8355	307	236	4.2
25	99.0	11444	490	259	6.1
35	51.6	5731	302	155	4.1
53	43.3	4615	257	397	4.4
59.5	556.2	4406	185	100	2.5
67.5	561.8	5149	130	140	2.6
74	210.4	5542	93	130	2.8
95	97.5	14934	231	191	4.0
105	53.3	8500	200	195	3.7

Tonnes per square km in top 1 m


As	Fe	Mn	P	Pb
47.0	2468	89	62	1.3

Concentrations Ascorbic Acid (g/tonne)

Depth (cm)	As	Fe	Mn	P
15	18.8	1322.8	197.9	42.9
15*	16.1	1296.6	211.3	37.3
25	13.3	1608.9	184.0	26.1
35	16.0	1677.8	165.3	29.6
53	16.1	1274.4	130.1	44.1
59.5	140.7	2123.1	164.1	39.7
66.5	112.7	1778.1	161.3	30.4
74	53.6	1593.0	75.3	31.9
95	24.7	2635.9	99.5	31.6
105	15.6	2053.8	154.4	57.3

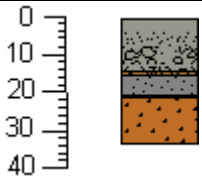

Core ID	Site Location	Grid S Grid E	Water Depth (m)	Core Length (m)
Ru 17	38 06 31.4534 S	6338838	7.36	0
	176 15 13.6437 E	2795460		

Core Stratigraphy

Stratigraphic Column	Description	Location Map
	Box Corer Nothing able to be recovered	

Core ID	Site Location	Grid S Grid E	Water Depth (m)	Core Length (m)
Ru 18	38 06 31.5133 S 176 14 49.2302E	6338859 2794866	2.46	0.33

Core Stratigraphy

Stratigraphic Column	Description	Location Map
	<p>Box Core</p> <p>0-14cm Well worked mud to fine gravel, gravel contains cm sized pumice and freshwater mussels</p> <p>14-15 cm Brown Gravel</p> <p>15-20cm Fine well worked sand</p> <p>20cm Black pea sized gravel this is a sharp boundary</p> <p>20-33cm fine orange/brown mud with black streaks</p>	

Concentrations (g/tonne)


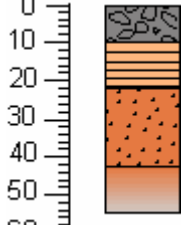

Depth (cm)	As	Fe	Mn	P	Pb
5	16	2610	79	76	1.7
12.5	47	6350	151	115	2.3
17.5	21	3820	70	49	0.9
26.5	104	10300	202	107	1.9

Tonnes per square km in top 1 m

As	Fe	Mn	P	Pb
27.3	2784	56	31	0.6

Core ID	Site Location	Grid S Grid E	Water Depth (m)	Core Length (m)
Ru 19	38 05 08.5834 S 176 17 35.5970 E	6341265 2799011	8.92	0.65

Core Stratigraphy

0-65	Stratigraphic Column	Description	Location Map
		<p>Box Core</p> <p>0-10cm fine gravel made of 3-5 mm pumice pebbles and minor grey band sharp boundary.</p> <p>10-22cm orangey laminated diatomaceous ooze</p> <p>22-43cm orangey grey mud with dark streaks.</p>	

Concentrations (g/tonne)

Depth (cm)	As	Fe	Mn	P	Pb
25	32.8	2786.5	29.7	52.3	2.1
46	43.6	7600.6	47.3	44.8	2.2

Tonnes per square km in top 1 m


As	Fe	Mn	P	Pb
11.8	1605	11.9	15.0	0.7

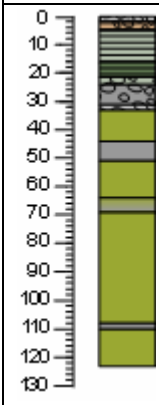

Concentrations Ascorbic Acid (g/tonne)

Depth (cm)	As	Fe	Mn	P
15	18.8	1322.8	197.9	42.9
15*	16.1	1296.6	211.3	37.3
25	13.3	1608.9	184.0	26.1

Core ID	Site Location	Grid S Grid E	Water Depth (m)	Core Length (m)
Ru 20	38 05 08.2889 S 176 18 17.3705 E	6341237 2800028	9.45	1.19

Core Stratigraphy

0-25	25-47	47-69	69-91	91-117
				

Stratigraphic Column	Description	Location Map
	<p>Piston Core</p> <p>0-2cm rice bubble size pumice with grey sand (reworked Kaharoa?)</p> <p>2-5cm black mud, orange contact with pumice</p> <p>5-16 cm grey mud with black laminations</p> <p>16-21cm black mud with grey laminations</p> <p>21-24.5cm rice bubble size pumice with greyish mud</p> <p>24.5-31 cm rice bubble size pumice with dark greyish sand.</p> <p>31-33 cm pumice.</p> <p>33-44 cm olive diatomaceous ooze.</p> <p>44-51 cm grey sand grading down from grey sandy silt.</p> <p>51-64 cm olive diatomaceous ooze.</p> <p>64-69 cm organic rich layer grading down into silt sandy at top contact.</p> <p>69-108 cm very sticky dense olive slightly sandy diatomaceous ooze.</p> <p>108-110 cm grey sand.</p> <p>110-123 cm very sticky silty olive diatomaceous ooze.</p>	

Concentrations (g/tonne)

Depth (cm)	As	Fe	Mn	P	Pb
1	192.9	16257	280	383	3.2
11.5	166.3	10555	216	174	2.3
29	62.9	6501	120	186	0.9
41.5	325.4	14595	322	248	3.2
47.5	36.8	8324	165	216	2.2
57.5	78.3	17307	550	1671	3.2
66.5	781.5	37498	372	316	3.4
79	49.6	18471	603	909	4.2
98.5	31.2	12951	485	480	3.8
109	25.4	14691	391	356	5.0
117	50.0	10925	348	460	2.8

Tonnes per square km in top 1 m

As	Fe	Mn	P	Pb
40	4716	125	189	1.0

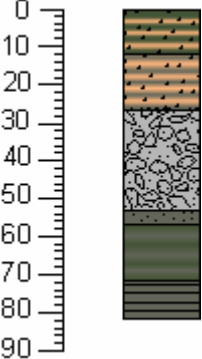

Concentrations Ascorbic Acid (g/tonne)

Depth (cm)	As	Fe	Mn	P
1	40.3	3044.2	80.3	136.6
11	65.8	3626.6	106.9	86.8
26	30.6	2346.6	54.2	55.2
40	49.4	3475.6	163.6	109.0
45.5	17.9	2118.6	65.6	65.2
57.5	45.3	7040.5	269.5	903.0
67	134.8	5100.8	186.6	92.9
79	21.8	4913.5	300.1	638.5
99	15.3	4284.1	194.8	256.6
109	13.6	3063.5	98.0	133.0
117	21.8	4000.7	160.4	271.1

Core ID	Site Location	Grid S Grid E	Water Depth (m)	Core Length (m)
Ru 21	38 05 08.8141 S	6341207	6.45	0.84
	176 18 57.1219 E	2800996		

Core Stratigraphy

0-27	27-54	54-80
		

Stratigraphic Column	Description	Location Map
	<p>Piston Core</p> <p>0-12cm dark olive mud, black patches, orange streaks</p> <p>12-27cm dark grey mud, black patches, orange streaks</p> <p>27-53cm sandy pumice</p> <p>53-57cm sandy mud, gritty, dark grey</p> <p>57-72cm dark grey & dark olive mud</p> <p>72-82cm dark grey mud with black laminations (hard).</p>	

Concentrations (g/tonne)

Depth (cm)	As	Fe	Mn	P	Pb
6	59.0	23595	603	899	11.5
19.5	40.2	19122	514	622	7.9
42	24.4	9634	167	195	2.1
69.5	7.8	18418	260	288	6.0

Tonnes per square km in top 1 m


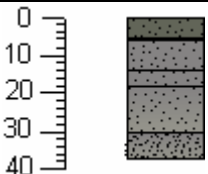

As	Fe	Mn	P	Pb
7.4	5101	96	119	1.8

Concentrations Ascorbic Acid (g/tonne)

Depth (cm)	As	Fe	Mn	P
6	40.3	3044.2	80.3	136.6
19.5	65.8	3626.6	106.9	86.8
42	30.6	2346.6	54.2	55.2
69.5	49.4	3475.6	163.6	109.0

Core ID	Site Location	Grid S Grid E	Water Depth (m)	Core Length (m)
Ru 22	38 05 08.5074 S 176 19 15.6219 E	6341178 2801446	0.51	0.36

Core Stratigraphy






0-36	Stratigraphic Column	Description	Location Map
		<p>Gravity Core</p> <p>Well worked sand</p> <p>Sand well sorted coarsening on top</p> <p>0-5cm oxidized dark colour</p> <p>14-18cm paler bands</p> <p>30-37cm siltier fine sand</p> <p>NOTE – looks as though 1 unit, looks to being actively wave worked.</p>	

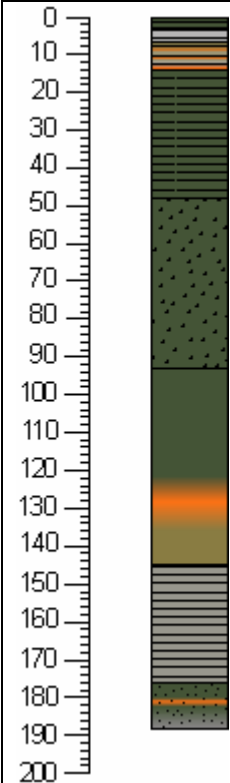

Concentrations (g/tonne)

Depth (cm)	As	Fe	Mn	P	Pb
5	4	4310	63	72	0.8
33.5	3	3900	61	65	1.2

Core ID	Site Location	Grid S Grid E	Water Depth (m)	Core Length (m)
Ru 23	38 05 07.8741 S 176 16 28.9905 E	6341346 2797389	15.48	1.57

Core Stratigraphy

0-35	35-68	68-95	95-120	120-150
				

Stratigraphic Column	Description	Location Map
	<p>Piston Core</p> <p>0-3cm diatomaceous ooze, dark olive, black laminations</p> <p>3-7cm light grey mud, black laminations (Tarawera)</p> <p>7-14cm olive diatomaceous ooze, orange, grey, dark grey, black laminations</p> <p>14-48cm dark olive diatomaceous ooze, black laminations</p> <p>48-93cm dark olive diatomaceous ooze with black patches</p> <p>95-145cm diatomaceous ooze dark olive orange band, fibrous black olive fluffy</p> <p>145-176cm light grey mud black laminations, gummy</p> <p>176-188 dark olive diatomaceous ooze, orange band dark grey firmer, black mud patches, irregular contacts.</p>	

Concentrations (g/tonne)

Depth (cm)	As	Fe	Mn	P	Pb
3.5	36.7	5017	156.3	228.9	4.4
13.5	69.3	5719	138.0	197.7	3.0
30	27.1	3539	100.3	310.8	7.1
50	33.9	3803	92.0	263.1	6.5
70	32.8	3874	68.5	240.2	5.3
87.5	27.2	2927	58.9	247.9	3.4
105	21.4	2906	106.1	413.9	3.0
122.5	43.4	4601	110.6	150.8	2.4
137.5	48.0	5392	139.3	196.6	2.9
160.5	22.4	6515	218.0	202.8	4.1
182.5	40.2	4536	129.4	227.8	3.1

Tonnes per square km in top 1 m

As	Fe	Mn	P	Pb
11.0	1212	29.4	81.1	1.6

Tonnes per square km above Tarawera tephra




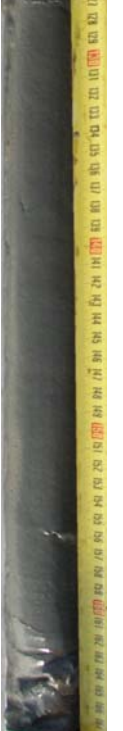
As	Fe	Mn	P	Pb
0.4	54	2	2	0.05

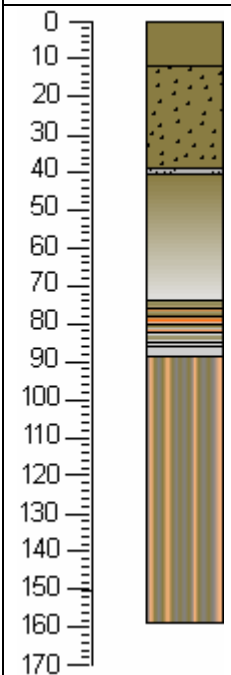

Concentrations Ascorbic Acid (g/tonne)

Depth (cm)	As	Fe	Mn	P
3.5	23.5	4197.7	270.3	94.0
13.5	52.4	6932.4	394.2	104.1
30	45.1	6035.3	288.6	128.3
50	63.4	7303.5	392.2	143.8
70	66.6	8698.3	355.1	154.2
87.5	59.3	7804.5	378.7	201.0
105	55.7	6576.2	367.0	307.8
122.5	77.0	9013.7	324.5	113.2
137.5	54.0	7594.4	360.9	118.6
160	15.9	4281.8	352.1	102.1
183	48.7	6080.6	353.0	171.1

Core ID	Site Location	Grid S Grid E	Water Depth (m)	Core Length (m)
Ru 24	38 05 07.8872 S 176 15 47.7497 E	6341329 2797844	20.09	1.6

Core Stratigraphy

0-37	37-74	74-115	115-156
			

Stratigraphic Column	Description	Location Map
	<p>Piston Core</p> <p>0-11cm olive diatomaceous ooze</p> <p>11-39.5cm olive diatomaceous ooze with thick black areas</p> <p>39.5-41cm fine pale grey silt with thin lower contact of fine sand (Tarawera)</p> <p>41-74cm olive to very pale grey diatomaceous ooze</p> <p>74-86 pale olive to pale grey diatomaceous ooze with olive to orange laminations</p> <p>86-88.5 pale grey diatomaceous ooze</p> <p>88.5-159.5cm dark grey diatomaceous ooze with vertical streaks of olive, pale grey and pale orange.</p>	

Concentrations (g/tonne)

Depth (cm)	As	Fe	Mn	P	Pb
10	29.1	4904	152.9	218.8	4.2
29.5	40.2	3872	93.6	128.9	2.0
40	11.0	2224	63.2	190.8	4.4
87.5	17.2	2657	64.5	179.0	4.4
27.5	21.9	3367	59.7	203.8	4.6
84	18.0	2655	53.6	219.8	3.0
104	15.1	2963	108.3	416.9	3.0
124	37.3	4638	111.7	147.2	2.3
146.5	42.2	5495	142.2	195.4	2.9

Tonnes per square km in top 1 m

As	Fe	Mn	P	Pb
7.7	1076	27.0	63.3	1.1

Tonnes per square km above Tarawera tephra





As	Fe	Mn	P	Pb
4.2	530	15	21	0.38

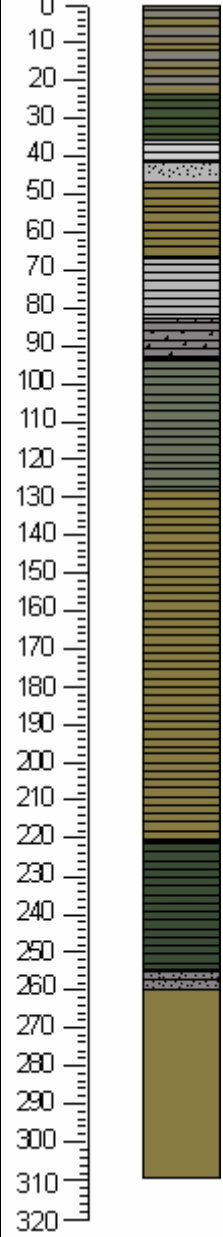

Concentrations Ascorbic Acid (g/tonne)

Depth (cm)	As	Fe	Mn	P
10	39.5	4008.2	262.0	165.7
30	38.9	5297.3	246.6	204.3
40	21.6	4281.3	180.1	224.0
49	35.5	3919.8	192.2	220.1
65	35.8	4064.3	187.2	199.1
84	43.6	4272.4	199.0	161.6
104	62.4	5599.3	205.7	224.9
124	52.9	4360.9	223.1	166.3
147	49.9	4422.2	260.5	159.3

Core ID	Site Location	Grid S Grid E	Water Depth (m)	Core Length (m)
Ru 25	38 05 08.0773S 176 15 07.5113 E	6341413 6341413	14.00	3.29

Core Stratigraphy

0-68	68-156	156-248	248-338
			

Stratigraphic Column	Description	Location Map
	<p>3-27cm olive diatomaceous ooze with dark grey and black laminations</p> <p>27-39cm dark olive diatomaceous ooze with black laminations</p> <p>39-44cm grey diatomaceous ooze with black laminations</p> <p>45-50cm silt, upper contact gradational lower contact sharp and slightly tilted (Tarawera)</p> <p>50-70cm Olive diatomaceous ooze with dark grey laminations</p> <p>78-94cm grey diatomaceous ooze with dark grey laminations</p> <p>94-115cm dark grey diatomaceous ooze with black laminations and black patches</p> <p>115-140cm grey olive diatomaceous ooze with dark grey laminations</p> <p>178-270cm uniform consistency, olive diatomaceous ooze with grey laminations</p> <p>277-312cm dark olive diatomaceous ooze with dark grey laminations</p> <p>312-317cm dark grey silt with black laminations, sharp contact at bottom (Kaharoa?)</p> <p>317-366cm olive diatomaceous ooze</p>	

Concentrations (g/tonne)

Depth (cm)	As	Fe	Mn	P	Pb
1	60	6720	319	600	17
3	60	6410	282	1000	14
5	60	9780	350	535	16
7	52	6660	312	589	17
9	43	5890	335	577	16
15	61	6860	324	619	14.3
55	83	6440	227	440	2.9
105	77	7150	233	374	2.6
155	47	6260	159	193	1.6
305	54	7340	174	200	1.7
355	54	5220	147	193	1.6

Tonnes per square km in top 1 m


As	Fe	Mn	P	Pb
24.1	2023	76	148	1.7

Tonnes per square km above Tarawera tephra

As	Fe	Mn	P	Pb
8.3	961.1	44.9	87.3	2.04






Core ID	Site Location	Grid S Grid E	Water Depth (m)	Core Length (m)
Ru 26	380556.7031S	6339906	11.77	0.38
	1761518.2584E	2795613		





Core Stratigraphy

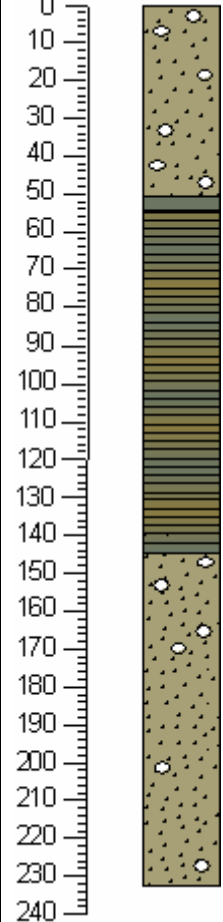

Stratigraphic Column	Description	Location Map
	Box core Sample bagged	

Core ID	Site Location	Grid S Grid E	Water Depth (m)	Core Length (m)
Ru 27	38 03 46.1214S	6343857	18.60	2.6
	176 16 39.0884E	2797728		

Core Stratigraphy

0-28	28-55	55-84	84-113	113-143
				

143-168	168-193	193-218	218-233
			

Stratigraphic Column	Description	Location Map
	<p>Piston Core</p> <p>0-51cm light olive diatomaceous ooze, contains black flecks and fibrous organic matter. Large air bubbles throughout and black patches</p> <p>51-55cm olive grey diatomaceous ooze</p> <p>55-145cm mottled olive diatomaceous ooze with laminations. Changes in colour.</p> <p>At 140cm is a 1 mm black tephra (Tarwera?).</p> <p>145-233cm light olive diatomaceous ooze with black flecks, organic matter and air bubbles - NO laminations</p>	

Concentrations (g/tonne)

Depth (cm)	As	Fe	Mn	P	Pb
5	8.51		78.80	235.97	8.94
15	10.31		106.40	290.52	11.16
25	10.21		105.44	264.83	11.33
35	10.06		91.49	234.27	10.75
45	10.09		88.81	201.64	11.17
52.5	9.80		107.58	223.12	10.95
65	9.38		94.44	223.86	9.91
82.5	9.53		87.39	150.12	9.78
112.5	9.88		87.09	122.19	10.11
135	10.60		81.21	137.66	10.93
155	6.29		79.04	105.99	8.37
175	6.29		58.29	86.35	8.63
195	6.35		45.86	66.51	8.44
212.5	5.22		48.05	82.24	8.55
232.5	6.67		34.21	56.63	8.83

Tonnes per square km in top 1 m

As	Fe	Mn	P	Pb
1.5		14.1	32.5	1.6

Tonnes per square km above Tarawera tephra

As	Fe	Mn	P	Pb
0.8		7.4	19.3	0.8

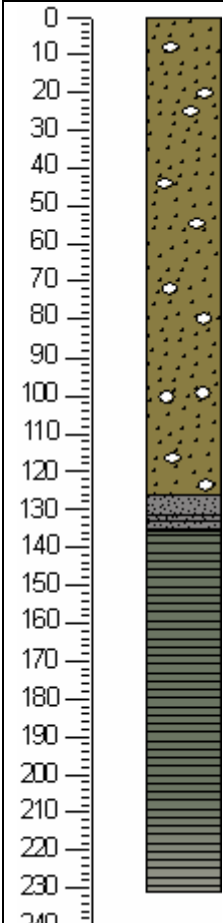

Concentrations Ascorbic Acid (g/tonne)

Depth (cm)	As	Fe	Mn	P
5	29.8	2492.0	302.6	192.4
15	27.0	1760.5	213.4	165.7
25	28.6	1727.0	193.8	149.5
35	31.1	1624.4	193.8	134.2
45	31.8	1821.4	191.3	128.7
53	24.8	1241.0	222.7	101.3
65	29.2	1619.2	230.9	153.4
88	24.4	983.7	247.2	113.1
113	24.3	1049.1	222.2	94.1
135	27.8	1229.8	176.1	68.1
155	26.9	1334.6	164.5	67.2
175	24.8	1197.2	145.9	63.0
195	28.7	1259.6	137.3	61.1
213	31.4	1329.0	131.6	58.0
233	33.0	1415.6	122.4	65.5

Core ID	Site Location	Grid S Grid E	Water Depth (m)	Core Length (m)
Ru 28	38 03 47.9495S 176 17 20.8080E	6343764 2798742	16.00	2.04

Core Stratigraphy

0-22	22-45	45-68	68-92	92-115
				
115-138	138-161	161-185	185-208	208-231
				

Stratigraphic Column	Description	Location Map
	<p>Piston Core</p> <p>0-126cm olive diatomaceous ooze with black patches. Fibrous with air bubbles. Very high water content. Erosional lower contact.</p> <p>126-131cm grey silt (Tarawera?)</p> <p>131-132cm grey silty sand with black clasts</p> <p>132-135cm grey silt with erosional lower contact</p> <p>135-231cm olive-grey diatomaceous ooze, some laminations, more compacted near base</p>	

Concentrations (g/tonne)

Depth (cm)	As	Fe	Mn	P	Pb
7.5	55.6	5556	136.9	439.3	6.4
22.5	33.5	3728	104.5	326.4	4.4
37.5	29.5	3402	105.5	408.8	4.0
55	10.4	4122	280.1	704.0	4.3
75	21.2	2571	95.5	321.2	2.1
95	24.8	2650	88.1	261.5	2.1
115.5	23.8	4130	96.1	300.8	2.7
130.5	16.5	8807	228.6	597.2	5.1
136.5	25.5	2546	93.0	345.8	1.7
148	20.4	4996	121.4	366.1	2.8
168	26.2	2450	85.0	256.6	1.4
188	23.3	2306	79.6	241.1	1.4

Tonnes per square km in top 1 m

As	Fe	Mn	P	Pb
8.6	1124	43.4	129.9	1.2

Tonnes per square km above Tarawera tephra





As	Fe	Mn	P	Pb
10.5	1433	51	153	1.39




Concentrations Ascorbic Acid (g/tonne)

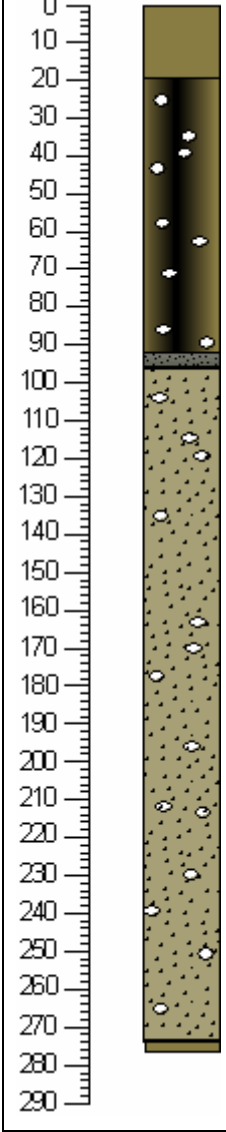

Depth (cm)	As	Fe	Mn	P
23	61.3	5391.5	390.3	215.8
35	61.7	5411.2	236.6	189.3
95	51.0	4045.3	307.2	245.2
115	30.7	3216.3	270.5	219.9
130	15.5	3280.5	235.4	237.7
147	28.4	1669.8	237.2	204.5
168	32.8	1483.0	215.7	165.9
188	27.8	1175.4	239.2	158.2
208	29.7	989.1	267.3	164.9
225	27.3	819.2	240.7	123.2

Core ID	Site Location	Grid S Grid E	Water Depth (m)	Core Length (m)
Ru 29	38 03 47.0243S 176 18 00.7964E	6343728 2799716	15.70	2.83

Core Stratigraphy

0-27	27-54	54-73	73-92
			

92-115	115-138	138-162	162-184
			

Stratigraphic Column	Description	Location Map
	<p>Piston core</p> <p>0-20cm olive diatomaceous ooze, high water content</p> <p>20-92cm centre of core black with margins olive. Fibrous organic matter. Several large air bubbles</p> <p>92-96cm grey silt with grey/black sands at base, erosional contact (Tarawera Tephra)</p> <p>96-273cm massive light olive diatomaceous ooze with air bubbles and black flecks.</p> <p>At 273cm 2mm layer of fine black sand pulled into a "U" by the coring equipment</p> <p>273-276cm olive diatomaceous ooze</p>	

Concentrations (g/tonne)

Depth (cm)	As	Fe	Mn	P	Pb
10	19.2	2852	97.7	341.4	4.2
30	21.8	2572	97.3	304.8	3.4
50	15.1	2181	79.9	230.7	2.1
70	29.5	4270	119.8	310.0	2.7
86	27.8	5868	127.7	383.2	3.6
94.5	12.5	9155	206.3	412.4	5.2
106.5	26.4	2822	80.2	251.7	1.8
131	32.2	2262	61.9	180.9	1.4
156	31.6	3162	84.9	216.7	1.6
175	27.8	3867	93.6	288.8	1.8
194	14.5	2282	62.5	127.0	0.7
214	13.2	2524	64.2	119.9	1.1
234	12.6	2977	71.0	96.7	1.7
254	16.1	3060	63.4	88.7	1.1
270	17.8	3391	70.7	118.3	1.4

Tonnes per square km in top 1 m

As	Fe	Mn	P	Pb
6.8	1119	33.1	96.3	1.0

Tonnes per square km above Tarawera tephra

As	Fe	Mn	P	Pb
6.3	952	29	88	0.90

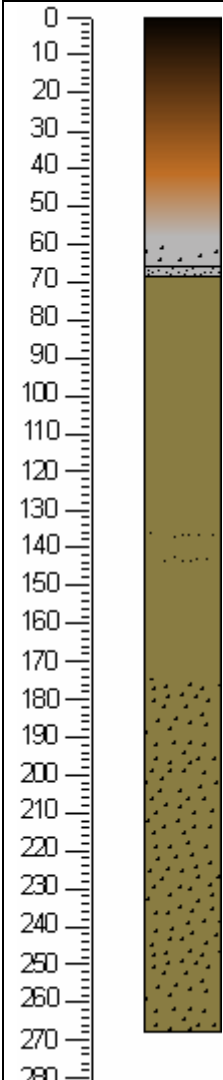

Concentrations Ascorbic Acid (g/tonne)

Depth (cm)	As	Fe	Mn	P
10	54.9	4812.8	442.6	356.0
30	34.1	3512.8	228.0	184.7
50	38.8	3490.5	278.8	183.3
70	37.5	3368.9	219.2	172.2
86	28.0	3280.6	231.3	162.5
95	19.4	3015.3	203.0	179.6
107	37.8	2051.5	199.1	180.4
131	46.1	1732.9	183.8	137.0
156	34.9	1461.7	199.3	105.8
175	32.9	1474.0	216.1	136.8
194	29.6	1312.4	188.2	87.7
214	26.3	1238.3	190.3	76.4
234	26.3	1320.9	187.3	63.9
254	28.0	1267.0	164.3	49.4
270	26.4	1351.6	151.4	54.3

Core ID	Site Location	Grid S Grid E	Water Depth (m)	Core Length (m)
Ru 30	38 03 46.9921S	6343718	11.90	2.92
	176 18 43.1133E	2800747		

Core Stratigraphy

0-24	24-48	48-67	67-85	85-109	109-133
					
133-157	157-175	175-199	199-224	224-247	247-268
					

Stratigraphic Column	Description	Location Map
	<p>Piston Core</p> <p>0-66cm brown-black diatomaceous ooze with ring of olive diatomaceous ooze at edges. Mottled grey for lower 5 cm</p> <p>66-69cm grey sandy silt with erosional contacts (Tarawera tephra)</p> <p>69-175cm massive olive diatomaceous ooze. At 137 cm and 144 cm there are thin 1 mm layers of black sand</p> <p>175-268cm massive olive diatomaceous ooze with some black flecks.</p>	

Concentrations (g/tonne)

Depth (cm)	As	Fe	Mn	P	Pb
10	16.7	2787	102.3	308.5	2.6
32.5	24.7	3910	103.0	218.1	1.3
55.5	27.9	6537	191.8	428.3	3.2
67.5	13.9	7280	171.1	226.5	2.6
77	38.6	4081	103.3	234.9	1.2
95	20.1	3589	89.0	185.6	0.9
115	14.1	2957	70.5	130.4	0.6
135	11.2	2595	69.9	112.6	0.4
155	11.6	2503	57.8	106.5	0.3
170	19.1	2714	51.0	85.5	0.2
185	15.7	2070	49.3	83.2	0.2

Tonnes per square km in top 1 m

As	Fe	Mn	P	Pb
7.7	1334	37.5	86.0	0.6

Tonnes per square km above Tarawera tephra

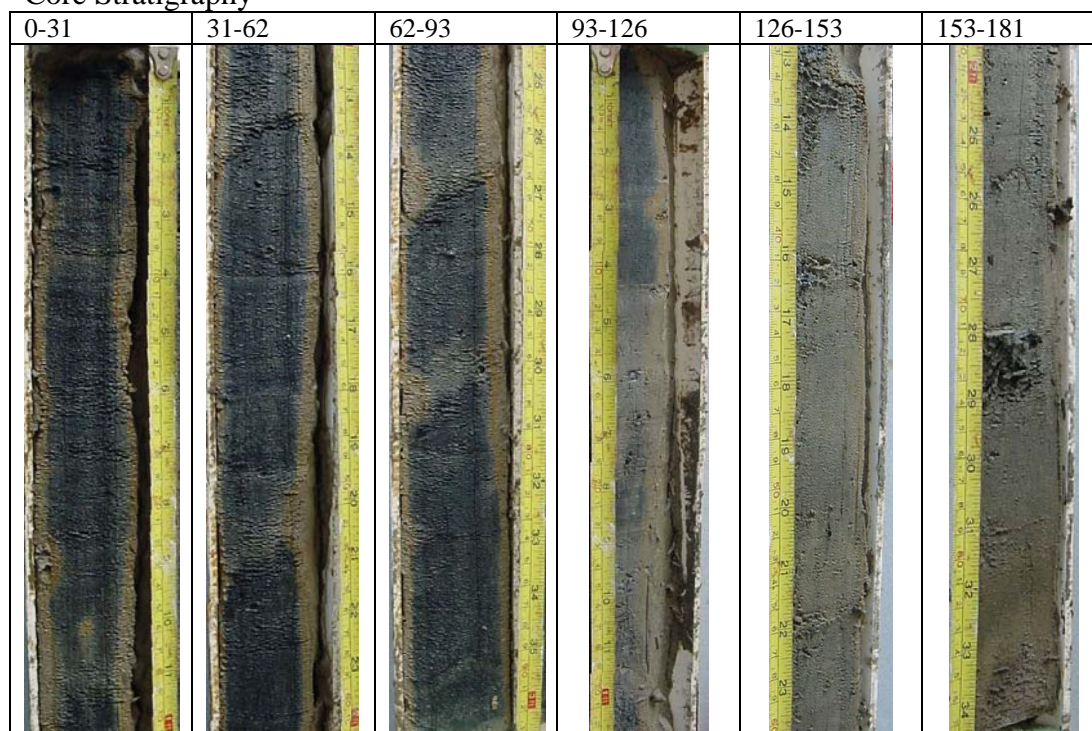
As	Fe	Mn	P	Pb
4.7	898	27	64	0.47

Concentrations Ascorbic Acid (g/tonne)

Depth (cm)	As	Fe	Mn	P
10	39.3	4530.5	228.9	150.6
33	37.1	3731.0	232.0	170.0
55	25.4	3629.5	229.8	111.2
68	18.1	1924.5	107.0	71.7
77	31.9	1257.2	183.3	72.6
95	32.0	1920.3	212.5	99.2
115	28.0	1759.0	189.2	75.9
135	30.5	1398.7	172.5	75.3
155	27.2	1164.5	152.2	59.0
170	35.4	1377.7	151.6	60.0
185	41.1	1338.3	143.8	63.1
205	35.7	1127.2	130.9	53.6
225	44.7	1547.9	110.1	62.2
245	42.7	1285.6	117.8	56.6
261	43.0	1379.6	103.9	56.5

Core ID	Site Location	Grid S Grid E	Water Depth (m)	Core Length (m)
Ru 31	38 03 46.0938S	6343725	7.90	2
	176 19 06.3696E	2801315		

Core Stratigraphy



Stratigraphic Column	Description	Location Map
	<p>Piston Core</p> <p>0-93cm black diatomaceous ooze with strong sulphur smell</p> <p>93-105cm black diatomaceous ooze</p> <p>105-125cm grey silt</p> <p>125-127cm grey sand (Tarawera?)</p> <p>127-180cm olive diatomaceous ooze. 2mm grey sand layer at 135cm. Organic rich 167-170cm</p> <p>180-181cm pumice (Kaharoa?)</p>	

Concentrations (g/tonne)

Depth (cm)	As	Fe	Mn	P	Pb
10	39.1	7387	110.0	351.0	2.0
30	25.2	5953	116.9	270.3	0.9
50	23.8	7037	149.2	369.0	2.6
70	30.5	6307	133.2	315.9	1.9
87	20.5	6192	141.0	282.8	2.3
99	24.0	6878	152.6	323.9	2.8
115	12.0	7367	169.7	355.5	3.7
126	9.1	6818	156.2	227.7	2.5
137	37.9	4968	112.2	194.3	1.1
157	51.1	6058	85.8	116.9	1.0

Tonnes per square km in top 1 m


As	Fe	Mn	P	Pb
8.8	2089	41.4	101.1	0.6

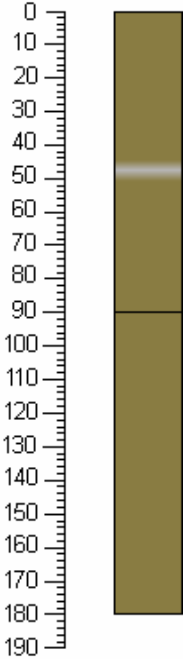

Tonnes per square km above Tarawera tephra

As	Fe	Mn	P	Pb
9.8	2608	53	126	0.9

Core ID	Site Location	Grid S Grid E	Water Depth (m)	Core Length (m)
Ru 32	38 03 15.2206S	6344698	15.40	1.8
	176 18 42.2416E	2800761		

Core Stratigraphy

0-90	90-120	120-150	150-180
No photos available Disturbed Not sampled			




Stratigraphic Column	Description	Location Map
	<p>Piston Core</p> <p>0-90cm disturbed after coring. High water contact, tephra at 50cm</p> <p>90-180cm olive diatomaceous ooze. High water Content.</p>	

Concentrations (g/tonne)

Depth (cm)	As	Fe	Mn	P	Pb
100	18.1	2887	68.6	225.3	0.9
120	23.9	2810	108.5	338.6	1.2
140	15.9	3369	79.1	352.3	0.9
160	11.6	2059	69.8	148.3	0.6
175	14.8	2685	72.5	182.6	0.8

Core ID	Site Location	Grid S Grid E	Water Depth (m)	Core Length (m)
Ru 33	38 02 42.5948S 176 18 45.0107E	6345700 2800867	17.00	0.53

Core Stratigraphy

0-53	Stratigraphic Column	Description	Location Map
		Piston Core 0-53cm olive diatomaceous ooze, very high water content	

Concentrations (g/tonne)

Depth (cm)	As	Fe	Mn	P	Pb
10	28.7	4651	116.5	426.7	3.4
30	32.5	6762	205.2	534.7	5.0
47	32.7	5117	115.5	393.8	4.7

Tonnes per square km in top 1 m

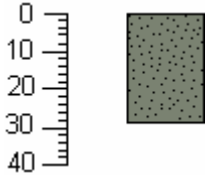

As	Fe	Mn	P	Pb
10.2	1822	49.0	150.5	1.4

Tonnes per square km above Tarawera tephra

As	Fe	Mn	P	Pb
3.28	601	17	51	0.44




Core ID	Site Location	Grid S Grid E	Water Depth (m)	Core Length (m)
Ru 34	38 03 43.9021S	6344106	1.00	0.28
	176 13 15.0460E	2792759		




Core Stratigraphy

Stratigraphic Column	Description	Location Map
	<p>Box Core</p> <p>0-28cm Grey sand</p>	

Core ID	Site Location	Grid S Grid E	Water Depth (m)	Core Length (m)
Ru 35	38 03 11.9424S	6345054	10.00	2.98
	176 13 57.6401E	2793833		

Core Stratigraphy

0-15	15-37	37-59	59-81	81-95	95-120	120-145
						
145-170	170-188	188-211	213-236	236-260	260-276	
						

Stratigraphic column	Description	Location Map
	<p>Piston Core</p> <p>0-5, black diatomaceous ooze</p> <p>5-7, grey silt with erosional lower contact (Tarawera)</p>  <p>7-15, black diatomaceous ooze</p> <p>15-24, olive black diatomaceous ooze</p> <p>24-33, olive diatomaceous ooze with abundant organic matter, whole twigs and leaves)</p> <p>33-95, olive diatomaceous ooze with layers of leaves at 40cm</p> <p>95-188 olive diatomaceous ooze with many gas bubbles</p> <p>188-235, olive diatomaceous ooze</p> <p>235-237, pumice Kaharoa?</p>  <p>237-276, olive diatomaceous ooze</p>	

Concentrations (g/tonne)

Depth (cm)	As	Fe	Mn	P	Pb
2.5	53.5	5905	202.6	341.9	2.6
6	53.9	9257	343.5	349.8	3.9
11	110.2	6150	125.2	271.4	1.3
19.5	65.4	3895	127.9	230.5	1.3
28.5	41.8	3547	138.0	238.3	1.5
43	40.2	4764	115.5	171.5	5.5
63	32.0	4263	113.2	154.3	1.1
83	41.4	4924	99.9	153.3	1.1
104	32.0	3489	70.7	116.5	0.6
125	31.8	3934	80.5	141.1	1.0
145	27.5	3794	72.0	136.2	0.7
165	26.5	3847	65.7	125.2	0.7
200.5	27.5	4554	62.6	136.4	0.6
220.5	27.0	3155	50.8	109.0	0.7
235.5	28.9	3163	58.9	160.4	0.9
244	18.5	2372	61.5	188.6	1.0
255	29.4	3947	76.7	134.0	1.0
270.5	38.7	4374	85.6	121.9	1.1

Tonnes per square km in top 1 m

As	Fe	Mn	P	Pb
14.6	1445	38	59	0.7

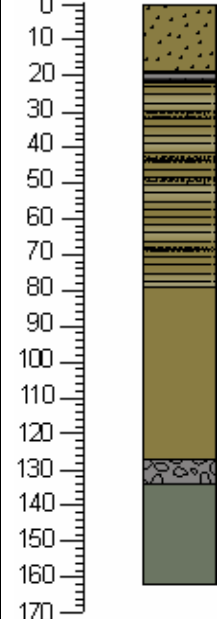

Tonnes per square km above Tarawera tephra

As	Fe	Mn	P	Pb
0.83	91	3.13	5.28	0.04

Core ID	Site Location	Grid S Grid E	Water Depth (m)	Core Length (m)
Ru 36	38 03 14.3S 176 14 38.0E	6344945 2794813	11.90	1.68

Core Stratigraphy

0-34	34-68	68-79
		
79-106	106-131	131-162
		

Stratigraphic Column	Description	Location Map
	<p>Piston Core</p> <p>0-19cm olive diatomaceous ooze with black flecks</p> <p>19-22cm grey silt with thin black sand layer at base (Tarawera tephra)</p> <p>22-79cm olive diatomaceous ooze with colour laminations and scattered organic matter</p> <p>79-127cm olive diatomaceous ooze</p> <p>127-134cm pumice layer (Kaharoa tephra)</p>	

Concentrations (g/tonne)

Depth (cm)	As	Fe	Mn	P	Pb
10	43.2	5680	170.2	251.3	1.9
21	32.9	9652	354.4	302.6	3.4
32	49.3	4019	88.8	154.1	0.6

Tonnes per square km in top 1 m

As	Fe	Mn	P	Pb
15	1416	35	56	0.30

Tonnes per square km above Tarawera tephra

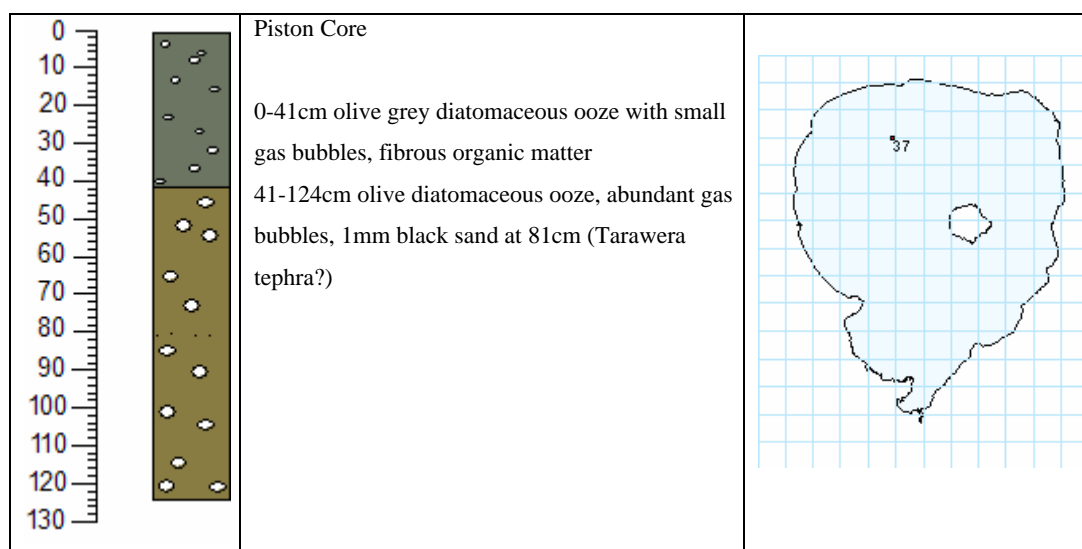
As	Fe	Mn	P	Pb
2.54	333.5	10.0	14.8	0.11

Core ID	Site Location	Grid S Grid E	Water Depth (m)	Core Length (m)
Ru 37	38 03 14.8321S 176 15 17.3987E	6344894 2795772	14.12	1.37

Core Stratigraphy

0-41	41-70	70-99	99-124
			

Stratigraphic Column	Description	Location Map
----------------------	-------------	--------------



Concentrations (g/tonne)

Depth (cm)	As	Fe	Mn	P	Pb
10	26.1	2289	95.9	188.0	
31	16.1	2292	75.2	136.7	
51	13.0	2398	84.6	147.9	
71	1.6	1211	51.6	80.8	
91	10.2	1665	63.3	86.5	
112	8.0	1227	43.8	58.9	

Tonnes per square km in top 1 m


As	Fe	Mn	P	Pb
4.2	611	23.0	39.9	

Tonnes per square km above Tarawera tephra

As	Fe	Mn	P	Pb
3.6	513.2	19.3	34.8	




Core ID	Site Location	Grid S Grid E	Water Depth (m)	Core Length (m)
Ru 38	38 03 14.8597S	6344814	17.43	0
	176 16 43.4195E	2797867		

Core Stratigraphy

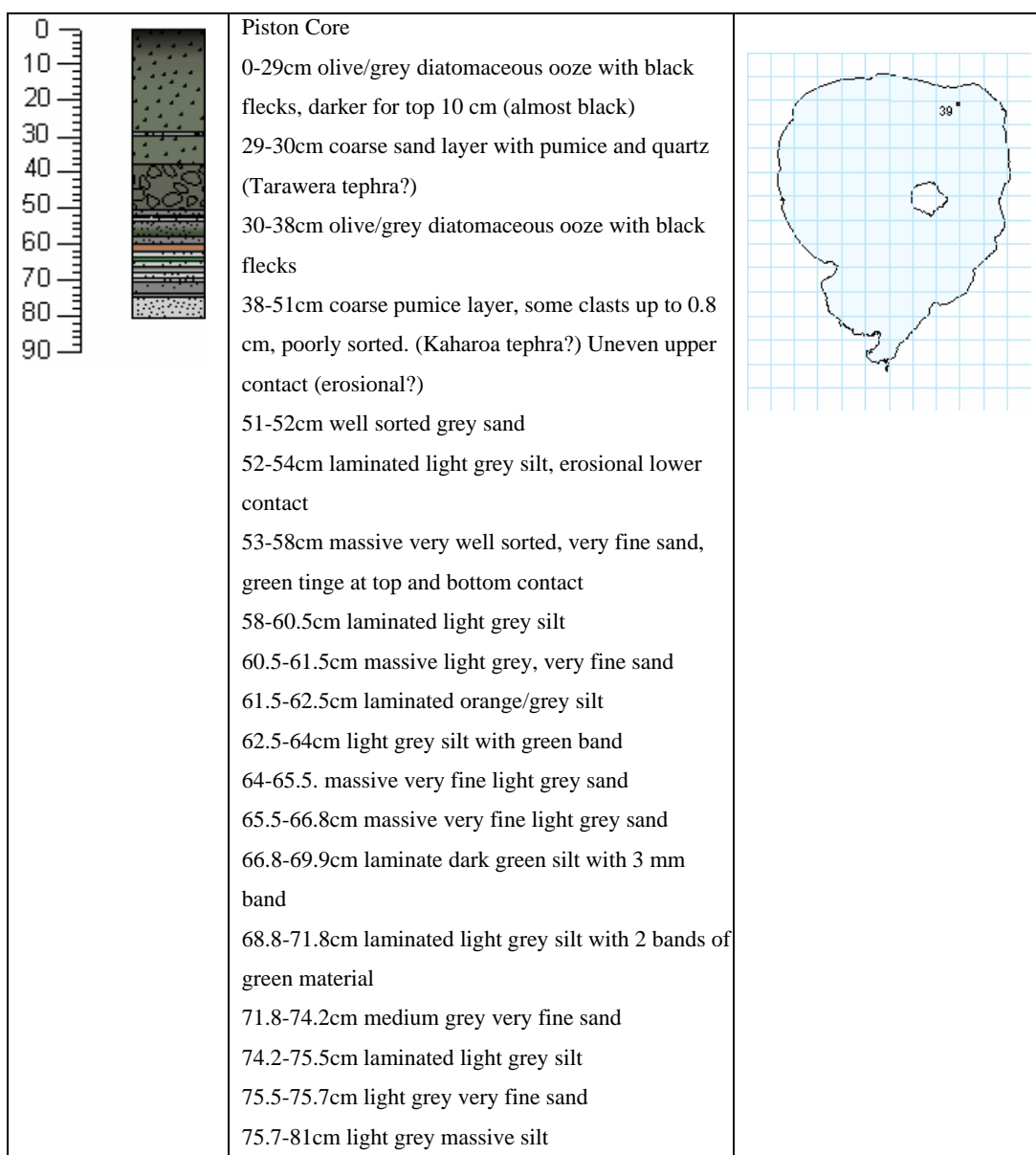
Stratigraphic Column	Description	Location Map
	No core recovered	

Core ID	Site Location	Grid S Grid E	Water Depth (m)	Core Length (m)
Ru 39	38 02 43.005 S	6345730	13.00	0.85
	176 17 58.3905 E	2799730		

Core Stratigraphy

0-25	25-50	50-80
		

Stratigraphic Column	Description	Location Map
----------------------	-------------	--------------



Concentrations (g/tonne)

Depth (cm)	As	Fe	Mn	P	Pb
5.0	35.5	4867	144.9	151.2	
15.0	50.1	5559	168.4	124.1	
20.0	38.9	4836	180.0	95.5	
29.5	24.2	4789	99.2	78.5	

Tonnes per square km in top 1 m


As	Fe	Mn	P	Pb
6.9	898	23.9	17.6	

Tonnes per square km above Tarawera tephra

As	Fe	Mn	P	Pb
3.7	457	15	11	




Core ID	Site Location	Grid S Grid E	Water Depth (m)	Core Length (m)
Ru 40	38 05 37.1674S	6340436	14.10	0
	176 16 38.8026E	2799730		




Core Stratigraphy

Stratigraphic Column	Description	Location Map
	No core recovered	

Core ID	Site Location	Grid S Grid E	Water Depth (m)	Core Length (m)
Ru 41	38 05 37.1533	6340435.87	14.32	1.78
	176 16 39.0798	2797601.42		

Core Stratigraphy

0-31	31-62	62-83
		

83-114	114-145	145-178
		

Stratigraphic Column	Description	Location Map
	<p>Piston Core</p> <p>0-29cm Olive diatomaceous ooze with large gas bubbles</p> <p>29-31cm Grey silt and sand (Tarawera Tephra)</p> <p>83-177cm olive diatomaceous ooze with very thin black tephra at 112 cm</p>	

Concentrations (g/tonne)

Depth (cm)	As	Fe	Mn	P	Pb
0-15	93.74	5831.11	298.78	530.13	5.07
15-27	116.77	8222.43	347.86	446.31	4.87
29-31	78.22	9306.12	341.46	402.54	5.30
31-50	110.50	5522.64	235.47	289.37	2.66
50-70	116.01	6909.72	218.09	263.18	2.18
70-83	80.04	7052.03	201.77	194.75	1.56
83-111	66.49	6123.55	185.89	163.20	1.73
111-113	37.01	4009.34	95.52	113.57	1.04
113-133	49.69	4237.24	143.43	103.30	1.29
133-153	61.19	4687.25	143.75	108.02	0.60
153-177	66.87	5312.19	134.52	105.82	1.31

Tonnes per square km in top 1 m

As	Fe	Mn	P	Pb
29.5	1989	74	93	0.89

Tonnes per square km above Tarawera tephra

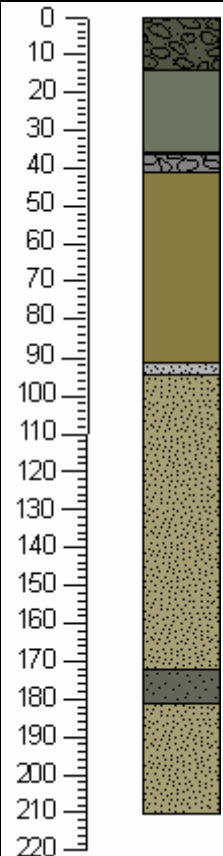


As	Fe	Mn	P	Pb
8.7	575	27	41	0.4

Core ID	Site Location	Grid S Grid E	Water Depth (m)	Core Length (m)
Ru 42	38 05 41.2993	6340269.78	8.21	2.1
	176 17 21.9037	2798639.36		

Core Stratigraphy

0-19	19-50	50-81	81-122

122-152	152-182	182-210

Stratigraphic Column	Description	Location Map
	<p>Piston Core</p> <p>0-14cm pumice with sand and diatomaceous ooze, ~1/2-1cm clast near top,fining down to ~3mm at base</p> <p>14-36cm olive/grey diatomaceous ooze</p> <p>36-41cm very dense grey layer rich in pumice clasts, fining upwards (see photo)</p>  <p>41-91cm olive diatomaceous ooze</p> <p>91-94cm fine grey sand</p>	

Concentrations (g/tonne)




Depth (cm)	As	Fe	Mn	P	Pb
0-14	29.45	2892.43	51.14	59.86	0.43
14-19	121.73	5192.71	276.29	154.13	1.96
19-36	40.27	4274.02	291.16	156.73	2.12
36-41	13.15	2599.14	80.08	96.49	0.57
41-61	28.01	5650.90	297.12	144.56	1.96
61-81	21.92	4473.69	265.11	109.75	1.63
81-91	16.18	6646.53	314.30	173.35	1.63
91-94	10.51	4253.72	143.65	88.63	1.68
94-122	29.51	7715.88	447.70	358.88	1.59
122-142	27.05	4193.20	301.68	248.44	1.30
142-162	29.63	3512.74	310.89	304.66	1.45
162-172	96.72	4585.76	312.25	242.91	1.40
172-181	18.46	8680.80	510.16	127.43	0.65
181-198	48.36	3451.18	308.16	78.25	0.79
198-210	26.13	3237.13	326.12	227.36	1.54

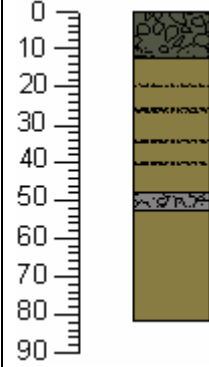

Tonnes per square km in top 1 m

As	Fe	Mn	P	Pb
0.956	142.1	7.128	3.957	0.047

Core ID	Site Location	Grid S Grid E	Water Depth (m)	Core Length (m)
Ru 43	38 05 39.9307	6340277.56	8.04	0.82
	176 18 00.1670	2799572.51		

Core Stratigraphy

0-30	30-60	60-82
		

Stratigraphic Column	Description	Location Map
	<p>Piston Core</p> <p>0-13cm pumice and diatomaceous ooze, fining downwards</p> <p>13-48cm olive diatomaceous ooze with scattered organic matter</p> <p>48-53cm grey pumice sand</p> <p>53-82cm olive diatomaceous ooze</p>	

Concentrations (g/tonne)






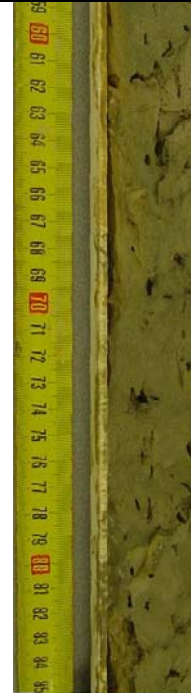

Depth (cm)	As	Fe	Mn	P	Pb
0-13	36.14	3625	54.6	68.03	0.561
13-30	49.41	3870	165.3	152.8	1.766
30-48	34.13	4332	190.4	131.7	1.704
48-53	9.969	2390	74.07	120.9	0.86
53-65	24.7	3580	165.6	206.4	1.168
65-82	53.58	5377	186.9	348	1.472

Tonnes per square km in top 1 m

As	Fe	Mn	P	Pb
0.983	104.2	3.856	4.588	0.034

Core ID	Site Location	Grid S Grid E	Water Depth (m)	Core Length (m)
Ru 44	38 05 39.8358	6340243.17	6.54	1.85
	176 18 41.5559	2800580.31		

Core Stratigraphy

0-30	30-60	60-75	75-105
			
105-134	134-160	160-170	
			

Stratigraphic Column	Description	Location Map
	<p>Piston Core</p> <p>0-32cm pumice and diatomaceous ooze, larger clasts ranging from 2mm to 2 cm</p> <p>32-36cm brown sand</p> <p>36-46cm pumice layer, fining downwards, uneven lower contact</p> <p>46-57cm olive diatomaceous ooze</p> <p>57-61cm sand layer, gradational upper contact</p> <p>61-63cm very fine black sand, unusual lower contact (see photo), very irregular</p> <p>63-119cm silty olive diatomaceous ooze</p> <p>119- 136cm silty olive green diatomaceous ooze</p> <p>136-139cm grey silt</p> <p>139-185cm olive green silty diatomaceous ooze with scattered organics</p>	<p>*the lower diatomaceous ooze layers in this core are very sticky</p>

Concentrations (g/tonne)





Depth (cm)	As	Fe	Mn	P	Pb
0-15	27.49	4520	188.9	244.6	0.87
15-32	40.58	4221	37.91	57.4	0.3
32-36	119	6592	48.18	52.14	1.184
36-46	68.83	8008	62.46	153.9	1.123
46-57	80.31	8472	83.44	69.95	1.915
57-61	38.14	4887	83.23	55.52	1.837
61-63	83.81	9599	84.89	66.52	1.304
75-95	23.51	2476	101.2	69.99	1.574
95-115	42.36	4360	115.2	112.5	0.846
115-136	22.44	2548	100.5	65.68	1.498
136-139	21.76	5361	133.4	77.07	2.467
139-175	7.761	2226	57.94	52.41	1.16
175-185	40.73	6136	140.9	121	1.975

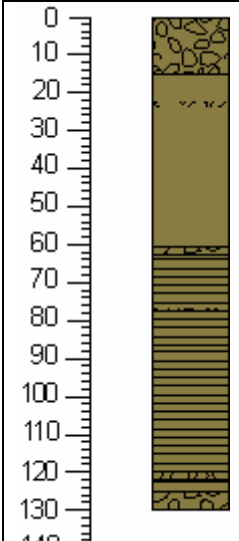

Tonnes per square km in top 1 m

As	Fe	Mn	P	Pb
1.421	152.9	2.854	3.278	0.031

Core ID	Site Location	Grid S Grid E	Water Depth (m)	Core Length (m)
Ru 45	38 04 19.2006	6342710.59	8.17	1.3
	176 19 00.0653	2801123.24		

Core Stratigraphy

0-40	40-70	70-100	100-130
			

Stratigraphic Column	Description	Location Map
	<p>Piston Core</p> <p>0-15cm coarse pumice layer with diatomaceous ooze</p> <p>15-61cm olive diatomaceous ooze, with possible very thin pumice layers at 23 and 37cm</p> <p>61-63cm diatomaceous ooze with small amount of pumice</p> <p>63-120cm laminated diatomaceous ooze with a thin pumice layer at 78cm</p> <p>120-122cm diatomaceous ooze with pumice</p> <p>122-125cm olive diatomaceous ooze</p> <p>125-130cm pumice with diatomaceous ooze</p>	

Concentrations (g/tonne)





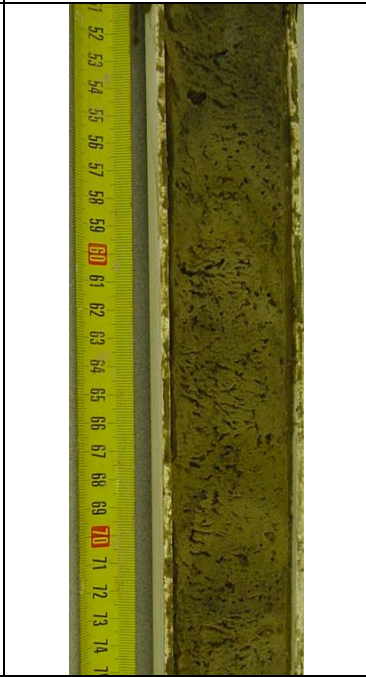

Depth (cm)	As	Fe	Mn	P	Pb
0-15	95.64	5591	54.77	77.55	0.161
15-30	83.63	5459	39.04	59.3	0.019
30-40	44.19	4034	77.52	84.75	0.863
40-61	70.46	5699	75.35	83.97	0.678
61-63	93.61	9794	52.15	80.35	0.243
63-83	65.4	6305	74.63	84.34	0.582
83-103	85.48	7323	71.69	81.62	0.752
103-120	100.3	3664	75.79	75.04	1.156
120-130	84.12	9239	60.58	87.86	0.403

Tonnes per square km in top 1 m

As	Fe	Mn	P	Pb
2.415	190.9	2.1	2.516	0.016

Core ID	Site Location	Grid S Grid E	Water Depth (m)	Core Length (m)
Ru 46	38 04 19.8010	6342726.14	13.6	1.58
	176 18 22.3785	2800204.72		

Core Stratigraphy

0-32	32-65	65-90
		
90-116	116-140	140-159
		

Stratigraphic Column	Description	Location Map
	<p>Piston Core</p> <p>0-93cm laminated olive diatomaceous ooze with very high water content</p> <p>93-95cm grey silt and sand (Tarawera tephra)</p> <p>95-108cm olive diatomaceous ooze</p> <p>108-109cm grey silt/black sand</p> <p>109-158cm laminated olive diatomaceous ooze, very thin tephra and ~118 cm</p>	

Concentrations (g/tonne)

Depth (cm)	As	Fe	Mn	P	Pb
0-25	50.29	4115	183.6	317.2	6.879
25-45	45.01	3103	158.7	246	3.966
45-65	60.29	5001	179.9	263.4	3.005
65-93	72.45	4939	156.9	185.3	1.856
93-95	107.8	9425	310.3	407.1	4.714
95-108	83.38	7439	274	371.2	4.072
108-109	100.2	7787	286.9	392.8	4.319
109-135	104.3	4558	137.6	185.2	1.546
135-158	45.57	2699	117.1	150.6	1.278

Tonnes per square km in top 1 m

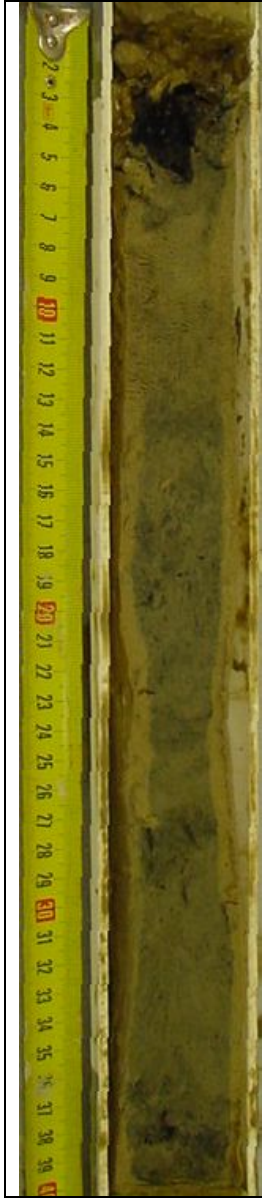



As	Fe	Mn	P	Pb
16.4	1267	50	74.5	1.16

Tonnes per square km above Tarawera tephra

As	Fe	Mn	P	Pb
14.4	1093	43.8	66.3	1.07

Core ID	Site Location	Grid S Grid E	Water Depth (m)	Core Length (m)
Ru 47	38 07 00.9774	6337853.55	8.07	1.25
	176 16 38.9546	2797503.53		

Core Stratigraphy

0-40	40-73	73-100	100-125
			

Stratigraphic Column	Description	Location Map
	<p>Piston Core</p> <p>0-6cm gravel with fresh water mussel</p> <p>6-106cm olive diatomaceous ooze</p> <p>106-125cm mottled grey diatomaceous ooze with one gravel chunk at the base</p>	

Concentrations (g/tonne)





Depth (cm)	As	Fe	Mn	P	Pb
0-6	29.1	2920	88.9	95.6	0.78
6-25	48.4	3889	185	134	1.65
25-40	35.9	4406	270	366	1.9
40-60	32.4	3271	159	190	1.86
60-80	41.3	4441	184	347	1.74
800-106	29.9	3101	144	280	1.56
106-125	35.7	4124	179	368	1.54




Tonnes per square km in top 1 m

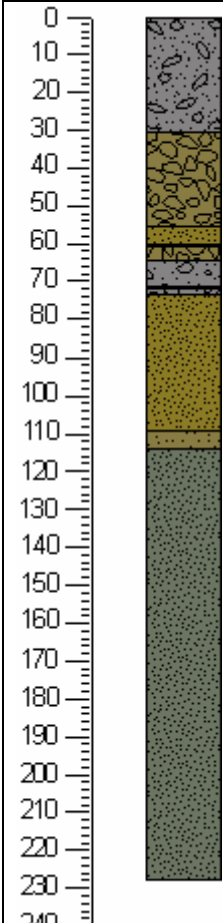

As	Fe	Mn	P	Pb
1.2	121	5.78	8.23	0.055

Core ID	Site Location	Grid S Grid E	Water Depth (m)	Core Length (m)
Ru 48	38 07 00.9521	6337626.58	7.28	2.31
	176 17 13.8446	2798326.83		

Core Stratigraphy

0-42	42-77	77-112	112-136
			

136-167	167-201	201-231
		

Stratigraphic Column	Description	Location Map
	<p>Piston Core</p> <p>0-30cm well sorted sand with occasional pumice clasts and organic matter. Part of mussel shell at the top</p> <p>30-55cm diatomaceous ooze with pumice</p> <p>55-60cm olive silty diatomaceous ooze</p> <p>60-64cm pumice with diatomaceous ooze</p> <p>64-71cm grey medium pumice sand</p> <p>71-73cm coarse pumice sand</p> <p>73-109cm silty olive diatomaceous ooze</p> <p>109-114cm diatomaceous ooze with sand</p> <p>114-228cm silty olive/grey diatomaceous ooze</p>	

Concentrations (g/tonne)







Depth (cm)	As	Fe	Mn	P	Pb
0-30	26.91	2527	28.33	80.55	0.772
30-55	104.8	2453	41.88	55.29	1.135
55-60	46.83	3440	83.25	118.4	1.257
60-73	57.4	7485	39.15	93.58	1.023
73-93	19.85	1597	60	75.18	0.98
93-109	29.84	3022	127.7	131.2	2.084
109-114	44.25	1835	56.81	44.89	1.539
114-134	55.09	4969	90.99	68.89	1.506
134-154	31.77	3517	111.8	64.5	1.507
154-174	44.39	5880	111.7	70.99	1.818
174-194	43.26	4902	103	64.65	1.34
194-214	33.2	3888	112.2	60.09	1.199
214-227	79.08	8165	85.9	72.39	1.322

Tonnes per square km in top 1 m

As	Fe	Mn	P	Pb
1.485	87.62	1.243	2.197	0.028

Core ID	Site Location	Grid S Grid E	Water Depth (m)	Core Length (m)
Ru 49	38 07 00.6834	6337935.27	5.05	1.54
	176 15 17.4004	2795518.85		

Core Stratigraphy

0-35	35-60	60-74
		
74-104	104-134	134-158
		

Stratigraphic Column	Description	Location Map
	<p>Piston Core</p> <p>0-2cm black diatomaceous ooze with sand</p> <p>2-80cm olive diatomaceous ooze with thin sand layer at ~73cm</p> <p>80-82cm black diatomaceous ooze with sand</p> <p>82-88cm olive diatomaceous ooze</p> <p>88-90cm black diatomaceous ooze with sand</p> <p>90-108cm olive diatomaceous ooze with thin sand at 96.5 cm</p> <p>108-109.5cm black sand</p> <p>109.5-133cm olive diatomaceous ooze</p> <p>133-136cm silty layer with organic matter</p> <p>136-148cm silty olive diatomaceous ooze</p> <p>148-140cm black sand</p> <p>140-154cm silty olive diatomaceous ooze</p> <p>*the lower silty diatomaceous oozes are very sticky</p>	

Concentrations (g/tonne)

Depth (cm)	As	Fe	Mn	P	Pb
0-2	26.03	112.3	0.39	96.61	1.875
2-20	25.82	3120.0	155.46	159.29	1.382
20-45	30.17	4271.0	177.37	209.65	1.974
45-70	21.00	3800.8	171.69	188.18	1.858
70-80	24.02	2846.6	141.82	108.96	1.310
80-82	23.91	2756.5	116.64	216.84	1.674
82-88	25.99	2937.5	145.14	138.81	0.505
88-90	25.37	2809.0	131.33	231.66	1.416
90-108	25.95	3273.5	156.87	314.79	1.535
108-110	34.97	3046.6	121.29	296.94	1.723
110-133	50.41	4379.6	170.86	437.96	1.280
133-136	33.40	3760.3	190.77	302.63	1.195
136-148	20.03	2505.1	116.93	346.25	1.327




Tonnes per square km in top 1 m

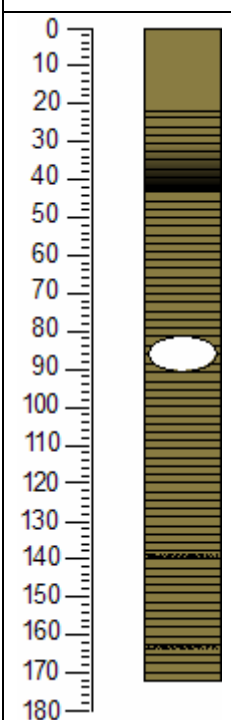

As	Fe	Mn	P	Pb
17.2	1791	75	85	0.84

Core ID	Site Location	Grid S Grid E	Water Depth (m)	Core Length (m)
Ru 50	38 05 39.3386	6340476.85	8.62	1.72
	176 14 37.3497	2794635.14		

Core Stratigraphy

0-16	16-50	50-82	82-110
			

110-139	139-170	170-182
		

Stratigraphic Column	Description	Location Map
	<p>Piston Core</p> <p>0-22cm olive diatomaceous ooze</p> <p>22-43cm olive/black laminated diatomaceous ooze</p> <p>43-172cm laminated olive diatomaceous ooze, large gas bubble from 85-93 cm, organic matter at 140cm and 163 cm..</p> <p>Tarawera Tephra not seen</p>	

Concentrations (g/tonne)








Depth (cm)	As	Fe	Mn	P	Pb
0-20	60.2	3315	118	329	7
20-40	70	4294	191	387	4.99
40-60	60.4	3864	165	294	7.71
60-80	60.7	4173	126	337	7.63
80-100	92.2	6341	185	532	11.4
100-120	77.1	4542	190	407	5.57
120-140	126	6693	255	353	4.66
140-160	79.1	5971	143	227	2.25
160-172	62.6	5499	130	205	2.59

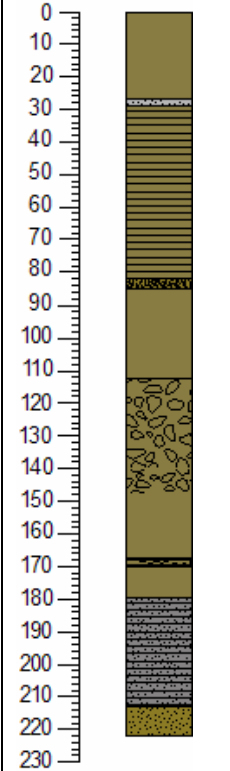

Tonnes per square km in top 1 m

As	Fe	Mn	P	Pb
21.0	1341	48	115	2.36

Core ID	Site Location	Grid S Grid E	Water Depth (m)	Core Length (m)
Ru 51	38 05 06.8822	6341478.25	10.45	2.21
	176 14 35.6718	2794630.64		

Core Stratigraphy

0-46	46-77	77-99	99-138
			
138-173	173-202	202-221	
			

Stratigraphic Column	Description	Location Map
	<p>Piston Core</p> <p>0-27cm olive diatomaceous ooze</p> <p>27-29cm grey silt (Tarawera)</p> <p>29-82cm laminated olive diatomaceous ooze</p> <p>82-85cm organic layer</p> <p>85-103cm olive diatomaceous ooze</p> <p>103-168cm olive diatomaceous ooze containing scattered pumice from 103-148cm</p> <p>168-170cm pumice with diatomaceous ooze</p> <p>170-180cm olive diatomaceous ooze</p> <p>180-213cm laminated grey/black silt (gap from 189-194 cm)</p> <p>213-221cm olive silty diatomaceous ooze</p>	

Concentrations (g/tonne)

Depth (cm)	As	Fe	Mn	P	Pb
0-27	51.74	3151	146.4	230.6	4.971
27-29	94.84	8165	417.1	276.2	5.461
29-46	195.1	10428	225.7	220.1	2.921
46-56	75.01	6438	147.3	128.9	1.615
56-82	54.79	4338	104.2	83.16	1.009
82-85	49.63	3441	80.27	71.6	0.908
85-103	44.95	2358	60.67	48.81	0.741
103-123	101	4401	69.42	73.22	0.717
123-138	94.63	3654	68.89	80.49	0.962
138-152	56.72	3570	75.48	62.1	0.779
152-168	42.16	2620	65.62	52.92	0.69
168-170	72.27	3261	68.83	65.48	0.871
170-180	80.11	3037	63.49	61.94	0.532
180-200	76.94	3716	89	91.53	1.285
200-213	49.46	4344	164.4	229	1.984
213-221	279.6	2337	84.05	67.55	0.944

Tonnes per square km in top 1 m




As	Fe	Mn	P	Pb
30.5	1869	50	53	0.86




Tonnes per square km above Tarawera tephra

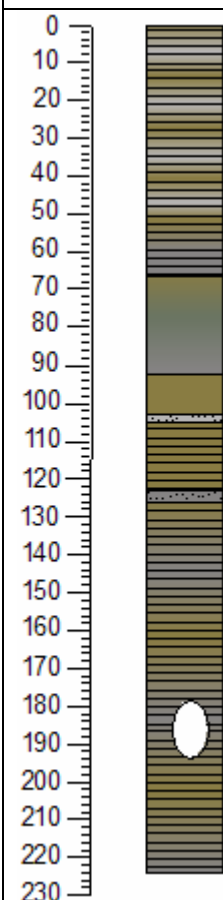

As	Fe	Mn	P	Pb
4.8	309	15	21	0.44

Core ID	Site Location	Grid S Grid E	Water Depth (m)	Core Length (m)
Ru 52	38 04 34.2559	6342484.20	12.08	2.24
	176 14 34.7743	2794645.32		

Core Stratigraphy

0-38	38-70	70-105	105-127
			

127-167	167-200	200-224
		

Stratigraphic Column	Description	Location Map
	<p>Piston Core</p> <p>0-66cm olive/dark grey laminated diatomaceous ooze grading into grey at the base</p> <p>66-92cm olive/dark grey diatomaceous ooze grading into grey at the base</p> <p>92-103cm olive diatomaceous ooze</p> <p>103-105cm grey silt (Tarawera)</p> <p>105-123cm olive laminated diatomaceous ooze</p> <p>123-126cm grey silt (Tephra?)</p> <p>126-224cm laminated olive/dark grey diatomaceous ooze.</p> <p>Large gap from 177-194cm (gas bubble?)</p>	

Concentrations (g/tonne)

Depth (cm)	As	Fe	Mn	P	Pb
0-20	38.8	1888	66.4	154	2.04
20-40	84.6	4795	115	225	2.42
40-60	70	4136	152	204	2.54
60-80	75.2	4288	154	254	2.96
80-103	84.6	6811	261	426	4.05
103-105	92.2	8600	376	437	4.53
105-123	110	5003	142	255	2.29
123-126	101	7639	339	474	6.2
126-146	57.7	3286	123	189	1.92
146-166	45.2	2262	118	244	5.48
166-210	48	2510	90.2	260	4.99
210-224	49.4	2195	134	275	3.6

Tonnes per square km in top 1 m




As	Fe	Mn	P	Pb
21.5	1337	46	77	0.86




Tonnes per square km above Tarawera tephra

As	Fe	Mn	P	Pb
22.3	1399	48	81	0.89

Core ID	Site Location	Grid S Grid E	Water Depth (m)	Core Length (m)
Ru 53	38 03 44.9686	6344001.01	11.22	2.13
	176 14 36.6150	2794745.35		

Core Stratigraphy

0-34	34-64	64-94	94-122
Photo missing			

122-153	153-184	184-216
		

Stratigraphic Column	Description	Location Map
	<p>Piston Core</p> <p>0-3cm olive diatomaceous ooze</p> <p>3-4cm grey silt (Tarawera)</p> <p>4-80cm olive diatomaceous ooze</p> <p>80-100cm pumice layer (Kaharoa)</p> <p>100-120cm olive/grey laminated silty diatomaceous ooze</p> <p>120-152cm motley black/grey diatomaceous ooze</p> <p>152-201cm laminated olive/grey diatomaceous ooze</p> <p>201-213cm grey silty diatomaceous ooze</p> <p>NB: The surface appears to have been eroded off or failed to be cored. This site should be reoccupied.</p>	

Concentrations (g/tonne)

Depth (cm)	As	Fe	Mn	P	Pb
0-3		7644.8	288.84	323.44	4.7547
3-4		11911	438.93	316.45	5.7511
4-20		5581.4	125.2	102.22	1.1017
20-34		3448.4	86.706	67.904	0.7755
34-54		3881	73.254	60.312	0.4906
54-80		3696	69.084	66.615	0.5313
80-100		3758.9	62.909	78.268	0.8485
100-120		5611.2	170.9	281.16	1.1469
120-140		5673.3	211.66	275.04	1.7826
140-160		5116.4	218.16	316.77	2.2766
160-180		3481	111.23	60.007	0.6826
180-200		4304.3	65.324	39.273	0.4648
200-213		9223	213.25	184.49	0.9121

Tonnes per square km in top 1 m






As	Fe	Mn	P	Pb
	130.2	2.794	2.588	0.028

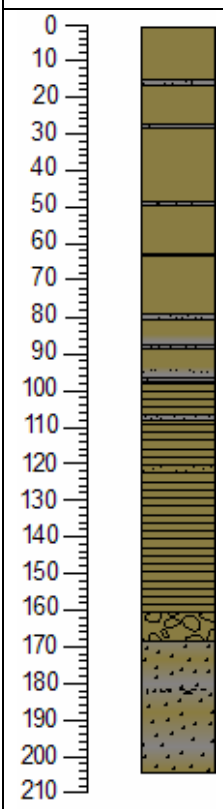

Tonnes per square km above Tarawera tephra

As	Fe	Mn	P	Pb
	71	3	3	0.04

Core ID	Site Location	Grid S Grid E	Water Depth (m)	Core Length (m)
Ru 54	38 03 46.8272	6343908.17	12.92	2.15
	176 15 16.7351	2795720.51		

Core Stratigraphy

0-32	32-64	64-76	76-107
			
107-140	140-170	170-200	200-215
			

Stratigraphic Column	Description	Location Map
	<p>Piston Core</p> <p>0-15cm olive diatomaceous ooze</p> <p>15-16cm grey silt and sand</p> <p>16-62cm olive diatomaceous ooze, at 28cm and 48cm are 1 mm thick grey silt layers</p> <p>62-63cm grey silt and sand</p> <p>63-79cm olive diatomaceous ooze</p> <p>79-80cm grey silt and sand</p> <p>80-87cm olive diatomaceous ooze (grading to grey above tephra)</p> <p>87-88cm grey silt and sand</p> <p>88-96cm olive diatomaceous ooze (grading to grey above tephra)</p> <p>96-97cm grey silt</p> <p>97-160cm olive laminated diatomaceous ooze, grey silt (1mm) at 107cm. black sand (1 mm) at 121cm</p> <p>170-178cm pumice and diatomaceous ooze layer</p> <p>168-204cm mottled grey/olive diatomaceous ooze, then pumice layer at 182cm.</p>	

Concentrations (g/tonne)

Depth (cm)	As	Fe	Mn	P	Pb
0-15		8589	164.4	264.8	2.895
15-16		12652	445.9	518.6	7.631
16-40		3806	107.6	216.8	0.915
40-62		4399	133.6	255.4	1.798
62-63		10092	355.8	527.4	5.763
63-79		3885	108	250.2	2.052
79-80		11470	413.4	540.7	6.843
80-87		7078	200.1	357.7	3.712
87-88		10003	345.9	469.3	5.968
88-96		4179	125.8	253.5	1.821
96-97		11587	414.7	491.3	6.841
97-120		7039	198.3	316.1	3.342
120-140		2974	51.83	73.68	0.227
140-160		3146	49.24	66.55	0.645
160-168		3038	38.75	203.5	0.248
168-180		5259	91.45	938.6	1.156
180-204		4538	63.52	310.4	1.154

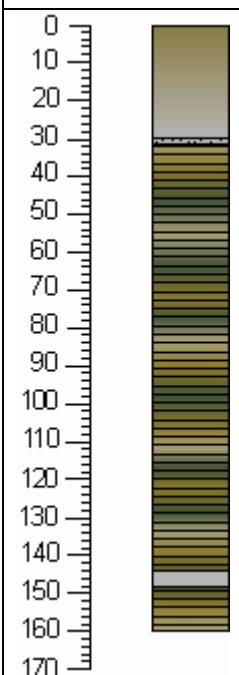


Tonnes per square km in top 1 m

As	Fe	Mn	P	Pb
	1600	44	80	0.65

Core ID	Site Location	Grid S Grid E	Water Depth (m)	Core Length (m)
Ru 55	38 03 45.9931	6343896.87	15.83	1.48
	176 15 58.3014	2796734		

Core Stratigraphy

0-21	21-49	49-77	77-94
			
94-118	118-142	142-161	
			

Stratigraphic Column	Description	Location Map
	<p>Piston Core</p> <p>0-30cm olive/grey diatomaceous ooze</p> <p>30-32cm grey silt and sand (Tarawera Tephra)</p>  <p>32-160cm olive laminated diatomaceous ooze, laminations are olive, light green and green.</p> <p>144-148cm is a band of grey diatomaceous ooze</p>	

Concentrations (g/tonne)

Depth (cm)	As	Fe	Mn	P	Pb
0-20		8603.4	164.64	265.24	2.8999
20-30		13897	489.72	569.55	8.3815
30-32		3588.3	101.42	204.46	0.863
32-52		4355.2	132.31	252.92	1.7807
52-72		9903	349.12	517.59	5.6551
72-92		3874.9	107.7	249.55	2.0462
92-112		11529	415.53	543.53	6.8781
112-132		7054.6	199.42	356.49	3.7
132-160		9719.5	336.14	455.99	5.7991

Tonnes per square km in top 1 m









As	Fe	Mn	P	Pb
	2389	73	112	1.20

Tonnes per square km above Tarawera tephra

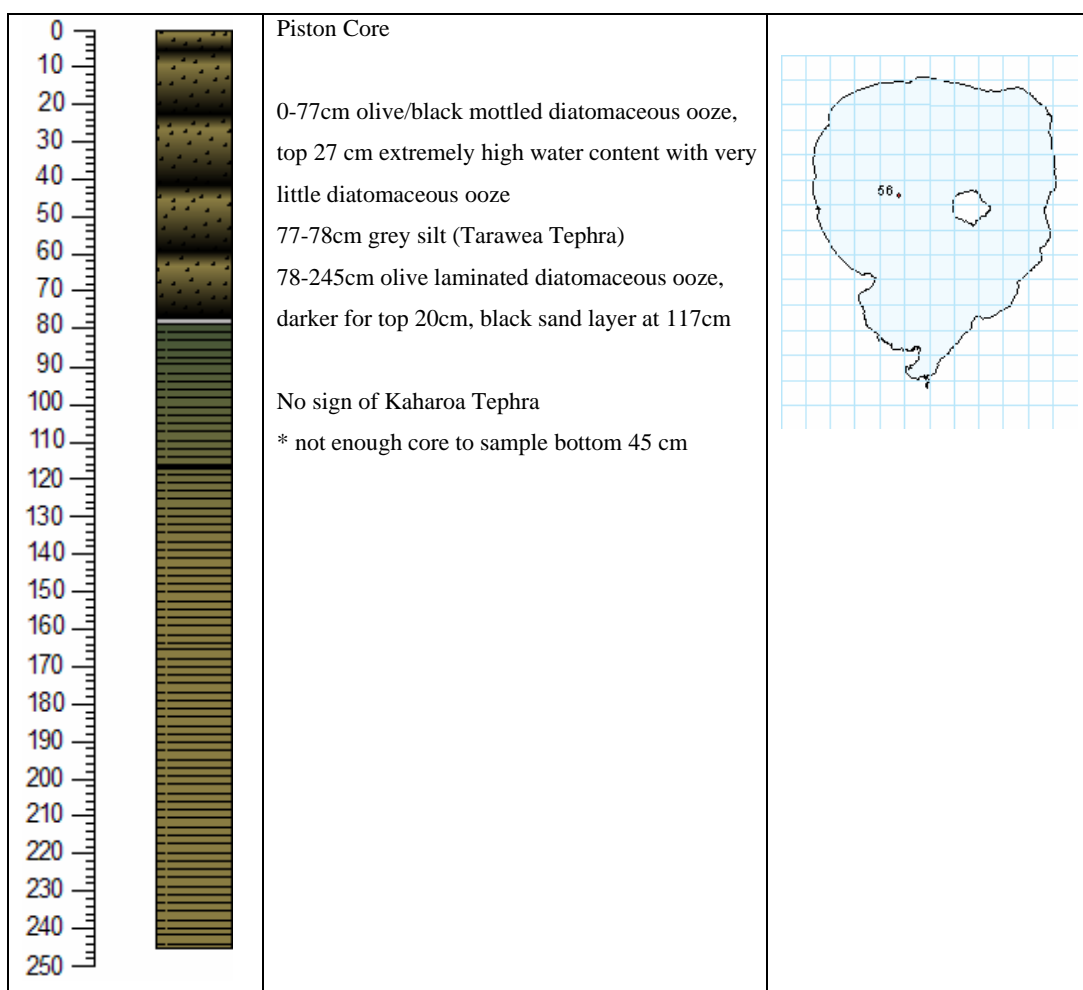
As	Fe	Mn	P	Pb
	961	25	34	0.44

Core ID	Site Location	Grid S Grid E	Water Depth (m)	Core Length (m)
Ru 56	38 04 35.1392	6342419.44	14.94	2.17
	176 15 17.1081	2795675.30		

Core Stratigraphy

0-25	25-50	50-75	75-100
			
100-126	126-157	157-188	188-217
			

Stratigraphic Column	Description	Location Map
----------------------	-------------	--------------



Concentrations (g/tonne)

Depth (cm)	As	Fe	Mn	P	Pb
0-12		3796	146.7	336.1	6.39
20-40		3273	128	207.1	1.824
40-60		5648	174.4	281.9	2.857
60-77		7241	218.2	320.6	3.648
77-78		13191	453.2	612.2	7.975
78-98		6470	148.3	222.4	1.682
98-118		4946	140.7	141.8	0.953
118-138		3330	89.46	99.12	0.771
138-158		2054	72.74	79.29	0.439
158-178		2894	105.9	115.2	0.82
178-198		5314	114.2	156.9	1.365

Tonnes per square km in top 1 m








As	Fe	Mn	P	Pb
	1637	51	84	1.01

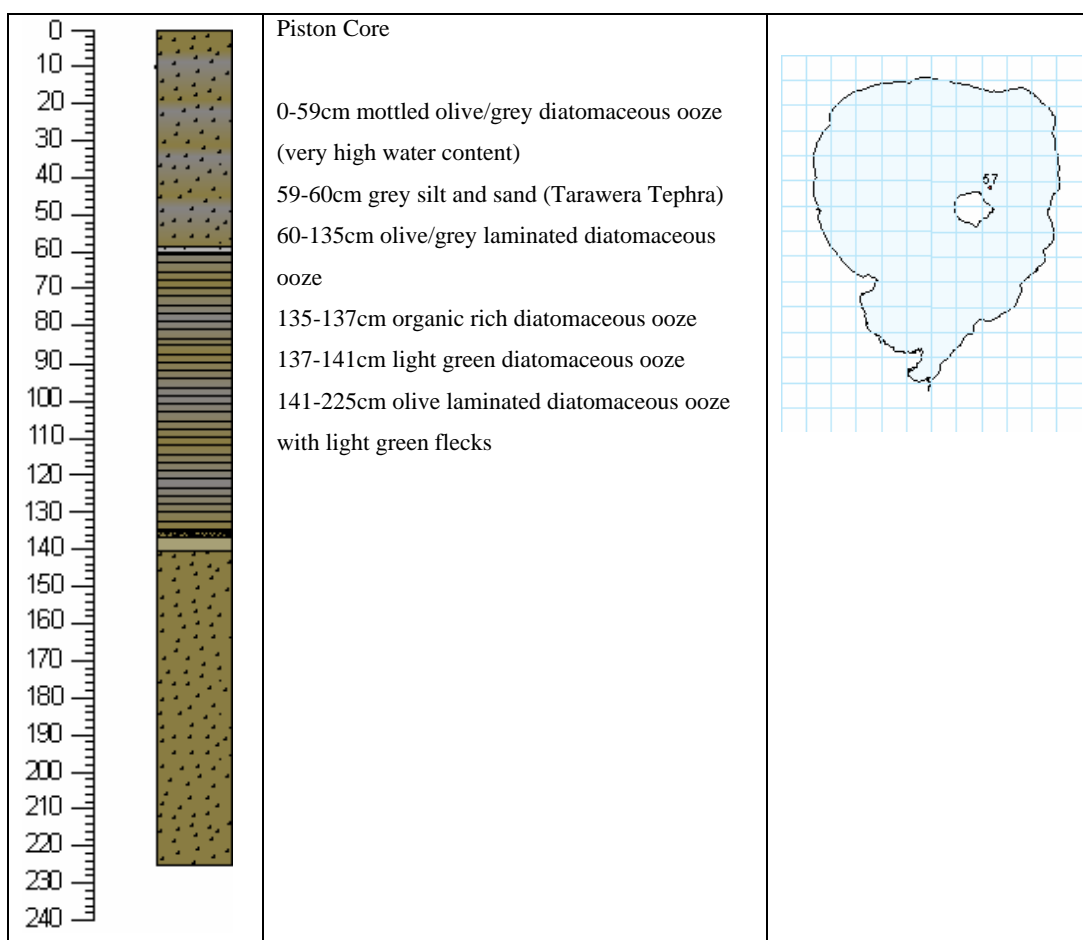
Tonnes per square km above Tarawera tephra

As	Fe	Mn	P	Pb
	1166	39	68	0.88

Core ID	Site Location	Grid S Grid E	Water Depth (m)	Core Length (m)
Ru 57	38 04 19.2982	6342779.87	15.75	2.25
	176 17 39.8995	2799170.74		

Core Stratigraphy

0-44	44-74	74-104	104-120
			
120-152	152-183	183-213	
			
Stratigraphic Column	Description	Location Map	



Concentrations (g/tonne)

Depth (cm)	As	Fe	Mn	P	Pb
0-20		6018	204.14	457.11	3.4565
20-40		4792.7	155.2	359.06	3.0237
40-59		7682.2	229.56	652.13	4.6729
59-60		14466	407.81	667.2	7.6428
60-80		2972	99.046	320.77	1.5826
80-100		3454	120.22	308.47	1.6995
100-120		3067.1	112	282.16	1.4213
120-140		3204	121.7	297.8	1.5954
140-160		2967.1	107.75	268.01	1.0034
160-180		2206	82.104	171.68	0.739
180-200		2810.4	116.59	241.16	1.2249
200-225		2290.3	105.34	213.82	0.7574

Tonnes per square km in top 1 m





As	Fe	Mn	P	Pb
	1561	50.5	130	0.9

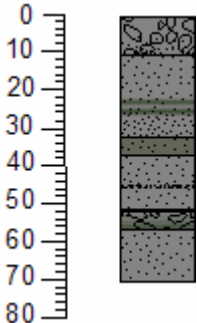

Tonnes per square km above Tarawera tephra

As	Fe	Mn	P	Pb
	1119	36	89	0.67

Core ID	Site Location	Grid S Grid E	Water Depth (m)	Core Length (m)
58	38 04 19.2982 176 17 39.8995	6342820.30 2798182.73	17.01	0.71

Core Stratigraphy

0-21	21-42	42-63	63-71
			

Stratigraphic Column	Description	Location Map
	<p>Piston Core</p> <p>0-10cm coarse pumice fining downwards, large clasts are ~1 cm (probably Kaharoa Lapilli)</p> <p>10-32cm coarse grey sand fining downwards, bands of green tinge at 24cm and 26cm</p> <p>32-37cm fine dark grey sand</p> <p>37-51cm coarse grey sand, black between 45-46cm with fibrous material</p> <p>51-56cm pumice rich layer, green at base</p> <p>56-70cm medium grey sand</p>	

Concentrations (g/tonne)






Depth (cm)	As	Fe	Mn	P	Pb
0-10		3165.3	85.044	54.535	0.1748
10-32		19644	698.57	317.07	0.9441
32-37		84.964	>d. lmt	>d. lmt	>d. lmt
37-51		9645.1	1726.8	128.33	0.7841
51-56		6924.3	192.59	81.277	0.4627
56-70		8308.6	270.61	127.93	0.8848





Tonnes per square km in top 1 m

As	Fe	Mn	P	Pb
308.84	16.457	4.7422	0.023	

Core ID	Site Location	Grid S Grid E	Water Depth (m)	Core Length (m)
Ru 59	38 03 14.0670	6344808.60	17.43	2.45
	176 17 18.6108	2798726.30		

Core Stratigraphy

0-34	34-67	67-75	75-105	105-135
				

135-161	161-194	194-221	221-247
			

Stratigraphic Column	Description	Location Map
	<p>Piston Core</p> <p>0-55cm laminated olive diatomaceous ooze, grading into grey near base. Fibrous for top 30cm, scattered organic matter</p> <p>55-57cm grey silt and sand (Tarawera Tephra)</p> <p>57-245cm laminated olive/grey diatomaceous ooze. Occasionally laminations are of light green or green.</p>	

Concentrations (g/tonne)

Depth (cm)	As	Fe	Mn	P	Pb
10	27.25	2483.5	142.5	289.0	6.061
30	38.82	5174.5	158.4	284.3	5.756
42.5	39.18	6179.0	229.6	453.4	8.696
56	29.56	9639.0	324.7	560.9	11.309
66	38.26	3813.1	131.6	394.0	5.443
85	42.68	3703.6	147.8	333.6	4.932
105	45.09	3445.5	151.4	309.9	4.260
125	24.44	2712.1	128.3	232.1	3.353
145	24.74	2573.4	124.6	214.1	3.611
165	38.30	2684.2	121.9	197.5	3.744
185	28.09	3436.7	161.1	189.7	4.860
205	20.94	2793.2	112.3	156.8	3.486

Tonnes per square km in top 1 m









As	Fe	Mn	P	Pb
11.4	1296	49	106	1.85

Tonnes per square km above Tarawera tephra

As	Fe	Mn	P	Pb
5.8	750	29	56	1.12

Core ID	Site Location	Grid S Grid E	Water Depth (m)	Core Length (m)
Ru 60	38 03 13.9885	6344771.25	17.79	2.37
	176 18 02.8520	2799804.13		

Core Stratigraphy

0-25	258-49	49-80	80-112
			
112-143	143-175	175-207	207-237
			

Stratigraphic Column	Description	Location Map
	<p>Piston Core</p> <p>0-86cm olive/dark grey laminated diatomaceous ooze</p> <p>86-88cm grey silt and sand (Tarawera Tephra)</p> <p>88-237cm olive laminated diatomaceous ooze, with light green algal clusters</p>	

Concentrations (g/tonne)

Depth (cm)	As	Fe	Mn	P	Pb
10	27.96	3379	188.1	366.0	7.892
30	22.31	2804	173.9	335.1	6.837
50	30.54	3284	166.2	287.9	6.190
68	45.27	8115	257.9	487.5	9.919
87	23.65	10330	422.0	699.8	13.067
98	29.17	3758	163.3	332.9	5.430
118	36.55	3165	147.2	334.5	5.021
138	39.00	3721	161.5	349.8	6.485
158	21.56	2918	125.1	229.0	4.947
178	21.96	2653	113.8	190.9	4.022
198	26.89	3069	139.0	241.6	4.682
223	27.80	3286	149.5	285.2	5.481

Tonnes per square km in top 1 m



As	Fe	Mn	P	Pb
8.3	1174	53.3	101	2.04

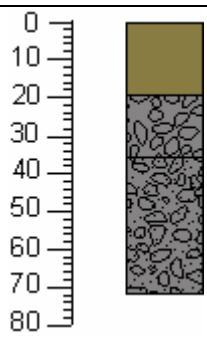
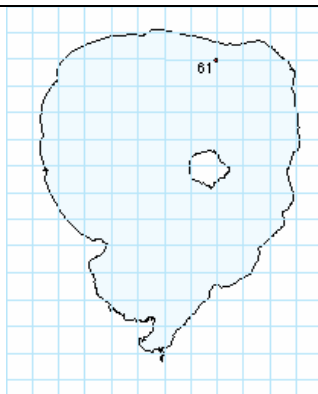
Tonnes per square km above Tarawera tephra

As	Fe	Mn	P	Pb
7.1	973	45	84	1.76

Core ID	Site Location	Grid S Grid E	Water Depth (m)	Core Length (m)
61	38 02 41.5693 176 17 19.5488	6345808.93 2798786.04	13.44	0.72

Core Stratigraphy

0-20	20-50	50-82
*Not recovered intact		

Stratigraphic Column	Description	Location Map
	<p>Piston Core</p> <p>*top ~20 cm diatomaceous ooze bagged , ~5cm Kaharoa lost during extrusion</p> <p>20-36cm pumice with clasts averaging ~3 mm (Kaharoa)</p> <p>36-72cm well sorted pumice rich sand</p>	

Concentrations (g/tonne)



Depth (cm)	As	Fe	Mn	P	Pb
10	42.91	5611	241.1	156.7	6.840
28	24.85	3295	42.2	59.7	1.887
41	8.30	7469	173.4	107.3	4.021
52	4.96	7087	501.5	172.0	3.151

Tonnes per square km in top 1 m

As	Fe	Mn	P	Pb
4.9	1941	108	45	1.17

Core ID	Site Location	Grid S Grid E	Water Depth (m)	Core Length (m)
Ru 62	38 02 40.4845	6345878.75	8.2	0.11
	176 16 38.9378	2797797.83		

Core Stratigraphy





Stratigraphic Column	Description	Location Map
	<p>Piston Core</p> <p>Lost most of the core as it was packed to tight to extrude. Had to wash out the bottom of the core. Bagged some of this material and retained the top of the core</p> <p>0-11cm pumice sand with diatomaceous ooze (pumice averaging ~2 mm)</p>	

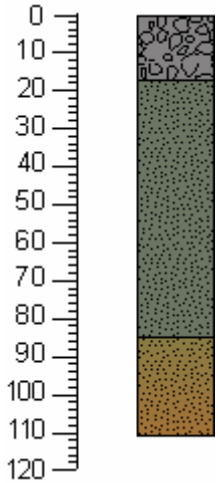

Concentrations (g/tonne)

Depth (cm)	As	Fe	Mn	P	Pb
0-11	17.03	2716	64.86	192.4	2.803

Core ID	Site Location	Grid S Grid E	Water Depth (m)	Core Length (m)
Ru 63	38 02 41.1072	6345895.97	9.92	1.11
	176 15 58.1752	2796804.00		

Core Stratigraphy

0-24	24-56	56-88	88-111
			

Stratigraphic Column	Description	Location Map
	<p>Piston Core</p> <p>0-17cm pumice (Kaharoa) with diatomaceous ooze</p> <p>17-85cm silty olive/grey diatomaceous ooze</p> <p>85-111cm olive/brown silty diatomaceous ooze</p>	

Concentrations (g/tonne)






Depth (cm)	As	Fe	Mn	P	Pb
8.5	28.33	2843	39.7	58.1	1.113
25	39.82	2732	127.7	98.4	5.279
43	26.35	4024	155.8	132.1	5.888
63	23.28	4244	171.4	170.5	5.851
83	41.91	2013	107.6	115.3	4.544

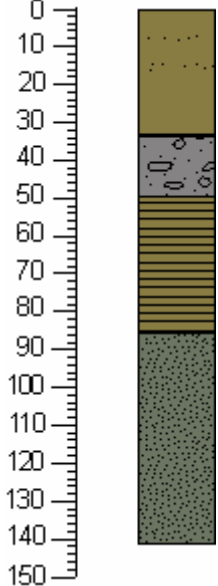

Tonnes per square km in top 1 m

As	Fe	Mn	P	Pb
9.0	908	35	33	1.31

Core ID	Site Location	Grid S Grid E	Water Depth (m)	Core Length (m)
Ru 64	38 02 41.7183	6345752.67	9.38	1.41
	176 18 16.9887	2800185.31		

Core Stratigraphy

0-24	24-48	48-83	83-118	118-141
				

Stratigraphic Column	Description	Location Map
	<p>Piston Core</p> <p>0-33cm olive diatomaceous ooze, sand layers at 7cm and 15cm, scattered organic material</p> <p>33-49cm pumice with diatomaceous ooze and organic matter</p> <p>49-85cm laminated olive diatomaceous ooze</p> <p>85-141cm silty olive/grey diatomaceous ooze</p>	

Concentrations (g/tonne)









Depth (cm)	As	Fe	Mn	P	Pb
7.5	49.64	6231	250.1	213.0	6.778
24	46.35	6651	141.3	164.2	5.740
41	44.37	5164	102.1	138.2	3.475
60	80.31	2123	106.4	91.1	4.179
78	72.53	7831	105.5	104.4	4.926
95	44.11	5953	130.6	108.9	4.661
115	28.61	4932	140.1	117.6	4.745
133	17.28	3813	150.3	122.7	5.219

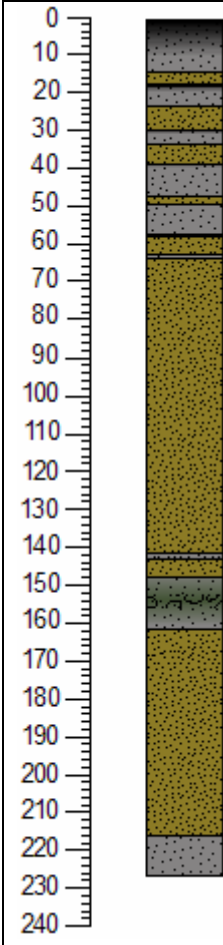

Tonnes per square km in top 1 m

As	Fe	Mn	P	Pb
14.6	1306	35	35	1.23

Core ID	Site Location	Grid S Grid E	Water Depth (m)	Core Length (m)
Ru 65	38 02 41.2469	6345964.75	5.36	2.26
	176 14 35.9335	2794800.11		

Core Stratigraphy

0-21	21-42	42-78	78-114
			
114-136	136-167	167-198	198-226
			

Stratigraphic Column	Description	Location Map
	<p>Piston Core</p> <p>* had fresh water muscle part way down</p> <p>0-14cm grey sand, black for top 5 cm, freshwater muscle at the top</p> <p>14-17cm olive silty diatomaceous ooze</p> <p>17-23cm grey sand, black from top 1 cm, freshwater muscle at the top</p> <p>23-29cm olive silty diatomaceous ooze</p> <p>29-33cm grey sand, black from top 1 cm, freshwater muscle at the top</p> <p>33-38cm olive silty diatomaceous ooze</p> <p>38-47cm grey sand, black from top 1 cm</p> <p>47-49cm olive silty diatomaceous ooze</p> <p>49-57cm grey sand</p> <p>57-62cm olive silty diatomaceous ooze</p> <p>62-63cm grey sand</p> <p>63-147cm olive silty diatomaceous ooze, thin tephra at 142 cm</p> <p>147-161cm grey sand with greenish tinge through middle section, 2 cm pumice clasts at the top</p> <p>161-215cm olive silty diatomaceous ooze (166-167cm sand layer)</p> <p>215-226cm grey sand, gradational upper boundary</p>	

Concentrations (g/tonne)

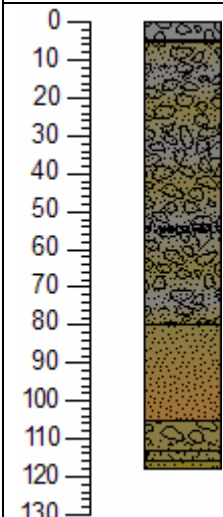

Depth (cm)	As	Fe	Mn	P	Pb
7	23.30	2273	41.1	91.9	1.301
15.5	26.14	nd	nd	83.2	3.477
20	43.42	4230	189.7	91.3	4.431
26	25.41	2698	92.8	76.4	2.848
30	17.88	1888	37.6	64.3	1.579
34.5	86.58	7374	223.4	104.5	4.528
42.5	20.62	2547	92.5	68.3	1.622
48	26.56	2623	52.8	81.9	2.122
53	25.11	2666	91.7	75.5	2.815
59.5	18.28	1900	30.8	64.1	1.171
63.5	52.45	6259	196.8	91.0	3.894
73	25.54	3085	72.2	64.2	2.143
93	45.27	5211	181.1	85.9	4.213
113	43.41	4845	138.2	71.2	3.963
130	22.54	2831	156.4	68.4	3.922
142	36.05	4501	105.2	68.6	3.900
154	29.04	4127	97.3	73.0	4.911
171	7.31	8112	106.6	50.7	3.907
191	24.29	4252	103.6	74.7	4.595
208	39.51	5553	100.6	73.3	4.031
221	35.83	4328	98.3	67.4	3.848

Tonnes per square km in top 1 m

As	Fe	Mn	P	Pb
10.7	1129	35	26	0.90

Core ID	Site Location	Grid S Grid E	Water Depth (m)	Core Length (m)
Ru 66	38 03 46.8437	6343980.09	9.32	1.18
	176 13 54.9329	2793727.96		

Core Stratigraphy

Stratigraphic Column	Description	Location Map
	<p>Piston Core</p> <p>0-5cm pumice (Reworked Kaharoa?) with diatomaceous ooze</p> <p>5-80cm olive/grey silty diatomaceous ooze with pumice and 55cm and scattered organic material</p> <p>80-105cm olive/brown silty diatomaceous ooze</p> <p>105-116cm pumice with diatomaceous ooze, fining downwards</p> <p>116-118cm olive silty diatomaceous ooze</p>	

Concentrations (g/tonne)






Depth (cm)	As	Fe	Mn	P	Pb
2.5	46.82	3612	54.6	53.9	1.715
15	61.27	2491	75.7	73.1	3.058
35	35.24	5010	128.0	88.2	4.186
55	14.59	4057	149.2	95.8	4.453
73	38.06	5615	121.8	94.2	4.031
93	3.76	3237	118.1	227.7	9.614
113	6.12	4389	52.5	56.1	2.675

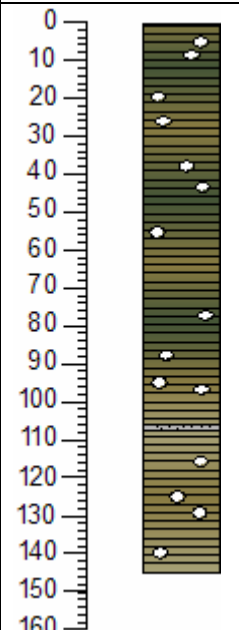

Tonnes per square km in top 1 m

As	Fe	Mn	P	Pb
9.5	1214	35	35	1.51

Core ID	Site Location	Grid S Grid E	Water Depth (m)	Core Length (m)
Ru 67	38 04 18.8450	6342994.45	11.4	1.45
	176 13 54.6378	2793685.05		

Core Stratigraphy

0-31	31-60	60-93	91-120	120-145
				

Stratigraphic Column	Description	Location Map
	<p>Piston Core</p> <p>0-145cm olive laminated diatomaceous ooze, some dark laminations.</p> <p>Large gas bubbles, extremely high water content.</p> <p>Thin silt at 107cm (Tarawera?).</p> <p>139-145cm has lighter green laminations</p>	

Concentrations (g/tonne)

Depth (cm)	As	Fe	Mn	P	Pb
10	35.11	2954	195.6	395.6	8.114
30	5.75	3805	208.7	411.9	11.251
50	10.26	4308	196.8	435.2	11.463
70	19.35	4632	186.6	489.2	12.410
90	7.57	2803	184.3	365.4	8.132
110	2.60	2695	160.4	302.8	5.814
133	5.30	3026	141.0	218.6	4.980

Tonnes per square km in top 1 m







As	Fe	Mn	P	Pb
4.76	1128	59.3	128	3.13

Tonnes per square km above Tarawera tephra

As	Fe	Mn	P	Pb
4.8	1186	63	134	3.26

Core ID	Site Location	Grid S Grid E	Water Depth (m)	Core Length (m)
Ru 68	38 04 51.2297	6341997.03	9.12	1.59
	176 13 54.3067	2793640.85		

Core Stratigraphy

0-28	28-56	56-74
		
73-105	105-131	131-159
		

Stratigraphic Column	Description	Location Map
	<p>Piston Core</p> <p>0-11cm olive diatomaceous ooze (darker for bottom 5cm)</p> <p>11-12cm grey silt</p> <p>12-159cm olive laminated diatomaceous ooze, organic matter at 57cm, 1mm thick silts at 121cm and 149cm. Darker (blackish) from 113cm to base.</p>	

Concentrations (g/tonne)

Depth (cm)	As	Fe	Mn	P	Pb
5.5		6327	163.9	251.7	7.108
12	19.21	7905	327.9	254.8	8.996
22	52.43	7254	154.6	199.3	3.258
42	18.46	6812	94.3	140.0	5.044
62	12.79	6786	101.1	124.1	4.490
82	9.61	5293	113.7	115.0	3.971
102	9.41	5298	192.4	267.6	8.573
122	9.80	4534	235.4	323.8	10.222
146	7.96	6740	220.8	279.2	8.561

Tonnes per square km in top 1 m










As	Fe	Mn	P	Pb
5.9	1960	39	51	1.5

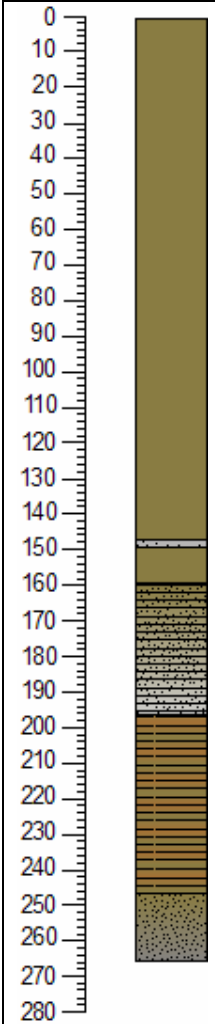

Tonnes per square km above Tarawera tephra

As	Fe	Mn	P	Pb
	212	5	8	0.24

Core ID	Site Location	Grid S Grid E	Water Depth (m)	Core Length (m)
Ru 69	38 04 11.2994	6343190.78	11.68	2.65
	176 14 35.5221	2794689.24		

Core Stratigraphy

0-32	32-64	64-82	82-116	116-150
				
150-176	176-207	207-238	238-265	
				

Stratigraphic Column	Description	Location Map
	<p>Piston Core</p> <p>0-147cm olive diatomaceous ooze, very high water content</p> <p>147-149cm sandy layer (Tarawera?)</p> <p>149-159cm olive diatomaceous ooze</p> <p>159-196cm laminated grey/olive silty diatomaceous ooze</p> <p>196-246cm olive/brown laminated diatomaceous ooze</p> <p>246-265cm silty grey/olive diatomaceous ooze</p>	

Concentrations (g/tonne)






Depth (cm)	As	Fe	Mn	P	Pb
10		2043	137.0	23.5	19.354
30	56.41	1866	96.5	154.8	4.284
50	21.44	1732	79.5	93.1	2.900
71	21.02	2210	95.3	76.0	2.664
92	25.18	1770	68.4	100.2	3.481
112	19.77	1346	56.1	70.3	2.522
135	14.72	1759	60.9	56.0	2.181
148	19.47	3818	81.3	56.0	2.317
153	82.13	1187	88.8	81.9	2.527
166	87.60	2356	148.3	77.5	3.184
186	37.18	6042	255.1	493.0	4.566
206	95.35	3330	108.0	224.6	2.370

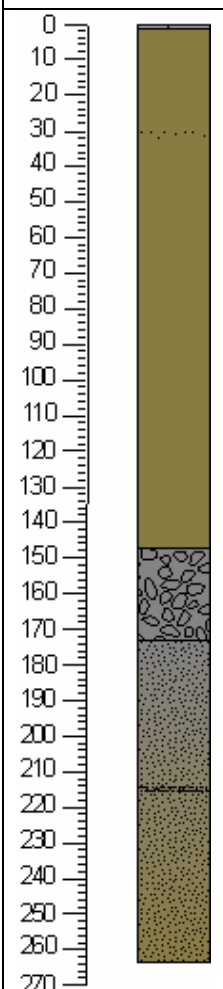

Tonnes per square km in top 1 m

As	Fe	Mn	P	Pb
9.3	729	35	34	2.23

Core ID	Site Location	Grid S Grid E	Water Depth (m)	Core Length (m)
Ru 70	38 04 10.5325	6343177.49	13.72	2.63
	176 15 17.1463	2795703.89		

Core Stratigraphy

0-34	34-67	67-103	103-139	139-160
				

Stratigraphic Column	Description	Location Map
	<p>Piston Core</p> <p>0-1cm grey silt (Tarawera ?) diatomaceous ooze was on top, but washed out due to high water content</p> <p>1-146cm mottled olive diatomaceous ooze with 1mm black sand at 32cm</p> <p>146-173cm pumice (Kaharoa?) within a diatomaceous ooze layer</p> <p>173-263cm mottled grey/olive silty diatomaceous ooze, organic matter at 215cm</p>	

Concentrations (g/tonne)








Depth (cm)	As	Fe	Mn	P	Pb
0.5	42.24	8229	348.4	316.1	8.853
11	59.84	5002	119.2	167.7	3.728
31	17.39	2595	78.0	75.5	1.990
54	27.29	2899	73.6	70.2	2.166
77	31.95	3176	87.9	94.0	2.751
97	28.20	2130	56.0	48.5	1.733
117	32.33	2878	61.3	105.5	1.780
137	139.56	4313	83.0	740.5	2.201
158	116.15	4238	88.1	532.5	1.555
180	93.18	4316	97.1	396.1	2.693
200	46.78	5344	246.1	561.4	3.422
220	57.10	7801	450.2	1234.3	2.924
240	41.28	5442	214.4	297.4	3.712
256	47.06	6327	261.2	571.6	3.138

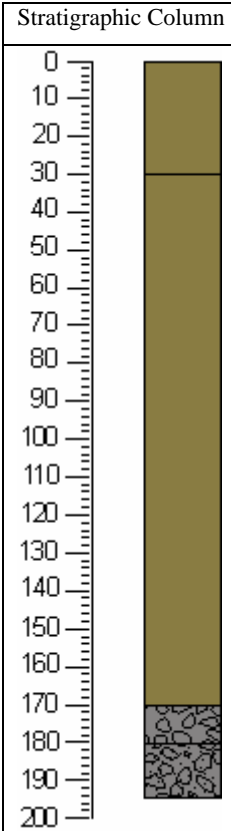

Tonnes per square km in top 1 m

As	Fe	Mn	P	Pb
10.1	1001	27	29	0.79

Core ID	Site Location	Grid S Grid E	Water Depth (m)	Core Length (m)
Ru 71	38 04 34.8989	6342353.61	19.56	1.94
	176 16 39.2735	2797676.57		

Core Stratigraphy

30-57	57-84	80-100	100-125
			
125-150	150-175	175-194	
			

Stratigraphic Column	Description	Location Map
	<p>Piston Core</p> <p>*bagged top ~30 cm (Tarawera not seen)</p> <p>30- approx 170cm olive diatomaceous ooze</p> <p>170-180cm pumice (clasts up to 1cm) Kaharoa</p> <p>180-194cm well sorted pumice rich sand</p> <p>* this core had dried out prior to sampling making it difficult to determine depths</p>	

Concentrations (g/tonne)





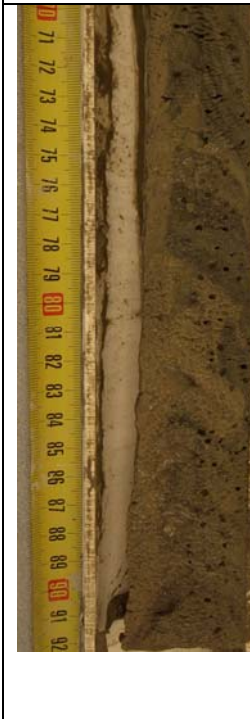



Depth (cm)	As	Fe	Mn	P	Pb
15	96.17	9972	396.0	202.8	6.401
45	66.94	8130	330.7	140.3	5.828
80	66.53	8554	317.1	93.5	5.688
115	51.89	6996	289.5	95.0	5.224
145	44.11	5994	268.0	63.8	4.203
165	33.52	3794	167.8	142.2	3.232
175	23.22	3003	169.4	129.1	3.535
187	17.60	10859	497.4	414.8	4.390

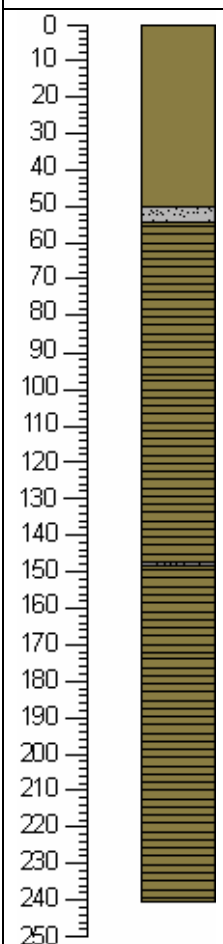


Tonnes per square km in top 1 m

As	Fe	Mn	P	Pb
23	2699	105	43	1.81

Core ID	Site Location	Grid S Grid E	Water Depth (m)	Core Length (m)
Ru 72	38 04 43.1662	6342025.72	14.32	2.40
	176 18 00.8496	2799653.78		

Core Stratigraphy

0-27	27-54	54-89	89-124
			
124-147	147-180	180-213	213-240
			

Stratigraphic Column	Description	Location Map
	<p>Piston Core</p> <p>0-50cm olive diatomaceous ooze, high water content</p> <p>50-54cm grey silt with black sand at base (Tarawera)</p>  <p>54-240cm laminated olive diatomaceous ooze with possible tephra at 148cm</p> <p>* whole core has a very high water content</p>	

Concentrations (g/tonne)

Depth (cm)	As	Fe	Mn	P	Pb
13	64.28	5821	350.7	461.1	12.733
38	62.40	7821	328.2	353.1	11.326
52	23.51	9969	338.7	221.8	10.033
64	87.51	6600	229.6	207.9	7.759
84	66.47	5487	192.8	171.6	6.862
107	62.76	7121	171.2	147.3	7.344
133	59.88	6823	116.1	100.9	7.180
157	57.67	6058	93.3	40.8	3.931
177	66.82	6511	86.7	57.7	4.276
200	81.83	7006	77.8	20.1	3.931
226	74.47	6456	77.8	27.3	3.746

Tonnes per square km in top 1 m




As	Fe	Mn	P	Pb
20.5	2023	85	91	2.99

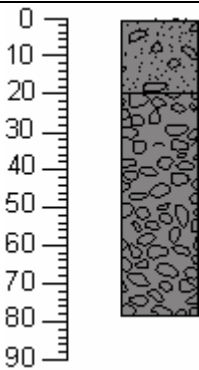


Tonnes per square km above Tarawera tephra

As	Fe	Mn	P	Pb
9.7	1034	52	62	1.84

Core ID	Site Location	Grid S Grid E	Water Depth (m)	Core Length (m)
Ru 73			8.97	0.78

Core Stratigraphy

0-31	31-62	62-80
		

Stratigraphic Column	Description	Location Map
	<p>Piston Core</p> <p>0-20cm well sorted grey sand with occasional pumice clasts. 3cm below surface is in intact fresh water mussel</p>  <p>20-78cm pumice- biggest clasts 4 mm, fragments of fresh water mussel</p>	

Concentrations (g/tonne)





Depth (cm)	As	Fe	Mn	P	Pb
10	41.45	10757	138.9	26.3	3.696
33	31.80	7947	103.6	19.7	2.931
63	30.51	8013	82.0	4.6	3.446



Tonnes per square km in top 1 m

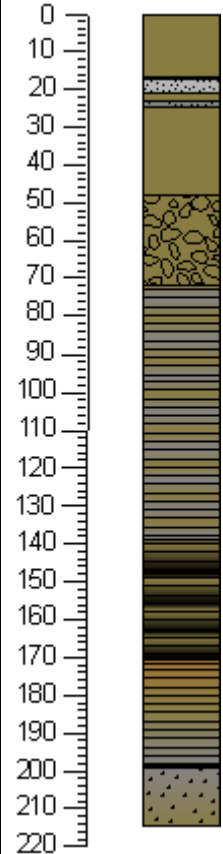

As	Fe	Mn	P	Pb
10.1	2606	30	4	1.03

Core ID	Site Location	Grid S Grid E	Water Depth (m)	Core Length (m)
Ru 74		6339700 2798500	13.0	2.15

Core Stratigraphy

0-45	45-79	79-113	113-140
			

140-171	171-202	202-218
		

Stratigraphic Column	Description	Location Map
	<p>Piston Core</p> <p>0-17cm olive diatomaceous ooze</p> <p>17-21cm grey silt (Tarawera)</p> <p>21-48cm olive diatomaceous ooze with possible tephra at 24cm</p> <p>48-72cm olive diatomaceous ooze with pumice clasts (eroded from Kaharoa elsewhere?)</p> <p>72-139cm olive and grey laminated diatomaceous ooze</p> <p>139-171cm black/olive laminated diatomaceous ooze</p> <p>171-199cm laminated diatomaceous ooze grading down from brown through olive to grey</p> <p>199-215cm mottled grey/olive diatomaceous ooze</p>	

Concentrations (g/tonne)

Depth (cm)	As	Fe	Mn	P	Pb
8.5	25.5	13791	642.1	410.4	17.1
19	44.4	9773	439.7	358.8	10.6
33	67.3	10036	355.3	244.0	9.0
59	74.2	8540	172.5	150.5	5.6
82	232.3	8428	233.6	936.2	4.7
102	170.2	9615	258.0	1142.1	3.9
126	83.6	7449	329.9	736.1	4.3
149	75.7	7439	360.9	535.6	4.9
169	175.5	10465	381.6	1807.8	4.9
189	159.7	11725	231.7	206.0	4.2
207	41.4	8291	377.3	367.9	5.6

Tonnes per square km in top 1 m








As	Fe	Mn	P	Pb
31.6	3061	101	143	2.55

Tonnes per square km above Tarawera tephra

As	Fe	Mn	P	Pb
1.34	724	34	22	0.9

Core ID	Site Location	Grid S Grid E	Water Depth (m)	Core Length (m)
Ru 75		6340000 2799500	8.00	2.08

Core Stratigraphy

0-40	40-76	76-112	112-133
			
133-163	163-193	193-210	
			

Stratigraphic Column	Description	Location Map
	<p>Piston Core</p> <p>0-30cm coarse gravel lag, predominately pumice.</p> <p>Sandier near the surface with organic matter scattered throughout</p> <p>30-40cm olive diatomaceous ooze</p> <p>40-82cm olive-grey silty diatomaceous ooze, more brown near the top</p> <p>82-83cm pumice layer</p> <p>83-107cm grey silty diatomaceous ooze</p> <p>107-110cm sandy pumice layer</p> <p>110-115cm silty diatomaceous ooze</p> <p>115-123cm sand layer</p> <p>123-127cm silty diatomaceous ooze</p> <p>127-132cm grey sand layer</p> <p>132-167cm olive-grey silty diatomaceous ooze, thin tephra at 162cm and 136cm</p> <p>167-208cm grey/dark grey silty diatomaceous ooze</p> <p>* from 82-132 cm it is difficult to determine the true thicknesses and depths due to dewatering and movement of sediment.</p>	

Concentrations (g/tonne)



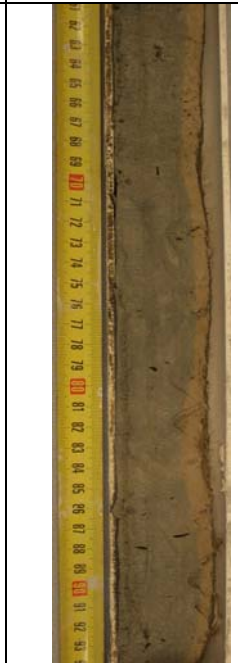

Depth (cm)	As	Fe	Mn	P	Pb
15	8.3	1959.5	36.3	84.2	0.4
35	108.5	6440.2	245.3	152.1	3.6
50	115.7	8058.5	295.1	189.5	4.6
71	22.9	5762.0	432.8	354.0	4.7
84	34.3	4708.2	238.7	211.3	2.5
96	33.1	5784.6	410.9	367.2	4.6
110	33.8	5582.2	309.3	267.3	3.6
120	24.2	4428.6	235.0	219.3	2.7
130	24.2	4592.1	198.6	171.5	3.4
142	18.9	6850.0	439.6	394.4	5.2
162	25.9	6963.7	438.5	397.6	4.3
182	60.4	6636.0	372.0	674.1	2.9
200	90.1	9405.2	314.3	367.3	3.2




Tonnes per square km in top 1 m

As	Fe	Mn	P	Pb
14.7	1582	79.9	67.3	0.99

Core ID	Site Location	Grid S Grid E	Water Depth (m)	Core Length (m)
Ru 76		6340000 2800500	6.50	2.23

Core Stratigraphy

0-30	30-61	61-94	94-120
			

120-150	150-179	179-223
		

Stratigraphic Column	Description	Location Map
	<p>Piston Core</p> <p>0-8cm coarse pumice lag</p> <p>8-12cm pumice sand with 2-3 mm clasts</p> <p>12-16cm pumice sand fining upwards</p> <p>16-35cm olive silty diatomaceous ooze</p> <p>35-40cm diatomaceous ooze with sand</p> <p>40-48cm dark grey slightly sandy diatomaceous ooze, very sharp lower contact</p> <p>48-223cm olive-grey silty diatomaceous ooze with green tint. Large gas bubble from 119-122cm, algal cluster at ~110cm, possible tephra at 216cm.</p>	

Concentrations (g/tonne)






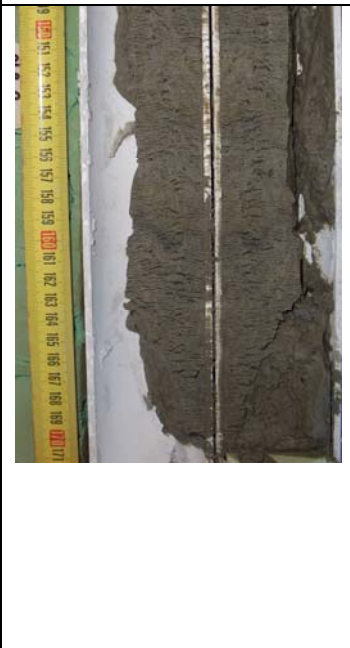
Depth (cm)	As	Fe	Mn	P	Pb
4	4.9	1953	84	121	0.68
10	26.9	4402	111	76	1.32
14	47.4	5051	67	30	1.83
26	31.8	3837	183	25	3.98
37.5	22.3	3693	116	15	3.55
44	125.6	14923	194	63	4.70
58	19.0	5167	217	82	4.23
81	12.8	4499	225	124	4.61
104	11.3	7410	367	261	4.78
124	8.2	6792	226	40	4.75
144	8.9	6826	267	135	5.15
166	9.5	7069	277	123	5.22
210	6.3	5338	317	193	4.50



Tonnes per square km in top 1 m

As	Fe	Mn	P	Pb
9.4	1677	59.3	26.9	1.2

Core ID	Site Location	Grid S Grid E	Water Depth (m)	Core Length (m)
Ru 77	38 06 42.9216 S	6338452	16.8	1.71
	176 16 13.112 E	2790896		

Core Stratigraphy

0-30	30-60	58-88
		
88-119	119-149	149-171
		

Stratigraphic Column	Description	Location Map
	<p>0-30cm Grey to light olive green diatomaceous ooze with very high water content. Water lost over time.</p> <p>30-59cm similar diatomaceous ooze but with lower water content</p> <p>59-63cm fine grey mud (Rotomahana mud unit of Tarawera) see photo below.</p>  <p>63cm 3mm thick coarse sand (Tarawera lapilli) abrupt transition</p> <p>63-171cm diatomaceous ooze with grey bands at 108-110cm and 135-138cm</p> <p>*No evidence of the Kaharoa</p> <p>Bottom 1m lost while raising the core.</p>	

Concentrations (g/tonne)

Depth (cm)	As	Cd	Fe	K	Mn	Na	P	S	Zn
5	74	4.5	5202	126	319	76.3	1039	4832	52.6
15	93	5.23	6991	216	412	176	891	4458	62.6
25	104	5.7	8402	311	424	259	705	4225	51.1
43.5	62.9	3.49	9621	300	403	245	667	5326	20.7
60	39.4	2.08	13952	472	450	427	605	1830	37.4
71.5	113	6.02	6787	162	255	111	382	5519	13.5
90	75.5	3.97	6579	156	210	80.2	370	7976	9.4
110	51.5	3.28	5337	124	244	88	286	5021	3.75
130	66.9	3.62	6501	153	294	67.6	180	9446	23.3
150	54.5	3.18	6388	143	237	124	190	4778	8.72
165.5	50.2	3.3	7903	156	272	77.7	213	7870	58.3

Tonnes per square km in top 1 m










As	Cd	Fe	K	Mn	Na	P	S	Zn
23	1.2	2135	62	90	47	168	1494	8.1

Tonnes per square km above Tarawera tephra

As	Fe	Mn	P	Pb
12.2	1382	64	126	

Core ID	Site Location	Grid S Grid E	Water Depth (m)	Core Length (m)
Ru 79	38 04 28.2149S 176 17 45.4014E	6342304 2799269	12.6	2.29

Core Stratigraphy

0-22	22-44	44-65	65-92.5
			
92.5-115	115-135	135-152.5	152.5-175
			
175-195	195-215	215-229	
			

Stratigraphic Column	Description	Location Map
	<p>Piston Core</p> <p>0-65cm Dark diatomaceous ooze</p> <p>65-67cm grey silt (Tarawera Tephra)</p> <p>67-77cm very sloppy diatomaceous ooze</p> <p>77-107cm sloppy diatomaceous ooze</p> <p>107-140cm brown diatomaceous ooze</p> <p>140-153cm diatomaceous ooze with many fine layers</p> <p>153-229cm diatomaceous ooze with numerous gas voids</p> <p>*no sign of Kaharoa Tephra</p>	

Concentrations (g/tonne) Aqua Regia Digestion

Depth (cm)	As	Cd	Fe	K	Mn	Na	P	S	Zn
5	57.9	3.4	6697	190	288	2465	770	2465	37.3
15	49.6	3.56	5223	153	267	2113	584	2113	31.6
30	79	3.94	7781	236	236	3030	610	3030	31.4
51.5	72.8	3.72	7565	241	232	3739	574	3739	29.6
65	47.2	2.45	14818	452	450	2738	1038	2738	42.4
78.5	82.6	4.09	10928	172	219	3573	666	3573	38.6
100	119	5.75	7439	128	151	3749	765	3749	12.7
120	105	5.64	6809	139	141	3336	677	3336	21.1
140	104	5.29	8682	159	233	5135	653	5135	11.8
160	67.4	3.64	6012	133	188	5064	490	5064	11.7
180	58.3	3.23	5271	139	187	6153	451	6153	16.8
200	66.6	3.61	6796	121	199	7969	743	7969	16.1
214.5	57.9	3.4	6697	190	232	2465	770	2465	37.3

Major elements by X-Ray Fluorescence

Depth (cm)	Na	Mg	Al	Si	P	S
5	1426	839	11249	309088	651	2526
15	2214	1234	11651	370934	518	2716
30	2054	938	14908	325286	409	2539
52	4545	1983	29661	342956	674	6812
65	7302	3032	51322	330825	1201	3930
79	2725	1595	18839	389375	730	4366
100	1650	1095	14597	377175	765	6157
120	1820	1399	17838	441545	752	6704
140	1980	1255	14966	399402	725	7827
160	905	577	11536	390988	467	6950
180	1863	1341	15352	461108	573	8433
200	2320	1067	15704	390357	908	7731
220	1735	1282	14424	455849	554	12272

Major elements by X-Ray Fluorescence (continued)

Depth (cm)	K	Ca	Ti	Mn	Fe
5	316	2103	512	419	6852
15	358	2302	546	555	6941
30	514	3006	688	345	9595
52	894	4384	808	665	13702
65	1461	5700	1129	722	18696
79	591	3952	792	487	11834
100	446	2937	655	465	10160
120	571	3803	644	480	10901
140	466	3383	675	642	10943
160	336	2115	495	384	8408
180	422	2531	623	631	9118
200	448	3053	681	595	9398
220	391	3078	593	528	9028

Minor Elements by X-Ray Fluorescence

Depth (cm)	Cl	V	Cr	Cu	Zn	Ga	Ge	As	Br	Rb	Sr	Y
5	78	32	6	6	41	5	14	39	7	15	17	5
15	147	38	1	5	41	6	16	39	8	18	21	6
30	53	42	0	5	35	7	15	58	7	25	27	8
52	104	22	2	5	44	9	11	54	8	44	41	11
65	158	32	2	6	49	13	6	55	6	73	51	14
79	123	50	2	3	28	7	11	64	6	33	49	9
100	113	40	4	3	26	7	14	102	7	25	30	8
120	135	15	2	4	33	9	15	104	8	32	42	10
140	175	40	0	4	31	8	15	103	8	26	40	9
160	98	25	2	4	22	6	19	61	8	18	23	7
180	119	39	0	5	31	8	20	76	11	24	31	10
200	123	40	0	4	27	8	13	66	9	23	29	10
220	123	29	0	4	26	7	23	51	11	22	27	9

Minor Elements by X-Ray Fluorescence (continued)

Depth (cm)	Zr	I	Cs	Ba	La	Ce	Pr	Nd	W	Pb	Th	U
5	26	4	13	84	19	22	24	16	25	6	3	2
15	26	5	17	87	28	34	35	22	25	6	4	4
30	37	3	13	97	12	14	12	14	27	6	4	3
52	52	5	23	157	26	33	32	20	24	9	6	4
65	72	5	24	213	28	39	35	35	24	11	8	4
79	47	4	16	119	26	32	26	34	24	7	5	3
100	42	5	20	133	21	31	28	39	32	6	4	3
120	52	5	21	151	29	50	32	28	34	7	5	3
140	43	3	13	138	20	28	19	20	30	5	3	2
160	33	6	22	119	35	47	48	34	25	5	4	3
180	44	4	15	119	18	26	15	0	25	5	3	3
200	40	5	19	143	27	33	33	30	30	6	5	4
220	43	4	15	117	17	23	15	17	25	6	5	4

Tonnes per square km in top 1 m


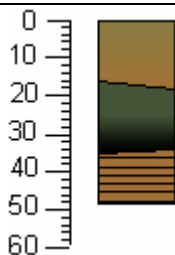

As	Cd	Fe	K	Mn	Na	P	S	Zn
76	4	8754	241	936	3240	936	3240	45

Tonnes per square km above Tarawera tephra

As	Fe	Mn	P	Pb
9.9	1128	40	99	

Core ID	Site Location	Grid S Grid E	Water Depth (m)	Core Length (m)
Ru 90	38 07.390S 176 15.917E	6337005.44 2796383.01	30.1	0.50

Core Stratigraphy

0-48	Stratigraphic Column	Description	Location Map
		<p>Gravity Core</p> <p>0-17cm Olive brown diatomaceous ooze, lower boundary at 45° (16-18 cm)</p> <p>17-34.5cm Dark olive green to black diatomaceous ooze, lower boundary at 30° in opposite direction to upper boundary</p> <p>34.5-48cm Laminated brown diatomaceous ooze.</p> <p>*No sign of Tarawera Tephra</p>	

Concentrations (g/tonne) Aqua Regia Digestion

Depth (cm)	As	Cd	Fe	K	Mn	Na	P	S	Zn
1	108	5.8	105?	263	192	105	1330	7615	105
3.5	109	5.7	10859	281	287	252	1163	7819	118
7.5	107	5.7	10572	232	274	212	1021	7156	106
12.5	101	5.4	11984	248	327	183	1138	8907	144
17.5	124	6.4	12055	238	297	165	883.9	8881	103
22.5	129	6.1	11259	255	305	173	897.4	7043	94
27.5	114	5.3	9661	240	317	133	1293	5654	78
35	138	6.9	10453	235	361	179	1116	6718	81
45	89	4.5	7774	221	339	149	792	5086	59

Tonnes per square km in top 1 m


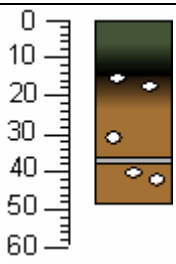

As	Cd	Fe	K	Mn	Na	P	S	Zn
31	2	2721	71	101	50	281	1851	23

Tonnes per square km above Tarawera tephra (at least)

As	Fe	Mn	P	Pb
17.7	1535	49	160	

Core ID	Site Location	Grid S Grid E	Water Depth (m)	Core Length (m)
Ru 91	38 05.667S 176 16.141E	6340178.34 2796826.78	21.4	0.50

Core Stratigraphy

0-48	Stratigraphic Column	Description	Location Map
		<p>Gravity Core</p> <p>0-14.5cm dark olive green/black diatomaceous ooze</p> <p>14.5-36cm gradual transition to paler brown diatomaceous ooze. Numerous gas voids, especially at 16, 19, 32, 40 & 42</p> <p>36-38cm grey band, possibly Tarawera Tephra</p> <p>38-48cm pale brown diatomaceous ooze as above</p>	

Concentrations (g/tonne) Aqua Regia Digestion

Depth (cm)	As	Cd	Fe	K	Mn	Na	P	S	Zn
1	90	5.5	8216	147	263	120	771.9	5275	56
3.5	67	3.9	7906	167	280	133	742.3	4218	33
7.5	82	4.6	7489	147	259	74.8	798.5	4723	37
12.5	69	4.0	7890	174	344	148	799.6	3986	65
17.5	96	5.2	8448	196	448	180	876.8	5599	94
22.5	117	6.0	8652	151	266	82.4	761.7	4533	47
27.5	131	6.9	10381	178	347	97.2	843	5937	53
35	96	5.3	9357	201	409	124	1084	5691	59
45	82	4.4	7879	189	413	156	1121	3538	44

Tonnes per square km in top 1 m


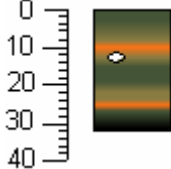

As	Cd	Fe	K	Mn	Na	P	S	Zn
27	1	2527	56	118	44	314	1282	15

Tonnes per square km above Tarawera tephra

As	Fe	Mn	P	Pb
10.1	914	35	89	

Core ID	Site Location	Grid S Grid E	Water Depth (m)	Core Length (m)
Ru 92	38 04.345S 176 16.705E	6342591.75 2797740.43	22.8	0.32

Core Stratigraphy

0-32	Stratigraphic Column	Description	Location Map
		<p>Gravity Core</p> <p>0-32cm dark olive green-black diatomaceous ooze with patches of paler green and orange. Gas void at 17 cm</p> <p>No sign of Tarawera Tephra</p>	

Concentrations (g/tonne) Aqua Regia Digestion

Depth (cm)	As	Cd	Fe	K	Mn	Na	P	S	Zn
1	91	6.6	19626	379	736		2436	7233	27
3.5	98	5.5	11263	205	220		1557	5195	23
7.5	80	4.8	9594	247	301		1162	5127	122
12.5	61	3.9	8565	134	229		685.4	5843	172
17.5	73	4.2	9226	86	142		544.9	5299	23
22.5	83	4.4	14231	151	251		540.1	9090	41
28.5	81	5.0	9938	124	204		559.3	6954	33

Tonnes per square km in top 1 m


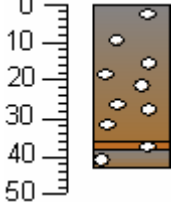

As	Cd	Fe	K	Mn	Na	P	S	Zn
25	2	3225	43	69		210	2127	14

Tonnes per square km above Tarawera tephra (at least)

As	Fe	Mn	P	Pb
8.0	1104	26	90	

Core ID	Site Location	Grid S Grid E	Water Depth (m)	Core Length (m)
Ru 93	38 04.072S	6343051.35	17.5	0.50
	176 17.542E	2798982.09		

Core Stratigraphy

0-48	Stratigraphic Column	Description	Location Map
		<p>Gravity Core</p> <p>0-36cm grey brown diatomaceous ooze with numerous gas voids</p> <p>36-38cm orange-brown diatomaceous ooze</p> <p>38-43cm laminated grey-brown diatomaceous ooze with gas voids on laminations</p> <p>43 – 47cm orange-brown diatomaceous ooze</p> <p>Gas voids at 4-5, 8,12, 17, 19, 21-22, 26, 28, 32-34, 39, 41, 43cm.</p>	

Concentrations (g/tonne) Aqua Regia Digestion

Depth (cm)	As	Cd	Fe	K	Mn	Na	P	S	Zn
1	103	5.9	21075	129	191	112	662.5	6417	42
3.5	74	4.3	17188	154	221	120	756.5	4353	30
7.5	79	4.3	16387	173	284	197	661.4	5333	65
12.5	86	4.6	14325	167	240	129	744.5	5151	58
17.5	80	4.3	14905	142	208	83.5	714.1	4232	42
22.5	89	4.9	18690	231	514	299	995.1	6332	55
27.5	91	5.2	15177	150	234	104	752.3	5127	54
35	80	4.3	14979	173	324	127	836	3758	44
41.5	67	4.0		179	303	157	787	3234	141

Tonnes per square km in top 1 m




As	Cd	Fe	K	Mn	Na	P	S	Zn
25	1	4610	53	95	42	250	1289	15

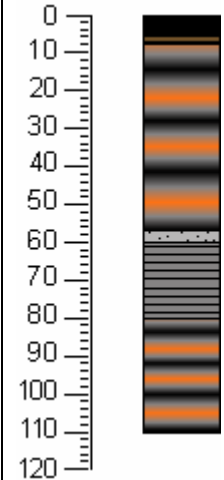

Tonnes per square km above Tarawera tephra (at least)

As	Fe	Mn	P	Pb
11.0	2007	39	105	

Core ID	Site Location	Grid S Grid E	Water Depth (m)	Core Length (m)
Ru 94	38 04.071S 176 17.545E	6343053.04 2798986.54	17.4	1.20

Core Stratigraphy

0-40	40-80	70-110
		

Stratigraphic Column	Description	Location Map
	<p>Box Core</p> <p>0-5cm black diatomaceous ooze</p> <p>5-7cm dark brown diatomaceous ooze</p> <p>7-57cm grey diatomaceous ooze with orange and black laminations</p> <p>57-60cm fine grey mud with a few sand sized grains</p> <p>60-80cm laminated grey diatomaceous ooze</p> <p>80-110cm sediment more compact but still with black and orange laminations (could have dewatered during core retrieval).</p>	

Concentrations (g/tonne) Aqua Regia Digestion

Depth (cm)	As	Cd	Fe	K	Mn	Na	P	S	Zn
25	69	3.8	15714	74	166	48.6	557.8	6029	38
35	84	4.6	20786	77	220	53.3	719.1	3981	52
45	80	4.4	15714	77	230	9.27	863.1	3107	27
55	79	4.3	12491	84	203	41.9	533.2	5260	46
65	75	4.4	10736	164	430	173	743.7	5570	73
75	66	3.8	7495	135	336	129	656.3	2822	59
85	62	3.5	8971	150	214	86.2	619.3	1676	31
95	50	2.8	9573	196	247	142	545.1	2241	50
105	70	3.7	16866	206	241	130	705	4545	28
115	41	2.4	13808	250	263	197	595	3125	24

Tonnes per square km in top 1 m


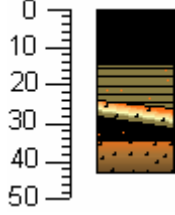

As	Cd	Fe	K	Mn	Na	P	S	Zn
19	1	3573	31	68	22	177	1119	13

Tonnes per square km above Tarawera tephra

As	Fe	Mn	P	Pb
13.0	2817	33	111	

Core ID	Site Location	Grid S Grid E	Water Depth (m)	Core Length (m)
Ru 96	38 02.646S	6345640.75	16.1	0.43
	176 18.402E	2800336.45		

Core Stratigraphy

0-43	Stratigraphic Column	Description	Location Map
		<p>Gravity Core</p> <p>0-14cm black diatomaceous ooze</p> <p>14-26cm laminated diatomaceous ooze with orange flecks</p> <p>24-30.5cm orange layer 20mm thick on an angle of 45° with dark flecks. Grades to yellow -olive green at base</p> <p>28-34cm black diatomaceous ooze with orange flecks</p> <p>34-43cm orange-brown diatomaceous ooze with dark flecks</p>	

Concentrations (g/tonne) Aqua Regia Digestion

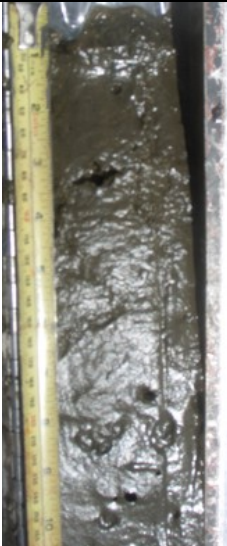

Depth (cm)	As	Cd	Fe	K	Mn	Na	P	S	Zn
1	76	5.6	15457	102	198		1526	4024	52
3.5	84	4.6	22308	290	724		1407	4921	51
7.5	74	4.2	18584	327	597		1320	5085	51
12.5	52	3.0	18584	288	350		1133	5123	60
18	49	2.9	16063	205	318		950.3	4311	60

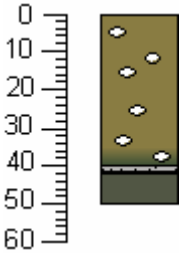

Tonnes per square km in top 1 m

As	Cd	Fe	K	Mn	Na	P	S	Zn
16	1	5096	67	107		310	1357	18

Core ID	Site Location	Grid S Grid E	Water Depth (m)	Core Length (m)
Ru 99	38 08152 S	6341744.46	7	0.5
	176 22764 E	2793252.09		

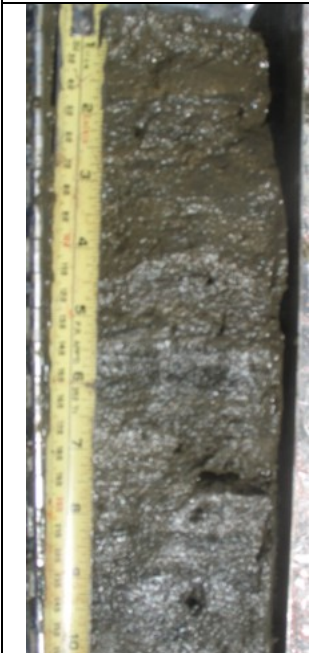

Core Stratigraphy

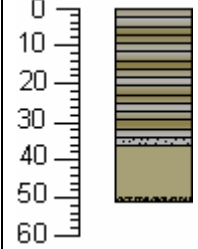

0-25	25-50
	

Stratigraphic Column	Description	Location Map
	<p>Box Core</p> <p>0-40 cm Loose olive ooze with gas voids</p> <p>40-41 cm Darker ooze(Tarawera Tephra)</p> <p>41-50 cm Darker olive grey ooze.</p> <p>More compact.</p> <p>No samples taken.</p>	

Core ID	Site Location	Grid S Grid E	Water Depth (m)	Core Length (m)
Ru 100	38 08152 S	6341744.46	7	0.51
	176 22764 E	2793252.09		



Core Stratigraphy

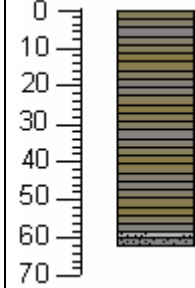
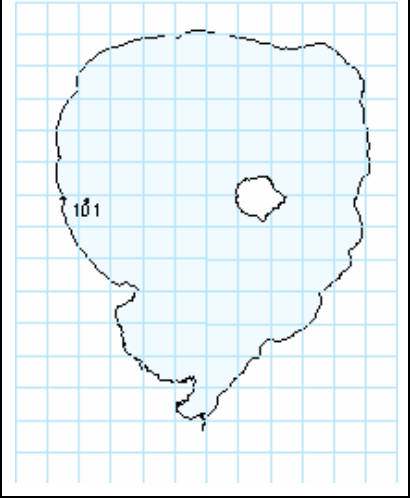
0-25	25-51
	

Stratigraphic Column	Description	Location Map
	<p>Box Core</p> <p>0-34 cm Laminated olive/grey diatomaceous ooze</p> <p>34-36 cm Dark grey silty material (Tarawera Tephra)</p> <p>36-51 cm Pale diatomaceous ooze. More compact. At 51 cm organic leaf material.</p> <p>No samples taken.</p>	

Core ID	Site Location	Grid S Grid E	Water Depth (m)	Core Length (m)
Ru 101	38 08152 S 176 22764 E	6341744.46 2793252.09	7	0.62


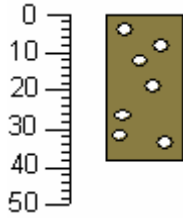

Core Stratigraphy

0-35	35-62
	

Stratigraphic Column	Description	Location Map
	<p>Box Core</p> <p>0-58 cm Laminated olive/dark grey diatomaceous ooze.</p> <p>58-60 cm Grey silt (Tarawera Tephra)</p> <p>60-62 cm Compact dark grey silty material.</p> <p>No samples taken.</p>	

Core ID	Site Location	Grid S Grid E	Water Depth (m)	Core Length (m)
Ru 102	38 08152 S 176 22764 E	6341744.46 2793252.09	7	0.38

Core Stratigraphy


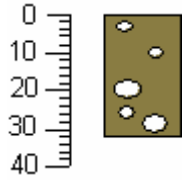
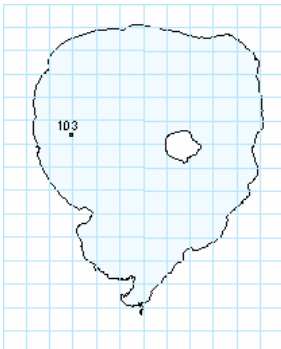
0-38 cm	Stratigraphic Column	Description	Location Map
		Gravity Core 0-38 cm Olive diatomaceous ooze with gas voids.	

Concentrations (g/tonne)

Depth (cm)	As	Fe	Mn	P	Pb
0-2	65.86	7776.44	486.25	813.66	12.86
2-4	94.41	9107.32	355.96	542.91	5.35
4-6	49.54	6628.97	380.65	925.70	6.63
6-8	47.70	6944.10	389.81	883.24	7.67
8-10	44.67	6939.59	450.42	1185.62	8.48
10-12	42.32	6012.32	396.30	998.75	6.80
12-14	41.97	5833.37	409.32	972.18	7.21
14-16	45.62	6605.34	411.16	924.21	8.42
16-18	57.96	8051.63	404.09	854.27	9.37
18-20	-	-	-	-	-
20-22	47.28	7049.56	458.24	845.60	12.63
22-24	52.47	7385.57	486.08	833.52	12.93

Core ID	Site Location	Grid S Grid E	Water Depth (m)	Core Length (m)
Ru 103	38 07578 S 176 23499 E	6342357.67 2793919.50	11.5	0.32

Core Stratigraphy


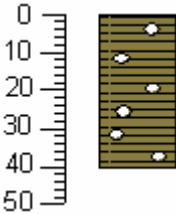

0-32 cm	Stratigraphic Column	Description	Location Map
		<p>Gravity Core</p> <p>0-32 cm Laminated olive diatomaceous ooze with gas voids. Large gas voids at 20 cm and 28 cm.</p> <p>Retained core top.</p>	

Concentrations (g/tonne)

Depth (cm)	As	Fe	Mn	P	Pb
0-2	-	-	-	-	-
2-4	72.81	7458.74	435.79	1322.84	7.62
4-6	66.60	7431.11	408.23	1067.14	7.99
6-8	54.08	7334.08	506.89	1104.37	9.20
8-10	47.60	6285.32	495.22	1014.79	7.28
10-12	64.47	6106.59	479.60	800.88	9.12
12-14	49.46	5956.29	482.58	963.59	8.32
14-16	50.87	5378.77	475.65	853.97	10.26
16-18	62.30	6769.22	463.99	1105.75	10.94
18-20	47.85	5174.66	389.67	890.27	11.74
20-22	63.21	6865.15	398.33	892.67	12.19
22-24	65.19	6502.08	409.58	1030.21	14.88
24-26	-	-	-	-	-
26-28	52.42	5093.00	378.65	854.50	15.31
28-30	46.15	4619.67	372.84	879.33	16.00

Core ID	Site Location	Grid S Grid E	Water Depth (m)	Core Length (m)
Ru 104	38 0751 S 176 2464 E	6342396.76 2794922.57	12.5	0.40

Core Stratigraphy


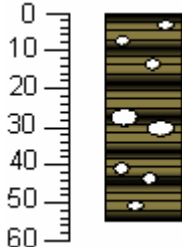
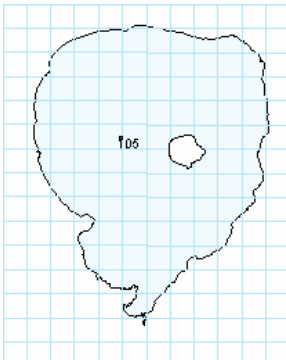
0-40 cm	Stratigraphic Column	Description	Location Map
		Gravity Core 0-40 cm Laminated olive diatomaceous ooze with gas voids. Core top retained.	

Concentrations (g/tonne)

Depth (cm)	As	Fe	Mn	P	Pb
0-2	67.30	6003.05	319.41	1185.18	90.47
2-4	43.79	5345.70	377.09	887.38	7.87
4-6	48.24	5400.43	419.62	899.14	7.90
6-8	40.28	4615.63	398.92	971.03	8.85
8-10	-	-	-	-	-
10-12	33.34	3691.06	334.81	823.89	6.70
12-14	47.20	4999.19	425.58	885.82	8.29
14-16	43.18	4715.66	388.21	903.85	8.98
16-18	41.41	4571.39	386.14	827.53	9.98
18-20	47.18	5540.45	380.37	757.17	11.18

Core ID	Site Location	Grid S Grid E	Water Depth (m)	Core Length (m)
Ru 105	38 07462 S 176 25782 E	6342413.51 2795925.72	15.5	0.55

Core Stratigraphy


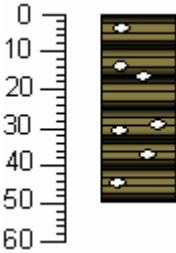
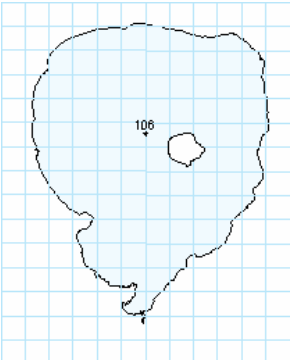
0-55 cm	Stratigraphic Column	Description	Location Map
		<p>Gravity Core</p> <p>0-55 cm Laminated olive and black diatomaceous ooze with large gas voids, particularly around the 30 cm range.</p> <p>Core top retained.</p>	

Concentrations (g/tonne)

Depth (cm)	As	Fe	Mn	P	Pb
0-2	56.60	6022.46	402.08	1144.03	7.51
2-4	60.25	6172.84	408.15	890.94	7.31
4-6	55.43	6544.43	399.24	992.68	7.22
6-8	52.45	5656.95	382.14	896.06	6.87
8-10	46.82	4041.14	324.11	633.91	6.43
10-12	69.52	6716.34	392.82	962.18	8.87
12-14	57.70	5624.10	343.05	706.69	9.01
14-16	38.65	4272.50	331.39	633.32	9.10
16-18	51.20	6210.81	373.15	760.71	11.61
18-20	51.62	5833.94	352.21	713.99	11.44

Core ID	Site Location	Grid S Grid E	Water Depth (m)	Core Length (m)
Ru 106	38 07325 S 176 72010 E	6342526.07 2797007.89	21.4	0.50

Core Stratigraphy


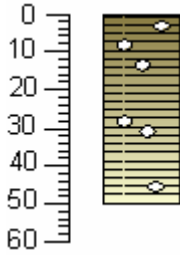
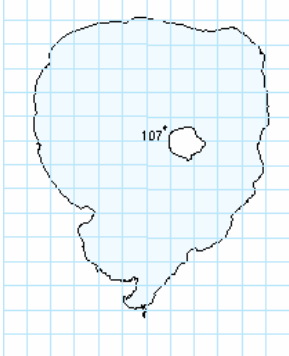
0-50 cm	Stratigraphic Column	Description	Location Map
		<p>Gravity Core</p> <p>0-50 cm Laminated olive and black diatomaceous ooze with gas voids.</p> <p>Core top retained.</p>	

Concentrations (g/tonne)

Depth (cm)	As	Fe	Mn	P	Pb
0-2	96.00	9069.31	498.35	1159.61	6.85
2-4	84.08	8202.01	533.18	958.44	8.89
4-6	62.31	7128.92	441.30	819.31	7.24
6-8	70.22	7218.57	424.52	834.52	7.12
8-10	63.27	6436.39	401.40	840.71	6.62
10-12	68.45	6639.42	436.10	886.67	8.07
12-14	67.64	6860.11	479.12	808.01	9.50
14-16	59.96	6307.35	379.18	677.95	9.13
16-18	103.03	8605.34	386.69	662.71	10.75
18-20	77.85	8224.62	489.64	902.95	12.19

Core ID	Site Location	Grid S Grid E	Water Depth (m)	Core Length (m)
Ru 107	38 07256 S 176 27891 E	6342574.26 2797783.10	22.7	0.50

Core Stratigraphy


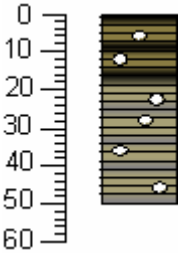

0-50 cm	Stratigraphic Column	Description	Location Map
		<p>Gravity Core</p> <p>0-50 cm Laminated olive diatomaceous ooze with gas voids. Becomes pale yellow at 20 cm deep.</p> <p>Core top retained.</p>	

Concentrations (g/tonne)

Depth (cm)	As	Fe	Mn	P	Pb
0-2	83.79	8570.33	527.89	1049.07	8.63
2-4	95.42	9582.82	532.05	859.95	7.71
4-6	102.56	12255.31	525.44	916.35	7.70
6-8	63.66	7595.61	543.68	837.67	8.53
8-10	60.67	5371.89	408.49	550.93	6.66
10-12	64.18	8536.83	457.83	635.29	8.91
12-14	73.82	10165.32	430.34	692.78	11.52
14-16	57.62	7159.36	502.37	702.58	10.96
16-18	78.18	7900.39	504.13	781.14	13.68
18-20	75.21	8000.98	623.81	1105.33	16.46

Core ID	Site Location	Grid S Grid E	Water Depth (m)	Core Length (m)
Ru 108	38 0719 S 176 2893 E	6342613.95 2798696.73	14.5	0.50

Core Stratigraphy


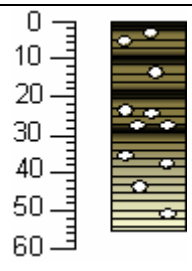

0-50 cm	Stratigraphic Column	Description	Location Map
		<p>Gravity Core</p> <p>0-50 cm Laminated olive and black diatomaceous ooze.</p> <p>Becomes paler at 20 cm deep.</p> <p>Tarawera Tephra at bottom of core.</p> <p>Core top retained.</p>	

Concentrations (g/tonne)

Depth (cm)	As	Fe	Mn	P	Pb
0-2	79.47	8789.75	328.12	1332.57	7.72
2-4	77.98	9090.25	472.31	1291.12	6.79
4-6	74.15	10072.60	466.46	996.84	6.29
6-8	77.32	10152.39	457.90	1016.03	5.84
8-10	64.84	9270.59	453.87	906.10	6.41
10-12	74.06	9536.44	406.55	893.37	6.68
12-14	61.74	7675.36	405.03	843.60	5.63
14-16	68.85	7753.30	486.52	1000.93	7.24
16-18	78.51	8123.88	465.58	885.10	7.97
18-20	69.77	7788.97	389.99	824.07	6.31

Core ID	Site Location	Grid S Grid E	Water Depth (m)	Core Length (m)
Ru 109	38 07202 S	6342565.21	13.8	0.55
	176 30025 E	2799656.26		

Core Stratigraphy


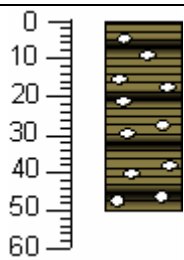

0-55 cm	Stratigraphic Column	Description	Location Map
		<p>Gravity Core</p> <p>0-55 cm Laminated olive and black diatomaceous ooze with many gas voids. Gas voids increase between 25-30 cm. Lighter colour at bottom of core.</p> <p>Core top retained.</p>	

Concentrations (g/tonne)

Depth (cm)	As	Fe	Mn	P	Pb
0-4	48.06	6206.07	334.01	1009.78	5.16
4-6	54.74	6505.51	336.33	894.10	6.97
6-8	71.60	7651.94	443.68	911.90	11.59
8-10	59.07	6855.21	427.83	899.80	11.40
10-12	41.87	5715.10	331.13	776.70	8.09
12-14	52.50	8386.35	337.34	782.07	8.79
14-16	51.59	6185.40	324.37	688.66	10.25
16-18	51.45	5835.08	260.64	617.05	8.99
19-20	56.21	5624.31	328.08	671.39	8.99

Core ID	Site Location	Grid S Grid E	Water Depth (m)	Core Length (m)
Ru 110	38 07123 S	6342619.82	12.4	0.50
	176 31042 E	2800551.15		

Core Stratigraphy


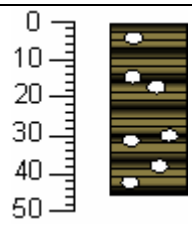

0-50 cm	Stratigraphic Column	Description	Location Map
		<p>Gravity Core</p> <p>0-50 cm Olive and black diatomaceous ooze, not as laminated as previous cores.</p> <p>Lots of gas voids, one gas bubble released which may have caused disturbance.</p> <p>Core top retained.</p>	

Concentrations (g/tonne)

Depth (cm)	As	Fe	Mn	P	Pb
0-2	30.42	5662.04	309.07	1323.26	6.75
2-4	80.98	7697.91	327.31	1083.85	6.83
4-6	40.65	6205.92	348.16	884.38	6.77
6-8	52.14	6448.90	382.59	829.93	6.44
8-10	61.50	8106.15	338.49	874.73	5.94
10-12	58.18	6975.07	381.06	803.18	8.58
12-14	53.60	7040.93	355.45	866.71	7.18
14-16	35.73	5450.81	297.33	702.84	7.04
16-18	44.70	6906.83	297.54	586.56	7.85
18-20	51.77	6600.74	323.81	556.58	11.90

Core ID	Site Location	Grid S Grid E	Water Depth (m)	Core Length (m)
Ru 111	38 07318 S 176 27041 E	6342532.84 2797035.36	21.7	0.45

Core Stratigraphy

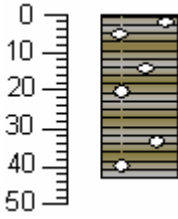

0-45 cm	Stratigraphic Column	Description	Location Map
		<p>Gravity Core</p> <p>0-45 cm Laminated olive and black diatomaceous ooze with gas voids.</p> <p>Core top retained.</p>	

Concentrations (g/tonne)

Depth (cm)	As	Fe	Mn	P	Pb
0-2	74.67	8542.58	463.50	814.74	7.11
2-4	67.33	6535.73	468.95	917.35	9.03
4-6	83.42	7609.00	502.57	825.59	8.61
6-8	71.62	6349.18	355.39	753.46	6.43
8-10	67.48	6004.92	344.06	702.74	5.96
10-15	52.95	5007.47	387.85	645.02	8.99
15-18	58.32	6133.36	358.26	673.63	6.40
18-20	83.14	7823.77	393.29	790.60	9.76
20-25	72.87	7222.47	493.92	989.66	10.21
25-30	71.21	7047.17	475.73	969.30	9.86
30-35	62.40	6163.24	451.85	863.24	9.01
35-40	97.88	8831.35	573.10	1075.96	11.54
40-45	90.60	7292.78	547.56	1007.69	9.57

Core ID	Site Location	Grid S Grid E	Water Depth (m)	Core Length (m)
Ru 112	38 06692 S 176 29616 E	6343144.07 2799318.56	16.4	0.43

Core Stratigraphy







Stratigraphic Column	Description	Location Map
	<p>Gravity Core</p> <p>0-43 cm Laminated olive and grey diatomaceous ooze. 1-2 cm thick laminations. Gas present.</p>	

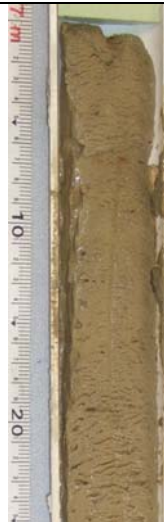





Concentrations (g/tonne)

Depth (cm)	As	Fe	Mn	P	Pb
0-2	61.19	6962.44	364.18	969.82	5.86
2-4	78.41	7924.59	395.88	992.08	5.49
4-6	79.40	9757.45	365.49	907.39	5.38
6-8	52.23	5330.31	324.25	788.91	4.83
8-10	60.93	6043.34	398.26	990.56	6.71
10-12	82.79	7504.75	420.35	912.55	8.81
12-14	55.20	6091.58	405.94	993.03	6.40
14-16	50.53	5090.89	384.21	807.64	6.05
16-18	60.48	7948.63	377.74	826.92	7.79
18-20	65.19	6561.81	337.87	804.89	7.45
20-25	65.96	6249.14	302.17	719.86	6.94
25-30	60.38	6086.84	338.74	759.50	10.40
35-40	75.83	6687.33	404.58	956.50	15.62
40-43	55.42	5762.15	362.64	998.97	7.47

Core ID	Site Location	Grid S Grid E	Water Depth (m)	Core Length (m)
Ru 113	38 04433 S 176 16178 E	6342457.33 S 2796964.41 E	21	1.10

Core Stratigraphy

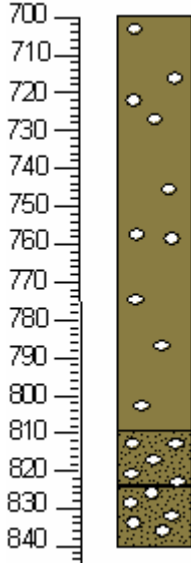
Thrust 2 300-330	330-350	342-355	355-370	370-390	390-410
					

Thrust 3 700-725	725-752	752-775	775-800	800-820	820-842
					

Stratigraphic Column	Description	Location Map
<p>Thrust 2</p>	<p>Piston Core</p> <p>Thrust 1</p> <p>Core lost 3m of penetration.</p> <p>Thrust 2</p> <p>300-306 cm Course grey pumice (Kaharoa Tephra). Large pumice clasts (5-10 mm diameter)</p> <p>306-309 cm Silty olive green/brown diatomaceous ooze.</p> <p>309-316 cm Laminated green/black diatomaceous ooze. Layering slightly dragged probably as a result of coring. Gas present.</p> <p>316-325 cm Unknown Tephra layer. Course grey ash grading to sand to very fine sand at 323 cm.</p> <p>325-330 cm Laminated olive green diatomaceous ooze.</p> <p>330-337 cm Olive green diatomaceous ooze with black oxidation throughout.</p> <p>337-341 cm Light grey mud.</p> <p>341-344 cm Unknown Tephra layer. Dark grey fine sand, grading downwards.</p> <p>344-350 cm Slightly courser white sandy, densely packed layer. Possibly pulverised pumice.</p> <p>350-410 cm Dark olive green diatomaceous ooze grading down to olive green. Very gaseous.</p>	

Concentrations Thrust 2 (g/tonne)

Depth (cm)	As	Fe	Mn	P	Pb
300-306	79.54	3426.40	73.49	587.05	1.62
306-309	318.06	23897.12	257.76	6512.07	4.44
309-316	183.44	7450.62	188.40	1384.90	2.29
316-325	178.36	6319.70	115.65	1129.58	2.07
325-330	198.44	8491.77	140.35	1385.89	2.24
330-337	153.57	8138.18	172.17	1270.43	2.39
337-341	44.39	6009.77	124.01	708.34	1.91
341-344	7.86	9327.16	203.80	171.00	2.04
344-350	21.20	4224.58	136.47	174.49	1.28
350-360	102.42	4178.07	181.77	162.17	2.13
360-370	134.66	4842.16	246.46	172.47	3.80
370-380	87.56	4446.46	221.57	162.52	2.21
380-390	98.22	4712.78	251.25	176.23	2.46
390-400	80.56	5062.33	267.91	197.22	2.73
400-410	72.39	4847.98	245.02	196.32	2.67

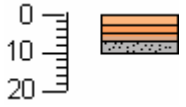

Stratigraphic Column	Description
<p>Thrust 3</p> 	<p>Core taken at approximately 7m depth.</p> <p>Photos not taken at time of sampling</p> <p>700-752 cm Massive olive diatomaceous ooze. Gas present. No tephra present.</p> <p>752-810 cm Continues massive olive diatomaceous ooze. Gas present.</p> <p>810-824 cm Olive diatomaceous ooze becomes silty with 1mm size pumice grains.</p> <p>Higher gas content than previous layers.</p> <p>824-824.5 cm Black pumice 5-6 mm thick (Unknown Tephra).</p> <p>824.5-842 cm Silty olive diatomaceous. High gas content.</p>

Concentrations Thrust 3 (g/tonne)

Depth (cm)	As	Fe	Mn	P	Pb
700-710	49.46	4342.55	205.16	186.16	5.38
710-720	47.30	4261.74	192.25	198.64	2.94
720-730	39.10	3808.18	182.57	200.88	3.19
730-740	38.78	3651.18	179.87	307.78	2.83
740-750	35.43	3215.05	151.79	190.93	2.40
750-760	44.08	3676.85	168.83	311.13	2.19
760-770	42.22	3332.67	146.98	220.50	2.20
770-780	39.95	3650.31	175.64	219.53	2.70
780-790	46.71	4165.79	194.12	186.78	2.73
790-800	53.24	4167.19	183.02	164.10	2.42
800-810	52.27	4597.47	207.20	174.50	2.57
810-820	36.91	6063.75	344.56	382.74	3.04
820-830	28.36	5929.29	365.60	346.66	2.97
830-842	29.19	6061.18	364.46	362.96	3.07

Core ID	Site Location	Grid S Grid E	Water Depth (m)	Core Length (m)
Ru 114	38 09706 S	6339804.23	11.9	0.1
	176 29528 E	2799118.00		

Core Stratigraphy

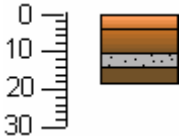

Stratigraphic Column	Description	Location Map
	<p>Gravity Core</p> <p>0-3 cm Loose orange diatomaceous ooze</p> <p>3 cm 1mm thick black band</p> <p>3-5 cm Darker orange diatomaceous ooze</p> <p>5-7 cm Gradation towards grey silt</p> <p>7-10 cm Grey silt (Tarawera Tephra)</p>	

Concentrations (g/tonne)

Depth (cm)	As	Fe	Mn	P	Pb
0	77.33	12943.63	1313.19	2937.35	10.38
0-2	40.77	7139.64	445.33	1318.83	6.21
2-4	124.32	16408.94	607.66	833.38	8.47
4-6	70.13	9646.92	620.41	481.14	5.26
6-8	61.76	12613.32	590.06	488.96	5.85

Core ID	Site Location	Grid S Grid E	Water Depth (m)	Core Length (m)
Ru 115	38 09507 S 176 28455 E	6340059.59 2798185.70	9.7	0.18

Core Stratigraphy

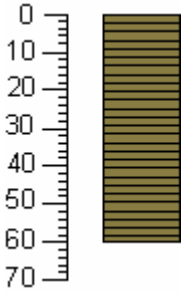

Stratigraphic Column	Description	Location Map
	<p>Gravity Core</p> <p>0-4 cm Loose orangey/brown diatomaceous ooze. Irregular black line at 4 cm.</p> <p>4-10 cm Diatomaceous ooze becomes darker brown and more compact.</p> <p>10-14 cm Irregular dark grey sand (Tarawera tephra).</p> <p>14-18 cm Dark brown diatomaceous ooze.</p>	

Concentrations (g/tonne)

Depth (cm)	As	Fe	Mn	P	Pb
0	98.30	15254.99	1788.80	3565.74	8.72
0-2	54.47	9137.28	550.47	1573.11	5.81
2-4	63.44	9163.33	432.90	1161.08	6.34
4-6	94.91	15135.10	485.21	688.14	8.67
6-8	121.25	17300.34	817.54	531.03	7.59
8-10	84.78	13134.00	402.39	375.45	3.92
10-12	60.49	9999.70	305.81	257.83	2.31
12-14	94.75	10548.80	211.52	306.90	1.92
14-16	95.58	11539.80	298.11	301.00	1.81
16-18	85.95	9632.94	331.76	251.11	1.74

Core ID	Site Location	Grid S Grid E	Water Depth (m)	Core Length (m)
Ru 116	38 09324 S	6340302.04	21	0.6
	176 29528 E	2797118.11		

Core Stratigraphy

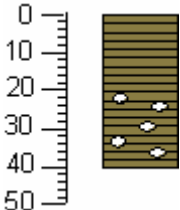

Stratigraphic Column	Description	Location Map
	<p>Gravity Core</p> <p>0-60 cm Laminated olive and black diatomaceous ooze.</p> <p>Core top might not be included.</p>	

Concentrations (g/tonne)

Depth (cm)	As	Fe	Mn	P	Pb
0-2	57.37	6851.53	447.46	870.25	7.74
2-4	58.53	5716.19	362.09	715.74	8.13
4-6	63.75	7105.75	421.79	862.43	8.74
6-8	72.84	7668.40	466.16	1039.21	10.10
8-10	67.28	6817.67	394.27	857.34	9.38
10-12	56.00	6048.67	367.23	719.19	8.96
12-14	41.60	4802.88	340.72	587.71	8.44
14-16	42.82	4485.13	311.45	509.41	8.18
16-18	54.16	6029.44	366.26	591.71	9.36
18-20	57.80	5816.77	345.69	601.28	9.16
20-22	39.64	4117.45	244.03	441.95	7.31
22-24	38.75	4132.40	304.88	516.41	7.72
24-26	49.74	5444.55	340.40	584.79	9.31
26-28	36.20	3722.58	244.36	407.77	7.83
28-30	39.80	4239.58	256.75	426.45	8.73
30-32	42.55	4712.60	346.04	584.54	11.05
32-34	45.31	4798.95	317.91	586.13	10.77
34-36	45.47	4964.28	341.41	656.50	10.72
36-38	41.46	5316.83	404.28	698.82	12.36
38-40	25.17	3757.82	304.46	470.43	9.30
40-42	43.45	4396.81	288.80	547.27	10.46
42-44	70.50	5656.45	257.10	632.75	9.85
44-46	86.06	7571.56	413.93	847.12	13.24

Core ID	Site Location	Grid S Grid E	Water Depth (m)	Core Length (m)
Ru 117	38 09324 S 176 29528 E	6340302.04 2797118.11	21	0.4

Core Stratigraphy

Stratigraphic Column	Description	Location Map
	<p>Gravity Core</p> <p>0-40 cm Laminated olive and black diatomaceous ooze.</p> <p>Gas present below 20 cm.</p>	

Concentrations (g/tonne)

Depth (cm)	As	Fe	Mn	P	Pb
0-2	89.78	10291.63	473.94	1167.87	6.64
2-4	51.79	7266.15	426.38	1145.23	8.91
4-6	44.13	4952.16	263.73	641.06	5.08
6-8	58.19	8414.74	445.32	930.52	7.82
8-10	48.24	7214.88	485.08	744.66	6.52
10-12	68.67	8966.31	412.27	732.91	7.34
12-14	57.09	6469.18	499.00	913.83	10.73
14-16	61.90	5478.56	405.35	796.93	7.42
16-18	66.72	6388.69	382.26	789.11	8.48
18-20	59.38	6014.85	402.26	883.22	8.14
20-22	51.67	5909.29	391.11	890.39	9.68
22-24	41.65	5069.15	381.54	782.02	9.72
24-26	34.91	3721.49	328.46	653.14	8.00
26-28	46.80	5000.02	324.93	581.95	9.12
28-30	44.74	5911.30	321.77	638.31	10.18
30-32	45.68	5447.88	334.44	689.51	10.34
32-34	64.38	6837.80	393.17	780.07	11.86
34-36	53.03	5789.75	390.16	725.32	11.00
36-38	71.06	6615.30	360.76	675.65	12.43
38-40	43.52	4891.39	363.55	660.67	13.92

Core ID	Site Location	Grid S Grid E	Water Depth (m)	Core Length (m)
Ru 118	38 09162 S	6339804.23	17.6	0.36
	176 26004 E	2799118.00		

Core Stratigraphy

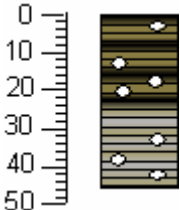

Stratigraphic Column	Description	Location Map
	<p>Gravity Core</p> <p>0-2 cm Loose orange diatomaceous ooze, gas present.</p> <p>2-4 cm Black diatomaceous ooze, gas present.</p> <p>4-36 cm Laminated black, pale olive, green diatomaceous ooze, 1-2 cm thick, gas present.</p>	

Concentrations (g/tonne)

Depth (cm)	As	Fe	Mn	P	Pb
0	34.36	5581.48	379.78	1902.81	7.24
0-2	45.28	4884.73	298.62	1274.63	5.23
2-4	66.17	6726.83	300.05	784.63	6.58
4-6	42.66	5080.48	344.32	706.99	7.24
6-8	58.19	6979.88	372.50	684.82	8.16
8-10	43.71	5430.08	332.89	623.44	7.34
10-12	41.31	3956.32	274.87	542.57	6.34
12-14	61.58	6678.09	355.18	724.10	9.31
14-16	41.85	5182.89	342.32	626.57	8.88
16-18	32.93	4112.93	298.25	515.42	9.30
18-20	46.15	5559.19	314.03	551.63	10.08
20-22	51.85	6077.27	331.20	600.73	11.91
22-24	51.83	5328.54	332.91	569.97	12.23
24-26	51.27	5614.60	382.15	632.82	15.37
26-28	46.89	5213.62	383.73	691.29	14.39
28-30	55.77	5224.82	349.61	626.63	14.57
30-32	73.09	6316.21	388.65	735.99	13.43
32-34	59.16	5496.14	355.66	687.09	12.79
34-36	65.29	5617.26	328.29	534.01	10.64

Core ID	Site Location	Grid S Grid E	Water Depth (m)	Core Length (m)
Ru 119	38 08863 S 176 24895 E	6340888.05 2795091.48	12.3	0.46

Core Stratigraphy

Stratigraphic Column	Description	Location Map
	<p>Gravity Core</p> <p>0-46 cm Laminated olive and black diatomaceous ooze becoming lighter at bottom of the core. 1 cm thick laminations.</p> <p>Gas present through core.</p>	

Concentrations (g/tonne)

Depth (cm)	As	Fe	Mn	P	Pb
0-4	48.33	4991.54	320.73	682.50	8.57
4-6	56.51	6021.02	332.86	637.66	8.71
6-8	40.87	4650.25	372.18	667.64	9.08
8-10	36.97	4369.64	296.68	552.06	7.56
10-12	35.70	4195.73	255.46	454.45	7.99
12-14	43.00	5123.96	286.12	471.74	9.65
14-16	44.72	5489.11	233.39	450.85	9.63
16-18	45.09	4702.84	312.11	547.99	12.61
18-20	31.52	3100.12	234.67	381.80	10.86
20-22	45.75	4908.18	337.34	582.56	17.66
22-24	34.07	3652.68	263.68	494.16	14.20
24-26	30.23	3245.41	281.42	493.34	12.29
26-28	61.39	5382.56	363.23	708.06	15.06
28-30	43.29	4256.90	306.55	511.80	12.32
28-30	63.75	5200.78	335.39	639.12	12.93
30-32	37.06	4032.07	334.79	501.92	8.84
32-34	38.18	4021.08	322.02	658.98	8.24
34-36	34.13	3385.20	296.42	496.70	6.61
36-38	21.11	2794.69	250.70	450.78	4.77
38-40	46.08	5318.99	282.40	591.39	5.94
40-42	49.64	4649.97	265.82	529.12	4.94
42-44	48.33	4991.54	320.73	682.50	8.57

Core ID	Site Location	Grid S Grid E	Water Depth (m)	Core Length (m)
Ru 120	38 05705 S	6344424.18	10.2	0.3
	176 23838 E	2794292.12		

Core Stratigraphy

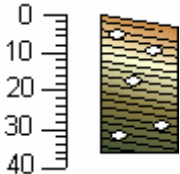

Stratigraphic Column	Description	Location Map
	<p>Gravity Core</p> <p>0-2 cm Very loose flaky dark olive green diatomaceous ooze</p> <p>2-3 cm Finer pale yellow diatomaceous ooze</p> <p>3-5 cm Loose flaky dark olive green diatomaceous ooze.</p> <p>5-7 cm Finer pale yellow diatomaceous ooze</p> <p>7-13 cm Laminated mid-olive green to yellow brown.</p> <p>13-23 cm Massive fine grained pale olive diatomaceous ooze</p> <p>23-29 cm Similar to above, yellow in colour, gritty at bottom. Up to 1 cm clasts (Kaharoa Tephra).</p>	

Concentrations (g/tonne)

Depth (cm)	As	Fe	Mn	P	Pb
0-2	29.00	4505.10	316.23	1431.92	13.44
2-4	32.88	4462.26	294.76	815.05	9.92
4-6	35.21	4695.30	342.97	568.95	9.76
6-8	43.23	5754.95	358.77	526.65	8.30
8-10	48.51	5883.11	383.30	468.93	9.91
10-12	86.39	11083.14	284.20	418.92	12.05
12-14	73.27	9125.33	296.32	386.66	9.79
14-16	87.37	9916.26	295.29	348.50	7.18
16-18	143.79	14765.27	465.71	232.81	3.56
18-20	118.49	12714.71	180.61	186.57	2.48
20-22	146.05	15738.88	252.36	233.80	3.24
22-24	83.56	8415.59	125.22	138.34	1.70
24-26	72.25	7418.13	109.79	118.73	1.57
26-28	40.55	3964.32	57.64	66.93	0.98

Core ID	Site Location	Grid S Grid E	Water Depth (m)	Core Length (m)
Ru 121	38 05886 S 176 24683 E	6344196.52 2795025.82	11.9	0.36

Core Stratigraphy

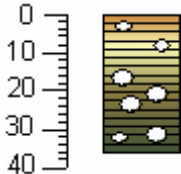

Stratigraphic Column	Description	Location Map
	<p>Gravity Core</p> <p>Core on 30° angle</p> <p>0-36 cm Laminated brown and yellow to olive green, dark olive green diatomaceous ooze, 1 cm thick.</p> <p>Gas present throughout core.</p>	

Concentrations (g/tonne)

Depth (cm)	As	Fe	Mn	P	Pb
0-2	29.90	3750.08	300.71	1160.40	6.27
2-4	32.63	3608.09	223.27	759.51	6.47
4-6	40.61	4514.75	312.61	756.59	8.51
6-8	28.01	3150.17	248.42	508.23	6.13
8-10	69.41	6335.08	425.21	750.44	6.92
10-12	59.67	6696.42	473.33	893.44	7.44
12-14	97.62	10137.53	472.96	1210.79	8.63
14-16	95.52	8524.35	375.85	1345.45	5.31
16-18	45.96	5345.11	367.06	1391.49	4.97
18-20	30.78	3656.59	215.17	944.64	3.30
20-22	41.12	4022.41	332.31	549.90	14.27
22-24	48.19	4898.22	339.67	583.81	16.63
24-26	60.81	5914.41	336.54	584.86	17.30
26-28	49.11	4535.78	350.57	571.10	14.76
28-30	67.68	6941.07	390.41	611.19	12.51
30-32	73.99	7036.54	346.76	633.01	13.62
32-34	54.21	6121.98	332.49	591.46	10.87
34-36	30.86	3377.18	305.62	511.14	11.50
36-38	45.66	5058.31	355.50	661.32	9.36
38-40	61.56	6383.15	378.13	771.63	9.73
40-42	42.32	4027.50	356.49	637.68	7.56

Core ID	Site Location	Grid S Grid E	Water Depth (m)	Core Length (m)
Ru 122	38 06079 S 176 25546 E	6343954.90 2795774.78	13.4	0.36

Core Stratigraphy

Stratigraphic Column	Description	Location Map
	<p>Gravity Core</p> <p>0-36 cm Laminated brown and yellow to dark olive green diatomaceous ooze, 1-3 cm thick.</p> <p>Gas present, major gas at 17, 21, 25 and 32 cm.</p> <p>Core becoming more compact with depth.</p>	

Concentrations (g/tonne)

Depth (cm)	As	Fe	Mn	P	Pb
0-2	44.24	4944.39	393.76	709.08	7.42
2-4	57.93	6411.11	444.22	817.60	8.37
4-6	68.39	6777.63	315.71	810.92	7.21
6-8	55.09	4849.75	251.80	893.57	7.91
8-10	32.27	4240.70	322.38	1738.07	4.93
10-12	5.17	701.30	49.51	306.48	1.25
12-14	56.26	4279.08	248.88	486.09	11.76
14-16	42.38	3853.85	284.97	484.32	13.79
16-18	38.07	3782.63	303.29	521.11	16.97
18-20	41.18	4072.24	286.62	486.07	15.90
20-22	44.38	4143.53	256.60	448.91	15.30
22-24	45.40	4200.11	264.99	476.64	15.55
24-26	48.35	5563.18	256.41	482.95	12.81
26-28	50.57	5862.98	241.08	444.87	10.84
28-30	34.61	4452.12	235.58	396.21	8.99
30-32	31.16	3712.82	248.64	481.80	7.86
32-34	30.83	3618.42	248.82	463.13	7.75

Core ID	Site Location	Grid S Grid E	Water Depth (m)	Core Length (m)
Ru 123	38 06245 S 176 26501 E	6343740.20 2796605.46	15.9	0.34

Core Stratigraphy

Stratigraphic Column	Description	Location Map
	<p>Gravity Core</p> <p>0-1 cm Very loose flaky yellow grey diatomaceous ooze.</p> <p>1-2 cm Yellow diatomaceous ooze, more compact</p> <p>2-8 cm Laminated, very dark diatomaceous ooze, lots of gas</p> <p>8-28 cm Laminated black to dark olive green to mid-yellow. Paler towards the base.</p> <p>28-34 cm Fine grained, faint 1 cm thick laminations pale olive to yellow.</p>	

Concentrations (g/tonne)

Depth (cm)	As	Fe	Mn	P	Pb
0-2	31.29	3188.27	293.64	536.97	6.99
2-4	45.56	5893.75	307.53	615.93	7.74
4-6	33.79	4294.66	271.22	607.13	6.99
6-8	31.60	4204.92	281.44	823.57	6.64
8-10	34.10	5259.32	468.61	1814.62	5.90
10-12	1.97	338.36	44.71	153.74	0.49
12-14	62.17	6395.84	325.64	519.48	8.32
14-16	47.74	4702.26	404.46	520.66	9.85
16-18	51.90	4643.69	335.34	529.77	13.07
18-20	61.41	5947.61	350.15	643.01	15.62
20-22	45.61	4404.76	363.47	555.13	13.68
22-24	48.38	4760.66	413.40	569.20	17.26
24-26	47.61	4569.46	303.40	472.05	14.15
26-28	53.07	5265.25	361.88	541.53	17.32
28-30	39.73	4082.94	325.24	498.20	14.24
30-32	44.64	5180.66	341.65	577.62	12.95
32-34	72.79	7779.45	342.63	626.75	13.39

Core ID	Site Location	Grid S Grid E	Water Depth (m)	Core Length (m)
Ru 124	38 06603 S 176 27568 E	6343308.88 2797526.50	20.4	0.36

Core Stratigraphy

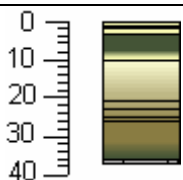

Stratigraphic Column	Description	Location Map
	<p>Gravity Core</p> <p>1-10 cm Disturbed by gas release. Very loose flaky material.</p> <p>0-4 cm orange to yellow to black flaky diatomaceous ooze</p> <p>4-8 cm Very dark laminated material, gas present.</p> <p>8-20 cm Laminated black to mid-olive green to pale yellow diatomaceous ooze.</p> <p>Full of gas. Denser as depth increases.</p> <p>20-36 cm Laminated to mid-olive green diatomaceous ooze. 2 cm thick lamination.</p> <p>Lots of gas.</p>	

Concentrations (g/tonne)

Depth (cm)	As	Fe	Mn	P	Pb
0-2	89.59	11252.54	579.66	964.40	19.19
2-4	39.75	4791.00	328.12	538.56	10.74
4-6	33.08	4069.85	300.14	540.77	8.53
6-8	30.96	3609.28	290.98	549.52	7.34
8-10	39.52	4411.47	327.29	605.85	7.59
10-12	40.33	4569.95	328.60	657.69	7.09
12-14	91.29	11276.17	356.22	712.59	6.80
14-16	49.13	5598.67	400.39	737.42	7.77
16-18	57.60	5656.06	384.22	733.50	8.40
18-20	71.36	6475.05	383.37	695.55	6.94
20-22	48.58	5005.19	371.61	653.85	8.34
22-24	56.04	5519.26	343.09	598.99	9.06
24-26	65.59	8052.74	330.74	569.06	9.92
26-28	72.23	7405.80	410.90	640.83	11.29
28-30	58.52	6172.91	365.15	603.98	12.60
30-32	66.26	6572.72	313.81	537.97	15.11
32-34	55.18	5497.98	318.08	548.57	14.25

Core ID	Site Location	Grid S Grid E	Water Depth (m)	Core Length (m)
Ru 125	38 06850 S 176 28568 E	6343002.71 2798393.23	21.4	0.37

Core Stratigraphy

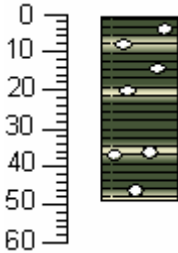
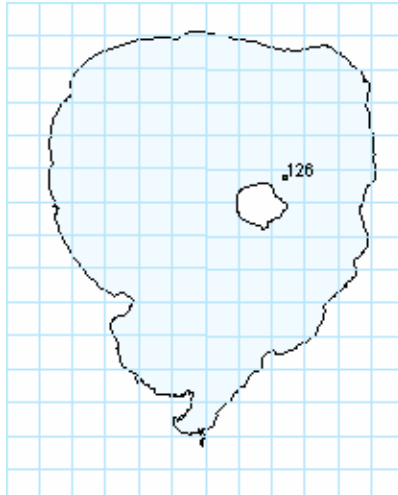
Stratigraphic Column	Description	Location Map
	<p>Gravity Core</p> <p>0-0.1 Reddy brown loose flaky diatomaceous ooze.</p> <p>0-1 cm Fine 2mm thick laminations, yellow and black.</p> <p>1-2 cm Yellow diatomaceous ooze.</p> <p>2-3 cm Laminated dark olive green to dark yellow diatomaceous ooze.</p> <p>3-10 cm Dark olive green massive diatomaceous ooze, mottled yellow towards bottom.</p> <p>10-26 cm Yellow olive green diatomaceous ooze with dark mottles at the top. Faint lamination towards the bottom.</p> <p>26-36 cm Massive mid-olive green diatomaceous ooze becoming darker towards the bottom.</p> <p>36-37 cm Grey sand (Tarawera Tephra).</p>	

Concentrations (g/tonne)

Depth (cm)	As	Fe	Mn	P	Pb
0	55.48	8430.47	847.70	3242.84	9.92
0-2	39.60	5333.94	509.66	1740.69	5.43
2-4	52.25	5463.87	313.19	966.94	5.14
4-6	52.82	6092.65	375.41	771.22	7.64
6-8	59.96	6446.75	429.47	651.67	8.56
8-10	56.53	6221.64	367.83	570.16	8.31
10-12	40.79	5218.00	380.38	799.63	8.58
12-14	45.35	5751.55	422.48	582.42	7.59
14-16	64.31	7213.54	397.79	713.95	8.06
16-18	38.69	4758.25	449.26	532.99	7.13
18-20	45.70	4598.89	468.04	478.71	6.07
20-22	30.16	6019.48	643.51	1368.55	5.32
22-24	42.39	5174.95	539.98	709.61	5.30
24-26	71.67	6550.59	497.95	434.81	4.53
26-28	76.97	6896.00	547.11	350.38	4.12
28-30	79.22	6949.15	411.49	311.50	3.38
30-32	95.51	8369.88	385.93	305.57	3.36
32-34	102.21	8680.98	381.67	377.62	3.97
34-36	62.13	8170.12	381.72	352.67	3.81

Core ID	Site Location	Grid S Grid E	Water Depth (m)	Core Length (m)
Ru 126	38 07070 S 176 29611 E	6342725.01 2799298.70	16	0.48

Core Stratigraphy

Stratigraphic Column	Description	Location Map
	<p>Gravity Core</p> <p>Core top lost.</p> <p>0-48 Laminated dark olive green diatomaceous ooze with flecks of yellow.</p> <p>1-2 cm thick laminations. Core becomes more yellow down the core. Full of gas, as large as 2 cm in diameter across core.</p>	

Concentrations (g/tonne)

Depth (cm)	As	Fe	Mn	P	Pb
0-2	109.74	9201.62	381.26	980.46	6.71
2-4	70.40	7956.64	404.44	869.05	7.65
4-6	64.30	6839.12	366.07	697.14	6.64
6-8	51.68	6423.03	372.66	666.63	6.75
8-10	74.58	8166.00	370.90	696.70	6.59
10-12	59.19	6760.21	365.92	618.38	6.89
12-14	37.34	4133.33	358.10	654.80	7.68
14-16	45.05	4588.53	366.74	622.90	7.82
16-18	43.69	5063.04	327.02	604.43	7.10
18-20	38.92	4447.59	329.51	539.13	8.31
20-22	49.61	6623.23	385.67	550.71	10.08
22-24	57.13	7761.45	342.06	514.93	10.02
24-26	94.75	9053.30	370.75	562.25	10.64
26-28	57.73	7122.91	372.79	582.95	11.31
28-30	74.11	7646.54	395.98	556.63	11.33
30-32	63.86	6431.88	386.45	574.36	13.78
32-34	67.07	7156.08	326.02	500.33	14.65
34-36	58.34	6361.68	344.19	574.17	15.14
36-38	53.95	5843.37	361.30	538.43	14.05
38-40	67.23	6698.31	407.04	603.31	15.19
40-42	93.38	9283.78	388.09	673.56	13.74
42-44	85.59	8818.42	361.65	630.31	13.20

Core ID	Site Location	Grid S Grid E	Water Depth (m)	Core Length (m)
Ru 127	38 07277 S 176 30628 E	6342462.47 2800181.85	13.5	0.3

Core Stratigraphy

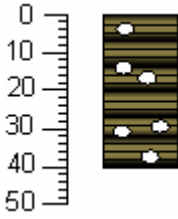

Stratigraphic Column	Description	Location Map
	<p>Gravity Core</p> <p>0-2 cm Loose flaky yellow diatomaceous ooze.</p> <p>2-7 cm Dark olive green massive diatomaceous ooze, gas present from 2 cm onwards.</p> <p>7-30 cm Yellow diatomaceous ooze with faint black laminations 1 cm apart.</p>	

Concentrations (g/tonne)

Depth (cm)	As	Fe	Mn	P	Pb
0-2	59.75	6745.16	419.03	1216.47	7.48
2-4	98.26	9393.58	389.50	874.00	7.61
4-6	53.43	7462.14	433.39	782.05	8.32
6-8	49.60	5935.40	362.01	571.68	6.81
8-10	60.88	7691.03	304.35	499.81	7.74
10-12	57.50	6924.20	438.61	502.66	10.23
12-14	54.92	7444.61	311.10	443.35	9.48
14-16	52.98	6284.72	348.25	447.52	11.16
16-18	70.86	6684.06	370.75	500.42	11.54
18-20	59.12	5948.89	368.81	521.00	13.15
20-22	51.21	5929.04	393.72	522.67	15.89
22-24	57.92	5934.20	358.44	574.17	14.28
24-26	45.00	5074.01	312.36	502.69	14.18
26-28	90.63	8235.78	358.39	606.15	12.64
28-30	76.05	6382.77	467.80	736.01	12.72

Core ID	Site Location	Grid S Grid E	Water Depth (m)	Core Length (m)
Ru 128	38 07318 S 176 27041 E	6342532.84 2797035.36	21	0.40

Core Stratigraphy


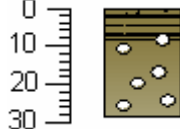

Stratigraphic Column	Description	Location Map
	<p>Gravity Core</p> <p>0-40 cm Laminated olive and black diatomaceous ooze with gas voids.</p> <p>Core top retained.</p>	

Concentrations (g/tonne)

Depth (cm)	As	Fe	Mn	P	Pb
0-2	91.90	9570.68	383.28	589.02	9.57
2-4	68.33	7474.05	387.80	621.55	10.45
4-6	53.65	6192.58	412.76	632.57	11.75
6-8	61.64	6480.19	440.90	681.62	14.74
8-10	67.43	7222.14	415.94	605.53	15.36
10-12	71.55	7183.91	416.73	648.99	14.86
12-14	49.26	6059.82	501.39	893.79	14.30
14-16	52.91	5712.31	484.95	740.55	15.12
16-18	79.74	6871.03	412.65	695.91	13.80
18-20	61.30	5948.70	413.58	733.00	12.48
20-22	77.46	6305.91	411.44	713.96	12.10
22-24	76.00	6648.99	408.65	651.44	10.30
24-26	99.12	8157.03	507.64	859.58	12.77
26-28	85.31	8661.62	499.94	889.46	11.14
28-30	66.16	6370.85	471.47	786.99	9.11
30-32	69.84	6731.20	514.31	840.46	7.86
32-34	62.85	5447.50	405.81	769.26	6.08
34-36	78.98	7408.99	489.82	831.25	6.31
36-38	51.87	7173.44	643.03	1203.64	7.12
38-40	38.44	4826.94	428.79	789.60	5.69

Core ID	Site Location	Grid S Grid E	Water Depth (m)	Core Length (m)
Ru 129	38 07 26.8553 S 176 16 30.8872 E	6336867 2797252	11.4	0.28

Core Stratigraphy


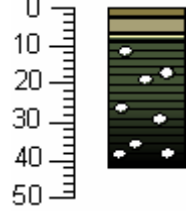

0-28 cm	Stratigraphic Column	Description	Location Map
		<p>Gravity Core</p> <p>0-1 cm Very loose olive diatomaceous ooze with black flecks (nepheloid layer).</p> <p>1-7 cm Laminated olive/black diatomaceous ooze.</p> <p>7-8 cm Light olive diatomaceous ooze with gas.</p> <p>8-28 cm Olive diatomaceous ooze with gas becoming lighter at bottom of core.</p>	

Concentrations (g/tonne)

Depth (cm)	As	Fe	Mn	P	Pb
0-2	66.59	10146.62	453.21	1475.66	11.26
2-4	107.11	11684.04	423.17	1369.65	16.04
4-6	107.49	10957.30	447.30	1572.42	20.42
6-8	82.27	10425.02	481.70	1374.97	17.63
8-10	106.56	12302.78	402.08	1362.09	17.34
10-12	78.58	10450.99	381.77	1297.11	14.78
12-14	109.47	12170.45	444.84	1649.02	17.82
14-16	105.72	13006.87	431.02	1575.63	18.92
16-18	75.05	8954.92	392.44	1378.93	17.75
18-20	104.35	11059.13	437.37	1639.23	19.34

Core ID	Site Location	Grid S Grid E	Water Depth (m)	Core Length (m)
Ru 130	38 07 08.6680 S 176 15 59.8429 E	6337455 2796517	21.4	0.42

Core Stratigraphy


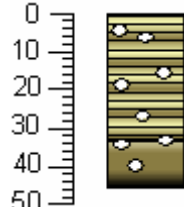

0-42 cm	Stratigraphic Column	Description	Location Map
		<p>Gravity Core</p> <p>0-3 cm Very loose olive diatomaceous ooze (nepheloid layer).</p> <p>3-7 cm Pale olive green diatomaceous ooze.</p> <p>7-9 cm Yellow diatomaceous ooze with dark bands.</p> <p>9-42 cm Dark olive black diatomaceous ooze with faint laminations and significant gas.</p>	

Concentrations (g/tonne)

Depth (cm)	As	Fe	Mn	P	Pb
0-2	102.54	10015.35	746.33	2979.22	7.87
2-4	82.99	10382.19	501.65	2107.08	12.35
4-6	87.94	10906.18	393.65	1607.35	12.79
6-8	70.16	8504.02	408.42	1612.12	11.28
8-10	119.12	13219.95	437.70	1649.23	13.69
10-12	132.20	14344.45	493.17	1717.12	14.29
12-14	98.92	11998.85	561.89	1750.77	14.35
14-16	114.63	12100.80	634.27	1903.64	16.94
16-18	140.62	11851.10	560.79	1640.35	14.43
18-20	128.85	13385.80	745.52	2220.85	18.65

Core ID	Site Location	Grid S Grid E	Water Depth (m)	Core Length (m)
Ru 131	38 06 33.0313 S 176 16 07.5584 E	6338546 2796745	17.9	0.46

Core Stratigraphy

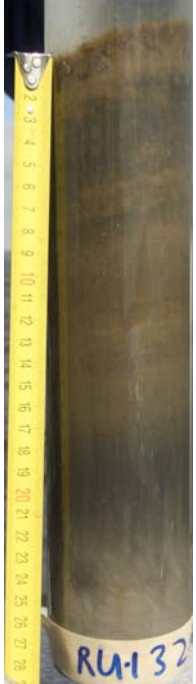
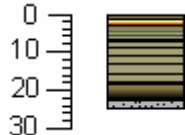

0-46 cm	Stratigraphic Column	Description	Location Map
		<p>Gravity Core</p> <p>0-33 cm Laminated yellow, black and olive diatomaceous ooze. Approximately 1 cm laminations.</p> <p>33-46 cm Becomes more muted, olive diatomaceous ooze. Lots of gas present.</p>	

Concentrations (g/tonne)

Depth (cm)	As	Fe	Mn	P	Pb
0-2	70.87	7781.86	466.64	1130.44	16.64
2-4	75.74	8061.13	467.78	1451.11	10.43
4-6	87.51	9962.87	445.38	1155.44	9.46
6-8	78.40	9357.62	447.19	936.12	9.75
8-10	99.05	11074.35	492.39	960.83	10.76
10-12	65.28	7271.51	560.94	909.43	11.41
12-14	81.19	7756.89	447.77	797.70	10.63
14-16	68.16	7317.53	459.93	790.29	12.91
16-18	68.50	7665.05	403.96	651.86	13.20
18-20	81.75	8836.60	448.41	760.14	14.12

Core ID	Site Location	Grid S Grid E	Water Depth (m)	Core Length (m)
Ru 132	38 06 00.6018 S	6339472	13	0.24
	176 16 50.2276 E	2798770		

Core Stratigraphy


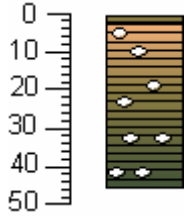

0-24 cm	Stratigraphic Column	Description	Location Map
		<p>Gravity Core</p> <p>0-1 cm Loose olive nepheloid layer</p> <p>2-3 cm Pale yellow orange diatomaceous ooze.</p> <p>3-7 cm Dark olive diatomaceous ooze with pale laminations 1 cm apart.</p> <p>7-18 cm Muted pale olive diatomaceous ooze with faint laminations.</p> <p>18-23 Uniform olive black diatomaceous ooze.</p> <p>23-24 cm Pale grey gritty (Tarawera tephra).</p>	

Concentrations (g/tonne)

Depth (cm)	As	Fe	Mn	P	Pb
0-2	50.79	6298.73	465.79	1509.07	6.14
2-4	69.13	9345.13	539.29	1073.41	8.77
4-6	86.05	11932.94	545.39	695.22	11.00
6-8	89.48	12286.58	481.72	556.20	11.45
8-10	99.07	12975.70	546.99	624.01	10.04
10-12	79.26	10287.00	527.65	654.98	9.35
12-14	75.65	9293.09	585.14	545.01	7.69
14-16	120.59	14357.69	484.14	418.13	5.67
16-18	146.07	14813.84	753.28	467.31	5.64
18-20	80.26	9420.09	663.80	478.49	5.72

Core ID	Site Location	Grid S Grid E	Water Depth (m)	Core Length (m)
Ru 133	38 05 54.0029 S 176 15 53.3854 E	6339761 2796444	18.5	0.45

Core Stratigraphy


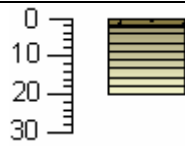
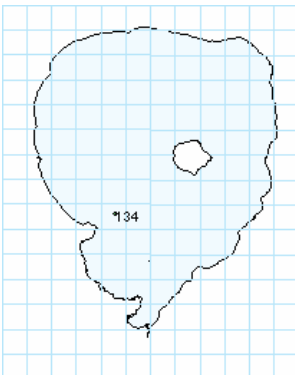
0-45 cm	Stratigraphic Column	Description	Location Map
		<p>Gravity Core</p> <p>0-2 cm Olive loose flakey nepheloid layer.</p> <p>2-45 cm Laminated pale orange to dark olive green. 2 cm thick laminations.</p> <p>Extensive gas throughout core. Signs of disturbance.</p>	

Concentrations (g/tonne)

Depth (cm)	As	Fe	Mn	P	Pb
0-2	58.98	6766.27	433.05	2182.52	6.37
2-4	51.87	6103.65	473.40	1455.31	7.45
4-6	92.41	10281.28	499.39	1150.50	10.00
6-8	96.59	9783.48	502.43	886.93	9.13
8-10	75.61	10052.44	547.94	968.35	9.59
10-12	71.03	9881.49	531.45	875.31	9.96
12-14	70.33	10059.05	535.58	833.70	10.48
14-16	121.67	9677.42	476.40	749.26	10.55
16-18	77.36	9731.68	487.13	729.22	11.71
18-20	66.66	8596.90	480.68	669.78	12.17

Core ID	Site Location	Grid S Grid E	Water Depth (m)	Core Length (m)
Ru 134	38 05 54.1702 S	6339787	13	0.25
	176 15 18.3556 E	2795591		

Core Stratigraphy


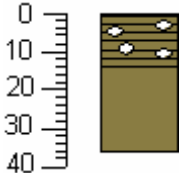
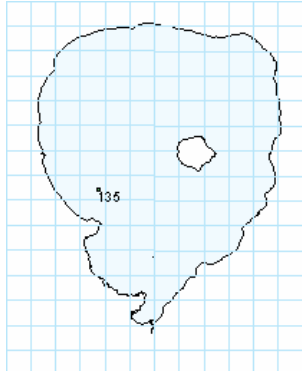
0-25 cm	Stratigraphic Column	Description	Location Map
		<p>Gravity Core</p> <p>0-2 cm Loose mottled pale olive diatomaceous ooze (nepheloid layer) extending upwards into the water column.</p> <p>2-20 cm Olive/yellow diatomaceous ooze with few laminations.</p>	

Concentrations (g/tonne)

Depth (cm)	As	Fe	Mn	P	Pb
0-2	62.19	8742.22	380.54	1500.43	10.18
2-4	59.26	8587.60	403.31	1104.14	10.53
4-6	66.51	8948.03	393.04	952.95	10.89
6-8	63.58	8548.96	481.78	1021.94	13.46
8-10	57.92	8099.57	423.69	945.72	13.53
10-12	61.70	9754.07	390.74	740.94	14.30
12-14	69.51	11590.75	396.60	724.21	15.35
14-16	80.13	12206.97	366.68	814.65	17.99
16-18	65.01	9561.55	409.83	824.01	18.10
18-20	60.19	8298.45	486.00	876.74	20.30

Core ID	Site Location	Grid S Grid E	Water Depth (m)	Core Length (m)
Ru 135	38 05 38.8801 S 176 14 42.3268 E	6340290 2794731	9.4	0.36

Core Stratigraphy


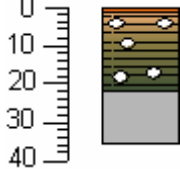
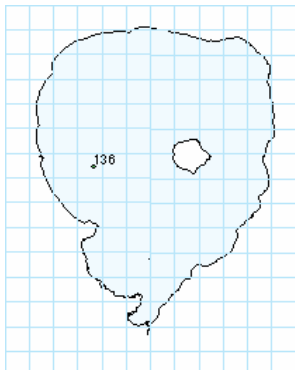
0-36 cm	Stratigraphic Column	Description	Location Map
		<p>Gravity Core</p> <p>0-14 cm Laminated black/olive diatomaceous ooze. Gas present.</p> <p>14-36 cm Massive dull olive green diatomaceous ooze. No gas.</p>	

Concentrations (g/tonne)

Depth (cm)	As	Fe	Mn	P	Pb
0-2	79.34	10055.16	517.68	2118.19	9.61
2-4	67.18	8734.22	462.74	1580.96	10.14
4-6	64.77	9537.82	444.87	1249.84	11.48
6-8	59.15	9158.70	498.05	1049.13	11.93
8-10	63.45	9180.09	505.27	1152.50	12.60
10-12	57.31	8368.10	495.52	1042.35	11.90
12-14	51.85	7567.31	464.13	968.82	13.03
14-16	69.38	11064.44	363.99	750.86	13.36
16-18	70.55	11092.83	393.29	817.73	16.61
18-20	65.94	9513.40	438.41	780.50	16.95

Core ID	Site Location	Grid S Grid E	Water Depth (m)	Core Length (m)
Ru 136	38 04 57.9861 S	6341553	12	0.36
	176 14 38.7610 E	2794690		

Core Stratigraphy


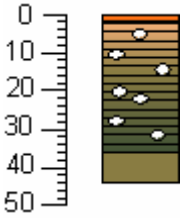


0-36 cm	Stratigraphic Column	Description	Location Map
		<p>Gravity Core</p> <p>0-2 cm Olive black to orange flakey nepheloid layer.</p> <p>2-22 cm Laminated pale orange to dark olive green diatomaceous ooze. 2 cm thick laminations. Little gas.</p> <p>22-36 cm Massive pale grey.</p>	

Concentrations (g/tonne)

Depth (cm)	As	Fe	Mn	P	Pb
0-2	50.36	6993.54	434.96	2275.60	6.83
2-4	57.47	5936.67	360.27	1540.73	5.91
4-6	97.88	10328.43	419.60	1278.08	8.28
6-8	65.38	9604.66	469.12	1182.83	9.97
8-10	56.92	7531.82	457.40	987.63	8.94
10-12	61.08	7936.38	444.68	969.47	9.08
12-14	75.31	10720.55	451.38	908.64	9.82
14-16	61.69	7508.50	492.46	888.01	10.13
16-18	63.01	7658.35	489.04	849.98	10.61
18-20	62.26	7514.48	460.03	784.80	9.74

Core ID	Site Location	Grid S Grid E	Water Depth (m)	Core Length (m)
Ru 137	38 04 01.2836 S 176 18 02.4294 E	6343118 2793714	11.2	0.44

Core Stratigraphy


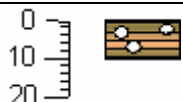

0-44 cm	Stratigraphic Column	Description	Location Map
		<p>Gravity Core</p> <p>0-2 cm Laminated orange diatomaceous ooze (see image).</p>  <p>2-36 cm Pale orange to dark olive laminated diatomaceous ooze. Laminations 2 cm thick. Full of gas.</p> <p>36-44 cm Uniform olive diatomaceous ooze.</p>	

Concentrations (g/tonne)

Depth (cm)	As	Fe	Mn	P	Pb
0-2	43.21	6362.72	412.53	2487.62	6.21
2-4	49.50	6051.23	363.83	1562.53	6.17
4-6	86.10	10118.07	392.95	1258.86	7.47
6-8	74.49	10119.46	456.74	930.37	8.73
8-10	59.25	7648.73	470.83	862.93	8.32
10-12	91.55	11620.90	518.13	907.10	9.22
12-14	64.77	8373.68	537.94	890.00	9.63
14-16	59.30	7682.74	598.01	981.54	10.83
16-18	70.51	10274.95	622.45	1110.95	12.06
18-20	55.32	6726.40	448.68	720.80	9.47

Core ID	Site Location	Grid S Grid E	Water Depth (m)	Core Length (m)
Ru 138	38 05 02.44675 S	6341380	16.1	0.10
	176 15 18.8838 E	2795662		

Core Stratigraphy


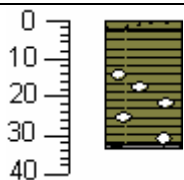

0-10 cm	Stratigraphic Column	Description	Location Map
		<p>Gravity Core</p> <p>0-10 cm Laminated pale orange to pale olive diatomaceous ooze. Gas present. Large nepheloid layer extending upwards into the water column.</p> <p>First three samples are nepheloid layer.</p>	

Concentrations (g/tonne)

Depth (cm)	As	Fe	Mn	P	Pb
0-2	70.50	8394.22	308.06	1134.82	10.43
2-4	77.79	8968.98	341.05	1211.75	10.35
4-6	77.00	8855.84	436.30	986.81	9.95
6-8	82.87	9848.20	457.88	770.92	14.72
8-10	106.75	12643.50	683.57	1125.09	16.69
10-12	93.69	10505.21	612.12	1026.29	12.71
12-13	100.82	11843.47	771.84	1173.01	15.52

Core ID	Site Location	Grid S Grid E	Water Depth (m)	Core Length (m)
Ru139	38 03 33.7410 S 176 14 04.1373 E	6344179 2793941	9.8	0.33

Core Stratigraphy

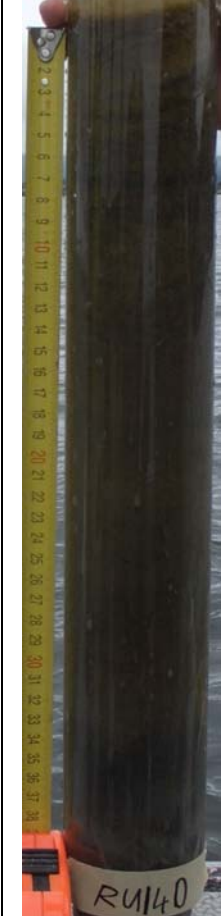
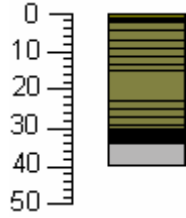
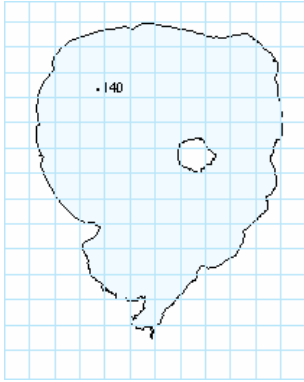
0-33 cm	Stratigraphic Column	Description	Location Map
		<p>Gravity Core</p> <p>0-2 cm Olive diatomaceous ooze with black flecks and white algal mat.</p> <p>2-32 cm Olive/black laminated diatomaceous ooze. Gas present from 13 cm onwards throughout the core.</p> <p>32-33 cm Grey pumice (Kaharoa).</p>	

Concentrations (g/tonne)

Depth (cm)	As	Fe	Mn	P	Pb
0-2	41.45	5776.81	475.06	1601.56	6.51
2-4	63.08	7399.31	459.92	1142.68	9.16
4-6	59.96	8628.08	506.83	953.86	9.31
6-8	72.61	10150.74	528.43	763.96	9.01
8-10	46.14	5980.29	436.87	589.24	8.22
10-12	53.29	6291.53	448.85	524.28	10.44
12-14	64.41	7880.77	353.25	654.26	12.37
14-16	67.48	7436.82	532.74	733.42	16.83
16-18	67.55	6929.23	461.23	692.66	18.94
18-20	48.58	5595.51	518.10	755.43	17.25

Core ID	Site Location	Grid S Grid E	Water Depth (m)	Core Length (m)
Ru140	38 03 23.4341 S	6344467	11.5	0.40
	176 14 37.5324 E	2794766		

Core Stratigraphy


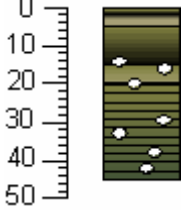

0-40 cm	Stratigraphic Column	Description	Location Map
		<p>Gravity Core</p> <p>0-1 cm Olive green nephroid layer.</p> <p>1-2 cm Black diatomaceous ooze.</p> <p>2-15 cm laminated olive diatomaceous ooze.</p> <p>15-23 cm massive olive diatomaceous ooze.</p> <p>23-30 cm laminated black and olive diatomaceous ooze with 1cm wide laminations.</p> <p>30-34 cm Black diatomaceous ooze.</p> <p>34-40 cm Light grey diatomaceous ooze.</p>	

Concentrations (g/tonne)

Depth (cm)	As	Fe	Mn	P	Pb
0-2	34.77	4698.01	428.38	1994.97	6.07
2-4	42.00	5853.78	462.27	1470.11	7.07
4-6	58.13	6763.22	526.82	955.59	9.77
6-8	62.87	8462.63	540.25	893.91	11.73
8-10	56.98	7255.11	478.73	656.54	11.93
10-12	65.06	8428.19	553.53	767.42	15.61
12-14	58.66	6729.97	526.33	676.82	18.16
14-16	60.02	6621.36	510.47	675.55	19.33
16-18	51.13	5601.92	600.61	710.62	18.26
18-20	64.00	7047.57	601.84	767.97	18.17

Core ID	Site Location	Grid S Grid E	Water Depth (m)	Core Length (m)
Ru141	38 03 21.3354 S 176 15 30.1053 E	6344485 2796049	14.1	0.45

Core Stratigraphy


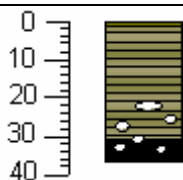

0-45 cm	Stratigraphic Column	Description	Location Map
		<p>Gravity Core</p> <p>0-5 cm Loose olive, black and light olive diatomaceous ooze.</p> <p>5-15 cm More compact olive/black diatomaceous ooze. Gas present from 12 cm onwards.</p> <p>15-20 cm Olive to light olive diatomaceous ooze.</p> <p>20-45 cm Laminated olive, dark olive and black diatomaceous ooze. 2 cm thick laminations.</p>	

Concentrations (g/tonne)

Depth (cm)	As	Fe	Mn	P	Pb
0-2	53.82	5662.51	405.68	2215.07	6.19
2-4	63.71	7015.77	464.68	1423.14	7.22
4-6	55.76	8144.04	547.25	1206.42	9.10
6-8	51.78	6765.20	567.04	987.31	8.99
8-10	71.21	8104.30	514.56	933.98	8.16
10-12	60.71	8483.19	558.22	932.55	9.16
12-14	45.89	4778.76	422.28	913.08	9.18
14-16	55.12	6186.99	439.97	987.34	10.63
16-18	38.58	4208.11	342.54	670.20	9.30
18-20	60.97	7175.37	356.02	714.30	11.24

Core ID	Site Location	Grid S Grid E	Water Depth (m)	Core Length (m)
Ru142	38 03 15.2614 S	6344638	16.1	0.36
	176 16 44.4610 E	2796989		

Core Stratigraphy


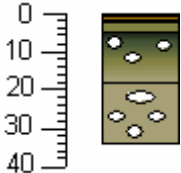

0-36 cm	Stratigraphic Column	Description	Location Map
		<p>Gravity Core</p> <p>0-1 cm Very loose olive green diatomaceous ooze.</p> <p>1-30 cm Olive black diatomaceous ooze with light olive laminations.</p> <p>Large gas void at 22 cm.</p> <p>Many smaller gas voids from 25 cm downwards throughout the core.</p> <p>30-36 cm Black diatomaceous ooze with gas.</p>	

Concentrations (g/tonne)

Depth (cm)	As	Fe	Mn	P	Pb
0-2	93.43	8337.82	375.80	1857.17	6.34
2-4	76.12	9633.15	422.01	1165.35	8.12
4-6	61.83	7380.31	451.38	1005.84	7.93
6-8	60.75	7813.48	463.15	1008.53	7.85
8-10	72.83	8000.97	399.00	848.02	7.07
10-12	52.61	6224.38	474.64	1011.39	9.43
12-14	54.04	6405.64	420.55	950.89	9.53
14-16	44.99	5433.63	414.97	827.25	10.43
16-18	50.68	5775.02	400.11	721.34	10.51
18-20	90.86	9317.63	448.19	841.29	13.24

Core ID	Site Location	Grid S Grid E	Water Depth (m)	Core Length (m)
Ru143	38 03 16.2609 S 176 16 44.4610 E	6344575 2797866	17.4	0.35

Core Stratigraphy


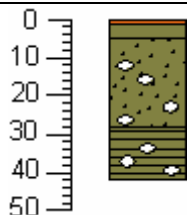

0-35 cm	Stratigraphic Column	Description	Location Map
		<p>Gravity Core</p> <p>0-1 cm Dark olive nepeloid layer extruding upwards into the water column.</p> <p>1 cm White algae mat</p> <p>1-2 cm Orange brown diatomaceous ooze.</p> <p>2-3 cm Black diatomaceous ooze.</p> <p>3-5 cm Olive diatomaceous ooze.</p> <p>5-18 cm Olive black diatomaceous ooze becoming lighter down the core. Gas present.</p> <p>18-34 cm Light olive diatomaceous ooze with gas. Large gas void at 23 cm.</p>	

Concentrations (g/tonne)

Depth (cm)	As	Fe	Mn	P	Pb
0-2	95.70	9068.57	504.39	2930.21	5.10
2-4	49.16	6817.06	545.49	2367.27	6.38
4-6	110.93	9238.13	438.36	1572.14	5.27
6-8	106.28	11297.12	455.23	1603.84	6.29
8-10	79.92	10260.93	465.49	1273.72	7.48
10-12	103.97	8894.92	461.75	1097.95	6.69
12-14	65.36	8580.07	493.58	1088.44	8.37
14-16	57.51	7524.40	418.23	776.00	10.60
16-18	69.52	9728.85	448.42	813.98	11.43
18-20	69.13	7871.88	429.05	788.32	11.69

Core ID	Site Location	Grid S Grid E	Water Depth (m)	Core Length (m)
Ru144	38 03 17.4277 S	6344507	18	0.42
	176 17 20.2300 E	2798736		

Core Stratigraphy


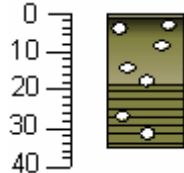
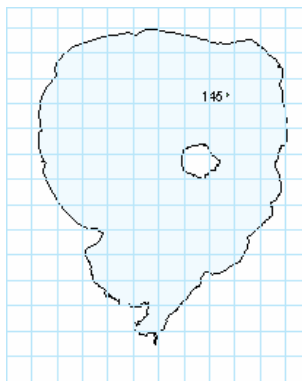
0-42 cm	Stratigraphic Column	Description	Location Map
		<p>Gravity Core</p> <p>0-1 cm Orange nepeloid layer with white algae mat.</p> <p>1-2 cm Black very loose diatomaceous ooze.</p> <p>2-5 cm Loose olive diatomaceous ooze.</p> <p>5-28 cm Mottled olive black diatomaceous ooze. Gas present from 10 cm downwards throughout core.</p> <p>28-42 cm Laminated black olive diatomaceous ooze.</p>	

Concentrations (g/tonne)

Depth (cm)	As	Fe	Mn	P	Pb
0-2	79.04	8957.15	575.71	2953.21	5.78
2-4	67.72	7940.97	503.62	1850.04	6.58
4-6	104.64	9964.20	398.08	1246.52	6.38
6-8	67.23	8375.59	452.60	1052.49	7.63
8-10	69.83	9195.12	446.81	1003.71	7.93
10-12	96.47	12176.01	483.33	1053.47	7.96
12-14	65.12	8345.19	465.63	930.94	8.30
14-16	98.85	10506.46	581.35	1193.04	10.04
16-18	98.96	10879.53	549.20	1096.13	10.21
18-20	80.29	10041.29	593.01	1250.41	10.89

Core ID	Site Location	Grid S Grid E	Water Depth (m)	Core Length (m)
Ru145	38 03 16.1091 S 176 18 00.7005 E	6344502 2799723	17.9	0.35

Core Stratigraphy


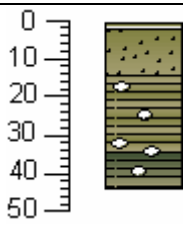

0-35 cm	Stratigraphic Column	Description	Location Map
		<p>Gravity Core</p> <p>0-1 cm Light olive diatomaceous ooze.</p> <p>1-19 cm Olive black diatomaceous ooze becoming lighter at bottom. Gas present.</p> <p>19-35 cm Olive black diatomaceous ooze with 1 cm laminations. Gas present.</p>	

Concentrations (g/tonne)

Depth (cm)	As	Fe	Mn	P	Pb
0-2	68.15	8823.23	426.52	922.29	7.96
2-4	64.55	9812.65	445.25	915.83	9.93
4-6	84.05	9336.65	518.75	1167.03	9.93
6-8	64.83	7605.38	474.20	987.69	9.11
8-10	58.69	6844.00	456.79	903.73	9.43
10-12	57.98	7096.79	455.17	767.59	10.26
12-14	69.84	8630.21	494.29	816.54	11.48
14-16	105.55	10465.35	430.84	818.68	11.57
16-18	89.91	9694.24	426.52	907.74	12.99
18-20	74.07	8190.57	404.74	819.56	11.58

Core ID	Site Location	Grid S Grid E	Water Depth (m)	Core Length (m)
Ru146	38 03 11.9124 S	6344606	15.9	0.43
	176 18 38.9959E	2800661		

Core Stratigraphy


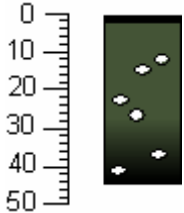

0-43 cm	Stratigraphic Column	Description	Location Map
		<p>Gravity Core</p> <p>0-2 Very loose olive diatomaceous ooze. White algae mat on top.</p> <p>2-14 cm Olive to light olive diatomaceous ooze with black mottles.</p> <p>14-34 cm Laminated olive and light olive diatomaceous ooze. 1cm thick laminations. Gas present.</p> <p>34-43 cm Dark olive to light olive diatomaceous ooze. Slightly laminated. Gas present.</p> <p>Sample 0-2 cm lost.</p>	

Concentrations (g/tonne)

Depth (cm)	As	Fe	Mn	P	Pb
0-2					
2-4	70.46	8345.70	349.02	975.93	6.47
4-6	54.12	8179.27	380.53	777.67	7.59
6-8	47.82	7391.24	422.16	822.30	7.85
8-10	68.53	8797.26	395.44	723.69	7.66
10-12	55.50	7567.92	444.81	812.34	9.86
12-14	50.07	6901.15	408.43	735.76	8.53
14-16	47.96	7142.72	387.53	623.41	8.90
16-18	48.19	8237.67	336.09	542.57	9.61
18-20	62.93	9952.91	371.62	628.49	10.81

Core ID	Site Location	Grid S Grid E	Water Depth (m)	Core Length (m)
Ru147	38 02 47.9268 S 176 17 58.4586 E	6345338 2800875	16.7	0.44

Core Stratigraphy


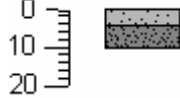

0-44 cm	Stratigraphic Column	Description	Location Map
		<p>Gravity Core</p> <p>0-2 cm Very loose olive black diatomaceous ooze.</p> <p>2-44 cm Dark olive black diatomaceous ooze with gas present from 10 cm onwards down the core.</p>	

Concentrations (g/tonne)

Depth (cm)	As	Fe	Mn	P	Pb
0-2	54.89	7758.65	403.04	1438.07	7.30
2-4	61.81	8350.94	393.70	964.38	5.98
4-6	81.17	10250.87	406.06	940.23	6.45
6-8	44.04	8783.11	532.52	1102.12	7.74
8-10	58.74	9657.41	458.80	812.50	6.89
10-12	43.06	8375.57	547.88	1047.18	7.37
12-14	63.10	9228.14	528.28	923.39	7.66
14-16	74.08	9240.49	515.42	937.86	7.80
16-18	79.11	10690.55	592.18	1035.33	9.35
18-20	58.64	8620.40	549.70	949.25	8.45

Core ID	Site Location	Grid S Grid E	Water Depth (m)	Core Length (m)
Ru148	38 02 36.3538 S	6345738	10.6	0.11
	176 17 58.4586 E	2799714		

Core Stratigraphy


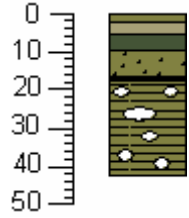
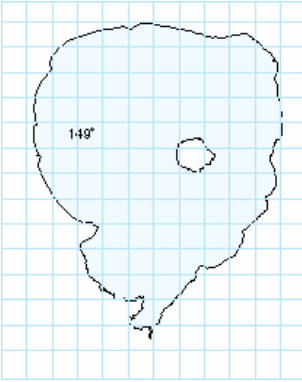
0-11 cm	Stratigraphic Column	Description	Location Map
		<p>Gravity Core</p> <p>0-0.1 cm Orange organics</p> <p>0.1 -4.5 cm Grey sand with black flecks.</p> <p>4.5-10 cm Darker grey silty sand.</p>	

Concentrations (g/tonne)

Depth (cm)	As	Fe	Mn	P	Pb
0-2	39.58	7222.00	292.32	290.88	2.81
2-4	34.07	6150.62	266.28	254.25	3.02
4-6	56.35	6315.49	314.40	259.15	3.50
6-8	42.07	5631.42	376.06	256.63	3.35
8-10	41.73	5740.78	322.51	258.30	3.41

Core ID	Site Location	Grid S Grid E	Water Depth (m)	Core Length (m)
Ru149	38 04 14.6855 S 176 14 31.9651 E	6342893 2794573	11.7	0.42

Core Stratigraphy


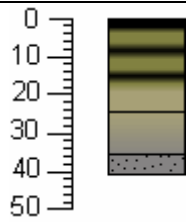
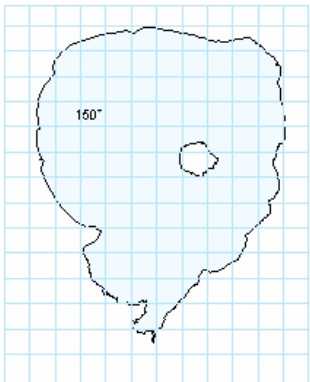
0-42 cm	Stratigraphic Column	Description	Location Map
		<p>Gravity Core</p> <p>0-2 cm Very loose olive nepeloid layer.</p> <p>2-5 cm Light olive diatomaceous ooze.</p> <p>5-9 cm dark olive diatomaceous ooze.</p> <p>9-16 cm Olive diatomaceous ooze with light olive mottles.</p> <p>16-17 cm Black diatomaceous ooze.</p> <p>17-42 cm Olive diatomaceous ooze with faint laminations. Gas present with large gas void at 27 cm.</p>	

Concentrations (g/tonne)

Depth (cm)	As	Fe	Mn	P	Pb
0-2	64.08	6869.94	414.61	1988.10	6.73
2-4	45.33	5890.72	375.48	1809.39	6.31
4-6	67.56	7216.06	338.69	877.15	7.16
6-8	50.07	6484.32	408.47	765.34	8.31
8-10	49.93	5953.75	437.03	716.11	8.48
10-12	53.73	6228.18	405.45	669.11	7.97
12-14	58.09	6100.98	427.86	655.29	8.95
14-16	70.50	7222.30	446.12	681.79	9.84
16-18	50.06	5689.11	392.09	570.88	9.42
18-20	47.95	5500.00	341.71	479.48	9.44

Core ID	Site Location	Grid S Grid E	Water Depth (m)	Core Length (m)
Ru150	38 03 45.9785 S	6343771	11.6	0.40
	176 14 39.1851E	2794781		

Core Stratigraphy


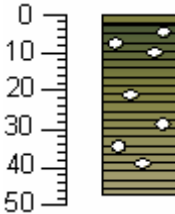

0-40 cm	Stratigraphic Column	Description	Location Map
		<p>Gravity Core</p> <p>0-0.5 cm Olive green nepeloid layer extending upwards in to water column.</p> <p>0.5-1 cm black diatomaceous ooze.</p> <p>1-24 cm Olive black diatomaceous ooze becoming lighter at bottom.</p> <p>24-35 cm Light olive to grey diatomaceous ooze.</p> <p>35-40 Grey gritty material.</p>	

Concentrations (g/tonne)

Depth (cm)	As	Fe	Mn	P	Pb
0-2	57.26	5456.83	396.48	1880.21	5.48
2-4	54.37	6396.82	438.02	925.80	7.49
4-6	71.36	9733.01	421.64	507.14	11.74
6-8	72.78	9399.81	496.14	525.97	14.41
8-10	73.72	8553.13	576.11	544.60	17.58
10-12	75.29	8007.91	521.99	530.42	20.11
12-14	79.30	7862.67	570.71	529.38	17.30
14-16	82.76	8876.91	537.10	477.03	14.16
16-18	100.96	12098.46	523.56	488.82	9.71
18-20	65.16	7588.80	516.31	442.79	7.72

Core ID	Site Location	Grid S Grid E	Water Depth (m)	Core Length (m)
Ru151	38 04 11.0173 S 176 15 19.3433 E	6342964 2795731	14.4	0.47

Core Stratigraphy


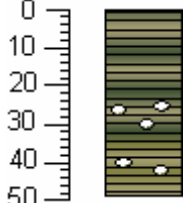

0-47 cm	Stratigraphic Column	Description	Location Map
		<p>Gravity Core</p> <p>0-2 cm Very loose olive diatomaceous ooze.</p> <p>2-47 cm Dark to pale olive diatomaceous ooze with laminations 4 cm thick. Full of gas.</p>	

Concentrations (g/tonne)

Depth (cm)	As	Fe	Mn	P	Pb
0-2	46.81	7527.71	476.58	2039.00	8.82
2-4	79.18	8764.85	420.75	1153.75	8.54
4-6	69.18	9408.60	438.62	910.79	9.67
6-8	58.73	7117.82	490.58	748.61	9.26
8-10	62.45	7406.40	465.13	717.29	8.96
10-12	66.38	8917.87	436.68	677.15	9.23
12-14	60.61	6820.78	470.76	740.25	10.17
14-16	72.78	8456.42	442.22	728.46	10.80
16-18	57.58	6911.19	425.10	666.39	10.51
18-20	47.00	6058.21	422.73	546.82	11.66

Core ID	Site Location	Grid S Grid E	Water Depth (m)	Core Length (m)
Ru152	38 03 43.9755 S	6343761	16.2	0.48
	176 15 59.8898 E	2796749		

Core Stratigraphy


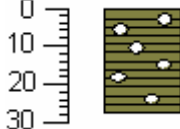

0-48 cm	Stratigraphic Column	Description	Location Map
		<p>Gravity Core</p> <p>Core top lost.</p> <p>0-48 cm Laminated dark olive, black and light olive diatomaceous ooze.</p> <p>Laminations typically 3 cm thick. Core becomes lighter at bottom. Gas present from 24 cm to bottom of core.</p>	

Concentrations (g/tonne)

Depth (cm)	As	Fe	Mn	P	Pb
0-2	78.20	9458.97	490.94	781.97	9.29
2-4	71.79	8223.42	412.37	708.77	8.24
4-6	95.09	10986.73	464.82	697.53	8.36
6-8	59.57	6702.03	459.82	678.78	8.88
8-10	87.81	9169.46	537.58	812.25	11.91
10-12	60.53	7530.38	437.71	679.06	10.47
12-14	48.83	6455.31	435.65	632.52	10.89
14-16	46.60	5934.93	419.20	567.46	11.81
16-18	67.45	9542.78	469.89	955.12	13.35
18-20	101.41	11528.53	576.22	1728.93	13.58

Core ID	Site Location	Grid S Grid E	Water Depth (m)	Core Length (m)
Ru153	38 03 46.0421 S 176 16 23.7979 E	6343676 2797329	20.1	0.27

Core Stratigraphy


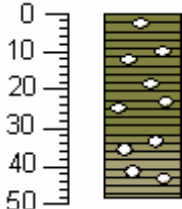


0-27 cm	Stratigraphic Column	Description	Location Map
		<p>Gravity Core</p> <p>0-27 Very loose on top. Nepeloid layer extending upwards into water column. Laminated olive/black diatomaceous ooze. Laminations typically 5 cm thick. Full of gas.</p>	

Concentrations (g/tonne)

Depth (cm)	As	Fe	Mn	P	Pb
0-2	120.64	13252.05	570.14	1143.37	8.20
2-4	151.89	13401.19	482.93	1031.43	7.49
4-6	78.99	11448.10	641.51	1121.92	10.32
6-8	103.10	11317.95	610.87	959.75	8.54
8-10	67.37	9193.02	604.00	890.89	8.28
10-12	101.70	11296.80	588.60	883.23	8.48
12-14	104.54	13742.71	553.86	775.55	8.21
14-16	74.04	9210.75	563.59	776.89	8.96
16-18	93.15	10072.68	607.70	868.67	9.99
18-20	97.96	10940.17	624.84	930.26	10.68

Core ID	Site Location	Grid S Grid E	Water Depth (m)	Core Length (m)
Ru154	38 03 47.4102 S 176 17 21.7095 E	6343582 2798738	20.4	0.48

Core Stratigraphy




0-48 cm	Stratigraphic Column	Description	Location Map
		<p>Gravity Core</p> <p>Core top lost.</p> <p>0-48 Loose on top. Laminated olive/black diatomaceous ooze becoming lighter at 38 cm. Laminations typically 5 cm thick. Full of gas. Gas being the possible cause for the coring problems.</p>  <p>Large gas bubbles can be seen at the surface while coring.</p>	

Concentrations (g/tonne)

Depth (cm)	As	Fe	Mn	P	Pb
0-2	82.16	10271.03	600.33	911.40	9.08
2-4	112.14	11441.37	478.76	764.13	7.65
4-6	87.14	11044.31	538.68	749.32	8.64
6-8	89.44	8671.14	513.85	754.49	8.93
8-10	92.54	9167.42	481.46	767.80	8.83
10-12	93.95	8660.23	445.20	676.71	8.48
12-14	75.25	8267.82	487.63	634.33	11.79
14-16	62.38	8884.34	432.96	561.37	11.19
16-18	84.29	11358.61	402.16	552.47	10.65
18-20	72.66	8801.85	392.10	515.76	10.42

Core ID	Site Location	Grid S Grid E	Water Depth (m)	Core Length (m)
Ru155	38 03 46.0589 S 176 18 01.3479 E	6343588 2799705	16.6	0.07

Core Stratigraphy


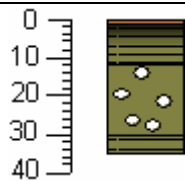

0-7 cm	Stratigraphic Column	Description	Location Map
		<p>Gravity Core</p> <p>0-0.1 cm dark brown, thin layers of white and orange algal mat. 10 cm thick seston above the sediment water interface.</p> <p>0.1-7 cm Olive diatomaceous ooze with black flecks.</p>	

Concentrations (g/tonne)

Depth (cm)	As	Fe	Mn	P	Pb
0-2	87.19	10164.75	467.06	1230.35	8.38
2-4	78.31	9317.68	458.19	648.19	15.20
4-6	76.45	8803.33	445.12	656.09	13.51
6-8	59.67	7056.97	455.69	644.34	9.68

Core ID	Site Location	Grid S Grid E	Water Depth (m)	Core Length (m)
Ru156	38 03 47.6356 S	6343500	12.4	0.35
	176 18 45.0645 E	2800768		

Core Stratigraphy


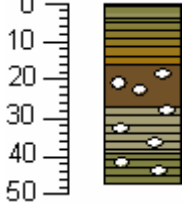

0-35 cm	Stratigraphic Column	Description	Location Map
		<p>Gravity Core</p> <p>0-1 cm Orange diatomaceous ooze, very loose.</p> <p>1-12 cm Laminated black to olive diatomaceous ooze.</p> <p>12-30 cm Massive olive diatomaceous ooze. Lots of gas present.</p> <p>30-35 Black laminations in massive olive diatomaceous ooze.</p>	

Concentrations (g/tonne)

Depth (cm)	As	Fe	Mn	P	Pb
0-2	53.48	7866.12	434.98	1445.65	7.81
2-4	75.89	9295.98	386.01	930.14	11.97
4-6	80.10	9468.25	512.09	1068.07	11.97
6-8	97.62	9568.99	545.15	1210.63	11.18
8-10	133.21	14209.54	631.56	1329.12	14.01
10-12	88.05	10889.73	470.17	877.13	13.20
12-14	92.12	11024.01	526.94	924.16	17.34
14-16	65.48	10090.72	527.14	1110.46	20.30
16-18	118.67	15694.46	761.25	1660.36	25.78
18-20	62.56	9288.64	682.05	1240.88	18.56

Core ID	Site Location	Grid S Grid E	Water Depth (m)	Core Length (m)
Ru157	38 04 43.1276 S 176 18 02.3336 E	6341829 2799664	14.2	0.47

Core Stratigraphy


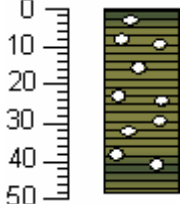
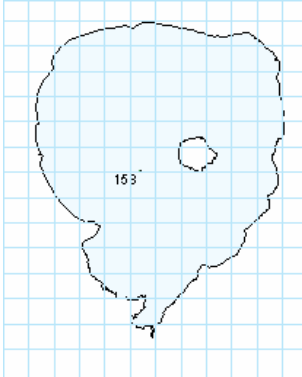
0-47 cm	Stratigraphic Column	Description	Location Map
		<p>Gravity Core</p> <p>0-1 cm Black and light brown diatomaceous ooze.</p> <p>1-4 cm Olive diatomaceous ooze becoming lighter at the bottom.</p> <p>4-16 cm Laminated black to olive and mid-olive brown diatomaceous ooze. Laminations typically 4 cm thick.</p> <p>16-27 cm Dark brown massive diatomaceous ooze. Gas present.</p> <p>27-39 cm Laminated light olive and black diatomaceous ooze with gas present.</p> <p>39-47 cm Laminations become darker. Gas present.</p>	

Concentrations (g/tonne)

Depth (cm)	As	Fe	Mn	P	Pb
0-2	119.49	11339.89	459.60	1288.48	8.74
2-4	70.47	9271.36	496.21	1234.79	7.75
4-6	67.77	8351.05	454.26	1006.20	7.75
6-8	54.05	7093.38	468.03	1003.36	7.64
8-10	96.26	10631.80	457.36	1022.43	7.64
10-12	63.49	7906.57	416.29	860.86	7.41
12-14	76.21	7259.95	448.41	962.05	7.94
14-16	86.15	8422.75	496.41	1165.76	10.07
16-18	93.38	8361.84	474.99	1060.11	9.21
18-20	78.41	9143.67	504.40	1223.31	9.92

Core ID	Site Location	Grid S Grid E	Water Depth (m)	Core Length (m)
Ru158	38 05 06.3571 S	6341233	20.8	0.48
	176 15 48.7156 E	2796384		

Core Stratigraphy


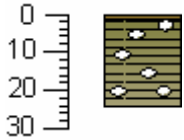
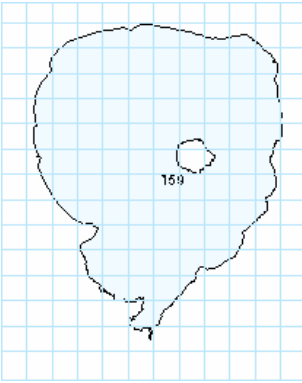
0-48 cm	Stratigraphic Column	Description	Location Map
		<p>Gravity Core</p> <p>0-48 cm Laminated olive black diatomaceous ooze. Darker at 3-5 cm and 41-45 cm. Laminations are 2 cm thick. Lots of gas.</p>	

Concentrations (g/tonne)

Depth (cm)	As	Fe	Mn	P	Pb
0-2	87.15	8935.74	510.30	1109.98	8.24
2-4	113.59	11166.62	522.94	1139.01	9.58
4-6	116.26	15981.46	559.83	1211.10	9.58
6-8	77.96	8349.86	543.32	1072.77	8.98
8-10	107.59	8514.61	575.91	1220.85	10.86
10-12	104.37	8986.90	539.20	1178.31	10.31
12-14	85.38	8398.93	528.55	1028.74	10.50
14-16	62.77	6222.76	477.40	844.61	11.15
16-18	72.16	8724.92	481.01	853.26	11.89
18-20	92.70	9393.13	504.80	941.61	13.25

Core ID	Site Location	Grid S Grid E	Water Depth (m)	Core Length (m)
Ru159	38 05 07.8424 S 176 16 30.4689 E	6341150 2797399	16.6	0.24

Core Stratigraphy


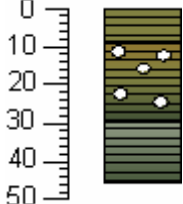

0-24 cm	Stratigraphic Column	Description	Location Map
		<p>Gravity Core</p> <p>Thick nepeloid layer extending 15cm into the water column.</p> <p>0-1 cm Very loose brown diatomaceous ooze.</p> <p>1-1.5 cm Loose black diatomaceous ooze.</p> <p>1.5-24 cm Laminated black to pale olive diatomaceous ooze. Laminations 5 cm thick. Gas present.</p>	

Concentrations (g/tonne)

Depth (cm)	As	Fe	Mn	P	Pb
0-2	81.59	10287.69	438.91	1381.94	11.73
2-4	83.92	10854.12	605.71	1553.56	9.18
4-6	76.57	9467.25	613.57	1150.74	9.18
6-8	76.82	9838.92	638.63	1124.41	10.64
8-10	61.95	7182.89	512.29	903.83	9.05
10-12	102.75	10394.30	482.13	1028.21	9.51
12-14	119.04	13395.43	517.83	1089.02	11.01
14-16	85.03	10816.49	470.16	862.30	14.93
16-18	80.02	8703.75	490.99	816.83	20.25
18-20	64.16	7231.14	464.16	703.50	19.12

Core ID	Site Location	Grid S Grid E	Water Depth (m)	Core Length (m)
Ru160	38 05 37.3836 S 176 15 56.6249 E	6340233 2797554	15.2	0.46

Core Stratigraphy


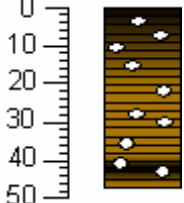

0-46 cm	Stratigraphic Column	Description	Location Map
		<p>Gravity Core</p> <p>0-9 cm Very loose olive and black laminated diatomaceous ooze.</p> <p>9-30 cm Denser light brown to dark olive laminated diatomaceous ooze. 4 cm thick laminations. Large gas voids.</p> <p>30-46 cm Becoming increasingly darker and more compact. Olive grey to dark olive with 1 cm thick laminations.</p>	

Concentrations (g/tonne)

Depth (cm)	As	Fe	Mn	P	Pb
0-2	71.93	7690.44	419.06	1614.30	9.89
2-4	73.66	8665.62	465.12	1495.93	10.55
4-6	66.74	8466.86	464.14	1251.41	10.55
6-8	69.65	8137.53	476.02	1103.10	10.16
8-10	94.00	10653.21	418.39	989.75	9.25
10-12	61.42	7895.95	478.26	1019.42	9.96
12-14	64.14	7557.05	497.71	1196.72	11.78
14-16	74.49	8453.36	552.85	1195.11	12.53
16-18	83.90	10018.81	578.04	1437.22	14.40
18-20	85.57	8620.35	465.71	1083.35	13.48

Core ID	Site Location	Grid S Grid E	Water Depth (m)	Core Length (m)
Ru161	38 05 28.1034 S 176 15 52.1452 E	6340560 2796443	21	0.47

Core Stratigraphy


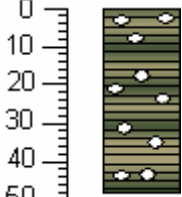
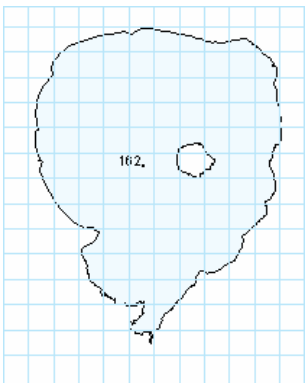
0-47 cm	Stratigraphic Column	Description	Location Map
		<p>Gravity Core</p> <p>0-47 cm Laminated black to pale orange brown diatomaceous ooze.</p> <p>Laminations typically 1 cm thick.</p> <p>Many large gas voids. Dark patches at 5-7 cm and 40-45 cm.</p>	

Concentrations (g/tonne)

Depth (cm)	As	Fe	Mn	P	Pb
0-2	85.70	10321.11	521.24	1065.95	9.15
2-4	82.75	7519.67	496.93	988.84	9.31
4-6	118.65	9446.20	471.32	1036.24	9.31
6-8	89.38	8506.33	597.19	1420.66	11.68
8-10	70.08	7352.52	457.62	960.34	10.06
10-12	48.66	5516.08	423.19	812.72	9.34
12-14	53.23	5792.35	429.26	810.19	10.46
14-16	77.62	8930.05	448.76	851.98	11.77
16-18	78.63	8193.51	517.62	967.69	12.65
18-20	88.82	8386.58	491.12	942.17	13.83

Core ID	Site Location	Grid S Grid E	Water Depth (m)	Core Length (m)
Ru162	38 04 52.6900 S 176 15 56.6249 E	6341647 2796592	21.6	0.48

Core Stratigraphy


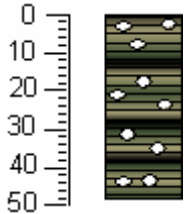

0-48 cm	Stratigraphic Column	Description	Location Map
		<p>Gravity Core</p> <p>0-48 cm Laminated dark olive diatomaceous ooze with minor pale olive bands. Laminations are 1-2 cm thick. Many large gas voids. Pale band at 42-43 cm.</p>	

Concentrations (g/tonne)

Depth (cm)	As	Fe	Mn	P	Pb
0-2	103.18	8336.12	505.49	946.83	9.59
2-4	112.94	9588.37	561.23	1084.85	10.08
4-6	102.56	9804.59	652.26	1467.40	10.08
6-8	70.70	7330.97	480.40	868.26	8.84
8-10	66.20	7284.54	493.53	795.16	9.94
10-12	87.05	10878.35	540.49	885.24	11.24
12-14	105.59	10711.24	537.07	966.71	13.57
14-16	90.02	8849.51	462.62	841.55	12.82
16-18	92.64	9621.18	664.45	1115.16	17.37
18-20	138.03	13235.43	764.13	1309.91	23.51

Core ID	Site Location	Grid S Grid E	Water Depth (m)	Core Length (m)
Ru163	38 02 56.6198 S 176 15 54.1675 E	6342552 2796663	19.4	0.48

Core Stratigraphy

0-48 cm	Stratigraphic Column	Description	Location Map
		<p>Gravity Core</p> <p>0-48 cm Laminated dark olive green diatomaceous ooze with minor pale olive and black bands.</p> <p>Laminations are 1-2 cm thick. Large gas voids.</p>	

Concentrations (g/tonne)

Depth (cm)	As	Fe	Mn	P	Pb
0-2	81.13	8620.74	536.13	1102.94	7.56
2-4	109.90	12746.34	488.59	1002.75	9.68
4-6	82.96	10728.27	569.47	1147.68	9.68
6-8	94.18	7799.70	503.11	974.32	8.24
8-10	100.91	8672.97	525.53	1067.78	9.85
10-12	83.31	8052.91	466.54	1003.73	9.61
12-14	77.15	8348.25	536.44	1047.54	12.29
14-16	57.53	6467.30	569.11	1220.86	10.70
16-18	93.91	10751.11	577.52	1068.90	13.49
18-20	109.68	11811.28	510.84	1002.06	14.32

APPENDIX TWO:
BULK DENSITY



APPENDIX TWO- BULK DENSITY OF GRAVITY CORES

Bulk densities of the diatomaceous sediments were calculated from the weights recorded from the gravity cores. Samples were weighed to give a total sediment weight/porewater before the samples were centrifuged to separate the porewater from the sediment. Once the porewater was separated, the sediment samples were weighed again to give a percentage of pore water recovered. The samples were then dried and reweighed to give the dry weight of the sediment. Total porewater was calculated as sediment and porewater weight minus the dry sediment weight.

Cores Ru102-Ru138 were sampled with a core barrel that has internal volume for the 2 cm separations of 61.36 cm³. The internal volume of the core barrel for cores Ru139-Ru163 is 52.84 cm³ for the 2 cm separations.

Bulk density (g/cm³) is calculated by the dry sediment weight (g) divided by the volume of the sample (cm³). Bulk density (g/g) is calculated by the dry sediment weight (g) divided by the total weight of the sediment containing pore water (g).

Ru102

Depth	Sediment and pore water (g)	Pore water (g)	Dry Sediment (g)	% water (w/w)	Bulk Density (g/cm ³)	Bulk Density (g/g)
0-2	53.50	46.95	6.55	88	0.053	0.126
2-4	51.32	40.73	10.59	79	0.173	0.206
4-6	52.40	45.79	6.61	87	0.108	0.126
6-8	51.03	43.88	7.15	86	0.116	0.140
8-10	50.97	43.80	7.17	86	0.117	0.141
10-12	48.94	42.41	6.54	87	0.107	0.134
12-14	49.73	42.82	6.91	86	0.113	0.139
14-16	54.99	46.24	8.75	84	0.143	0.159
16-18	55.85	47.23	8.62	85	0.140	0.154
18-20	48.73	41.72	7.01	86	0.114	0.144
20-22	55.87	46.31	9.56	83	0.156	0.171
22-24	50.64	41.07	9.57	81	0.156	0.189

Ru103

Depth	Sediment and pore water (g)	Pore water (g)	Dry Sediment (g)	% water (w/w)	Bulk Density (g/cm³)	Bulk Density (g/g)
0-2	-	-	-	-	-	-
2-4	49.08	46.02	3.06	94	0.050	0.062
4-6	46.66	43.92	2.75	94	0.045	0.059
6-8	46.67	43.38	3.30	93	0.054	0.071
8-10	46.11	42.00	4.11	91	0.067	0.089
10-12	36.57	32.90	3.66	90	0.060	0.100
12-14	53.28	48.56	4.72	91	0.077	0.089
14-16	49.46	44.42	5.04	90	0.082	0.102
16-18	16.63	15.03	1.61	90	0.026	0.097
18-20	25.57	22.88	2.70	89	0.044	0.105
20-22	38.64	34.61	4.04	90	0.066	0.104
22-24	54.81	48.62	6.19	89	0.101	0.113
24-26	-	-	-	-	-	-
26-28	34.65	28.98	5.67	84	0.092	0.164
28-30	46.46	39.15	7.31	84	0.119	0.157

Ru104

Depth	Sediment and pore water (g)	Pore water (g)	Dry Sediment (g)	% water (w/w)	Bulk Density (g/cm³)	Bulk Density (g/g)
0-2	49.30	46.59	2.72	94	0.044	0.055
2-4	40.88	37.78	3.10	92	0.050	0.076
4-6	33.26	30.55	2.71	92	0.044	0.081
6-8	33.04	30.36	2.68	92	0.044	0.081
8-10	-	-	-	-	-	-
10-12	53.44	49.43	4.00	93	0.065	0.075
12-14	53.22	48.80	4.42	92	0.072	0.083
14-16	50.83	47.01	3.83	92	0.062	0.075
16-18	38.35	35.43	2.91	92	0.047	0.076
18-20	26.97	24.38	2.60	90	0.042	0.096

Ru105

Depth	Sediment and pore water (g)	Pore water (g)	Dry Sediment (g)	% water (w/w)	Bulk Density (g/cm ³)	Bulk Density (g/g)
0-2	22.78	21.11	1.67	93	0.027	0.073
2-4	45.86	42.17	3.68	92	0.060	0.080
4-6	44.57	40.30	4.27	90	0.070	0.096
6-8	48.95	44.94	4.01	92	0.065	0.082
8-10	51.36	47.31	4.05	92	0.066	0.079
10-12	46.58	42.23	4.35	91	0.071	0.093
12-14	52.11	47.67	4.44	91	0.072	0.085
14-16	56.57	51.08	5.49	90	0.089	0.097
16-18	50.01	45.27	4.74	91	0.077	0.095
18-20	54.59	48.97	5.62	90	0.092	0.103

Ru106

Depth	Sediment and pore water (g)	Pore water (g)	Dry Sediment (g)	% water (w/w)	Bulk Density (g/cm ³)	Bulk Density (g/g)
0-2	50.17	47.48	2.69	95	0.044	0.054
2-4	56.03	52.08	3.95	93	0.064	0.070
4-6	31.23	28.74	2.49	92	0.041	0.080
6-8	46.11	42.79	3.32	93	0.054	0.072
8-10	50.53	46.78	3.75	93	0.061	0.074
10-12	50.35	45.62	4.72	91	0.077	0.094
12-14	50.90	46.69	4.22	92	0.069	0.083
14-16	56.11	50.98	5.13	91	0.084	0.091
16-18	49.69	45.38	4.32	91	0.070	0.087
18-20	50.01	44.73	5.28	89	0.086	0.106

Ru107

Depth	Sediment and pore water (g)	Pore water (g)	Dry Sediment (g)	% water (w/w)	Bulk Density (g/cm ³)	Bulk Density (g/g)
0-2	54.39	49.09	5.30	90	0.086	0.097
2-4	30.80	27.80	3.00	90	0.049	0.097
4-6	56.87	51.84	5.04	91	0.082	0.089
6-8	50.44	46.19	4.25	92	0.069	0.084
8-10	53.00	48.40	4.60	91	0.075	0.087
10-12	56.67	51.01	5.66	90	0.092	0.100
12-14	56.35	49.70	6.65	88	0.108	0.118
14-16	54.13	47.53	6.60	88	0.107	0.122
16-18	49.02	43.43	5.59	89	0.091	0.114
18-20	53.17	45.15	8.03	85	0.131	0.151

Ru108

Depth	Sediment and pore water (g)	Pore water (g)	Dry Sediment (g)	% water (w/w)	Bulk Density (g/cm³)	Bulk Density (g/g)
0-2	53.78	51.42	2.36	96	0.038	0.044
2-4	48.73	45.08	3.65	93	0.059	0.075
4-6	51.73	46.91	4.82	91	0.079	0.093
6-8	47.40	42.39	5.01	89	0.082	0.106
8-10	56.28	50.72	5.56	90	0.091	0.099
10-12	40.51	36.85	3.66	91	0.060	0.090
12-14	49.79	45.41	4.38	91	0.071	0.088
14-16	54.58	48.68	5.90	89	0.096	0.108
16-18	52.86	47.77	5.09	90	0.083	0.096
18-20	53.67	49.78	3.89	93	0.063	0.073

Ru109

Depth	Sediment and pore water (g)	Pore water (g)	Dry Sediment (g)	% water (w/w)	Bulk Density (g/cm³)	Bulk Density (g/g)
0-4	101.08	101.08	8.54	100	0.070	0.084
4-6	50.68	46.62	4.06	92	0.066	0.080
6-8	53.56	48.00	5.55	90	0.090	0.104
8-10	49.87	45.29	4.59	91	0.075	0.092
10-12	50.99	46.72	4.27	92	0.070	0.084
12-14	55.93	50.12	5.82	90	0.095	0.104
14-16	54.27	48.77	5.51	90	0.090	0.101
16-18	53.98	47.51	6.47	88	0.105	0.120
18-20	54.85	48.85	6.00	89	0.098	0.109

Ru110

Depth	Sediment and pore water (g)	Pore water (g)	Dry Sediment (g)	% water (w/w)	Bulk Density (g/cm³)	Bulk Density (g/g)
0-2	37.87	36.29	1.58	96	0.026	0.042
2-4	56.76	51.68	5.08	91	0.083	0.090
4-6	57.03	50.90	6.12	89	0.100	0.107
6-8	55.38	49.56	5.82	89	0.095	0.105
8-10	55.70	49.81	5.88	89	0.096	0.106
10-12	53.15	47.58	5.58	90	0.091	0.105
12-14	58.25	51.13	7.13	88	0.116	0.122
14-16	55.43	48.13	7.30	87	0.119	0.132
16-18	54.49	46.22	8.26	85	0.135	0.152
18-20	52.38	44.25	8.12	84	0.132	0.155

Ru111

Depth	Sediment and pore water (g)	Pore water (g)	Dry Sediment (g)	% water (w/w)	Bulk Density (g/cm ³)	Bulk Density (g/g)
0-2	28.23	26.34	1.89	93	0.031	0.067
2-4	47.17	43.55	3.63	92	0.059	0.077
4-6	52.89	48.54	4.35	92	0.071	0.082
6-8	57.16	53.44	3.72	93	0.061	0.065
8-10	52.08	49.00	3.08	94	0.050	0.059
10-15	93.59	86.30	7.29	92	0.059	0.078
15-18	105.69	97.33	8.35	92	0.068	0.079
18-20	56.13	51.12	5.01	91	0.082	0.089
20-25	110.83	101.00	9.83	91	0.080	0.089
25-30	104.63	92.69	11.94	89	0.097	0.114
30-35	112.20	99.19	13.00	88	0.106	0.116
35-40	110.71	98.67	12.04	89	0.098	0.109
40-45	96.51	84.80	11.71	88	0.095	0.121

Ru112

Depth	Sediment and pore water (g)	Pore water (g)	Dry Sediment (g)	% water (w/w)	Bulk Density (g/cm ³)	Bulk Density (g/g)
0-2	20.51	19.12	1.39	93	0.023	0.068
2-4	55.38	51.49	3.88	93	0.063	0.070
4-6	55.16	50.48	4.68	92	0.076	0.085
6-8	55.79	51.18	4.60	92	0.075	0.083
8-10	58.43	52.66	5.77	90	0.094	0.099
10-12	53.68	48.99	4.69	91	0.076	0.087
12-14	48.29	44.69	3.60	93	0.059	0.075
14-16	57.77	52.07	5.70	90	0.093	0.099
16-18	56.11	50.84	5.27	91	0.086	0.094
18-20	57.71	52.67	5.04	91	0.082	0.087
20-25	113.89	100.79	13.09	89	0.107	0.115
25-30	110.41	94.91	15.49	86	0.126	0.140
30-35	110.19	95.93	14.25	87	0.116	0.129
35-40	109.31	94.62	14.69	87	0.120	0.134
40-43	105.07	89.91	15.16	86	0.124	0.144

Ru114

Depth	Sediment and pore water (g)	Pore water (g)	Dry Sediment (g)	% water (w/w)	Bulk Density (g/cm³)	Bulk Density (g/g)
0	43.82	43.69	0.13	100	0.002	0.003
0-2	50.86	48.58	2.28	96	0.037	0.045
2-4	50.47	44.85	5.62	89	0.092	0.111
4-6	57.83	45.26	12.57	78	0.205	0.217
6-8	69.10	40.23	28.87	58	0.471	0.418

Ru115

Depth	Sediment and pore water (g)	Pore water (g)	Dry Sediment (g)	% water (w/w)	Bulk Density (g/cm³)	Bulk Density (g/g)
0	23.33	23.28	0.05	100	0.001	0.002
0-2	44.92	43.44	1.48	97	0.024	0.033
2-4	42.22	39.70	2.52	94	0.041	0.060
4-6	51.74	45.14	6.60	87	0.108	0.128
6-8	47.42	37.96	9.46	80	0.154	0.200
8-10	71.96	41.28	30.68	57	0.500	0.426
10-12	67.70	38.82	28.88	57	0.471	0.427
12-14	61.74	40.38	21.36	65	0.348	0.346
14-16	58.91	39.21	19.70	67	0.321	0.334
16-18	34.17	20.83	13.34	61	0.217	0.390

Ru116

Depth	Sediment and pore water (g)	Pore water (g)	Dry Sediment (g)	% water (w/w)	Bulk Density (g/cm³)	Bulk Density (g/g)
0-2	42.83	39.24	3.59	92	0.059	0.084
2-4	55.71	50.01	5.70	90	0.093	0.102
4-6	50.93	46.10	4.83	91	0.079	0.095
6-8	45.21	41.20	4.02	91	0.065	0.089
8-10	54.37	49.97	4.40	92	0.072	0.081
10-12	56.28	51.12	5.16	91	0.084	0.092
12-14	54.84	50.46	4.38	92	0.071	0.080
14-16	52.79	47.88	4.91	91	0.080	0.093
16-18	44.55	41.18	3.37	92	0.055	0.076
18-20	54.65	50.79	3.85	93	0.063	0.071
20-22	56.71	49.35	7.35	87	0.120	0.130
22-24	57.14	48.28	8.86	84	0.144	0.155
24-26	50.72	44.56	6.15	88	0.100	0.121
26-28	57.33	48.88	8.45	85	0.138	0.147
28-30	57.24	47.52	9.72	83	0.158	0.170
30-32	56.39	45.50	10.89	81	0.177	0.193
32-34	54.34	43.19	11.15	79	0.182	0.205
34-36	53.24	43.68	9.56	82	0.156	0.180
36-38	48.88	41.29	7.58	84	0.124	0.155
38-40	55.46	45.38	10.08	82	0.164	0.182
40-42	55.05	45.62	9.43	83	0.154	0.171
42-44	55.26	46.40	8.86	84	0.144	0.160
44-46	45.47	38.84	6.63	85	0.108	0.146

Ru117

Depth	Sediment and pore water (g)	Pore water (g)	Dry Sediment (g)	% water (w/w)	Bulk Density (g/cm³)	Bulk Density (g/g)
0-2	46.67	44.40	2.27	95	0.037	0.049
2-4	51.53	48.28	3.25	94	0.053	0.063
4-6	56.42	52.34	4.08	93	0.066	0.072
6-8	53.76	49.68	4.07	92	0.066	0.076
8-10	52.84	49.42	3.42	94	0.056	0.065
10-12	55.15	50.95	4.20	92	0.068	0.076
12-14	55.30	51.00	4.31	92	0.070	0.078
14-16	52.26	47.96	4.31	92	0.070	0.082
16-18	53.86	48.93	4.93	91	0.080	0.092
18-20	55.48	50.90	4.58	92	0.075	0.083
20-22	48.68	44.86	3.83	92	0.062	0.079
22-24	55.04	50.63	4.40	92	0.072	0.080
24-26	49.92	45.83	4.09	92	0.067	0.082
26-28	53.32	47.82	5.50	90	0.090	0.103
28-30	50.03	45.99	4.04	92	0.066	0.081
30-32	53.52	48.65	4.88	91	0.079	0.091
32-34	55.49	49.70	5.80	90	0.094	0.104
34-36	56.63	50.81	5.82	90	0.095	0.103
36-38	55.25	50.13	5.12	91	0.083	0.093
38-40	53.32	46.37	6.95	87	0.113	0.130

Ru118

Depth	Sediment and pore water (g)	Pore water (g)	Dry Sediment (g)	% water (w/w)	Bulk Density (g/cm³)	Bulk Density (g/g)
0-2	18.83	18.72	0.11	99	0.002	0.006
2-4	53.79	51.97	1.82	97	0.030	0.034
4-6	51.17	48.18	2.99	94	0.049	0.058
6-8	53.79	50.19	3.59	93	0.059	0.067
8-10	52.60	48.61	3.99	92	0.065	0.076
10-12	42.66	40.12	2.54	94	0.041	0.060
12-14	52.14	47.50	4.64	91	0.076	0.089
14-16	54.56	50.34	4.22	92	0.069	0.077
16-18	44.51	42.12	2.38	95	0.039	0.054
18-20	53.43	49.19	4.24	92	0.069	0.079
20-22	56.50	52.19	4.32	92	0.070	0.076
22-24	57.47	51.63	5.84	90	0.095	0.102
24-26	55.40	50.25	5.15	91	0.084	0.093
26-28	57.07	49.10	7.97	86	0.130	0.140
28-30	58.77	50.86	7.91	87	0.129	0.135
30-32	55.50	49.05	6.44	88	0.105	0.116
32-34	55.89	49.35	6.54	88	0.107	0.117
34-36	54.70	47.65	7.06	87	0.115	0.129

Ru119

Depth	Sediment and pore water (g)	Pore water (g)	Dry Sediment (g)	% water (w/w)	Bulk Density (g/cm ³)	Bulk Density (g/g)
0-4	100.12	92.93	7.19	93	0.059	0.072
4-6	56.83	52.70	4.13	93	0.067	0.073
6-8	57.89	53.13	4.76	92	0.078	0.082
8-10	53.23	48.59	4.65	91	0.076	0.087
10-12	56.16	51.46	4.70	92	0.077	0.084
12-14	57.22	54.94	2.28	96	0.037	0.040
14-16	55.51	49.21	6.30	89	0.103	0.113
16-18	58.89	52.28	6.61	89	0.108	0.112
18-20	56.27	45.80	10.46	81	0.171	0.186
20-22	54.71	46.68	8.04	85	0.131	0.147
22-24	58.47	49.83	8.65	85	0.141	0.148
24-26	56.08	48.19	7.89	86	0.129	0.141
26-28	55.41	48.72	6.69	88	0.109	0.121
28-30	57.13	49.54	7.58	87	0.124	0.133
30-32	57.91	48.77	9.14	84	0.149	0.158
32-34	58.16	49.51	8.65	85	0.141	0.149
34-36	58.71	49.96	8.75	85	0.143	0.149
36-38	54.87	48.11	6.76	88	0.110	0.123
38-40	59.17	47.30	11.87	80	0.193	0.201
40-42	58.35	46.19	12.16	79	0.198	0.208
42-44	57.25	44.98	12.27	79	0.200	0.214

Ru120

Depth	Sediment and pore water (g)	Pore water (g)	Dry Sediment (g)	% water (w/w)	Bulk Density (g/cm ³)	Bulk Density (g/g)
0-2	49.32	49.30	0.02	100	0.000	0.000
2-4	46.84	45.69	1.15	98	0.019	0.025
4-6	48.35	45.40	2.96	94	0.048	0.061
6-8	52.17	47.50	4.67	91	0.076	0.090
8-10	51.40	47.13	4.27	92	0.070	0.083
10-12	45.04	40.13	4.91	89	0.080	0.109
12-14	53.78	46.22	7.56	86	0.123	0.141
14-16	59.84	50.37	9.48	84	0.154	0.158
16-18	50.25	41.38	8.87	82	0.145	0.176
18-20	63.60	48.65	14.94	77	0.244	0.235
20-22	54.77	38.31	16.46	70	0.268	0.300
22-24	57.80	44.45	13.36	77	0.218	0.231
24-26	59.80	46.32	13.48	77	0.220	0.225
26-28	63.76	47.83	15.92	75	0.260	0.250

Ru121

Depth	Sediment and pore water (g)	Pore water (g)	Dry Sediment (g)	% water (w/w)	Bulk Density (g/cm³)	Bulk Density (g/g)
0-2	44.74	43.25	1.49	97	0.024	0.033
2-4	49.24	47.00	2.24	95	0.037	0.046
4-6	54.65	51.34	3.31	94	0.054	0.061
6-8	55.48	51.91	3.57	94	0.058	0.064
8-10	50.32	47.01	3.30	93	0.054	0.066
10-12	55.31	51.02	4.29	92	0.070	0.078
12-14	55.80	51.10	4.71	92	0.077	0.084
14-16	54.50	50.16	4.34	92	0.071	0.080
16-18	52.63	48.42	4.21	92	0.069	0.080
18-20	58.42	53.68	4.74	92	0.077	0.081
20-22	57.19	51.69	5.50	90	0.090	0.096
22-24	54.67	50.24	4.44	92	0.072	0.081
24-26	56.65	50.96	5.69	90	0.093	0.100
26-28	56.28	49.69	6.60	88	0.107	0.117
28-30	56.80	50.84	5.96	90	0.097	0.105
30-32	54.06	48.93	5.13	91	0.084	0.095
32-34	55.65	50.29	5.36	90	0.087	0.096
34-36	55.02	49.17	5.85	89	0.095	0.106
36-38	54.36	48.46	5.90	89	0.096	0.109
38-40	59.17	51.85	7.32	88	0.119	0.124
40-42	54.67	47.88	6.79	88	0.111	0.124

Ru122

Depth	Sediment and pore water (g)	Pore water (g)	Dry Sediment (g)	% water (w/w)	Bulk Density (g/cm ³)	Bulk Density (g/g)
0	8.92	8.82	0.10	99	0.002	0.011
0-2	55.85	53.96	1.89	97	0.031	0.034
2-4	54.15	51.35	2.80	95	0.046	0.052
4-6	57.62	53.58	4.04	93	0.066	0.070
6-8	55.36	51.86	3.50	94	0.057	0.063
8-10	52.49	48.67	3.82	93	0.062	0.073
10-12	57.03	51.99	5.04	91	0.082	0.088
12-14	53.56	49.48	4.07	92	0.066	0.076
14-16	55.13	50.58	4.56	92	0.074	0.083
16-18	55.06	50.61	4.46	92	0.073	0.081
18-20	55.51	50.42	5.09	91	0.083	0.092
20-22	55.04	50.23	4.81	91	0.078	0.087
22-24	56.85	50.31	6.54	88	0.107	0.115
24-26	55.59	48.85	6.74	88	0.110	0.121
26-28	56.83	50.51	6.32	89	0.103	0.111
28-30	55.85	49.72	6.13	89	0.100	0.110
30-32	57.26	50.50	6.77	88	0.110	0.118
32-34	59.11	50.79	8.33	86	0.136	0.141

Ru123

Depth	Sediment and pore water (g)	Pore water (g)	Dry Sediment (g)	% water (w/w)	Bulk Density (g/cm ³)	Bulk Density (g/g)
0	20.63	20.50	0.13	99	0.002	0.006
0-2	51.25	49.80	1.45	97	0.024	0.028
2-4	50.13	47.93	2.20	96	0.036	0.044
4-6	54.79	51.57	3.22	94	0.052	0.059
6-8	55.06	51.15	3.91	93	0.064	0.071
8-10	55.03	51.59	3.44	94	0.056	0.063
10-12	56.08	52.31	3.77	93	0.061	0.067
12-14	57.71	53.19	4.52	92	0.074	0.078
14-16	53.32	49.04	4.28	92	0.070	0.080
16-18	55.21	51.54	3.68	93	0.060	0.067
18-20	54.12	50.08	4.04	93	0.066	0.075
20-22	52.51	48.48	4.03	92	0.066	0.077
22-24	56.53	51.63	4.89	91	0.080	0.087
24-26	56.98	52.50	4.48	92	0.073	0.079
26-28	55.95	50.10	5.85	90	0.095	0.104
28-30	58.69	49.75	8.94	85	0.146	0.152
30-32	53.84	46.22	7.62	86	0.124	0.142
32-34	45.48	39.56	5.92	87	0.096	0.130

Ru124

Depth	Sediment and pore water (g)	Pore water (g)	Dry Sediment (g)	% water (w/w)	Bulk Density (g/cm ³)	Bulk Density (g/g)
0	55.33	55.31	0.02	100	0.000	0.000
0-2	54.49	53.93	0.57	99	0.009	0.010
2-4	36.23	35.31	0.92	97	0.015	0.025
4-6	53.74	51.93	1.81	97	0.030	0.034
6-8	54.16	50.85	3.31	94	0.054	0.061
8-10	55.28	51.21	4.07	93	0.066	0.074
10-12	55.32	51.62	3.70	93	0.060	0.067
12-14	54.78	50.95	3.82	93	0.062	0.070
14-16	55.64	51.67	3.97	93	0.065	0.071
16-18	51.66	47.43	4.23	92	0.069	0.082
18-20	50.15	47.35	2.81	94	0.046	0.056
20-22	52.55	49.11	3.44	93	0.056	0.065
22-24	56.78	51.91	4.87	91	0.079	0.086
24-26	57.88	52.69	5.19	91	0.085	0.090
26-28	55.88	50.75	5.13	91	0.084	0.092
28-30	55.30	50.15	5.15	91	0.084	0.093
30-32	56.57	48.45	8.12	86	0.132	0.144
32-34	56.57	48.92	7.65	86	0.125	0.135

Ru125

Depth	Sediment and pore water (g)	Pore water (g)	Dry Sediment (g)	% water (w/w)	Bulk Density (g/cm ³)	Bulk Density (g/g)
0	51.18	51.13	0.05	100	0.001	0.001
0-2	51.81	49.97	1.84	96	0.030	0.035
2-4	54.41	52.10	2.31	96	0.038	0.042
4-6	52.99	49.31	3.68	93	0.060	0.069
6-8	53.99	49.23	4.76	91	0.078	0.088
8-10	56.35	51.48	4.88	91	0.079	0.087
10-12	55.35	51.36	3.99	93	0.065	0.072
12-14	56.98	50.24	6.74	88	0.110	0.118
14-16	57.64	50.42	7.22	87	0.118	0.125
16-18	56.46	50.30	6.16	89	0.100	0.109
18-20	55.24	49.50	5.74	90	0.094	0.104
20-22	60.93	51.66	9.28	85	0.151	0.152
22-24	55.34	47.56	7.78	86	0.127	0.141
24-26	56.91	48.93	7.98	86	0.130	0.140
26-28	59.80	50.12	9.68	84	0.158	0.162
28-30	58.84	49.72	9.11	85	0.149	0.155
30-32	58.47	47.51	10.96	81	0.179	0.187
32-40	61.13	47.11	14.01	77	0.228	0.229

Ru126

Depth	Sediment and pore water (g)	Pore water (g)	Dry Sediment (g)	% water (w/w)	Bulk Density (g/cm ³)	Bulk Density (g/g)
0-2	44.96	42.37	2.59	94	0.042	0.058
2-4	35.39	33.07	2.32	93	0.038	0.065
4-6	56.74	52.28	4.46	92	0.073	0.079
6-8	55.20	50.62	4.57	92	0.075	0.083
8-10	56.73	52.89	3.84	93	0.063	0.068
10-12	57.47	52.90	4.56	92	0.074	0.079
12-14	57.16	52.50	4.65	92	0.076	0.081
14-16	54.91	49.94	4.97	91	0.081	0.090
16-18	55.68	51.38	4.30	92	0.070	0.077
18-20	54.77	50.32	4.45	92	0.073	0.081
20-22	56.97	51.60	5.37	91	0.088	0.094
22-24	58.27	53.18	5.09	91	0.083	0.087
24-26	53.18	48.23	4.95	91	0.081	0.093
26-28	58.74	52.37	6.36	89	0.104	0.108
28-30	57.73	52.16	5.57	90	0.091	0.097
30-32	58.16	51.83	6.32	89	0.103	0.109
32-34	58.71	49.37	9.33	84	0.152	0.159
34-36	58.63	50.42	8.21	86	0.134	0.140
36-38	55.69	47.99	7.71	86	0.126	0.138
38-40	59.84	52.10	7.73	87	0.126	0.129
40-42	57.21	49.82	7.39	87	0.120	0.129
42-44	54.15	46.83	7.32	86	0.119	0.135

Ru127

Depth	Sediment and pore water (g)	Pore water (g)	Dry Sediment (g)	% water (w/w)	Bulk Density (g/cm ³)	Bulk Density (g/g)
0	54.30	54.25	0.05	100	0.001	0.001
0-2	55.41	52.95	2.47	96	0.040	0.045
2-4	57.23	53.12	4.10	93	0.067	0.072
4-6	55.79	50.68	5.11	91	0.083	0.092
6-8	58.17	53.09	5.07	91	0.083	0.087
8-10	56.80	51.58	5.22	91	0.085	0.092
10-12	57.21	51.54	5.67	90	0.092	0.099
12-14	55.84	50.16	5.69	90	0.093	0.102
14-16	57.57	50.67	6.90	88	0.112	0.120
16-18	56.30	49.65	6.65	88	0.108	0.118
18-20	53.79	47.77	6.01	89	0.098	0.112
20-22	50.92	42.36	8.55	83	0.139	0.168
22-24	56.87	48.35	8.52	85	0.139	0.150
24-26	56.52	48.27	8.25	85	0.134	0.146
26-28	56.11	47.33	8.78	84	0.143	0.156
28-30	24.24	20.37	3.88	84	0.063	0.160

Ru128

Depth	Sediment and pore water (g)	Pore water (g)	Dry Sediment (g)	% water (w/w)	Bulk Density (g/cm³)	Bulk Density (g/g)
0-2	52.86	48.10	4.76	91	0.078	0.090
2-4	50.86	45.74	5.12	90	0.083	0.101
4-6	55.21	50.83	4.39	92	0.071	0.079
6-8	57.16	52.76	4.40	92	0.072	0.077
8-10	59.46	51.18	8.28	86	0.135	0.139
10-12	57.73	50.72	7.02	88	0.114	0.122
12-14	58.32	51.96	6.36	89	0.104	0.109
14-16	58.80	53.04	5.76	90	0.094	0.098
16-18	58.10	52.71	5.39	91	0.088	0.093
18-20	56.21	50.36	5.85	90	0.095	0.104
20-22	55.04	49.28	5.76	90	0.094	0.105
22-24	57.90	52.17	5.73	90	0.093	0.099
24-26	59.00	51.27	7.73	87	0.126	0.131
26-28	59.20	51.60	7.59	87	0.124	0.128
28-30	57.46	50.60	6.86	88	0.112	0.119
30-32	57.31	50.89	6.41	89	0.105	0.112
32-34	57.36	50.94	6.42	89	0.105	0.112
34-36	59.10	52.54	6.55	89	0.107	0.111
36-38	61.26	52.60	8.66	86	0.141	0.141
38-40	55.71	48.07	7.63	86	0.124	0.137

Ru129

Depth	Sediment and pore water (g)	Pore water (g)	Dry Sediment (g)	% water (w/w)	Bulk Density (g/cm³)	Bulk Density (g/g)
0-2	51.53	47.11	4.42	91	0.072	0.086
2-4	53.69	47.19	6.51	88	0.106	0.121
4-6	42.14	37.85	4.29	90	0.070	0.102
6-8	51.74	45.41	6.33	88	0.103	0.122
8-10	48.85	43.12	5.72	88	0.093	0.117
10-12	50.97	44.87	6.10	88	0.099	0.120
12-14	50.09	44.56	5.53	89	0.090	0.110
14-16	56.58	50.23	6.35	89	0.104	0.112
16-18	50.48	45.05	5.43	89	0.088	0.108
18-20	53.81	46.63	7.18	87	0.117	0.133

Ru130

Depth	Sediment and pore water (g)	Pore water (g)	Dry Sediment (g)	% water (w/w)	Bulk Density (g/cm ³)	Bulk Density (g/g)
0-2	46.03	45.36	0.67	99	0.011	0.014
2-4	59.55	55.71	3.84	94	0.063	0.064
4-6	54.97	49.63	5.33	90	0.087	0.097
6-8	57.05	52.47	4.57	92	0.075	0.080
8-10	49.95	45.60	4.35	91	0.071	0.087
10-12	58.79	54.07	4.73	92	0.077	0.080
12-14	45.96	41.54	4.42	90	0.072	0.096
14-16	57.81	50.18	7.64	87	0.124	0.132
16-18	54.38	48.84	5.54	90	0.090	0.102
18-20	57.98	50.81	7.17	88	0.117	0.124

Ru131

Depth	Sediment and pore water (g)	Pore water (g)	Dry Sediment (g)	% water (w/w)	Bulk Density (g/cm ³)	Bulk Density (g/g)
0-2	42.83	40.37	2.46	94	0.040	0.057
2-4	55.71	52.72	2.99	95	0.049	0.054
4-6	50.93	47.40	3.54	93	0.058	0.069
6-8	45.21	41.37	3.85	91	0.063	0.085
8-10	54.37	50.12	4.24	92	0.069	0.078
10-12	56.28	51.82	4.46	92	0.073	0.079
12-14	54.84	49.73	5.11	91	0.083	0.093
14-16	52.79	48.74	4.04	92	0.066	0.077
16-18	44.55	39.42	5.14	88	0.084	0.115
18-20	54.65	49.93	4.72	91	0.077	0.086

Ru132

Depth	Sediment and pore water (g)	Pore water (g)	Dry Sediment (g)	% water (w/w)	Bulk Density (g/cm ³)	Bulk Density (g/g)
0-2	46.67	44.51	2.15	95	0.035	0.046
2-4	51.53	47.81	3.72	93	0.061	0.072
4-6	56.42	51.43	4.99	91	0.081	0.088
6-8	53.76	47.89	5.87	89	0.096	0.109
8-10	52.84	45.48	7.37	86	0.120	0.139
10-12	55.15	48.25	6.90	87	0.112	0.125
12-14	55.30	46.51	8.80	84	0.143	0.159
14-16	52.26	40.41	11.85	77	0.193	0.227
16-18	53.86	38.66	15.21	72	0.248	0.282
18-20	55.48	39.31	16.17	71	0.264	0.291

Ru133

Depth	Sediment and pore water (g)	Pore water (g)	Dry Sediment (g)	% water (w/w)	Bulk Density (g/cm³)	Bulk Density (g/g)
0-2	18.83	17.56	1.27	93	0.021	0.067
2-4	53.79	51.70	2.09	96	0.034	0.039
4-6	51.17	47.38	3.78	93	0.062	0.074
6-8	53.79	49.74	4.05	92	0.066	0.075
8-10	52.60	48.35	4.25	92	0.069	0.081
10-12	42.66	39.27	3.39	92	0.055	0.080
12-14	52.14	47.72	4.42	92	0.072	0.085
14-16	54.56	50.84	3.72	93	0.061	0.068
16-18	44.51	41.06	3.44	92	0.056	0.077
18-20	53.43	49.13	4.30	92	0.070	0.080

Ru134

Depth	Sediment and pore water (g)	Pore water (g)	Dry Sediment (g)	% water (w/w)	Bulk Density (g/cm³)	Bulk Density (g/g)
0-2	100.12	99.13	0.99	99	0.016	0.010
2-4	56.83	54.43	2.40	96	0.039	0.042
4-6	57.89	53.84	4.06	93	0.066	0.070
6-8	53.23	48.14	5.10	90	0.083	0.096
8-10	56.16	49.86	6.30	89	0.103	0.112
10-12	57.22	50.82	6.40	89	0.104	0.112
12-14	55.51	49.00	6.51	88	0.106	0.117
14-16	58.89	51.63	7.26	88	0.118	0.123
16-18	56.27	49.44	6.83	88	0.111	0.121
18-20	54.71	46.83	7.88	86	0.128	0.144

Ru135

Depth	Sediment and pore water (g)	Pore water (g)	Dry Sediment (g)	% water (w/w)	Bulk Density (g/cm³)	Bulk Density (g/g)
0-2	49.32	47.67	1.65	97	0.027	0.033
2-4	46.84	43.50	3.35	93	0.055	0.071
4-6	48.35	43.75	4.61	90	0.075	0.095
6-8	52.17	46.47	5.70	89	0.093	0.109
8-10	51.40	46.49	4.92	90	0.080	0.096
10-12	45.04	39.81	5.22	88	0.085	0.116
12-14	53.78	47.69	6.09	89	0.099	0.113
14-16	59.84	53.14	6.71	89	0.109	0.112
16-18	50.25	42.79	7.46	85	0.122	0.148
18-20	63.60	56.59	7.00	89	0.114	0.110

Ru136

Depth	Sediment and pore water (g)	Pore water (g)	Dry Sediment (g)	% water (w/w)	Bulk Density (g/cm ³)	Bulk Density (g/g)
0-2	44.74	43.05	1.69	96	0.027	0.038
2-4	49.24	47.30	1.94	96	0.032	0.039
4-6	54.65	51.18	3.47	94	0.056	0.063
6-8	55.48	52.00	3.48	94	0.057	0.063
8-10	50.32	46.23	4.09	92	0.067	0.081
10-12	55.31	51.37	3.94	93	0.064	0.071
12-14	55.80	51.66	4.14	93	0.067	0.074
14-16	54.50	50.27	4.23	92	0.069	0.078
16-18	52.63	47.28	5.36	90	0.087	0.102
18-20	58.42	53.69	4.73	92	0.077	0.081

Ru137

Depth	Sediment and pore water (g)	Pore water (g)	Dry Sediment (g)	% water (w/w)	Bulk Density (g/cm ³)	Bulk Density (g/g)
0-2	89.18	87.66	1.52	98	0.025	0.017
2-4	55.85	53.98	1.87	97	0.030	0.033
4-6	54.15	51.83	2.32	96	0.038	0.043
6-8	57.62	54.62	3.00	95	0.049	0.052
8-10	55.36	51.72	3.64	93	0.059	0.066
10-12	52.49	48.81	3.68	93	0.060	0.070
12-14	57.03	53.62	3.41	94	0.056	0.060
14-16	53.56	48.76	4.80	91	0.078	0.090
16-18	55.13	50.48	4.66	92	0.076	0.084
18-20	55.06	51.09	3.97	93	0.065	0.072

Ru138

Depth	Sediment and pore water (g)	Pore water (g)	Dry Sediment (g)	% water (w/w)	Bulk Density (g/cm ³)	Bulk Density (g/g)
0-2	20.63	20.37	0.25	99	0.004	0.012
2-4	51.25	50.90	0.35	99	0.006	0.007
4-6	50.13	48.71	1.41	97	0.023	0.028
6-8	54.79	51.43	3.36	94	0.055	0.061
8-10	55.06	47.39	7.67	86	0.125	0.139
10-12	55.03	45.19	9.85	82	0.160	0.179
12-13	56.08	53.70	2.38	96	0.039	0.042

Ru139

Depth	Sediment and pore water (g)	Pore water (g)	Dry Sediment (g)	% water (w/w)	Bulk Density (g/cm³)	Bulk Density (g/g)
0-2	39.48	38.11	1.36	97	0.026	0.035
2-4	47.62	45.35	2.27	95	0.043	0.048
4-6	48.47	45.45	3.02	94	0.057	0.062
6-8	54.84	50.84	4.00	93	0.076	0.073
8-10	52.78	48.47	4.31	92	0.082	0.082
10-12	58.62	53.52	5.10	91	0.097	0.087
12-14	53.81	49.04	4.77	91	0.090	0.089
14-16	52.60	46.45	6.14	88	0.116	0.117
16-18	57.86	50.30	7.56	87	0.143	0.131
18-20	49.41	43.89	5.52	89	0.105	0.112

Ru140

Depth	Sediment and pore water (g)	Pore water (g)	Dry Sediment (g)	% water (w/w)	Bulk Density (g/cm³)	Bulk Density (g/g)
0-2	42.21	40.78	1.43	97	0.027	0.034
2-4	47.12	44.99	2.13	95	0.040	0.045
4-6	49.66	46.16	3.51	93	0.066	0.071
6-8	55.17	50.60	4.57	92	0.086	0.083
8-10	52.54	48.04	4.50	91	0.085	0.086
10-12	51.66	46.63	5.03	90	0.095	0.097
12-14	54.28	48.13	6.15	89	0.116	0.113
14-16	53.00	46.98	6.02	89	0.114	0.114
16-18	49.92	44.86	5.06	90	0.096	0.101
18-20	51.08	45.41	5.67	89	0.107	0.111

Ru141

Depth	Sediment and pore water (g)	Pore water (g)	Dry Sediment (g)	% water (w/w)	Bulk Density (g/cm³)	Bulk Density (g/g)
0-2	50.41	49.39	1.03	98	0.019	0.020
2-4	48.68	46.57	2.12	96	0.040	0.043
4-6	44.99	42.70	2.29	95	0.043	0.051
6-8	47.77	44.62	3.15	93	0.060	0.066
8-10	51.39	48.35	3.04	94	0.058	0.059
10-12	50.74	47.43	3.31	93	0.063	0.065
12-14	55.19	50.71	4.48	92	0.085	0.081
14-16	54.79	50.79	4.00	93	0.076	0.073
16-18	56.59	51.73	4.85	91	0.092	0.086
18-20	51.15	47.06	4.09	92	0.077	0.080

Ru142

Depth	Sediment and pore water (g)	Pore water (g)	Dry Sediment (g)	% water (w/w)	Bulk Density (g/cm ³)	Bulk Density (g/g)
0-2	49.29	47.91	1.38	97	0.026	0.028
2-4	47.43	44.87	2.56	95	0.048	0.054
4-6	57.86	53.62	4.24	93	0.080	0.073
6-8	51.73	47.89	3.84	93	0.073	0.074
8-10	51.70	48.09	3.61	93	0.068	0.070
10-12	52.23	48.00	4.23	92	0.080	0.081
12-14	53.18	48.53	4.65	91	0.088	0.087
14-16	51.54	47.61	3.92	92	0.074	0.076
16-18	56.18	51.54	4.64	92	0.088	0.083
18-20	56.47	50.93	5.54	90	0.105	0.098

Ru143

Depth	Sediment and pore water (g)	Pore water (g)	Dry Sediment (g)	% water (w/w)	Bulk Density (g/cm ³)	Bulk Density (g/g)
0-2	39.76	39.10	0.65	98	0.012	0.016
2-4	53.39	51.49	1.90	96	0.036	0.036
4-6	55.38	53.02	2.37	96	0.045	0.043
6-8	55.13	52.62	2.51	95	0.048	0.046
8-10	55.22	51.91	3.30	94	0.062	0.060
10-12	55.69	52.39	3.31	94	0.063	0.059
12-14	57.40	52.96	4.44	92	0.084	0.077
14-16	55.00	50.18	4.82	91	0.091	0.088
16-18	54.94	50.31	4.63	92	0.088	0.084
18-20	48.35	44.53	3.82	92	0.072	0.079

Ru144

Depth	Sediment and pore water (g)	Pore water (g)	Dry Sediment (g)	% water (w/w)	Bulk Density (g/cm ³)	Bulk Density (g/g)
0-2	44.66	43.85	0.81	98	0.015	0.018
2-4	51.70	49.17	2.53	95	0.048	0.049
4-6	55.32	52.27	3.05	94	0.058	0.055
6-8	55.92	51.87	4.05	93	0.077	0.072
8-10	56.97	51.50	5.48	90	0.104	0.096
10-12	50.07	46.68	3.40	93	0.064	0.068
12-14	52.93	48.64	4.29	92	0.081	0.081
14-16	49.20	45.26	3.94	92	0.075	0.080
16-18	53.93	48.47	5.47	90	0.103	0.101
18-20	52.52	48.47	4.05	92	0.077	0.077

Ru145

Depth	Sediment and pore water (g)	Pore water (g)	Dry Sediment (g)	% water (w/w)	Bulk Density (g/cm³)	Bulk Density (g/g)
0-2	41.43	39.76	1.67	96	0.032	0.040
2-4	50.86	46.45	4.41	91	0.084	0.087
4-6	56.28	51.02	5.26	91	0.100	0.093
6-8	57.18	51.82	5.36	91	0.102	0.094
8-10	55.53	51.02	4.52	92	0.085	0.081
10-12	54.02	48.62	5.40	90	0.102	0.100
12-14	55.84	49.98	5.86	90	0.111	0.105
14-16	54.79	49.43	5.36	90	0.101	0.098
16-18	47.77	42.06	5.71	88	0.108	0.120
18-20	51.10	44.59	6.52	87	0.123	0.127

Ru146

Depth	Sediment and pore water (g)	Pore water (g)	Dry Sediment (g)	% water (w/w)	Bulk Density (g/cm³)	Bulk Density (g/g)
0-2	-	-	-	-	-	-
2-4	53.46	49.20	4.26	92	0.081	0.080
4-6	56.09	49.99	6.10	89	0.115	0.109
6-8	47.37	43.26	4.11	91	0.078	0.087
8-10	54.91	49.82	5.09	91	0.096	0.093
10-12	54.77	49.21	5.55	90	0.105	0.101
12-14	51.60	46.07	5.53	89	0.105	0.107
14-16	53.63	47.23	6.40	88	0.121	0.119
16-18	52.28	44.22	8.06	85	0.153	0.154
18-20	49.04	41.67	7.37	85	0.139	0.150

Ru147

Depth	Sediment and pore water (g)	Pore water (g)	Dry Sediment (g)	% water (w/w)	Bulk Density (g/cm³)	Bulk Density (g/g)
0-2	43.86	41.60	2.26	95	0.043	0.051
2-4	46.22	42.72	3.49	92	0.066	0.076
4-6	55.17	49.63	5.54	90	0.105	0.100
6-8	52.56	45.85	6.71	87	0.127	0.128
8-10	49.70	43.39	6.31	87	0.119	0.127
10-12	55.62	48.69	6.93	88	0.131	0.125
12-14	51.25	45.46	5.79	89	0.110	0.113
14-16	56.49	50.53	5.96	89	0.113	0.106
16-18	51.90	44.61	7.30	86	0.138	0.141
18-20	50.64	44.40	6.24	88	0.118	0.123

Ru148

Depth	Sediment and pore water (g)	Pore water (g)	Dry Sediment (g)	% water (w/w)	Bulk Density (g/cm ³)	Bulk Density (g/g)
0-2	78.53	35.77	42.76	46	0.809	0.545
2-4	82.42	37.90	44.52	46	0.842	0.540
4-6	66.82	36.61	30.21	55	0.572	0.452
6-8	48.45	27.06	21.40	56	0.405	0.442
8-10	37.67	20.88	16.79	55	0.318	0.446

Ru149

Depth	Sediment and pore water (g)	Pore water (g)	Dry Sediment (g)	% water (w/w)	Bulk Density (g/cm ³)	Bulk Density (g/g)
0-2	48.66	47.55	1.12	98	0.021	0.023
2-4	59.00	56.83	2.17	96	0.041	0.037
4-6	58.71	56.36	2.36	96	0.045	0.040
6-8	58.92	55.59	3.32	94	0.063	0.056
8-10	58.91	55.81	3.10	95	0.059	0.053
10-12	54.43	51.13	3.30	94	0.062	0.061
12-14	48.97	45.13	3.84	92	0.073	0.078
14-16	56.94	53.12	3.81	93	0.072	0.067
16-18	57.03	52.98	4.05	93	0.077	0.071
18-20	58.64	53.74	4.91	92	0.093	0.084

Ru150

Depth	Sediment and pore water (g)	Pore water (g)	Dry Sediment (g)	% water (w/w)	Bulk Density (g/cm ³)	Bulk Density (g/g)
0-2	48.30	47.66	0.64	99	0.012	0.013
2-4	55.71	53.29	2.41	96	0.046	0.043
4-6	49.05	45.67	3.38	93	0.064	0.069
6-8	55.72	51.54	4.18	93	0.079	0.075
8-10	53.16	48.51	4.65	91	0.088	0.087
10-12	57.13	51.21	5.92	90	0.112	0.104
12-14	53.53	48.83	4.70	91	0.089	0.088
14-16	56.74	51.12	5.62	90	0.106	0.099
16-18	56.70	50.39	6.31	89	0.119	0.111
18-20	56.28	50.47	5.81	90	0.110	0.103

Ru151

Depth	Sediment and pore water (g)	Pore water (g)	Dry Sediment (g)	% water (w/w)	Bulk Density (g/cm³)	Bulk Density (g/g)
0-2	34.03	32.79	1.24	96	0.024	0.037
2-4	56.64	53.90	2.74	95	0.052	0.048
4-6	52.71	49.58	3.13	94	0.059	0.059
6-8	55.44	51.36	4.07	93	0.077	0.073
8-10	56.07	52.62	3.45	94	0.065	0.062
10-12	53.93	50.37	3.55	93	0.067	0.066
12-14	55.29	51.06	4.24	92	0.080	0.077
14-16	48.61	44.83	3.78	92	0.072	0.078
16-18	47.76	44.74	3.02	94	0.057	0.063
18-20	57.72	52.88	4.84	92	0.092	0.084

Ru152

Depth	Sediment and pore water (g)	Pore water (g)	Dry Sediment (g)	% water (w/w)	Bulk Density (g/cm³)	Bulk Density (g/g)
0-2	27.84	25.78	2.06	93	0.039	0.074
2-4	52.24	48.05	4.19	92	0.079	0.080
4-6	49.57	46.02	3.55	93	0.067	0.072
6-8	53.57	49.55	4.02	93	0.076	0.075
8-10	48.75	44.31	4.43	91	0.084	0.091
10-12	54.54	50.96	3.58	93	0.068	0.066
12-14	50.54	47.26	3.28	94	0.062	0.065
14-16	58.65	53.57	5.08	91	0.096	0.087
16-18	57.18	52.31	4.87	91	0.092	0.085
18-20	57.11	51.87	5.24	91	0.099	0.092

Ru153

Depth	Sediment and pore water (g)	Pore water (g)	Dry Sediment (g)	% water (w/w)	Bulk Density (g/cm³)	Bulk Density (g/g)
0-2	43.95	41.91	2.04	95	0.039	0.047
2-4	49.07	46.27	2.80	94	0.053	0.057
4-6	53.46	49.99	3.47	94	0.066	0.065
6-8	56.07	52.64	3.43	94	0.065	0.061
8-10	53.71	50.06	3.65	93	0.069	0.068
10-12	49.26	46.05	3.21	93	0.061	0.065
12-14	57.26	53.37	3.89	93	0.074	0.068
14-16	50.23	46.47	3.77	93	0.071	0.075
16-18	54.81	50.42	4.39	92	0.083	0.080
18-20	53.05	49.55	3.50	93	0.066	0.066

Ru154

Depth	Sediment and pore water (g)	Pore water (g)	Dry Sediment (g)	% water (w/w)	Bulk Density (g/cm ³)	Bulk Density (g/g)
0-2	45.61	41.88	3.73	92	0.071	0.082
2-4	55.79	52.50	3.28	94	0.062	0.059
4-6	57.12	52.84	4.28	93	0.081	0.075
6-8	49.49	45.80	3.69	93	0.070	0.075
8-10	58.08	52.87	5.21	91	0.099	0.090
10-12	57.26	53.11	4.14	93	0.078	0.072
12-14	49.31	44.88	4.43	91	0.084	0.090
14-16	56.67	50.32	6.35	89	0.120	0.112
16-18	55.40	48.75	6.65	88	0.126	0.120
18-20	57.16	49.51	7.65	87	0.145	0.134

Ru155

Depth	Sediment and pore water (g)	Pore water (g)	Dry Sediment (g)	% water (w/w)	Bulk Density (g/cm ³)	Bulk Density (g/g)
0-2	55.72	54.57	1.15	98	0.022	0.021
2-4	59.46	53.76	5.70	90	0.108	0.096
4-6	52.75	45.55	7.20	86	0.136	0.136
6-8	50.49	42.83	7.66	85	0.145	0.152

Ru156

Depth	Sediment and pore water (g)	Pore water (g)	Dry Sediment (g)	% water (w/w)	Bulk Density (g/cm ³)	Bulk Density (g/g)
0-2	50.88	48.45	2.44	95	0.046	0.048
2-4	54.35	50.39	3.97	93	0.075	0.073
4-6	60.35	52.96	7.38	88	0.140	0.122
6-8	55.12	49.09	6.03	89	0.114	0.109
8-10	58.19	52.81	5.38	91	0.102	0.093
10-12	57.24	47.75	9.49	83	0.180	0.166
12-14	54.61	44.23	10.38	81	0.196	0.190
14-16	56.57	45.17	11.40	80	0.216	0.202
16-18	54.48	44.46	10.02	82	0.190	0.184
18-20	55.97	44.99	10.99	80	0.208	0.196

Ru157

Depth	Sediment and pore water (g)	Pore water (g)	Dry Sediment (g)	% water (w/w)	Bulk Density (g/cm ³)	Bulk Density (g/g)
0-2	47.98	44.72	3.26	93	0.062	0.068
2-4	54.33	50.06	4.27	92	0.081	0.079
4-6	58.85	54.08	4.77	92	0.090	0.081
6-8	55.64	51.48	4.16	93	0.079	0.075
8-10	55.22	51.15	4.07	93	0.077	0.074
10-12	55.44	51.39	4.05	93	0.077	0.073
12-14	49.54	45.98	3.56	93	0.067	0.072
14-16	58.21	52.95	5.26	91	0.100	0.090
16-18	57.49	52.81	4.68	92	0.089	0.081
18-20	47.29	44.02	3.26	93	0.062	0.069

Ru158

Depth	Sediment and pore water (g)	Pore water (g)	Dry Sediment (g)	% water (w/w)	Bulk Density (g/cm ³)	Bulk Density (g/g)
0-2	38.52	35.69	2.83	93	0.054	0.073
2-4	51.34	48.46	2.88	94	0.055	0.056
4-6	51.48	48.14	3.34	94	0.063	0.065
6-8	58.13	53.93	4.19	93	0.079	0.072
8-10	58.63	53.31	5.32	91	0.101	0.091
10-12	54.58	50.56	4.03	93	0.076	0.074
12-14	47.91	45.20	2.72	94	0.051	0.057
14-16	56.21	52.16	4.05	93	0.077	0.072
16-18	55.36	51.43	3.92	93	0.074	0.071
18-20	57.50	53.43	4.07	93	0.077	0.071

Ru159

Depth	Sediment and pore water (g)	Pore water (g)	Dry Sediment (g)	% water (w/w)	Bulk Density (g/cm ³)	Bulk Density (g/g)
0-2	54.54	53.67	0.88	98	0.017	0.016
2-4	54.44	51.94	2.49	95	0.047	0.046
4-6	57.85	54.05	3.80	93	0.072	0.066
6-8	53.40	49.60	3.79	93	0.072	0.071
8-10	57.06	53.33	3.72	93	0.070	0.065
10-12	58.50	55.03	3.47	94	0.066	0.059
12-14	59.50	55.55	3.95	93	0.075	0.066
14-16	56.76	51.76	5.00	91	0.095	0.088
16-18	55.22	48.74	6.48	88	0.123	0.117
18-20	56.07	48.21	7.86	86	0.149	0.140

Ru160

Depth	Sediment and pore water (g)	Pore water (g)	Dry Sediment (g)	% water (w/w)	Bulk Density (g/cm ³)	Bulk Density (g/g)
0-2	53.23	50.93	2.30	96	0.044	0.043
2-4	50.00	46.61	3.40	93	0.064	0.068
4-6	55.88	51.69	4.19	93	0.079	0.075
6-8	53.84	50.10	3.73	93	0.071	0.069
8-10	58.03	54.36	3.66	94	0.069	0.063
10-12	56.22	52.41	3.81	93	0.072	0.068
12-14	55.87	51.50	4.37	92	0.083	0.078
14-16	57.49	52.46	5.03	91	0.095	0.087
16-18	56.75	51.18	5.57	90	0.105	0.098
18-20	56.51	52.34	4.17	93	0.079	0.074

Ru161

Depth	Sediment and pore water (g)	Pore water (g)	Dry Sediment (g)	% water (w/w)	Bulk Density (g/cm ³)	Bulk Density (g/g)
0-2	49.23	45.55	3.68	93	0.070	0.075
2-4	51.70	47.59	4.11	92	0.078	0.079
4-6	57.04	52.46	4.58	92	0.087	0.080
6-8	53.34	49.28	4.07	92	0.077	0.076
8-10	51.39	48.37	3.02	94	0.057	0.059
10-12	58.30	54.32	3.98	93	0.075	0.068
12-14	56.95	52.49	4.46	92	0.084	0.078
14-16	57.12	53.02	4.10	93	0.078	0.072
16-18	55.67	51.04	4.63	92	0.088	0.083
18-20	58.21	52.71	5.50	91	0.104	0.095

Ru162

Depth	Sediment and pore water (g)	Pore water (g)	Dry Sediment (g)	% water (w/w)	Bulk Density (g/cm ³)	Bulk Density (g/g)
0-2	54.33	50.11	4.23	92	0.080	0.078
2-4	47.27	43.45	3.83	92	0.072	0.081
4-6	57.66	53.38	4.28	93	0.081	0.074
6-8	56.44	53.17	3.27	94	0.062	0.058
8-10	54.81	50.60	4.21	92	0.080	0.077
10-12	54.52	50.59	3.93	93	0.074	0.072
12-14	51.64	47.77	3.88	92	0.073	0.075
14-16	59.74	54.30	5.44	91	0.103	0.091
16-18	56.02	51.36	4.66	92	0.088	0.083
18-20	56.54	50.38	6.16	89	0.117	0.109

Ru163

Depth	Sediment and pore water (g)	Pore water (g)	Dry Sediment (g)	% water (w/w)	Bulk Density (g/cm³)	Bulk Density (g/g)
0-2	45.05	42.18	2.87	94	0.054	0.064
2-4	54.18	50.76	3.42	94	0.065	0.063
4-6	55.88	52.00	3.88	93	0.073	0.069
6-8	57.42	53.52	3.90	93	0.074	0.068
8-10	57.34	52.71	4.63	92	0.088	0.081
10-12	54.56	50.59	3.97	93	0.075	0.073
12-14	58.05	54.27	3.78	93	0.072	0.065
14-16	48.68	45.11	3.56	93	0.067	0.073
16-18	58.20	52.98	5.22	91	0.099	0.090
18-20	55.60	50.53	5.07	91	0.096	0.091

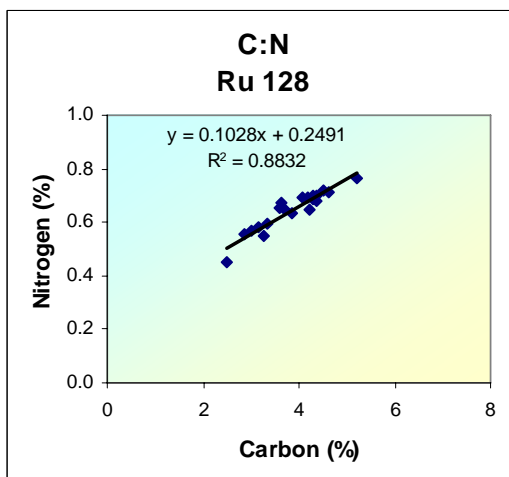
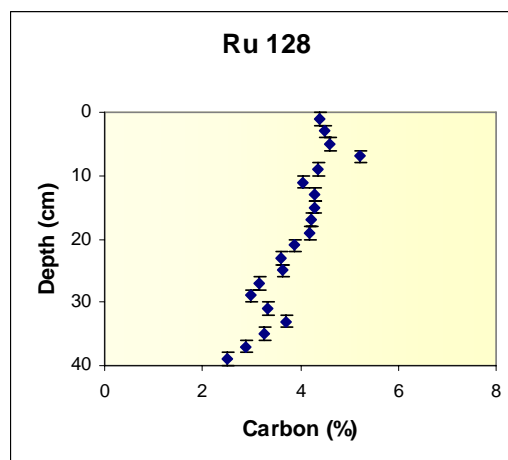
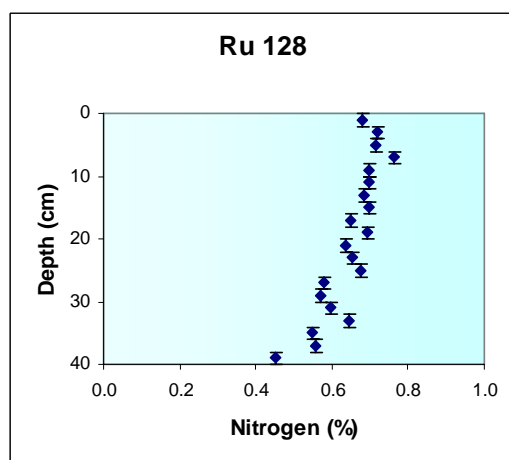
APPENDIX THREE:

CARBON AND NITROGEN



APPENDIX THREE- CARBON AND NITROGEN

Sample	% N	% C	C:N Ratio
1	0.68	4.39	6.47
3	0.72	4.50	6.27
5	0.72	4.62	6.45
7	0.76	5.22	6.82
9	0.70	4.35	6.24
11	0.70	4.06	5.84
13	0.68	4.30	6.29
15	0.70	4.29	6.13
17	0.65	4.21	6.50
19	0.69	4.18	6.02
21	0.64	3.87	6.09
23	0.66	3.61	5.51
25	0.67	3.64	5.40
27	0.58	3.15	5.44
29	0.57	3.00	5.28
31	0.60	3.35	5.60
33	0.65	3.70	5.73
35	0.55	3.27	5.98
37	0.56	2.87	5.15
39	0.45	2.50	5.52



APPENDIX FOUR:

SUB-BOTTOM TRACK DESCRIPTIONS



APPENDIX FOUR- SUB-BOTTOM PROFILING TRACK DESCRIPTIONS

Sub-bottom profile tracks were run simultaneously with the multibeam survey. The echo sounder produces an image of the stratigraphy of the sediment directly below the boat. The descriptions made and images produced are from the lower 33 kHz frequency, which gives better definition of sediment stratigraphy.

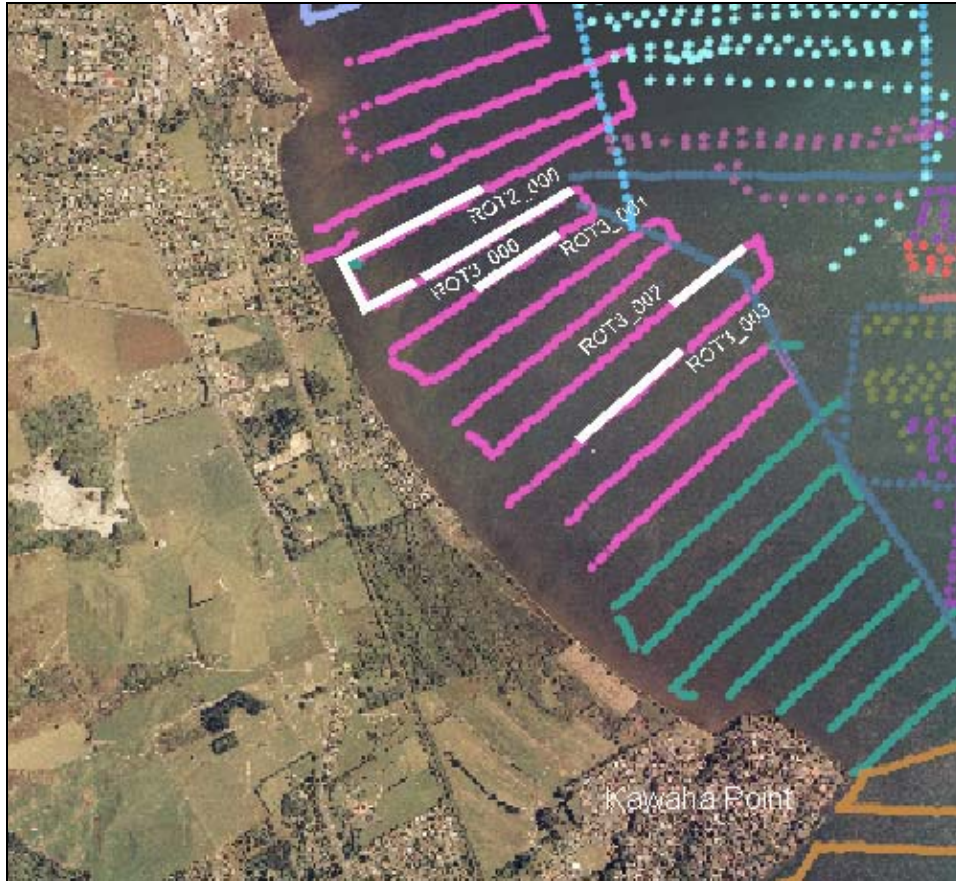
Data processing of the sub-bottom profile tracks was undertaken by Brad Scarfe, (Coastal Marine Group at the University of Waikato). The sub-bottom data is saved as text files and converted into *ArcGIS* format to produce an *ArcMap* file and *ArcGIS* geodatabase file, which is used to locate the sub-bottom profile tracks on Lake Rotorua.

Post Survey was used to view the tracks from the echo-sounder to describe the tracks and identify features of interest on the lake bed. The date and time parameter in NZST or NZDT was recorded for the start and end of the track and converted to UTC (NZST-12h). In *ArcMap* the track lines can be identified by selecting the times between the beginning and end of the track in the attribute table. Select 'Selection' off the task bar and click on 'zoom to selected features' and the track will be highlighted. Zooming in closer will reveal more information. Track lines are identified in white and labeled with the track file name at the start of the track.

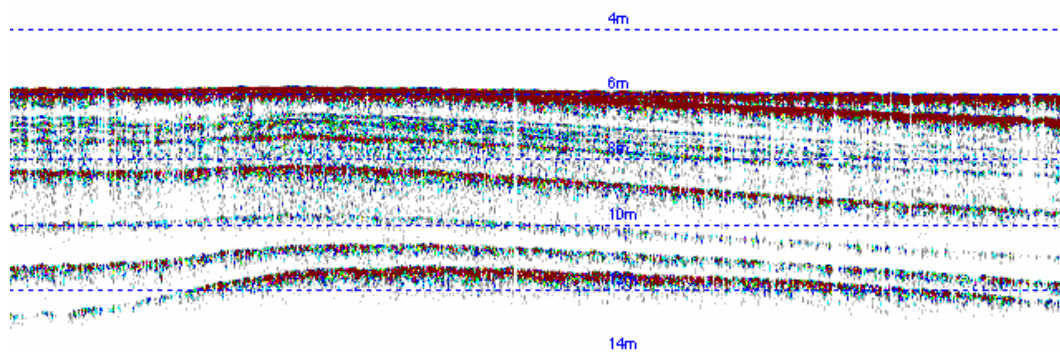
The track lines (which can be viewed using Sounder Suite software), the *ArcMap* document and associated files are included on DVD at the back of this thesis. Not all track lines were recorded for sub-bottom profiling, therefore unless identified it is not possible to view the sub-bottom track.

DAY 1 29th August 2006

Day 1 tracks are located north of Kawaha Point. Water depth ranges from 2.5 to 10 m. The lake sediment is predominantly coarse sands and gravels in this area.



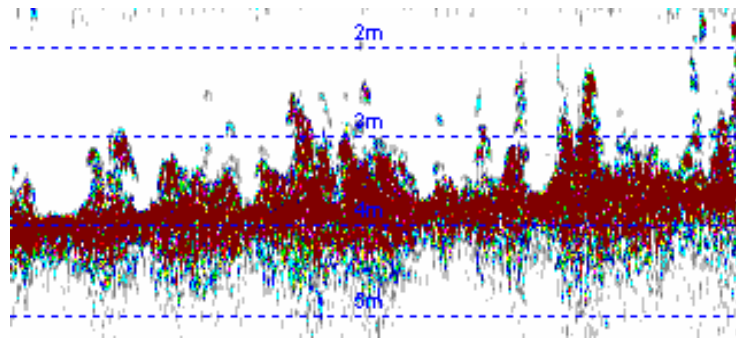
ROT1_000 6 m water depth. Stratigraphy visible for 6 m below surface.



ROT2_000 Short track in less than 2 m water depth. No stratigraphy visible.

ROT3_000 From 4 m to 8 m water depth. No stratigraphy. Not well defined lake floor.

ROT3_001 Short track 4 m water depth. Interference with lake weed.

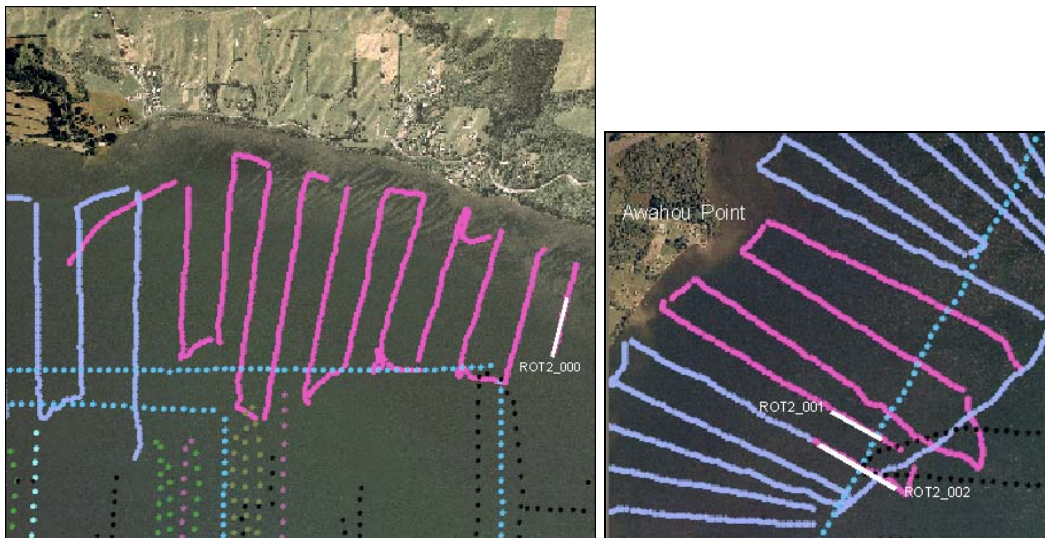


ROT3_002 Short track in 10 m of water. Faint stratigraphy 1m and 2 m below sediment surface.

ROT3_003 7 m water depth. Stratigraphy visible until decreases to 1 m water depth.

DAY 2 30th August 2006

ROT2_000 is located to the north of the lake, east of Hamurana, in water depths reaching 15 m. The remainder of the Day 2 tracks are situated off Awahou Point. The water depths in this area reach 10 m. The lake sediment is predominantly coarse sands and gravels in this area.



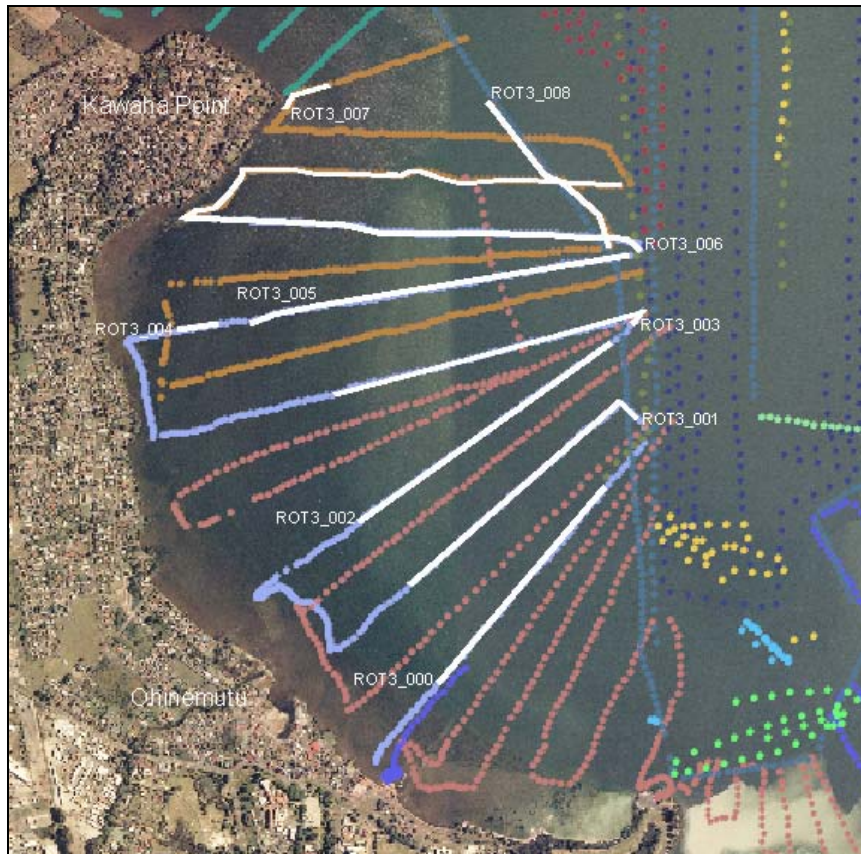
ROT2_000 Less than 1 m water depth. No stratigraphy.

ROT2_001 Decreasing from 4 m to 10 m water depth. No stratigraphy

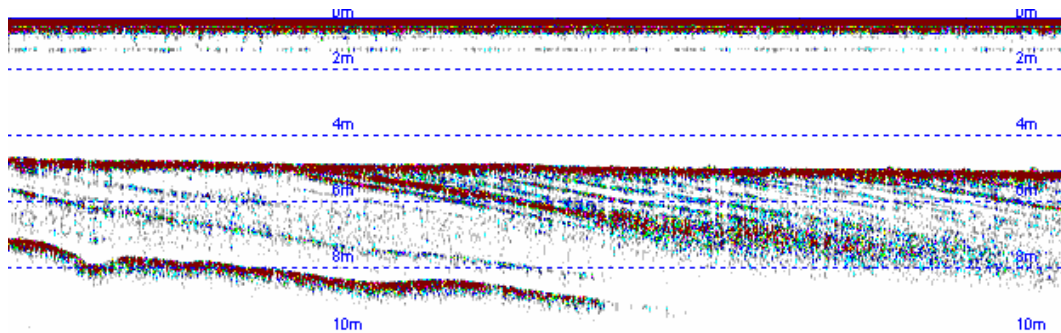
ROT2_002 10 m water depth. Transition from gas filled sediment to sediment with out gas. Stratigraphy not very visible.

DAY 3 31st August 2006

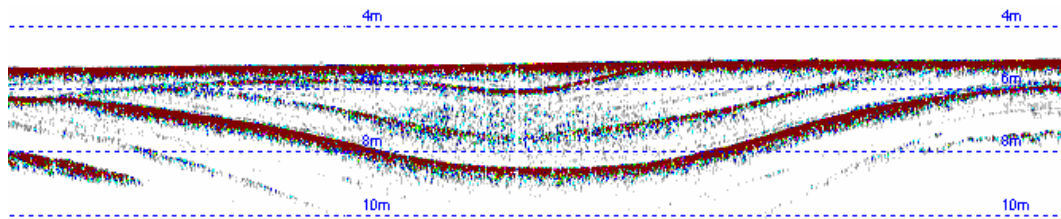
Day 3 tracks are located on the western side of the lake between Ohinemutu and Kawaha Point. The tracks are in shallow water reaching 10 m. The lake sediment is predominantly coarse sands and gravels in this area.



ROT3_000 5 m water depth. Stratigraphy on a 25-30° angle sloping towards the deeper water. Transition to gas sediment where stratigraphy lost.



ROT3_001 8 m decreasing to 4 m water depth. Stratigraphy visible showing depressions that have been infilled and areas that have had erosion of the surface sediment before being buried under new sediment.

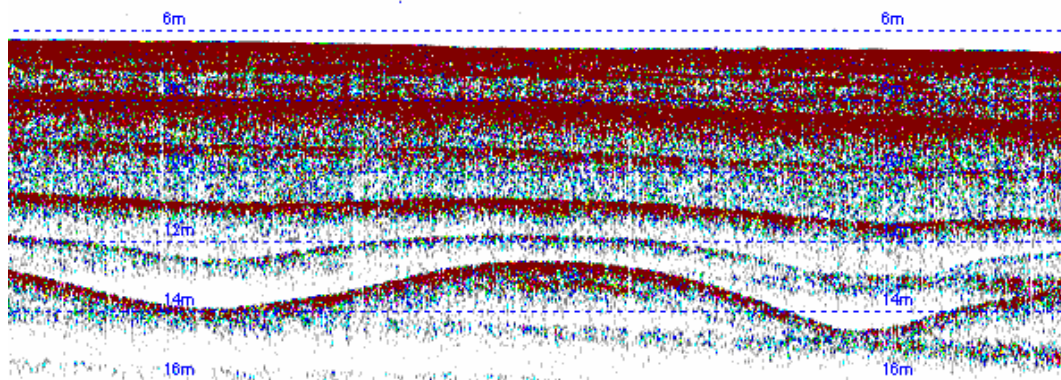


ROT3_002 6 m to 10 m water depth. Stratigraphy visible but frequency too high for a clear image of the sediment. Possibility of multiples interfering with record in the shallow water.

ROT3_003 Very short track over lake weed.

ROT3_004 Very short track over lake weed.

ROT3_005 6 m to 10 m water depth. Stratigraphy showing depressions 6 m below sediment surface that have been infilled to a flat surface at the water interface. Up to 6 layers of sediment visible.



ROT3_006 8 m water depth. Stratigraphy visible. One distinct layer 3 m below surface possibly Kaharoa.

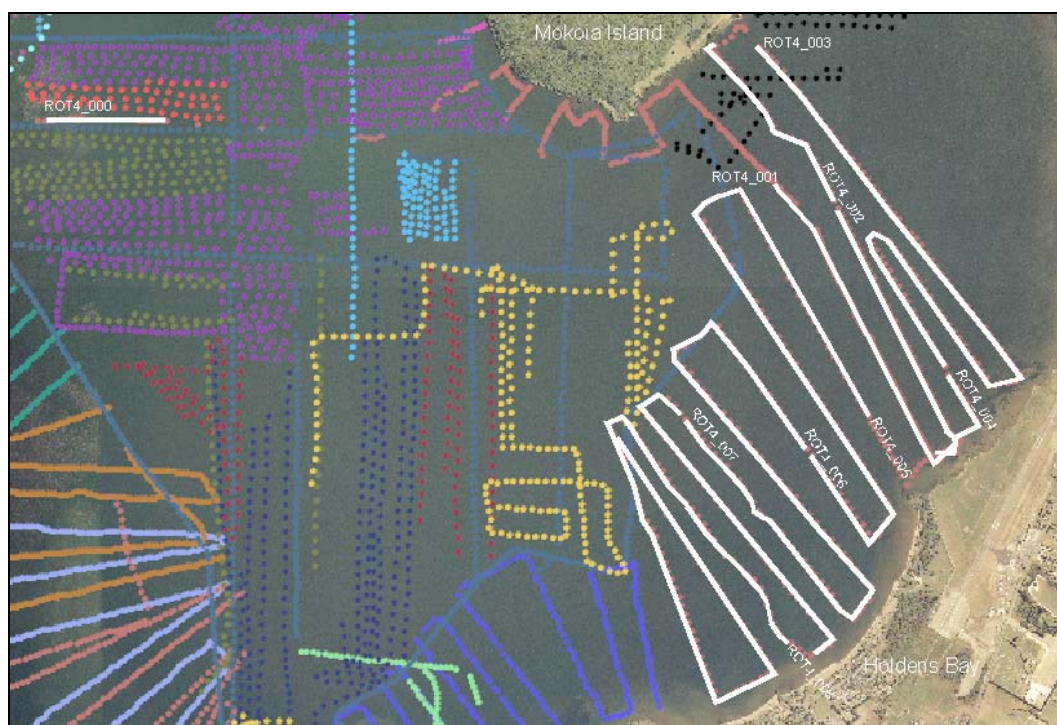
ROT3_007 Short profile in 3 m water. Stratigraphy visible.

ROT3_008 8 m of water depth showing shallow stratigraphy 2 m below the sediment interface.

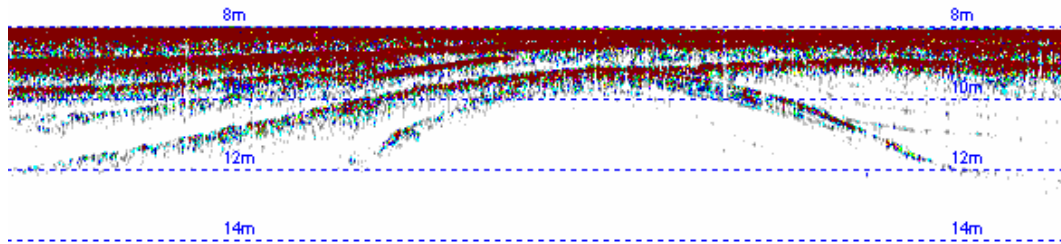
DAY 4 7th September 2006

Day 4 tracks are located from Hinemoa point to Hannahs Bay, with the exception of ROT4_000, which is found on the western side of the lake. The sediment is dominated by sands and gravels near shore and transition into diatomaceous

sediment at approximately 10 m water depth. Most of the track lines extend from the shore to the 10 m depth contour.

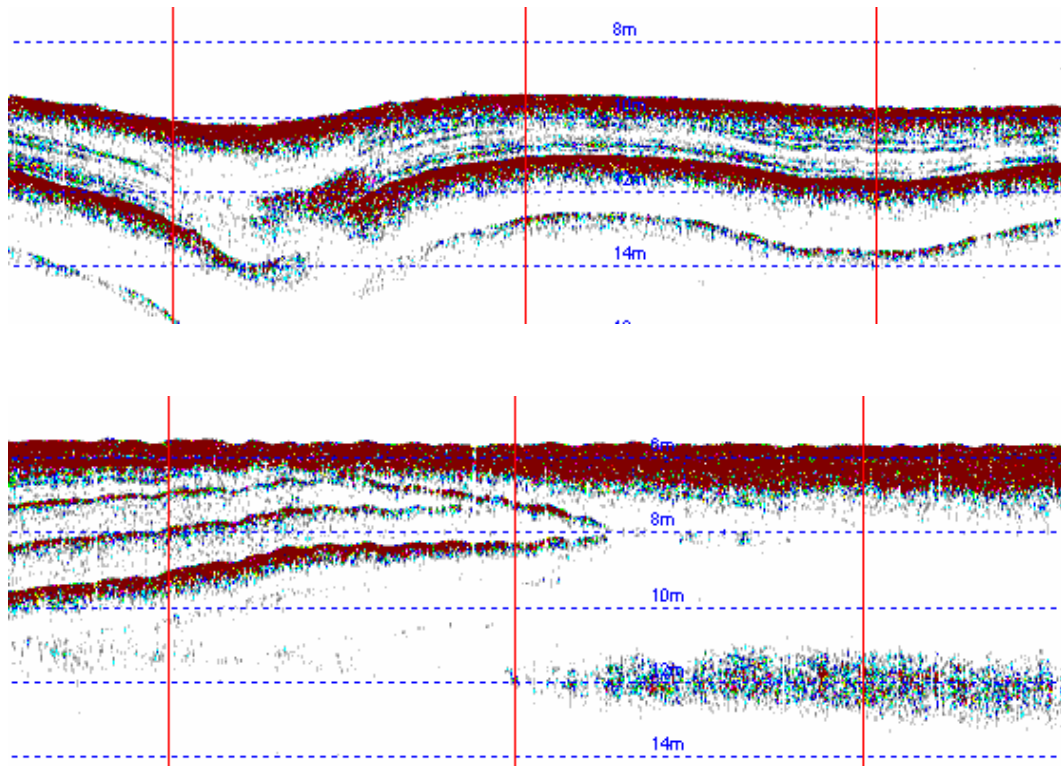


ROT4_000	14 m of water over lying gas filled sediment, stratigraphy not visible.
ROT4_001	8 m of water showing stratigraphy. Predominantly linear with few depressions that have been infilled.
ROT4_002	8 m water depth decreasing to 12 m. Transition from non gaseous sediment to gas filled sediment where stratigraphy is masked. Multiples of lake floor present.
ROT4_003	16 m of water decreasing to 9 m. Gas filled sediment to non gas sediment where stratigraphy visible. 2 distinct layers within 3 m of sediment-water interface. Track line crosses an area in 4 m water depth showing same stratigraphy as the deeper water.
ROT4_004	6 m of water decreasing to 3 m. Stratigraphy visible.
ROT4_005	8 m of water. Stratigraphy shows mounds and depressions in the multiple sediment layers that have been buried as sediment surface is flat. Prograding layers at the top of the mounds.

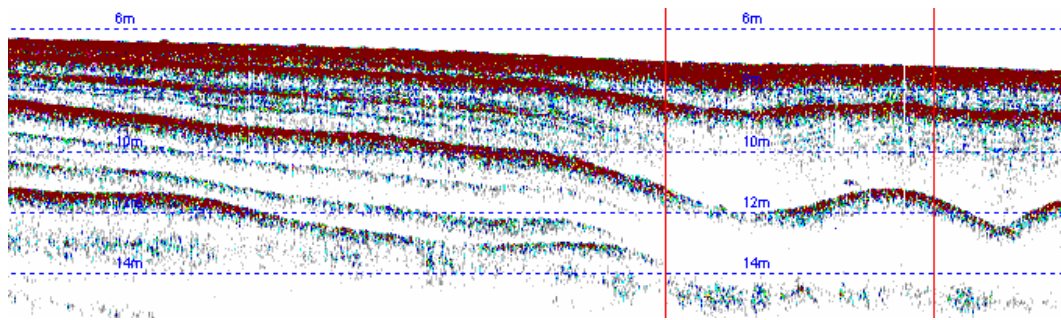


ROT4_006 Generally between 8 and 5 m water depth although does decrease to 2 m in middle of track line. Stratigraphy visible. and depressions in the multiple sediment layers that have been buried as sediment surface is flat.

ROT4_007 10 m rising to 6 m water depth. Depressions in the sediment which is matched by the stratigraphy. Stratigraphy is lost and reflection multiples are seen.



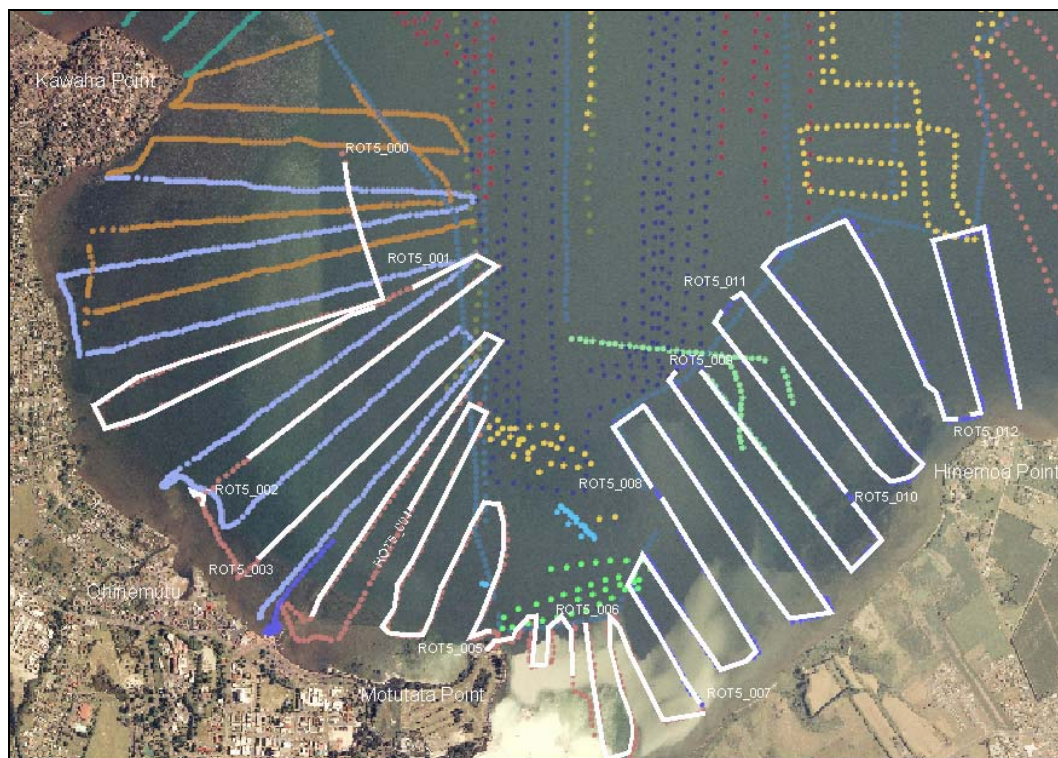
ROT4_008 3 m water depth and increases to 8 m. Stratigraphy flat until depth increases and mounds and depressions are seen in buried layers. Multiple layers seen up to 8 m into the sediment.



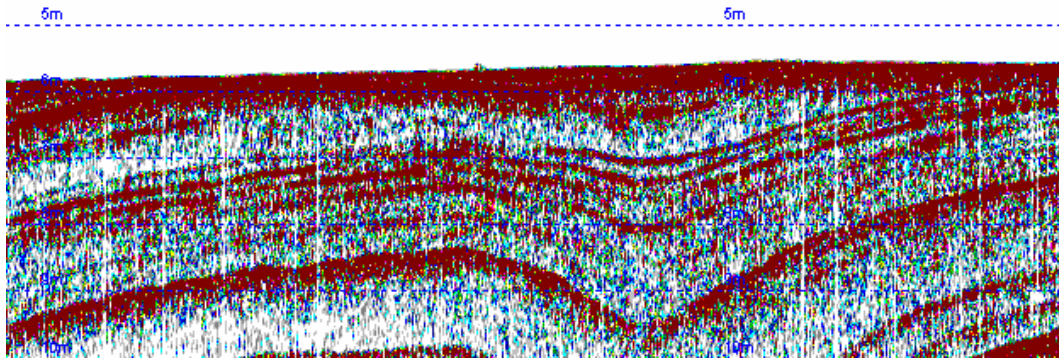
ROT4_009 Short track in 9 m water depth. Stratigraphy visible.

DAY 5 8th September 2006

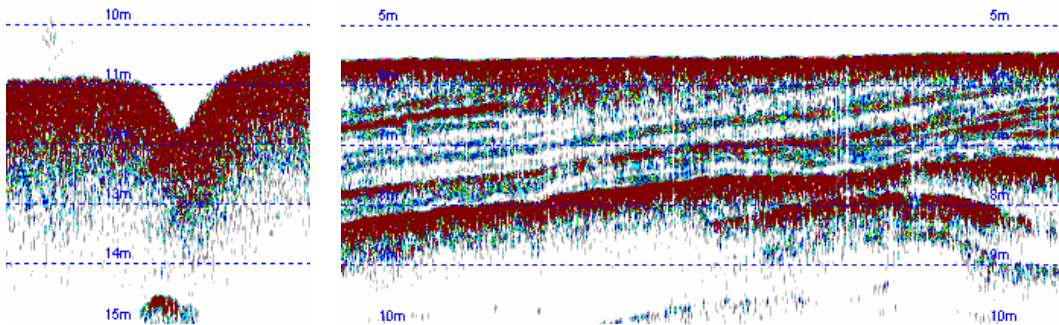
Day 5 tracks are located at the southern end of the lake. The sediment is dominated by sands and gravels near shore and transition into diatomaceous sediment at approximately 10 m water depth. Most of the track lines extend from the shore to the 10 m depth contour.



ROT5_000 5 to 6 m water depth showing stratigraphy. Multiples of surface seen at 10-12 m depth.



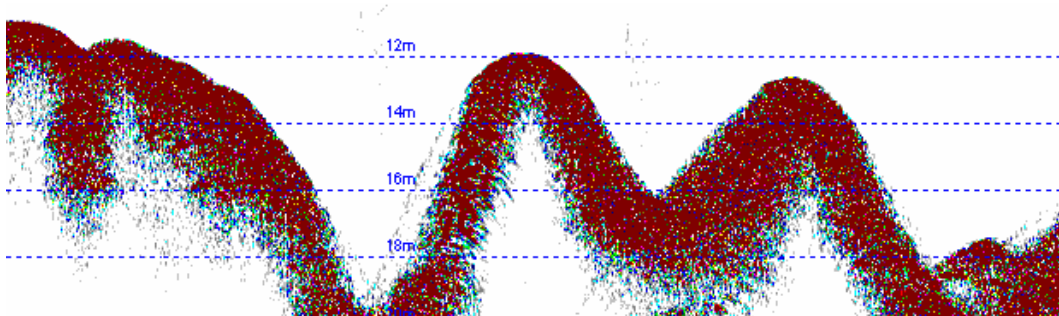
ROT5_001 12 m water depth decreasing to 5 m. Gas in sediment deeper than 7 m so stratigraphy not seen. Small pock marks present where gas has escaped from the sediment making underlying stratigraphy visible and a small depression at the sediment surface. Sediment laminated on an approximate 25° angle.



ROT5_002 Short transect in 3 m water depth. Stratigraphy not well defined.

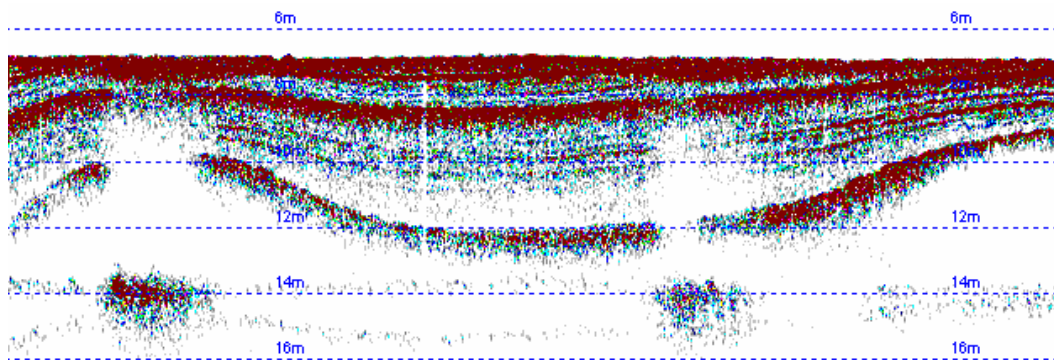
ROT5_003 5 to 10 m water depth. Interference with gas and lake weed affects visibility of sediment layers.

ROT5_004 Stratigraphy not seen. 14 m water depth with abrupt changes in water depth, possibly pockmarks or in an area with hydrothermal disturbance.



ROT5_005 2-3 m water depth. Stratigraphy hard to determine. Abrupt changes in water depth to 12 m, where stratigraphy is masked by gas in the sediment.

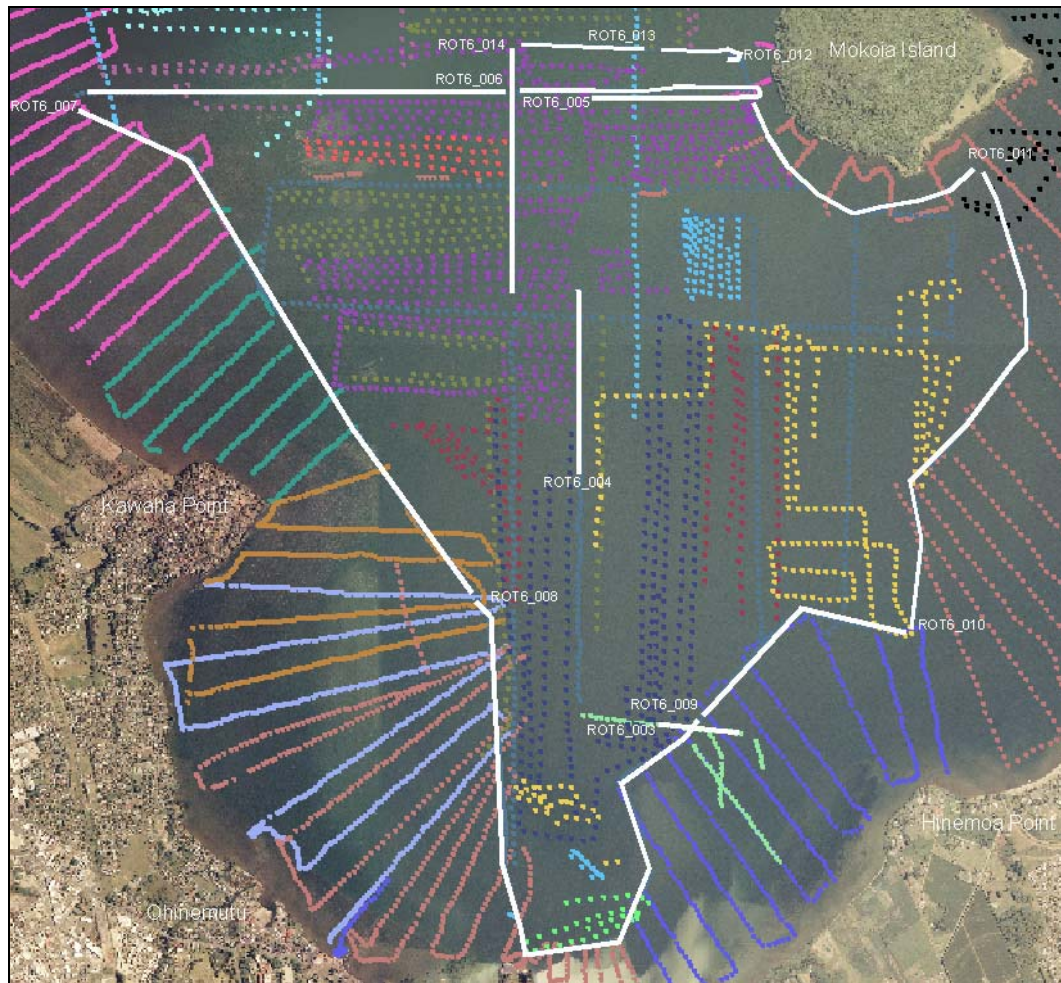
- ROT5_006 Gas filled sediment in 3 to 12 m water depth. Many multiples.
- ROT5_007 Stratigraphy not visible clearly due to shallowness of water depth.
- ROT5_008 Stratigraphy not visible clearly for first half of track possibly due to lake weed. In 7 m water depth buried depressions visible.



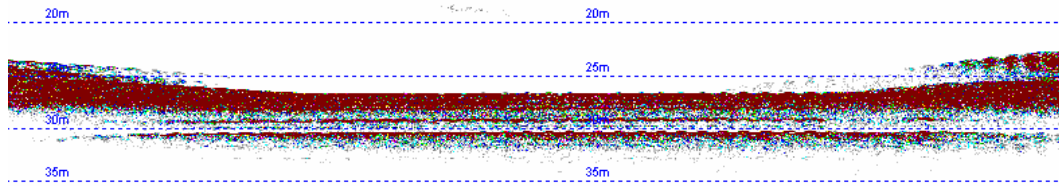
- ROT5_009 In 9 m water depth buried depressions visible. Look very similar to above image.
- ROT5_010 Very shallow dropping to 8 m water depth. Stratigraphy shows faint linear laminations with few depressions that have been infilled.
- ROT5_011 Between 8 and 10 m water depth. Stratigraphy shows faint linear laminations with few depressions that have been infilled.
- ROT5_012 Between 5 and 10 m water depth. Stratigraphy shows faint linear laminations with some 4 m deep depressions that have been infilled.

DAY 6 12th September 2006

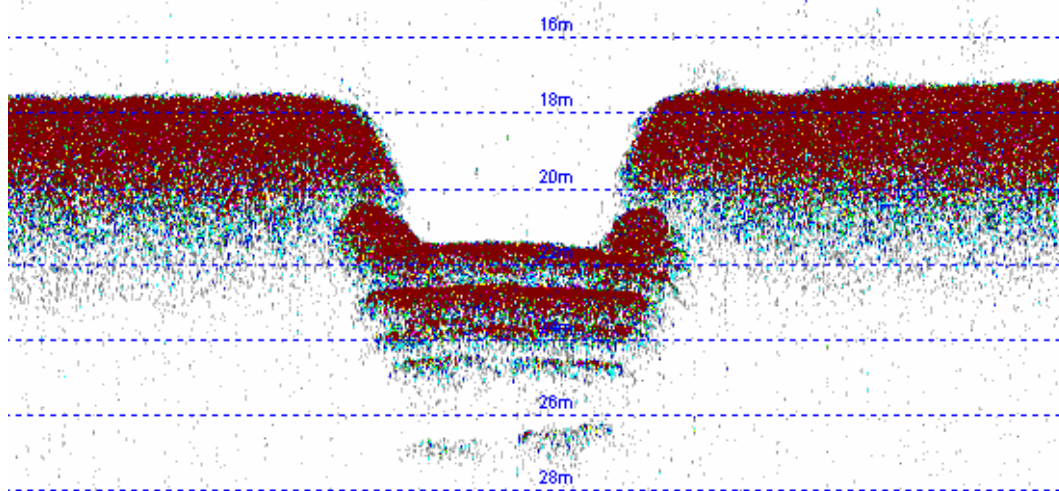
Day 6 tracks are located from Mokoia Island to the south of the lake. The majority of the track lines follow the 10 m depth contour. The sediment transitions from coarse gravels to diatomaceous ooze in water depths greater than 10 m.



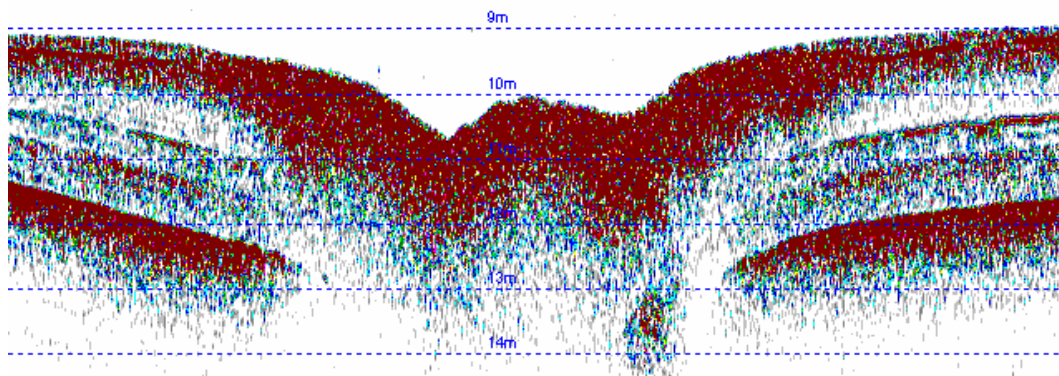
- ROT6_000 Water depths greater than 20 m. Gas filled sediment.
- ROT6_001 Water depths reach 40 m. Sediment surface very uneven as this area crosses hydrothermal explosion craters near the southern end of the lake. Sediment shows no stratigraphy and is possibly fill with gas.
- ROT6_002 7 m water depth showing shallow stratigraphy. Multiples present.
- ROT6_003 Stratigraphy seen from 9 to 10 m water depth lost as water depths increase deeper than 16 m.
- ROT6_004 20 m water depth. No clear image seen.
- ROT6_005 Around 20 m water depth. Very large, approximately 5 m deep pock mark at 25.5 m water depth. Stratigraphy can be seen under pockmark suggesting gas had been lost from the sediment. The location of this site is to the west of Mokoia Island, close to the island.



ROT6_006 20 m water depth. No stratigraphy seen due to the presence of gas. Large pock mark present which is approximately 4 m deep.

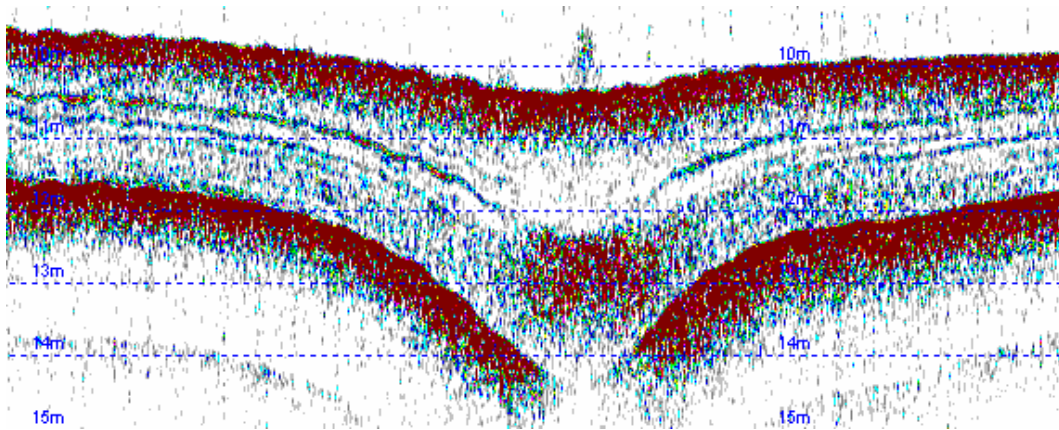


ROT6_007 Complex stratigraphy in water depths 10 -12 m deep. Sediment is often saturated with gas. There are areas where stratigraphy visibility is lost and sediment surface becomes uneven.

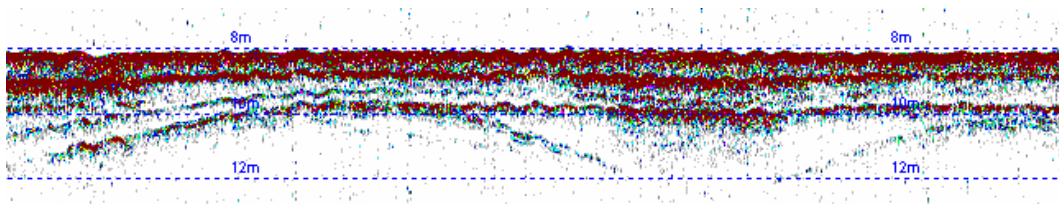


ROT6_008 Gas filled and uneven surfaces make stratigraphy impossible to see clearly.

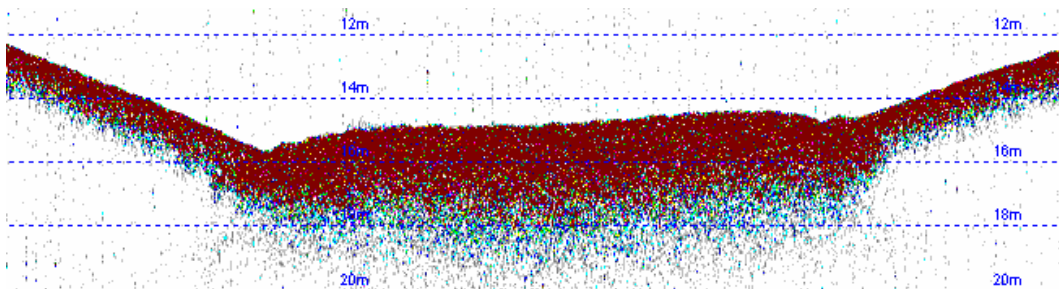
ROT6_009 10 m water depth. Series of mounds that stratigraphy is lost below. Suggests areas have gas in the sediment. Possible discharge of gas from the sediment visible in the following image.



ROT6_010 Water depths around 8 to 10 m. Sediment stratigraphy clear showing 2 clear layers that follow the incline of the sediment surface. A layer under these has large depressions which have been filled in before the deposition of the above layers.



ROT6_011 Section similar to previous track in 10 m of water. There are 2 depressions that seem to have accumulated a larger amount of softer sediment.



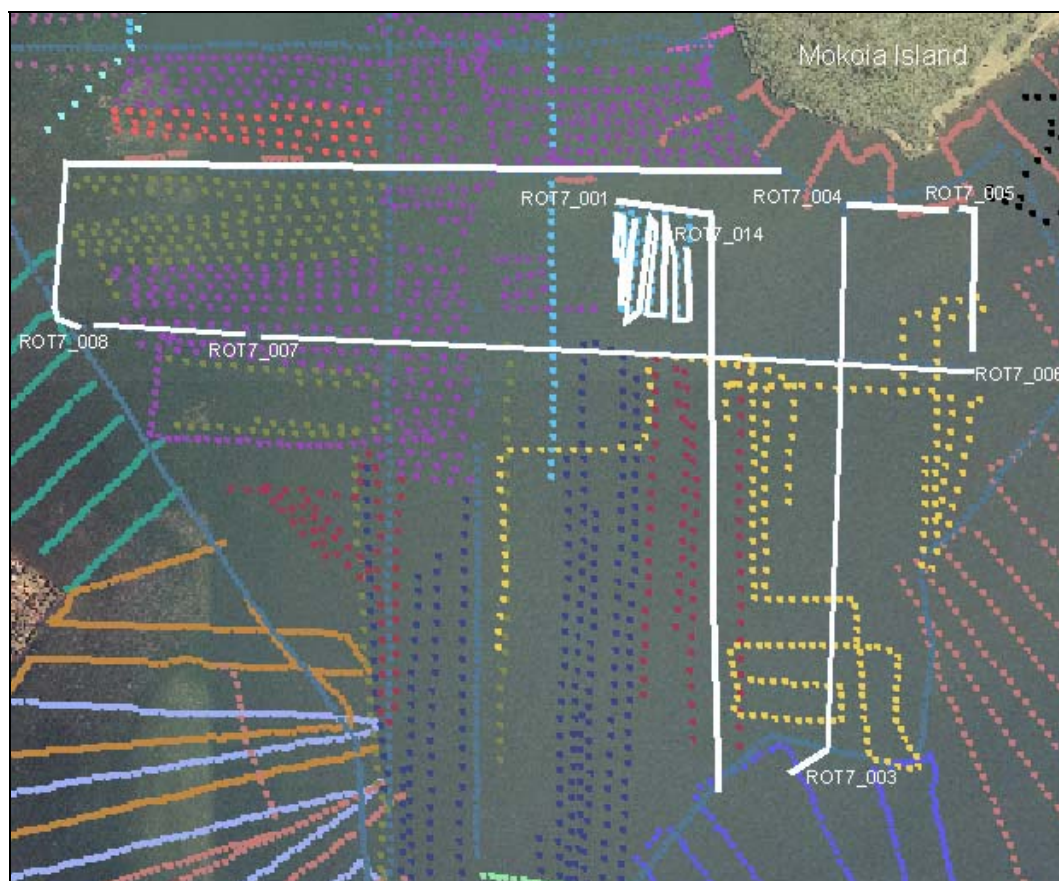
ROT6_012 18 to 24 m water depth. Thick soft sediment. No stratigraphy visible.

ROT6_013 22 m water depth. Thick soft sediment. No stratigraphy visible.

ROT6_014 Decreases in water depth from 18 m to 14m. At 14m water depth stratigraphy is visible showing at least 4 distinct layers. Transitions into a water depth of 10 m where stratigraphy is lost and sediment becomes obviously softer as thickness of surface increases.

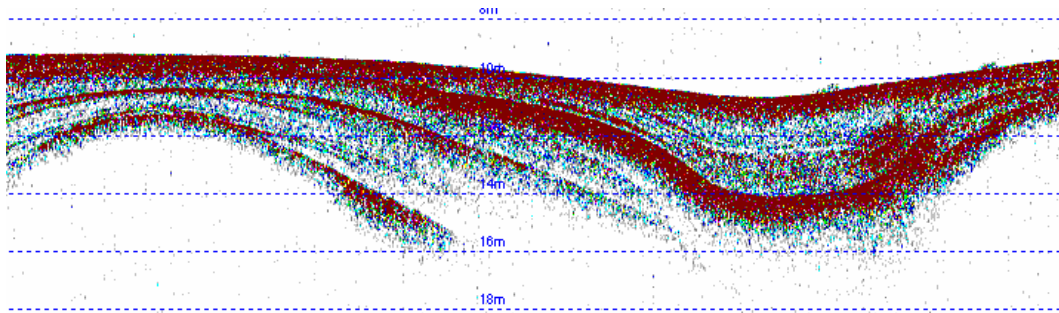
DAY 7 13th September 2006

Day 7 tracks are located south of Mokoia Island in water depths greater than 10 m. The sediment in this area is diatomaceous ooze.

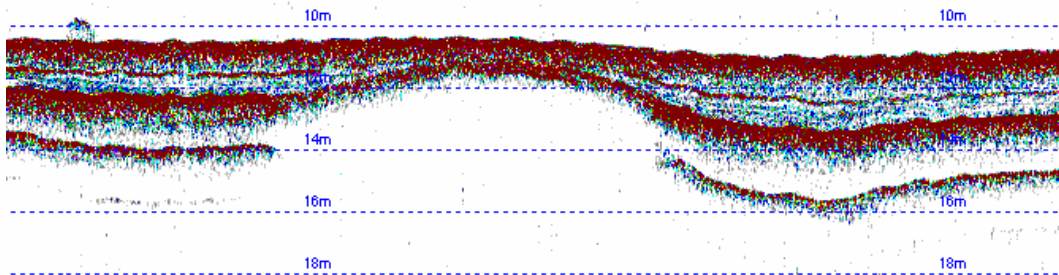


- ROT7_000 Stratigraphy not visible for most of track. Water depths range from 8 m to 20 m. Stratigraphy visible for 8 m into the sediment in middle of track between 12-14 m of water.
- ROT7_001 Mostly gaseous sediment in 14 m of water. Stratigraphy visible in areas that are possibly small pockmarks as sediment surface has depressions.
- ROT7_002 No track.
- ROT7_003 Complex stratigraphy of mounds and depressions that have been infilled to leave a flat sediment surface in 9 m water depth (see image). Depressions become smooth liner lines as water depth increases. At 14 m water depth sediment contains gas and

stratigraphy lost. As water shallows again stratigraphy becomes visible showing flat layers.

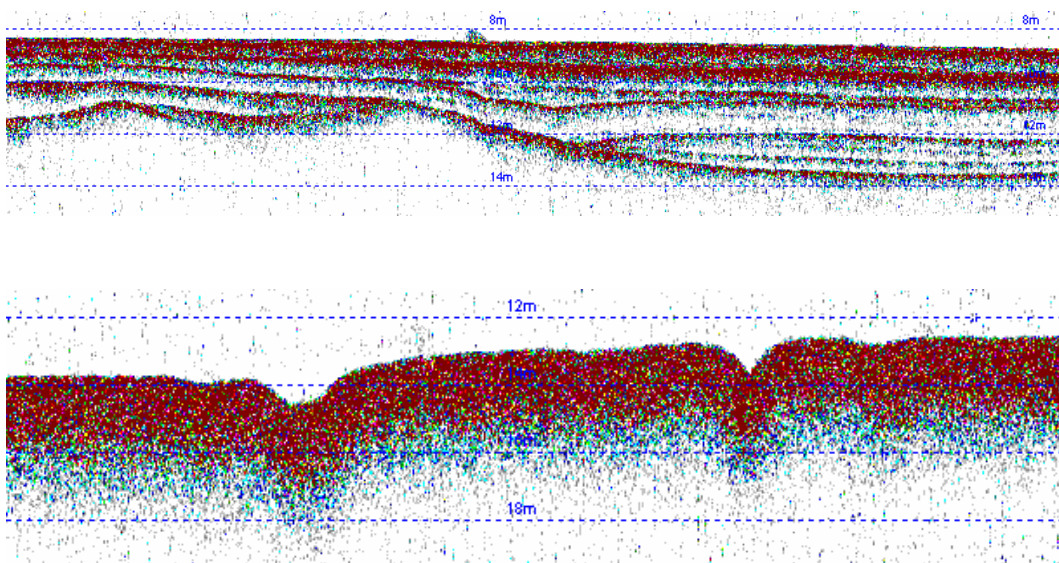


ROT7_004 Short track in 11 m water depth.



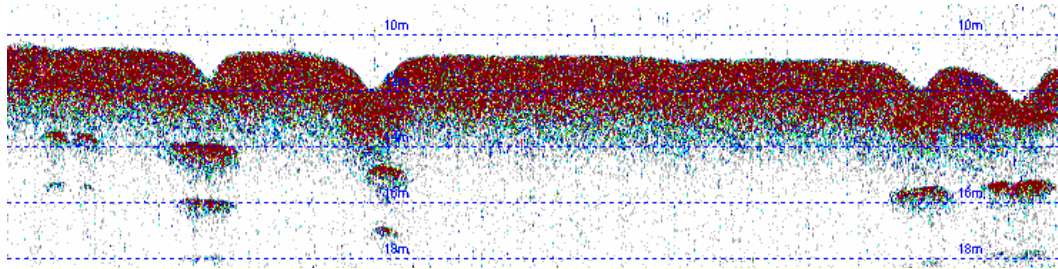
ROT7_005 Sediment in 14 m water depth is gaseous masking reflections until water depth decreases to 10 m. Stratigraphy shows similar to image in ROT6_010.

ROT7_006 Stratigraphy visible in water depth from 9 to 12m. Sediment becomes gaseous and reflection is lost. Gaseous sediment contains small depressions on the surface but stratigraphy is not visible below.

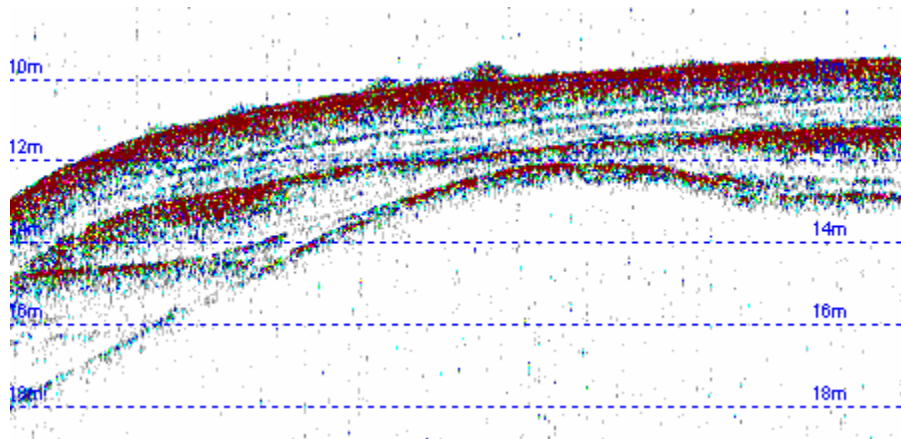


ROT7_007 Short track in 11 m water depth. Sediment gaseous same as image above. One larger pockmark larger showing one layer underneath.

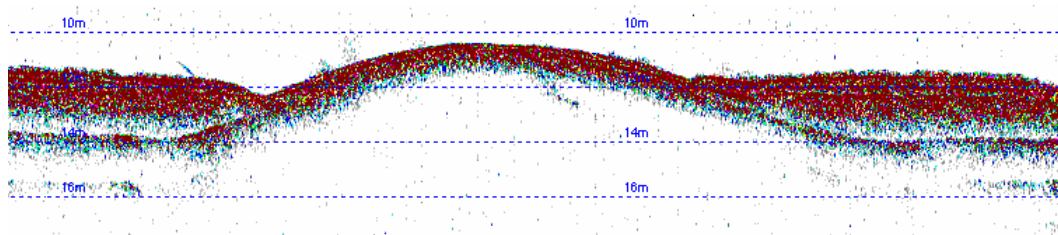
ROT7_008 Sediment pockmarked showing two layers of sediment below in 11 m water depth.



ROT7_009 Short track shown in image. 10 m water depth.

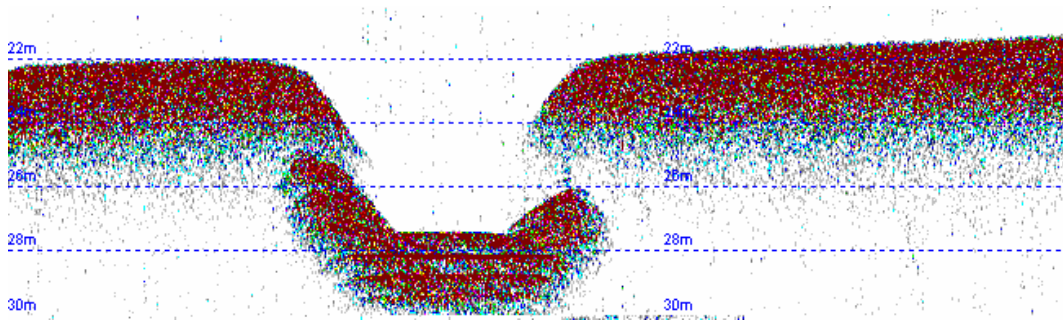


ROT7_010 Complex stratigraphy transitioning to areas with and without gas. When stratigraphy is seen it contains depressions and mounds. Areas of gas contain small pockmarks.



ROT7_011 Stratigraphy shows three main layers in 10 m water depth. Bottom layer contains more depressions that have been filled in but in places all sediment layers follow the pattern. Transition to gaseous sediment that contains small pockmarks. Large pockmark visible but shows no stratigraphy below.

ROT7_012 22 m water depth. Gaseous sediment. Large pockmark approximately 5.5 m deep.



ROT7_013 Gaseous sediment in 12-14 m water depth. Sediment surface reflects gently rolling hills. In the lower depressions sediment is less compacted and probably accumulates sediment at a faster rate.

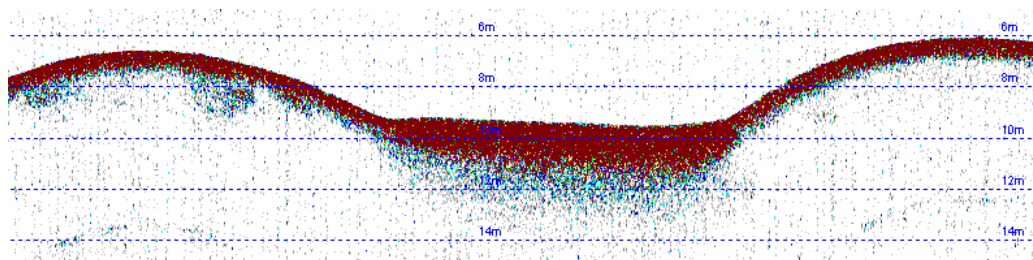
ROT7_014 No stratigraphy seen. Covers a large range of water depths as sediment depth increases and decreases gently.

DAY 8 14th September 2006

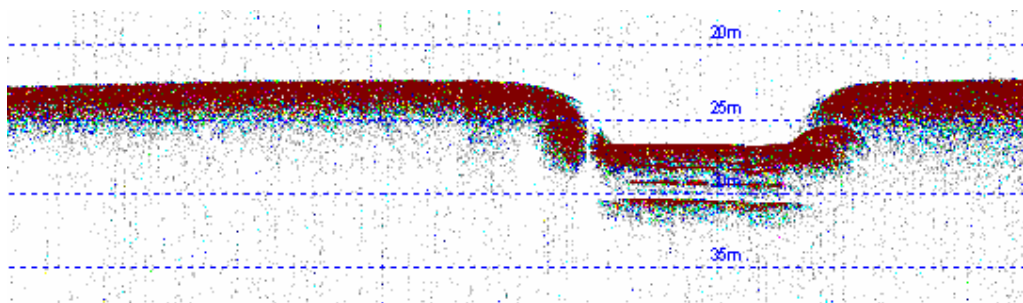
Day 8 tracks are located on the western side of Lake Rotrua. The sediment is predominantly diatomaceous ooze in water depths greater than 10 m.



- ROT8_000 Gaseous sediment in 18 to 16 m of water. No stratigraphy visible.
- ROT8_001 Short track in 18 m water depth. No stratigraphy visible.
- ROT8_002 Water depth changes steeply to form depressions. Stratigraphy visible in some areas as water depth decreases.
- ROT8_003 6 to 11 m water depth. Limited stratigraphy. Mounding seen as above but not as steep, with a change of only 2 m instead of 8 m as seen in the image above. Area in depression has a lower density than that on the mounds.



- ROT8_004 Gaseous sediment in 10 m water depth. Small pockmarks. Stratigraphy not visible.
- ROT8_005 Gaseous sediment in 13 m water depth. Small pockmarks. Stratigraphy not visible.
- ROT8_006 6 to 10 m water depth. Mounding present again with sediment usually visible at the bottom of the depression.
- ROT8_007 18 to 22 m water depth. Stratigraphy not seen.
- ROT8_008 Short track in 18 m water depth. Stratigraphy not visible.
- ROT8_009 22 to 16 m water depth. Stratigraphy not seen. Few small pockmarks present.
- ROT8_010 23 m water depth. No stratigraphy seen except below two large pock marks. Both approximately 4-5 m deep.

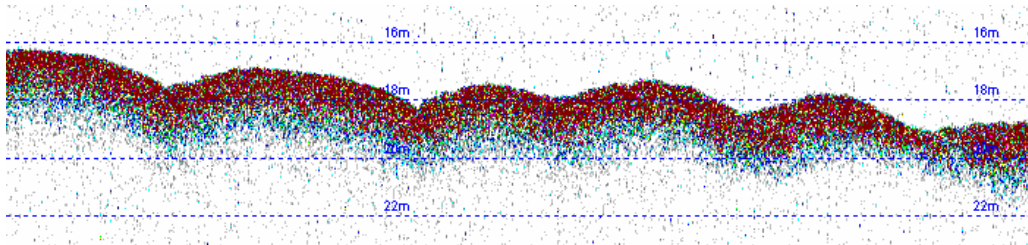


- ROT8_011 Short track 18-20 m water depth. Stratigraphy not seen due to the presence of gas.

ROT8_012 Stratigraphy not seen. Sediment surface has large mound from 18 to 15 m water depth.

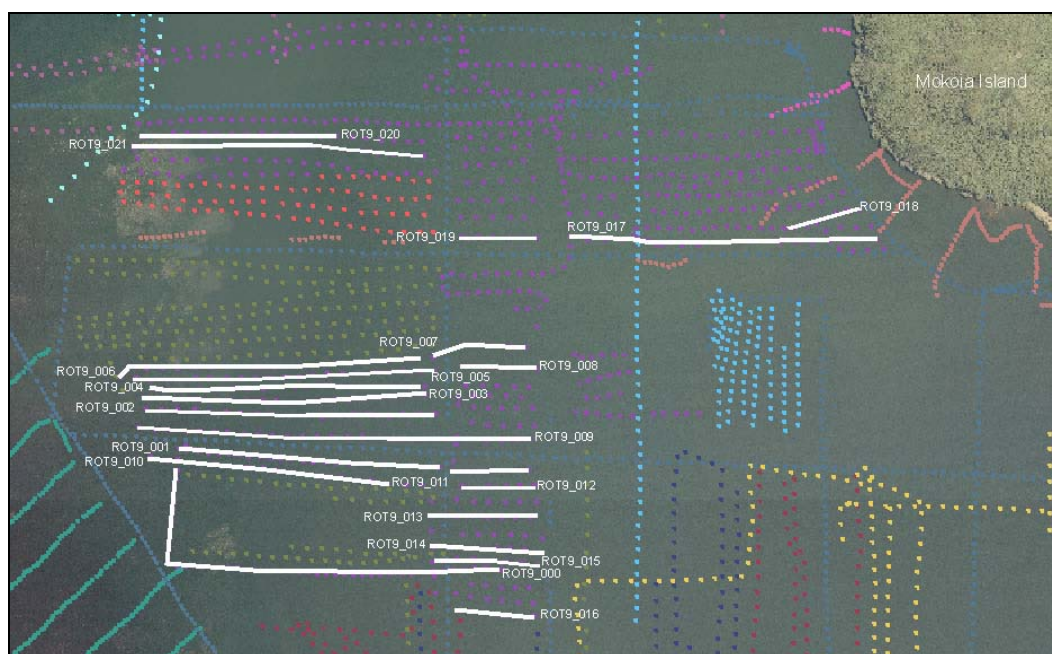
ROT8_013 Stratigraphy not seen. Sediment surface similar to ROT8_012.

ROT8_014 18 m of water depth. Area of very uneven surface.



DAY 9 15th September 2006

Day 9 tracks are located west of Ngongotaha in diatomaceous sediment.



ROT9_000 12-14 m water depth. Stratigraphy not seen. Small pockmarks.

ROT9_001 12-20 m water depth. Stratigraphy not seen. Small pockmarks.

ROT9_002 10-20 m water depth. Stratigraphy not seen. Small pockmarks.

ROT9_003 20-10 m water depth. Stratigraphy not seen. Small pockmarks.

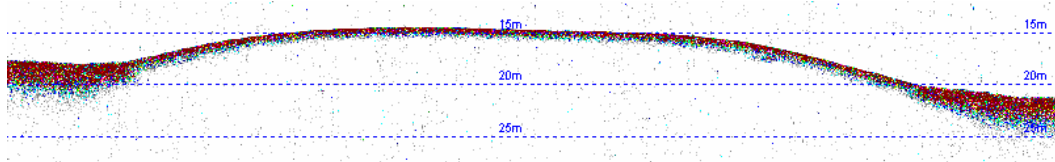
ROT9_004 12-20 m water depth. Stratigraphy not seen. Small pockmarks.

ROT9_005 20-10 m water depth. Stratigraphy not seen. Small pockmarks.

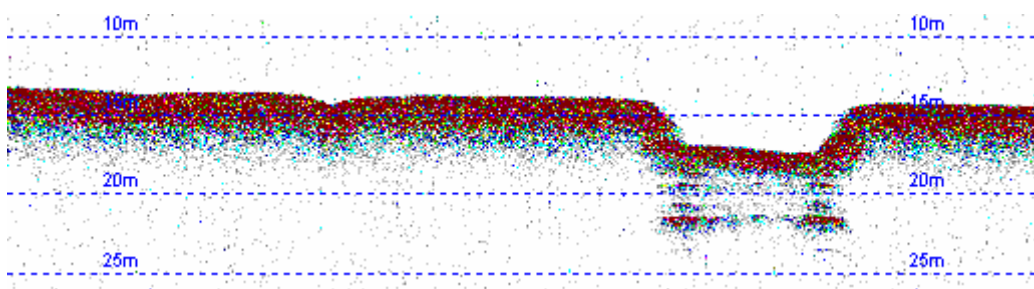
ROT9_006 10-20 m water depth. Stratigraphy not seen. Small pockmarks.

ROT9_007 Small track line in 20 m water depth. Stratigraphy not seen.

- ROT9_008 Small track line in 20 m water depth. Stratigraphy not seen.
- ROT9_009 18-10 m water depth. Stratigraphy not seen.
- ROT9_010 12-15 m water depth. Stratigraphy not seen.
- ROT9_011 Short track. Stratigraphy not seen. Mound of denser material in 15-20 m water depth.

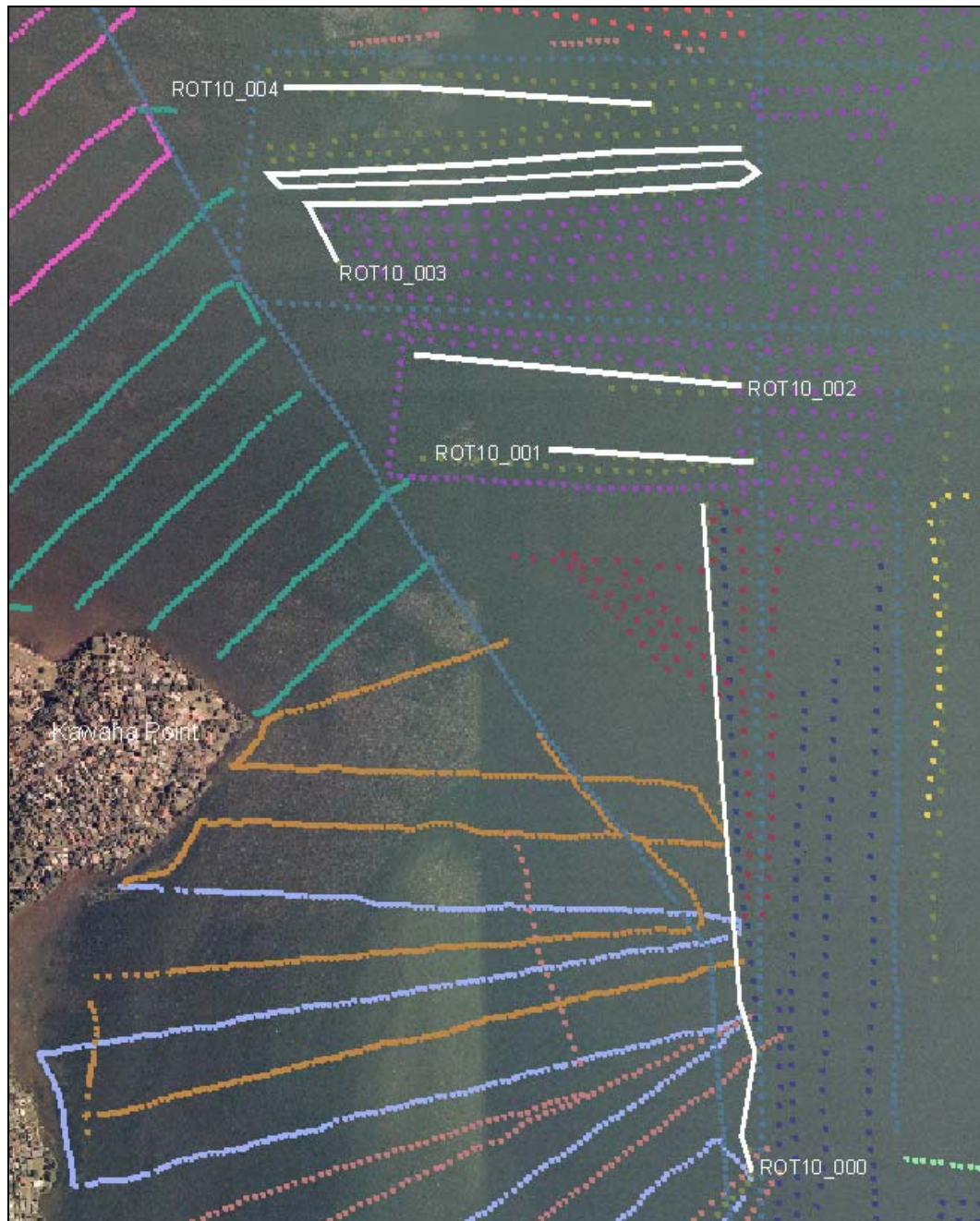


- ROT9_012 Short track. Stratigraphy not seen. 15-20 m water depth.
- ROT9_013 Short track. Stratigraphy not seen. 18-20 m water depth.
- ROT9_014 Short track. Stratigraphy not seen. 18-20 m water depth.
- ROT9_015 Short track. Stratigraphy not seen. 15 m water depth.
- ROT9_016 15-20 m water depth. Density of material higher in the shallower water depths. No Stratigraphy seen.
- ROT9_017 25-12.5 m water depth. Uneven sediment surface. Stratigraphy not seen.
- ROT9_018 Short track. Stratigraphy not seen. 20-16 m water depth.
- ROT9_019 Short track. Stratigraphy not seen. 20 m water depth.
- ROT9_020 Short track. Stratigraphy not seen. 15-13 m water depth.
- ROT9_021 15 m water depth. Stratigraphy not seen except under one large pock mark.

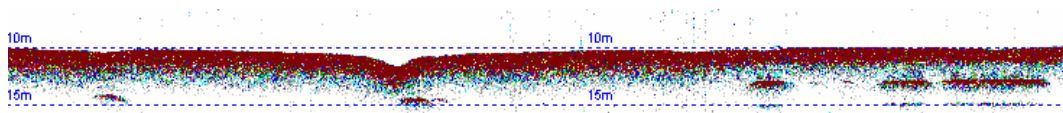


DAY 10 1st November 2006

Day 10 tracks are located in water depths between 10 and 18 m near Kawaha Point. The dominant sediment type is diatomaceous ooze.



ROT10_000 Water depth changes between 10-15 m. Stratigraphy generally not seen except in small areas.



ROT10_001 Water depth 12.5 m. Stratigraphy not seen.

ROT10_002 12-15 m water depth. Stratigraphy not seen except under small pock marks.

ROT10_003 10-18 m water depth. Stratigraphy not seen except under small pock marks.

ROT10_004 12-18 m water depth. Stratigraphy not seen except under small pock marks.

DAY 11 12th November 2006

Tracks recorded on day 11 are located in the deepest part of the lake west of Mokoia Island. The sediment type is diatomaceous ooze.

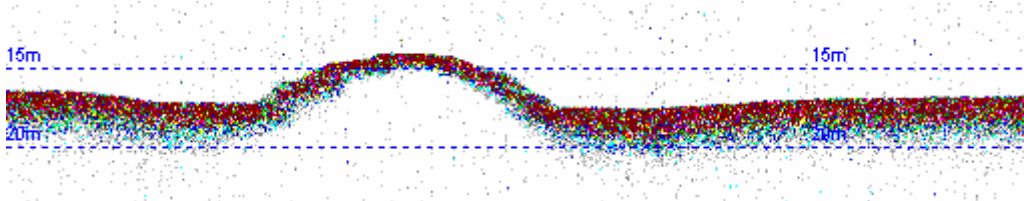


ROT11_000 20-16 m water depth. Stratigraphy not seen.

ROT11_001 22-16 m water depth. Stratigraphy not seen.

ROT11_002 16-24 m water depth. Stratigraphy not seen.

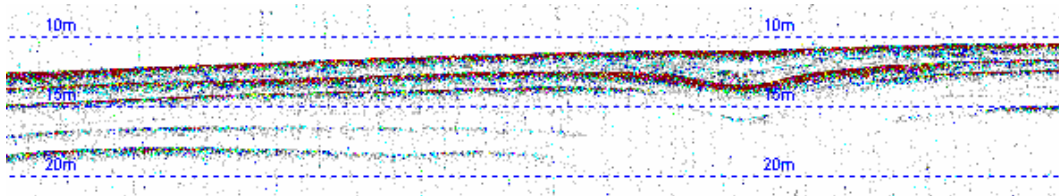
ROT11_003 12 m water depth. Stratigraphy not seen. Mound in sediment.



ROT11_004 Water depth range from 10-25 m. Smooth sediment surface with few mounds and depressions. Stratigraphy not seen.

ROT11_005 22-18 m water depth. Stratigraphy not seen.

ROT11_006 22-10 m water depth. Stratigraphy not seen until the end of the track line in 12 m water depth.



ROT11_007 10-20 m water depth. Thin stratigraphy seen until 15 m water depth.

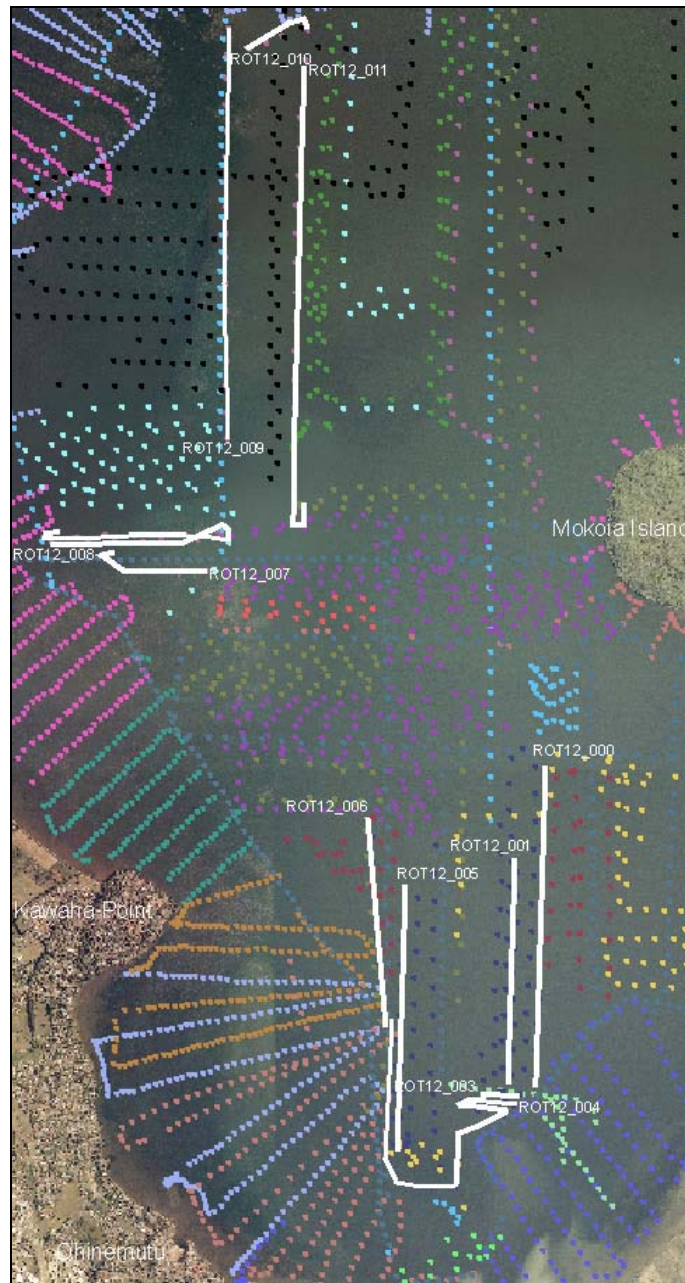
ROT11_008 Short track in 25 m water depth. No Stratigraphy.

ROT11_009 25-18 m water depth. Stratigraphy not seen.

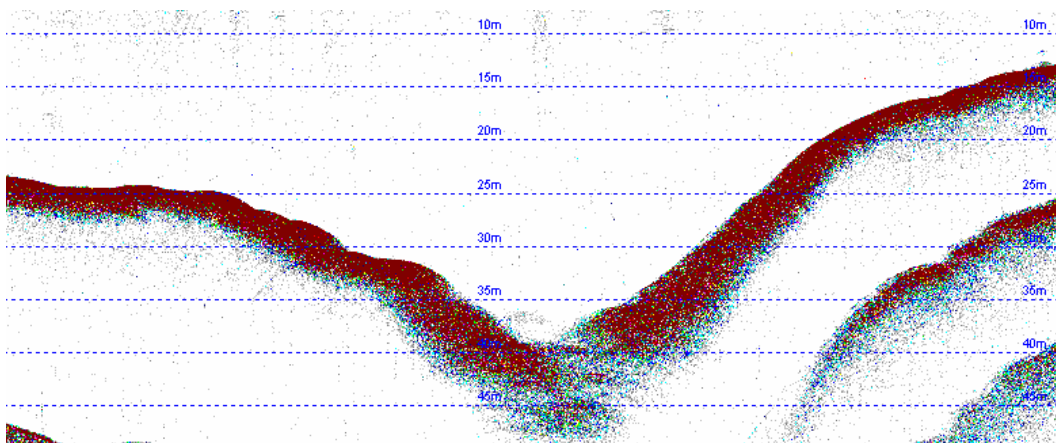
ROT11_010 16-20 m water depth. Stratigraphy not seen.

DAY 12 3rd November 2006

Day 12 tracks are recorded to the west of Mokoia Island. The tracks are located in water depths ranging from 8 to 18 m. The sediment type is diatomaceous ooze. Coarse sediments may be encountered close to the 10 m depth contour.

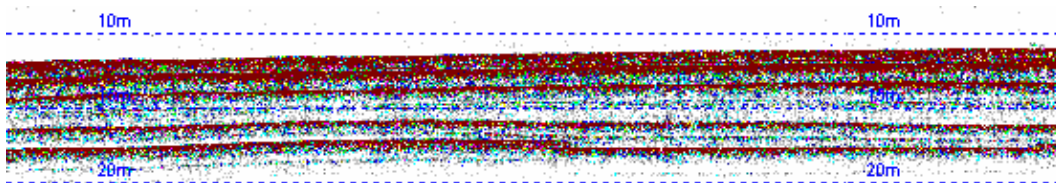


- ROT12_000 18-10 m water depth. Stratigraphy not seen until 15 m water depth at the end of the track line.
- ROT12_001 18-12 m water depth. Stratigraphy not seen.
- ROT12_002 Short track. 12-18 m water depth. Stratigraphy not seen.
- ROT12_003 Short track. 12-14 m water depth. Stratigraphy not seen.
- ROT12_004 Multiples of the sediment surface are seen on this track. Water depth ranges from 10-40 m. Steep drop in water depth shown in image. Location most possibly just north of Sulphur Point as it is the deepest part of the lake.



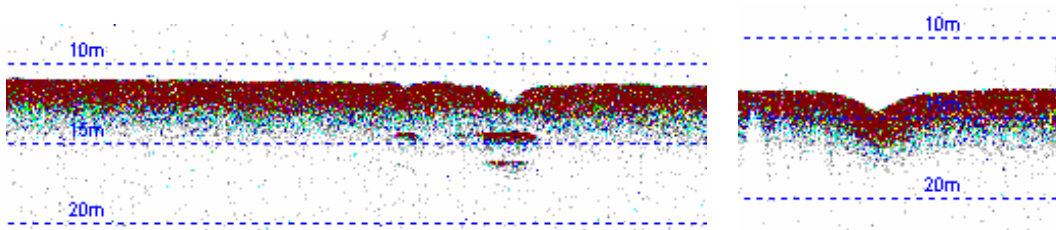
ROT12_005 13-18 m water depth. Stratigraphy not seen in most areas except at start of track line. No change in water depth while this occurs.

ROT12_006 15-12 m water depth. Stratigraphy seen in 12 m water depth. Flat laminated stratigraphy showing 4 distinct layers.



ROT12_007 18 m water depth. Stratigraphy not seen except in very small areas.

ROT12_008 10-13 m water depth. Stratigraphy not seen except under some of the small pockmarks.



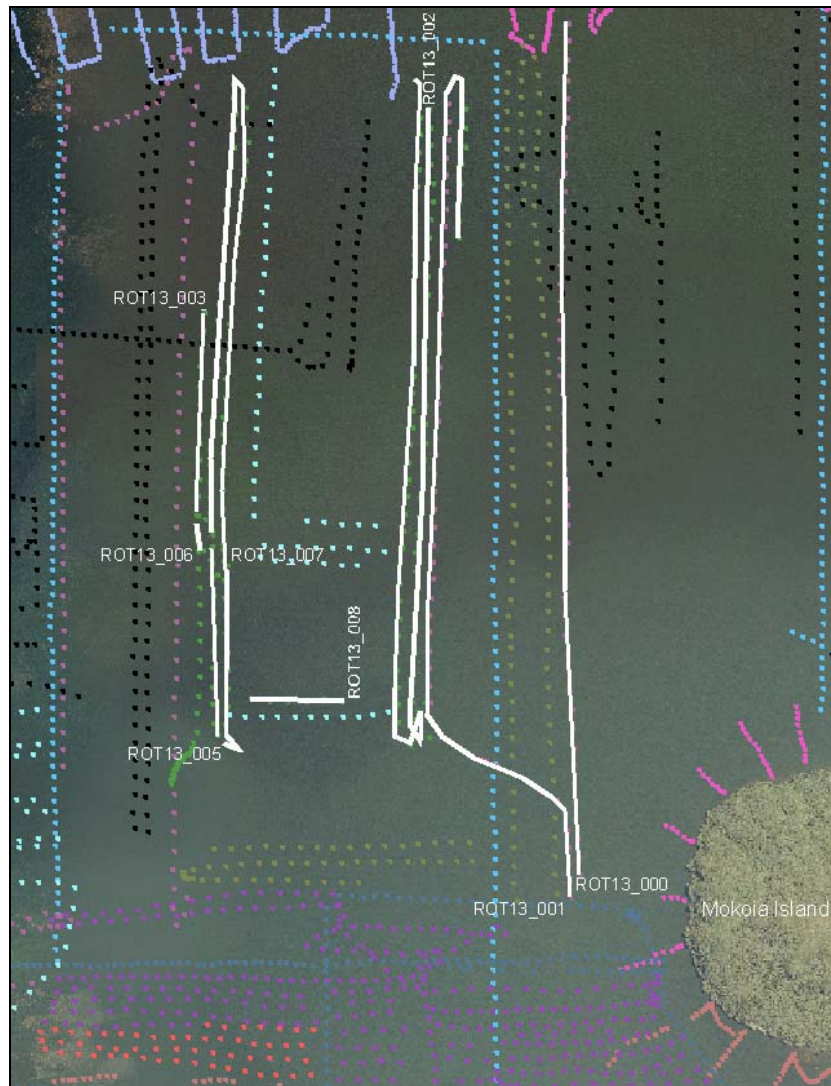
ROT12_009 Water depth 10-12 m. Stratigraphy not seen until end of track line. Small pockmarks present in gaseous sediment.

ROT12_010 12-8 m water depth. Stratigraphy not seen.

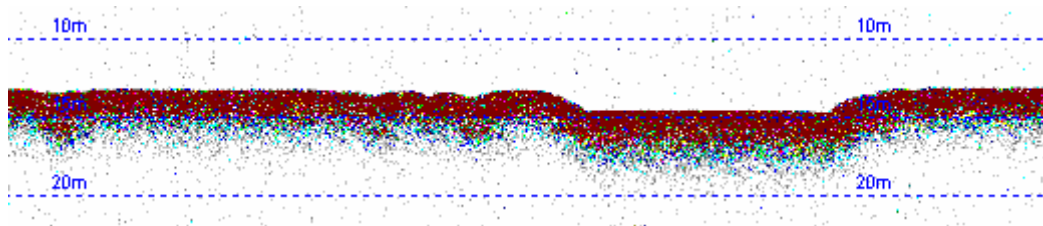
ROT12_011 15 m water depth. Sediment stratigraphy not seen except under one small pockmark.

DAY 13 4th November 2006

Day 13 tracks are located to the northwest in Lake Rotorua in water depths greater than 10 m. The sediment type is diatomaceous ooze.

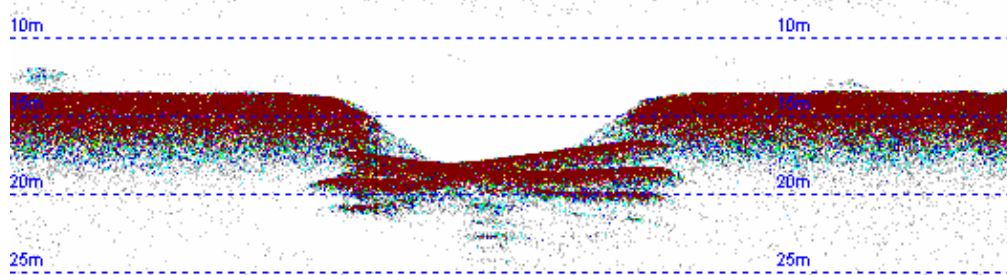


- ROT13_000 23-15 m water depth. Stratigraphy not seen. One small pockmark.
- ROT13_001 24-15 m water depth. Stratigraphy not seen.
- ROT13_002 8-20 m water depth. Stratigraphy not seen. Few small pockmarks.
- ROT13_003 14 m water depth. Stratigraphy not seen. Small pockmarks present. One large pock mark approximately 2 m deep. Stratigraphy not seen underneath.



- ROT13_004 No profile.
- ROT13_005 15 m water depth. Few small pockmarks. Stratigraphy not seen.

ROT13_006 Short track. One large pockmark showing underlying stratigraphy.
14 m water depth. Pockmark approximately 5 m deep.



ROT13_007 14 m water depth with mound in the middle of the track decreasing to 10 m water depth. Stratigraphy not seen. Many small pockmarks present.

ROT13_008 16 m water depth. Small pockmarks. No stratigraphy seen.

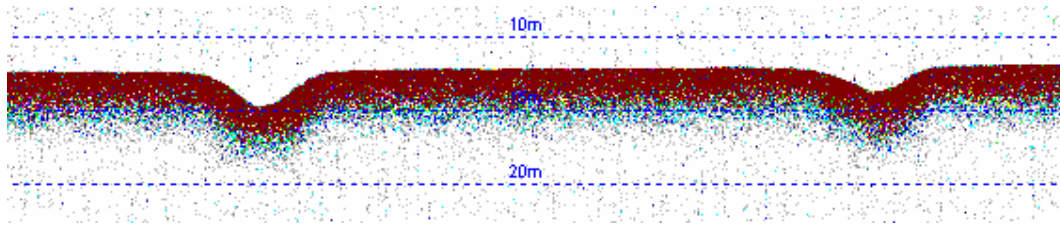
DAY 14 5th November 2006

Day 14 tracks are located east of Ngongotaha is water depths greater than 12 m. The sediment in this area is predominantly diatomaceous ooze.



ROT14_000 12-14 m water depth. Small pockmarks. No stratigraphy seen.

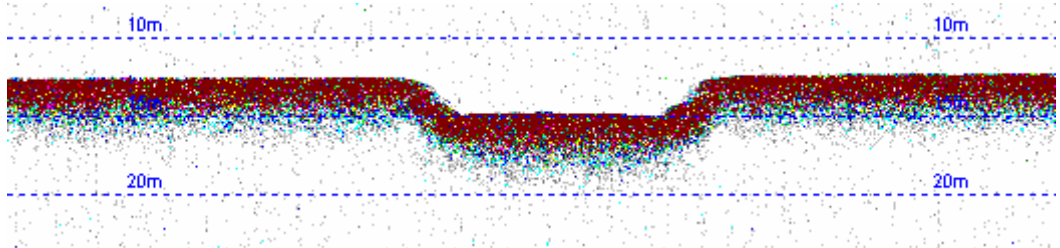
ROT14_001 12.5 m water depth. No stratigraphy seen. Larger pockmarks present.



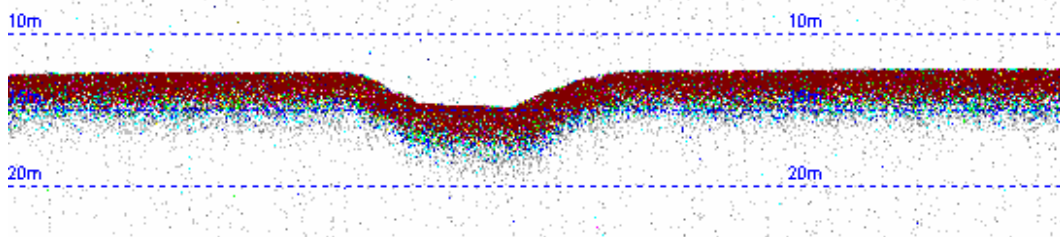
ROT14_002 12 m water depth. Stratigraphy not seen.

ROT14_003 12 m water depth. Stratigraphy not seen. Few small pockmarks.

ROT14_004 12.5 m water depth. One large pockmark. Stratigraphy not seen.



ROT14_005 12 m water depth. One large pockmark. Stratigraphy not seen.

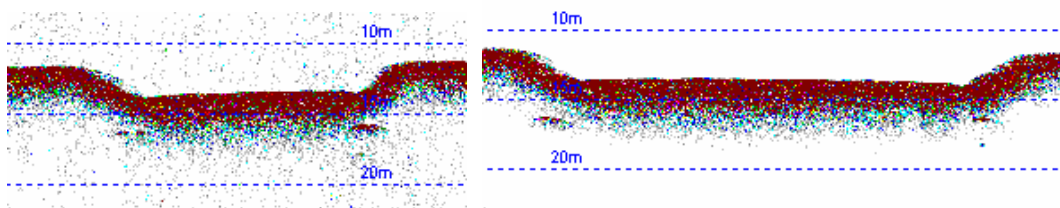


ROT14_006 12 m water depth. two large pockmarks. Stratigraphy not seen.

ROT14_007 12 m water depth. Stratigraphy not seen. Few small pockmarks.

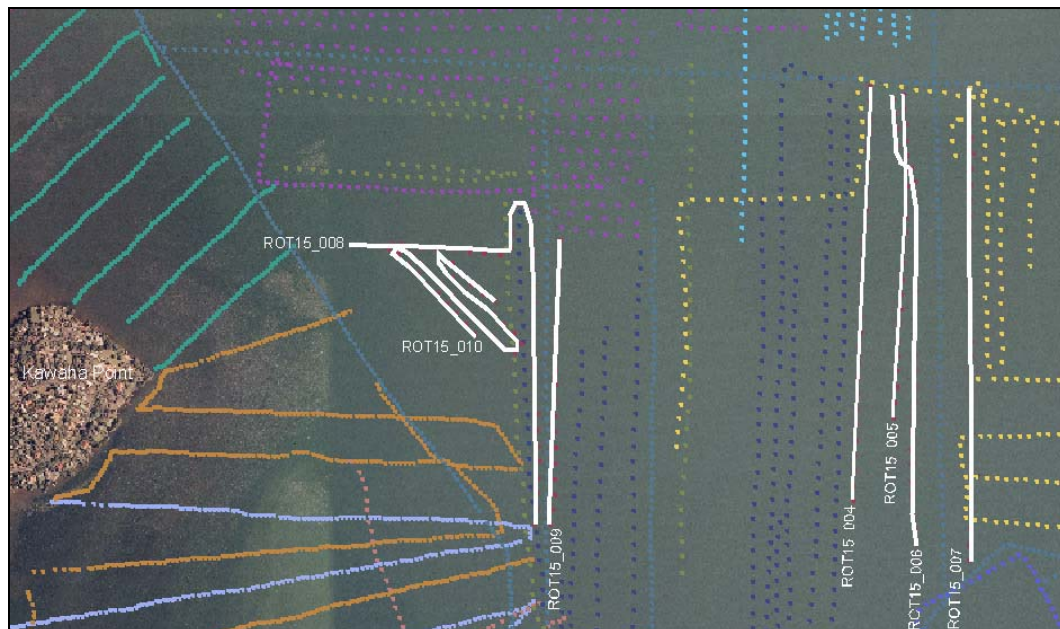
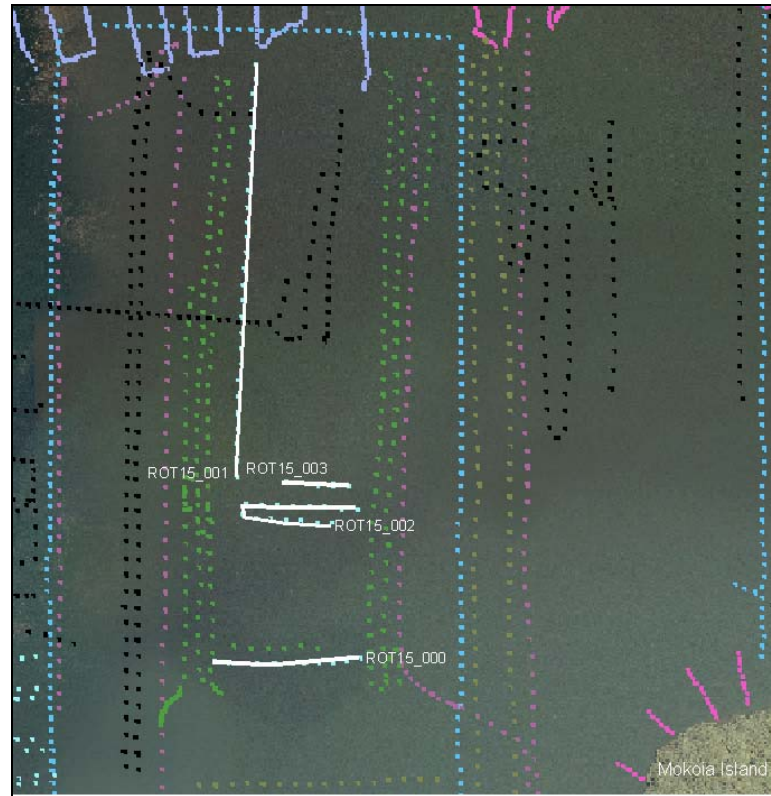
ROT14_008 12 m water depth. One large pockmark. Stratigraphy not seen.

ROT14_009 Short track. Two large pock marks, but track covers over the same pockmark twice. Stratigraphy not seen.

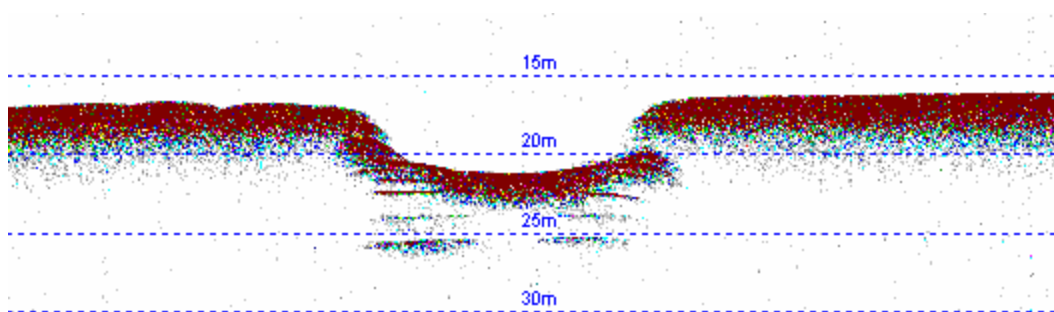


DAY 15 6th November 2006

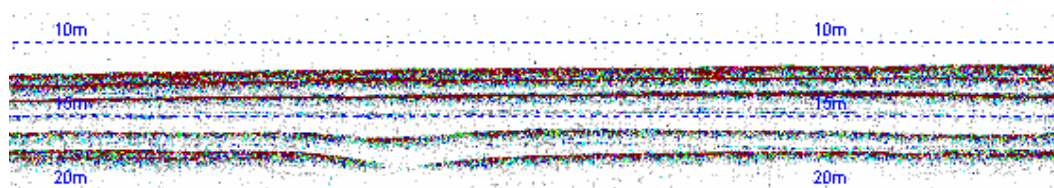
Day 15 tracks are located to the northwest of Mokoia Island and east of Kawaha Point. The sediment type is diatomaceous ooze.



ROT15_000 18-15 m water depth. One large pock mark approximately 5 m deep showing underlying stratigraphy.



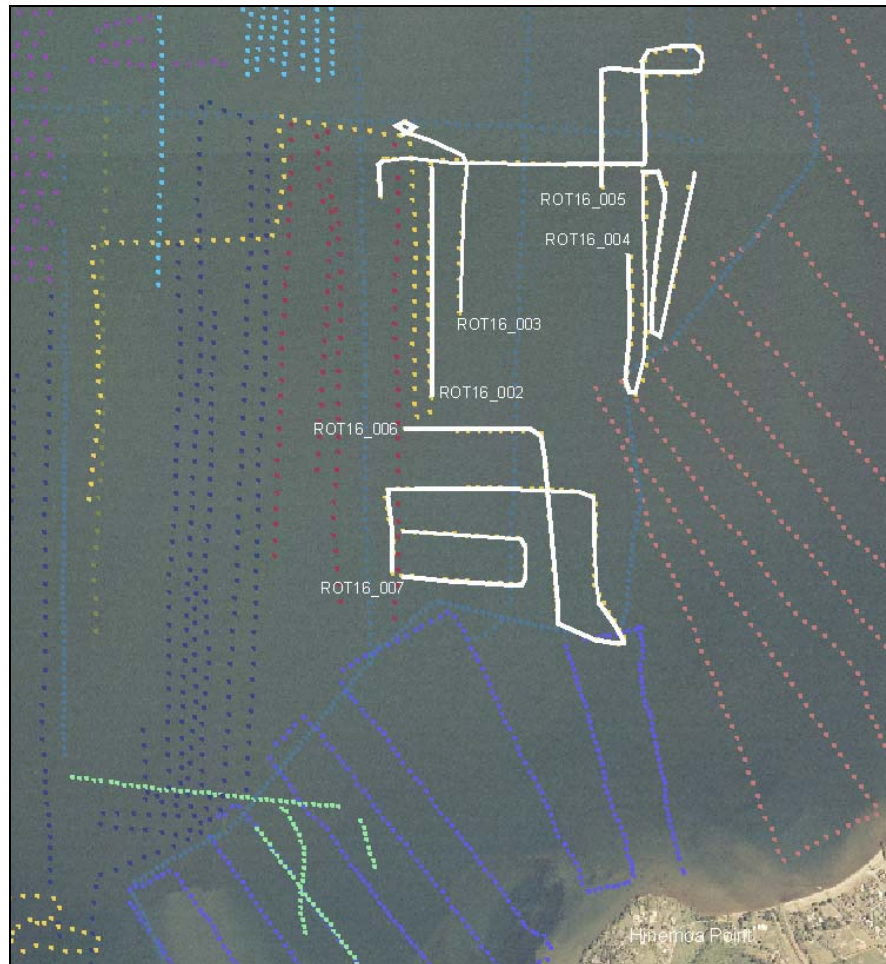
- ROT15_001 14 m water depth. Stratigraphy not seen. Few small pockmarks.
- ROT15_002 16 m water depth. Stratigraphy not seen. Few small pockmarks.
- ROT15_003 15 m water depth. Stratigraphy not seen.
- ROT15_004 15-18 m water depth. Undulating sediment surface. Stratigraphy not seen.
- ROT15_005 15 m water depth. Stratigraphy not seen. Few small pockmarks.
- ROT15_006 In 12 m water depth at start of track stratigraphy is visible showing two distinct layers. Transitions into gas filled sediment with no change in water depth and stratigraphy is no longer visible. Few small pockmarks present.
- ROT15_007 In 12 m water depth at start of track stratigraphy is visible showing two distinct layers. Mounds present in the sediment of a denser material. Transitions into gas filled sediment in 15 m water depth and stratigraphy is no longer visible. Few small pockmarks present.
- ROT15_008 10-15 m water depth with few small pockmarks. Stratigraphy not seen until water depth decreases to 14m at the end of the track line. 4 distinct layers present.



- ROT15_009 12 m water depth stratigraphy visible, similar to above image. Stratigraphy not seen after water depth increases to 15 m at the end of the track.
- ROT15_010 12 m water depth stratigraphy visible in most areas. Part of track stratigraphy masked by the presence of gas in the sediment. Small pockmarks present in these areas.

DAY 16 11th December 2006

Day 16 tracks are located north of Hinemoa Point. The sediment is dominated by sands and gravels near shore and transition into diatomaceous sediment. The water depth is less than 14 m for these tracks.

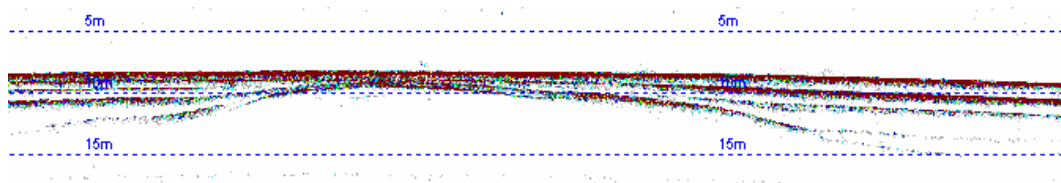


ROT16_002 No data at low frequency.

ROT16_003 No data at low frequency.

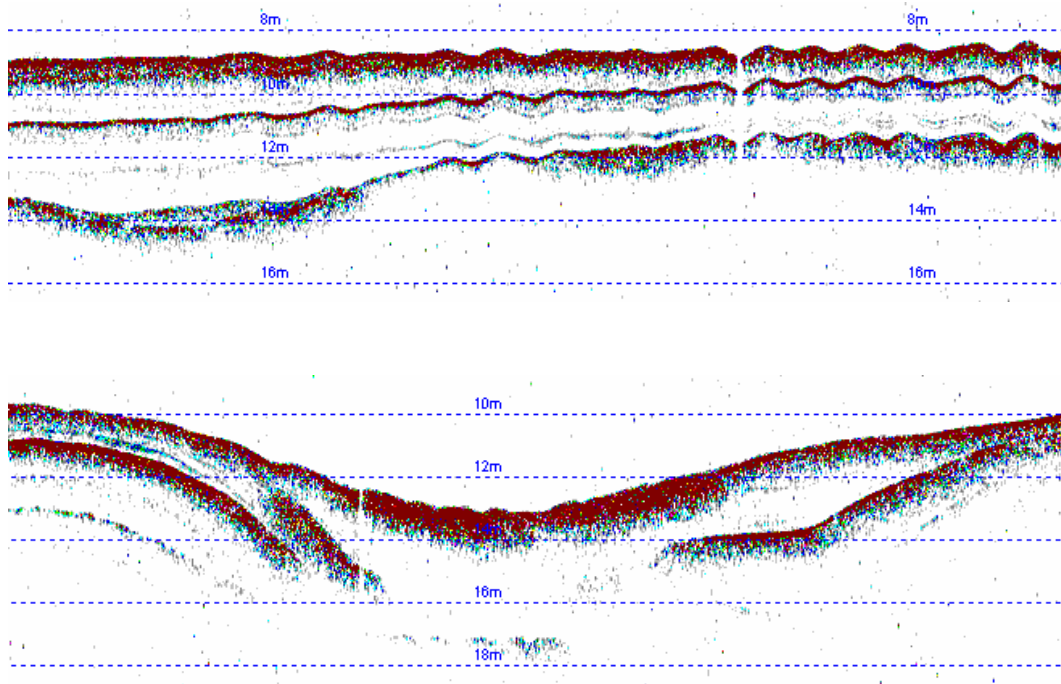
ROT16_004 No data at low frequency.

ROT16_005 Less than 10 m water depth. 3 distinct layers present.

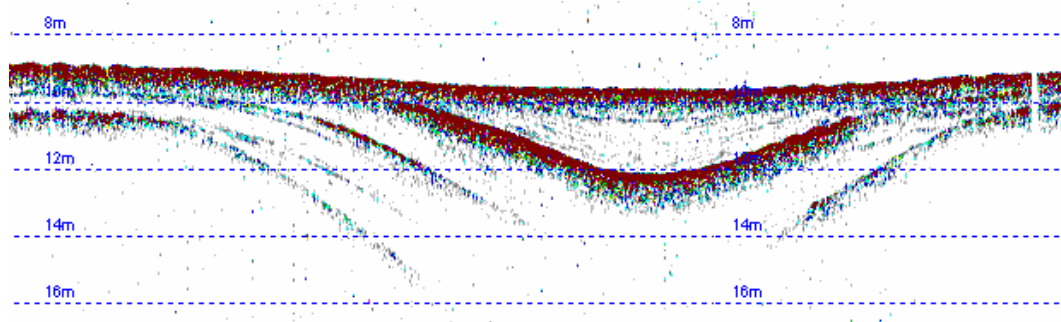


ROT16_006 Less than 10 m water depth. Sediment surface changes from a flat surface to a wavy surface shown in the image. Stratigraphy is visible. There are three large depressions in the sediment across the

track before gas charged sediment blocks the stratigraphy in 14 m water depth.

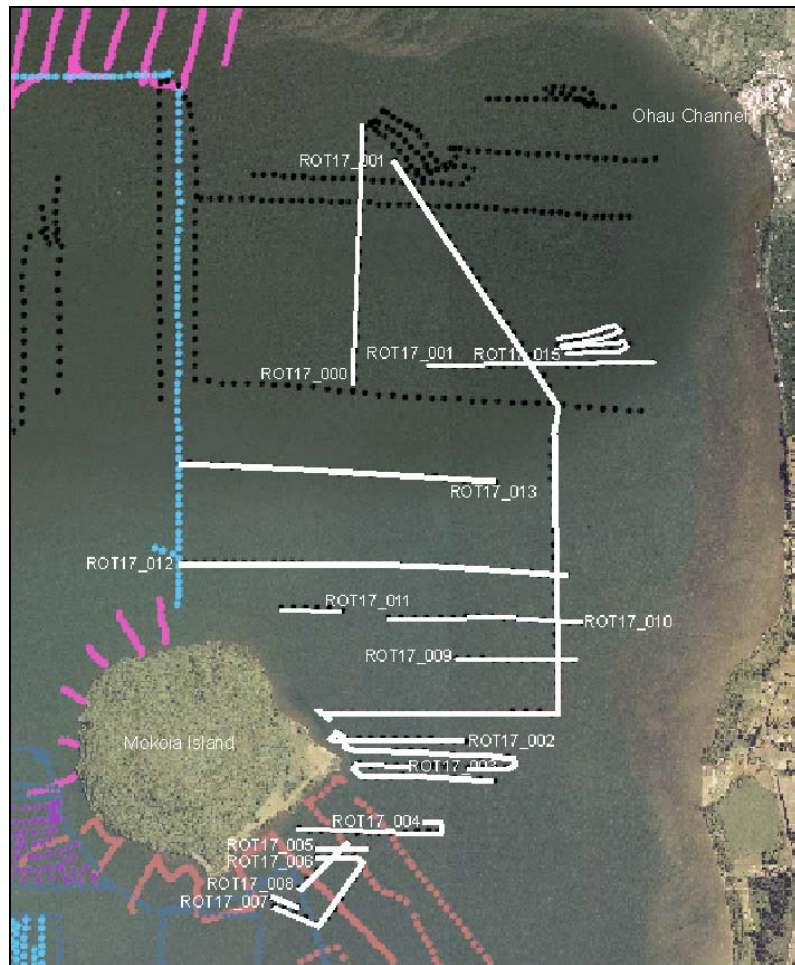


ROT16_007 7-12 m water depths. Stratigraphy visible showing areas of infilled depressions.



DAY 17 12th December 2006

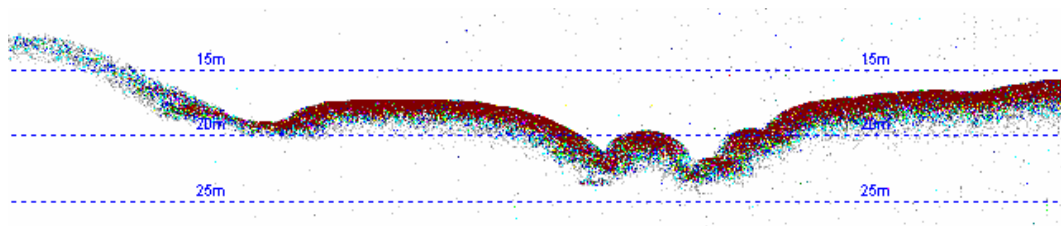
Day 17 tracks are on the eastern side of Lake Rotorua. The tracks are in varying water depths and sediment type.



ROT17_000 17-8 m water depth. Stratigraphy not seen.

ROT17_001 17-8 m water depth. Stratigraphy not seen. Mounds of sediment present at the end of the track line.

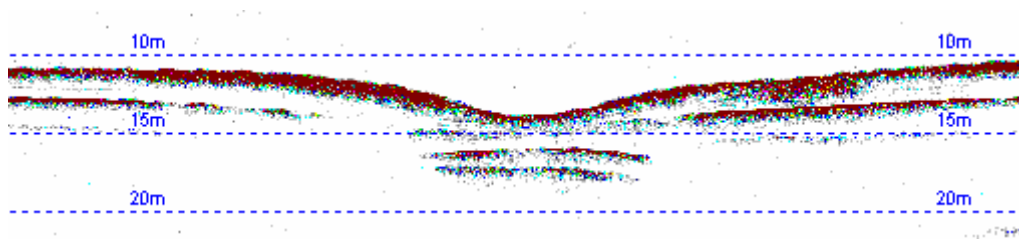
ROT17_002 12-20 m water depth. Stratigraphy not seen. Uneven sediment surfaces in the deeper water. Possibly pockmarks.



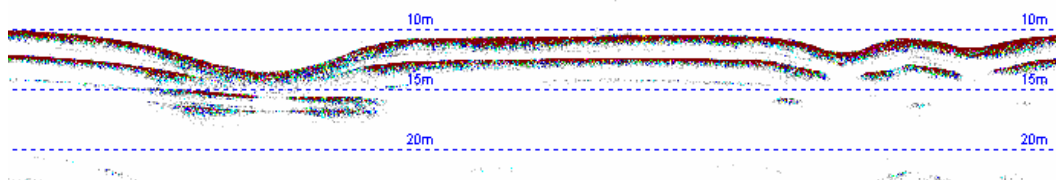
ROT17_003 14-10 m water depth. Stratigraphy not seen. Uneven sediment surfaces in some areas. Possibly pockmarks.

ROT17_004 10 m water depth. Faint stratigraphy visible.

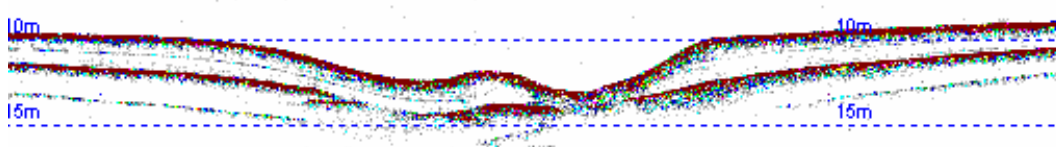
ROT17_005 11 m water depth. Faint stratigraphy visible. Feature that resembles a pockmark but stratigraphy is visible on either side.



ROT17_006 11 m water depth. Faint stratigraphy visible. Features similar to that of previous track.



ROT17_007 Short track in 10 m water depth. Depression in sediment surface is not represented in underlying layer.



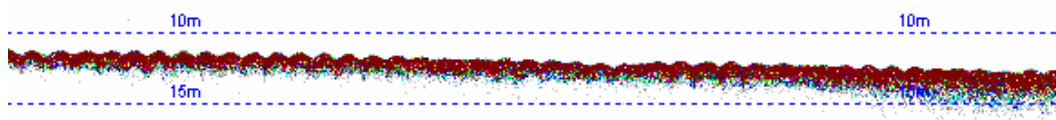
ROT17_008 Short track in 10 -14 m of water. Stratigraphy visible.

ROT17_009 14-10 m water depth. Stratigraphy not visible.

ROT17_010 14-10 m water depth. Stratigraphy not visible.

ROT17_011 10-15 m water depth. Stratigraphy not visible. Small pockmark present.

ROT17_012 12-15 m water depth. Stratigraphy not visible. Sediment surface is wavy. This could be a result of wave action on the sediment as winds mix the water.



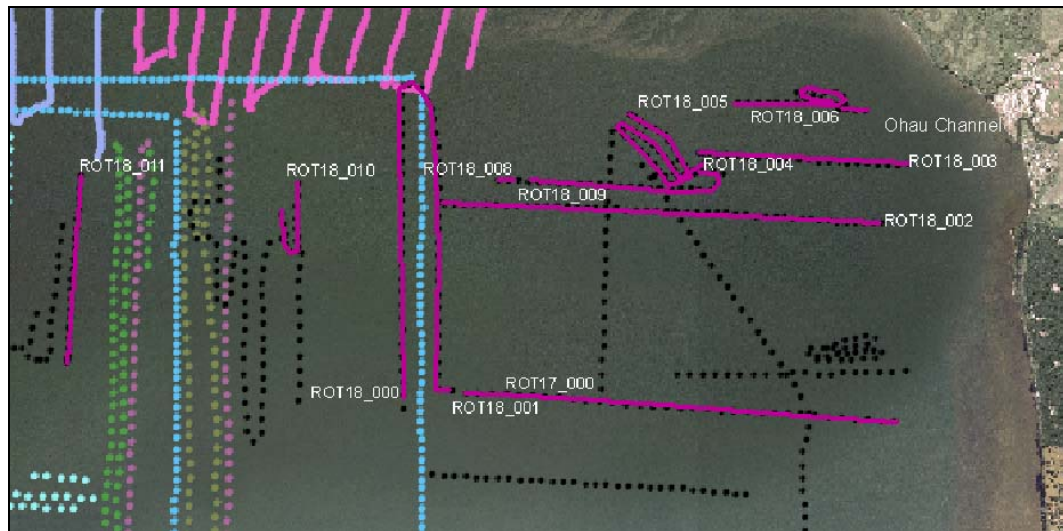
ROT17_013 15-20 m water depth. Stratigraphy not visible.

ROT17_014 15-11 m water depth. Stratigraphy not visible. Small pockmark present.

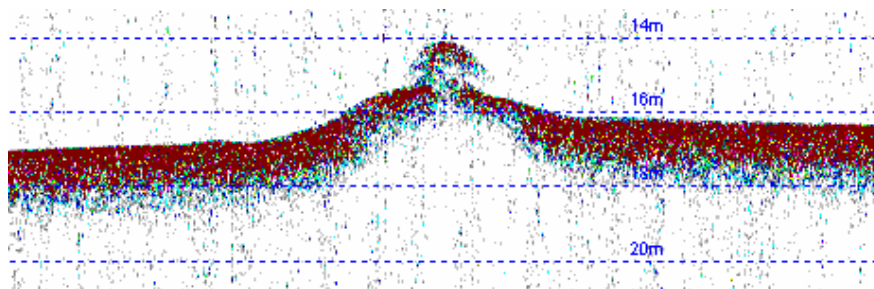
ROT17_015 8-15 m water depth as mounds are visible. No stratigraphy.

DAY 18 14th December 2006

Day 18 tracks are located in the north eastern corner of the lake.



- ROT18_000 18-8 m water depth as sediment rises in mounds. Stratigraphy not visible.
- ROT18_001 20-14 m water depth. Stratigraphy not visible. Small pockmarks present.
- ROT18_002 12-20 m water depth. Stratigraphy not visible. Small pockmarks present.
- ROT18_003 13-20 m water depth. Stratigraphy not visible.
- ROT18_004 15-20 m water depth. Stratigraphy not visible. Small pockmarks present.
- ROT18_005 15-20 m water depth. Stratigraphy not visible. Small pockmarks present. Mounds in the sediment surface.

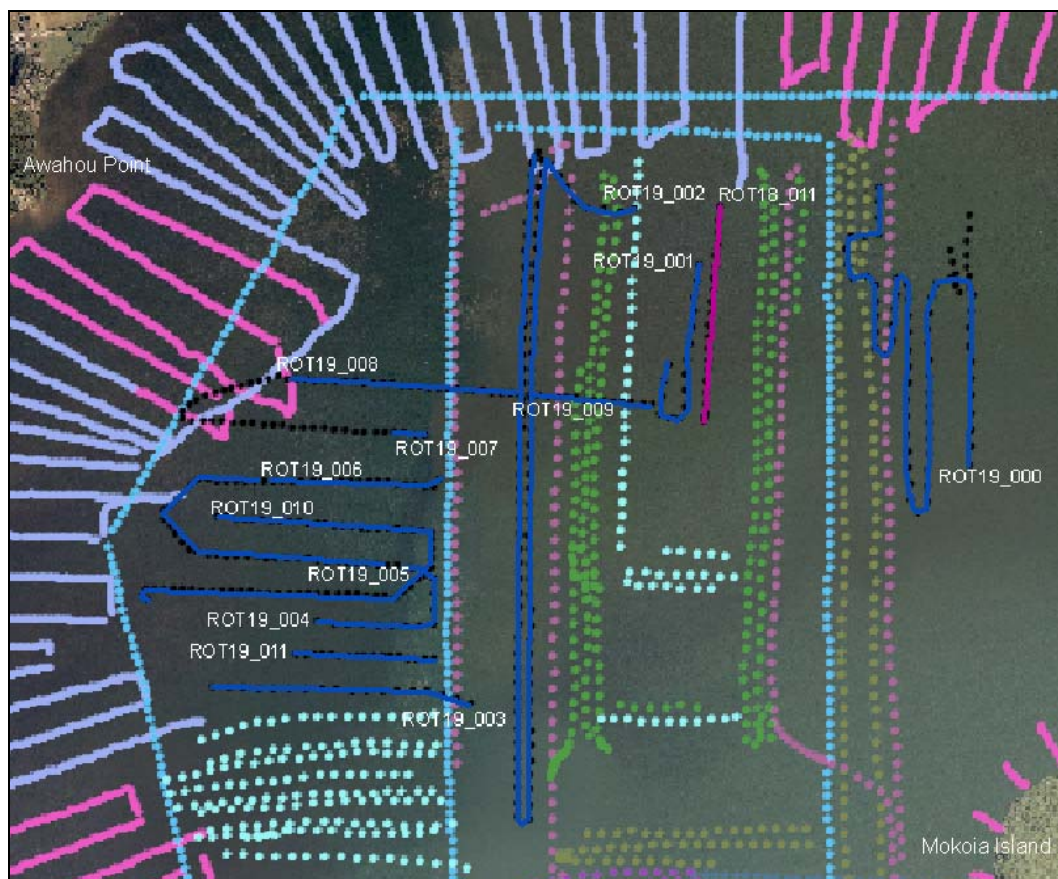


- ROT18_006 10-20 m water depth. Undulating sediment surface. Stratigraphy not visible.
- ROT18_007 16-20 m water depth. Stratigraphy not visible. Small pockmarks present.
- ROT18_008 Short track. 20 m water depth. Stratigraphy not visible.

- ROT18_009 18-21 m water depth. Stratigraphy not visible. Undulating sediment surface. Small pockmarks present.
- ROT18_010 16 m water depth. Stratigraphy not visible. 3 pockmarks present that drop the sediment surface by 2 m in the middle of the pockmark.
- ROT18_011 16-15 m water depth. Stratigraphy not visible. Small pockmarks present.

DAY 19 15th December 2006

Day 19 tracks are located in water depths greater than 10 m in the north western part of the lake near Awahou Point. The sediment type is predominantly diatomaceous ooze.



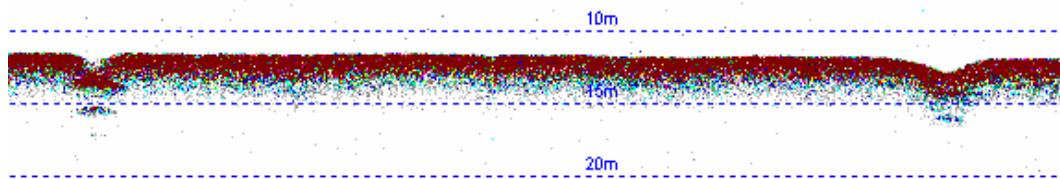
- ROT19_000 20-15 m water depth. Stratigraphy not visible. Small pockmarks present.

ROT19_001 15 m water depth. Stratigraphy not visible. Small pockmarks present.

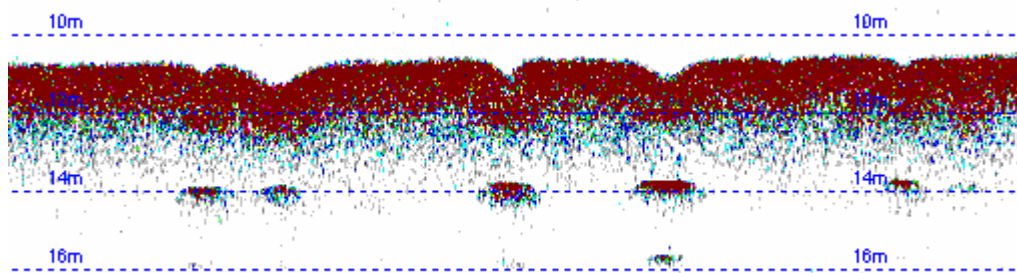
ROT19_002 15-12 m water depth. Stratigraphy not visible. Small pockmarks present.

ROT19_003 14-11 m water depth. Stratigraphy not visible. Small pockmarks present.

ROT19_004 12 m water depth. Stratigraphy not visible. Small pockmarks present to show slight stratigraphy underneath.



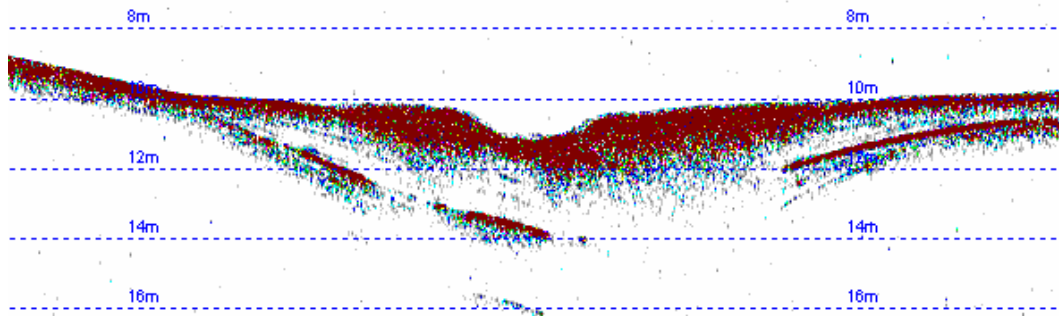
ROT19_005 12 m water depth. Stratigraphy not visible. Small pockmarks present to show slight stratigraphy underneath.



ROT19_006 11 m water depth. Stratigraphy not visible. Small pockmarks present to show slight stratigraphy underneath.

ROT19_007 12 m water depth. Stratigraphy not visible. Small pockmarks present to show slight stratigraphy underneath. At the end of the track line sediment becomes denser and mounds are found.

ROT19_008 8 to 12 m water depth. Stratigraphy visible until half way through the track line where sediment becomes gas filled and the stratigraphy is masked. Areas of infilling in depressions are found at the start of the track.



- ROT19_009 12-10 m water depth. Sediment transitions from gas filled to non gaseous and stratigraphy becomes visible. Two distinct layers are present. Small pockmarks present in areas with gas in the sediment.
- ROT19_010 10-12 m water depth. Sediment stratigraphy not visible. Small pockmarks present. Stratigraphy visible underneath some pockmarks.
- ROT19_011 11 m water depth. Sediment stratigraphy not visible. Small pockmarks present.